



# Interagency Flood Risk Management (InFRM)

## Watershed Hydrology Assessment for the Nueces River Basin

March 2025

# Table of Contents

- The InFRM Team..... 7**
- Executive Summary ..... 8**
- 1 Study Background and Purpose ..... 15**
  - 1.1 The National Flood Insurance Program..... 15
  - 1.2 The Challenge and Importance of Hydrology..... 16
  - 1.3 Purposes of the Watershed Hydrology Assessment..... 16
  - 1.4 Study Team Members ..... 17
  - 1.5 Technical Review Process..... 18
- 2 Nueces River Basin..... 19**
  - 2.1 Watershed and River System Description ..... 19
  - 2.2 Climate ..... 22
  - 2.3 Major Floods in the Nueces River Basin ..... 22
    - 2.3.1 The Flood of July 1932..... 23
    - 2.3.2 The Flood of June 1935 ..... 24
    - 2.3.3 The Flood of September 1955 ..... 24
    - 2.3.4 The Flood of September 1967 – Hurricane Beulah..... 24
  - 2.4 Previous Studies and Currently Effective FEMA Flows..... 25
  - 2.5 The Effects of Future Conditions ..... 26
- 3 Methodology..... 28**
- 4 Data Sources..... 29**
  - 4.1 Spatial Tools and Reference..... 29
  - 4.2 Digital Elevation Model (DEM) ..... 29
  - 4.3 Vector and Raster Geospatial Data ..... 29
  - 4.4 Aerial Images ..... 29
  - 4.5 Soil Data..... 30
  - 4.6 Precipitation Data..... 30
    - 4.6.1 Radar Data for Observed Storms ..... 30

4.6.2 NOAA Atlas 14 Frequency Point Rainfall Depths..... 30

4.7 Stream Flow and Stage Data ..... 30

4.8 Reservoir Physical Data ..... 32

4.9 Software ..... 34

**5 Statistical Hydrology..... 35**

5.1 Statistical Methods..... 38

5.2 Stream Gage Data and Statistical Flow Frequency Results ..... 41

5.3 Changes to Flood Flow Frequency Estimates Over Time ..... 55

**6 Rainfall-Runoff Modeling in HEC-HMS ..... 66**

6.1 Existing HEC-HMS Models..... 66

6.2 Updates to the HEC-HMS Model..... 68

6.3 HEC-HMS Model Initial Parameters..... 72

6.3.1 Subbasin and Routing Initial Parameters ..... 72

6.3.2 Initial Reservoir Data ..... 74

6.4 HEC-HMS Model Calibration ..... 75

6.4.1 Calibration Storms..... 76

6.4.2 Calibration Methodology ..... 95

6.4.3 Calibrated Parameters ..... 99

6.4.4 Calibration Results ..... 99

6.5 Final Model Parameters ..... 110

6.6 Uniform Rainfall Frequency Storms..... 115

6.6.1 Point Rainfall Depths for the Uniform Frequency Storms..... 115

6.6.2 Frequency Storm Results – Uniform Rainfall Method..... 116

6.6.3 Uniform Rainfall Frequency Results versus Drainage Area ..... 133

**7 Elliptical Frequency Storms in HEC-HMS ..... 135**

7.1 Introduction To Elliptical Storms ..... 135

7.2 Elliptical Storm Parameters AND METHODOLOGY ..... 136

7.2.1	Elliptical Storm Area .....	138
7.2.2	Storm Ellipse Ratio .....	138
7.2.3	Elliptical Storm Rainfall Depths .....	138
7.2.4	Storm Depth Area Reduction (DAR) Factors .....	138
7.2.5	Storm Temporal Pattern / Hyetograph.....	144
7.2.6	Geospatial Process for Building the Elliptical Storms .....	145
7.3	Optimization of the Storm Center Location.....	146
7.3.1	Global Optimization .....	148
7.3.2	Shuffled Complex Evolution .....	148
7.4	Elliptical Storm Locations.....	149
7.5	Elliptical Frequency Storm Loss Rates .....	149
7.6	Elliptical Frequency Storm Results – Peak Flow .....	149
7.6.1	Tabular Results.....	149
7.6.2	Map Results .....	156
7.7	Elliptical Frequency Storm Results Versus Drainage Area.....	161
7.8	Elliptical Storm Versus Uniform Rain Frequency Results .....	162
<b>8</b>	<b>RiverWare Analysis.....</b>	<b>164</b>
8.1	Introduction to Riverware Modeling .....	164
8.1.1	USACE Models .....	164
8.1.2	Model Description .....	165
8.2	Data Sources Used in the Riverware Model .....	168
8.3	Period of Record Hydrology Development .....	170
8.3.1	Methodology Used to Develop Period of Record Hydrology.....	170
8.3.2	Period of Record Hydrology for the Nueces River Basin .....	173
8.4	Water Control Plans for the Nueces Usace Reservoirs .....	174
8.5	Riverware Operational Model Application.....	175
8.6	Model Calibration Results and Discussion .....	177

8.6.1 Choke Canyon Reservoir Model Performance .....177

8.6.2 Lake Corpus Christi Model Performance .....185

8.7 Final Riverware Model Period of Record Results .....195

8.8 Conversion of Daily Discharges to Peak Instantaneous Discharges.....200

8.9 Streamgage Data and Statistical Flood Flow Frequency Results.....207

**9 Reservoir Analyses..... 224**

9.1 Introduction.....224

9.2 Watershed Description.....225

9.2.1 Nueces River Watershed Gages .....226

9.3 Climate .....227

9.4 Runoff.....227

9.5 Methods .....228

9.5.1 Empirical Stage-Frequency .....228

9.5.2 Risk Management Center - Reservoir Frequency Analysis (RMC-RFA) .....228

9.5.3 Volume-Sampling Approach.....228

9.6 Data Analysis and Model Input.....229

9.6.1 Inflow Hydrograph and Pool Stage .....229

9.6.2 Historical Discharge Peak Estimates .....232

9.6.3 Daily Average AMS Estimates.....232

9.7 Critical Inflow Duration Analysis .....232

9.7.1 Volume/Flow Frequency Statistical Analysis .....234

9.7.2 Bulletin 17B/C.....235

9.7.3 HEC-SSP Computations.....235

9.8 RMC-RFA Data Input.....236

9.8.1 Inflow Hydrographs.....236

9.8.2 Volume Frequency Curve Computation.....237

9.9 RMC-RFA Analyses.....239

9.9.1	Flood Seasonality .....	239
9.9.2	Reservoir Starting Stage .....	241
9.9.3	Empirical Frequency Curve .....	243
9.9.4	Reservoir Model.....	245
9.10	Results .....	249
9.10.1	Choke Canyon Reservoir .....	249
9.10.2	Lake Corpus Christi .....	252
9.11	Results Validation.....	254
<b>10</b>	<b>2-Dimensional HEC-RAS Analysis of the Turkey Creek Watershed .....</b>	<b>254</b>
10.1	Introduction.....	254
10.2	HEC-HMS Model Development and Calibration.....	255
10.3	2D HEC-RAS Model Development and Calibration.....	257
10.3.1	Terrain and 2D Computational Mesh.....	257
10.3.2	Unsteady Flow Files and Boundary Conditions.....	259
10.3.3	National Land Cover Database (NLCD).....	260
10.3.4	Manning’s n Values .....	262
10.4	HEC-RAS Results And Adjusting Parameters In Hec-Hms.....	262
10.4.1	Transform Parameter Analysis.....	262
10.4.2	Routing Parameter Analysis.....	264
10.4.3	2D-Informed Updates to the InFRM HEC-HMS Model.....	266
10.5	Limitations and Opportunities for Improvement .....	269
10.6	Conclusions.....	270
<b>11</b>	<b>Comparison of Frequency Flow Estimates.....</b>	<b>271</b>
11.1	Frequency Flow Comparisons.....	271
11.2	Lake Elevation Comparisons .....	317
<b>12</b>	<b>Frequency Flow Recommendations.....</b>	<b>321</b>
<b>13</b>	<b>Conclusions.....</b>	<b>338</b>
<b>14</b>	<b>References and Resources.....</b>	<b>340</b>

14.1	References.....	340
14.2	Software .....	344
14.3	Data Sources, Guidance & Procedures.....	345
15	Terms of Reference.....	347

## Appendices

Appendix A: Statistical Hydrology

Appendix B: HEC-HMS Model Development and Uniform Rainfall Frequency Results

Appendix C: Elliptical Frequency Storms in HEC-HMS

Appendix D: RiverWare Analysis

Appendix E: Reservoir Analyses

Appendix F: 2D HEC-RAS Analysis of the Turkey Creek Watershed

Appendix G: Peer Review Comments & Responses

## The InFRM Team

As flooding remains the leading cause of natural-disaster loss across the United States, the Interagency Flood Risk Management (InFRM) team brings together federal agencies with mission areas in water resources, hazard mitigation, and emergency management to leverage their unique skillsets, resources, and expertise to reduce long term flood risk throughout the region. The Federal Emergency Management Agency (FEMA) Region VI began sponsorship of the InFRM team in 2014 to better align Federal resources across the States of Texas, Oklahoma, New Mexico, Louisiana, and Arkansas. The InFRM team is comprised of FEMA, the U.S. Army Corps of Engineers (USACE), the US Geological Survey (USGS), and the National Weather Service (NWS), which serves under the National Oceanic and Atmospheric Administration (NOAA). One of the first initiatives undertaken by the InFRM team was performing Watershed Hydrology Assessments for large river basins in the region.

The Federal Emergency Management Agency (FEMA) funded the Watershed Hydrology Assessments to leverage the technical expertise, available data, and scientific methodologies for hydrologic assessment through the InFRM team. This partnership allows FEMA to draw from the local knowledge, historic data and field staff of its partner agencies and develop forward leaning hydrologic assessments at a river basin level. These studies provide outcomes based on all available hydrologic approaches and provide suggestions for areas where the current flood hazard information may require update. FEMA will leverage these outcomes to assess the current flood hazard inventory, communicate areas of change with community technical and decision makers, and identify/prioritize future updates for Flood Insurance Rate Maps (FIRMs).

The U.S. Army Corps of Engineers (USACE) has participated in the development of the Watershed Hydrology Assessments as a study manager and member of the InFRM team. USACE served in an advisory role in this study where USACE's expertise in the areas of hydraulics, hydrology, water management, and reservoir operations was required. USACE's primary scientific contributions to the study have been in rainfall runoff watershed modeling and reservoir analyses. The reservoir analyses in this study are based on USACE's firsthand reservoir operations experience and the latest scientific techniques from USACE's Dam Safety program.

The U.S. Geological Survey (USGS) Texas Water Science Center has participated in the development of this study as an adviser and member of the InFRM team. USGS served in an advisory role for this study where USGS' expertise in stream gaging, modeling, and statistics was requested. USGS's primary scientific contribution to the study has been statistical support for flood flow frequency analysis. This flood flow frequency analysis included USGS firsthand stream gaging expertise as well as advanced statistical science.

NOAA National Weather Service (NWS) has participated in the development of this study as an adviser and member of the InFRM team. NOAA NWS served in an advisory role of this study where expertise in NOAA NWS' area of practice in water, weather and climate was requested. NOAA's primary scientific contribution to the study has been the NOAA Atlas 14 precipitation frequency estimates study for Texas. This precipitation-frequency atlas was jointly developed by participants from the InFRM team and published by NOAA. NOAA Atlas 14 is intended as the U.S. Government source of precipitation frequency estimates and associated information for the United States and U.S. affiliated territories.

More information on the InFRM team and its current initiatives can be found on the InFRM website at [www.InFRM.us](http://www.InFRM.us).

## EXECUTIVE SUMMARY

The Federal Emergency Management Agency (FEMA) administers the National Flood Insurance Program (NFIP), which was created in 1968 to guide new development (and construction) away from flood hazard areas and to help transfer the costs of flood damages to the property owners through the payment of flood insurance premiums. The standard that is generally used by FEMA in regulating development and in publishing flood insurance rate maps is the 1% annual chance (100-yr) flood. The 100-yr flood is defined as a flood which has a 1% chance of happening in any year. The factor that has the greatest influence on the depth and width of the 100-yr flood zone is the expected 1% annual chance (100-yr) flow value.

This report summarizes new analyses that were completed as part of a study to estimate the 1% annual chance (100-yr) flow, along with other frequency flows, for various stream reaches throughout the Nueces River Basin in Texas. This study was conducted for FEMA Region VI by an Interagency Flood Risk Management (InFRM) team. The InFRM team is a partnership of federal agencies that includes subject matter experts (SME) from FEMA, the U.S. Army Corps of Engineers (USACE), the U.S. Geological Survey (USGS), and the National Weather Service (NWS). In addition to the federal partners of the InFRM team, regional stakeholders such as the Nueces River Authority, Bureau of Reclamation, City of Corpus Christi, and the Texas Water Development Board (TWDB) also participated in the progress updates and review processes for this study. This study represents a significant step forward towards increasing resiliency against flood hazards in the Nueces River basin.

The InFRM team used several hydrologic methods, including statistical hydrology, rainfall-runoff modeling, period of record simulations, and reservoir analyses, to estimate the 1% annual chance (100-yr) flow and then compared those results to one another. The purpose of the study is to produce 100-yr flow values that are consistent and defensible across the basin.

The InFRM team used up-to-date statistical analysis along with state-of-the-art rainfall-runoff watershed modeling and reservoir analyses to estimate the 1% annual chance (100-yr) flow values throughout the Nueces River Basin. In the statistical analysis, the gage records were updated through the year 2020 to include all recent major flood events. However, since statistical estimates inherently change with each additional year of data, their results were compared to the results of a detailed watershed model, which is less likely to change over time.

Significant downward trends in streamflow were observed at a few of the gage locations in the Nueces River basin. These downward trends primarily occurred in portions of the basin with wide irrigated floodplains and significant irrigation withdrawals from the river channels. Figure ES.1 gives an example of these downward streamflow trends in the annual peak streamflow data for the Nueces River at Cotulla, Texas. More information on the declining flow trends can be found in Chapter 5.

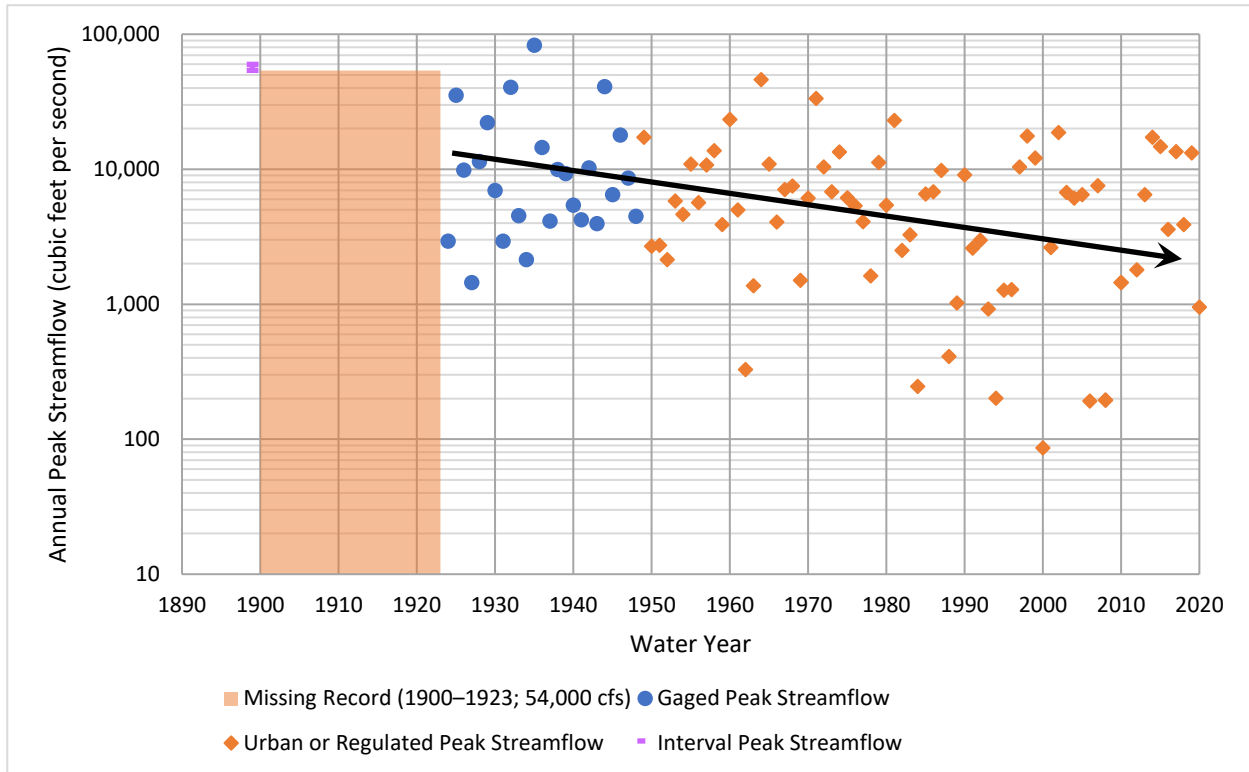


Figure ES.0.1 Example of Declining Streamflow Trends for the Nueces River at Cotulla, TX

Rainfall-runoff watershed modeling is used to simulate the physical processes that occur during storm events including how water moves across the land surface and through the streams and rivers. A watershed model was built for the Nueces River Basin with input parameters that represented the physical characteristics of the watershed. After building the model, the InFRM team calibrated the model to verify that it was accurately simulating the response of the watershed to a range of observed flood events, including large events similar to a 1% annual chance (100-yr) flood. A total of 16 recent storm events spanning from 1996 to 2018 were used to fine tune the model.

For the 16 storm events used to fine tune the model, the availability of National Weather Service (NWS) hourly rainfall radar data allowed for more detailed calibration of the watershed model than would have been possible during earlier modeling efforts. The final watershed model accurately simulated the response of the Nueces watershed, as it reproduced the timing, shape, and magnitudes of the observed floods very well. Figure ES.2 gives an example of the results from one of those calibrations showing how the model results matched the observed streamflow very well.

The model calibration and verification process undertaken during this study substantially exceeds the standard of a typical FEMA floodplain study. Because these rainfall-runoff models have been calibrated to observed watershed responses to storm events, there is more assurance that these models, when paired with best available precipitation frequency information, provide the best available representation of flood risk.

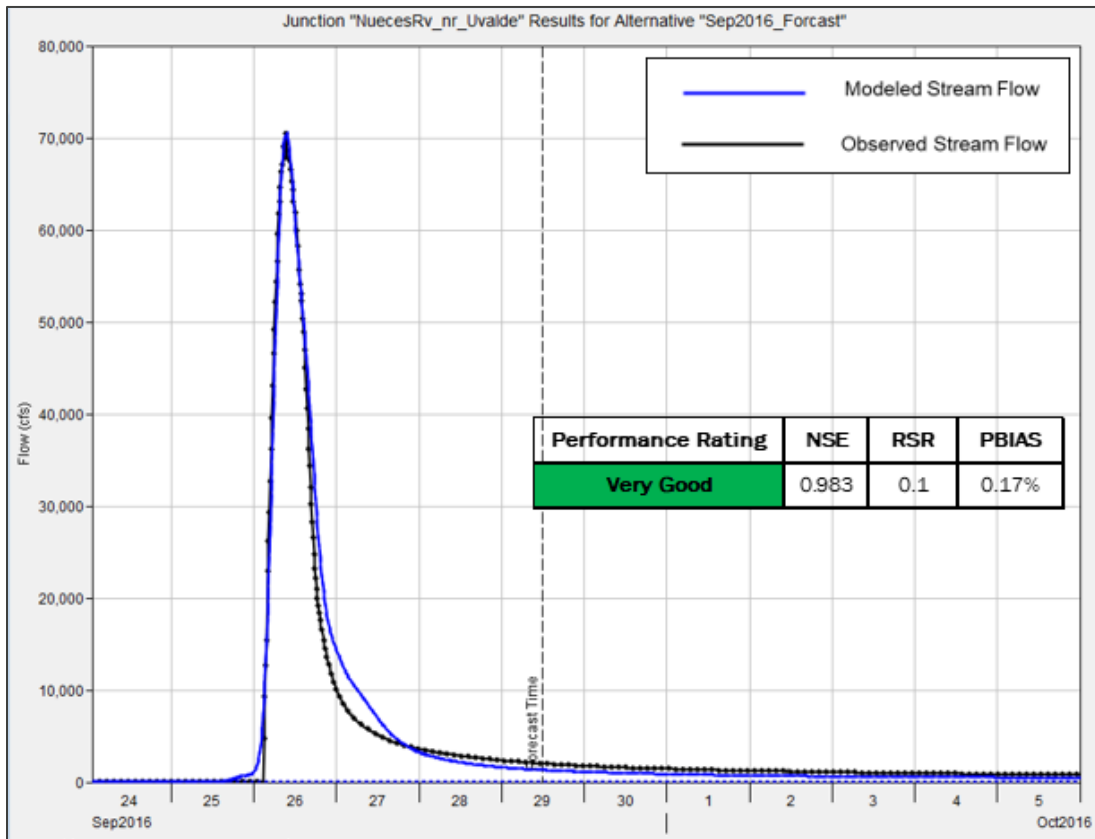


Figure ES.0.2 Example of Watershed Model Results versus Recorded Flow at the Streamgage

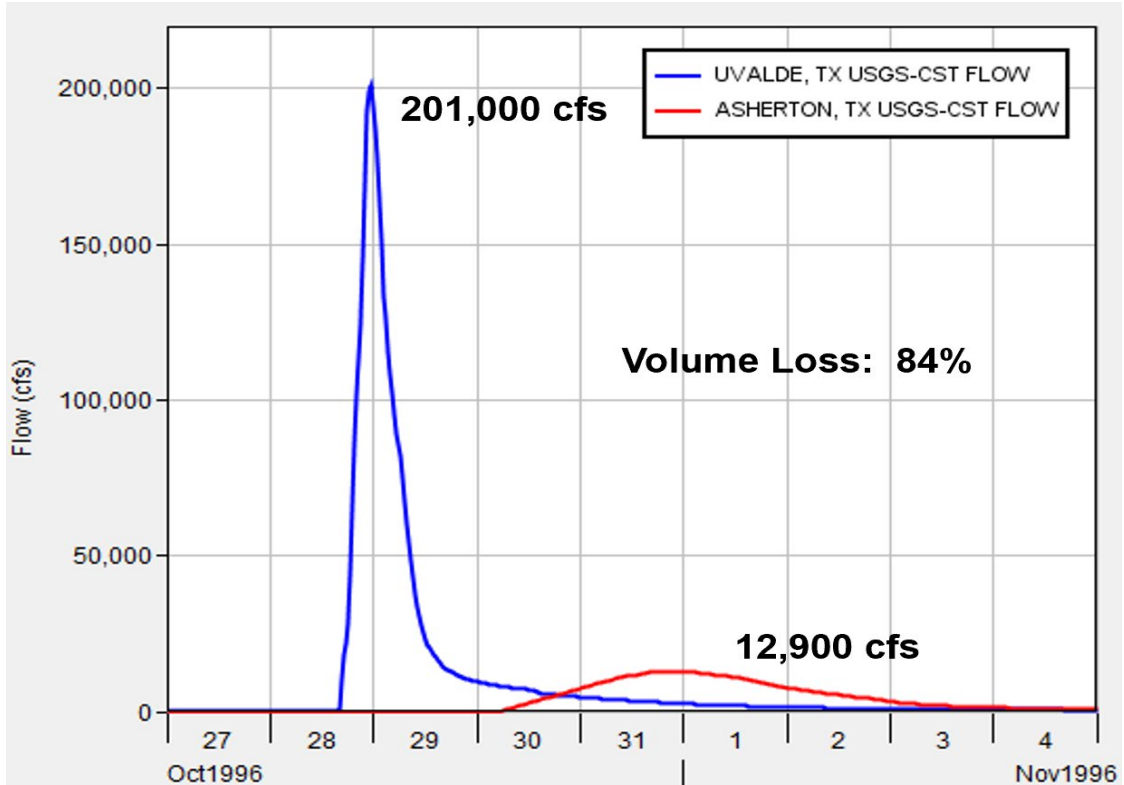


Figure ES.0.3: Example of Recorded Streamflows Decreasing from Upstream to Downstream

One other unique aspect of the hydrology of the Nueces River basin is that peak flows have been observed to decrease dramatically from upstream to downstream. Figure ES.3 illustrates one example of this decrease in streamflow by comparing the observed streamflows at the Nueces River USGS gages at Uvalde and Asherton during the 1996 flood event. Asherton is located approximately 60 miles downstream of Uvalde. This phenomenon is primarily observed at the locations where the streams abruptly transition from steep, narrow hill country watersheds to wide irrigated floodplains. These dramatic decreases in streamflow are likely due to a combination of factors including aquifer recharge, irrigation withdrawals and floodplain attenuation. For these reaches, part of the model calibration process involved calibrating the channel losses along the losing reaches of the rivers. After calibrating those channel loss parameters, the watershed model results matched the observed data at the downstream gages very well. See Chapter 6 for more information on the channel losses.

After completing the model calibration process, the 1% annual chance (100-yr) flow values were then calculated by applying a 100-yr storm to the watershed model. Rainfall estimates for the 100-yr storm are considered more reliable than statistical estimates for the 100-year flow due to the larger number of rainfall stations and the longer periods of time during which rainfall measurements have been made. The accuracy of those rainfall frequency estimates was further advanced by the release of NOAA Atlas 14 for Texas in 2018 (NOAA, 2018). NOAA Atlas 14 is the U.S. Government source of precipitation frequency estimates and is the most accurate, up-to-date, and comprehensive study of rainfall depths in Texas. The regional approach used in NOAA Atlas 14 incorporated at least 1,000 cumulative years of daily data into each location's rainfall estimate, yielding better estimates of rare rainfall depths such as the 100-yr storm. These new rainfall depths from NOAA Atlas 14 were applied to the calibrated watershed model for the Nueces River basin.

After completing the model runs, the watershed model results were compared to previous studies and to the results of other hydrologic methods. Where there were significant differences, investigations were made into the drivers of those differences. Extensive comparisons were made between the watershed model results, the USGS gage record results, the flood of record, and previously published flow values, which can be found in Chapter 11 of this report. The expected impacts of reservoir operations for Choke Canyon Reservoir and Lake Corpus Christi were also analyzed in detail for this study, and the frequency dam releases and pool elevations that resulted from the reservoir analyses were recommended for the reaches immediately upstream and downstream of the dams.

The final recommendations for the Nueces Watershed Hydrology Assessment were formulated through a rigorous process which required technical feedback and collaboration between all of the InFRM subject matter experts. This process included the following steps: (1) comparing the results of the various hydrologic methods to one another, (2) performing an investigation into the reasons for the differences in results at each location in the watershed, (3) selecting of the draft recommended methods, (4) performing internal and external technical reviews of the hydrologic analyses and the draft recommendations, and finally, (5) finalizing the study recommendations. After completing this process, the flows that were recommended for adoption by the InFRM team came from a combination of watershed model results using NOAA Atlas 14 uniform rainfall, elliptical storms, and reservoir analysis techniques.

Figure ES.4 shows the trends in the recommended 1% AEP (100-year) peak flows versus drainage area for all the analyzed locations in the Nueces River basin. This figure shows that the discharges followed generally expected patterns of increasing peak flow with drainage area for similar watershed types. The relative magnitudes of the 1% AEP (100-year) discharges of different watershed types in this graph generally make sense. For example, the steep headwater basins in the upper portions of the study area had the highest peak discharges relative to their drainage areas, while the streams with wide, irrigated floodplains in the middle and lower portions of the basin, on the other hand, had the lowest peak discharges relative to their drainage areas. For the large majority of the Nueces River basin, no effective FEMA FIS flows have been published, so the results from this study provide a significant step forward in accurately mapping flood risk in the Nueces River basin by providing detailed

information about the hydrology of the significant streams in the basin. For the limited locations where effective FIS flows were available, the new flow frequency results were significantly higher than the effective FIS discharges in some areas, while they were lower in other areas. However, many of those effective FIS discharges have not been updated since the 1970s or 1980s (see section 2.4 of this report) and were based on much more limited data than the current study.

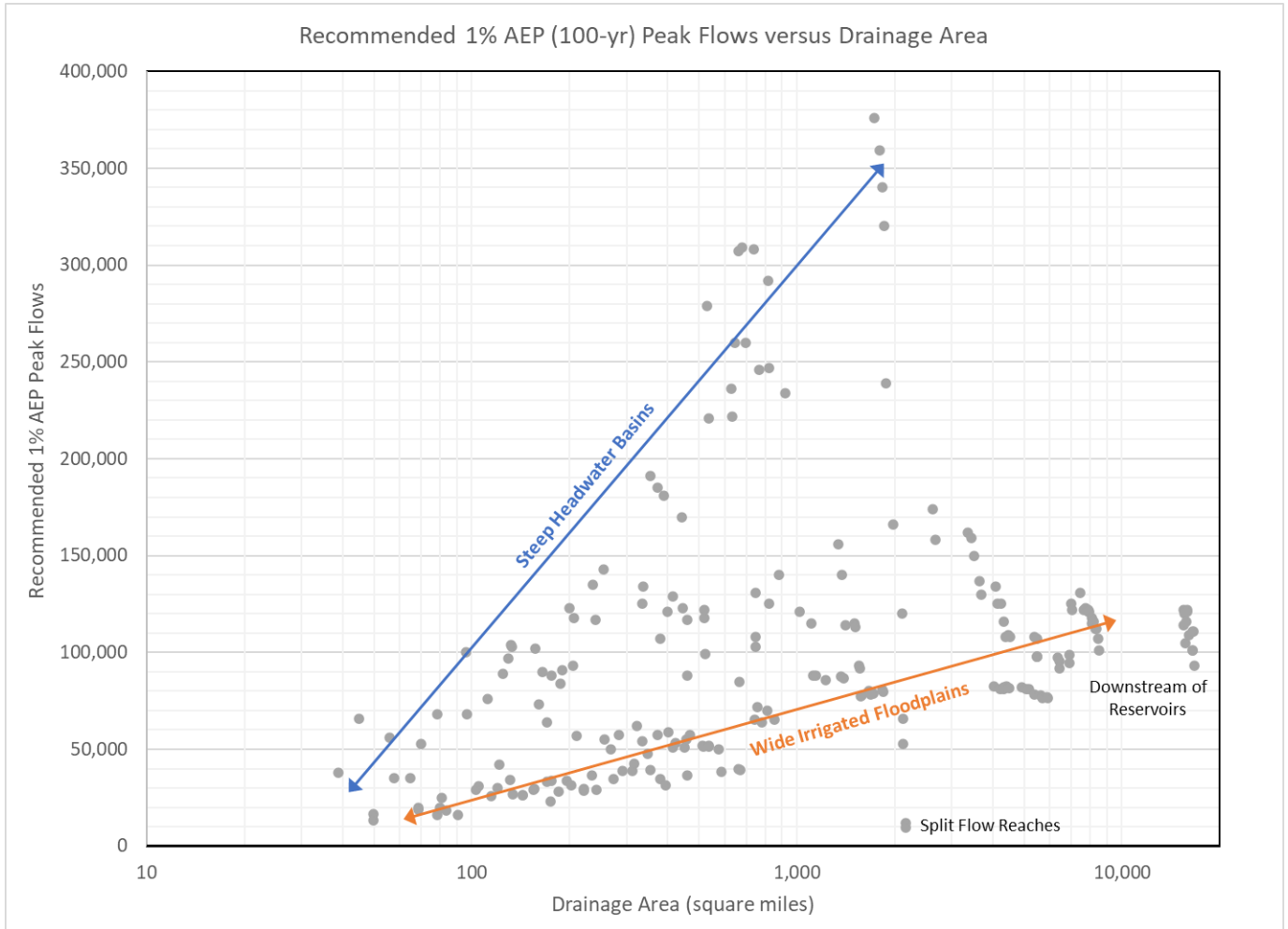
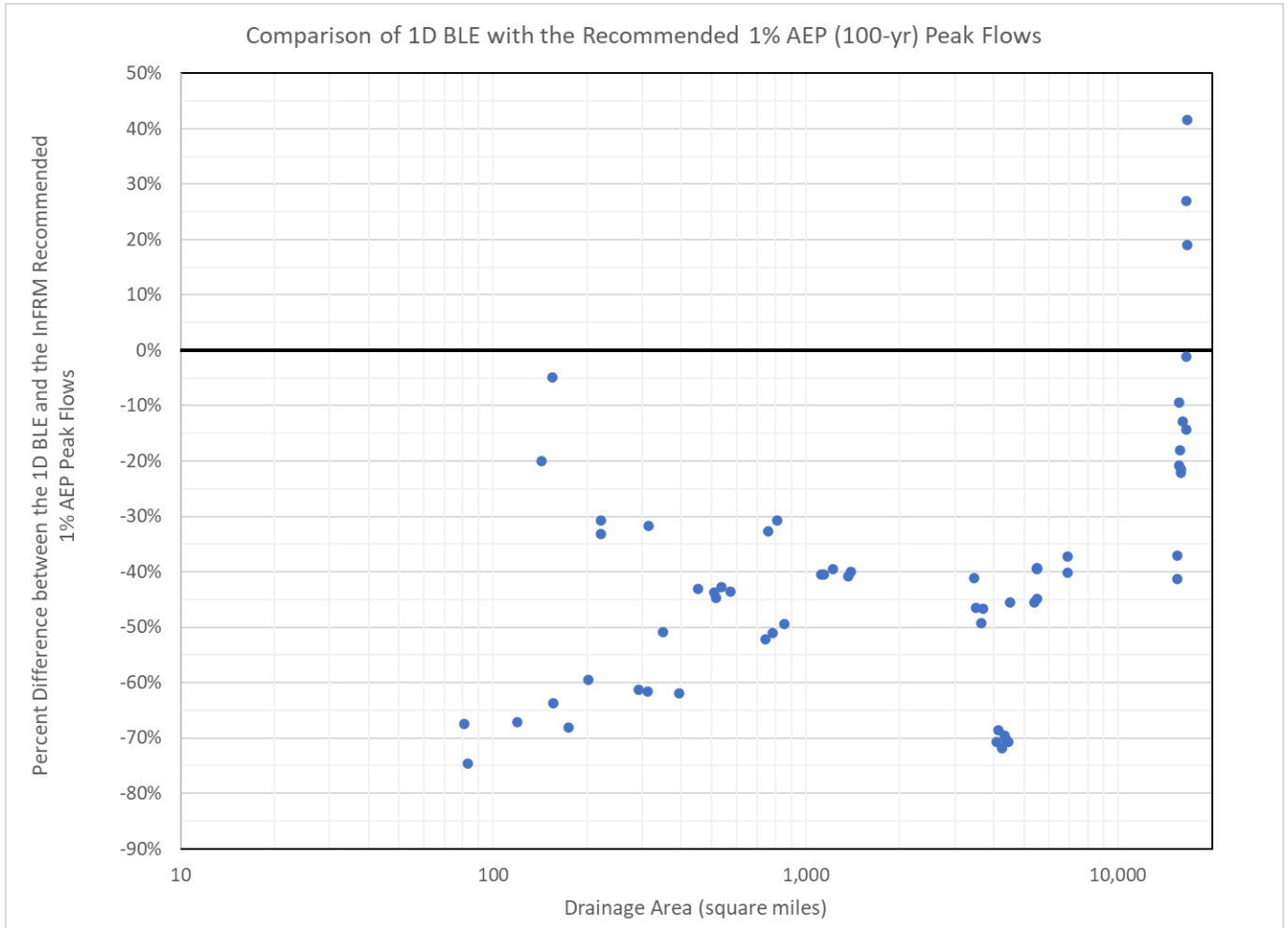


Figure ES.0.4: Recommended 1% AEP (100-year) Peak Flows versus Drainage Area

Base Level Engineering (BLE) data was available for a significant portion of the Nueces River basin at the time of this report publication, including the Lower Frio River, San Miguel Creek, the Atascosa River and the Lower Nueces River. However, all of the available BLE data was only from 1D HEC-RAS modeling using a combination of regional regression equations and statistical analyses at the gages for the hydrology. The results of this study showed that the 1D BLE data grossly underestimated the flood risk for the unregulated areas of Nueces River basin while overestimating the frequency discharges on the lower Nueces River downstream of the major reservoirs, as shown on Figure ES.5. On this figure, negative values indicate that the 1D BLE data is lower than the new recommended peak flows. Figure ES.5 shows that 1D BLE peak discharges were 40% to 70% lower than the new recommended 1% AEP peak flows for most of the locations in the Nueces River basin. The only locations where the 1D BLE was higher than the recommended peak discharges were for the locations on the lower Nueces River that were downstream of Lake Corpus Christi. This likely because the 1D BLE data did not properly account for the effects of reservoir regulation.



**Figure ES.0.5: Comparison of 1D BLE with Recommended 1% Annual Chance (100-yr) Flow Results**

Given the severe loss of life and property due to flooding that has occurred multiple times throughout the history of Texas, it is imperative that future updates to the published flood insurance rate maps for the Nueces River Basin accurately reflect the levels of flood risk in the basin. The recommended results from this study represent the best available estimate of flood risk for the larger streams in the Nueces River basin, based on a range of hydrologic methods performed by an expert team of engineers and scientists from multiple federal agencies. For smaller tributaries in the Nueces basin, the recommended results from the watershed model provide a good starting point which could be further refined by adding additional subbasins and using methodologies that are consistent with this study.

As a result of the level of investment, analyses, and collaboration that went into this Watershed Hydrology Assessment, the flood risk estimates contained in this report are recommended as the basis for future NFIP studies or other federal flood risk studies within the Nueces River basin. These federally developed modeling results form a consistent understanding of hydrology across the Nueces watershed, which is a key requirement outlined in FEMA's General Hydrologic Considerations Guidance. Furthermore, the models and data used to produce these flood risk estimates are available upon request, at no charge, to communities, local stakeholders, and architecture engineering firms. Models can be requested through the InFRM website at [www.InFRM.us](http://www.InFRM.us).

While the results from this study should be considered the best available estimates of flood risk for many areas of the Nueces River basin, significant uncertainty still remains, as it does in any hydrologic study. Because of this uncertainty and because of the potential impacts these estimates can have on life and property, the InFRM team strongly recommends and supports local communities that implement higher standards, such as additional freeboard requirements, floodplain management practices based on standards greater than the 1% annual chance flood, and/or “no valley storage loss” criteria.

# 1 Study Background and Purpose

## 1.1 THE NATIONAL FLOOD INSURANCE PROGRAM

The National Flood Insurance Program (NFIP) was created in 1968 to guide new development (and construction) away from flood hazard areas and to help transfer the costs of flood damages to the property owners through the payment of flood insurance premiums. The NFIP program is administered by FEMA within the Department of Homeland Security. The NFIP is charged with determination of the 1% and 0.2% annual chance flood risk and with mapping that flood risk on the Flood Insurance Rate Maps (FIRMs). FEMA Region 6 has an inventory of hundreds of thousands of river miles across Texas, Louisiana, Arkansas, Oklahoma, and New Mexico that are in need of flood risk mapping updates or validation. The current flood hazard inventory is available for viewing on FEMA's National Flood Hazard Layer (NFHL) Viewer at <https://msc.fema.gov/nfhl>.

FEMA's inventory is focused on determining the extent and areas that are vulnerable to flooding during the 1% annual chance (1 in 100 chance of occurrence each calendar year) and 0.2% chance (1 in 500 chance of occurrence each calendar year). Flood hazards are assessed along natural drainage elements such as rivers, streams, and creeks. The program focuses on comprehensive and broad analysis to define, determine and communicate flooding potential.

The Flood Insurance Rate Maps (FIRMs) published by FEMA define the area where flood insurance purchase is mandatory. The mandatory purchase area includes insurable structures within the defined 1% annual chance floodplain with federally backed mortgages. However, the engineering modeling and the flood extents produced and released on FIRMs do not describe the full potential for flooding, as the FIRMs focus on natural streams, creeks and rivers that traverse the watershed and generally do not determine flood hazards related to highly urbanized flooding problems from man-made drainage systems such as sewers and pipe networks.

The standard that is generally used by FEMA in publishing Flood Insurance Rate Maps (FIRMs) for the NFIP is the 1% annual exceedance probability (AEP) flood, also known as the 100-year flood. The 1% AEP, or 100-year flood is defined as a 1 in 100 chance of occurrence each calendar year. The chance of a 100-year flood occurring during the life of a 30-year mortgage or over the life of a structure is much more probable than its name suggests, as shown in Figure 1.1. These statistics underline the need to minimize uncertainty in flood frequency estimates.

Engineering modeling prepared by Federal, State, local, academic and private industry utilize standard engineering practices to determine:

- **Hydrologic Conditions in a Study Area.** In a hydrologic analysis, ground slope, land use, soil types and climatic factors are analyzed to determine how much flood water is expected to collect on the landscape. This flood volume is entered into hydraulic engineering models.
- **Hydraulic Conditions.** Hydraulic engineering efforts generalize stream and channel geometries utilizing ground elevation information to define the areas available to convey flood volumes. These analyses describe stream cross-sections that are analyzed to determine how high the water will rise in the stream channel and/or if it will expand into the natural floodplain areas adjacent to these stream channels. The output of these analysis is a series of calculated water surface elevations.
- **Flood Extent.** The water surface elevations determined by the hydraulic analysis are then reviewed against ground elevation information to define the areas which are prone to flooding during the analyzed event.



Figure 1.1: Probabilities of the 100-yr Flood

## 1.2 THE CHALLENGE AND IMPORTANCE OF HYDROLOGY

In standard engineering practice, the factor that has the greatest influence on the depth and width of the 100-year floodplain is the 1% annual chance (100-yr) flow estimate. As a result, hydrology remains the single largest source of uncertainty in the estimation of flood risk. The challenge of hydrology is that there are many different commonly used and accepted methods for estimating the 1% annual chance flow, and every method will result in a different answer. In Texas, where the climate can cause dramatic shifts between drought and flood cycles, the variation in flood risk estimation can be quite extreme. The challenge of climactic and hydrologic variation points to the need for a more thorough approach to hydrology using multiple scientific methods.

In addition to the natural variation described above, urbanization and reservoir regulation provide additional challenges to hydrology and the estimation of flood risk. For basins which include major reservoirs, such as the Nueces River basin, first-hand knowledge of reservoir operations and additional analysis is needed for accurate flood risk estimation. For basins experiencing major population growth and urban development, land use change must also be considered in the analysis.

## 1.3 PURPOSES OF THE WATERSHED HYDROLOGY ASSESSMENT

The InFRM Watershed Hydrology Assessment for the Nueces River Basin summarizes new analyses that were completed as part of a study to estimate the 1% annual chance (100-yr) flow, along with other frequency flows, for various stream reaches across the river basin. This study also produces greatly refined meteorologic and hydrologic tools, analysis and data, including verification studies that ensure that the tools accurately reflect the basin's response to intense rainfall events. The tools, analyses and data produced in this study can be leveraged by local communities to manage their growth and development and to better estimate the risk of flooding associated with constructing infrastructure and urban development in the vicinity of significant streams and rivers.

This study was conducted for FEMA Region 6 by the InFRM team. The InFRM team includes subject matter experts (SME) from USACE, the USGS, and the NWS. The Watershed Hydrology Assessment employed a thorough approach to the hydrology of the Nueces River basin. The multi-layered analysis used in this assessment applied a range of hydrologic methods, including rainfall runoff modeling, statistical hydrology, period-of-record simulations, and reservoir analyses, and then compared the results of those methods to one another. This type of multi-layered analysis helped to reduce the uncertainty in the 1% annual chance (100-yr) flow estimates by ensuring that all possible variables affecting flood risk in the basin have been examined. The analysis also accounts for the impacts of non-stationary factors, such as reservoir regulation and climate variation, which helps to tell the story of how the 1% annual chance flow estimate has changed over time.

The purpose of this study is to produce 1% annual chance and other frequency flows that are consistent and defensible across the Nueces River basin based on analyses from multiple methods. The end product of this hydrology assessment will include a hydrology report for use as a reference to evaluate against existing studies and to support new local studies. The results of the watershed hydrology assessment will provide FEMA suggested 1% and 0.2% peak flow rates along the major rivers and tributaries and will inform future updates to Flood Insurance Rate Maps (FIRMs). These analyses will allow Federal, State and Local entities to leverage these basin wide results in a variety of ways.

FEMA will leverage the outcomes from this study to assess the current flood hazard inventory, communicate areas of change with community technical staff and decision makers, and identify/prioritize future updates for FIRMs. This watershed hydrology assessment also provides the recommended hydrologic methods and results needed for use on local studies, which may add the detail necessary to develop frequency flows at a smaller scale. The watershed assessment gives a consistent avenue of updating the hydrology for large, complex river systems, such as the Nueces River basin, much of which is either mapped with approximate methods or has not had its hydrology updated in decades.

This report summarizes all of the hydrologic analyses that were completed to estimate frequency peak stream flows for significant stream reaches throughout the Nueces River Basin. The results of all hydrologic analyses and the recommended frequency discharges are summarized herein. Additional technical detail is also available in the appendices to this report.

## 1.4 STUDY TEAM MEMBERS

The following table lists the primary InFRM team members who participated in the development of the InFRM Watershed Hydrology Assessment for the Nueces River Basin. Max Strickler, Lead Engineer in the USACE Fort Worth District Water Management Section, served as the team lead for this study. In addition to those listed, the InFRM team would also like to acknowledge the many others who served supervisory and support roles during this effort.

**Table 1.1: Study Team Members**

	<u>Name</u>	<u>Agency</u>	<u>Office</u>
1	Allen Avance, P.E.	USACE	RMC
2	Diana Hanbali, EIT	USACE	Fort Worth
3	Simeon Benson, P.E.	USACE	Fort Worth
4	Christopher Chiu, P.E.	USACE	Fort Worth
5	Landon Erickson, P.E.	USACE	Fort Worth
6	Heitem Ghanuni, P.E.	USACE	Fort Worth
7	Timothy Helms, EIT	USACE	Fort Worth
8	Seongwon Hong	USACE	Fort Worth

	<u>Name</u>	<u>Agency</u>	<u>Office</u>
9	Bret Higginbotham, P.E., CFM	USACE	Fort Worth
10	Diane Howe	FEMA	Region 6
11	Kris Lander, P.E.	NWS	WGRFC
12	Molly Milmo	USGS	Fort Worth
13	Helena Mosser, P.E.	USACE	Fort Worth
14	Stephen Pilney	USACE	Fort Worth
15	Max Strickler, P.H., CFM	USACE	Fort Worth
16	Jon Thomas	USGS	Fort Worth
17	Larry Voice	FEMA	Region 6
18	Sam Wallace	USGS	Fort Worth

## 1.5 TECHNICAL REVIEW PROCESS

The InFRM Watershed Hydrology Assessments undergo a rigorous review process. Numerous peer reviews are performed by InFRM team members throughout the study. Each model, analysis, and technical product is peer reviewed as it is developed by an InFRM Subject Matter Expert (SME). Any technical issues that are discovered during the review process are thoroughly discussed and resolved, often with input from multiple team members. This same review process is also applied to the process of comparing the results from different methods. Any significant differences in the results are thoroughly investigated and discussed with multiple team members, which sometimes leads to changes in the assumptions of the analyses. After completing all the comparisons and investigations, the draft results are shared with the rest of the InFRM team, and input is solicited from multiple subject matter experts. The draft study recommendations are then documented in the draft report, which is sent out for peer review.

Representatives from the following entities were invited to participate as peer reviewers of the InFRM Watershed Hydrology Assessment of the Nueces River basin: Nueces River Authority, Bureau of Reclamation, City of Corpus Christi, Texas Water Development Board (TWDB), the Texas Department of Transportation (TxDOT), and the InFRM Academic Council. The InFRM Academic Council is comprised of a select group of professors from local universities with unique skillsets and regional expertise in water resources and hydrology. Their involvement provides an independent and unbiased review of the InFRM team's methods and results. Collaboration with the InFRM Academic Council also helps the InFRM team to stay abreast with the latest advances in hydrologic science and technology. The primary InFRM Academic Council reviewers for the Nueces Watershed Hydrology Assessment include Dr. Nick Fang and Dr. Shannon Abolmaali from the University of Texas at Arlington and Dr. Philip Bedient from Rice University. The peer review comments that were received for this study and the responses from the InFRM team have been documented in Appendix H.

## 2 Nueces River Basin

The Nueces River basin was selected for study by FEMA based upon their NFIP mapping needs and the availability of existing models and LiDAR (Light Detection and Ranging) data. USACE already had sufficiently detailed modeling products available as a starting point for the Nueces Watershed Hydrology Assessment from USACE's Corps Water Management System (CWMS) Implementation program. CWMS is the automated decision support tool developed by the Hydrologic Engineering Center (HEC) for USACE Water Managers. In 2013, USACE began a national implementation effort to have all watersheds containing USACE managed flood control systems (dams, levees, etc.) fully modeled within CWMS. The models that were developed for the national CWMS implementation included basin-wide models for surface water hydrology in HEC-HMS (Hydrologic Modeling System), reservoir operations in HEC-ResSim (Reservoir System Simulation), river hydraulics in HEC-RAS (River Analysis System), and economic flood damages in HEC-FIA (Flood Impact Analysis). For the Nueces River basin, CWMS implementation modeling was completed in 2020, and representatives of FEMA Region 6 attended the CWMS handoff meeting.

### 2.1 WATERSHED AND RIVER SYSTEM DESCRIPTION

The Nueces River begins in Edwards County approximately 110 miles southeast of San Angelo, Texas (15 miles east of Rocksprings, TX). The Nueces River is located in South Texas and is the fifth largest river basin in the state, with a drainage area totaling 16,675 square miles. The watershed spans Edwards, Real, Kerr, Bandera, Kinney, Uvalde, Medina, Bexar, Maverick, Zavala, Frio, Atascosa, Wilson, Karnes, Dimmit, La Salle, McMullen, Live Oak, Bee, Webb, Duval, Jim Wells, San Patricio, and Nueces Counties. The Nueces River Basin drains all or parts of 24 counties and 29 municipalities. The basin is approximately 230 miles long, with a maximum width of 115 miles, and includes about 6.2 percent of the total land area of Texas. The Nueces River is entirely freshwater and impounds 963,000 acre-feet of freshwater including Choke Canyon and Lake Corpus Christi. The Nueces River discharges into Nueces Bay before the Corpus Christi Bay and finally the Gulf of Mexico. See Figure 2.1 for a location map of the Nueces River basin.

The Edwards Aquifer cuts the upper Nueces River Basin watershed through Kinney, Uvalde, and Medina Counties. Downstream, the Carrizo-Wilcox Aquifer cuts through the watershed along the borders of Medina/Frio Counties, Uvalde/Zavala Counties, and Maverick/Dimmit Counties. The Nueces River consists of rolling plains dissected by numerous streams that have cut shallow and relatively narrow valleys. The watershed ends in the coastal plains near Corpus Christi Bay. The elevations in this region vary from 2,200 to 600 feet North American Vertical Datum 1988 (NAVD 88) with most of the watershed at or below 1,000 feet. The topography of the coastal terrace near the Corpus Christi Bay is nearly level and is part of the Texas Coastal Bend. Although the Nueces River is not the only river that feeds the Corpus Christi Bay, the Nueces River provides most of the freshwater inflow to the bay.

The surface mantle of the Nueces River consists largely of soils, composed principally of sand and clay in varying mixtures. The topsoils are usually shallow to very shallow, and weathering of the underlying rocks is generally deep. The topsoils are well-drained in the upper part of the watershed due to the Edwards aquifer and the Carrizo-Wilcox aquifer. Aquifers within the Nueces River have been observed diverting flow from surface water to groundwater. Discussion of how aquifers were accounted for in this study can be found in the HEC-HMS Appendix B. A large majority of the land in the Nueces River watershed is used for agriculture. Cropland, pastureland, and/or orchards are located on the deeper soils along major drainage ways or on high divides. The Coastal Terrace is composed largely of sand, loam, and marine deposits of upper Cretaceous and younger age. The areas from Nueces Bay and upstream to the greater Corpus Christi area have become suburban with industrial development. The soils near the Corpus Christi Bay are thickly covered with gulf cordgrass and are not suitable for cultivation due to sediment deposits from the Corpus Christi Ship Channel.

Choke Canyon Dam and Reservoir are located approximately four miles West of Three Rivers in Live Oak County on the Frio River, a major tributary of the Nueces River. The total drainage area above Choke Canyon dam is 4,667 square miles, and deliberate impoundment began in October of 1982. The reservoir was built by the Bureau of Reclamation and is owned and operated by the City of Corpus Christi and the Nueces River Authority for municipal water supply and recreational purposes. According to TWDB 2012 survey, Choke Canyon Reservoir has a storage capacity of approximately 662,821 acre-feet encompassing a surface area of 25,438 acres at top of the conservation pool elevation, 220.5 feet above mean sea level.

Wesley E. Seale Dam and Lake Corpus Christ Lake are located on the Nueces River about four miles west of Mathis, TX, at the intersection of Live Oak, San Patricio, and Jim Wells County lines. The total drainage area above Wesley E. Seale Dam is 16,656 square miles. Deliberate impoundment began in April of 1958. Wesley E. Seale Dam and Lake Corpus Christi are a multi-purpose project used for water supply and recreation. The reservoir is owned and operated by the city of Corpus Christi. According to 2012 TWDB survey, the reservoir has a capacity of 254,732 acre-feet encompassing a surface area of 18,700 acres at the conservation pool elevation of 94.0 feet above mean sea level.

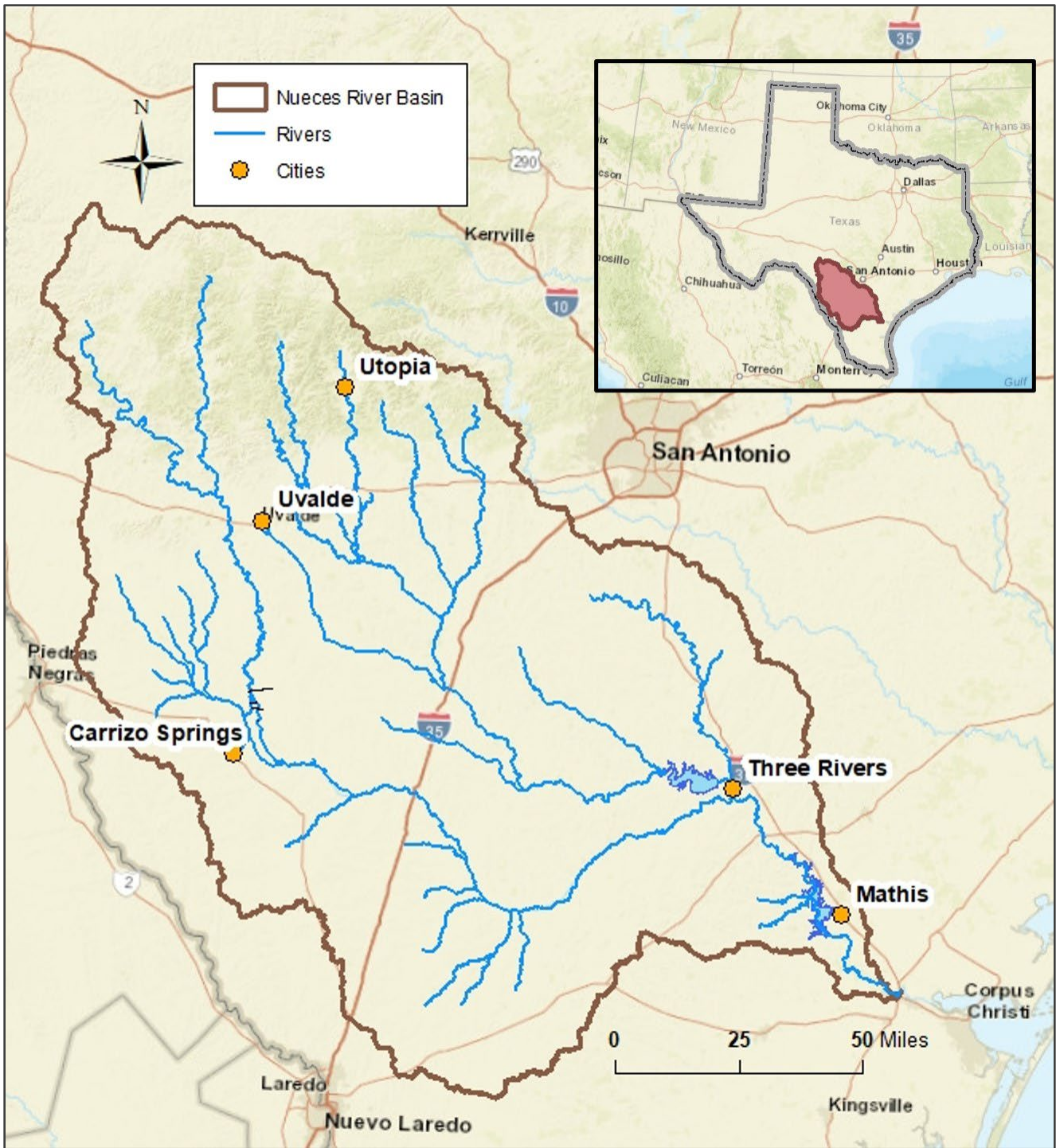


Figure 2.1: Nueces River Basin Location

## 2.2 CLIMATE

The climate over the entire Nueces River watershed is sub-humid to semi-arid, and temperatures are mild. Single digit temperatures have been recorded in the upper and middle sections of the basin but are relatively rare. Snowfall is negligible. The mean annual temperature is about 70 degrees Fahrenheit. January, the coldest month, has an average minimum daily temperature of about 40 degrees; August, the warmest month, has an average minimum daily temperature of about 95 degrees. Temperatures in the watershed have ranged from maximum of 116 degrees recorded at Cotulla La Salle County Airport to a minimum of 4 degrees recorded at Hondo. The prevailing winds over the watershed are from the south or southeast. During the winter months, the prevailing winds typically shift direction and originate from a high-pressure system in the northwest. Average annual precipitation over the Nueces River Basin varies from 24 inches along the western boundary of the basin to 32 inches at the downstream end of the basin where the Nueces River enters Corpus Christi Bay based on climatological data from 1991 - 2020 (NCEI, 2021). While the climate of the Nueces River basin is generally mild, like most of Texas, it is also subject to a variety of extreme weather events, including hurricanes, tornadoes, droughts, heat waves, cold waves, and intense precipitation (NCEI, 2017).

## 2.3 MAJOR FLOODS IN THE NUECES RIVER BASIN

The Nueces River Watershed is subject to three general types of flood-producing rainfall: thunderstorms, frontal rainfall, and tropical cyclones. Most of the flood producing storms are experienced in the spring and fall, usually occurring in May, June, and September. Most of the higher floods that have occurred in the general geographical region have resulted from generally heavy rains during this time. However, severe flooding can be produced by intense local thunderstorms. Although thunderstorms occur more frequently during the spring and summer months in this area of south Texas, they may occur at any time.

In the Edwards Plateau region of the basin, extremely high peak discharges have occurred such as those experienced during the floods of June 1935 and September 1955. These floods produced some of the highest peak discharges ever recorded in the state from drainage areas of comparable size. The gaging station at Laguna on the Nueces River recorded its maximum discharge of 307,000 cfs and gage height of 32.70 feet during the flood of September 24, 1955. This was the greatest known river stage since 1866. On the West Nueces River north of Brackettville, which has a drainage area of only 400 square miles, the June 1935 storm produced a peak flow of 580,000 cfs. This is the highest discharge ever recorded for a watershed of that size.

Downstream from the Balcones Fault Zone, the Nueces River and its tributaries cross various permeable formations and have small channel capacities with wide flood plains. As flood peaks cross the fault zone, there are substantial reductions in peak flow due to in-channel losses and losses to overbank storage.

The lower part of the basin has been significantly affected by floods associated with hurricanes and tropical storms moving inland from the coast. The maximum stage of the Nueces River since 1875 at the gaging station near Three Rivers was reached during the flood of September 1967. The river, which rose to a gage height of 49.21 feet and maximum discharge of 141,000 cfs, was swollen by tremendous rainfalls associated with Hurricane Beulah.

The Nueces River basin has a history of flooding that spans back to 1866. The following sections summarize information on some of the major floods in the Nueces basin, including the July 1932, June 1935, September 1955, and September 1967 floods on the Nueces River and its tributaries. Other major floods at significant stream gages in the Nueces River basin are listed in Table 2.1.

**Table 2.1: Major Floods in the Nueces River Basin**

Date of Flood	Observed Peak Flow (cfs)			
	Nueces River at Laguna, TX	West Nueces River nr Brackettville, TX	Nueces River bl Uvalde, TX	Nueces River nr Three Rivers, TX
	USGS 08190000	USGS 08190500	USGS 08192000	USGS 08210000
	737 sq mi	694 sq mi	1,861 sq mi	15,427 sq mi
Jun 1913	210,000	-	-	-
Sep 1919	-	-	-	85,000
Sep 1923	160,000	-	-	-
Jun 1930	87,200	-	68,200	10,100
Jul 1932	-	-	-	56,000
Sep 1932	67,400	-	207,000	-
Jun 1935	213,000	550,000	616,000	66,700
Sep 1936	114,000	-	74,800	-
Jul 1939	222,000	-	89,000	-
Jul 1942	-	-	-	55,000
Sep 1955	307,000	150,000	189,000	3,360
Feb 1958	-	-	-	56,500
Jun 1958	45,100	104,000	146,000	-
Sep 1964	108,000	246,000	188,000	21,200
Sep 1967	-	-	-	141,000
Aug 1971	72,000	37,500	90,600	30,400
Oct 1973	150,000	52,700	144,000	16,400
Oct 1996	142,000	230,000	201,000	2,420
Aug 1998	81,700	46,400	83,200	9,900
Sep 2002	-	-	-	48,500
Oct 2018	71,500	35,300	105,000	7,500

### 2.3.1 The Flood of July 1932

Torrential rains fell over the upper watershed of the Nueces River from June 30 to July 3, 1932. In Kerr, Real and Bandera Counties, the rainfall was from 20 to 35 inches from June 30 to July 3. The floods in the Frio River, which is tributary to the Nueces River, were the highest known. Considerable damage was done to property along the streams in the upper reaches of the Frio River and its tributaries. In its lower reaches, where the river flows through the relatively flat Coastal Plain, wide areas were overflowed, inundating several small towns and many farms and rural homes. The town of Three Rivers, at the junction of the Frio and Atascosa Rivers with the Nueces River, was inundated with the exception of the Murray Hill section and the highway. The flood in the Nueces River was unusually high below the mouth of the Frio River at Three Rivers. Many acres of farmland were submerged with damage to cotton and corn crops. The peak discharge on the Frio River for this flood was estimated to be 162,000 cfs at Concan, 148,000 cfs near Uvalde, and 230,000 cfs near Derby. The peak discharge for this flood was estimated to be 60,000 cfs at Sabinal River at Sabinal, 74,800 cfs at Hondo Creek at Hondo, and 35,800 cfs at Seco Creek near D'Hanis. The peak discharge for this flood was 56,000 cfs at Nueces River near Three Rivers.

### 2.3.2 The Flood of June 1935

The heaviest rain of the June storm fell over the upper part of the West Nueces River basin, and most of the flood in the Nueces River came from this tributary. This flood resulted from the storm of June 9-15, 1935. According to an isohyetal map, there was a 16-inch storm center in the upper part of the West Nueces River Basin. There were no gaging stations on the West Nueces River in June 1935. The peak discharge of 550,000 cfs at the West Nueces River near Brackettville gage was based on slope-area measurements of 580,000 cfs at site 33 miles upstream from gage, and 536,000 cfs at site 24 mi downstream from gage, present site and datum. The maximum gage height of about 40 feet on June 14, 1935 was from gage-height relation of 1935 and 1955 flood peaks at site 0.6 mi upstream. The flood of June 1935 was the greatest ever known on the West Nueces River, according to statements of ranchmen who have been living near the stream for many years. No one could be found who had ever heard of a flood that was comparable in extreme magnitude with this one. The peak discharge for this flood was estimated to be 213,000 cfs at Laguna, 616,000 cfs near Uvalde, 82,600 cfs at Cotulla, and 66,700 cfs near Three Rivers on the Nueces River.

### 2.3.3 The Flood of September 1955

Rain in large amounts and of severe intensity fell during the period September 23 -25, 1955, over the extreme upper end of the Nueces River basin. A 10-inch center northeast of Brackettville and west of Laguna contributed to the flood on the West Nueces River. A 24-inch center on the Nueces River, at the mouth of Hackberry Creek at the Edwards-Real County line southeast of Rock Springs, was the principal contributor to the Nueces River flood. Most of the rain fell during the night of September 23 and the morning of September 24. The peak discharge for this flood was estimated to be 307,000 cfs at Nueces River at Laguna, 150,000 cfs at West Nueces River near Brackettville, 189,000 cfs at Nueces River near Uvalde, 15,100 cfs at Nueces River near Asherton, 10,900 cfs at Nueces River at Cotulla, and 3,360 cfs at Nueces River near Three Rivers. The peak was reduced from 307,000 cfs at Laguna to 3,360 cfs at Three Rivers, or a reduction of 98.9 percent in 271 miles.

### 2.3.4 The Flood of September 1967 – Hurricane Beulah

Torrential rainfall produced by Hurricane Beulah caused floods of record-breaking magnitude on many streams in south Texas and northeastern Mexico in September and October 1967. Beulah made landfall near Brownsville about daybreak on September 20, 1967, and dissipated in the mountains of northern Mexico on September 22. Rainfall during the storm period September 19 - 25 ranged from less than 5 inches at the headwaters to 25 inches in the lower part of the basin. The Nueces River basin had the greatest main stem flood in the lower basin since records began in 1919. In the drainage area upstream from the Atascosa River at Whitsett gage, rainfall ranged from less than 10 inches to more than 25 inches, with the heavier amounts occurring in the lower part of the watershed. The greatest 24- hour total reported from a regular weather station in Texas was 15.69 inches at Whitsett. At the Atascosa River at Whitsett gage, the peak discharge was 121,000 cfs. The stage was 0.3 foot higher than the previous maximum in 1881. Flooding along the Atascosa River was severe from Pleasanton to the mouth. In the Frio River watershed downstream from Derby, rainfall ranged from less than 10 inches at Derby to 19 inches at Three Rivers. At Derby, the peak discharge was only 3,880 cfs. Flooding was substantial but not record breaking in the Frio River watershed. The drainage area along the main stem of the Nueces River below Cotulla received rainfall ranging from less than 10 inches at Cotulla to about 25 inches near Mathis. Mathis reported a 2-day total for September 21-22 of 16.05 inches. At Cotulla, a peak discharge of 7,050 cfs was recorded. On the main stem Nueces at the Tilden gage, the peak discharge was 76,500 cfs. The stage was the greatest known since 1902 and was about 0.1 foot higher than the previous maximum in 1946. At Three Rivers, the combined flow of the Atascosa and Frio Rivers merged with the Nueces to produce the greatest flood since at least 1875. A peak discharge of 141,000 cfs occurred on September 23, 1967. The 1919 stage was exceeded by 3.2 feet. Flooding in the town of Three Rivers was nearly catastrophic. The entire business section, as well as most of the residential area, was inundated with floodwaters up to 6 feet deep. Corpus Christi Lake had a peak

elevation of 94.82 feet, which is the highest stage since the present dam was completed in 1958. The peak discharge from the lake, at about 1800 hours on September 24, was computed to be 138,000 cfs.

## 2.4 PREVIOUS STUDIES AND CURRENTLY EFFECTIVE FEMA FLOWS

The large majority of the Nueces River basin is currently mapped with approximate “Zone A” designations on the FEMA Flood Insurance Rate Maps (FIRMs), meaning that the hydrology for these portions of the basin has never been studied in detail. However, data and models from several existing hydrologic and hydraulic studies were available at the time of this study. Some of these studies used approximate methods, while others used detailed methods for limited portions of the basin. Table 2.2 below summarizes the most notable existing studies, models, and hydrologic information that were previously performed in the Nueces River basin. From this table, one can see that most of the frequency flow estimates in the basin that were calculated with detailed methods have not been updated since the 1970s or 1980s, including the hydrology behind the effective FEMA Flood Insurance Studies for Medina, San Patricio, Uvalde and Atascosa Counties.

**Table 2.2: Previous Hydrologic Studies in the Nueces River Basin**

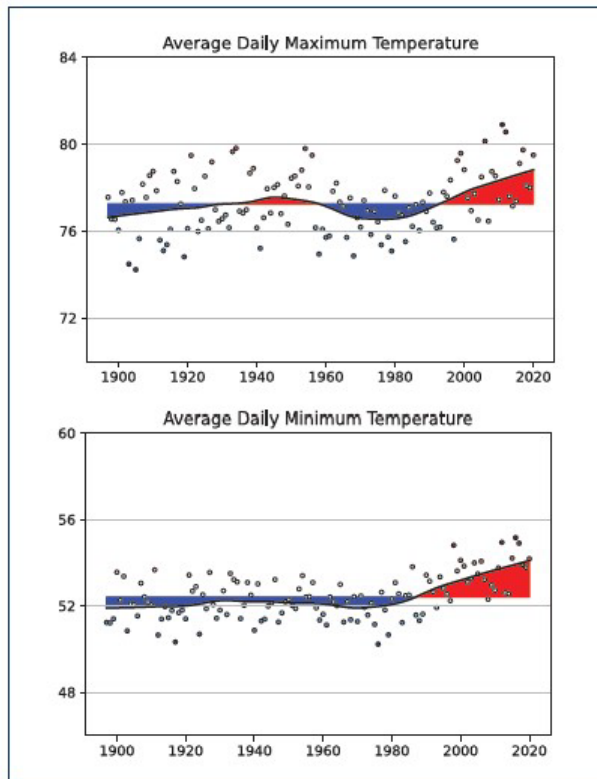
Study Name	River Extents	Frequency Flows	Hydrologic Methods	Description
Lower Frio Base Level Engineering (BLE) Results, 2020	Lower Frio River Basin	Yes	Regression equations, Statistical hydrology	Approximate 1D HEC-RAS models for the Lower Frio River basin with approximate hydrology
Atascosa Watershed Base Level Engineering (BLE) Results, 2020	Atascosa Watershed	Yes	Regression equations, Statistical hydrology	Approximate 1D HEC-RAS models for the Lower Frio River basin with approximate hydrology
San Miguel Watershed Base Level Engineering (BLE) Results, 2020	San Miguel Watershed	Yes	Regression equations, Statistical hydrology	Approximate 1D HEC-RAS models for the Lower Frio River basin with approximate hydrology
Lower Nueces Base Level Engineering (BLE) Results, 2020	Lower Nueces River Basin	Yes	Regression equations, Statistical hydrology	Approximate 1D HEC-RAS models for the Lower Frio River basin with approximate hydrology
Nueces CWMS Implementation Forecast Models, 2020	Nueces River Basin	No	Rainfall-runoff modeling	USACE reservoir forecast models and calibrated rainfall runoff models developed for the entire Nueces River Basin.
Medina County Flood Insurance Study (FIS), 2020	Hondo Creek and Seco Creek	Yes	Rainfall-runoff modeling	HEC-1 models from 1978.
San Patricio County Flood Insurance Study (FIS), 2019	Lower Nueces River at Calallen Dam	Yes	Regression Equations	1977 USGS regression equations
Jim Wells County Flood Insurance Study (FIS), 2017	Lower Nueces River at MOPAC railroad bridge	Yes	Statistical hydrology	2006 Bulletin 17B analysis
Uvalde County Flood Insurance Study (FIS), 2010	Leona River	Yes	Rainfall-runoff modeling	SCS TR-20 analysis from the previous 1986 FIS
Atascosa County Flood Insurance Study (FIS), 2010	Atascosa River	Yes	Rainfall-runoff modeling, Statistical hydrology	SCS method and a Bulletin 17B analysis from 1977.

Study Name	River Extents	Frequency Flows	Hydrologic Methods	Description
City of Corpus Christi Flood Insurance Study (FIS), 1992	Lower Nueces River at Mathis Dam	Yes	Regression Equations	1977 USGS regression equations
Interim Operating Procedures for Choke Canyon Lake Corpus Christi Reservoir System, 1990	Choke Canyon Reservoir and Lake Corpus Christi	No	Rainfall runoff modeling	Original spillway design floods from the Bureau of Reclamation

## 2.5 THE EFFECTS OF FUTURE CONDITIONS

Future conditions can impact the hydrology of a given watershed due to changes in both land use and climate. For the Nueces River Basin, which is primarily rural with approximately 30% of the basins population coming from the coastal city of Corpus Christi, future land use conditions are not expected to change substantially for the foreseeable future. Therefore, future land use change is not expected to cause significant changes to the hydrology of the Nueces River Basin.

Future climate change, on the other hand, is expected to increase the intensity and frequency of storms in Texas and in the Nueces River basin. Records from the National Centers for Environmental Information (NCEI) show that while temperatures in Texas have been slowly increasing since 1895, the increase has become more significant in recent decades. Since 1975, the increasing temperature trend in Texas has averaged about 0.61°F per decade, and this trend has been observed across all seasons and all regions of Texas (Nielsen-Gammon et al., 2021a). See Figure 2.2 for an illustration of the temperature trends in Texas. Higher temperatures will increase soil moisture loss during dry spells, increasing the intensity of naturally occurring droughts (NCEI, 2017).



Texas annual average statewide temperatures (°F)

Figure 2.2: Temperature Trends in Texas (Nielsen-Gammon et al., 2021a)

Basic physics tells us that warmer air can hold more moisture than cooler air. This means that as global temperatures increase, the total amount of water vapor that the atmosphere is capable of holding also increases (USGCRP, 2017). Since heavy rainfall events occur when the air in the atmosphere is almost completely saturated, the expected increase in atmospheric water vapor due to a warming climate directly translates to a similar increase in rainfall intensity. In other words, when rainfall does occur, the amount of rain falling in a given storm event tends to be greater due to the increased water vapor that is available. This is the physical driver to why heavy rainfall is expected to increase in intensity and frequency both globally and across Texas through the end of the century (USGCRP, 2017).

Many studies have documented an increase in extreme rainfall in Texas and the surrounding areas for a variety of durations and thresholds (Nielsen-Gammon et al., 2021a). For example, a median increase of about 7% has been observed in Texas since 1960 in the 1% AEP rainfall intensity, but this relatively small increase in rainfall intensity corresponds to a 30% increase in the frequency of the historic 100-year or 1% AEP rainfall depths (Nielsen-Gammon et al., 2021a).

Some of the extreme flood events that have occurred in the Nueces River Basin were due to hurricanes and tropical storms. As the climate warms, hurricane rainfall rates, storm surge height due to sea level rise, and the intensity of the strongest hurricanes are also projected to increase (NCEI, 2017).

While the predicted impacts of climate change on future rainfall intensity are fairly straightforward, the impacts of climate change on future riverine flooding in Texas are more complex and uncertain. Changes to streamflow and riverine flooding depend on many factors in addition to rainfall, including changes in land use, urbanization, reservoir regulation, evaporation and soil moisture conditions. Warmer temperatures directly lead to decreases in soil moisture content, which will lead to a greater threshold of rainfall being required to induce runoff over initially dry soils (Nielsen-Gammon & Jorgensen, 2021b). Based on limited modeling studies, the Texas State Climatologist concluded that the effects of increased rainfall intensity are likely to dominate over decreased soil moisture conditions for large flood events (Nielsen-Gammon et al., 2021a). This is because the increased soil moisture deficits are likely to have the greatest relative effect on small rainfall events, whereas for larger, more extreme rainfall events like the 100-yr storm, the initial soil moisture deficit becomes less significant relative to the total rainfall depth. This may mean that minor floods become less likely while major floods may become more likely in Texas under future climate conditions (Nielsen-Gammon & Jorgensen, 2021b).

Current research is rapidly improving estimates of future rainfall patterns. For example, in 2022, NOAA completed a pilot project testing new methods to incorporate a nonstationary climate into NOAA Atlas 14's frequency rainfall estimates (NOAA, 2022a). After the completion of that pilot project, NOAA's Hydrometeorological Design Study Center (HDSC) kicked off an effort to apply those recommended methods nationally and to estimate frequency rainfall depths under future climate conditions. The product of that effort will be called NOAA Atlas 15 (NOAA, 2022b). After its initial publication, Atlas 15 will continue to be updated on a 10-year cycle. NOAA Atlas 15 is one of the biggest research needs in flood hydrology as it will allow engineers to easily apply climate change informed future rainfall estimates to hydrologic rainfall-runoff models, just as they do now with existing conditions rainfall data. Once that future rainfall data becomes available, the other research need that quickly becomes apparent is how to alter the hydrologic model's loss parameters for future soil moisture conditions. More information and the current status of NOAA Atlas 15 can be found on their website: <https://water.noaa.gov/about/atlas15>

While there is strong scientific consensus that a warmer future climate will increase the intensity of future heavy rainfall events, additional research is needed to quantify the effects of these changes on flood frequency and severity. The InFRM team is currently waiting on additional guidance from NOAA Atlas 15 in order to quantify the effects of future climate change on the hydrology of Texas and the Nueces River basin. A quantitative

assessment of future climate conditions may be added as an addendum to this report when the appropriate data is available to support it.

### 3 Methodology

Assessing flood potential within complex river basins requires considerable expertise and experience. A multi-layered approach is essential due to the Nueces basin's complex hydrology, variable land use, and historical flood variability. Frequency flows in the Nueces River Basin were calculated through several different methods and their results were compared to one another before making final flow recommendations. The purpose of this analysis was to produce a set of frequency flows that are consistent and defensible across the basin.

The current study builds upon the information that was available from previous hydrology studies by combining detailed data from different models, utilizing land use data, calibrating the models to multiple recent flood events, and updating statistical analyses to include the most recent flood events.

The multi-layered analysis for the current study of the basin consists of four main components: (1) statistical analysis of the stream gages, (2) rainfall-runoff watershed modeling in the Hydrologic Engineering Center's Hydrologic Modeling System (HEC-HMS), (3) extended period-of-record modeling in RiverWare, and (4) reservoir analyses. Details on the methodology of each analysis are included in their respective report chapters and appendices.

After completing all of these different types of analyses, the final recommendations for the InFRM Watershed Hydrology Assessment were then formulated through a rigorous process which required technical feedback and collaboration between all of the InFRM subject matter experts. This process included the following steps at a minimum: (1) comparing the results of the various hydrologic methods to one another, (2) performing an investigation into the reasons for the differences in results at each location in the watershed, (3) selecting the draft recommended methods, (4) performing internal and external technical reviews of the hydrologic analyses and the draft recommendations, and finally, (5) finalizing the study recommendations. The comparisons of results are included in Chapter 11, and additional details on the process of selecting draft recommendations and finalizing the results can be found in Chapter 12.

## 4 Data Sources

This chapter provides a general summary of the data that was collected, reviewed, or utilized in the InFRM Watershed Hydrology Assessment of the Nueces River Basin, including geospatial and climatic information, field observations and previous reports. A more complete list of the data sources used in each type of analysis is included in their respective appendices.

### 4.1 SPATIAL TOOLS AND REFERENCE

ArcMap version 10.8.2 (developed by ESRI), together with HEC-GeoHMS version 10.8 were used to process and analyze the data necessary for hydrologic modeling and to generate the sub-basin boundaries. The geographic projection parameters used for this study are listed below:

- Horizontal Datum: North American Datum 1983 (NAD83)
- Projection: USA Contiguous Albers Equal Area Conic USGS version
- Vertical Datum: North American Vertical Datum, 1988 (NAVD 88)
- Linear Units: U.S. feet

### 4.2 DIGITAL ELEVATION MODEL (DEM)

As part of USACE's Corp Water Management System (CWMS) implementation for the Nueces River basin, 10-meter DEMs were collected from the seamless USGS National Elevation Dataset (NED, accessed June 2018) for the study watershed from the <http://seamless.usgs.gov> website. Limited high-resolution 1-meter LiDAR was also incorporated where available. The DEM's vertical units were converted from meters to feet, cell sizes resampled to 15-m, and the projection was converted to the standard USACE CWMS projection of Albers equal area. The watershed and subbasin delineations for the Nueces HEC-HMS model were performed using the combination of the 15-meter NED data and the resampled LiDAR data.

### 4.3 VECTOR AND RASTER GEOSPATIAL DATA

The mapping team member utilized web mapping services and downloaded the USGS hydrologic unit boundaries, USGS stream gages, USGS medium resolution National Hydrography Dataset (NHD), National Inventory of Dams (NID) data, National Levee Database (NLD) levee centerlines as well as general base map layers. Additional vector data were obtained from the ESRI database and used in figures prepared for the final report. Raster Data includes the National Land Cover Database (NLCD) 2016 land cover layers and percent imperviousness layers from the <https://seamless.usgs.gov> website, accessed October 2016 and August 2018.

### 4.4 AERIAL IMAGES

The Nueces CWMS implementation team utilized current high-resolution imagery from the National Aerial Imagery Program (NAIP) with a horizontal accuracy based upon National Map Accuracy Standards (NMAS), with 1"=200' scale (1-foot imagery) accuracy of +/- 5.0-feet and the 1"=100' scale (0.5-foot imagery) accuracy of +/- 2.5-feet.

Digital photos were used to verify watershed boundaries as well as delineate centerlines and other geographic features. In addition, Google Earth and Bing Maps were also used to locate important geographic features.

## 4.5 SOIL DATA

Gridded Soil Survey Geographic (SSURGO) datasets were obtained from the NRCS soil survey website during the Nueces CWMS implementation (NRCS, accessed Dec 2019). These datasets were used to estimate initial and constant loss rates for the frequency storm events in HEC-HMS and to calculate initial estimates of the Snyder's lag time. The lag times were modified during calibration. See Chapter 6 for more information.

## 4.6 PRECIPITATION DATA

### 4.6.1 Radar Data for Observed Storms

Historic precipitation data for observed storm events were collected from the NWS gridded precipitation data files. NEXRAD Stage IV grids were used for the basin. The NEXRAD Stage IV grids are stored in a binary file format called XMRG. The historical XMRG data were processed into hourly precipitation grids in HEC-DSS format using HEC-METVUE. This data was acquired from the NWS West Gulf River Forecasting Center (WGRFC) in GMT (Greenwich Mean Time) format. A time shift from GMT to CST (Central Standard Time) was later applied within HEC-HMS. The radar rainfall data has the spatial resolution of approximately a 4 km x 4 km grid, and the rainfall depths are calibrated by the NWS to on-the-ground observations at rainfall gages.

### 4.6.2 NOAA Atlas 14 Frequency Point Rainfall Depths

Frequency point rainfall depths of various durations and recurrence intervals were collected from NOAA Atlas 14. NOAA Atlas 14 contains precipitation frequency estimates for the United States along with their associated lower and upper 90% confidence bounds. The Atlas is divided into volumes based on geographic sections of the country. NOAA Atlas 14 is intended as the U.S. Government source of precipitation frequency estimates. NOAA Atlas 14 Volume 11, which covers the state of Texas, was published in September of 2018 (NOAA, 2018). The new rainfall depths that were published in NOAA Atlas 14 (NA14) were applied to the HEC-HMS model for this study, as they are the most up-to-date precipitation frequency estimates in Texas. NOAA Atlas 14 point rainfall depths from the annual maximum series for various durations and recurrence intervals were collected from the NA14 Precipitation Frequency Data Server (PFDS) for the centroid of each HEC-HMS subbasin (NOAA, 2020).

## 4.7 STREAM FLOW AND STAGE DATA

The USGS stream flow and reservoir pool elevation gages located in the basin are listed in Table 4.1. Table 4.1 also indicates whether the gage record was used in this study's statistical analysis or in the calibration of the HEC-HMS model. For these gage sites, annual peak flow data and 15-minute stream flow and stage data was collected from the USGS National Water Information System (NWIS) database (USGS, 2021).

**Table 4.1: USGS Stream Flow and Reservoir Pool Elevation Gages in the Nueces River Basin**

	USGS ID	Location Description	Drainage Area (sq mi)	Data Type	Used in HEC-HMS Calibration	Used for Statistical Analysis
1	818999010	W Nueces Rv nr Barksdale TX	351	Flow	Yes	
2	8189998	Nueces Rv at CR 414 at Montell TX	660	Flow	Yes	
3	8190000	Nueces Rv at Laguna TX	737	Flow	Yes	Yes
4	8190500	W Nueces Rv nr Brackettville TX	694	Flow	Yes	Yes
5	8192000	Nueces Rv bl Uvalde TX	1,861	Flow	Yes	Yes
6	8193000	Nueces Rv nr Asherton TX	4,082	Flow	Yes	Yes
7	8194000	Nueces Rv at Cotulla TX	5,171	Flow	Yes	Yes
8	8194200	San Casimiro Ck nr Freer TX	469	Flow	Yes	Yes
9	8194500	Nueces Rv nr Tilden TX	8,093	Flow	Yes	Yes
10	8195000	Frio Rv at Concan TX	389	Flow	Yes	Yes
11	8196000	Dry Frio Rv nr Reagan Wells TX	126	Flow	Yes	Yes
12	8196300	Dry Frio Rv at FM 2690 nr Knippa TX	176	Flow	Yes	
13	8197500	Frio Rv bl Dry Frio Rv nr Uvalde TX	631	Flow	Yes	Yes
14	8197936	Sabinal Rv bl Mill Ck nr Vaderpool TX	56	Flow	Yes	
15	8198000	Sabinal Rv nr Sabinal TX	206	Flow	Yes	Yes
16	8198500	Sabinal Rv at Sabinal TX	241	Flow	Yes	Yes
17	8200000	Hondo Ck nr Tarpley TX	96	Flow	Yes	Yes
18	8200720	Hondo Ck at SH 173 nr Hondo TX	157	Flow	Yes	Yes
19	8200977	Middle Verde Ck at SH 173 nr Bandera TX	39	Flow	Yes	
20	8201500	Seco Ck at Miller Rh nr Utopia TX	45	Flow	Yes	Yes
21	8202700	Seco Ck at Rowe Rh nr D'Hanis TX	168	Flow	Yes	Yes
22	8204005	Leona Rv nr Uvalde TX	132	Flow	Yes	
23	8205500	Frio Rv nr Derby TX	3,429	Flow	Yes	Yes
24	8206600	Frio Rv at Tilden TX	4,493	Flow	Yes	Yes
25	8206700	San Miguel Ck nr Tilden TX	783	Flow	Yes	Yes
26	8206900	Choke Canyon Res nr Three Rivers, TX	5,490	Elevation	Yes	
27	8206910	Choke Canyon Res OWC nr Three Rivers TX	5,490	Flow (outflow)	Yes	
28	8207500	Atascosa Rv nr McCoy TX	530	Flow	Yes	
29	8208000	Atascosa Rv at Whitsett TX	1,171	Flow	Yes	Yes
30	8210000	Nueces Rv nr Three Rivers TX	15,427	Flow	Yes	Yes
31	8210400	Lagarto Ck nr George West TX	155	Flow	Yes	Yes
32	8210500	Lk Corpus Christi nr Mathis TX	16,502	Elevation	Yes	Yes
33	8211000	Nueces Rv nr Mathis TX	16,503	Flow (outflow)	Yes	Yes
34	8211200	Nueces Rv at Bluntzer TX	16,611	Flow	Yes	
35	8211500	Nueces Rv at Calallen TX	16,684	Flow	Yes	Yes

## 4.8 RESERVOIR PHYSICAL DATA

According to the National Inventory of Dams (NID), over 400 dams exist within Nueces River basin, most of which are NRCS structures, irrigation dams, or other small dams. Of these, reservoir elements were used in the HEC-HMS rainfall-runoff model for two reservoirs in the Nueces basin. These dams were selected to be modeled in detail due to their sizable pool storage and their noticeable influence on discharges in the major rivers downstream. While flood control is not an authorized purpose of these reservoirs, they still have a noticeable effect on downstream peak discharges due to their large storage capacities. Table 4.2 summarizes the reservoir data obtained for these dams and their corresponding data sources, and Figure 4.1 illustrates their locations within the basin.

The two modeled reservoirs, Choke Canyon Dam and Lake Corpus Christi, were included in the model. The dams were modeled as reservoir elements in HEC-HMS.

The elevation-storage and elevation-discharge curves for Choke Canyon Dam were taken from the CWMS model. Both curves were based on data provided by the Bureau of Reclamation (USBR) to 233.0 ft. Values were estimated above 233.0 ft. The datum of data provided by the USBR cannot be confirmed. The curve input in HEC-HMS is in vertical datum NAVD88.

The elevation-storage and elevation-discharge curves for Lake Corpus Christi were taken from the CWMS model. The storage-elevation curve data was derived from the Texas Water Development Board (TWDB) survey from 2016.

The smaller dams were scattered throughout the rural areas of the basin. These dams were not modeled in detail but were accounted for in the model through adjustments to the subbasins' initial losses, peaking coefficients, and routing data. For more information on these adjustments, see Chapter 6. Data for these dams was obtained from the National Inventory of Dams (USACE, 2016).

**Table 4.2: Reservoir Data and Sources for Dams Modeled in Detail**

Reservoir Name	Data	Source(s)
Choke Canyon	Elevation-Storage, Elevation-Discharge rating	Bureau of Reclamation (USBR)
Lake Corpus Christi	Elevation-Storage, Elevation-Discharge rating	Texas Water Development Board (TWDB)

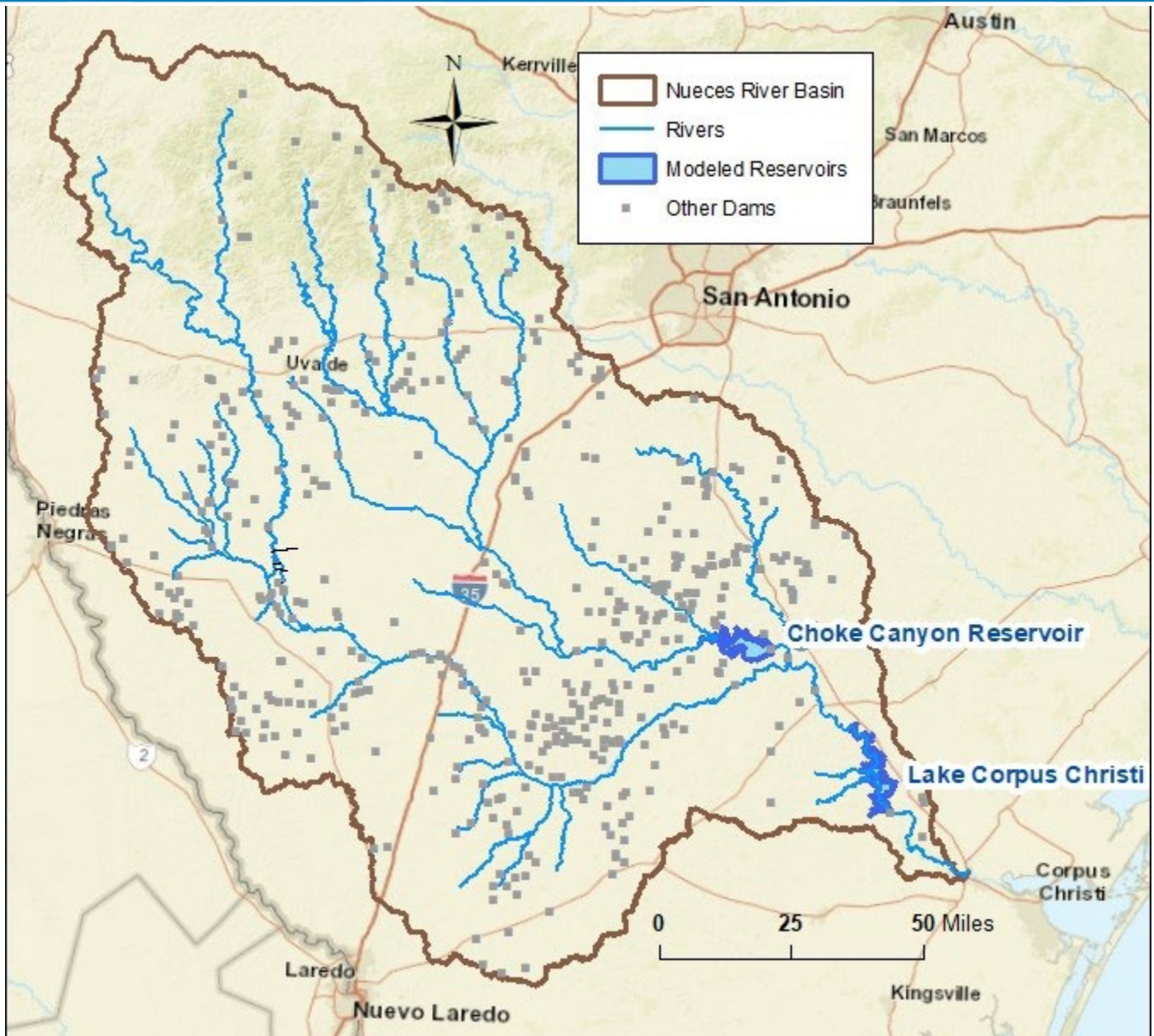


Figure 4.1: Locations of Reservoirs Modeled in HEC-HMS

## 4.9 SOFTWARE

The following table provides a summary of the significant computer software programs and versions that were used in in this study for the hydrologic analyses of the Nueces River basin.

**Table 4.3: Summary of Software Used in the Watershed Hydrology Assessment**

Program	Version	Capability	Developer
ArcMap	10.8.2	Geographical Information System	ESRI
HEC-DSSVue	3.2.3	Plot, tabulate, edit and manipulate data in HEC-DSS format	HEC
HEC-GeoHMS	10.8.2	Watershed delineation and generating HEC-HMS input	HEC
HEC-METVUE	3.0	Processing and viewing precipitation data	HEC
HEC-HMS	4.6.1, 4.11	Rainfall-Runoff Simulation	HEC
HEC-RAS	6.4.1	1D and 2D Hydraulic Routing	HEC
HEC-SSP	2.2	Statistical Software Package	HEC
RiverWare	8.0.1	River and Reservoir Simulation	CADSWES
RMC-RFA	1.1.0	Reservoir Frequency Analysis	RMC
PeakFQ	7.2	Statistical Analysis of Gage Records for Flood Frequency	USGS

## 5 Statistical Hydrology

Statistical analysis of the observational record from U.S. Geological Survey (USGS) streamgaging stations and other historical information provides an informative means of estimating flood flow frequency. Flood flow frequency is defined by values or quantiles of discharge for selected annual exceedance probabilities (AEPs) (England and others, 2019). The annual peak discharge data as part of systematic operation of a streamgaging station provides the foundation for a detailed analysis of peak discharge, but additional historical information pertaining to peak discharges also can be used. An annual peak discharge is defined as the maximum instantaneous discharge for a streamgaging station for a given water year, and annual peak discharge data for USGS streamgaging stations can be acquired through the USGS National Water Information System (NWIS) database (USGS, 2021). The statistical analyses are based on water-year increments. A water year is the 12-month period from October 1 of a given year through September 30 of the following year designated by the calendar year in which it ends.

For the statistical hydrology portion of the multi-layered analysis, InFRM team members from the USGS analyzed annual peak discharge records for the 25 USGS streamgaging stations (gages) shown on Figure 5.1. Information on the period of record data for those USGS gages are listed in Table 5.1 .

This chapter provides a general summary of the data, analyses and results of the statistical analyses of the stream gage records that were completed for the InFRM Watershed Hydrology Assessment of the Nueces River Basin. Additional details on the statistical analyses are available in Appendix A: Statistical Hydrology.

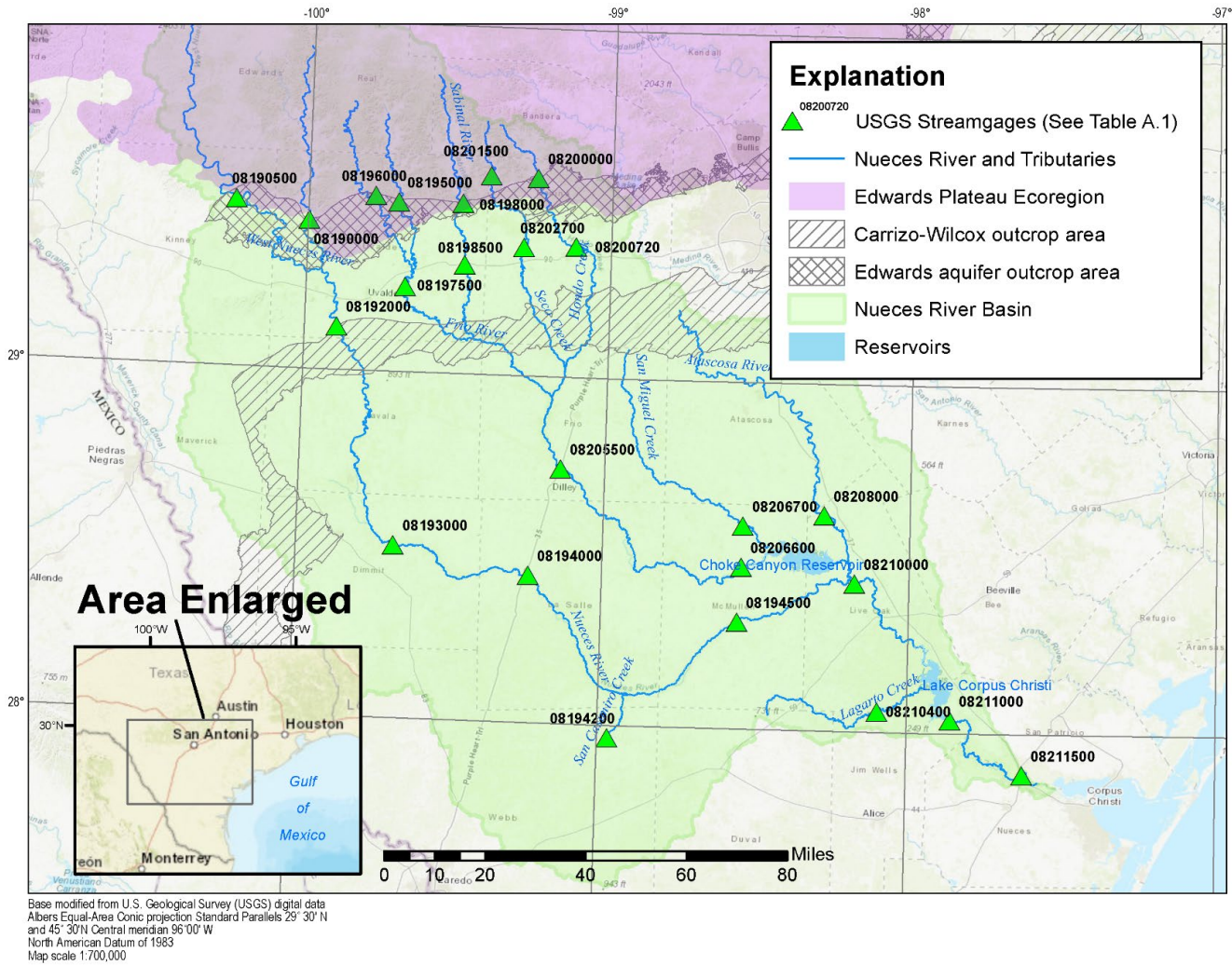


Figure 5.1: Map of U.S. Geological Survey (USGS) Streamgaging Stations included in the Statistical Analysis

**Table 5.1: Summary of the Twenty-Five Analyses for U.S. Geological Survey Streamgaging Stations in the Nueces River Basin Study Area, Texas with Ancillary Information Concerning Statistical Analyses**

[mi<sup>2</sup>, square miles; ft/mi, feet per mile; p-value, probability value; <, less than; --, not applicable]

USGS Streamgage number	USGS Streamgage name	Latitude	Longitude	Period of available annual peak streamflow	Period of analyzed annual peak streamflow	Contributing drainage area (mi <sup>2</sup> )	Station Skew (dimensionless)	Regional skew (Asquith and others, 2021) (dimensionless)	Stream slope (Asquith and Slade, 1997) (ft/mi)	Kendall's tau of analyzed annual peak streamflow (dimensionless)	Kendall's tau p-value of analyzed annual peak streamflow (dimensionless)	Kendall's tau Trend (p-value < 0.05, downward -, upward +) (dimensionless)	Change in Time Analysis (dimensionless)	Pettitt Test Change Point (p-value < 0.05) (water year)	Pettitt Test p-value of full peak streamflow record (dimensionless)
8190000	Nueces River at Laguna, Tex.	29.4283	-99.9969	1913–2020	1913–2020	737	-0.64	-0.46	17.21	-0.059	0.39	None	Yes	--	0.436
8192000	Nueces River below Uvalde, Tex.	29.1236	-99.8944	1928–2020	1928–2020	1,861	-0.74	-0.43	15.62	-0.102	0.149	None	Yes	--	0.185
8193000	Nueces River near Asherton, Tex.	28.5	-99.6817	1940–2020	1940–2020	4,082	0.12	-0.33	10.7	-0.086	0.262	None	Yes	--	0.19
8194000	Nueces River at Cotulla, Tex.	28.4261	-99.2397	1924–2020	1924–2020	5,171	-0.22	-0.29	9.15	-0.163	0.019	-	Yes	1982	0.014
8194500	Nueces River near Tilden, Tex.	28.3086	-98.5569	1935–2020	1935–2020	8,093	-0.51	-0.22	7.44	-0.209	0.007	-	Yes	1983	0.001
8210000	Nueces River near Three Rivers, Tex.	28.4272	-98.1778	1916–2020	1983–2020	15,247	-0.53	-0.19	6.88	0.018	0.88	None	Yes	1984	<0.001
8211000	Nueces River near Mathis, Tex.	28.0381	-97.86	1919–2020	1983–2020	16,503	0.22	-0.09	NA	-0.018	0.88	None	No	1982	<0.001
8211500	Nueces River at Calallen, Tex.	27.8828	-97.625	1983–2020	1983–2020	16,684	0.48	-0.04	NA	0.042	0.733	None	Yes	--	0.653
8194200	San Casimiro Creek near Freer, Tex.	27.9647	-98.9667	1954–2020	1954–2020	469	0.17	-0.19	9.03	-0.175	0.053	None	No	1988	0.044
8190500	West Nueces River near Brackettville, Tex.	29.4811	-100.2392	1900–2020	1900–2020	694	-0.87	-0.45	15.15	-0.059	0.463	None	No	--	0.565
8196000	Dry Frio River near Reagan Wells, Tex.	29.5044	-99.7811	1932–2020	1932–2020	126	-0.9	-0.47	26.7	-0.095	0.25	None	No	--	0.363
8195000	Frio River at Concan, Tex.	29.4883	-99.7044	1923–2020	1923–2020	389	-0.5	-0.47	22.73	0.03	0.667	None	Yes	--	0.386
8197500	Frio River below Dry Frio River near Uvalde, Tex.	29.2456	-99.6742	1894–2020	1894–2020	631	-1.05	-0.45	20.94	0.044	0.644	None	Yes	--	0.197
8205500	Frio River near Derby, Tex.	28.7364	-99.1444	1916–2020	1916–2020	3,429	0.11	-0.35	13.22	-0.088	0.184	None	No	--	0.426
8206600	Frio River at Tilden, Tex.	28.4672	-98.5472	1979–2020	1979–2020	4,493	-0.57	-0.24	10.11	-0.192	0.076	None	Yes	--	0.087
8206600	Frio River at Tilden, Tex. (alternative analysis)	28.4672	-98.5472	1979–2020	1925–2020	4,493	-0.06	-0.24	10.11	-0.175	0.012	-	Yes	--	0.087
8206700	San Miguel Creek near Tilden, Tex.	28.5872	-98.5456	1925–2020	1925–2020	783	-0.49	-0.27	8.05	-0.27	0.003	-	No	1994	0.001
8198000	Sabinal River near Sabinal, Tex.	29.4908	-99.4925	1932–2020	1932–2020	206	-0.02	-0.48	28.28	-0.02	0.796	None	No	--	0.412
8198500	Sabinal River at Sabinal, Tex.	29.3143	-99.4805	1932–2020	1932–2020	241	-0.17	-0.46	23	-0.07	0.4	None	Yes	--	0.411
8201500	Seco Creek at Miller Ranch near Utopia, Tex.	29.5731	-99.4028	1958–2020	1958–2020	45	-0.77	-0.49	40.29	-0.087	0.163	None	No	--	0.13
8202700	Seco Creek at Rowe Ranch near D'Hanis, Tex.	29.3706	-99.2875	1961–2020	1961–2020	168	-1	-0.46	24.79	0.195	0.05	None	No	--	0.337
8200000	Hondo Creek near Tarpley, Tex.	29.57	-99.2477	1932–2020	1932–2020	96	-0.78	-0.48	41.84	-0.155	0.063	None	No	--	0.076
8200720	Hondo Creek at S.H. 173 near Hondo, Tex.	29.3761	-99.1167	2007–2020	1961–2020	157	1.06	-0.46	--	-0.118	0.226	None	No	--	0.301
8208000	Atascosa River at Whitsett, Tex.	28.6219	-98.2811	1919–2020	1919–2020	1,171	-0.01	-0.24	6.33	-0.113	0.116	None	Yes	--	0.111
8210400	Lagarto Creek near George West, Tex.	28.0594	-98.0967	1971–2020	1971–2020	155	0.15	-0.12	12.15	-0.271	0.041	-	No	--	0.141

See Appendix A for more information on how the data for each gage was used in the analyses.

## 5.1 STATISTICAL METHODS

The statistical methods in this Appendix describe the fitting of a log-Pearson type III probability distribution (LPIII) to the annual peak streamflow data for the Nueces River Basin. The general purpose of fitting a probability distribution is to provide an objective mechanism to extrapolate to hazard levels (as represented by AEPs and equivalently expressed as annual recurrence interval or recurrence interval measured in years) beyond those represented by the sample size of annual peak streamflow data for a given streamgage. The LPIII distribution was fit to the logarithm (base-10) of the annual peak streamflow data. The USGS-PeakFQ software version 7.2 (Veilleux and others, 2013; USGS, 2014) provides the foundation for the results of the flood flow frequency estimates that are specified by average annual recurrence intervals computed and extracted from software output at 2, 5, 10, 25, 50, 100, 200, and 500 year recurrence intervals or respective AEPs of 0.500, 0.200, 0.100, 0.040, 0.020, 0.010, 0.005, and 0.002 along with the accompanying 95-percent confidence limits. The flood flow frequency graphs in this appendix were exported from PeakFQ (USGS, 2014) and depict the relation between annual peak streamflow and AEP for each streamgage. The terms “flow,” “streamflow,” and “discharge” are synonymous and used interchangeably in this report. All three terms refer to the volume of water that passes a given point within a given period of time; all are expressed in units of cubic feet per second (cfs) (Rantz and others, 1982).

A complementary statistical technique used for initial data analysis included the non-parametric rank-based Pettitt test (Pettitt, 1979). The Pettitt test is a commonly used statistical test for identifying an abrupt shift in a data series, such as annual peak streamflow data (Mallakpour and Villarini, 2016; Ryberg and others, 2020). For this analysis, the Pettitt test was used to aid in the determination of the point in time when a new reservoir or other climatic or hydrologic changes upstream from a streamgage began to have an effect on peak streamflow, referred to as the “change point” (Ryberg and others, 2020). The Pettitt test was used to identify the water year of the change point and provide measure of its statistical significance; a statistically significant change point was determined when the p-value for the Pettitt test at a given streamgage was less than 0.05. Considered in combination with a visual inspection of the plotted annual peak streamflow series, an analysis of the type and extent of the upstream reservoir (or reservoirs), and the size of the intervening drainage area between the upstream reservoir and streamgage among other considerations, the Pettitt test is a powerful tool for determining whether the NWIS code ‘6’ designation (discharge affected by regulation or diversion) has a measurable or statistically significant effect on streamflows at the gaged location (Ryberg and others, 2020). Table 5.1 lists the p-values of the Pettitt test for the streamflow records at each streamgage. These values and the specific change point indicated by the Pettitt test are discussed further in the next section with the flood flow frequency results for each streamgage.

A second statistical technique used for data evaluation included the nonparametric Kendall’s tau (correlation) test, which is a popular statistic technique for quantifying the presence of monotonic changes in the central tendency of streamflow data in time. The Kendall’s tau test (Hollander and Wolfe, 1973; Helsel and others, 2020) was used through the USGS-PeakFQ software to detect for the presence of monotonic trends (upward or downward changes over time in the annual peak streamflow data). The test was only applied to the peak streamflow data used in the analysis. For example, if a portion of the annual peak streamflow record was removed because it represents a period of record prior to reservoir impoundment (that is, the completion of reservoir construction and deliberate impoundment of water), then the test was only applied to the annual peak streamflow record after reservoir construction. The p-values of the Kendall’s tau test results are listed in Table 5.1, and a trend in annual peak streamflow was

detected at many of the streamgages at a 0.1 significance level (probability value [p-value] of 0.10). Because the Kendall's tau test is a two-tailed test, the p-value must be divided by two to determine whether the identified trend is a statistically significant upward or downward trend (Helsel and others, 2020). Therefore, a p-value of 0.05 was used as the threshold for determining whether there was an upward or downward trend in annual peak streamflow at the streamgages in the Nueces River basin; a statistically significant downward trend in annual peak streamflow was detected for 5 of these 21 streamgages as indicated by the negative tau values (no upward trends in annual peak streamflow were detected). A p-value greater than 0.05 indicates that any upward or downward changes in streamflow were not statistically significant.

Flood flow frequency analyses were made for the period of record through 2020 for the streamgages included in this study by using the annual peak streamflow data from the USGS NWIS database (USGS, 2021) augmented by historical observations of large flood events, which are also stored in NWIS. The Interagency Advisory Committee on Water Data (IACWD, 1982) describes the updated Bulletin 17C method (B17C) to conduct the frequency analysis (England and others, 2019) for the streamgages in the Nueces River Basin. Bulletin 17C includes improvements over the previous guidelines and methodologies; in particular, the expected moments algorithm (EMA) was used in the flood flow frequency analysis of all streamgage records during this study (England and others, 2019; USGS, 2014). The expected moments algorithm enables sophisticated interpretations of the historical record intended to enhance the estimates of peak streamflow, especially for the rare frequency events such as the 100-year streamflow (AEP of 0.01). Estimates of streamflow can be inferred from historical peak stages by using a present-day streamflow-discharge rating curve at a nearby USGS streamgage. In each flood frequency analysis in Section 1.3 in which the rating curve was used to estimate a historical streamflow, the most recently available rating curve at the time of data collection was used. Although the present stage-discharge relationship represented in the rating curve is almost certainly different than the relationship was during the historical event, the rating curve is used as a simple and efficient means of providing an estimate of streamflow for the historical event, albeit a rough estimate with very high uncertainty. The expected moments algorithm also permits inclusion of nonstandard information such as data censoring. For example, an annual peak streamflow might be known to be less than a specified streamflow threshold. The expected moments algorithm can also be used to accommodate time varying streamflow thresholds by assigning a streamflow threshold, otherwise known as a perception threshold, as a "highest since" value within discrete intervals of time. England and others, 2019, p. 56 explain a perception threshold is "the stage or flow above which it is estimated a source would provide information on the flood peak in any given year." Nonstandard information such as historical peak streamflows, perception thresholds, and special-use NWIS codes (refer to section 5.2) collectively can be thought of as a framework fostering record extension. Nonstandard information regarding rare frequency flood events was not available for all streamgages.

Low outliers within a time series of peak streamflow, such as zero or low flow annual peak streamflow that were likely caused by hydrometeorological processes that are unique from the processes that create the floods of interest for these flood frequency analyses, often need special consideration during the analysis that is done by using a form of conditional probability adjustment (England and others, 2019). PeakFQ and HEC-SSP incorporate the Multiple Grubbs Beck Test (MGBT) to detect potentially influential low floods (Cohn and others, 2013). The MGBT was used to identify and partially exclude potentially influential low floods from the analysis (the potentially influential low floods retain their plotting position but are not used in the fitting of the flood flow frequency curve). Within PeakFQ, those peaks identified as potentially influential low floods are recoded as less than a threshold streamflow and treated as interval data in the expected moments algorithm because potentially influential low floods do not convey meaningful information about the magnitude of floods with low AEPs (0.01 or less); but if retained in the

analysis, they can influence the frequency estimates of very low AEP floods. Refer to appendix 7 of Bulletin 17C (England and others, 2019) for more information on the treatment of potentially influential low floods in the expected moments algorithm. For streamgage-specific reasons, the analyst can manually specify a low-outlier threshold. Low-outlier threshold values for each streamgage are identified and discussed further in the individual writeups for each streamgage that follow in this section. Although the ultimate decision for specifying a low-outlier threshold to identify influential low floods is based on engineering judgment, Bulletin 17C provides some general guidelines for choosing an appropriate threshold (England and others, 2019). For each flood frequency analysis, the computed flood frequency curve is evaluated for its fit to the data. If the data appear to have a clear inflection point or shift in the ordered peaks that was not identified by applying the MGBT, then the low outlier may be adjusted (England and others, 2019). Skew is an expression of the curvature or shape of the LPIII distribution intended to mimic that of the data (Asquith, 2011a, 2011b). The importance of a regional skew is stressed in England and others (2019) to mitigate the sensitivity of modest streamgage record lengths to extreme events (Griffis and Stedinger, 2007). A substantial motivation for a regional skew is to compensate for inefficient estimation of the product moment skew for highly variable and skewed data such as annual peak streamflow. The generalized skew coefficient is a built-in feature of the USGS-PeakFQ software but can be overridden by the user. Asquith and others (2021) developed generalized skew coefficients throughout Texas, and these estimates may be considered contemporary, and therefore valid, for this study.

Asquith and others (2021) developed generalized skew coefficients throughout Texas that were used for selected streamgage records in conjunction with the station skew coefficient obtained from the PeakFQ software if the period of record was (1) too short, (2) truncated because a substantial number of low outliers were removed, or (3) influenced considerably by a single extreme event (Griffis and Stedinger, 2007; England and others, 2019). The period of record for remaining streamgages was deemed sufficient to use the station skew computed by PeakFQ. Where the period was relatively short, truncated, or influenced by regulation or natural processes, the computed PeakFQ skew was weighted with regional skew values from Asquith and others (2021). In order to use the regional skew values, the weighted-skew option in USGS-PeakFQ software was required in conjunction with manual entry of skew information (USGS, 2014). The Asquith and others (2021) regional skew values used are listed in Table 5.1. The choice of weighted or station skew is discussed below in the FFQ analysis description for each streamgage.

At each site, a cursory sensitivity analysis was done to determine the effects of the selected low-outlier threshold and selected skew on the flood frequency curve. For the low-outlier threshold, it was considered whether the threshold could be adjusted to improve the station skew, and if the threshold could be adjusted to bring the estimates more in line with flood frequency curves from upstream and downstream streamgages. These factors along with others are considered for the low-outlier threshold for each gaged location analyzed. Low-outlier threshold values for each streamgage are identified in Section 5.2. The sensitivity analysis considered (1) if the station skew value deviated appreciably from published regional skew values, (2) if the calculated flood frequency curve did not appear to fit the ordered peak floods well, or (3) if the calculated flood frequency curve produced estimates inconsistent with flood frequency estimates at upstream and downstream streamgages. Although a station skew value calculated by using PeakFQ that differs greatly from the regional skew estimate is cause for further investigation, it is not necessarily justification for weighting by the regional skew value. This is because the gaged location may have site-specific hydrological characteristics that differ from regional hydrological characteristics (Asquith, 2021). If a weighted skew value was used at a given streamgage, the details of how the weighted skew was determined as well as the selection of the low-outlier threshold are discussed in the analysis section for that streamgage (Section 5.2).

Confidence limits of flood flow frequency can be informative to decision makers that need to know the probability of an event as well as that probability's associated error. The lower and upper limits of 95-percent confidence intervals were computed for this study. Confidence intervals can be expected to encompass the true value 95 percent of the time (Good and Hardin, 2006).

Input data are plotted on a probability scale along with the computed frequency curve and confidence limits using plotting positions. Plotting positions do not have any influence on the computed frequency distribution but are an important tool in assessing the fitted frequency distribution. The Hirsch-Stedinger plotting position was used in this analysis, which is the recommended method in Bulletin 17C because of its correct interpretation of historical information conveyed by historical flood data, the recognition of the limited precision of the exceedance probability estimates for historical floods, and noted the relative imprecision of estimators (Hirsch and Stedinger, 1984; England and others, 2018).

## 5.2 STREAM GAGE DATA AND STATISTICAL FLOW FREQUENCY RESULTS

This section provides a summary of available stream gage data and graphical flow frequency results for five example stream gages in the Nueces River basin along with a summary of results for all gages in Table 5.2. A full description of the stream gage data and flow frequency results for all analyzed gages in the basin can be found in Appendix A.

### **08194000 Nueces River at Cotulla, Texas**

The period of record at USGS streamgage 08194000 Nueces River at Cotulla, Tex. (hereinafter referred to as the "Nueces River at Cotulla streamgage") was from 1924 through 2020. Historical documentation includes a peak stage in 1899 of 29.7 ft (Dalrymple, 1939) at the streamgage location, which ranks as the second largest peak on record through 2020. By extrapolating the 2021 USGS rating curve for the location, the peak from 1899 was estimated between 54,000 and 60,000 cfs, and an interval peak was added to the analysis for that year. Beginning in water year 1949, streamflow is qualified with peak code 6 in NWIS, indicating "streamflow [is] affected by regulation or diversion" (USGS, 2021). No statistically significant differences in peak streamflows before and after the 1949 water year were detected. A significant change point in water year 1982 that does not appear to be associated with reservoir construction was determined by applying the Pettitt test. Furthermore, a significant downward trend in the annual peak streamflow record was identified by applying the Kendall's tau test (Table 5.1).

The largest peak in the gaged period of record is the 1935 peak streamflow of 82,600 cfs at a stage of 32.40 ft. A log-normal plot of the peak streamflows for each water year at the Nueces River at Cotulla streamgage is presented in Figure 5.2, and the flood flow frequency is presented in Figure 5.3. The low-outlier threshold was computed as 2,130 cfs by applying the MGBT in PeakFQ. During the computation of the low-outlier threshold 1 zero-flow and 19 low outliers were identified.

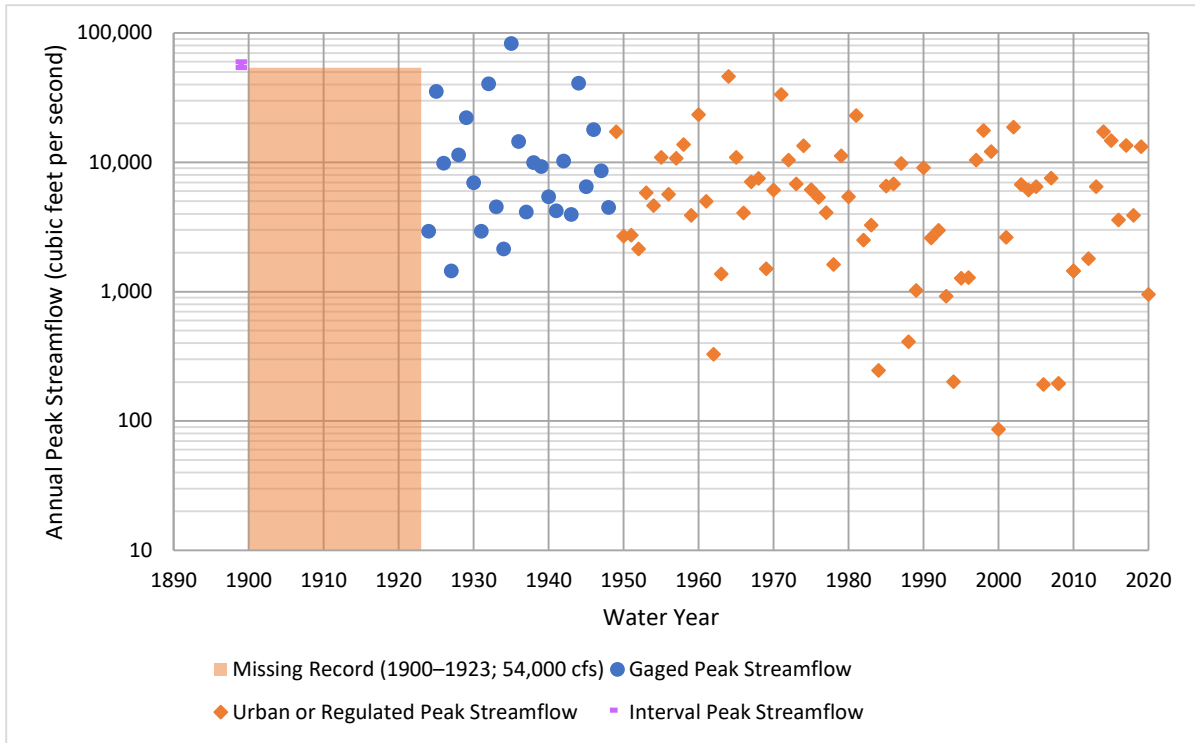


Figure 5.2: Annual Peak Streamflow Data for U.S. Geological Survey Streamgage 08194000 Nueces River at Cotulla, Texas.

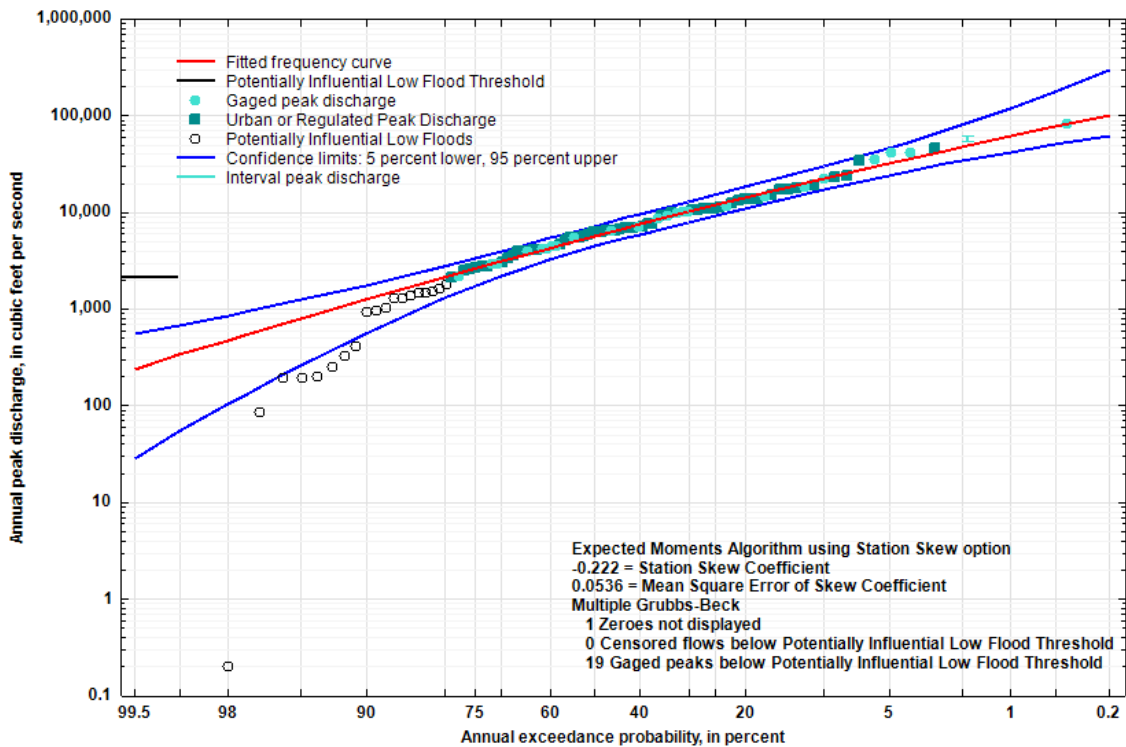


Figure 5.3: Flood Flow Frequency Curve for U.S. Geological Survey Streamgage 08194000 Nueces River at Cotulla, Texas.

**08198500 Sabinal River at Sabinal, Texas**

The period of record at USGS streamgage 08198500 Sabinal River at Sabinal, Tex. (hereinafter referred to as the “Sabinal River at Sabinal streamgage”) was from 1953 through 2020. A historical peak of 60,000 cfs was recorded in 1932 and was included in the analysis. Neither a statistically significant change point nor trend in the annual peak streamflow record were identified (Table 5.1).

The largest peak in the gaged period of record is the 2002 peak streamflow of 119,000 cfs at a stage of 39.00 ft. A log-normal plot of the peak streamflows for each water year at the Sabinal River at Sabinal streamgage is presented in Figure 5.4, and the flood flow frequency is presented in Figure 5.5. The skew was weighted by a regional value from Asquith and others (2021) (Table 5.1). It was determined that the MGBT choice of low-outlier threshold (3,380 cfs) missed a clear inflection point at approximately, 6,000 cfs. Therefore, the low-outlier threshold was manually set at 6,000 cfs, and 34 low outliers were identified.

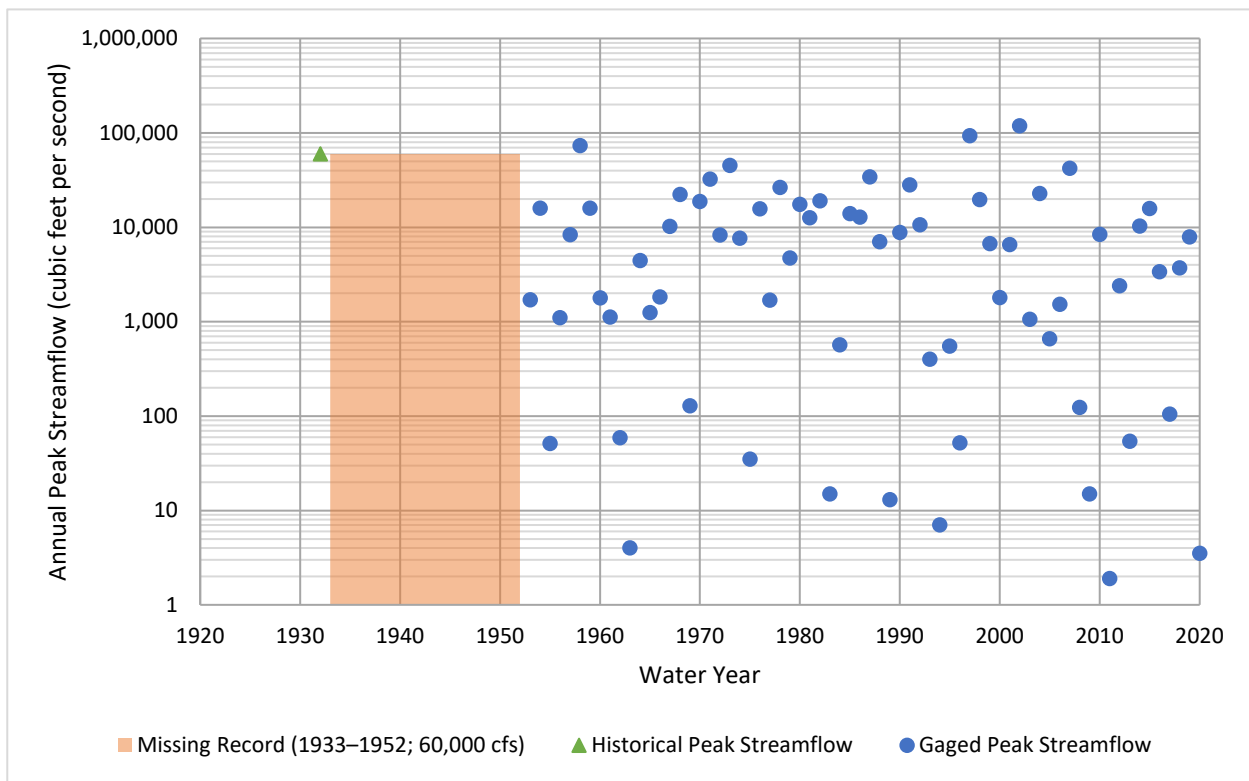


Figure 5.4: Annual Peak Streamflow Data for U.S. Geological Survey Streamgage 08198500 Sabinal River at Sabinal, Texas.

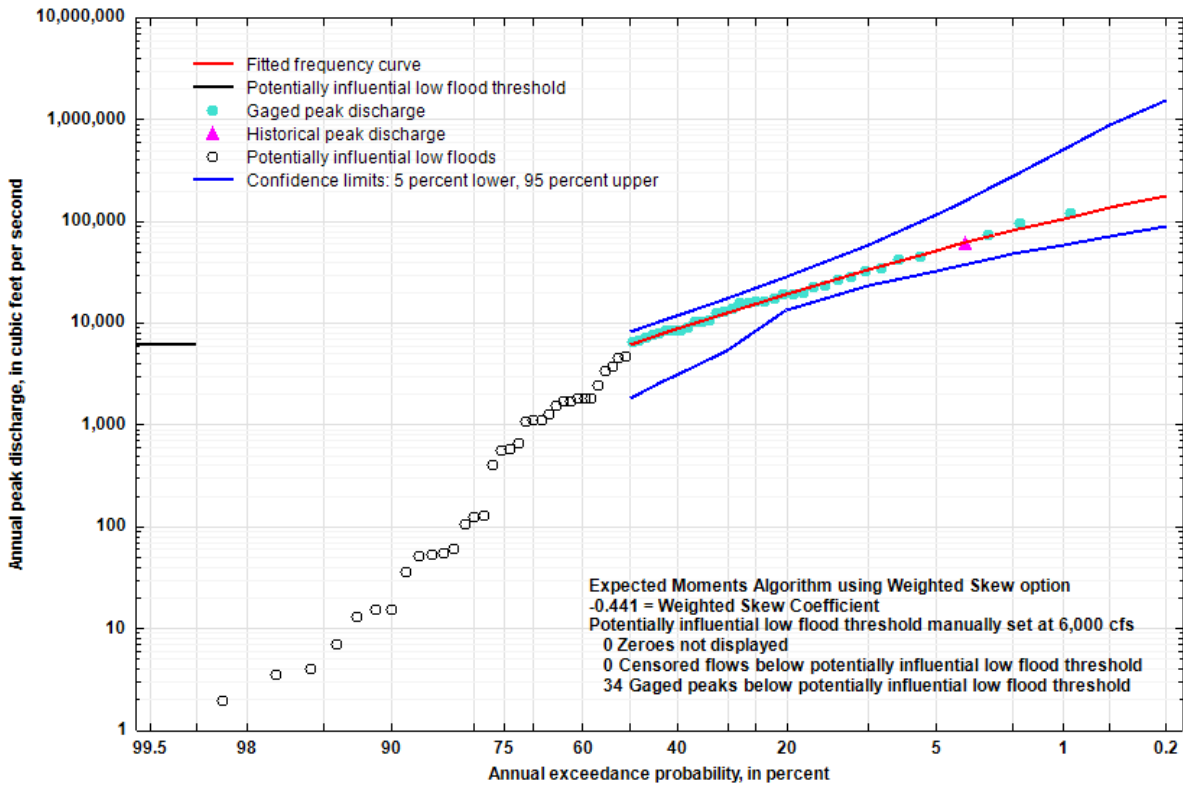


Figure 5.5: Flood Flow Frequency Curve for U.S. Geological Survey Streamgage 08198500 Sabinal River at Sabinal, Texas.

**08206600 Frio River at Tilden, Texas**

The period of record at USGS streamgage 08206600 Frio River at Tilden, Tex. (hereinafter referred to as the “Frio River at Tilden streamgage”) was from 1979 through 2020. A significant change point in the data was not identified. However, by applying the Kendall’s tau test a significant downward trend in the annual peak streamflow record was identified (Table 5.1).

The largest peak in the gaged period of record is the 2002 peak streamflow of 33,000 cfs at a stage of 30.29 ft. A log-normal plot of the peak streamflows for each water year at the Frio River at Tilden streamgage is presented in Figure 5.6, and the flood flow frequency is presented in Figure 5.7. The low-outlier threshold was computed as 476 cfs by applying the MGBT in PeakFQ. During the computation of the low-outlier threshold five low outliers were identified.

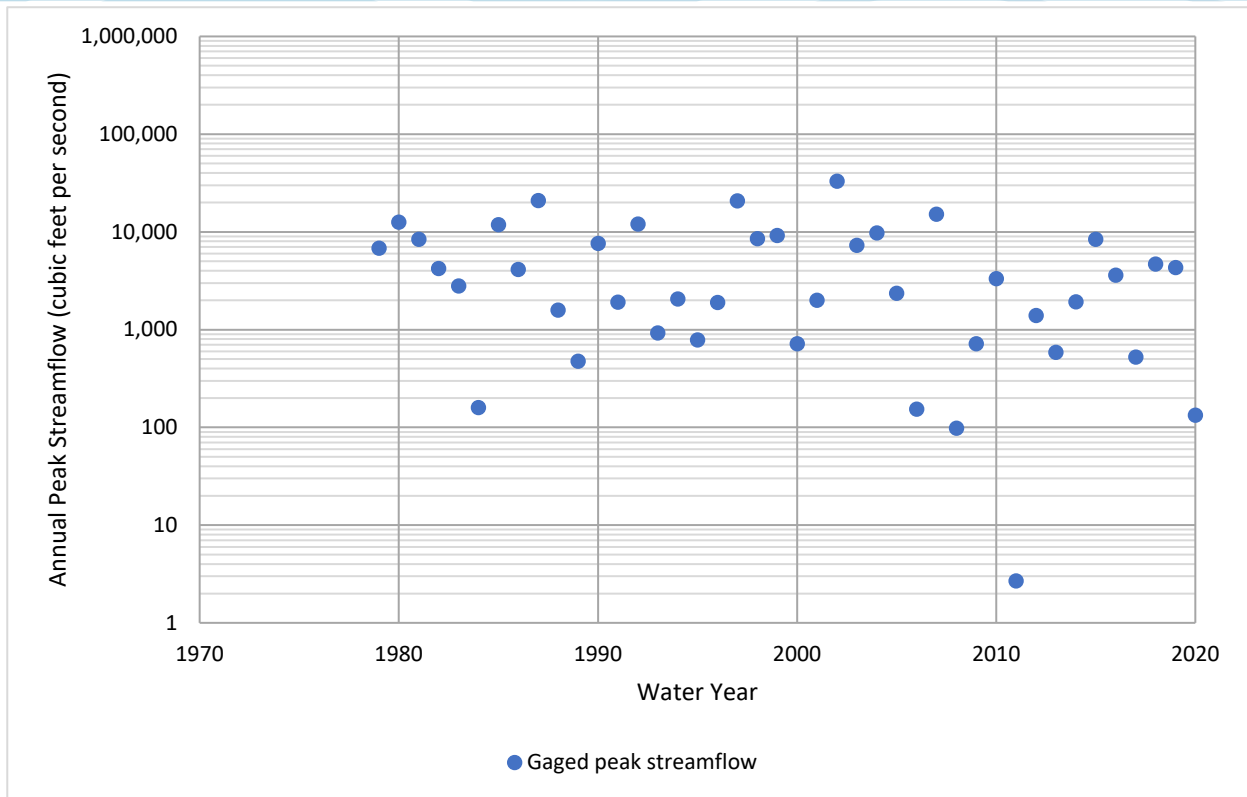


Figure 5.6: Annual Peak Streamflow Data for U.S. Geological Survey Streamgage 08206600 Frio River at Tilden, Texas.

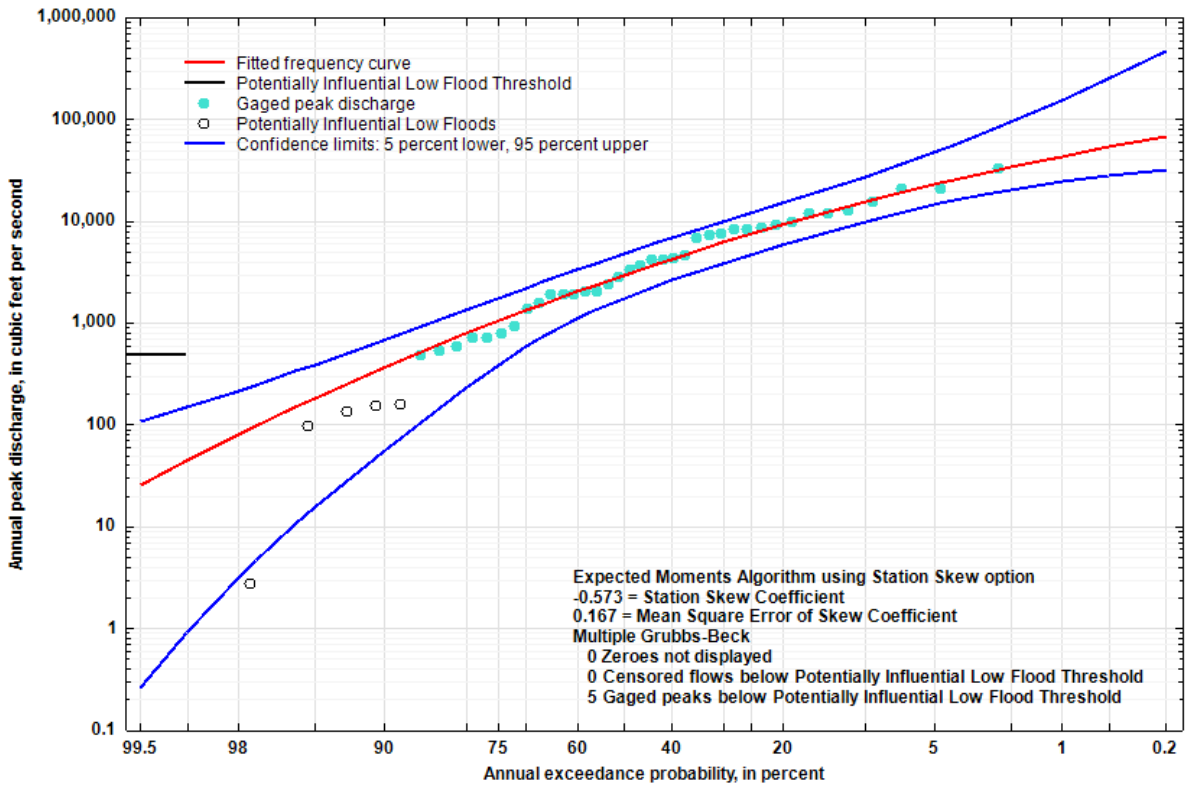


Figure 5.7: Flood Flow Frequency Curve for U.S. Geological Survey Streamgage 08206600 Frio River at Tilden, Texas.

**08206600 Frio River at Tilden, Texas (alternative analysis)**

In 1932, a peak stage of 38.44 ft was measured at the Frio River at Tilden streamgage. However, this peak is 8 ft greater than the next-highest recorded peak in 2002, and the rating curve at the streamgage (which terminates at 31 ft and 40,000 cfs) cannot be used to estimate the streamflow from this stage. To use the notable peak stage in 1932 and increase the reliability of the estimates at the Frio River at Tilden streamgage, record extension was performed with the MOVE.1 method (Hirsch, 1982; Hirsch and Gilroy, 1984; Vogel and Stedinger, 1985) using the USGS Streamflow Record Extension Facilitator (SREF) software (Granato, 2008). Two index stations were used: the upstream streamgage of 08205500 Frio River at Derby, Tex., and the streamgage downstream decommissioned as a result of the construction of Choke Canyon Reservoir, 08207000 Frio River at Calliham, Tex. The Frio River at Calliham streamgage was downstream from San Miguel Creek. Two other streamgages were considered as input for record extension but were not included because of poor correlation to the Frio River at Tilden streamgage. These were the Atascosa River at Whitsett streamgage and the Nueces River near Tilden streamgage. The extended period of record for the alternative analysis at the Frio River at Tilden was from 1925 through 2020.

Two Maintenance of Variance for Record Extension (MOVE) techniques were considered for extending records. Ultimately, the MOVE.1 method was chosen over MOVE.3 method (Vogel and Stedinger, 1985) for two reasons. First, because the MOVE.1 method provided higher streamflow estimates, which in turn should provide more conservative return interval estimates. Second, while both techniques can estimate records when the short-record site is missing data, the MOVE.1 method produces estimators from data sampled only during the concurrent period of record, while the MOVE.3 method uses the entire periods of record from both sites to produce estimators. In this analysis, only two index streamgages were used due to the lack of appropriate index streamgages nearby, and MOVE.1 was chosen to avoid using estimators from only one index streamgage. A simple drainage area ratio was applied to the Frio River at Calliham to estimate peak streamflow at the Nueces River at Tilden streamgage as well. However, the MOVE.1 methodology was considered to be more robust in this instance because it incorporates data from two streamgages instead of one and because of the unknown influence of San Miguel Creek, which enters between the two streamgages and only has records going back to 1964. Ultimately though, the two estimates produced similar results except for the 1932 peak of record, for which the two methods produced widely different estimates. This is most likely because of the unique characteristics of the 1932 flood. The flood of 1932 originated in early July of 1932 from heavy precipitation in the steeply sloped upstream part of the Nueces River watershed, which resulted in a flood wave that decreased in magnitude as it migrated downstream. The Frio River, Dry Frio River, Sabinal River, Seco Creek, and Hondo Creek all recorded noteworthy annual peak streamflows on either July 1 or July 2, 1932. On July 4, 1932, a peak streamflow of 230,000 cfs was recorded at the Frio River near Derby streamgage. Two days later, a peak of 80,200 cfs was recorded at the now defunct Frio River at Calliham streamgage. Therefore, the 1932 peak streamflow at Tilden was highly likely to be somewhere between these two values. Because the Tilden streamgage is approximately halfway between the Derby and Calliham streamgages (1,064 square mile [sq. mi.] increase in drainage area from Derby to Tilden; 998 sq. mi. drainage area increase from Tilden to Calliham), a simple average of the peak streamflows from the two streamgages was used to provide an estimate at Tilden. To accommodate this uncertainty, an interval peak streamflow was input into PeakFQ for the 1932 peak streamflow spanning the average estimate of 155,000 cfs to the MOVE.1 estimate of 162,000 cfs.

A log-normal plot of the peak streamflows for each water year at the Frio River at Tilden streamgage is presented in Figure 5.8, and the flood flow frequency is presented in Figure 5.9. The low-outlier threshold was computed as 1,375 cfs by applying the MGBT in PeakFQ. During the computation of the low-outlier

threshold 17 low outliers were identified. The alternative analysis maintains the original analysis' statistically significant downward trend.

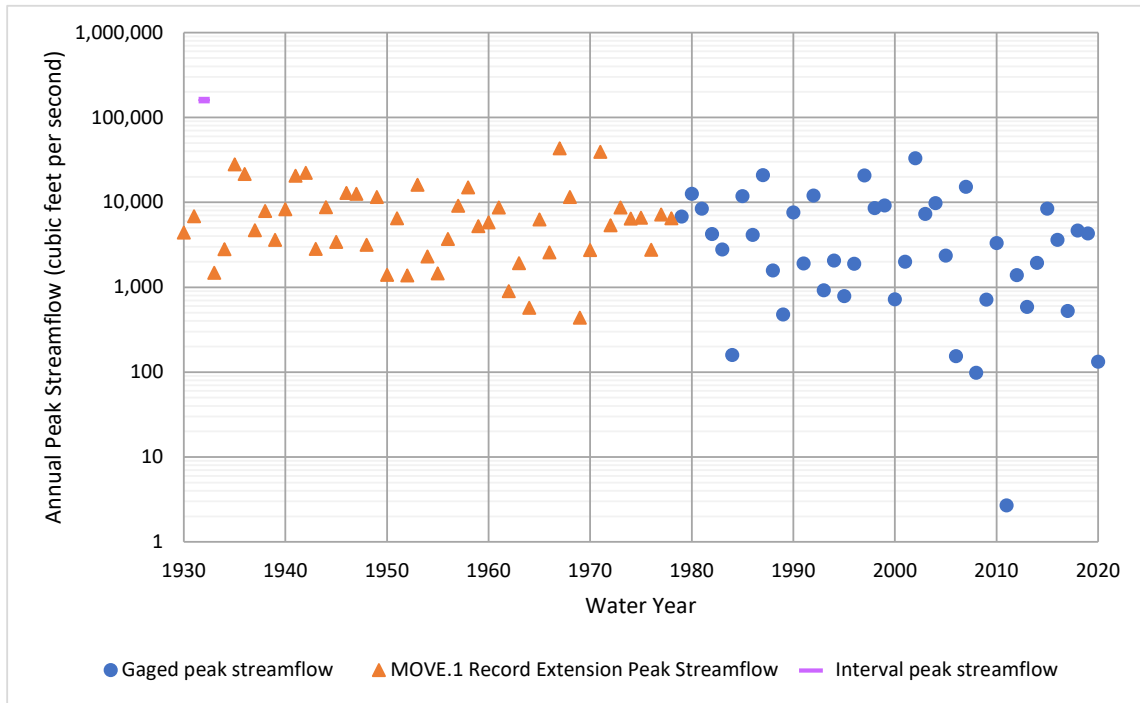


Figure 5.8: Annual Peak Streamflow Data for U.S. Geological Survey Streamgauge 08206600 Frio River at Tilden, Texas (alternative analysis).

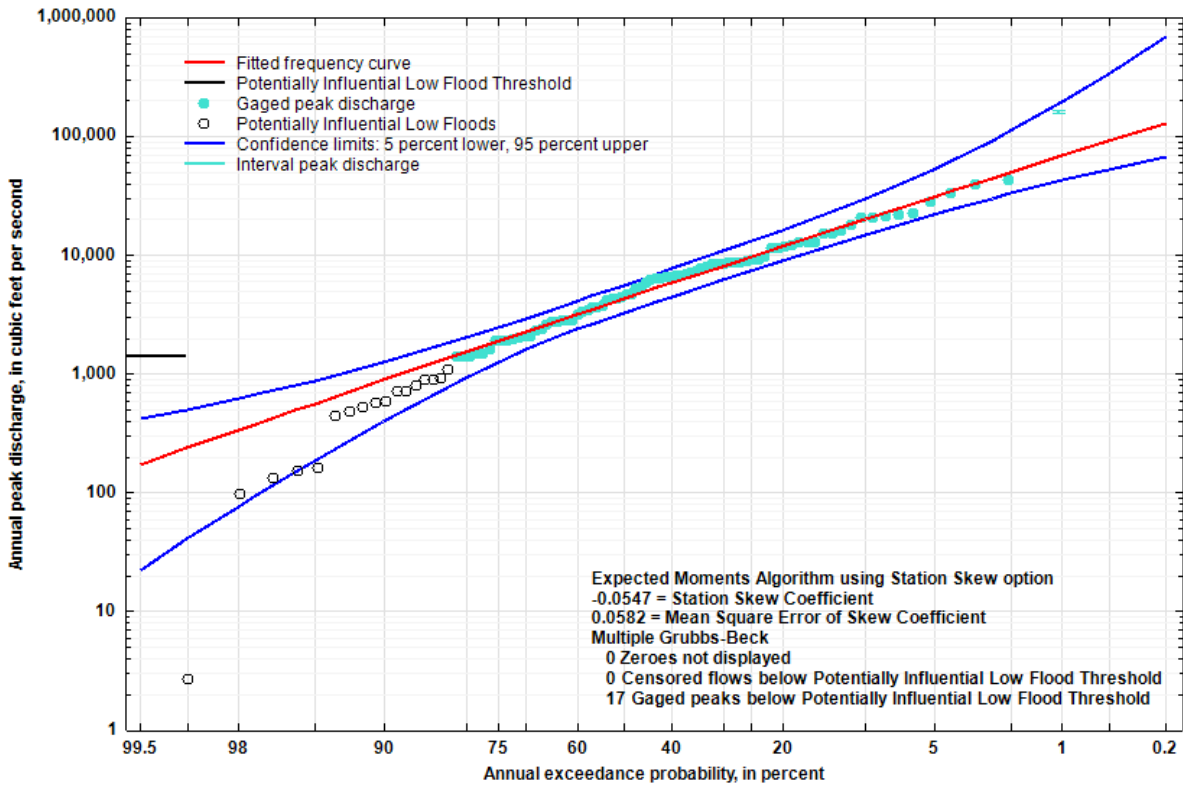


Figure 5.9: Flood Flow Frequency Curve for U.S. Geological Survey Streamgauge 08206600 Frio River at Tilden, Texas (alternative analysis).

**08211500 Nueces River at Calallen, Texas**

The period of record at USGS streamgauge 08211500 Nueces River at Calallen, Tex. (hereinafter referred to as the “Nueces River at Calallen streamgauge”) was from 1983 through 2020. All peak streamflow is qualified with peak code 6 in NWIS, indicating “streamflow [is] affected by regulation or diversion” (USGS, 2021). Annual peak streamflow is missing for water years 1990, 1992, and 2012. Using available peak stages, the USGS rating curve, and estimates of streamflow from upstream streamgages, perception thresholds of 12,000, 12,000, and 1,000 cfs were set for those three missing years respectively. Applying the Pettitt test did not identify a statistically significant change point because the period of record begins in 1983— after the construction in 1982 of Choke Canyon Reservoir upstream from this streamgauge (TWDB, 2022; Table 5.1). A statistically significant trend in the annual peak streamflow record was not identified by applying the Kendall’s tau test (Table 5.1).

The largest peak in the analyzed period of record is the 2002 peak streamflow of 49,000 cfs at a stage of 13.21 ft. A log-normal plot of the peak streamflows for each water year at the Nueces River at Calallen streamgauge is presented in Figure 5.10, and the flood flow frequency is presented in Figure 5.11. The skew was set to the station skew. The low-outlier threshold was manually set at 200 cfs, and one low outlier was identified.

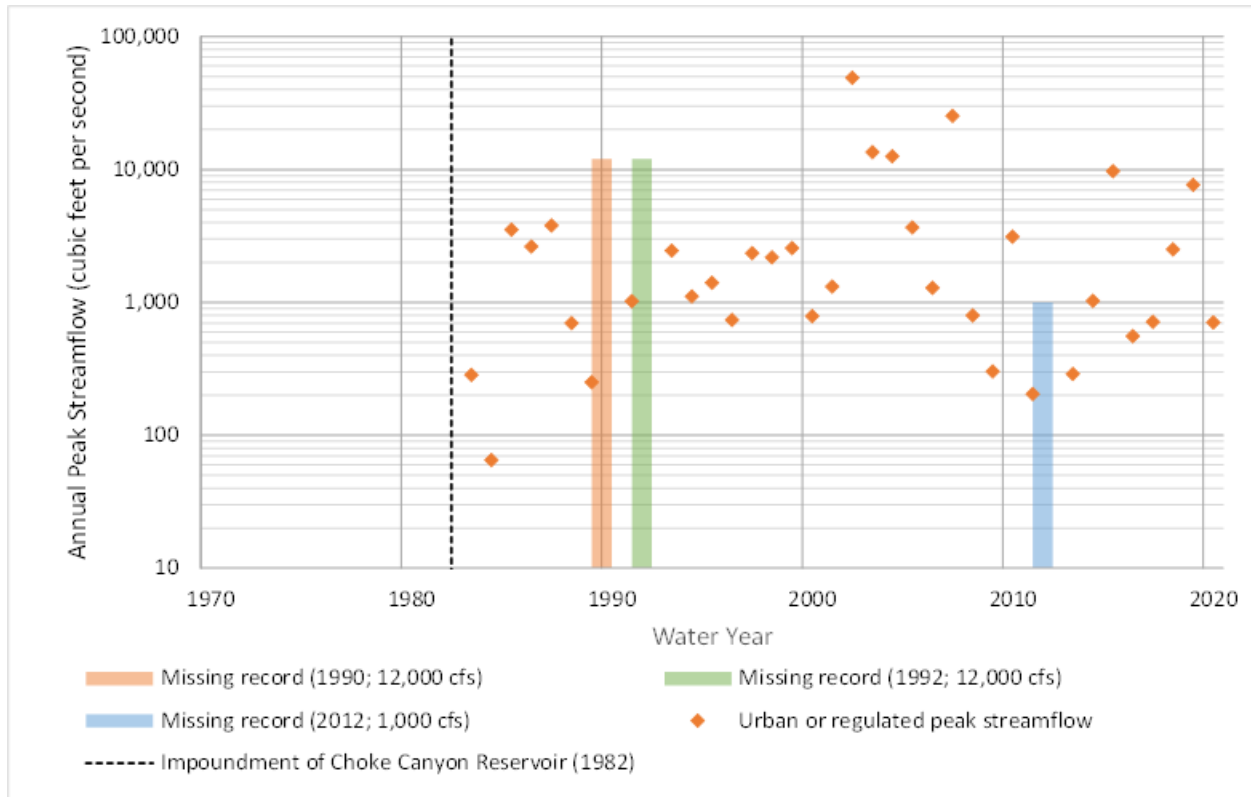


Figure 5.10: Annual Peak Streamflow Data for U.S. Geological Survey Streamgage 08211500 Nueces River at Calallen, Texas

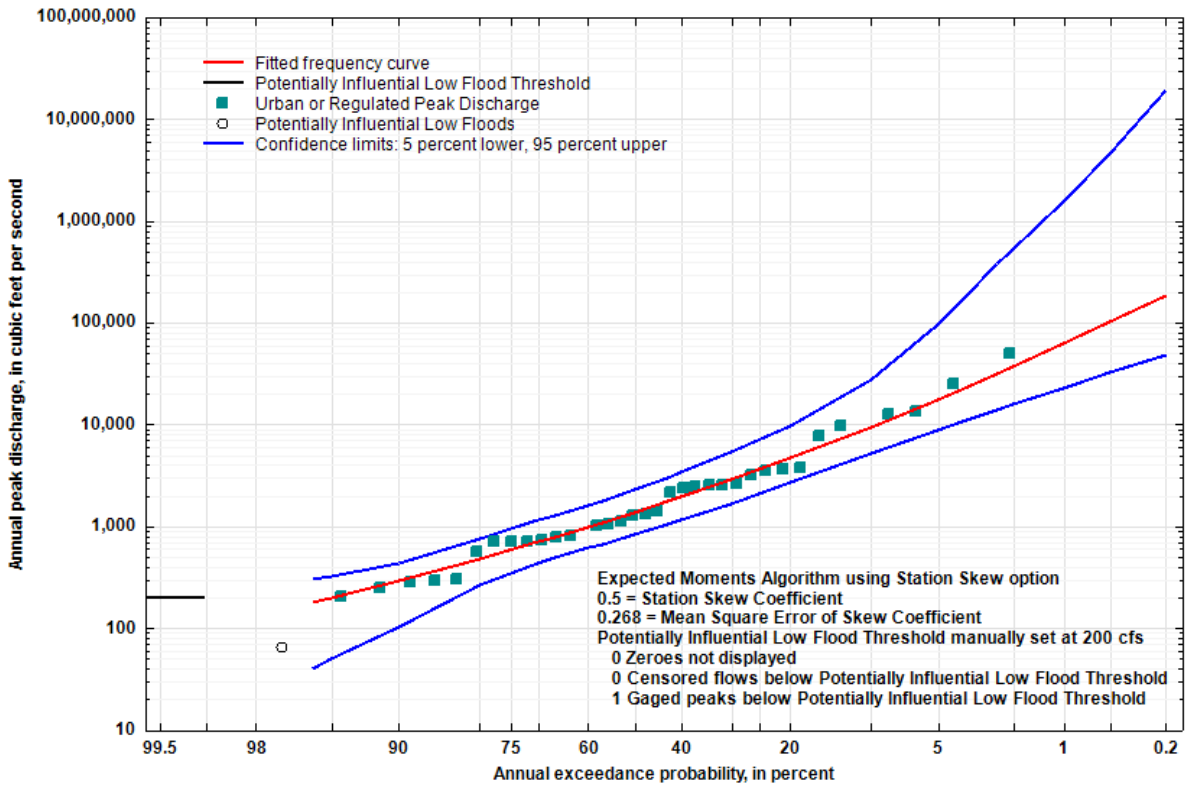


Figure 5.11: Flood Flow Frequency Curve for U.S. Geological Survey Streamgage 08211500 Nueces River at Calallen, Texas

**Table 5.2: Statistically Estimated Annual Flood Flow Frequency Results and Confidence Intervals for Twenty Five Analyses of the U.S. Geological Survey Streamgaging Stations in the Nueces River Basin, Texas Based on USGS-PeakFQ Software**

[USGS, U.S. Geological Survey; cfs, cubic feet per second; %, percent; CI, confidence interval; Note, table contents derived from EXP file (file extension name) of USGS-PeakFQ software output (USGS, 2014). The estimates are of primary interest and are accentuated using a bold typeface.]

USGS Station number and name	Flood flow frequency by corresponding average return period (recurrence interval) in years							
	2 year (cfs)	5 year (cfs)	10 year (cfs)	25 year (cfs)	50 year (cfs)	100 year (cfs)	200 year (cfs)	500 year (cfs)
<b>08190000 Nueces River at Laguna, Tex.</b>								
Lower 95%-CI	6,170	30,700	59,300	109,000	153,000	197,000	240,000	293,000
Estimate	<b>10,300</b>	<b>45,300</b>	<b>87,800</b>	<b>164,000</b>	<b>237,000</b>	<b>320,000</b>	<b>412,000</b>	<b>546,000</b>
Upper 95%-CI	15,400	67,400	134,000	277,000	450,000	712,000	1,100,000	1,920,000
<b>08192000 Nueces River below Uvalde, Tex.</b>								
Lower 95%-CI	3,780	32,000	65,400	125,000	177,000	232,000	285,000	350,000
Estimate	<b>9,310</b>	<b>49,500</b>	<b>103,000</b>	<b>201,000</b>	<b>294,000</b>	<b>401,000</b>	<b>519,000</b>	<b>686,000</b>
Upper 95%-CI	14,500	79,900	177,000	398,000	651,000	994,000	1,460,000	2,350,000
<b>08193000 Nueces River near Asherton, Tex.</b>								
Lower 95%-CI	3,990	8,200	12,200	19,000	25,500	33,500	43,100	58,800
Estimate	<b>4,710</b>	<b>9,590</b>	<b>14,900</b>	<b>25,200</b>	<b>36,500</b>	<b>51,900</b>	<b>73,100</b>	<b>113,000</b>
Upper 95%-CI	5,380	11,800	19,700	39,700	70,000	128,000	238,000	561,000
<b>08194000 Nueces River at Cotulla, Tex.</b>								
Lower 95%-CI	4,380	10,900	16,900	26,100	33,800	41,700	49,800	60,400
Estimate	<b>5,610</b>	<b>14,000</b>	<b>22,000</b>	<b>35,000</b>	<b>46,900</b>	<b>60,600</b>	<b>76,300</b>	<b>100,000</b>
Upper 95%-CI	7,130	18,100	29,400	52,100	79,200	119,000	176,000	292,000
<b>08194500 Nueces River near Tilden, Tex.</b>								
Lower 95%-CI	4,020	12,900	22,000	35,800	46,100	55,400	63,700	73,100
Estimate	<b>5,770</b>	<b>18,000</b>	<b>30,500</b>	<b>51,000</b>	<b>69,200</b>	<b>89,600</b>	<b>112,000</b>	<b>144,000</b>
Upper 95%-CI	8,140	25,000	44,400	86,500	135,000	202,000	296,000	477,000
<b>08210000 Nueces River near Three Rivers, Tex.</b>								
Lower 95%-CI	3,370	8,680	13,300	20,200	25,800	31,700	37,900	46,200
Estimate	<b>5,010</b>	<b>12,600</b>	<b>19,900</b>	<b>31,600</b>	<b>42,300</b>	<b>54,500</b>	<b>68,400</b>	<b>89,400</b>
Upper 95%-CI	7,230	19,700	34,000	62,200	92,600	133,000	187,000	282,000
<b>08211000 Nueces River near Mathis, Tex.</b>								
Lower 95%-CI	1,470	4,630	8,080	14,200	20,100	27,200	35,600	48,700
Estimate	<b>2,340</b>	<b>7,420</b>	<b>13,600</b>	<b>25,700</b>	<b>38,900</b>	<b>56,300</b>	<b>79,100</b>	<b>119,000</b>
Upper 95%-CI	3,700	13,300	27,800	64,000	113,000	192,000	317,000	592,000
<b>08211500 Nueces River at Calallen, Tex.</b>								
Lower 95%-CI	828	2,680	5,170	10,200	15,800	23,000	32,300	48,400
Estimate	<b>1,380</b>	<b>4,690</b>	<b>9,510</b>	<b>21,300</b>	<b>37,000</b>	<b>62,000</b>	<b>101,000</b>	<b>187,000</b>
Upper 95%-CI	2,310	9,700	27,800	151,000	527,000	1,560,000	4,600,000	19,300,000
<b>08190500 West Nueces River near Bracketville, Tex.</b>								
Lower 95%-CI	556	19,700	47,600	100,000	150,000	205,000	260,000	330,000
Estimate	<b>4,370</b>	<b>35,800</b>	<b>86,100</b>	<b>189,000</b>	<b>291,000</b>	<b>408,000</b>	<b>537,000</b>	<b>717,000</b>
Upper 95%-CI	7,920	66,800	198,000	909,000	2,340,000	4,170,000	6,770,000	11,600,000

**Table 5.2: (continued): Statistically Estimated Annual Flood Flow Frequency Results and Confidence Intervals for Twenty Five Analyses of the U.S. Geological Survey Streamgaging stations in the Nueces River Basin, Texas Based on USGS-PeakFQ Software**

USGS Station number and name	Flood flow frequency by corresponding average return period (recurrence interval) in years							
	2 year (cfs)	5 year (cfs)	10 year (cfs)	25 year (cfs)	50 year (cfs)	100 year (cfs)	200 year (cfs)	500 year (cfs)
<b>08194200 San Casimiro Creek near Freer, Tex.</b>								
Lower 95%-CI	1,480	5,200	9,940	19,300	29,100	41,500	56,600	81,100
Estimate	<b>2,250</b>	<b>8,100</b>	<b>16,200</b>	<b>34,600</b>	<b>57,000</b>	<b>89,900</b>	<b>137,000</b>	<b>231,000</b>
Upper 95%-CI	3,430	13,500	31,600	97,200	230,000	543,000	1,270,000	3,880,000
<b>08196000 Dry Frio River near Reagan Wells, Tex.</b>								
Lower 95%-CI	885	9,550	18,300	32,500	45,600	60,300	76,400	99,500
Estimate	<b>3,340</b>	<b>14,600</b>	<b>29,100</b>	<b>57,100</b>	<b>85,600</b>	<b>121,000</b>	<b>162,000</b>	<b>227,000</b>
Upper 95%-CI	4,970	22,500	51,800	140,000	275,000	507,000	877,000	1,670,000
<b>08195000 Frio River at Concan, Tex.</b>								
Lower 95%-CI	2,580	22,600	39,600	63,400	80,500	95,400	108,000	121,000
Estimate	<b>8,030</b>	<b>32,000</b>	<b>55,800</b>	<b>89,900</b>	<b>116,000</b>	<b>140,000</b>	<b>163,000</b>	<b>190,000</b>
Upper 95%-CI	11,600	47,000	92,000	197,000	314,000	437,000	541,000	653,000
<b>08197500 Frio River below Dry Frio River near Uvalde, Tex.</b>								
Lower 95%-CI	2,370	25,100	46,900	80,000	105,000	127,000	145,000	164,000
Estimate	<b>8,560</b>	<b>39,800</b>	<b>72,900</b>	<b>122,000</b>	<b>159,000</b>	<b>195,000</b>	<b>228,000</b>	<b>266,000</b>
Upper 95%-CI	14,000	64,600	132,000	313,000	560,000	745,000	941,000	1,210,000
<b>08205500 Frio River near Derby, Tex.</b>								
Lower 95%-CI	3,430	10,900	18,800	33,300	47,700	65,200	85,800	118,000
Estimate	<b>4,740</b>	<b>14,400</b>	<b>26,200</b>	<b>49,900</b>	<b>76,100</b>	<b>112,000</b>	<b>159,000</b>	<b>245,000</b>
Upper 95%-CI	6,190	20,400	40,200	94,600	185,000	376,000	783,000	2,130,000
<b>08206600 Frio River at Tilden, Tex.</b>								
Lower 95%-CI	1,740	5,770	9,710	15,700	20,100	24,100	27,500	31,300
Estimate	<b>2,950</b>	<b>9,150</b>	<b>15,300</b>	<b>25,200</b>	<b>33,700</b>	<b>43,000</b>	<b>53,000</b>	<b>67,000</b>
Upper 95%-CI	4,800	14,700	26,800	55,800	94,000	154,000	249,000	471,000
<b>08206600 Frio River at Tilden, Tex. (alternative analysis)</b>								
Lower 95%-CI	3,260	8,900	14,700	24,300	32,900	42,400	52,600	67,100
Estimate	<b>4,260</b>	<b>11,800</b>	<b>19,900</b>	<b>34,600</b>	<b>49,500</b>	<b>68,000</b>	<b>90,900</b>	<b>129,000</b>
Upper 95%-CI	5,570	16,000	29,200	62,300	110,000	193,000	333,000	679,000
<b>08206700 San Miguel Creek near Tilden, Tex.</b>								
Lower 95%-CI	2,010	6,240	10,500	17,000	21,900	26,400	30,200	34,500
Estimate	<b>3,000</b>	<b>8,940</b>	<b>14,900</b>	<b>24,500</b>	<b>33,000</b>	<b>42,400</b>	<b>52,800</b>	<b>67,700</b>
Upper 95%-CI	4,400	12,600	21,300	39,300	59,600	87,300	125,000	195,000
<b>08198000 Sabinal River near Sabinal, Tex.</b>								
Lower 95%-CI	3,250	12,200	18,800	29,300	38,700	49,400	61,100	78,300
Estimate	<b>6,320</b>	<b>15,800</b>	<b>25,400</b>	<b>42,100</b>	<b>58,400</b>	<b>78,400</b>	<b>103,000</b>	<b>142,000</b>
Upper 95%-CI	7,900	21,700	37,800	72,400	115,000	181,000	287,000	532,000

**Table 5.2: (continued): Statistically Estimated Annual Flood Flow Frequency Results and Confidence Intervals for Twenty Five Analyses of the U.S. Geological Survey Streamgaging stations in the Nueces River Basin, Texas Based on USGS-PeakFQ Software**

USGS Station number and name	Flood flow frequency by corresponding average return period (recurrence interval) in years							
	2 year (cfs)	5 year (cfs)	10 year (cfs)	25 year (cfs)	50 year (cfs)	100 year (cfs)	200 year (cfs)	500 year (cfs)
<b>08198500 Sabinal River at Sabinal, Tex.</b>								
Lower 95%-CI	1,810	13,200	22,900	35,900	46,800	58,600	71,000	88,300
Estimate	<b>5,990</b>	<b>19,200</b>	<b>33,200</b>	<b>57,100</b>	<b>79,300</b>	<b>105,000</b>	<b>134,000</b>	<b>177,000</b>
Upper 95%-CI	8,250	28,500	57,700	141,000	268,000	494,000	878,000	1,510,000
<b>08201500 Seco Creek at Miller Ranch near Utopia, Tex.</b>								
Lower 95%-CI	468	6,820	13,500	24,500	33,700	43,000	51,800	62,400
Estimate	<b>2,340</b>	<b>11,500</b>	<b>22,800</b>	<b>42,700</b>	<b>60,800</b>	<b>81,000</b>	<b>103,000</b>	<b>132,000</b>
Upper 95%-CI	3,890	20,400	47,500	135,000	276,000	494,000	777,000	1,230,000
<b>08202700 Seco Creek at Rowe Ranch near D'Hanis, Tex.</b>								
Lower 95%-CI	424	9,810	20,500	37,000	50,100	62,600	73,900	86,600
Estimate	<b>2,940</b>	<b>16,600</b>	<b>33,100</b>	<b>60,200</b>	<b>82,600</b>	<b>105,000</b>	<b>127,000</b>	<b>154,000</b>
Upper 95%-CI	4,970	26,100	60,000	255,000	458,000	716,000	1,030,000	1,540,000
<b>08200000 Hondo Creek near Tarpley, Tex.</b>								
Lower 95%-CI	2,780	12,400	22,500	38,800	51,700	63,500	73,800	84,900
Estimate	<b>4,820</b>	<b>18,900</b>	<b>33,900</b>	<b>58,100</b>	<b>78,600</b>	<b>100,000</b>	<b>123,000</b>	<b>152,000</b>
Upper 95%-CI	7,590	28,400	51,100	95,700	146,000	218,000	317,000	513,000
<b>08200720 Hondo Creek at S.H. 173 near Hondo, Tex.</b>								
Lower 95%-CI	1,140	15,200	28,200	41,500	50,000	56,800	62,200	68,200
Estimate	<b>6,370</b>	<b>24,200</b>	<b>41,100</b>	<b>64,200</b>	<b>81,000</b>	<b>96,500</b>	<b>110,000</b>	<b>126,000</b>
Upper 95%-CI	9,770	36,400	71,500	240,000	419,000	680,000	1,040,000	1,580,000
<b>08208000 Atascosa River at Whitsett, Tex.</b>								
Lower 95%-CI	3,160	8,960	15,100	25,500	35,000	45,800	57,700	75,000
Estimate	<b>4,190</b>	<b>12,000</b>	<b>20,700</b>	<b>37,200</b>	<b>54,200</b>	<b>76,000</b>	<b>104,000</b>	<b>151,000</b>
Upper 95%-CI	5,550	16,500	30,800	66,100	114,000	191,000	314,000	590,000
<b>08210400 Lagarto Creek near George West, Tex.</b>								
Lower 95%-CI	13	176	603	2,240	5,090	10,300	19,200	39,100
Estimate	<b>40</b>	<b>494</b>	<b>1,920</b>	<b>8,470</b>	<b>22,500</b>	<b>54,700</b>	<b>125,000</b>	<b>343,000</b>
Upper 95%-CI	113	1,660	8,830	89,700	666,000	6,520,000	41,900,000	399,000,000

NOTE: For more information on the analysis of each site, please see section 1.3 of Appendix A.

## 5.3 CHANGES TO FLOOD FLOW FREQUENCY ESTIMATES OVER TIME

Statistically based flood flow frequency estimates are dependent on observational data and historical information (England and others, 2019). Examples of changes to flood flow frequency estimates over time are provided for 5 streamgages in the Nueces River basin (Table 5.1). Collectively, these are shown in Figure 5.12 through Figure 5.16. The annual recurrence intervals of interest here are 2, 10, 100, and 500 years, which correspond to AEPs of 0.500, 0.100, 0.010, and 0.002, respectively.

Each of these examples is intended to illustrate that there is substantial variation in the statistical estimates over time especially for the rare frequencies. Peak streamflows outside the period of record are not shown. Because the data used to plot the values of the 2, 10, 100, and 500-year streamflow estimates in a given year are dependent on all data before that year, in general there is less variation in the annual chance exceedance estimates during the latter years of a given record (Figures 5.12 through 5.16). This decrease in the variation associated with annual chance exceedance occurs because the total sample size as a measure of information content of flood flows increases at a proportionally smaller rate with each additional year of data. For example, one more year of data for a sample of 10 years represents a 10-percent increase in information, whereas one more year of data for a sample of 50 years is only a 2-percent increase in information. In other words, as the record length increases given other factors remaining relatively constant (land use for example), the annual chance exceedance estimates are expected to vary year-to-year to a lesser degree for the simple reason that proportionally less information is included with each successive year.

Flood flow frequency estimates over time computations are performed in HEC-SSP and incorporate the Bulletin 17C analysis into a variable time window (England and others, 2019; USACE, 2023). Each analysis utilized an expanding time window with a minimum time period of 10 years and increments of 1 year. Therefore, the flood frequency estimates over time shown in the figures below begin 10 years after the availability of systematic record and provide estimates for each subsequent year through the present analysis (2020). See Appendix A for the results of all analyzed gages for flood flow frequency estimates over time.

**08194000 Nueces River at Cotulla, Tex.**

The relative effects of record length and magnitudes of substantial floods for the Nueces River at Cotulla streamgage are shown in Figure 5.12. In general, all return intervals appear to decrease over time similar to what is observed at upstream streamgages. A statistically significant change point was detected in water year 1982 (Table 5.1), and an increase in events less than 1,000 cfs is visually apparent beginning in the 1980s as well as a decrease in events greater than 20,000 cfs. The Kendall's *tau* test identified a statistically significant decrease in annual peak streamflow at the gaged location. Estimates of the annual chance exceedance appeared to continue to decline through 2021 except for the 50-percent annual chance exceedance and 10-percent annual chance exceedance estimates, which appear to have stabilized somewhat since about 1980. The 1-percent annual chance exceedance event decreases from 71,700 cfs in 2000 to 60,600 cfs in 2020. During the same time span, the 10-percent annual chance exceedance estimate decreases only from 23,700 cfs to 22,000 cfs, and the 50-percent annual chance exceedance estimate decreases only from 5,820 cfs to 5,610 cfs. However, prior to the observed increase in peak streamflow, less than 1,000 cfs the 50-percent annual chance exceedance estimate in 1980 is 6,490 cfs, which represents an approximately 14 percent decrease over four decades.

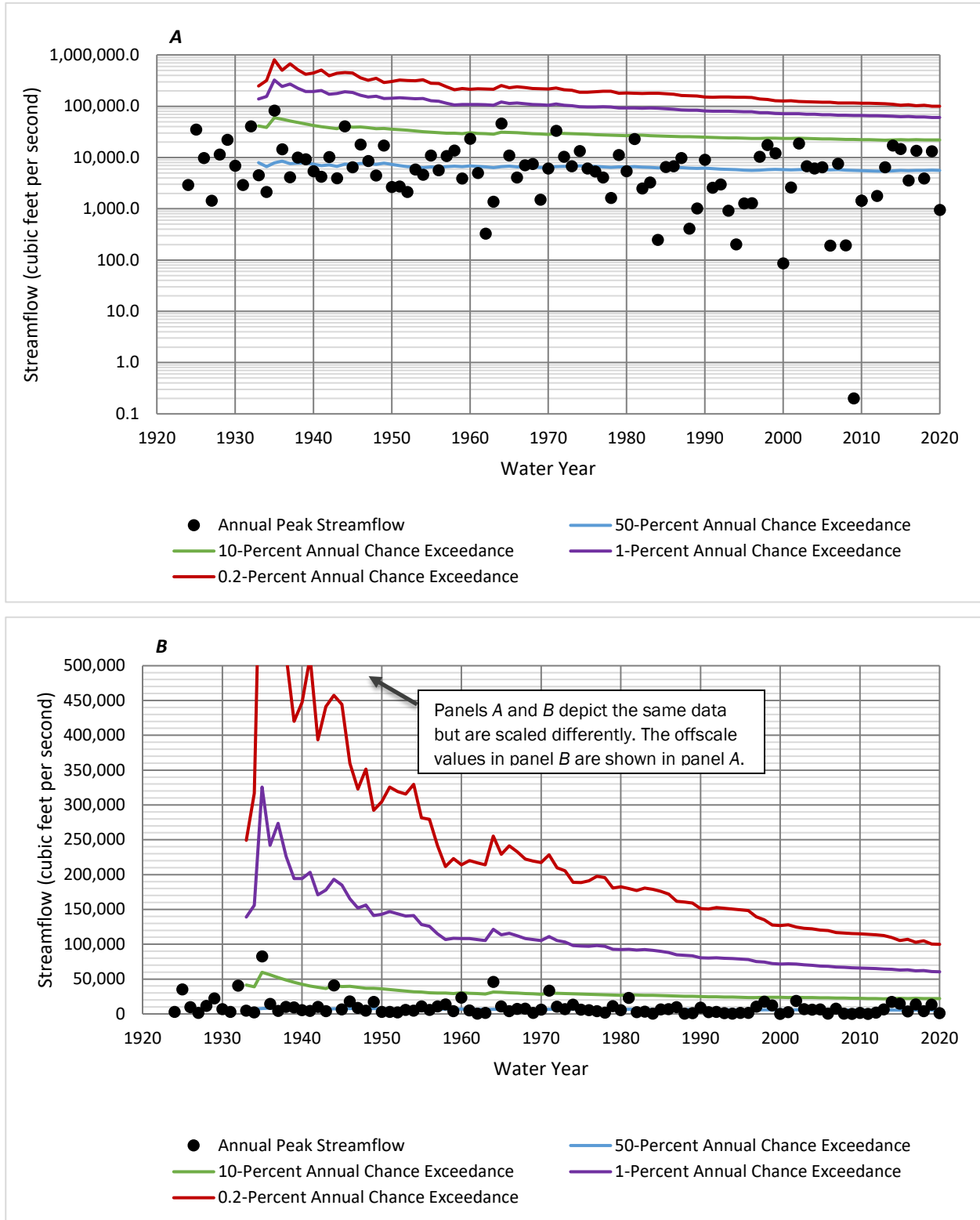


Figure 5.12: Statistical Frequency Flow Estimates versus Time in *A*, log y-axis and *B*, linear y-axis for U.S. Geological Survey Streamgauge 08194000 Nueces River at Cotulla, Texas.

**08211500 Nueces River at Calallen, Tex.**

The relative effects of record length and magnitudes of substantial floods for the Nueces River at Calallen streamgauge are shown in Figure 5.13. The 2002 annual peak streamflow of 49,000 cfs results in an increase in all estimates except the 50-percent annual chance exceedance. After the 2002 event, the 10-percent annual chance exceedance and 50-percent annual chance exceedance events have declined, and it is difficult to determine whether they have stabilized during the 18 years of record after the 2002 event that were considered for this analysis (2003–20). However, the 1-percent annual chance exceedance estimate appears relatively stable since water year 2010. The 1-percent annual chance exceedance event decreases from 63,100 cfs in 2011 to 60,600 cfs in 2020. During the same time span, the 10-percent annual chance exceedance estimate decreases slightly from 10,500 cfs to 9,620 cfs, and the 50-percent annual chance exceedance estimate also decreases slightly from 1,620 cfs to 1,420 cfs.

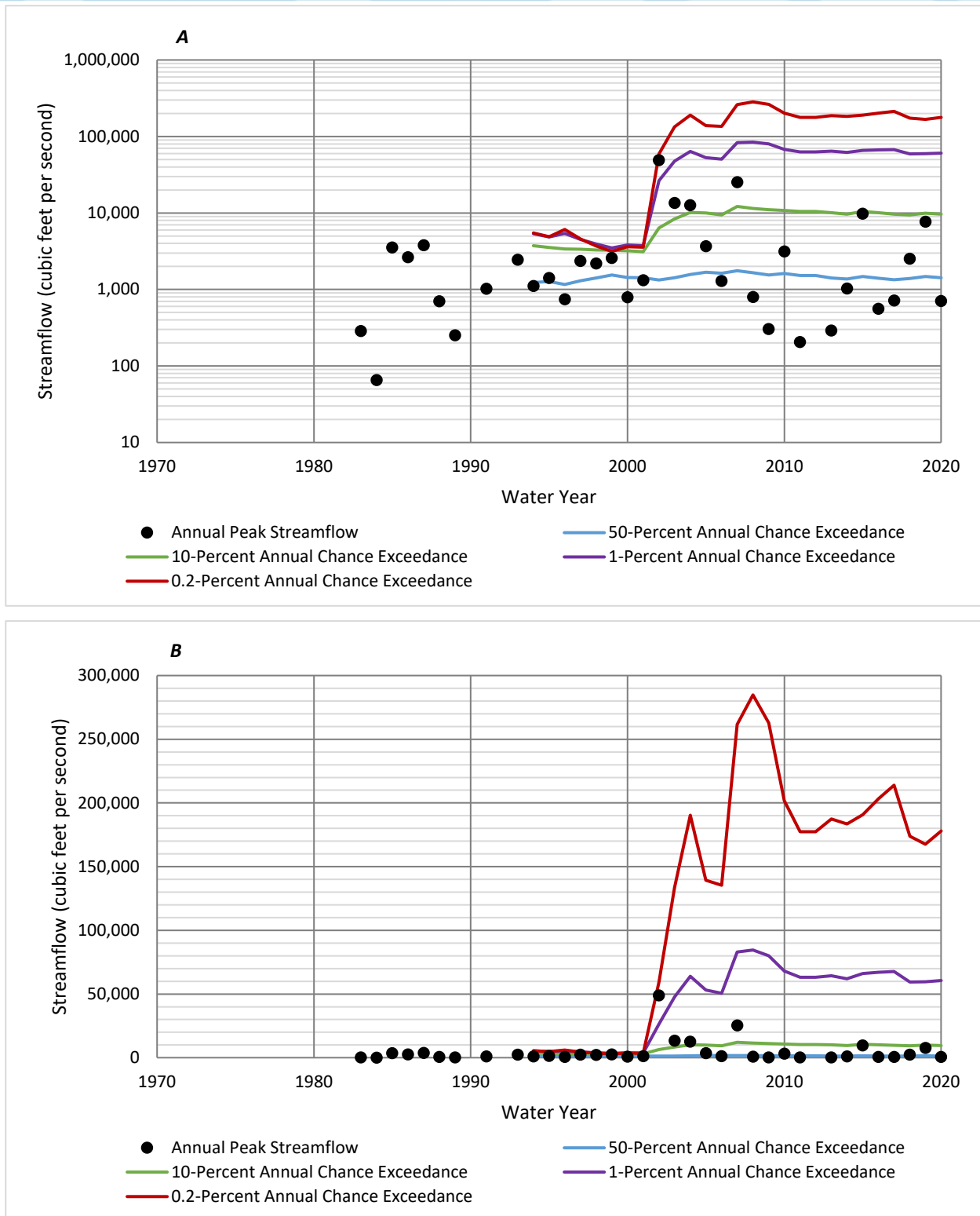


Figure 5.13: Statistical Frequency Flow Estimates versus Time in *A*, log y-axis and *B*, linear y-axis for U.S. Geological Survey Streamgauge 08211500 Nueces River at Calallen, Texas.

**08197500 Frio River below Dry Frio River near Uvalde, Tex.**

The relative effects of record length and magnitudes of substantial floods for the Frio River near Uvalde streamgage are shown in Figure 5.14. The 2002 extreme annual peak streamflow of 189,000 cfs results in an increase in all annual chance exceedance estimates compared to those for the years prior to this flood event. After the 2002 flood event, all annual chance exceedance estimates decreased, although it is difficult to determine whether they have stabilized given there were only 18 years of record (2003–20) since the 2002 event. The 1-percent annual chance exceedance event decreased from 212,000 cfs in 2010 to 195,000 cfs in 2020. During the same time span, the 10-percent annual chance exceedance estimate decreased from 81,200 cfs to 72,900 cfs.

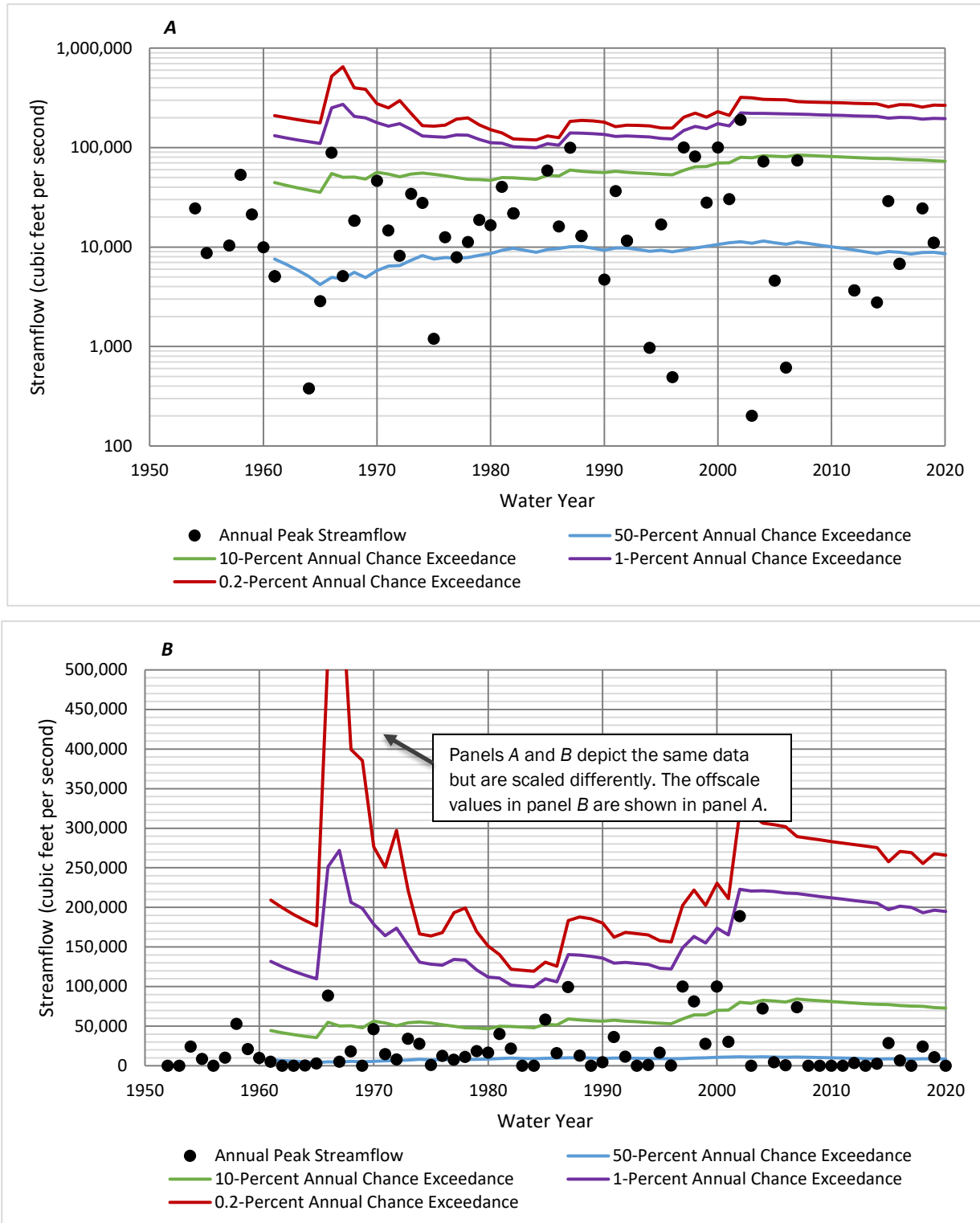


Figure 5.14: Statistical Frequency Flow Estimates versus Time in *A*, log y-axis and *B*, linear y-axis for U.S. Geological Survey Streamgauge 08197500 Frio River below Dry Frio River near Uvalde, Texas. Note: zero-flow values plotted in panel B (linear scale) are missing from panel A (log scale) because the logarithm of zero cannot be defined.

**08206600 Frio River at Tilden, Tex.**

The relative effects of record length and magnitudes of substantial floods for the Frio River at Tilden streamgage are shown in Figure 5.15. After a slight increase associated with the 2002 event, all estimates appear to decline only slightly, although it is difficult to determine whether they have stabilized with only 18 years of record after the 2002 event. The 1-percent annual chance exceedance (ACE) event decreases from 46,500 cfs in 2010 to 43,000 cfs in 2020. During the same time span, the 10-percent annual chance exceedance estimate decreases from 17,900 cfs to 15,300 cfs.

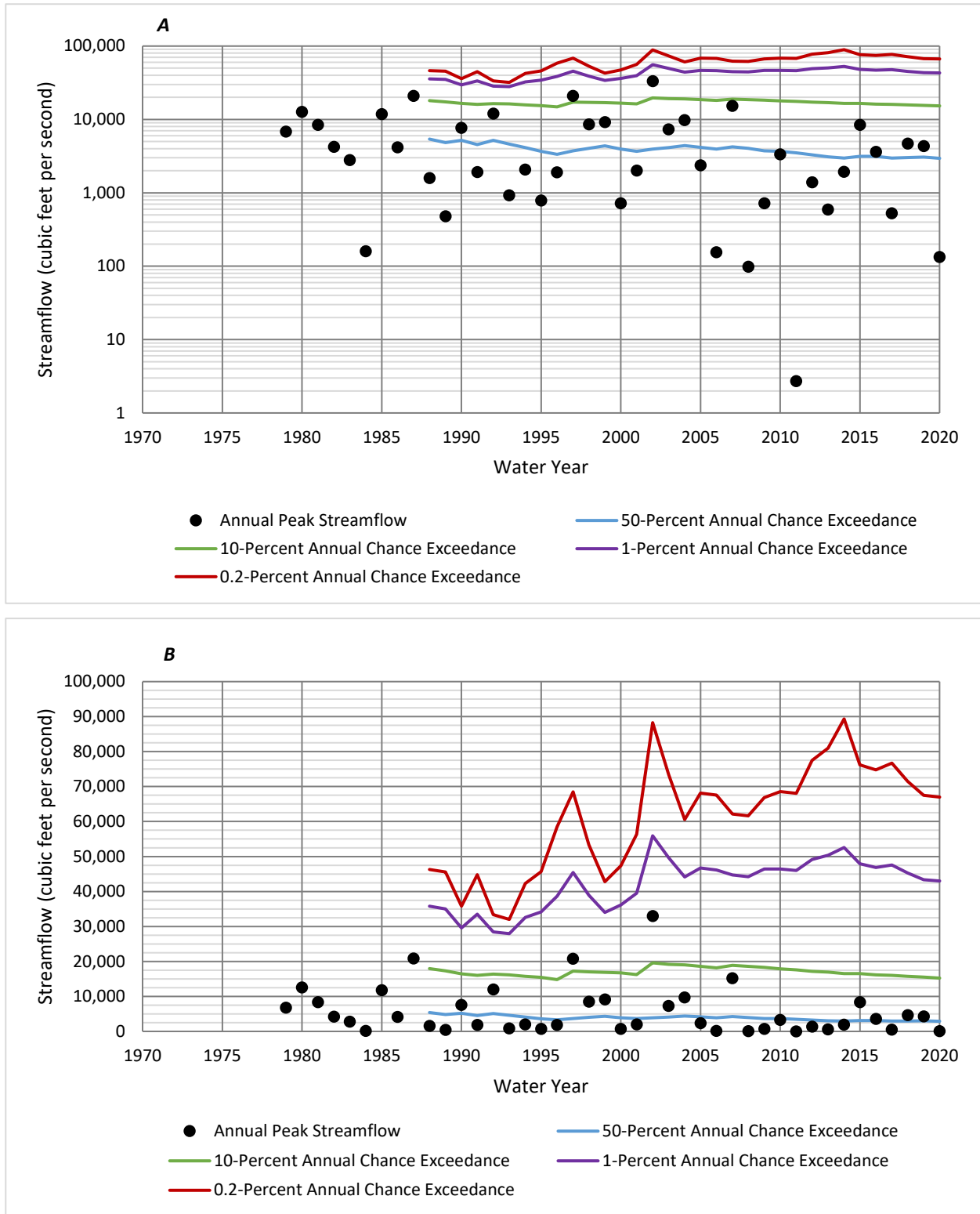


Figure 5.15: Statistical Frequency Flow Estimates versus Time in *A*, log y-axis and *B*, linear y-axis for U.S. Geological Survey Streamgage 08206600 Frio River at Tilden, Texas.

**08198500 Sabinal River at Sabinal, Tex.**

The relative effects of record length and magnitudes of substantial floods for the Sabinal River at Sabinal streamgage are shown in Figure 5.16. After marked increases in the 1-percent and 0.2-percent annual chance exceedance events following the notable 1997 and 2002 events, all estimates appear to have stabilized, although it is difficult to determine whether they have stabilized with only 18 years of record (2003–20) since the 2002 event. The 1-percent annual chance exceedance (ACE) event decreases from 114,000 cfs in 2010 to 105,000 cfs in 2020. During the same time span, the 10-percent annual chance exceedance estimate decreases from 37,400 cfs to 33,200 cfs.

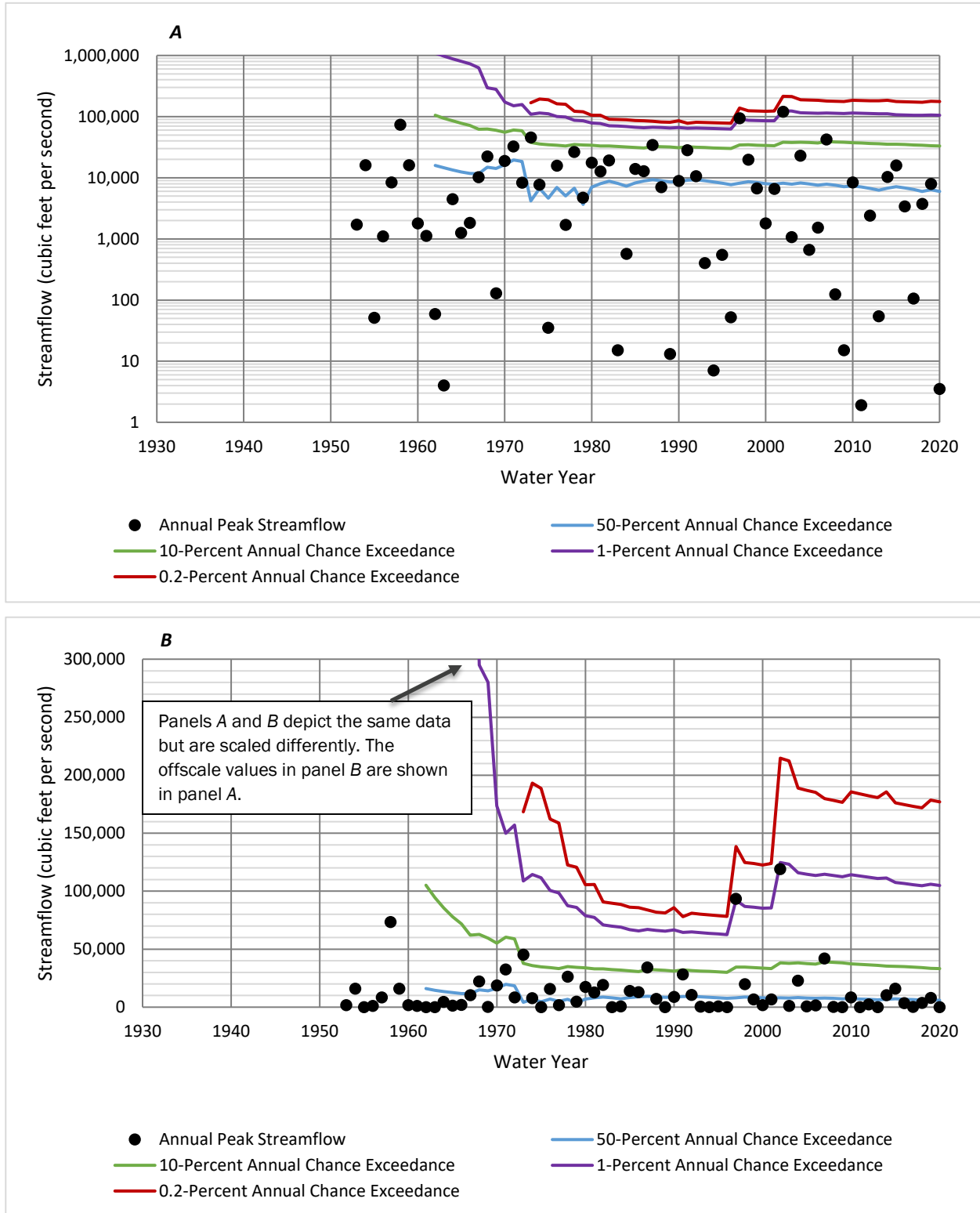


Figure 5.16: Statistical Frequency Flow Estimates versus Time in A, log y-axis and B, linear y-axis for U.S. Geological Survey Streamgage 08198500 Sabinal River at Sabinal, Texas.

## 6 Rainfall-Runoff Modeling in HEC-HMS

Rainfall-runoff watershed modeling is used to simulate the physical processes that occur during storm events that move water across the land surface and through the streams and rivers. While the statistical analyses of the gage records from the previous chapter are a valuable means of estimating the magnitude of flood frequency flows at the gages, watershed rainfall-runoff modeling is often used to estimate the rare frequency events whose return periods exceed the gaged period of record as well as to account for non-stationary watershed conditions such as urban development, reservoir storage and regulation, and climate variability. Rainfall-runoff modeling also provides a means of estimating flood frequency flows at other locations throughout the watershed that do not coincide with a stream flow gage.

In this phase of the multi-layered hydrologic analysis, a rainfall-runoff model was developed for the Nueces River Basin with input parameters that represented the physical characteristics of the watershed. The rainfall-runoff model for the basin was completed using the basin-wide Hydrologic Engineering Center – Hydrologic Modeling System (HEC-HMS) model developed for USACE’s 2020 Nueces River Basin Corps Water Management System (CWMS) Implementation as a starting point (USACE, 2020). This model was further refined by adding additional detailed data, updating the land use, and calibrating the model to multiple recent flood events. Through calibration, the updated HEC-HMS model was verified to accurately reproduce the response of the watershed to multiple recent observed storm events, including those similar in magnitude to a 1% annual chance (100-yr) storm. Finally, frequency storms were built using the depth area analysis in HEC-HMS and the latest published frequency rainfall depths from National Oceanic and Atmospheric Administration (NOAA) Atlas 14 (NOAA, 2018). These frequency storms were run through the calibrated model, yielding consistent estimates of the 1% annual chance (100-yr) and other frequency peak flows at various locations throughout the basin.

This chapter provides a general summary of the model development, calibration and results of the HEC-HMS rainfall runoff modeling that was completed for the InFRM Watershed Hydrology Assessment of the Nueces River Basin, but additional details on the development and application of the HEC-HMS model are available in Appendix B: HEC-HMS Model Development and Uniform Rainfall Frequency Results. In addition to the uniform rainfall frequency storm results presented in this chapter, the InFRM team also developed elliptical frequency storms for stream reaches with drainage areas greater than 400 square miles in the Nueces River Basin. The results from the elliptical frequency storms in HEC-HMS are presented in Chapter 7 of this report and in Appendix C: Elliptical Frequency Storms in HEC-HMS.

### 6.1 EXISTING HEC-HMS MODELS

The existing HEC-HMS model from the Nueces CWMS Implementation was used as the starting point for the current study. The CWMS model contained 100 subbasins in the Nueces River Basin with an average size of 165 square miles. The watershed drains into the Gulf of Mexico in Corpus Christi, Texas and totals approximately 16,675 square miles. The subbasins were delineated using the HEC-GeoHMS program and utilized terrain data in the form of a Digital Elevation Model (DEM) with a 15-meter grid cell size. The 15-meter DEM was derived from a combination of 10-meter seamless USGS National Elevation Data (NED) and limited high resolution LiDAR data where available. The vertical elevation units of the DEM was converted from meters to feet and the projection was converted to the standard USACE CWMS projection of Albers equal area.

The Nueces CWMS HEC-HMS model used the following methods:

- Losses – Deficit and Constant

- Transform – ModClark
- Baseflow – Recession
- Routing – Modified Puls and Muskingum
- Computation Interval – 60 minutes

A map of the Nueces CWMS subbasins is shown in Figure 6.1. More information on the CWMS model development is given in the final CWMS implementation report for the Nueces River Basin (USACE, 2020).

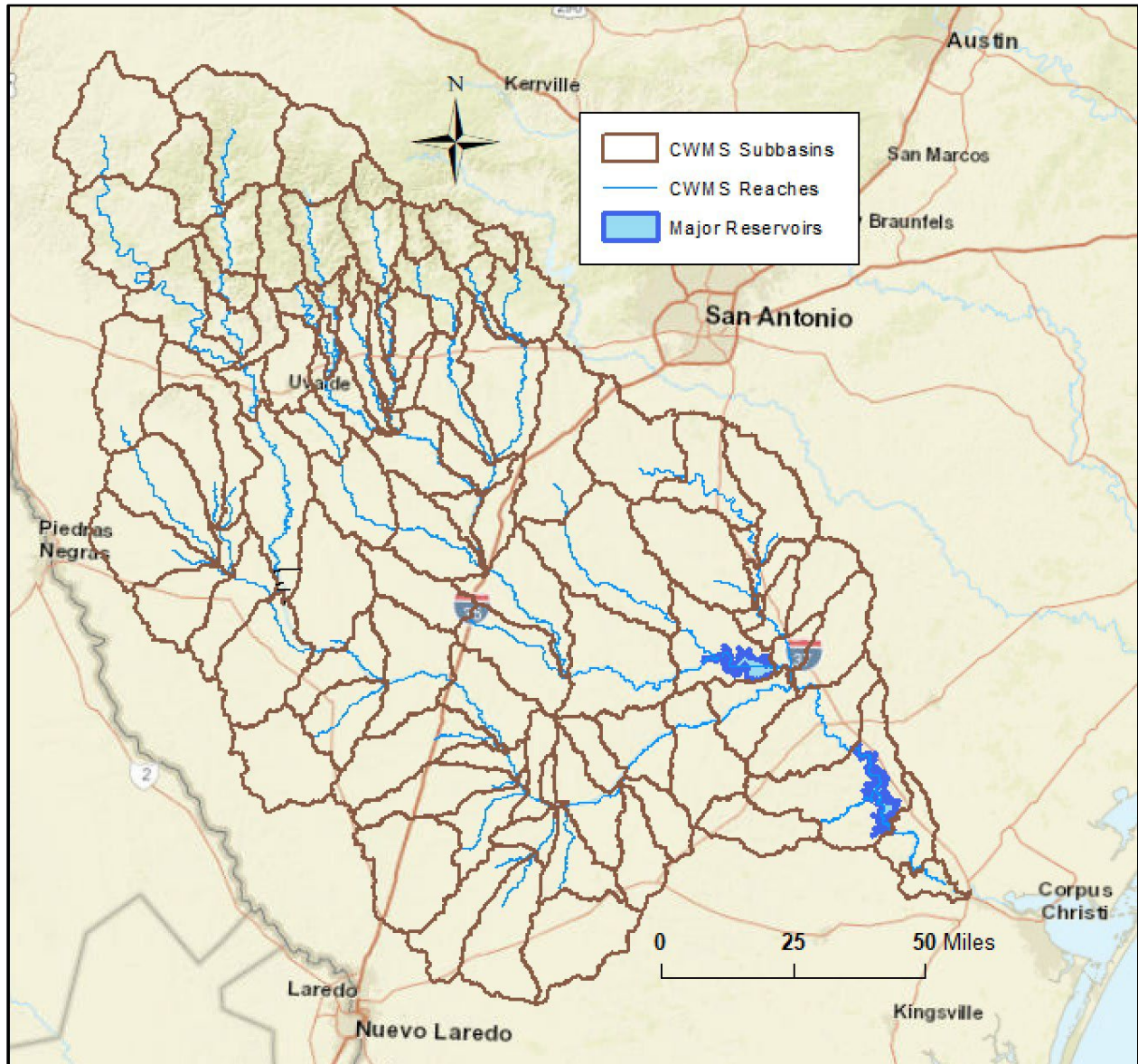


Figure 6.1: Existing CWMS Subbasins for the Nueces River Basin

## 6.2 UPDATES TO THE HEC-HMS MODEL

To better define the hydrology of the Nueces River Basin, additional subbasin breaks were added to the original CWMS delineation in order to have better definition of the flow change locations. The number of subbasins in the basin was increased from 100 to 199, with break points primarily at major tributaries, major roads and stream gages. Figure 6.2 shows the final HEC-HMS subbasin delineation for the InFRM Watershed Hydrology Assessment for the Nueces River basin. The subbasin sizes in the final HEC-HMS model varied from 2 to 282 square miles, with a mean subbasin size of 84 square miles.

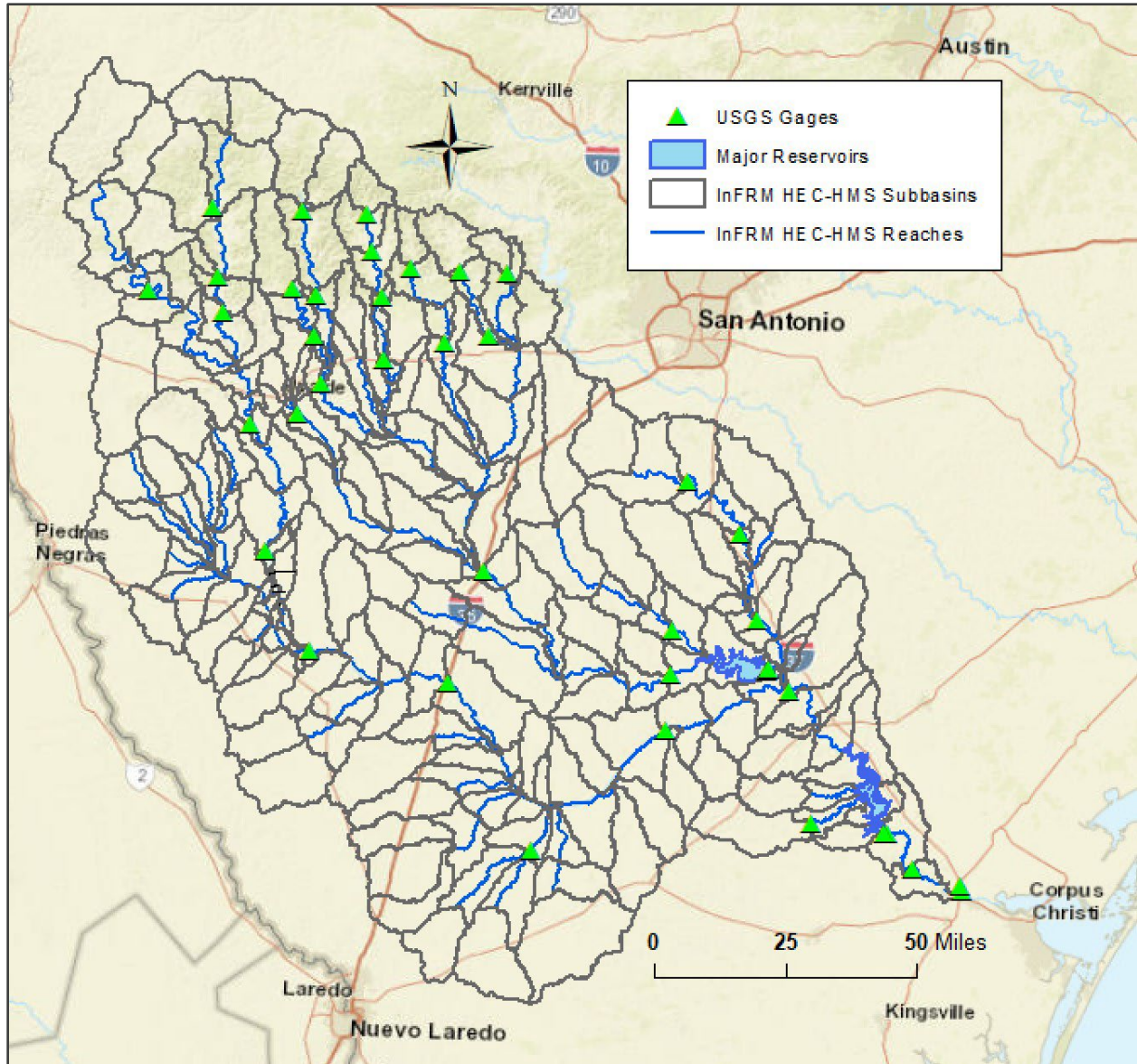


Figure 6.2: Final InFRM HEC-HMS Subbasins for the Nueces River Basin

After breaking out the additional subbasins, detailed routing data was added to the HEC-HMS model for the associated new river reaches. New detailed Modified Puls routing data was developed for portions of the basin using high resolution LiDAR elevation data and FEMA's Base Level Engineering (BLE) data, where available. The Modified-Puls routing method calculates the change in flow through the reach based

on the volume of floodplain storage through that reach. For the additional river reaches, the new detailed Modified Puls routing data was used to replace the existing Muskingum routing data.

During the CWMS implementation, the CWMS team noted that they were unable to correctly delineate or calibrate a split flow area on the Nueces River near Crystal City, Texas. In this area, the Nueces River at Crystal City splits into two rivers: the Nueces River and Espantosa Slough. Espantosa Slough merges with Turkey Creek to form Soldier Slough. Soldier Slough reconnects with the Nueces River approximately 20 miles downstream near Asherton, Texas. In addition, there are several small irrigation dams and irrigation diversion channel located along these split flow reaches. Therefore, special attention was paid to this area in the development of the InFRM HEC-HMS model. First, the terrain was reconditioned during the HEC-GeoHMS process to correctly delineate both flow paths and their associated subbasins. Second, a new 2D HEC-RAS model of the split flow area was developed from the BLE LiDAR terrain data. The new 2D HEC-RAS model was used to calculate an inflow-diversion curve at the split flow location, which was input into HEC-HMS as a Diversion element, as well as to calculate the Modified Puls storage-discharge relationships along each reach of the split flow paths. The diversion and split flow reaches were then calibrated to the observed hydrographs at Asherton, as will be described in a later section of this chapter.

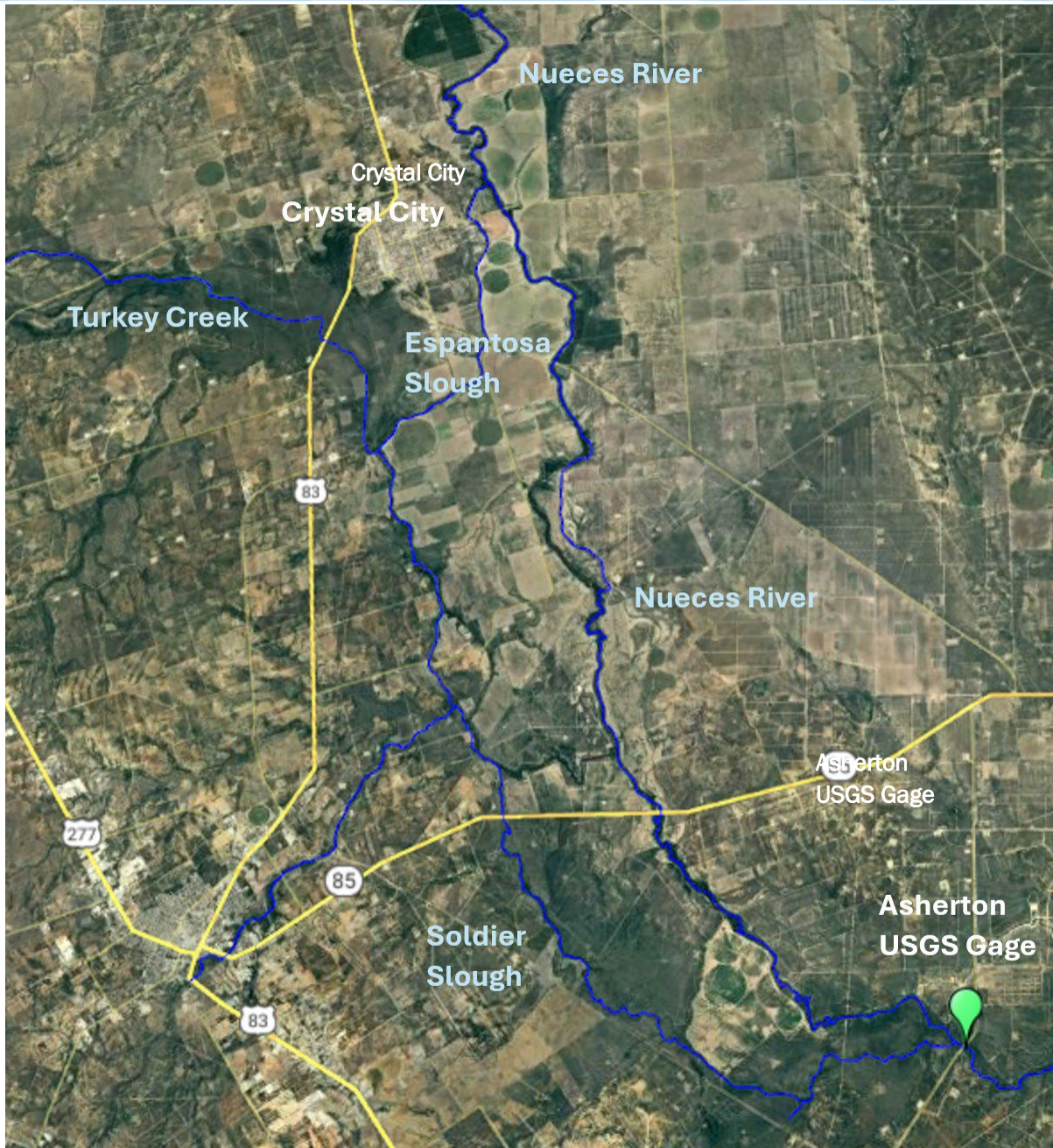
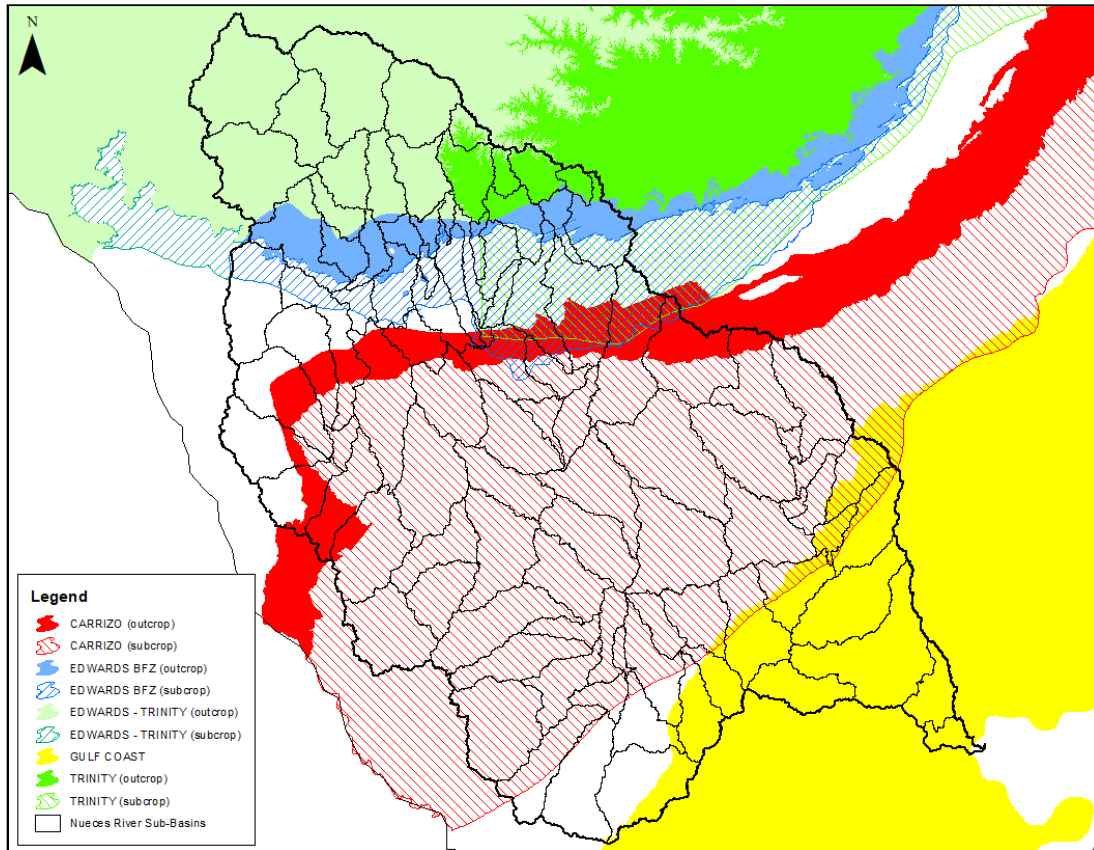


Figure 6.3: Split Flow Area on the Nueces River between Crystal City and Asherton, TX

Thirdly, the channel loss data was updated for the HEC-HMS reaches in areas where the reaches cross the aquifer outcrops and where routing losses have been observed in the USGS stream gage data. There are several major aquifers within this watershed that divert flow from surface water to groundwater. Part of the flow of the Nueces River and its headwater tributaries enters the Carrizo and Edwards aquifers and their associated limestones in the Balcones Fault Zone. After entering these aquifers, water moves slowly toward lower lying places and eventually is discharged from the aquifer from springs, seeps into streams, or is withdrawn from the ground by wells. A map of the major aquifers in the Nueces River Basin is shown in Figure 6.4. For these reaches, the constant channel loss method was applied in HEC-HMS

which diverts a constant baseflow into the ground as well as a fraction of the overall inflow hydrograph. More information on the development and calibration of these channel losses is included in Appendix B.



**Figure 6.4: Major Aquifers in the Nueces River Watershed.**

Finally, after adding all of the above detailed data, the loss method was updated from deficit constant to initial and constant, since the focus of this study is on single storm events, whereas the original CWMS model was used for multi-storm event real-time forecasting. Both of these methods have been found to adequately capture the range of observed losses experienced in Texas from extreme drought to 100% saturated soil conditions and are also simple to adjust for real-time forecasting purposes.

The computation interval of the model was also decreased from 60 to 15 minutes to show more refinement of the hydrographs on the smaller tributaries. The final Nueces HEC-HMS model was run in HEC-HMS version 4.6.1 and used the following methods:

- Losses – Initial and Constant
- Transform – Snyder
- Baseflow – Recession
- Routing – Modified Puls and Muskingum
- Computation Interval – 15 minutes

The Nueces HEC-HMS model also includes two significant reservoirs, which were modeled as reservoir elements in HEC-HMS. These reservoirs are Choke Canyon Reservoir and Lake Corpus Christi. While the National Inventory of Dams (NID) shows that over 400 small dams exist within Nueces River basin, these

two reservoirs were selected to be modeled in detail due to their sizable flood storage and their noticeable influence on discharges in the major rivers downstream.

## 6.3 HEC-HMS MODEL INITIAL PARAMETERS

### 6.3.1 Subbasin and Routing Initial Parameters

The Nueces River HEC-HMS model contains 199 subbasins totaling about 16,675 square miles on the Nueces River. The subbasins were delineated using the HEC-GeoHMS program and utilized 15-meter DEM terrain data. The Nueces River HEC-HMS model used initial and constant losses, Snyder transform, recession baseflows, and Modified Puls / Muskingum routing. The sources of the initial estimates for these parameters are described below.

- **Initial Loss and Constant Loss Rate** – For calibration, the initial and constant losses were initially set to a moderate loss of 2 inches of initial loss and the constant losses were calculated from the SSURGO soils data based on their Hydrologic Soil Group and the guidance included in the HEC\_HMS technical reference manual. The initial and constant losses were then adjusted according to the antecedent conditions of particular storm events during calibration. The calibrated initial and constant losses varied for each calibration event based on the soil moisture condition. For the frequency storms, the initial and constant loss rates were calculated based on the SSURGO soil type, according to the Fort Worth District Loss Rate equations, which vary the loss rates by frequency.
- **Percent Impervious** – The percent impervious values were developed based on the 2016 National Land Cover Database (NLCD) percent developed impervious dataset, which was the dataset that was available at the beginning of this study, and was adjusted to account for Open Water surface in the river basin.
- **Snyder's Transform Parameters** – Transform parameters were initially developed from regional equations for the Snyder's unit hydrograph method based on watershed characteristics such as length of longest flow path and stream slope that were extracted from ArcGIS. From this data, two regional equations were used to develop initial estimates of lag time for the Snyder unit hydrographs.

The regional equations that were used to develop initial estimates of lag time for the Snyder unit hydrograph was from the U.S. Army Corps of Engineers (USACE) Fort Worth District San Antonio Steep-Area (Upper Salado) and San Antonio Rolling – and Flatter-Area (Lower Salado) urban studies (Nelson, 1979) (Rodman, 1977). These equations estimate subbasin lag time based on the length and slope of the watershed, and the percent urban values taken from land cover data. The San Antonio Steep-Area equation was used for subbasins with mean percent rise in slope greater than 6 percent. The remaining subbasins used the San Antonio Rolling-and Flatter-Area equation.

The following San Antonio Steep-Area regional equation was used to calculate subbasin lag times for steep subbasins:

$$\log(T_p) = .36\log(L \cdot L_{ca}/(S^{.5})) + \log(.29) - (BW \cdot \text{PercentUrban.}/100)$$

where:  $T_p$  = Snyder's lag time (hours)

$L$  = longest flow path within the subbasin (miles)

$L_{ca}$  = distance along the stream from the subbasin centroid to outlet (miles)

S = stream slope over reach between 0% and 100% of L (feet per feet)

BW = log(tp) bandwidth between 0% and 100% urbanization = 0.30 (log hours)

Urban. = percentage urbanization factor

The following San Antonio Rolling-and Flatter-Area regional equation was used to calculate subbasin lag times for flatter subbasins:

$$\log(T_p) = .367\log(L * L_{ca} / (S^{.5})) + \log(.51) - (BW * \text{PercentUrban.} / 100)$$

where:  $T_p$  = Snyder's lag time (hours)

L = longest flow path within the subbasin (miles)

$L_{ca}$  = distance along the stream from the subbasin centroid to outlet (miles)

S = stream slope over reach between 0% and 100% of L (feet per feet)

BW = log(tp) bandwidth between 0% and 100% urbanization = 0.32 (log hours)

Urban. = percentage urbanization factor

The Snyder's peaking coefficients for steep subbasins were set to a value of 0.86 for subbasins with mean percent rise in slope greater than 15 percent and a value of 0.78 for subbasins with mean percent rise in slope greater than 6 percent but less than 15 percent. The Snyder's peaking coefficients for flatter subbasins were set to a value of 0.70 for subbasins with mean percent rise in slope less than 6 percent.

- Baseflow Parameters** – Initial baseflow parameters were taken from the existing USACE Nueces CWMS HEC-HMS model. For the entire watershed, the recession baseflows were set at 0.1 cfs/square mile of initial baseflow, 0.7 for the recession constant, and 0.1 for the ratio to peak. These values were later adjusted during calibration.
- Routing Parameters (Modified Puls)** – Storage-discharge curves for the Modified Puls routing were extracted from new or existing 1D and 2D hydraulic routing models in HEC-RAS, which were developed from the available LiDAR data. The existing 1D HEC-RAS models that were available for the basin included the CWMS HEC-RAS model and FEMA's BLE HEC-RAS models. New 2D HEC-RAS models were also developed from the LiDAR data for key locations in watershed, including the split flow area above Asherton and the reaches of the Nueces and Frio Rivers where the stream reaches suddenly transition from steep hilly reaches to wide irrigated floodplains. Initial subreach values were estimated based on the reach length and an average travel time through the reach.
- Routing Parameters (Muskingum)** – Muskingum routing parameters were calculated from basin geometry and adjusted to fall within the feasible region, prescribed by the HEC-HMS Technical Reference Manual. Muskingum K was estimated, as recommended by EM 1110-2-1417, by dividing the flood wave velocity from the length of the reach. The flood wave velocity was estimated to be 1.5 times the average velocity, which was 1 mph for the entire basin. Muskingum X values range between 0.0 and 0.5 and was estimated to be equivalent to the slope. Number of subreaches was initially set to equal the Muskingum K in hours. Parameters were adjusted during calibration to best represent attenuation while remaining in a feasible range of values.

The initial subbasin and routing parameters that were entered into the HEC-HMS model can be seen in Tables B.1 through B.4 of Appendix B. Some of these parameters were adjusted during calibration.

### 6.3.2 Initial Reservoir Data

According to the National Inventory of Dams (NID), over 400 dams exist within Nueces River basin, most of which are NRCS structures, irrigation dams, or other small dams. Of these, reservoir elements were used in the HEC-HMS rainfall-runoff model for two reservoirs in the Nueces basin. These dams were selected to be modeled in detail due to their sizable flood storage and their noticeable influence on discharges in the major rivers downstream. Table 6.1 summarizes the reservoir data obtained for these dams and their corresponding data sources, and Figure 6.5 illustrates their locations within the basin.

The two modeled reservoirs, Choke Canyon Dam and Lake Corpus Christi, were included in the model. The dams were modeled as reservoir elements in HEC-HMS.

The elevation-storage and elevation-discharge curves for Choke Canyon Dam were taken from the CWMS model. Both curves were based on data provided by the Bureau of Reclamation (USBR) to 233.0 ft. Values were estimated above 233.0 ft. The curve input in HEC-HMS is in vertical datum NAVD88.

The elevation-storage and elevation-discharge curves for Lake Corpus Christi were taken from the CWMS model. The storage-elevation curve data was derived from the Texas Water Development Board (TWDB) survey from 2016.

The smaller dams were scattered throughout the rural areas of the basin. These dams were not modeled in detail but were accounted for in the model through adjustments to the subbasins' initial losses, peaking coefficients, and routing data. These adjustments were made through the model calibration process. Data for these dams was obtained from the National Inventory of Dams (USACE, 2016). Please see section 6.4 for more information.

**Table 6.1: Reservoir Data and Sources for Dams Modeled in HEC-HMS**

Reservoir Name	Data	Source(s)
Choke Canyon	Elevation-Storage, Elevation-Discharge rating	Bureau of Reclamation (USBR)
Lake Corpus Christi	Elevation-Storage, Elevation-Discharge rating	Texas Water Development Board (TWDB)

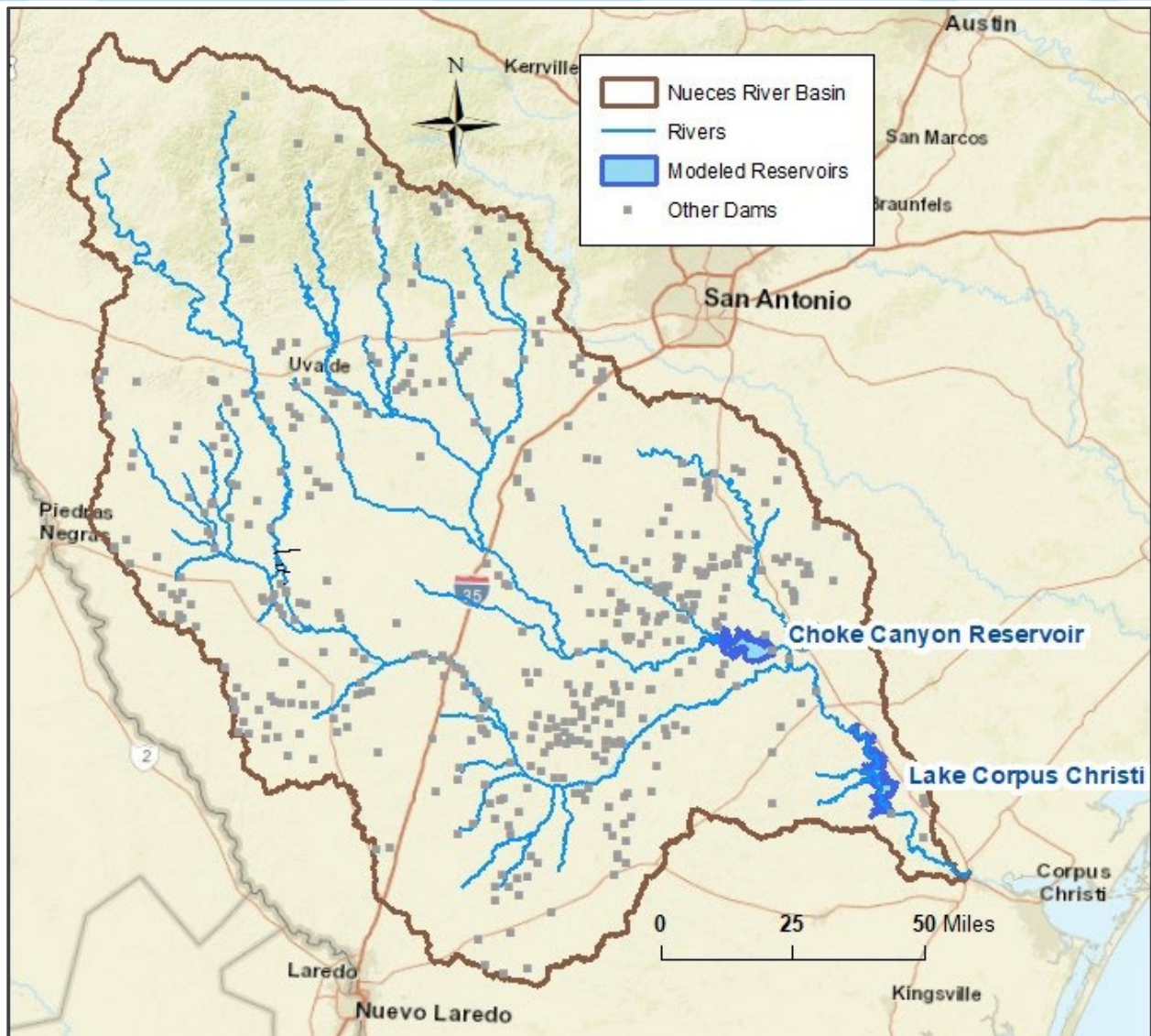


Figure 6.5: Locations of Reservoirs Modeled in HEC-HMS

## 6.4 HEC-HMS MODEL CALIBRATION

After building the more detailed HEC-HMS model with its initial parameters, the model was calibrated to ensure that it would accurately simulate the response of the watershed to a range of observed flood events, including large events similar to a 1% annual chance (100-yr) flood. The goal of calibration is to accurately simulate the response of the watershed to a given storm by reproducing the timing, shape, and magnitudes of the observed flows at the stream gages. A total of sixteen recent storm events were used throughout different parts of the watershed to calibrate the model. For these storms, the National Weather Service (NWS) hourly rainfall radar data allowed the team to fine tune the rainfall runoff model through detailed calibration. This radar rainfall data is a gridded product with a spatial resolution of approximately 4 km x 4 km cell sizes, and the rainfall depths are calibrated by the NWS to on-the-ground observations at rainfall gages. Prior to the late 1990s, the NWS radar data was not available for use during earlier modeling efforts. The model calibration and verification process undertaken during this study exceeds the standards of a typical FEMA floodplain study.

## 6.4.1 Calibration Storms

Table 6.2 lists the storms that were used to calibrate the Nueces HEC-HMS model, and Figure 6.6 through Figure 6.21 illustrate the total depth of rain for the major calibration storms and how that rain was distributed spatially throughout the Nueces River watershed. These plots were extracted from the HEC-MetVue meteorological program for visualizing and processing rainfall data. These storms were selected as the largest available storms during the time that NWS radar data was available. Since the rain fell on different parts of the basin from one historic storm event to another, the calibration of each storm was focused on those areas of the basin that received the greatest and most intense rainfall. Calibration was also only performed when the USGS stream gages were recording and experienced a significant peak flow for that event. Table 6.3 shows which storms were calibrated for each USGS stream and reservoir gage location.

**Table 6.2: Storm Events Used for Model Calibration**

Historic Storm Event	Simulation Period
Oct 1996	October 27 - November 9
Jun 1997	June 20 - July 6
Aug 1998	August 20 - September 2
Nov 2001	November 13 - November 21
Jul 2002	June 29 - July 13
Sep 2002 TS Fay	September 6 - September 29
Jun 2007	June 19 - July 19
Jul 2007 (short)	July 17 - July 23
Jul 2007 (late)	July 23 - August 5
Jul 2007 (long)	July 17 - August 12
May 2015 middle	May 11 - May 22
May 2015	May 20 - May 27
Sep 2016	September 24 - October 9
Oct 2018 (early)	October 7 - October 13
Oct 2018 middle	October 14 - October 20
Oct 2018 entire	October 7 - November 24

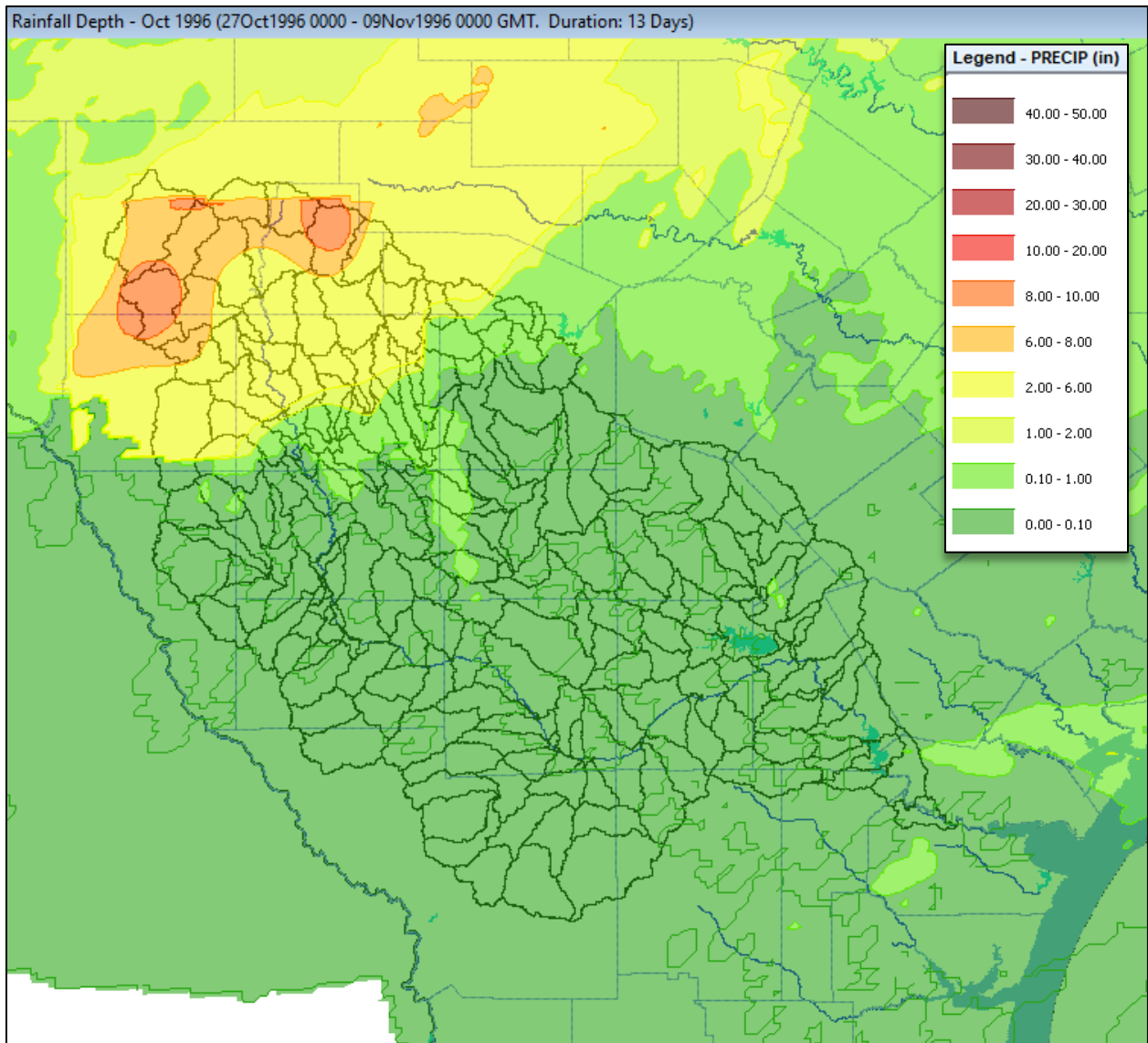


Figure 6.6: Total Rainfall Depths (inches) for the October 1996 Calibration Storm

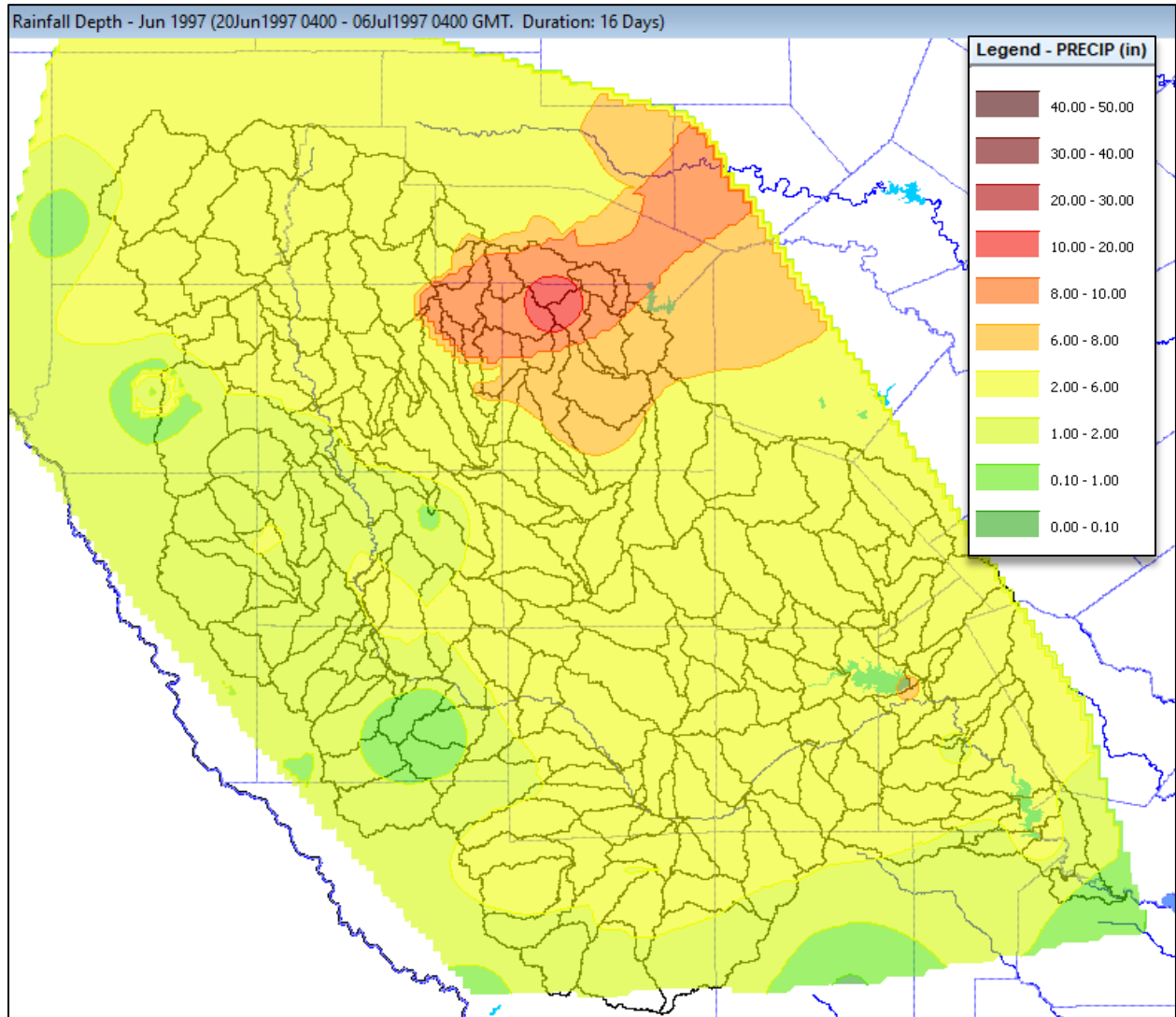


Figure 6.7: Total Rainfall Depths (inches) for the June 1997 Calibration Storm

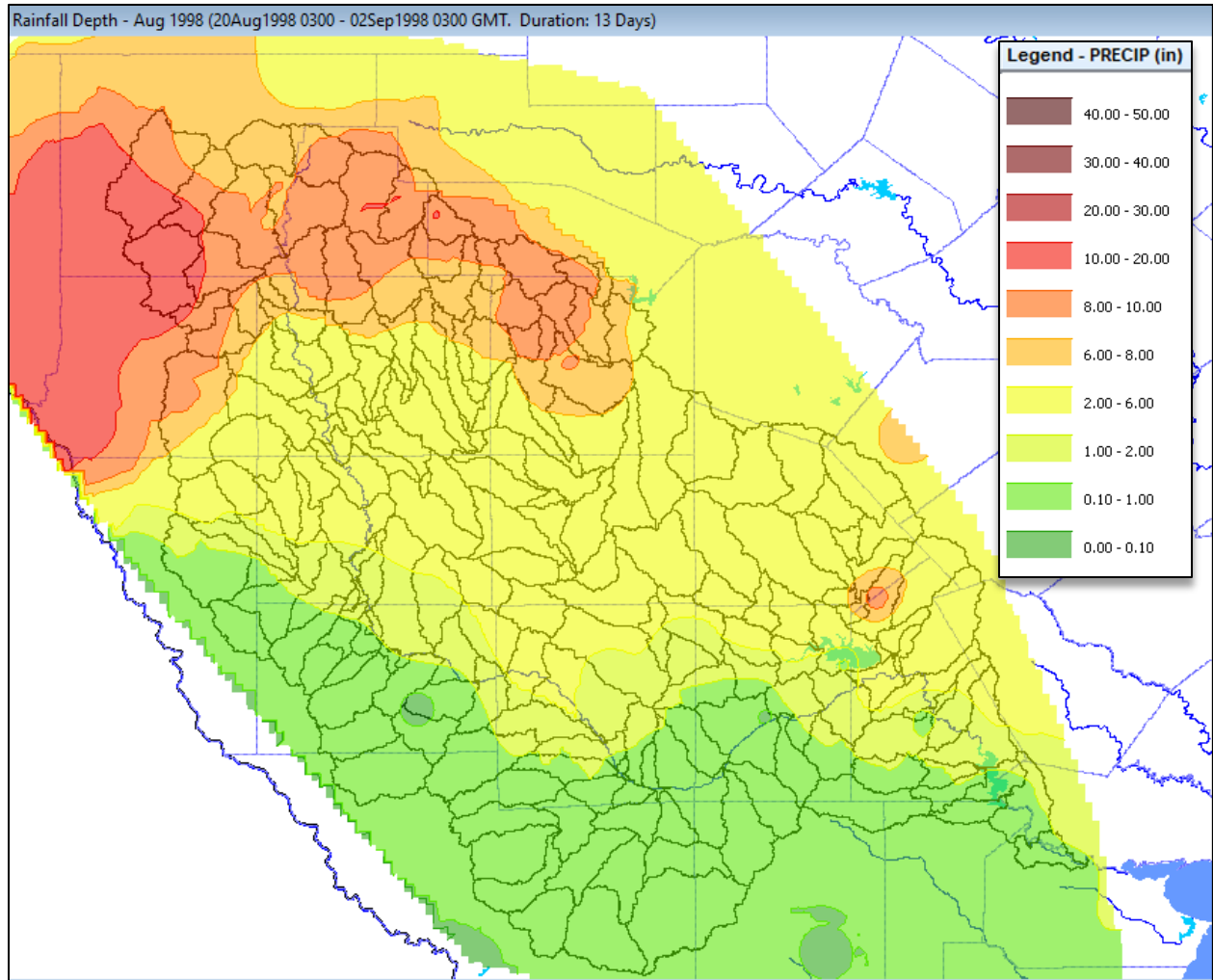


Figure 6.8: Total Rainfall Depths (inches) for the August 1998 Calibration Storm

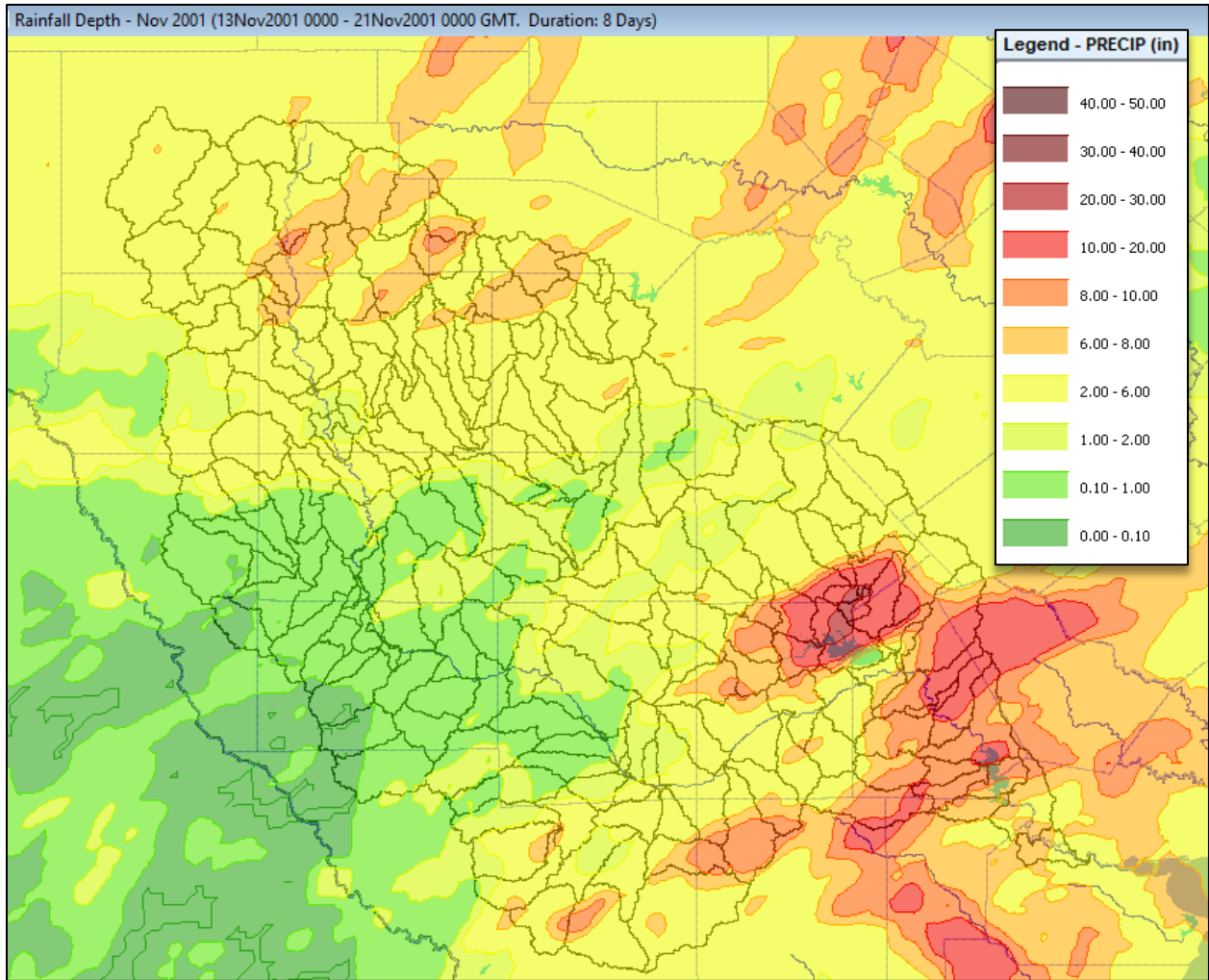


Figure 6.9: Total Rainfall Depths (inches) for the November 2001 Calibration Storm

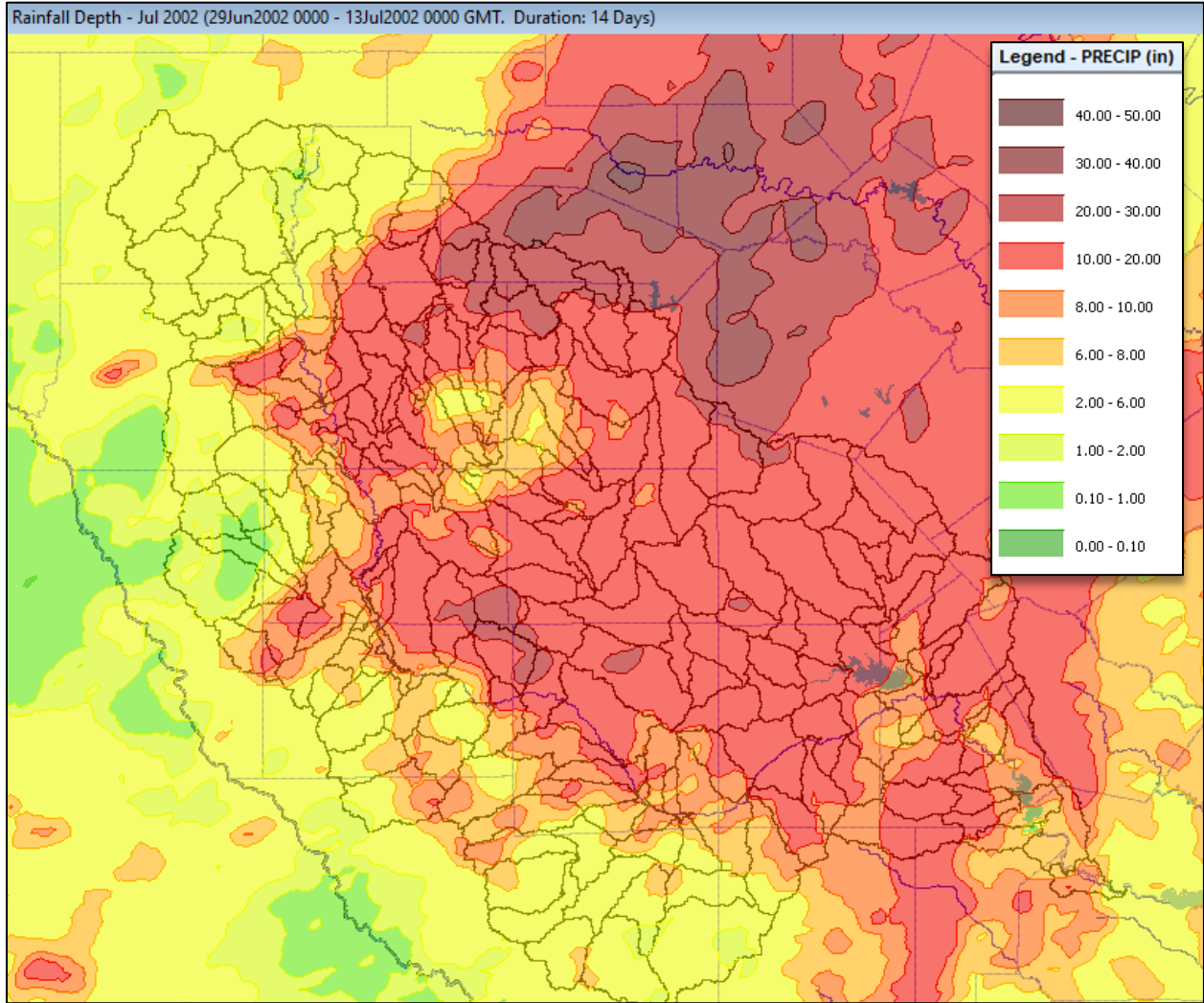


Figure 6.10: Total Rainfall Depths (inches) for the July 2002 Calibration Storm

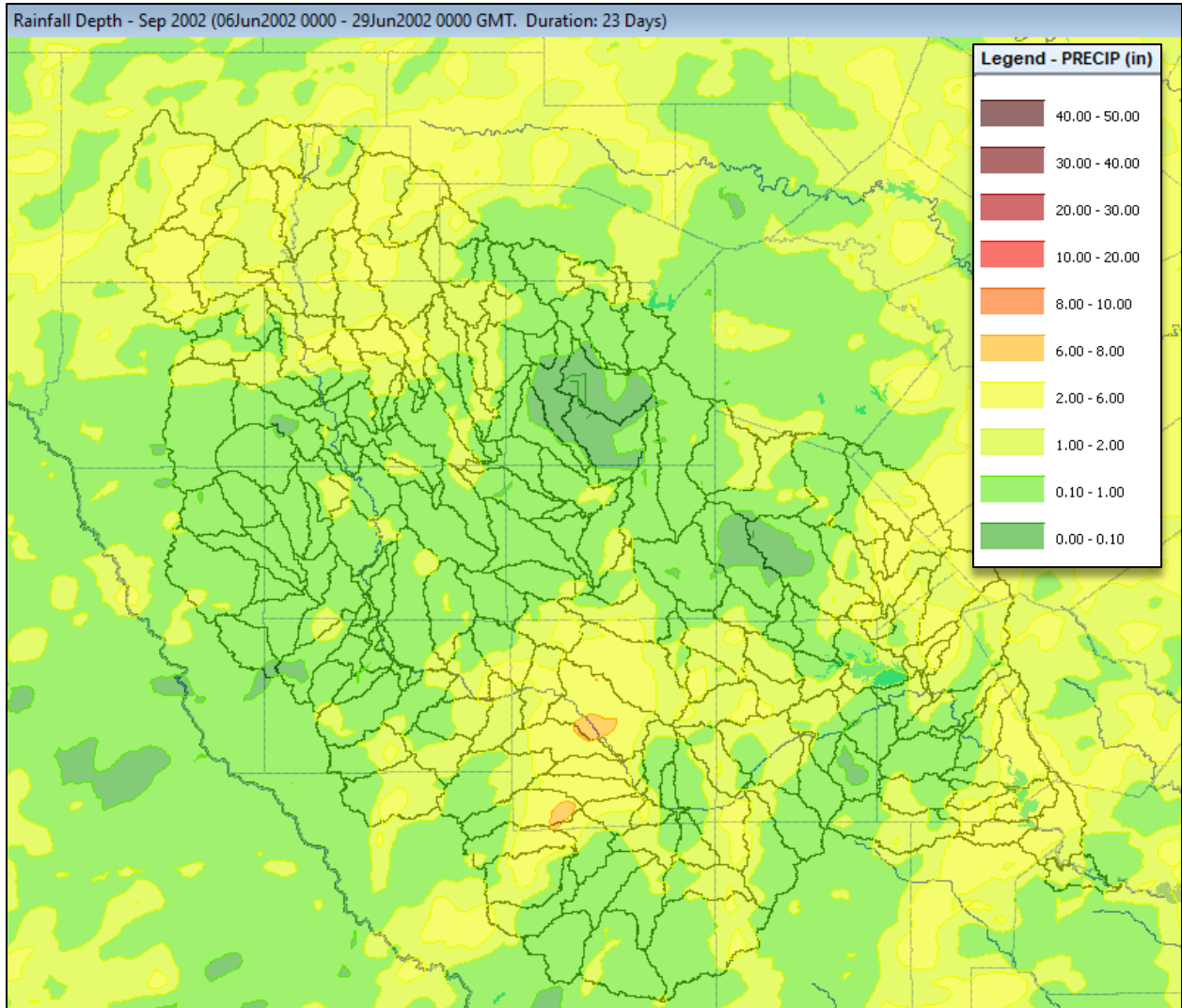


Figure 6.11: Total Rainfall Depths (inches) for the September 2002 TS Fay Calibration Storm

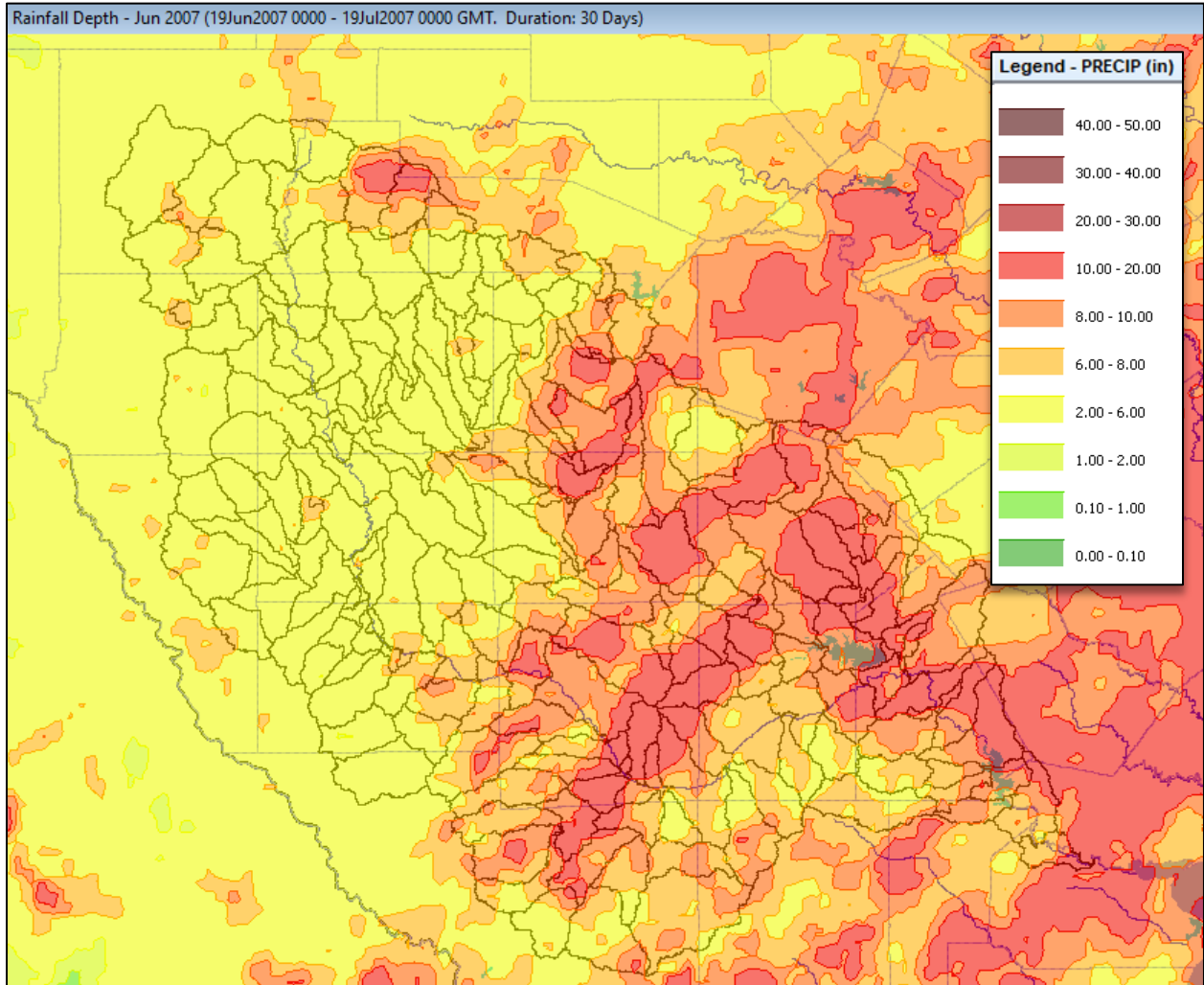


Figure 6.12: Total Rainfall Depths (inches) for the June 2007 Calibration Storm

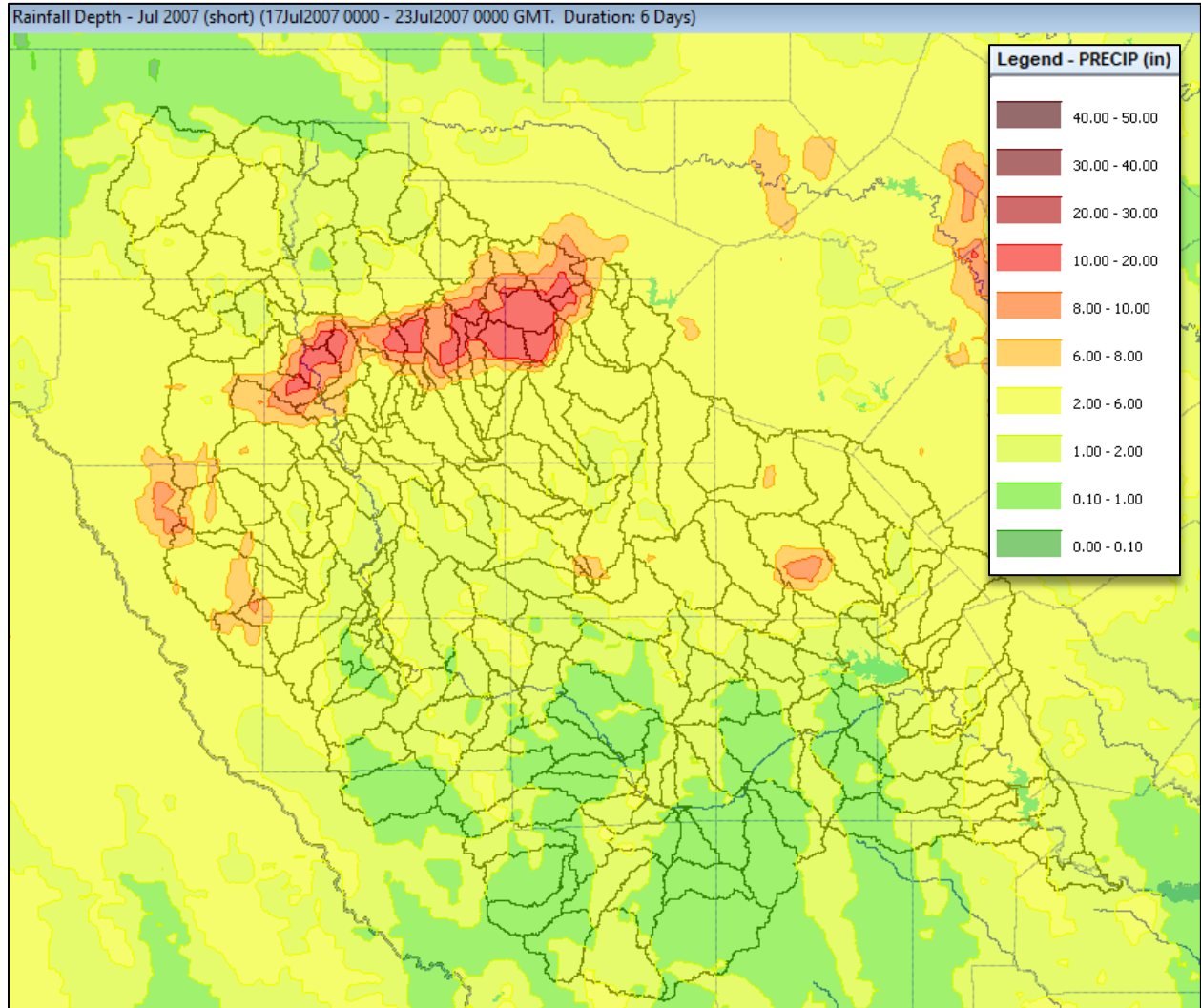


Figure 6.13: Total Rainfall Depths (inches) for the July 2007 (short) Calibration Storm

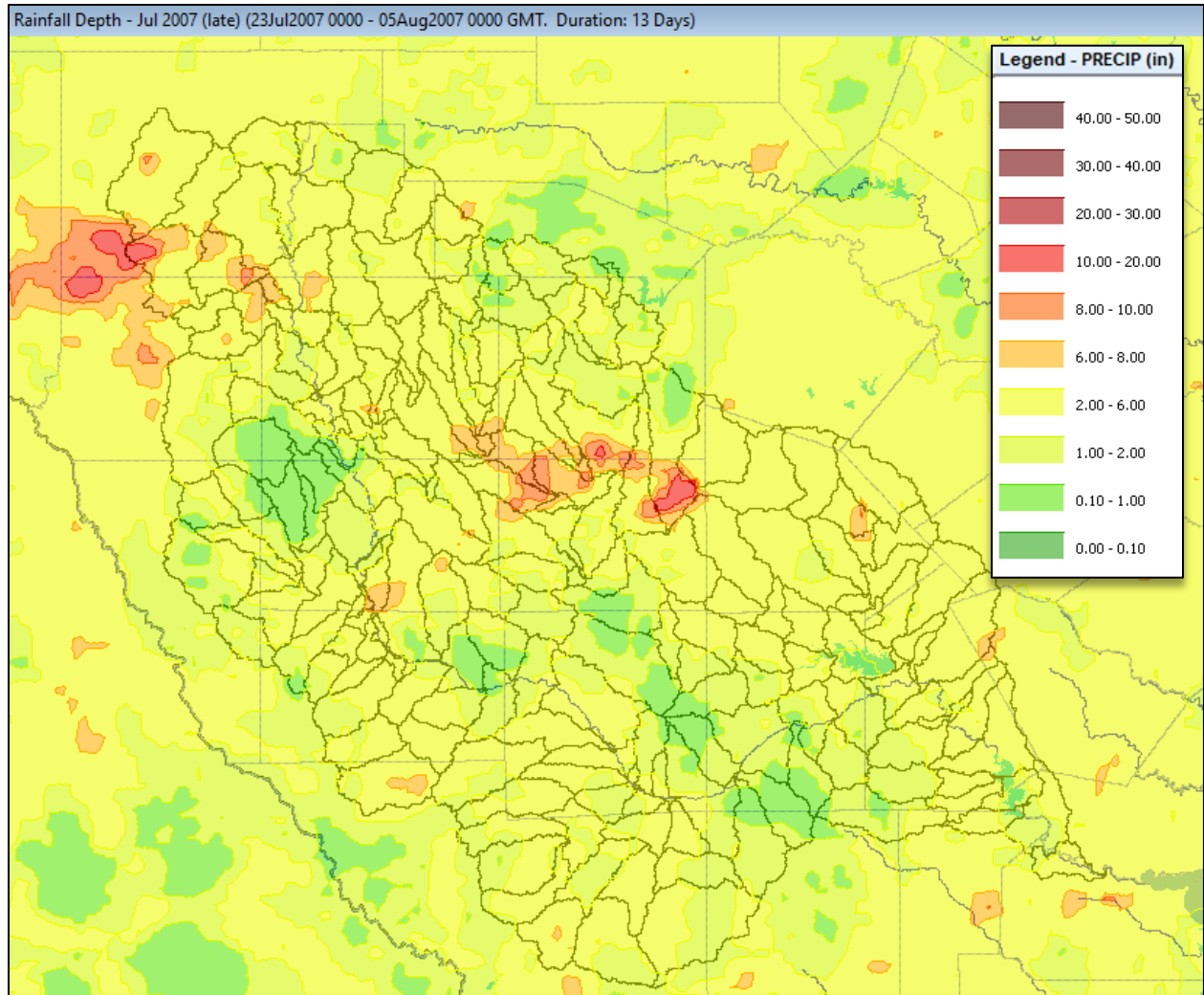


Figure 6.14: Total Rainfall Depths (inches) for the July 2007 (late) Calibration Storm

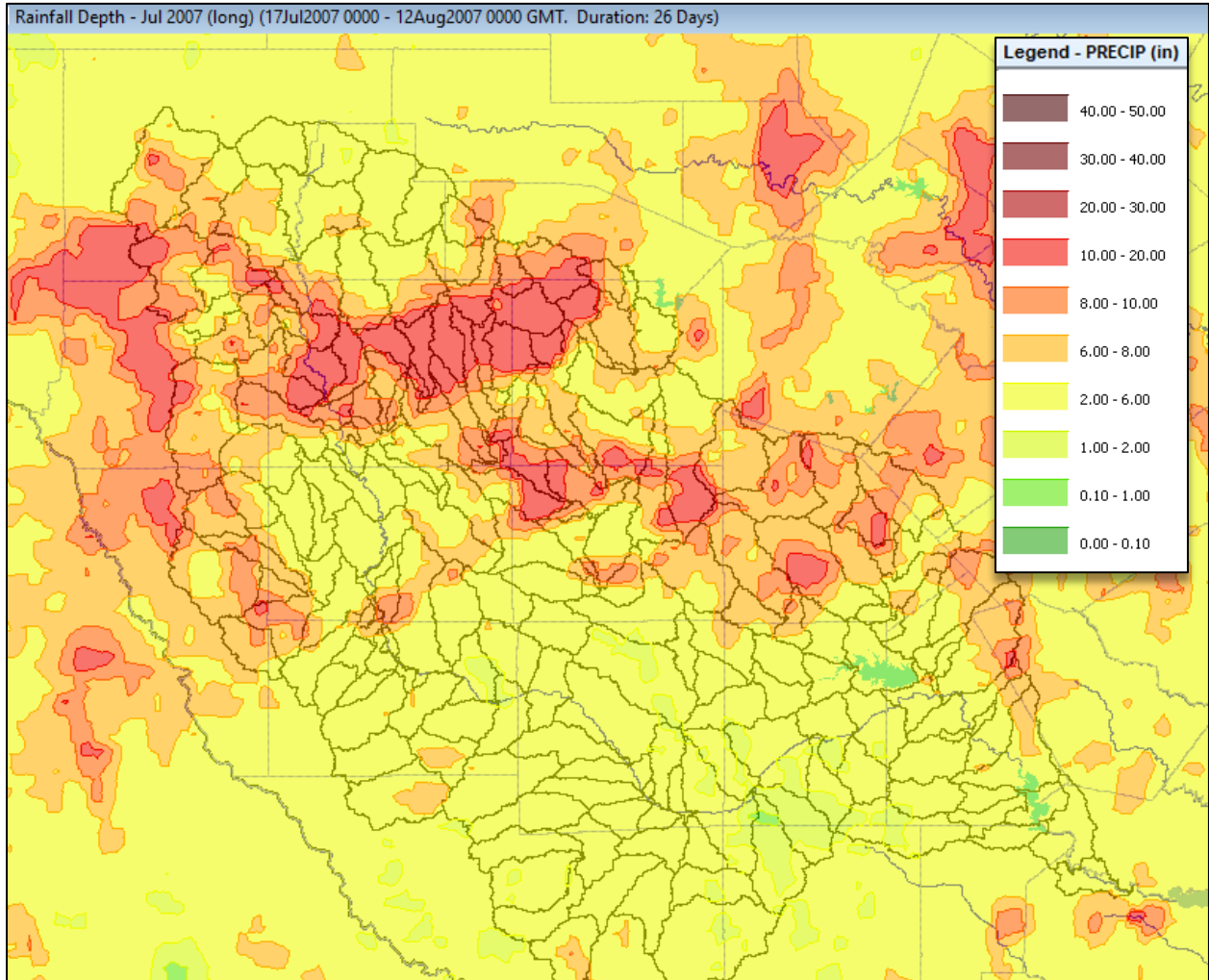


Figure 6.15: Total Rainfall Depths (inches) for the July 2007 (long) Calibration Storm

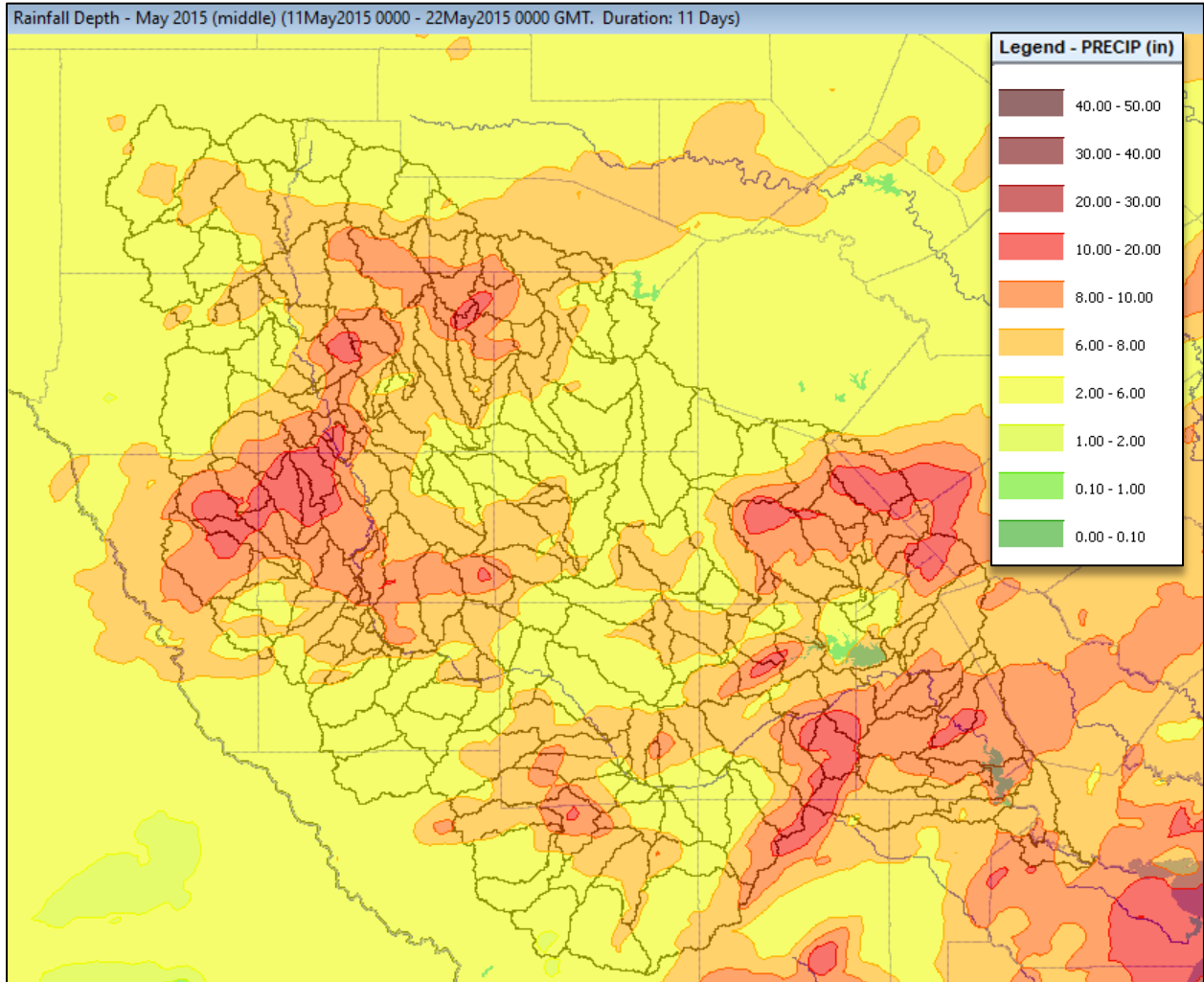


Figure 6.16: Total Rainfall Depths (inches) for the May 2015 middle Calibration Storm

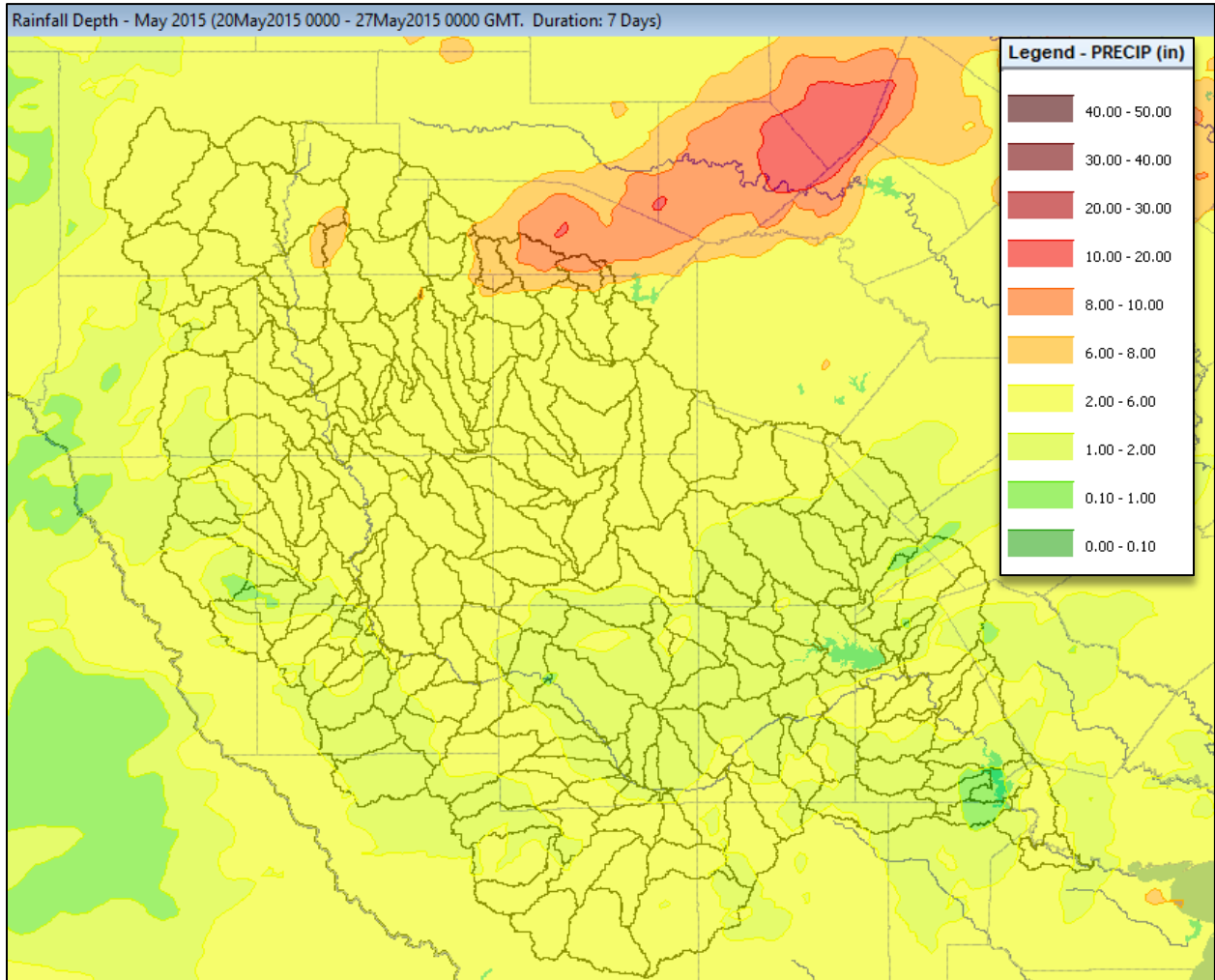


Figure 6.17: Total Rainfall Depths (inches) for the May 2015 Calibration Storm

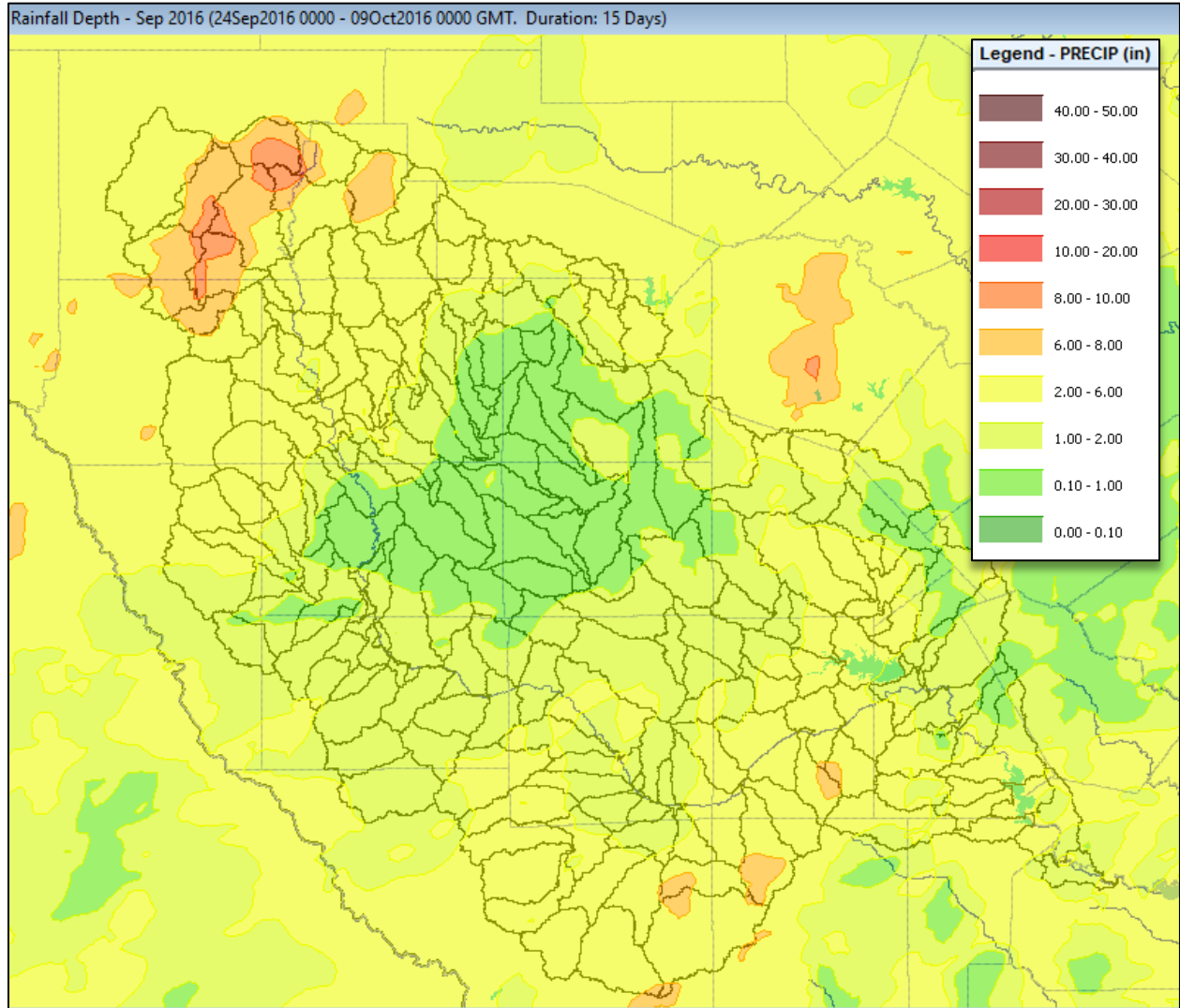


Figure 6.18: Total Rainfall Depths (inches) for the September 2016 Calibration Storm

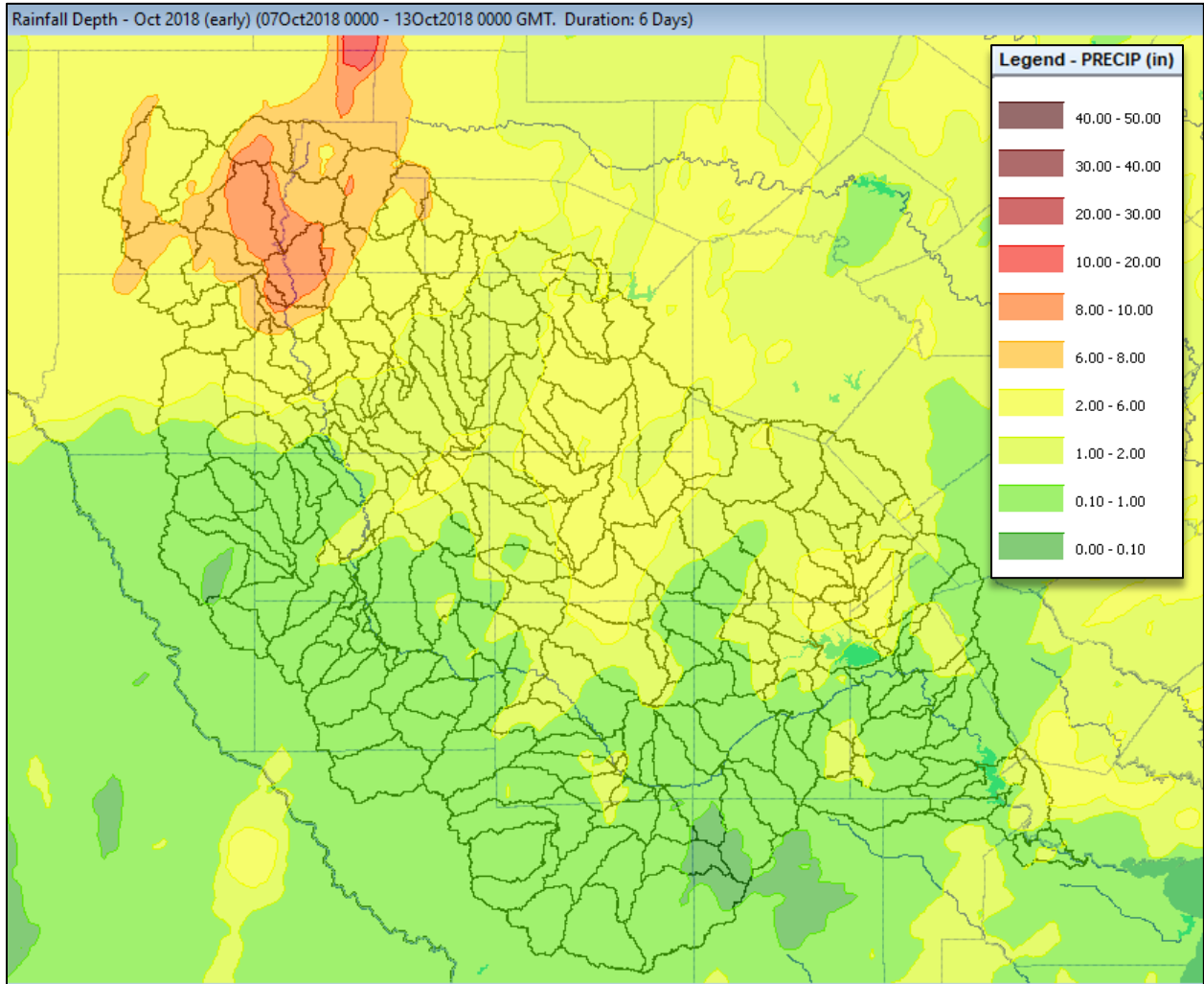


Figure 6.19: Total Rainfall Depths (inches) for the October 2018 (early) Calibration Storm

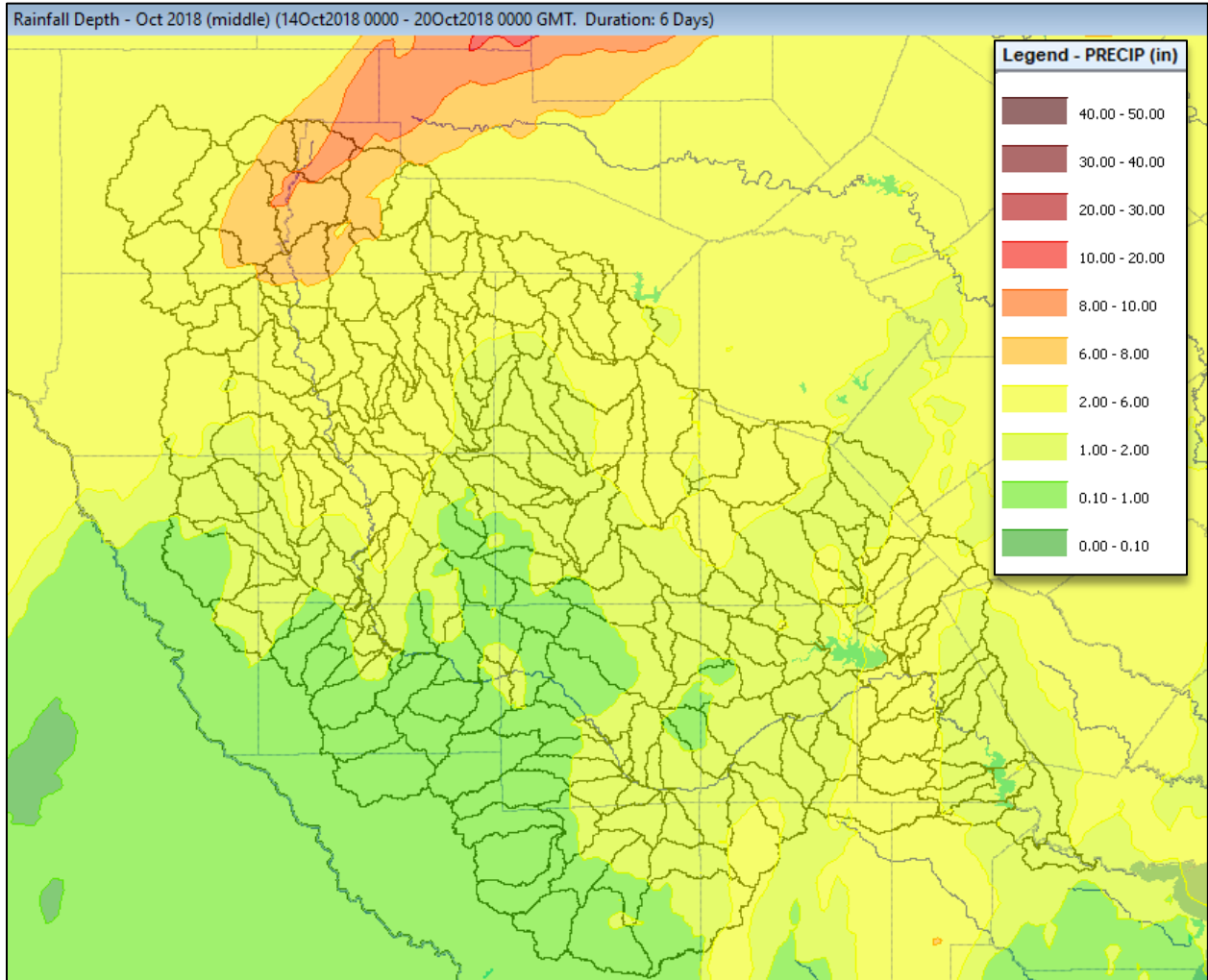


Figure 6.20: Total Rainfall Depths (inches) for the October 2018 middle Calibration Storm

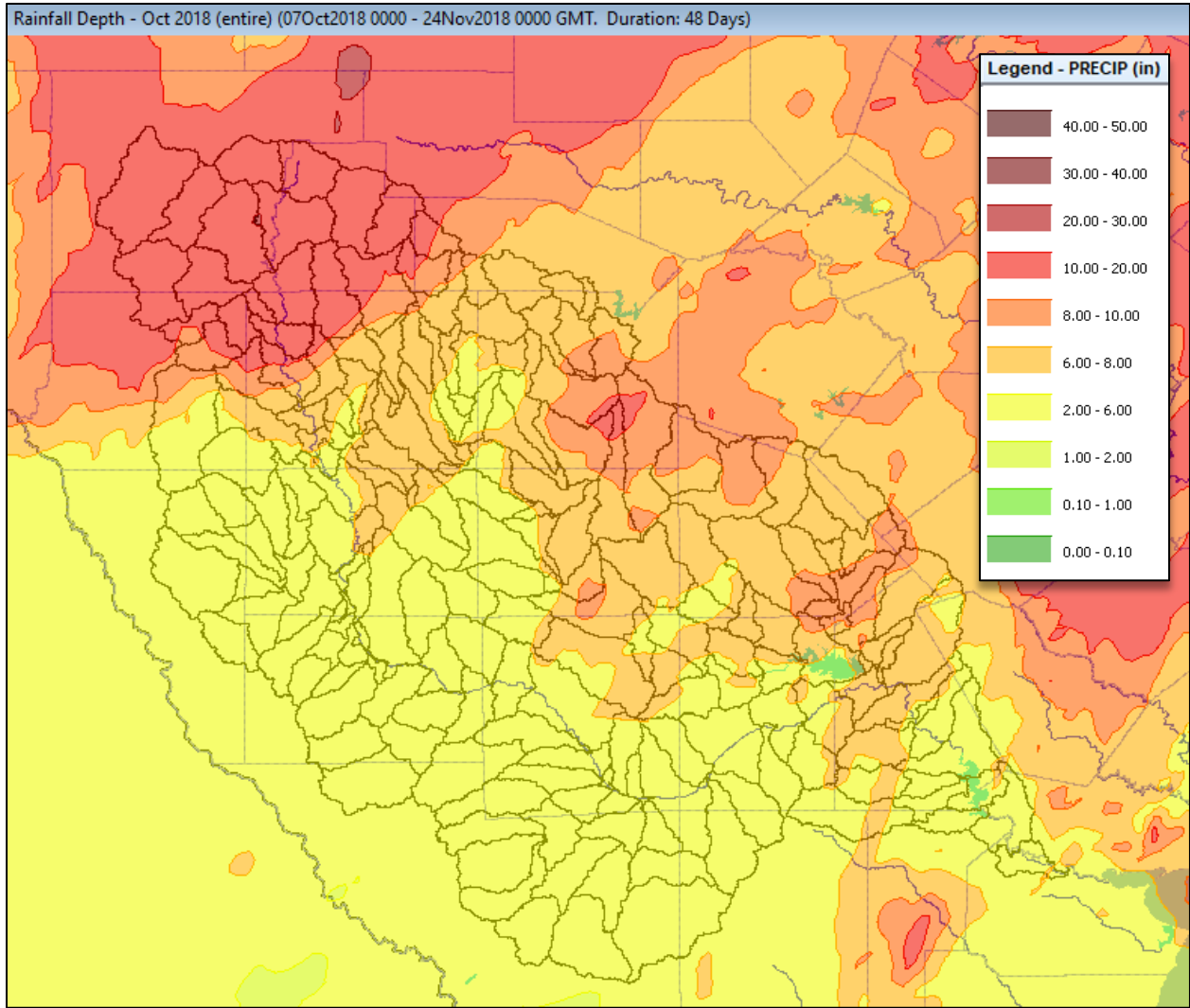


Figure 6.21: Total Rainfall Depths (inches) for the October 2018 entire Calibration Storm

Table 6.3 Calibrated Storm Events for Specific Gage Locations

USGS Gage Location	Oct 1996	Jun 1997	Aug 1998	Nov 2001	Jul 2002	Sep 2002 TS Fay	Jun 2007	Jul 2007 Short
Nueces Rv at Laguna TX	142,000	139,000	82,000	69,600	13,200			26,500
W Nueces Rv nr Brackettville TX	230,000	72,300	46,400	43,600				
Nueces Rv bl Uvalde TX	201,000	102,000	83,200	63,500	21,700			80,100
Nueces Rv nr Asherton TX					12,600			
Nueces Rv at Cotulla TX					18,100			
San Casimiro Ck nr Freer TX				12,000	15,600	9,380	6,990	
Nueces Rv nr Tilden TX					31,500			
Frio Rv at Concan TX	47,500	56,200	59,900		42,100		36,400	
Dry Frio Rv nr Reagan Wells TX	55,000	31,900	25,500		97,900			12,000
Dry Frio Rv at FM 2690 nr Knippa TX								
Frio Rv bl Dry Frio Rv nr Uvalde TX	66,800	100,000	81,200		189,000			74,100
Sabinal Rv bl Mill Ck nr Vaderpool TX								
Sabinal Rv nr Sabinal TX		52,500	18,500		108,000			19,600
Sabinal Rv at Sabinal TX	5,910	93,500	19,700		119,000			42,000
Hondo Ck nr Tarpley TX		76,900	16,400		24,000			51,100
Hondo Ck at SH 173 nr Hondo TX		63,600	12,600		31,600			60,400
Middle Verde Ck at SH 173 nr Bandera TX								2,240
Seco Ck at Miller Rh nr Utopia TX		64,900	13,000		36,500			
Seco Ck at Rowe Rh nr D'Hanis TX		51,400	19,200		15,300			52,200
Leona Rv nr Uvalde TX								
Frio Rv nr Derby TX		56,400			44,300			
Frio Rv at Tilden TX		20,800			33,000	30,800		
San Miguel Ck nr Tilden TX					16,800	29,500		4,200
Choke Canyon Res nr Three Rivers, TX					221.33	223.59	222.42	
Choke Canyon Res OWC nr Three Rivers TX								
Atascosa Rv nr McCoy TX						5,060	2,600	2,340
Atascosa Rv at Whitsett TX				18,200	10,600	13,200	12,700	9,360
Nueces Rv nr Three Rivers TX					39,800	48,500	19,900	
Lagarto Ck nr George West TX								
Lk Corpus Christi nr Mathis TX					94.55	94.36	94.42	
Nueces Rv nr Mathis TX								
Nueces Rv at Bluntzer TX								
Nueces Rv at Calallen TX					38,500	47,800	25,300	

USGS Gage Location	Jul 2007 Late	Jul 2007 Long	May 2015 middle	May 2015	Sep 2016	Oct 2018 early	Oct 2018 middle	Oct 2018 entire
Nueces Rv at Laguna TX				16,400	42,200	71,500	71,300	
W Nueces Rv nr Brackettville TX	8,460				46,500	35,300	8,400	
Nueces Rv bl Uvalde TX				11,200	70,400	105,000	102,000	
Nueces Rv nr Asherton TX		6,100			7,650	11,800		
Nueces Rv at Cotulla TX		7,550						13,200
San Casimiro Ck nr Freer TX		2,090			1,130			
Nueces Rv nr Tilden TX								10,600
Frio Rv at Concan TX				20,600	14,000	23,300		
Dry Frio Rv nr Reagan Wells TX				10,600		13,000		
Dry Frio Rv at FM 2690 nr Knippa TX								
Frio Rv bl Dry Frio Rv nr Uvalde TX				28,900		11,000		
Sabinal Rv bl Mill Ck nr Vaderpool TX						5,630		
Sabinal Rv nr Sabinal TX				14,700		8,980		
Sabinal Rv at Sabinal TX				15,800		7,890		
Hondo Ck nr Tarpley TX				42,000				
Hondo Ck at SH 173 nr Hondo TX				29,100				
Middle Verde Ck at SH 173 nr Bandera TX				11,700				
Seco Ck at Miller Rh nr Utopia TX				12,900				
Seco Ck at Rowe Rh nr D'Hanis TX				19,500				
Leona Rv nr Uvalde TX	19,400		N/A					
Frio Rv nr Derby TX		38,600		16,400				
Frio Rv at Tilden TX		15,200						
San Miguel Ck nr Tilden TX	6,670			5,350				
Choke Canyon Res nr Three Rivers, TX		221.78		200.38				
Choke Canyon Res OWC nr Three Rivers TX								
Atascosa Rv nr McCoy TX	4,890		6,330					
Atascosa Rv at Whitsett TX			16,800					
Nueces Rv nr Three Rivers TX		14,700	15,000					9,940
Lagarto Ck nr George West TX								
Lk Corpus Christi nr Mathis TX		94.15	94.45					94.23
Nueces Rv nr Mathis TX								
Nueces Rv at Bluntzer TX			7,820					6,890
Nueces Rv at Calallen TX		16,700	9,730					7,680

## 6.4.2 Calibration Methodology

Following the initial parameter estimates, calibration simulations were made using observed hourly Next-Generation Radar (NEXRAD) Stage IV gridded precipitation data obtained from the West Gulf River Forecast Center (WGRFC). For each storm event, the model's calculated flow hydrographs were compared to the observed USGS stream flow data at the gages. The model's parameters were then adjusted to improve the match between the simulated and observed hydrographs for the observed events. Calibration was performed for the 16 storm events previously listed in Table 6.2. Subbasin parameters that were adjusted during calibration included the subbasins' initial and constant loss rates, Snyder lag and peaking coefficients, and baseflow parameters. For the routing reaches, the Modified Puls number of subreaches and Muskingum routing parameters were adjusted as needed.

Calibration was generally performed from upstream to downstream, with all subbasins upstream of a specific gage receiving uniform adjustments, unless specific rainfall or observed flow patterns necessitated adjusting subbasin parameters on an individual basis. Generally, subbasin parameters were adjusted in a consistent order: first baseflow parameters, then subbasin loss rates and channel losses, and then Snyder lag and peaking coefficients. Modified Puls Routing subreaches and Muskingum routing parameters were the last to be adjusted. The methods of adjustment for each parameter are summarized in Table 6.4.

To the extent possible, effort was made to calibrate the model's results to the volume, timing, peak magnitude, and shape of the observed flow hydrograph. However, imperfections in the observed rainfall data and streamflow data did not always allow for a perfect match. For example, the gridded NEXRAD rainfall data from the National Weather Service was only available on an hourly basis. This meant that intense bursts of rain that occurred in 15-min or 30-min timespans might not be adequately represented in the hourly rainfall data. It also meant that even though the model was being run on a 15-min time step, the timing of the hydrographs could only be calibrated to the nearest hour. Likewise, the observed flow values at the gages are calculated indirectly from the observed stage and a limited number of flow measurements. While abundant flow measurements were usually available in the low flow range, the number and quality of USGS flow measurements were often very limited in the high flow range, leading to uncertainty in some of the observed flow hydrographs. In cases where all aspects of the observed flow hydrograph could not be matched simultaneously, priority was given to matching the peak flow magnitude first, followed by the peak timing, which are the aspects of model calibration that are most relevant to the final frequency flow estimation.

**Table 6.4: HEC-HMS Calibration Approach**

Parameter	Calibration Approach
Baseflow Parameters	First, the baseflow parameters were adjusted to match the observed flow rates at the start and end of each model simulation period. The initial discharges for the subbasins upstream of a certain gage were adjusted uniformly up or down to match the initial observed discharge at that gage. Similarly, the recession constant was adjusted to match the slope of the recession limb of the observed hydrograph, and the ratio to peak was adjusted to match the observed discharge at the end of the calibration event. All baseflow parameters were adjusted uniformly for all subbasins upstream of a given gage.
Initial Loss (in)	After adjusting the baseflow parameters, the initial and constant losses were adjusted to calibrate the total volume of the flood hydrograph. The initial loss was adjusted according to the antecedent soil moisture conditions at the beginning of each observed storm event. The initial loss was increased or decreased until the timing and volume of the initial runoff generally matched the observed arrival of the flow hydrograph at the nearest downstream gage. All subbasins that were upstream of each gage were generally adjusted uniformly, unless specific rainfall and observed flow patterns necessitated adjusting the subbasin initial losses on an individual basis.
Constant Loss Rate (in/hr)	After adjusting the baseflow and initial loss parameters, the constant losses were adjusted to calibrate the total volume of the flood hydrograph. The subbasins' constant loss rates were increased or decreased until the volume and magnitude of the simulated hydrographs generally matched the observed volume of the flow hydrograph at the nearest downstream gage. The combination of the adjusted baseflow and loss rate parameters led to the total calibrated volume of runoff at the gage.
Channel Loss (cfs) and Fraction	After adjusting the subbasin loss rates, the channel losses were adjusted as needed to calibrate the total volume of the flood hydrograph at the downstream gage. In general, channel losses were adjusted to account for the loss in observed stream flow volume in acre-feet from one upstream gage to the next downstream gage. The channel losses were adjusted uniformly for all reaches above a given stream gage.
Snyder Lag (hours)	After adjusting the loss rates, the Snyder Lags ( $T_p$ ) were the next parameters to be adjusted upstream of an individual gage. The Snyder Lags were adjusted to match the timing of the observed peak flow at the gage. Normally, all of the subbasin $T_p$ 's upstream of an individual gage were adjusted uniformly and proportionally to their initial values, unless the magnitude or shape of the observed hydrograph necessitated making individual adjustments. Efforts were also made to ensure that the adjusted $T_p$ 's still fell within a reasonable range, using the equivalent Snyder's lag times from the Fort Worth District Fort Worth District San Antonio Steep-Area (Upper Salado) and San Antonio Rolling - and Flatter-Area (Lower Salado) urban studies as a guide.
Snyder Peaking Coefficient	Snyder Peaking Coefficients ( $C_p$ ) were adjusted to match the general shape of the observed flow hydrograph as higher peaking coefficients produce steeper, narrower flood hydrographs, and lower peaking coefficients produce flatter, wider flood hydrographs. An attempt was made to use the same peaking coefficient for all subbasins with similar watershed characteristics. For example, steep, hilly subbasins were given a higher peaking coefficient, whereas flatter subbasins, such as those near the coast, were given lower peaking coefficients. Efforts were also made to ensure that the adjusted peaking coefficients fell within the typical range of 0.4 to 0.8. In most cases, peaking coefficients were adjusted once and left alone between subsequent events.
Modified Puls Routing Subreaches	The number of subreaches in the Modified Puls routing reaches were the final parameters to be adjusted when necessary. Calibration of routing parameters focused on storms that fell near the upstream end of the watershed and were routed downstream with little intervening subbasin flow. Adjustments to the number of subreaches in a given routing reach were made in order to match the amount of attenuation in the peak flow that occurred from the upstream end of a reach to the downstream gage. In a very few cases, where an adjustment to the subreaches was not sufficient

Parameter	Calibration Approach
	to match the observed downstream hydrograph, a factor was also applied to the reach's storage volume in the storage-discharge curve.
Muskingum Routing Parameters	For areas of the model that included Muskingum routing, the Muskingum k, X and subreach values were adjusted as needed. Calibration of the routing parameters focused on storms that fell near the upstream end of the watershed and were routed downstream with little intervening local flow. The Muskingum k values were adjusted to match the timing of the observed peak flow at the gage, while the Muskingum X values were adjusted to match the relative flatness or steepness of the hydrograph. Finally, adjustments to the number of subreaches were made in order to match the amount of attenuation in the peak flow that occurred from the upstream end of a reach to the downstream gage.

In addition to the calibration methods described above, some non-conventional calibration methods were needed to calibrate portions of the Nueces River basin. As discussed in section 6.2, a split flow area is located on the Nueces River between Crystal City and Asherton. A 2D HEC-RAS analysis was developed to calculate an inflow-diversion curve at the split flow location as well as to calculate the Modified Puls storage-discharge relationships for the routing reaches along each reach of the split flow paths. This more detailed modeling of the split flow area helped to better calibrate the downstream Asherton gage.

A 2D HEC-RAS analysis was also performed on the ungaged Turkey Creek watershed above Asherton. Turkey Creek is an ungaged portion of the Nueces River basin that encompasses approximately 2,000 square miles of drainage area. With no observed data available to help calibrate the HEC-HMS model, it was a prime candidate for a 2D runoff analysis. In addition, no existing hydraulic models were available within the Turkey Creek watershed to develop Modified Puls routing data for HEC-HMS. Therefore, a 2D HEC-RAS model was developed for the Turkey Creek watershed upstream of Highway 83, and the model was used to estimate Modified Puls routing parameters and to calibrate the Snyder's subbasin transform parameters. For more information on the 2D HEC-RAS analysis, see Appendix F.

Another issue that needed special attention was the calibration of channel losses in the HEC-HMS model. A unique aspect of the hydrology of the Nueces River basin is that peak flows have been observed to decrease dramatically from upstream to downstream along certain stream reaches. Figure 6.22 illustrates one example of this decrease in streamflow by comparing the observed stream flows at the Nueces River USGS gages at Uvalde and Asherton during the 1996 flood event. Asherton is located approximately 60 miles downstream of Uvalde, and as one can see from this figure, the 201,000 cfs observed peak flow at Uvalde was reduced to only 12,900 cfs by the time the flood reached the Asherton gage. In addition, 84% of the total volume of water that passes the upstream gage never reaches the gage at Asherton. This phenomenon is observed at multiple locations throughout the Nueces River basin, primarily at the locations where the streams cross the aquifer outcrops and where the streams abruptly transition from steep, narrow hill country watersheds to wide, irrigated floodplains. These dramatic decreases in streamflow are likely due to a combination of factors including aquifer recharge, irrigation withdrawals and floodplain attenuation. For these reaches, part of the model calibration process involved calibrating the channel losses along the losing reaches of the rivers. The constant loss method was used in HEC-HMS for these reaches, and the constant flow rate along with the fraction of inflow to be lost were adjusted through calibration to multiple flood events. After calibrating those channel loss parameters, the watershed model results matched the observed data at the downstream gages very well. More information on the results of those calibrations is included in Appendix B.

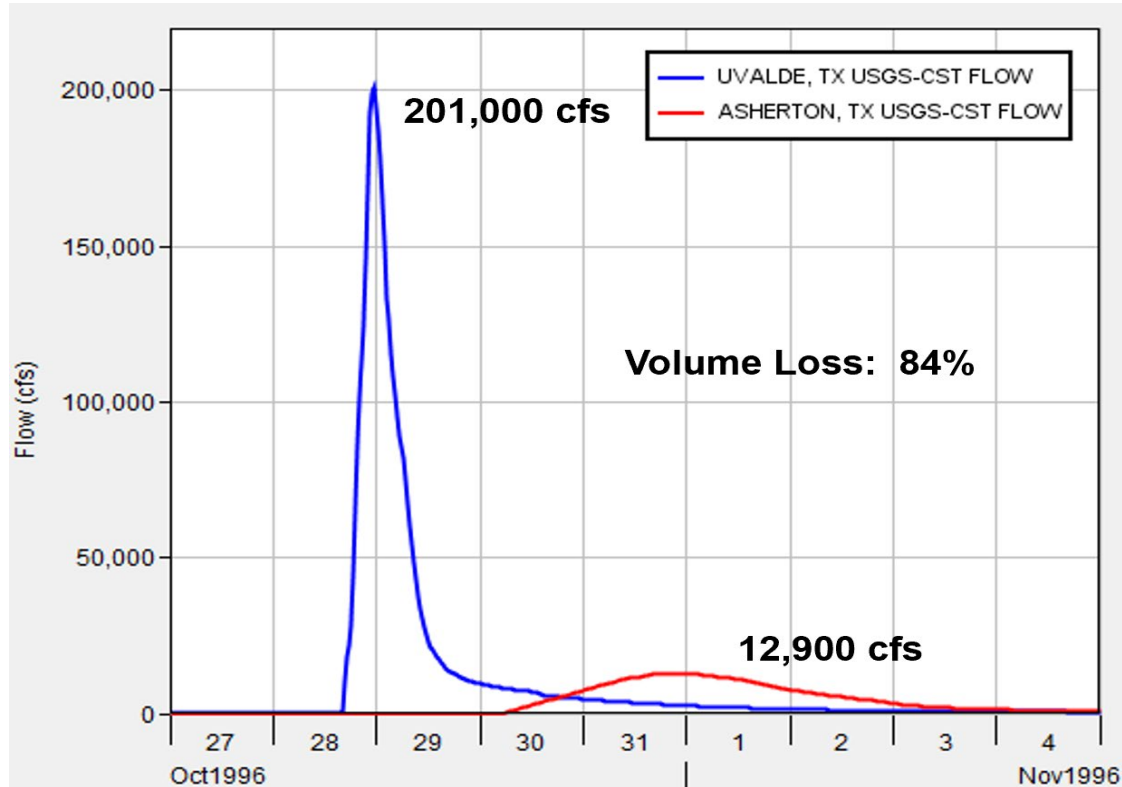


Figure 6.22: Decreasing Streamflows on the Nueces River between Uvalde and Asherton.

### 6.4.3 Calibrated Parameters

The resulting calibrated subbasin and routing reach parameters that were adjusted for each storm event can be seen in Tables B.10 through B.22 of Appendix B.

### 6.4.4 Calibration Results

The final calibration results showed that the HEC-HMS model was able to accurately simulate the response of the watershed, as it reproduced the volume, timing, shape, and peak magnitudes of most observed floods very well. The resulting hydrograph comparisons can be seen in the following figures of this section. The figures show the HEC-HMS computed versus the USGS observed flow hydrographs at each stream gage location. For each reservoir, the figures show the HEC-HMS computed pool elevation versus the USGS observed pool elevation. Calibration figures are only shown for the locations where the USGS stream gages were recording for that event and where the magnitude of the flow was significant enough to warrant calibration.

In addition to graphical comparisons of simulated to observed flow hydrographs, statistical tests were also employed in evaluating model performance. The statistical metrics used to evaluate the HEC-HMS model performance included the Nash-Sutcliffe Efficiency (NSE), the Root Mean Square Error – Observed Standard Deviation Ratio (RSR), and the Percent Bias (PBIAS). For the purposes of this study, the performance metrics were evaluated using the performance ratings shown in Table 6.5. These performance ratings are consistent with standard practices in watershed modeling (Moriassi, 2007) (Moriassi, 2012). In cases where each metric

had a different performance rating, the overall performance rating for that calibration was assigned as the lowest of the three ratings, which is the strictest method of assigning performance ratings.

**Table 6.5: HEC-HMS Model Calibration Evaluation Metrics**

Performance Rating	NSE	RSR	PBIAS
Very Good	$0.80 \leq \text{NSE} < 1.00$	$0 \leq \text{RSR} \leq 0.50$	$0 \leq \text{PBIAS} \leq \pm 5$
Good	$0.70 \leq \text{NSE} < 0.80$	$0.50 < \text{RSR} \leq 0.60$	$\pm 5 < \text{PBIAS} < \pm 10$
Satisfactory	$0.50 \leq \text{NSE} < 0.70$	$0.60 < \text{RSR} \leq 0.70$	$\pm 10 \leq \text{PBIAS} \leq \pm 25$
Unsatisfactory	$\text{NSE} < 0.50$	$\text{RSR} > 0.70$	$\text{PBIAS} > \pm 25$

Table 6.6 contains a summary of the model performance ratings for all the HEC-HMS calibrations performed for this study. The statistical metrics used to assign these performance ratings are shown on the figures for each individual calibration.

As shown in Table 6.6, over 51% of the all of the HEC-HMS model calibrations were rated as Good or Very Good. These ratings indicate that the HEC-HMS model performed very well in all three metrics when compared to observed data. For most of the other calibrations, there were missing observed data or inaccuracies in the rainfall data that resulted in a lower performance rating for the calibrations. Therefore, these lower performance ratings are not an accurate representation of the quality of those calibrations.

For the sake of brevity, only a handful of calibration plots have been included as examples in this section of the report. The resulting hydrograph comparisons for all of the calibrations performed for this study have been included in Appendix B.

**Table 6.6: Summary of HEC-HMS Model Calibration Performance Ratings**

<b>USGS Gage Location</b>	<b>Oct 1996</b>	<b>Jun 1997</b>	<b>Aug 1998</b>	<b>Nov 2001</b>	<b>Jul 2002</b>	<b>Sep 2002 TS Fay</b>	<b>Jun 2007</b>	<b>Jul 2007 Short</b>
Nueces Rv at Laguna TX	Very Good	Good	Satisfactory	Satisfactory	Very Good			Good
W Nueces Rv nr Brackettville TX	Very Good	Satisfactory	Unsatisfactory	Satisfactory				
Nueces Rv bl Uvalde TX	Very Good		Very Good	Unsatisfactory	Satisfactory			Good
Nueces Rv nr Asherton TX					Very Good			
Nueces Rv at Cotulla TX					Very Good			
San Casimiro Ck nr Freer TX				Satisfactory	Very Good	Very Good	Very Good	
Nueces Rv nr Tilden TX					Very Good			
Frio Rv at Concan TX	Very Good	Very Good	Satisfactory		Unsatisfactory		Unsatisfactory	Unsatisfactory
Dry Frio Rv nr Reagan Wells TX	Unsatisfactory	Unsatisfactory	Unsatisfactory		Unsatisfactory			Unsatisfactory
Dry Frio Rv at FM 2690 nr Knippa TX								
Frio Rv bl Dry Frio Rv nr Uvalde TX	Very Good	Satisfactory	Unsatisfactory		N/A			Satisfactory
Sabinal Rv bl Mill Ck nr Vaderpool TX								
Sabinal Rv nr Sabinal TX		Good	Very Good		Satisfactory			Very Good
Sabinal Rv at Sabinal TX	Satisfactory	Good	Satisfactory		Unsatisfactory			Good
Hondo Ck nr Tarpley TX		Unsatisfactory	Unsatisfactory		Satisfactory			Very Good
Hondo Ck at SH 173 nr Hondo TX		Satisfactory	Good		Unsatisfactory			Very Good
Middle Verde Ck at SH 173 nr Bandera TX								Satisfactory
Seco Ck at Miller Rh nr Utopia TX		Unsatisfactory	Unsatisfactory		Satisfactory			
Seco Ck at Rowe Rh nr D'Hanis TX		Unsatisfactory	Satisfactory		Very Good			Good
Leona Rv nr Uvalde TX								
Frio Rv nr Derby TX		Very Good			Unsatisfactory			
Frio Rv at Tilden TX		Satisfactory			Very Good	Very Good		
San Miguel Ck nr Tilden TX					Good	Very Good		Very Good
Choke Canyon Res nr Three Rivers, TX					Very Good	Unsatisfactory	Very Good	
Choke Canyon Res OWC nr Three Rivers TX								
Atascosa Rv nr McCoy TX						Very Good	Satisfactory	Very Good
Atascosa Rv at Whitsett TX				Very Good	Satisfactory	Satisfactory	Good	Unsatisfactory
Nueces Rv nr Three Rivers TX					Very Good	Satisfactory	Satisfactory	
Lagarto Ck nr George West TX								
Lk Corpus Christi nr Mathis TX					Very Good	Unsatisfactory	Unsatisfactory	
Nueces Rv nr Mathis TX								
Nueces Rv at Bluntzer TX								
Nueces Rv at Calallen TX					Good	Satisfactory	Satisfactory	

USGS Gage Location	Jul 2007 Late	Jul 2007 Long	May 2015 middle	May 2015	Sep 2016	Oct 2018 early	Oct 2018 middle	Oct 2018 entire
Nueces Rv at Laguna TX				Very Good	Very Good	Very Good	Very Good	
W Nueces Rv nr Brackettville TX	Good				Very Good	Good	Very Good	
Nueces Rv bl Uvalde TX				Very Good	Very Good	Good	Very Good	
Nueces Rv nr Asherton TX		Unsatisfactory			Very Good	Very Good		
Nueces Rv at Cotulla TX		Very Good						Very Good
San Casimiro Ck nr Freer TX		Unsatisfactory			Unsatisfactory			
Nueces Rv nr Tilden TX								Good
Frio Rv at Concan TX				Very Good	Very Good	Good		
Dry Frio Rv nr Reagan Wells TX				Unsatisfactory		Satisfactory		
Dry Frio Rv at FM 2690 nr Knippa TX								
Frio Rv bl Dry Frio Rv nr Uvalde TX				Good		Good		
Sabinal Rv bl Mill Ck nr Vaderpool TX						Satisfactory		
Sabinal Rv nr Sabinal TX				Good		Very Good		
Sabinal Rv at Sabinal TX				Satisfactory		Good		
Hondo Ck nr Tarpley TX				Satisfactory				
Hondo Ck at SH 173 nr Hondo TX				Very Good				
Middle Verde Ck at SH 173 nr Bandera TX				Satisfactory				
Seco Ck at Miller Rh nr Utopia TX				Very Good				
Seco Ck at Rowe Rh nr D'Hanis TX				Unsatisfactory				
Leona Rv nr Uvalde TX	Satisfactory		Unsatisfactory					
Frio Rv nr Derby TX		Good		Very Good				
Frio Rv at Tilden TX		Satisfactory						
San Miguel Ck nr Tilden TX	Unsatisfactory			Unsatisfactory				
Choke Canyon Res nr Three Rivers, TX		Unsatisfactory		Good				
Choke Canyon Res OWC nr Three Rivers TX								
Atascosa Rv nr McCoy TX	Very Good		Very Good					
Atascosa Rv at Whitsett TX			Satisfactory					
Nueces Rv nr Three Rivers TX		Very Good	Satisfactory					Satisfactory
Lagarto Ck nr George West TX								
Lk Corpus Christi nr Mathis TX		Unsatisfactory	Very Good					Unsatisfactory
Nueces Rv nr Mathis TX								
Nueces Rv at Bluntzer TX			Satisfactory					Good
Nueces Rv at Calallen TX		Satisfactory	Satisfactory					Very Good

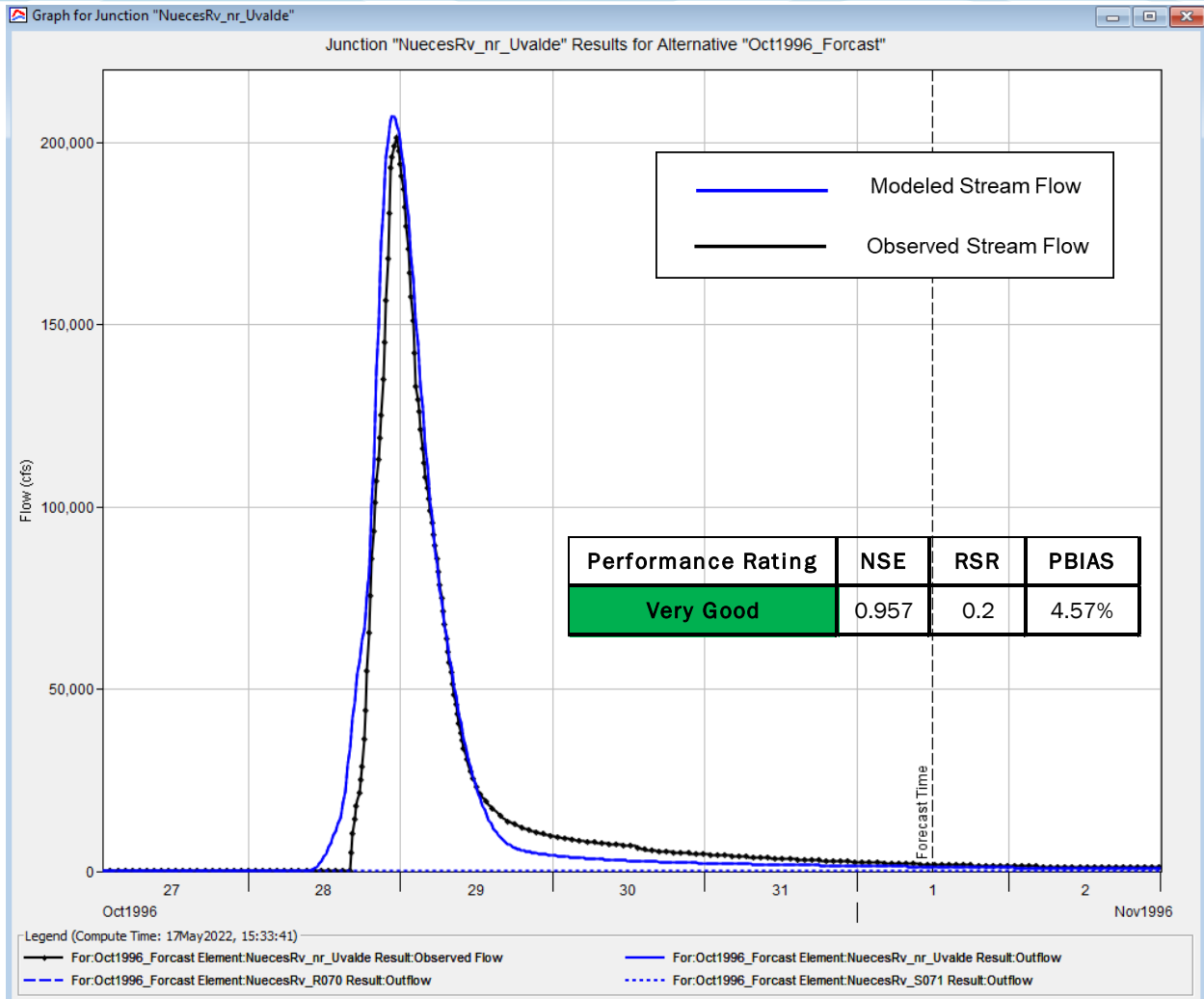


Figure 6.23: October 1996 Calibration Results for Nueces River below Uvalde USGS Gage

The Nueces River below Uvalde calibration achieved a “Very Good” performance rating. The HEC-HMS model matched the observed timing, shape and magnitude of the observed hydrograph very well. Muskingum routing, channel loss and initial losses were adjusted to achieve the calibration. The Nueces River below Uvalde plot is shown above.

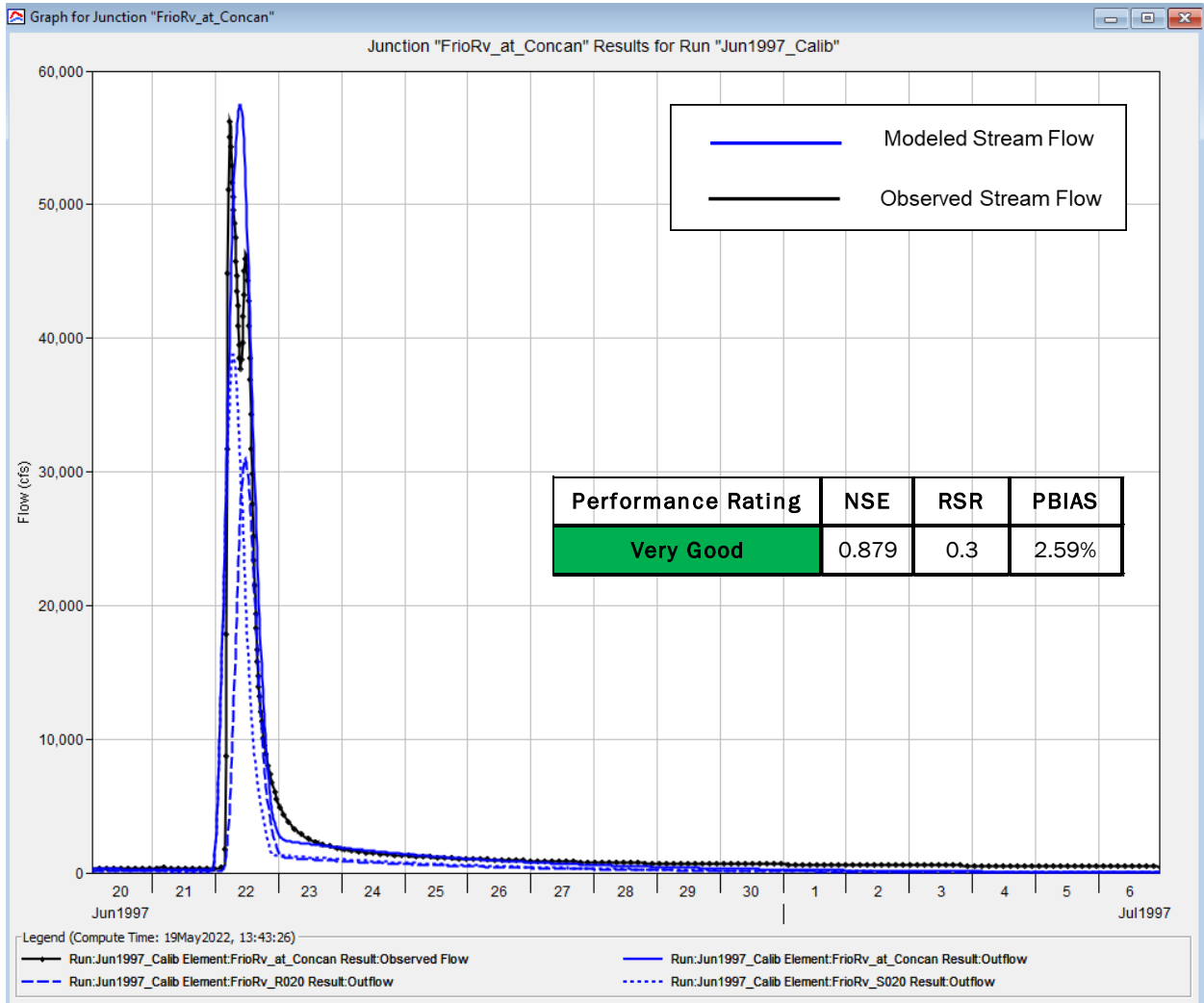


Figure 6.24: June 1997 Calibration Results for Frio River at Concan USGS Gage

The Frio River at Concan achieved a “Very Good” performance rating for the 1997 event. HEC-HMS matched the timing and magnitude of the observed hydrograph very well but could not match the shape of the double peak in the observed hydrograph most likely due to errors in the precipitation intensity and or distribution. The Frio River at Concan plot is shown above.

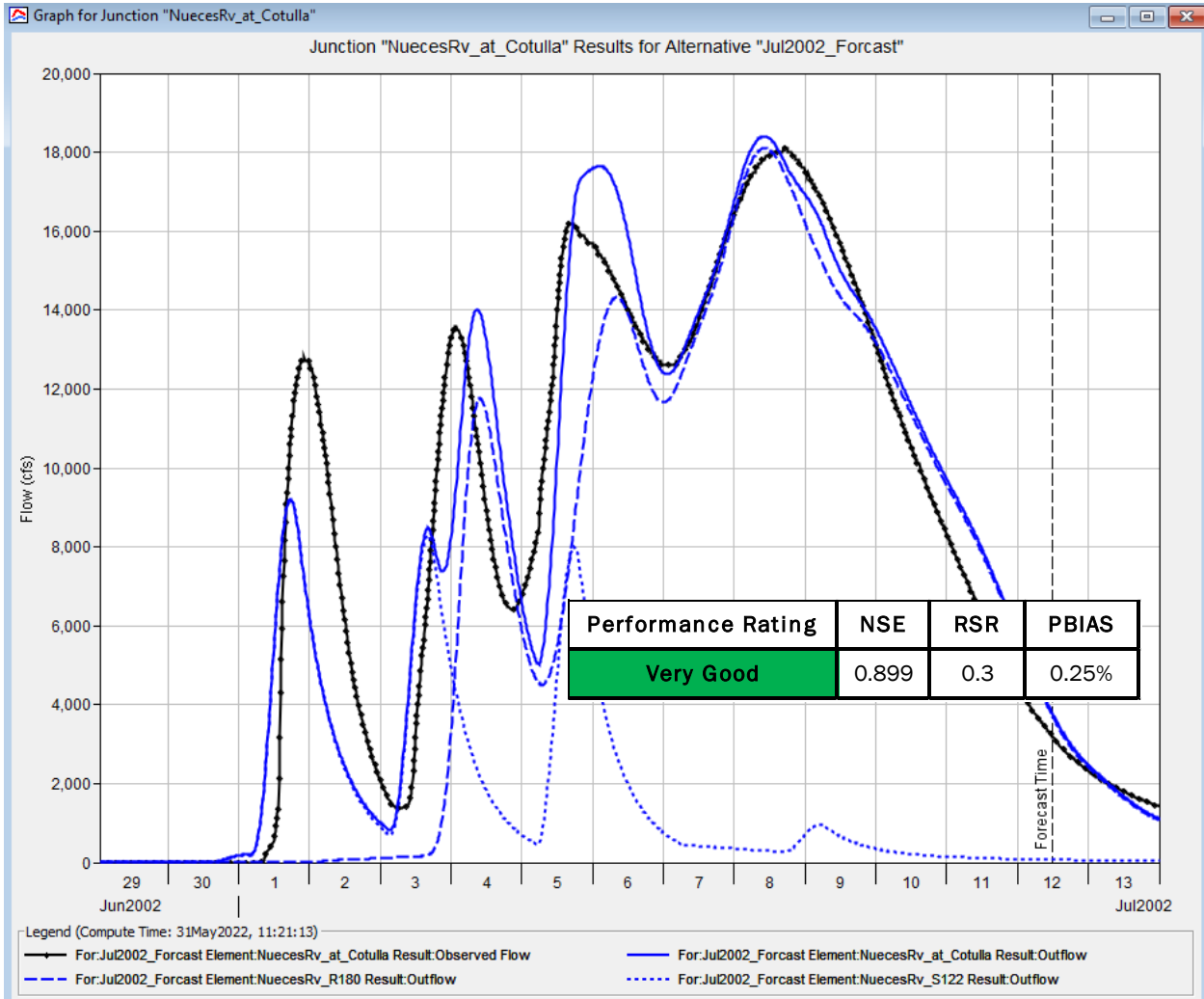


Figure 6.25: July 2002 Calibration Results for the Nueces River at Cotulla, TX USGS Gage

The Nueces River at Cotulla gage achieved a “Very Good” performance rating for the July 2002 event. The HEC-HMS model matched the timing, magnitude, shape and volume of the observed hydrograph fairly well. The July 2002 event has multiple individual storms occurring over several days. Since it was difficult to match all the peaks with a single set of loss rates, the calibration focused on the largest peak in the event. The Nueces River at Cotulla plot is shown above.

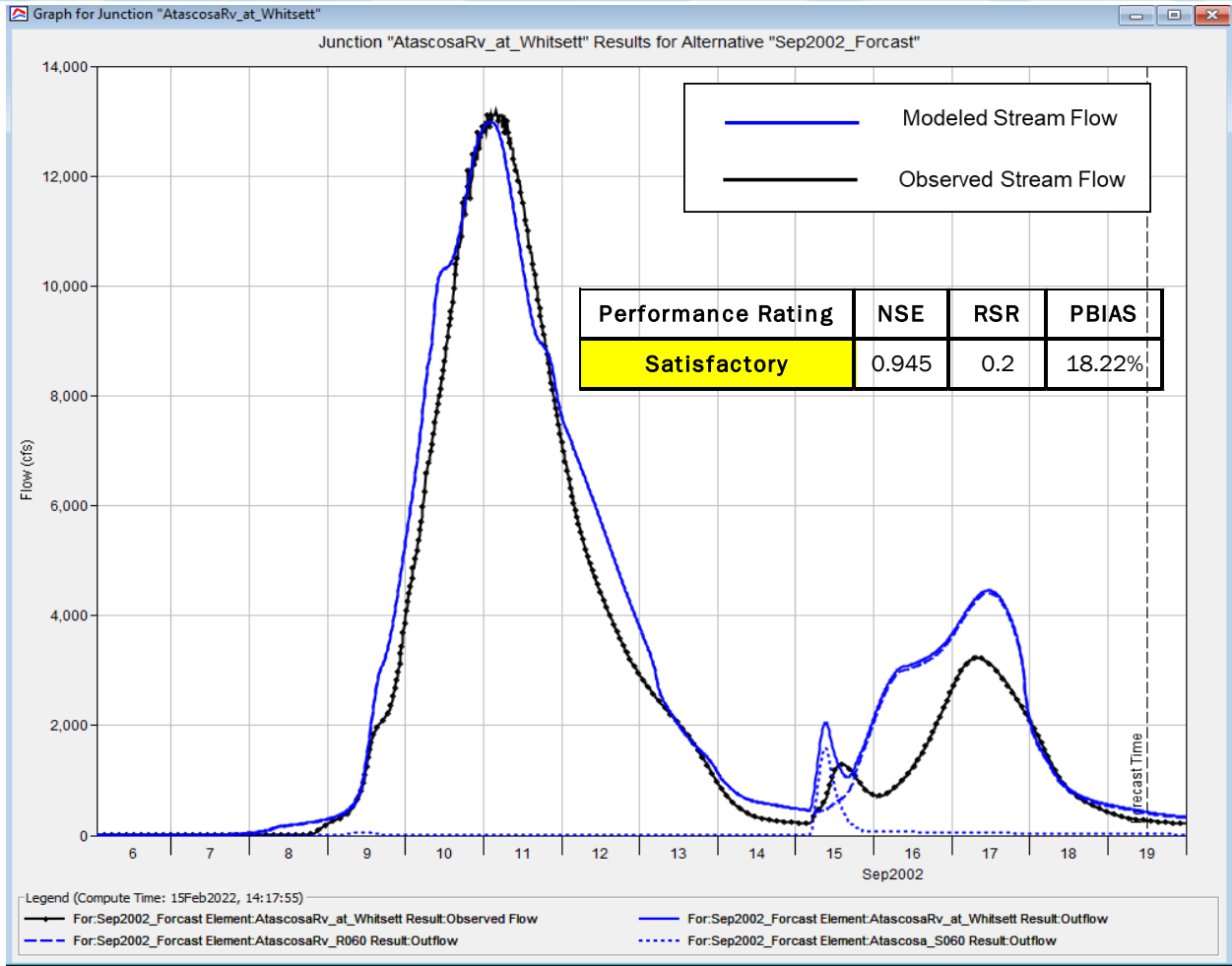


Figure 6.26: September 2002 Calibration Results for Atascosa River near Whitsett USGS Gage

The Atascosa River near Whitsett gage achieved a “Satisfactory” performance rating for the September 2002 event. The HEC-HMS model matched the timing, magnitude, shape and magnitude of the main peak very well. The satisfactory performance rating was caused by the computed volume of the second smaller peak being too high, so it is not an accurate representation of the calibration of the main portion of the flood. Atascosa River near Whitsett plot is shown above.

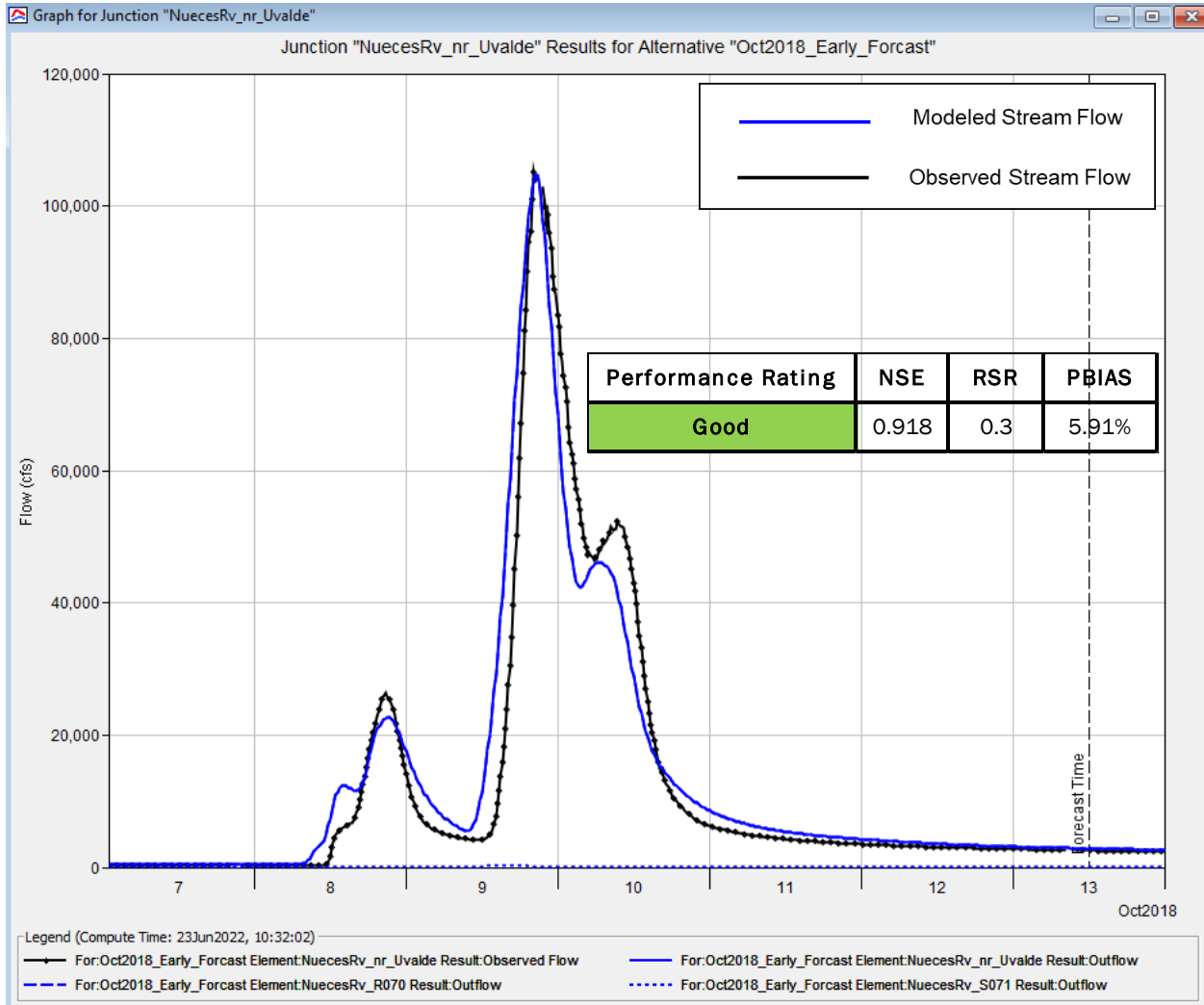


Figure 6.27: October 2018 (early) Calibration Results for Nueces River below Uvalde Gage

The October 2018 calibration for the Nueces River below Uvalde resulted in a “Good” performance rating. The model matched the observed peak flow and timing very well, but the percent bias was slightly higher than 5%. Forecast mode with blending is used for upstream gage in HEC-HMS. The Nueces River below Uvalde plot is shown above.

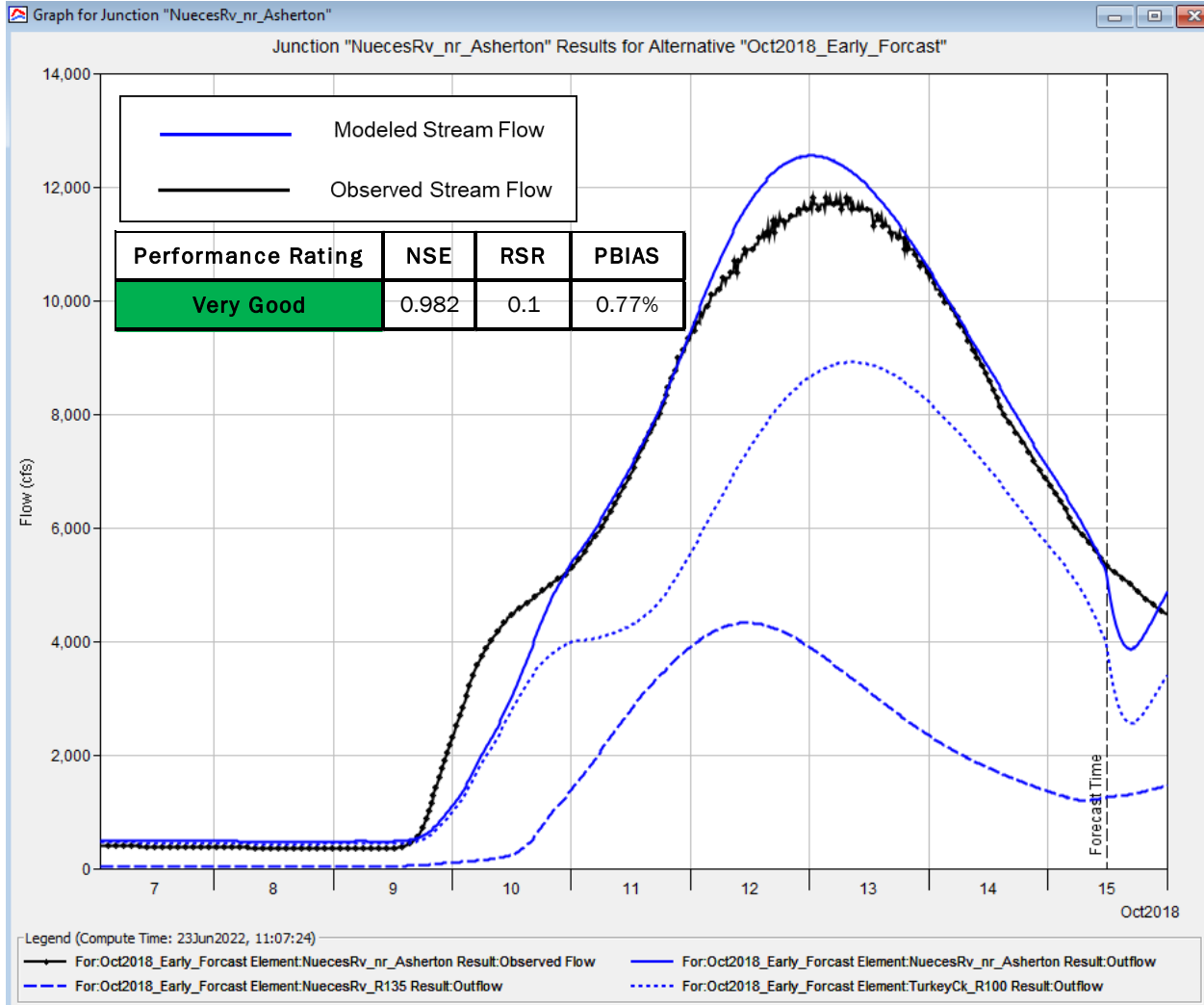


Figure 6.28: October 2018 (early) Calibration Results for Nueces River near Asherton Gage

The Nueces River near Asherton calibration for October 2018 achieved a “Very Good” performance rating. The HEC-HMS model matched the timing, shape, magnitude and volume of the observed hydrograph very well. Detailed modeling of the split flow area along with adjusting the channel losses on the Nueces River downstream of Uvalde helped to achieve this calibration. There is a split flow between the Nueces River and Espantosa Slough/Soldier Slough starting near the town of Crystal City to just upstream of the Nueces River near Asherton gage (State Hwy 190). Espantosa Slough/Soldier Slough has three low water dams and the Nueces River also has three dams. In the HEC-HMS model, a diversion element was set up with diversion method “Inflow Function”. The Inflow-Diversion Function, total inflow versus diversion, was estimated with 2D HEC-RAS. It was determined that Espantosa Slough/Soldier Slough is the main channel with most of the flow. The 2D HEC-RAS analysis showed that one of the dams on the Nueces River blocks the flow and only lets a small portion of the flow continue down the Nueces River flow path. The final Nueces River near Asherton plot is shown above. The final Nueces River near Asherton plot is shown above.

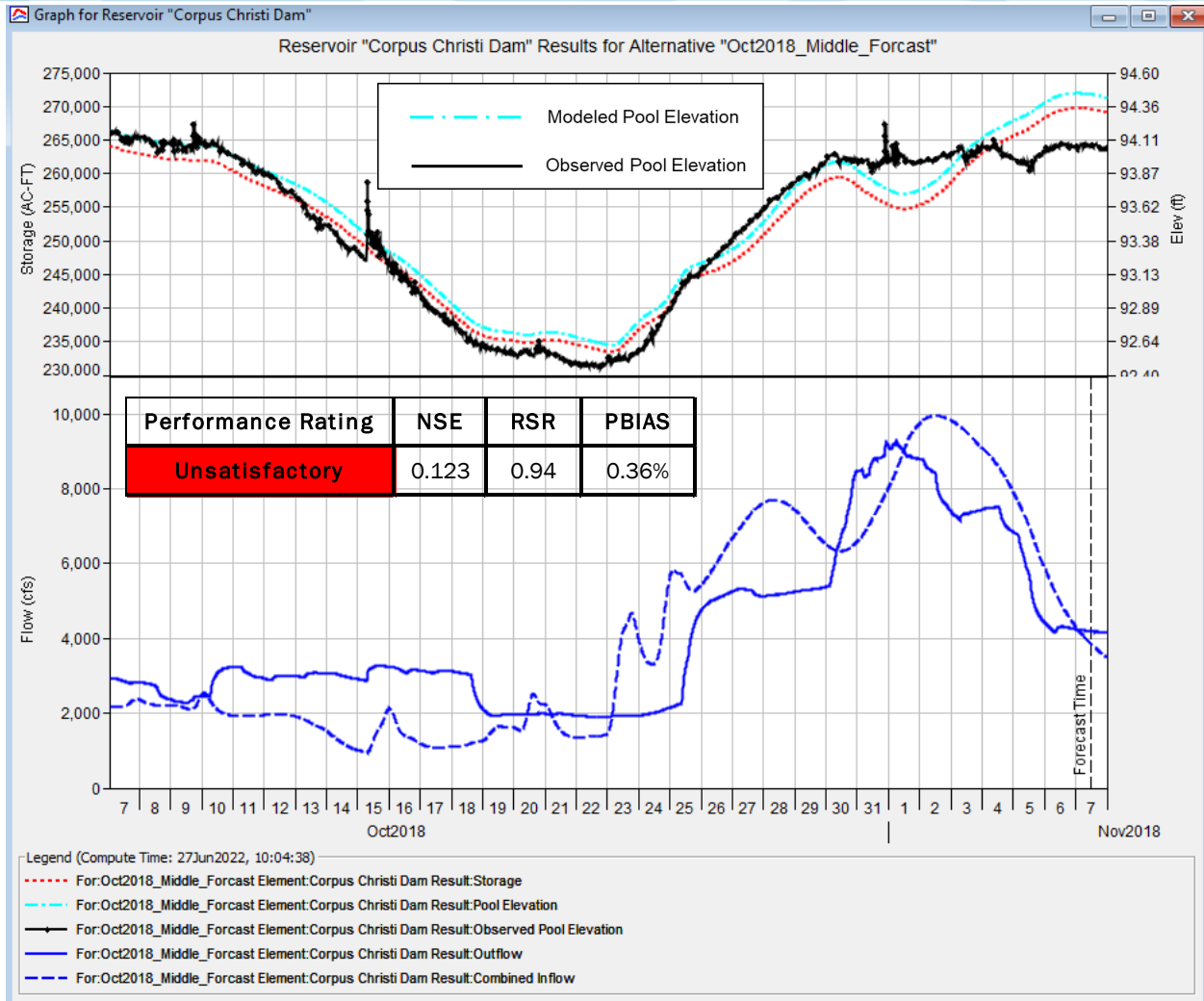


Figure 6.29: October 2018 (entire) Calibration Results for Lake Corpus Christi

The Lake Corpus Christi calibration for October 2018 had an "Unsatisfactory" performance rating. However, the HEC-HMS model matched the timing, shape, magnitude and volume of the observed pool elevation very well until the last week of the event when the computed pool elevation continued to rise. Lake Corpus Christi has a poor performance rating mainly because of its level pool operations, so it is not an accurate representation of the quality of the calibration. The observed pool elevation of the lake only varied by 1.5 feet throughout the entire event. This results in poor statistics for even small deviations from the observed pool elevation. For example, the figure above shows that the computed pool elevation was within 0.2 feet of observed for the entire event, but it still resulted in a poor performance rating. The Lake Corpus Christi plot is shown above.

## 6.5 FINAL MODEL PARAMETERS

After the initial parameter estimates were made and the calibration process was completed, the final model parameters were established. Tables of all final parameters are located in Section 1.5 of Appendix B. The final Snyder's lag times and peaking coefficients were developed by taking a weighted average of those parameters from the calibration events. The peak discharge from the subbasin for that event was used to weight the calibrated lag times. This method has the effect of granting a higher weight to the lag times and peaking coefficients that were calibrated from larger, more intense storms, and it ignores the storms that generated no runoff from a particular subbasin.

The final baseflow parameters were selected based on the results of the calibration runs. Specifically, the initial flows per square miles were selected based on typical flow rates observed on each reach of the river prior to a large storm event, and the recession constant and ratio to peak were selected based on the slope and shape of the receding limb of the hydrograph at the downstream gages.

The Modified Puls storage discharge relationships were calculated from the best available HEC-RAS models, and the final number of subreaches were selected based on calibration to the observed attenuation of the flood hydrograph in between stream gages. Once again, the final subreach values were calculated from a weighted average based on the peak magnitude of the flow through the reach for a given storm event. Similar to the Modified Puls routing, the final Muskingum K, X and subreach values were calculated from a weighted average based on the peak magnitude of the flow through the reach for a given storm event.

The final channel loss parameters were also selected based on the results of the calibration runs. The final channel loss values were calculated from a weighted average based on the peak magnitude of the flow through the reach for a given storm event.

In observed storm events, the initial and constant losses vary from storm to storm according to the antecedent moisture conditions of the soil. Therefore, the final set of loss rates was not directly calculated from the calibration results. Instead, the losses for the frequency storms were initially developed using the regional USACE Fort Worth District Method for determining losses based on soil type (percent sand) (Rodman, 1977). After calculating the default frequency loss rates based on soil type, three additional adjustments were made to the loss rate parameters. First, an adjustment was made to the initial deficits to account for the presence of NRCS flood control structures in the watershed that have not been modeled in detail. Second, a climate adjustment was made to both the initial deficits and constant losses to better align them with the observed "average" to "wet" loss rates from recent storm events for different regions of the basin. Third and finally, a Bulletin 17C adjustment was made to the loss rates of the frequent storm events (50% to 4% AEP) to better align the HEC-HMS results with the statistical results at the gages.

The USACE Fort Worth District Method for determining losses method produces a default set of loss rates for each frequency event, based on the soil type in each subbasin (Rodman, 1977). The method assumes that the antecedent moisture conditions become wetter, and the losses decrease as the rarity of the flood event increases, which is consistent with other research (McEnroe, 2003). In general, the 50% AEP loss rates are intended to correspond to an "average" or "normal" antecedent soil moisture condition, and the 0.2% AEP loss rates should correspond to a "wet" soil moisture condition. Table 6.7 summarizes the range of default loss rates of the Fort Worth District method by frequency and soil type. A geospatial grid of percent sand for the State of Texas developed by the USACE Fort Worth District was used to spatially calculate the percent sand for each subbasin. That percent sand value was then used to interpolate between the 0% and 100% sand loss rate values in Table 6.7 to assign the default initial and constant loss rates to each subbasin.

**Table 6.7: Default Frequency Loss Rates by Soil Type for the USACE Fort Worth District Method**

Annual Exceedance Probability (AEP) %	Initial Abstraction (inches) for Soil with 0% Sand	Infiltration Rate (inches per hour) for Soil with 0% Sand	Initial Abstraction (inches) for Soil with 100% Sand	Infiltration Rate (inches per hour) for Soil with 100% Sand
50%	1.50	0.20	2.10	0.26
20%	1.30	0.16	1.80	0.21
10%	1.12	0.14	1.50	0.18
4%	0.95	0.12	1.30	0.15
2%	0.84	0.10	1.10	0.13
1%	0.75	0.07	0.90	0.10
0.5%	0.61	0.06	0.73	0.09
0.2%	0.50	0.05	0.60	0.08

After calculating the default frequency loss rates based on soil type, three additional adjustments were made to the loss rate parameters. First, the default initial deficits were increased to account for the presence of NRCS type flood control structures in the watershed that have not been modeled in detail. This adjustment for the NRCS flood control structures was made based on data from the National Inventory of Dams (NID) (USACE, 2016). In this case, the percent of each subbasin area that was controlled by NRCS type structures was multiplied by the inches of runoff that can typically be stored between the riser and spillway of the NRCS structures in that basin (typically up to 4 inches of runoff). For the frequent storm events (50% to 4% AEP), the initial loss due to the NRCS structures was decreased in proportion to the total depth of rain for that event.

Second, a climate adjustment was made to both the initial deficits and constant losses to better align them with the observed “average” to “wet” loss rates from recent storm events for different regions of the basin. This adjustment was made by adding a factor to the previously calculated loss rates in order to ensure that the range of frequency loss rates (from 50% to 0.2% AEP) lined up well with the observed loss rates from the calibration storms for “average” to “wet” antecedent conditions. However, the InFRM team recognized that the calibration events represent a relatively small sample of observed storm events and may not always include enough data to accurately represent the true range of possible loss rates from “dry” to “wet.” Therefore, this adjustment was applied on a regional basis rather than by individual subbasin in order to reduce the possible sample bias.

Third and finally, a Bulletin 17C adjustment was made to the loss rates to better align the HEC-HMS results with the statistical results for the frequent storm events (50% to 4% AEP) at the gages. A comparison was made between the preliminary HEC-HMS results with the calculated frequency loss rates and the statistical flow frequency curves from the USGS gage records. A final adjustment was then made to the initial deficits and constant losses for the 50% through 10% AEP storms in order to have a better correlation with the statistical frequency curves estimated from the USGS gage records. This step was performed because of the increased confidence level in the gage records’ statistical frequency curves for the 50% through 10% AEP range. The 4% AEP losses were also adjusted when needed to create a smoother transition between the 2% and 10% AEP flow values. Loss rates for events with an AEP at or below 2% were not adjusted based on the statistical frequency curves because stream gage records in Texas are not long enough and there is too

much variability in the rare AEP statistical flow estimates over time (see the change over time plots in Appendix A) to justify adjusting the rare AEP loss rates. Generally, a stream gage record that is 3 to 4 times the length of the return period being estimated is needed before the statistical results can be considered reliable enough for this type of adjustment. For the 1% AEP event, this would require a stream gage record of 300 to 400 years in length, which is not available anywhere in Texas.

Based on the range of observed initial and constant losses from the calibration storms, the adopted losses for the frequency storms could be characterized to represent “average” to “wet” conditions (the “average” moisture conditions being applied to the 50% AEP storm, and “wet” moisture conditions being applied to the 0.2% AEP storm), which are appropriate assumptions for modeling hypothetical flood events. However, none of the adopted frequency losses are at the extreme wet or extreme dry ends of the range of calibrated losses.

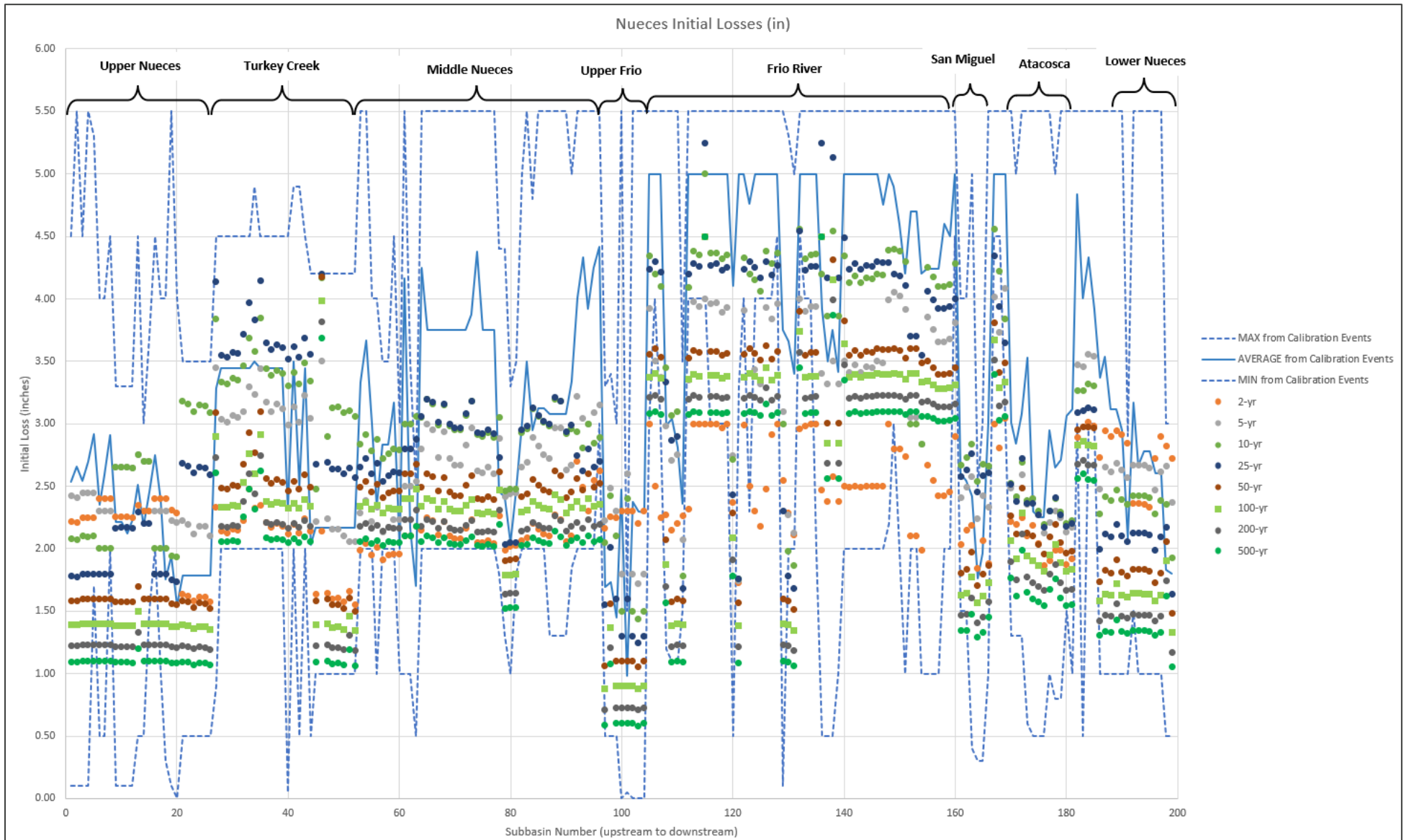


Figure 6.30: Comparison of Adopted versus Calibrated Initial Losses (inches)



Figure 6.31: Comparison of Adopted versus Calibrated Constant Losses (inches per hour)

## 6.6 UNIFORM RAINFALL FREQUENCY STORMS

After finalizing the model's parameters based on the calibration events, the frequency flow values were then calculated in HEC-HMS by applying frequency rainfall depths to the final watershed basin models through a series of depth-area analyses. This rainfall pattern is referred to as the uniform rainfall method because the assigned point rainfall depths for each subbasin are reduced uniformly over the entire watershed based on the published depth-area reduction factors from Figure 15 of the National Weather Service TP-40 publication (Herschfield, 1961). A depth area analysis was set up for every junction and node of interest within the HEC-HMS model in order to apply the appropriate depth-area reduction for each drainage area of interest.

A 2-day duration frequency storm with a 50% intensity position and a 15-minute intensity duration was adopted in the HEC-HMS model. Sensitivity tests were also run for durations ranging from 24-hours to 7-days and for intensity positions ranging from 25% to 75%, but in most cases, the peak flow results were not particularly sensitive to these settings (generally within +/- 5%). Additional information on the sensitivity tests results is provided in Appendix B.

### 6.6.1 Point Rainfall Depths for the Uniform Frequency Storms

NOAA Atlas 14 contains precipitation frequency estimates for the United States along with their associated lower and upper 90% confidence bounds. The Atlas is divided into volumes based on geographic sections of the country. NOAA Atlas 14 is intended as the U.S. Government source of precipitation frequency estimates. NOAA Atlas 14 Volume 11, which covers the state of Texas, was published in 2018 (NOAA, 2018). The point rainfall depths that were published in NOAA Atlas 14 (NA14) were applied to the HEC-HMS model for this study, as they are the most up-to-date precipitation frequency estimates in Texas.

NOAA Atlas 14 point rainfall depths from the annual maximum series for various durations and recurrence intervals were collected from the NA14 Precipitation Frequency Data Server (PFDS) for the centroid of each subbasin (NOAA, 2020). This method resulted in 199 separate point rainfall tables being applied in Nueces River basin, one for each subbasin. The appropriate point rainfall depth table was assigned to each subbasin within the HEC-HMS frequency storm editor. It should be noted that precipitation frequency estimates from NOAA Atlas 14 are point estimates and are not directly applicable to larger areas. The conversion from a point to an areal estimate was accomplished for the uniform rainfall method by using the depth area analyses in HEC-HMS with the default TP-40 area reduction curves.

Figure 6.32 illustrates how the NA14 1% Annual Exceedance Probability (AEP) point rainfall depths for the 48-hour durations vary spatially across the Nueces River basin. As one can see from this figure, the 1% AEP 48-hr depth varies from 11 inches in the middle portion of the basin to over 15 inches in the upper and lower portions of the basin. The two areas that receive the most rainfall are the steep hill country area near Utopia, TX and the downstream area near the Gulf of Mexico. Geographically, it makes sense that these areas would receive the most rainfall. The downstream end of the basin receives more rainfall because of its proximity to the large source of moisture at the Gulf of Mexico, while the steep hill country reaches near Utopia cause an orographic uplift effect which increases rainfall amounts in that area.

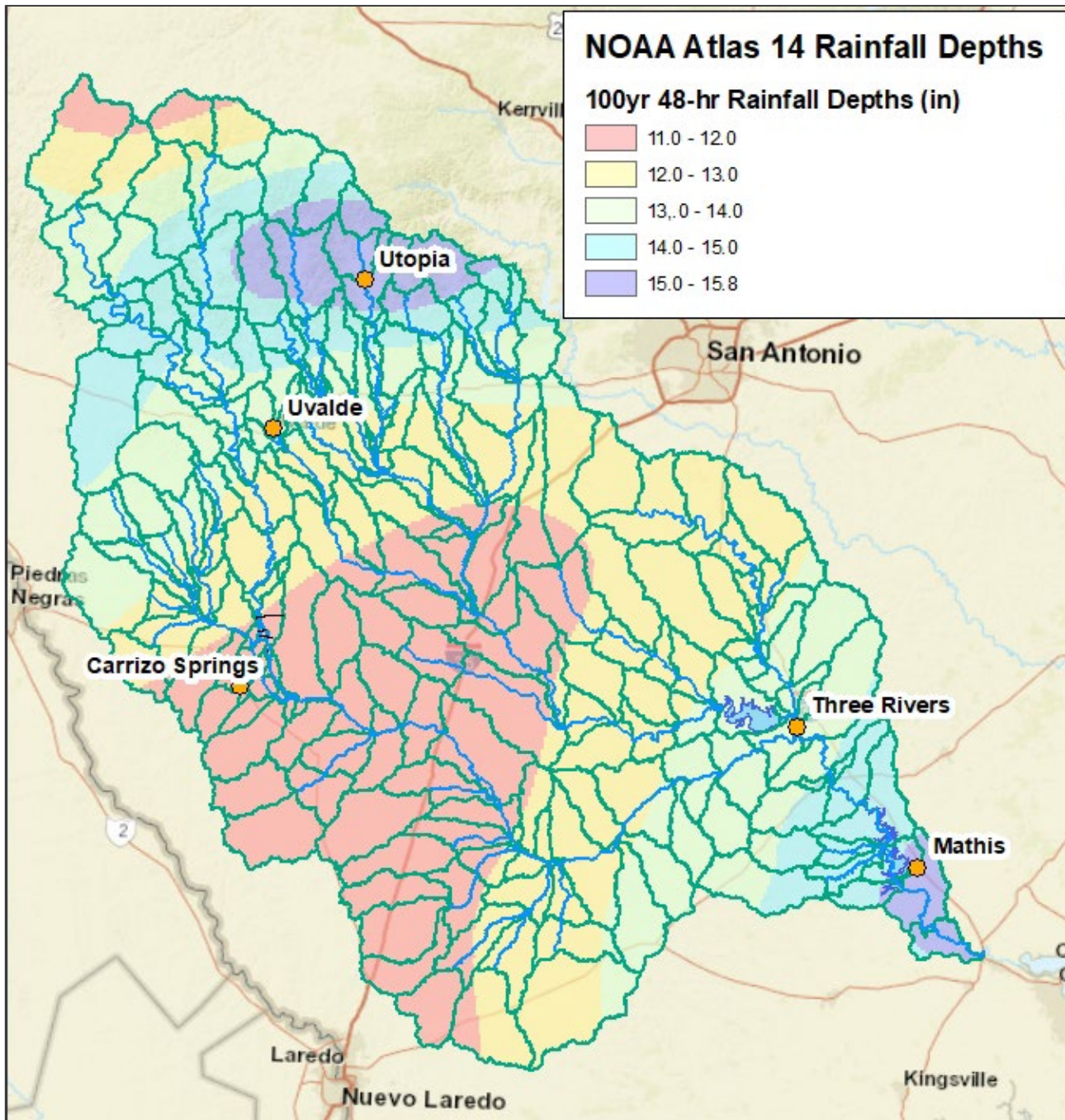


Figure 6.32: 1% AEP, 48-hour Rainfall Depths for the Nueces River Basin from NOAA Atlas 14

### 6.6.2 Frequency Storm Results – Uniform Rainfall Method

The final frequency results for the uniform rainfall method were then computed in HEC-HMS by applying the NOAA Atlas 14 frequency rainfall depths to the final watershed model through a series of depth-area analyses of the applied frequency storms. This rainfall pattern is referred to as the uniform rainfall method because the assigned point rainfall depths for each subbasin are reduced uniformly over the entire watershed.

The final uniform rain HEC-HMS frequency flow results for significant locations throughout the watershed model can be seen in Table 6.8. In this table, the highlighted rows indicate calibrated gage locations. The final uniform rain HEC-HMS frequency pool elevation results are summarized in Table 6.9. These results were then compared to the elliptical shaped storm results from HEC-HMS along with other methods from this study, as shown in Chapter 11 of the main report.

In some cases, one may observe in Table 6.8 that the simulated peak discharge decreases in the downstream direction. It is not an uncommon phenomenon to see decreasing frequency peak discharges for some river reaches as flood waters spread out into the floodplain and the hydrograph becomes dampened as it moves downstream. This can be due to a combination of peak attenuation due to river routing as well as the difference in timing between the peak of the main stem river versus the runoff from the local tributaries and subbasins.

Table 6.8: Summary of Peak Discharges (cfs) from the HEC-HMS Uniform Rainfall Frequency Storms

		AEP	50%	20%	10%	4%	2%	1%	0.5%	0.2%	
Location Description	HMS Element Name	Drainage Area (sq mi)	2-yr	5-yr	10-yr	25-yr	50-yr	100-yr	200-yr	500-yr	Method
West Nueces River at Indian Creek	W_NuecesRv+IndianCk	373.49	3,070	28,900	66,300	111,800	146,000	185,000	224,000	281,000	Uniform Rain
West Nueces River above Sycamore Creek	W_NuecesRv_abv_SycamoreCk	535.95	3,440	32,300	74,200	128,000	170,000	221,000	271,000	345,000	Uniform Rain
West Nueces River Below Sycamore Creek	W_NuecesRv_blw_SycamoreCk	646.40	4,060	37,000	85,100	148,200	199,000	260,000	320,000	409,000	Uniform Rain
West Nueces River near Brackettville (USGS gage 08190500)	W_NuecesRv_nr_Brackettville	693.94	4,050	36,800	84,400	147,000	197,000	260,000	321,000	412,000	Uniform Rain
West Nueces River above Sycamore Creek	W_NuecesRv_abv_Live OakCk	767.91	3,820	34,900	79,900	139,000	187,000	246,000	304,000	391,000	Uniform Rain
West Nueces River Below Sycamore Creek	W_NuecesRv_blw_Live OakCk	820.22	3,830	35,100	80,400	139,700	188,000	247,000	307,000	396,000	Uniform Rain
West Nueces River above Nueces River	W-NuecesRv_abv_NuecesRv	918.29	3,590	33,000	75,500	131,300	177,000	234,000	292,000	379,000	Uniform Rain
Hackberry Creek at East Prong Nueces River	HackberryCk+E_Prong_NuecesRv	199.93	4,300	19,900	40,200	76,800	101,000	123,000	144,000	172,000	Uniform Rain
Nueces River above Pulliam Creek	NuecesRv_abv_PulliamCk	354.34	6,520	29,300	58,900	113,600	154,000	191,000	226,000	276,000	Uniform Rain
Nueces River below Pulliam Creek	NuecesRv_blw_PulliamCk	529.82	8,830	41,400	83,800	162,500	222,000	279,000	334,000	411,000	Uniform Rain
Nueces River at CR414 at Montell (USGS gage 08189998)	NuecesRv_at_Cr414_at_Montell	659.62	9,170	43,200	87,600	172,700	241,000	307,000	372,000	463,000	Uniform Rain
Nueces River below Montell Creek	NuecesRv_blw_MontellCk	679.24	9,190	43,300	87,800	173,200	242,000	309,000	374,000	467,000	Uniform Rain
Nueces River at Laguna (USGS gage 08190000)	NuecesRv_at_Laguna	736.17	9,090	42,900	86,900	171,600	241,000	308,000	373,000	468,000	Uniform Rain
Nueces River above West Nueces River	NuecesRv_abv_W_NuecesRv	815.94	8,520	40,600	82,300	162,400	228,000	292,000	356,000	449,000	Uniform Rain
Nueces River below West Nueces River	NuecesRv_blw_W_NuecesRv	1734.22	11,000	63,600	135,400	255,400	357,000	473,000	588,000	758,000	Uniform Rain

		AEP	50%	20%	10%	4%	2%	1%	0.5%	0.2%	
Location Description	HMS Element Name	Drainage Area (sq mi)	2-yr	5-yr	10-yr	25-yr	50-yr	100-yr	200-yr	500-yr	Method
Nueces River below Indian Creek	NuecesRv+IndianCk	1802.06	10,440	60,600	128,900	243,300	340,000	451,000	563,000	726,000	Uniform Rain
Nueces River at Highway 90	NuecesRv_at_HWY-90	1838.04	9,860	57,600	122,400	231,100	323,000	429,000	536,000	693,000	Uniform Rain
Nueces River near Uvalde (USGS gage 08192000)	NuecesRv_nr_Uvalde	1861.45	9,320	54,600	116,200	219,300	307,000	408,000	510,000	660,000	Uniform Rain
Nueces River at Highway 83	NuecesRv_at_HWY-83	1885.45	6,880	40,200	88,200	164,400	232,000	309,000	388,000	503,000	Uniform Rain
Nueces River at Highway 57	NuecesRv_at_HWY-57	1981.12	4,500	26,700	57,600	122,700	172,000	231,000	291,000	380,000	Uniform Rain
Nueces River at FM 1025 nr Crystal City (USGS gage 08192550)	NuecesRv_at_FM-1025_nr_Cryst	2102.48	2,590	14,200	29,600	68,600	132,000	179,000	228,000	301,000	Uniform Rain
Nueces River at The Turkey Creek/Espantosa Slough Split	NuecesRv_TurkeyCk_Split	2122.77	1,870	10,000	20,000	41,000	75,000	130,000	168,000	226,000	Uniform Rain
Turkey Creek/Espantosa Slough Diversion	TurkeyCk_Diversion	2122.77	1,380	7,230	13,100	29,600	62,000	116,000	153,000	210,000	Uniform Rain
Nueces River Split	NuecesRv_Split_J010	2165.25	1,330	3,540	6,600	10,000	12,000	13,000	16,000	21,000	Uniform Rain
Nueces River above Turkey Creek	NuecesRv_abv_TurkeyCk	2165.25	710	2,740	5,400	8,800	11,000	12,000	13,000	14,000	Uniform Rain
Elm Creek and Stricklin Creek	ElmCk+StricklinCk	254.90	1,590	4,200	15,600	46,000	103,000	143,000	182,000	233,000	Uniform Rain
Chacon Creek at Highway 57	ChaconCk_at_HWY-57	337.55	1,770	4,220	10,800	35,200	90,000	134,000	177,000	233,000	Uniform Rain
Palo Blanco Creek at Highway 57	Palo_BlancoCk_at_HWY-57	69.98	2,430	5,170	10,700	22,200	41,000	53,000	66,000	82,000	Uniform Rain
Palo Blanco Creek above Chacon Creek	Palo_BlancoCk_abv_Chacnck	121.24	1,120	2,650	6,500	15,100	31,000	42,000	55,000	73,000	Uniform Rain
Palo Blanco Creek below Chacon Creek	Palo_BlancoCk_blw_Chacnck	520.34	1,690	4,220	10,600	30,100	78,000	122,000	170,000	234,000	Uniform Rain
Palo Blanco Creek above Picoso Creek	Palo_BlancoCk_abv_PicosacK	520.34	1,280	3,360	8,900	29,300	76,000	118,000	166,000	230,000	Uniform Rain

		AEP	50%	20%	10%	4%	2%	1%	0.5%	0.2%	
Location Description	HMS Element Name	Drainage Area (sq mi)	2-yr	5-yr	10-yr	25-yr	50-yr	100-yr	200-yr	500-yr	Method
Picosa Creek and Chueco Creek	PicosaCk+ ChuecoCk	190.28	2,020	5,890	13,500	31,900	66,000	91,000	115,000	148,000	Uniform Rain
Palo Blanco Creek below Picosa Creek	Palo_BlancoCk_ blw_PicosaCk	744.76	1,880	5,590	15,300	43,000	103,000	157,000	222,000	315,000	Uniform Rain
Palo Blanco Creek above Comanche Creek	Palo_BlancoCk_ abv_ComancheC	744.76	1,840	5,500	15,000	42,600	103,000	157,000	221,000	314,000	Uniform Rain
Comanche Creek at Highway 277	ComancheCk_at _HWY-277	78.18	1,430	3,940	10,300	24,900	51,000	68,000	83,000	105,000	Uniform Rain
Palo Blanco Creek Below Comanche Creek	Palo_BlancoCk_ blw_ComancheC	822.94	2,000	6,250	17,800	51,700	126,000	186,000	248,000	345,000	Uniform Rain
Turkey Creek and Wood Slough	TurkeyCk+ Wood_Slough	111.93	1,380	3,190	9,480	26,100	56,000	76,000	95,000	120,000	Uniform Rain
Turkey Creek at Highway 57	TurkeyCk_at_ HWY-57	170.51	1,090	2,360	6,210	16,200	41,000	64,000	88,000	122,000	Uniform Rain
Turkey Creek above Chaparrosa Creek	TurkeyCk_abv_ _ChaparrosaCk	210.04	780	1,680	4,490	14,000	36,000	57,000	81,000	117,000	Uniform Rain
Chaparrosa Creek and Muela Creek	ChaparrosaCk+ MuelaCk	132.77	3,370	7,290	18,300	41,900	80,000	103,000	126,000	157,000	Uniform Rain
Chaparrosa Creek above Turkey Creek	ChaparrosaCk_ abv_TurkeyCk	204.55	1,120	2,980	9,800	26,300	63,000	93,000	122,000	161,000	Uniform Rain
Turkey Creek below Chaparrosa Creek	TurkeyCk_blw_ _ChaparrosaCk	414.59	1,730	3,800	13,000	35,800	87,000	129,000	174,000	248,000	Uniform Rain
Turkey Creek above Picosa Creek	TurkeyCk_abv_ _PicosaCk	459.10	1,070	2,710	8,800	25,700	60,000	88,000	124,000	179,000	Uniform Rain
Turkey Creek below Picosa Creek	TurkeyCk_blw_ _PicosaCk	1376.61	2,880	8,520	25,400	72,200	170,000	258,000	351,000	482,000	Uniform Rain
Turkey Creek at Highway 83 (New USGS gage)	TurkeyCk_at_ HWY-83	1554.98	2,640	6,070	19,800	61,600	158,000	242,000	334,000	461,000	Uniform Rain
Turkey Creek above Turkey Split	TurkeyCk_abv_ _Turkey_Split	1563.55	2,410	6,030	19,700	61,000	156,000	238,000	328,000	453,000	Uniform Rain
Turkey Creek below Turkey Split	TurkeyCk_blw_ _Turkey_Split	1568.83	3,260	11,400	24,900	67,900	165,000	248,000	341,000	499,000	Uniform Rain
Turkey Creek above Carrizo Creek	TurkeyCk_abv_ _CarrizoCk	1581.46	3,220	10,600	23,800	64,200	150,000	232,000	330,000	482,000	Uniform Rain

		AEP	50%	20%	10%	4%	2%	1%	0.5%	0.2%	
Location Description	HMS Element Name	Drainage Area (sq mi)	2-yr	5-yr	10-yr	25-yr	50-yr	100-yr	200-yr	500-yr	Method
Carrizo Creek at Highway 83	CazzinoCk_at_HWY-83	49.73	1,790	3,030	3,640	7,400	12,800	16,500	20,400	26,200	Uniform Rain
Turkey Creek below Carrizo Creek	TurkeyCk_blw_CarrizoCk	1662.70	3,930	10,600	23,900	64,700	152,000	233,000	333,000	486,000	Uniform Rain
Turkey Creek above El Barrosa Creek	TurkeyCk_abv_El_BarrosaCk	1687.81	3,900	9,400	21,300	61,900	142,000	227,000	320,000	463,000	Uniform Rain
Turkey Creek below El Barrosa Creek	TurkeyCk_blw_El_BarrosaCk	1718.21	4,630	9,400	21,400	62,000	142,000	227,000	321,000	464,000	Uniform Rain
Turkey Creek and El Moro Creek	TurkeyCk+El_MoroCk	1836.07	6,450	9,900	21,000	62,300	143,000	229,000	323,000	467,000	Uniform Rain
Turkey Creek above Nueces River	TurkeyCk_abv_NuecesRv	1847.03	5,280	9,000	20,700	62,200	143,000	228,000	323,000	466,000	Uniform Rain
Nueces River near Asherton (USGS gage 08193000)	NuecesRv_nr_Asherton	4024.67	5,620	10,900	24,900	66,500	149,000	237,000	333,000	478,000	Uniform Rain
Nueces River above Arroyo Negro	NuecesRv_abv_Arroyo_Negro	4213.49	5,810	10,900	24,800	66,200	147,000	232,000	325,000	465,000	Uniform Rain
Nueces River below Arroyo Negro	NuecesRv_blw_Arroyo_Negro	4333.02	5,980	11,000	24,900	66,700	148,000	233,000	327,000	467,000	Uniform Rain
Nueces River above Appurceon Creek	NuecesRv_abv_AppurceonCk	4333.02	5,900	11,000	24,800	66,100	146,000	230,000	322,000	460,000	Uniform Rain
Nueces River below Appurceon Creek	NuecesRv_blw_AppurceonCk	4411.17	5,950	11,000	24,900	66,400	147,000	231,000	323,000	461,000	Uniform Rain
Nueces River above San Roque Creek	NuecesRv_abv_San_RoqueCk	4488.43	5,780	11,000	24,700	65,200	143,000	224,000	312,000	444,000	Uniform Rain
San Roque Creek and Canyon Creek	San_RoqueCk+CanyonCk	255.77	3,650	11,100	14,500	28,800	41,000	55,000	69,000	90,000	Uniform Rain
San Roque Creek below Highway 83	San_RoqueCk_blw_HWY-83	333.91	3,550	10,900	14,300	28,500	40,000	54,000	69,000	90,000	Uniform Rain
San Roque Creek above Nueces River	SanRoqCk_abv_NuecesRV	415.48	3,250	10,000	13,100	26,300	37,000	51,000	65,000	84,000	Uniform Rain
Nueces River below San Roque Creek	NuecesRv_blw_San_RoqueCk	4903.91	6,150	15,600	25,300	66,700	146,000	227,000	317,000	450,000	Uniform Rain
Nueces River and Espio Creek	NuecesRv+EspioCk	5084.65	6,080	15,200	25,200	66,100	144,000	223,000	310,000	441,000	Uniform Rain

		AEP	50%	20%	10%	4%	2%	1%	0.5%	0.2%	
Location Description	HMS Element Name	Drainage Area (sq mi)	2-yr	5-yr	10-yr	25-yr	50-yr	100-yr	200-yr	500-yr	Method
Nueces River at Cotulla (USGS gage 08194000)	NuecesRv_at_Cotulla	5172.43	5,930	14,600	24,900	64,700	140,000	216,000	299,000	423,000	Uniform Rain
Nueces River above La Raices Creek	NuecesRv_abv_La_RaicesCk	5366.43	5,750	13,900	24,400	62,600	135,000	205,000	282,000	398,000	Uniform Rain
La Raices Creek at IH-35	La_RaicesCk_at_IH-35	175.31	560	2,500	6,040	14,100	24,700	33,900	43,200	56,100	Uniform Rain
La Raices Creek above Nueces River	La_RaicesCk_abv_NuecesRv	272.12	560	2,500	6,090	14,400	25,200	34,800	44,500	58,100	Uniform Rain
Nueces River below La Raices Creek	NuecesRv_blw_La_RaicesCk	5638.55	5,750	13,900	24,400	62,600	135,000	205,000	282,000	398,000	Uniform Rain
Nueces River above Calman Creek	NuecesRv_abv_CalmanCk	5705.26	5,670	13,700	24,200	61,600	132,000	200,000	274,000	386,000	Uniform Rain
Tecolote Creek and Chucareto Creek	TecoloteCk+ChucaretoCk	115.03	690	2,340	4,990	11,000	19,000	26,000	33,000	42,000	Uniform Rain
Calman Creek above Nueces River	CalmanCk_abv_NuecesRv	185.52	890	2,840	5,520	12,100	21,000	28,000	36,000	47,000	Uniform Rain
Nueces River below Calman Creek	NuecesRv_blw_CalmanCk	5890.78	5,680	13,700	24,200	61,700	132,000	200,000	274,000	387,000	Uniform Rain
Nueces River above Los Olmos Creek	NuecesRv_abv_Los_OlmosCk	5898.22	5,650	13,600	24,100	61,400	131,000	198,000	272,000	383,000	Uniform Rain
Carrizitos Creek above Venado Creek	CarrizitosCk_abv_VenadoCk	90.70	780	2,190	3,670	7,250	11,900	16,000	20,000	25,800	Uniform Rain
Los Olmos Creek and Carrizitos Creek	Los_OlmosCk+CarrizitosCk	322.57	1,720	6,100	12,100	26,700	46,000	62,000	78,000	101,000	Uniform Rain
Los Olmos Creek above TX-44	Los_OlmosCk_J010	403.09	1,700	5,900	11,500	25,100	43,100	58,900	74,600	97,100	Uniform Rain
Los Olmos Creek above Nueces River	Los_OlmosCk_abv_NuecesRv	455.53	1,660	5,600	10,800	23,600	40,500	55,200	70,100	91,400	Uniform Rain
Nueces River below Los Olmos Creek	NuecesRv_blw_Los_OlmosCk	6353.75	5,670	13,700	24,100	61,400	131,000	198,000	272,000	383,000	Uniform Rain
Nueces River and Sauz Creek	NuecesRv+ SauzCk	6419.66	5,640	13,600	24,000	61,100	131,000	197,000	270,000	380,000	Uniform Rain
Nueces River above San Casimiro Creek	NuecesRv_abv_San_CasimiroCk	6445.15	5,620	13,500	24,000	60,800	130,000	195,000	267,000	376,000	Uniform Rain

		AEP	50%	20%	10%	4%	2%	1%	0.5%	0.2%	
Location Description	HMS Element Name	Drainage Area (sq mi)	2-yr	5-yr	10-yr	25-yr	50-yr	100-yr	200-yr	500-yr	Method
Salado Creek and Gato Creek	SaladoCk+GatoC	170.00	800	3,300	7,800	17,300	24,600	33,100	42,300	53,500	Uniform Rain
Beccerra Creek and Pato Creek	BeccerraCk+PatoCk	105.24	1,870	5,100	9,400	17,800	23,800	30,900	37,900	47,500	Uniform Rain
San Casimiro Creek near Freer (USGS gage 08194200)	San_CasimiroCk_nr_Freer	467.65	2,310	7,800	16,300	33,600	46,500	62,000	78,600	100,000	Uniform Rain
San Casimiro Creek above Nueces River	San_CasimiroCk_abv_NuecesRv	537.34	2,150	7,300	15,100	31,100	43,100	57,600	73,200	93,600	Uniform Rain
Nueces River below San Casimiro Creek	NuecesRv_blw_San_CasimiroCk	6982.49	5,650	18,300	36,700	77,900	130,000	196,000	268,000	377,000	Uniform Rain
Nueces River above Black Creek	NuecesRv_abv_BlackCk	7007.66	5,630	18,000	35,900	76,300	130,000	195,000	266,000	374,000	Uniform Rain
Black Creek near Biel Lake	BlackCk_J010	282.58	1,760	6,030	12,000	25,600	43,000	57,600	72,600	92,800	Uniform Rain
Black Creek at Highway 44	BlackCk_at_HWY-44	373.84	1,760	5,990	11,900	25,300	42,600	57,300	72,700	94,200	Uniform Rain
Black Creek above Nueces River	BlackCk_abv_NuecesRv	423.47	1,670	5,600	11,000	23,400	39,500	53,400	68,100	88,700	Uniform Rain
Nueces River below Black Creek	NuecesRv_blw_BlackCk	7431.13	6,330	20,400	40,300	85,600	137,000	195,000	267,000	375,000	Uniform Rain
Nueces River above Ygnacio Creek	NuecesRv_abv_YgnacioCk	7611.07	6,180	19,700	38,200	80,600	130,000	188,000	256,000	359,000	Uniform Rain
Nueces River below Ygnacio Creek	NuecesRv_blw_YgnacioCk	7754.47	6,190	19,700	38,300	80,800	130,000	188,000	257,000	359,000	Uniform Rain
Nueces River above San Jose Creek	NuecesRv_abv_San_JoseCk	7754.47	6,170	19,600	38,100	80,400	129,000	188,000	256,000	358,000	Uniform Rain
Nueces River below San Jose Creek	NuecesRv_blw_San_JoseCk	7857.73	6,170	19,600	38,200	80,500	129,000	188,000	256,000	358,000	Uniform Rain
Nueces River above Green Branch	NuecesRv_abv_GreenBr	7857.73	6,140	19,500	37,900	79,800	128,000	187,000	254,000	356,000	Uniform Rain
Nueces River below Green Branch	NuecesRv_blw_GreenBr	7943.10	6,150	19,500	37,900	79,900	128,000	187,000	254,000	356,000	Uniform Rain
Nueces River near Tilden (USGS gage 08194500)	NuecesRv_nr_Tilden	8105.85	6,040	19,100	37,000	77,800	125,000	184,000	250,000	349,000	Uniform Rain

		AEP	50%	20%	10%	4%	2%	1%	0.5%	0.2%	
Location Description	HMS Element Name	Drainage Area (sq mi)	2-yr	5-yr	10-yr	25-yr	50-yr	100-yr	200-yr	500-yr	Method
Nueces River above Cow Creek	NuecesRv_abv_CowCk	8105.85	5,960	18,800	36,400	76,500	123,000	182,000	247,000	345,000	Uniform Rain
Nueces River below Cow Creek	NuecesRv_blw_CowCk	8182.92	5,960	18,800	36,400	76,600	123,000	182,000	247,000	345,000	Uniform Rain
Nueces River above Old River	NuecesRv_abv_OldRv	8275.85	5,830	18,400	35,500	74,500	121,000	179,000	243,000	339,000	Uniform Rain
Old River and Hill Creek	OldRv+HillCk	78.22	310	1,560	4,320	8,710	12,200	15,900	19,900	26,000	Uniform Rain
Nueces River below Old River	NuecesRv_blw_OldRv	8354.07	5,830	18,400	35,500	74,500	121,000	179,000	243,000	339,000	Uniform Rain
Nueces River and White Creek	NuecesRv+WhiteCk	8464.98	5,630	17,700	34,100	71,500	118,000	174,000	236,000	329,000	Uniform Rain
Nueces River above Atascosa River	NuecesRv_abv_AltascosaRv	8519.43	5,380	16,900	32,400	68,000	115,000	169,000	228,000	317,000	Uniform Rain
Frio River and East Frio River	FrioRv+East_FrioRv	96.68	4,670	16,000	27,200	41,900	55,000	68,000	81,000	98,000	Uniform Rain
Frio River at Leakey (USGS gage 08194840)	FrioRv_at_Leakey	235.06	6,840	27,600	49,300	81,500	108,000	135,000	160,000	196,000	Uniform Rain
Frio River at Concan (USGS gage 08195000)	FrioRv_at_Concan	389.64	7,960	33,300	60,200	103,400	142,000	181,000	219,000	272,000	Uniform Rain
Frio River above Dry Frio River	FrioRv_abv_Dry_FrioRv	441.57	7,150	30,800	55,700	95,700	132,000	170,000	207,000	259,000	Uniform Rain
Dry Frio River near Reagan Wells (USGS gage 08196000)	Dry_FrioRv_nr_Reagan_Wells	124.55	3,510	15,200	30,000	53,000	71,000	89,000	107,000	132,000	Uniform Rain
Dry Frio River at FM 2690 (USGS gage 08196300)	Dry_FrioRv_at_FM_2690	176.10	2,790	14,000	27,900	50,500	69,000	88,000	107,000	135,000	Uniform Rain
Dry Frio River above Frio River	Dry_FrioRv_abv_FrioRv	187.17	2,490	13,100	26,100	47,500	65,000	84,000	102,000	129,000	Uniform Rain
Frio River below Dry Frio River	FrioRv_blw_Dry_FrioRv	628.74	9,220	42,400	79,300	138,900	192,000	248,000	303,000	380,000	Uniform Rain
Frio River near Uvalde (USGS gage 08197500)	FrioRv_nr_Uvalde	633.06	8,590	39,800	74,500	130,700	181,000	234,000	286,000	359,000	Uniform Rain

		AEP	50%	20%	10%	4%	2%	1%	0.5%	0.2%	
Location Description	HMS Element Name	Drainage Area (sq mi)	2-yr	5-yr	10-yr	25-yr	50-yr	100-yr	200-yr	500-yr	Method
Frio River above Blanco Creek	FrioRv_abv_BlancoCk	745.82	4,150	27,000	52,000	94,400	131,000	173,000	217,000	276,000	Uniform Rain
Blanco Creek at Highway 90	BlancoCk_at_HWY-90	64.51	310	1,790	3,910	12,800	24,900	35,100	45,000	57,800	Uniform Rain
Blanco Creek above Frio River	BlancoCk_abv_FrioRv	133.59	210	990	2,440	9,100	18,600	26,900	35,500	47,400	Uniform Rain
Frio River below Blanco Creek	FrioRv_blw_BlancoCk	879.41	4,240	27,300	52,800	98,000	140,000	186,000	234,000	299,000	Uniform Rain
Sabinal River near Vanderpool (USGS gage 08197936)	SabinalRv_nr_Vanderpool	55.75	4,070	9,800	16,400	31,300	46,000	56,000	67,000	81,000	Uniform Rain
Sabinal River at Utopia (USGS gage 08197970)	SabinalRv_at_Utopia	129.54	6,430	16,600	27,400	50,600	77,000	97,000	116,000	143,000	Uniform Rain
Sabinal River near Sabinal (USGS gage 08198000)	SabinalRv_nr_Sabinal	205.92	6,590	18,400	31,300	59,500	92,000	118,000	144,000	179,000	Uniform Rain
Sabinal River at Sabinal (USGS gage 08198500)	SabinalRv_at_Sabinal	240.56	6,080	18,000	31,000	58,600	91,000	117,000	143,000	180,000	Uniform Rain
Rancheros Creek and Elm Creek	RancherosCk +ElmCk	79.64	430	1,180	2,190	7,060	13,800	19,600	25,800	34,200	Uniform Rain
Sabinal River and Rancheros Creek	SabinalRv + RancherosCk	333.99	5,410	16,800	29,300	58,800	95,000	125,000	156,000	198,000	Uniform Rain
Sabinal River above East Elm Creek	SabinalRv_abv_East_ElmCk	398.47	4,810	15,200	27,000	55,300	91,000	121,000	151,000	194,000	Uniform Rain
Sabinal River below East Elm Creek	SabinalRv_blw_East_ElmCk	446.58	4,830	15,200	27,000	55,700	92,000	123,000	154,000	198,000	Uniform Rain
Sabinal River above Frio River	SabinalRv_abv_FrioRv	459.21	4,490	14,300	25,500	52,600	87,000	117,000	147,000	190,000	Uniform Rain
Frio River below Sabinal River	FrioRv_blw_SabinalRv	1338.62	7,010	27,100	52,800	103,600	158,000	212,000	269,000	351,000	Uniform Rain
Frio River above Elm Creek	FrioRv_abv_ElmCk	1411.00	4,800	23,900	45,600	91,000	145,000	204,000	264,000	346,000	Uniform Rain
Frio River below Elm Creek	FrioRv_blw_ElmCk	1499.66	4,810	23,900	45,700	92,000	147,000	208,000	269,000	354,000	Uniform Rain

		AEP	50%	20%	10%	4%	2%	1%	0.5%	0.2%	
Location Description	HMS Element Name	Drainage Area (sq mi)	2-yr	5-yr	10-yr	25-yr	50-yr	100-yr	200-yr	500-yr	Method
Frio River above Hondo Creek	FrioRv_abv_HondoCk	1514.24	4,670	22,300	43,800	90,500	145,000	206,000	267,000	352,000	Uniform Rain
Hondo Creek near Tarpley (USGS gage 8200000)	HondoCk_nr_Tarpley	96.07	4,840	20,000	37,600	63,100	81,000	100,000	118,000	143,000	Uniform Rain
Hondo Creek at Hwy 173 nr Hondo, TX (USGS Gage 08200720)	HondoCk_at_HWY-173	156.45	5,180	19,900	36,000	61,100	80,000	102,000	122,000	150,000	Uniform Rain
Hondo Creek above Verde Creek	HondoCk_abv_VerdeCk	160.76	3,890	13,900	24,900	42,600	57,000	73,000	88,000	109,000	Uniform Rain
Middle Verde Ck at SH 173 nr Bandera (USGS gage 08200977)	M_Verde_at_SH173_nr Bandera	38.90	1,180	2,900	6,300	16,600	29,000	38,000	46,000	56,000	Uniform Rain
Middle Verde Creek and East Verde Creek	M_VerdCk+E_VerdeCk	57.54	1,090	2,330	5,130	14,200	25,700	35,100	43,600	54,300	Uniform Rain
Verde Creek below Quihi Creek	VerdeCk_blw_QuihiCk	143.13	1,190	1,870	3,110	9,700	18,600	26,100	33,500	43,600	Uniform Rain
Hondo Creek below Verde Creek	HondoCk_blw_VerdeCk	379.80	4,480	14,700	27,400	54,300	81,000	107,000	133,000	168,000	Uniform Rain
Hondo Creek and Live Oak Creek	HondoCk+ Live_OakCk	521.81	3,710	11,300	21,400	45,800	72,700	99,100	126,000	163,000	Uniform Rain
Hondo Creek above Seco Creek	HondoCk_abv_SecoCk	666.04	2,890	8,700	16,700	37,500	61,200	84,600	109,000	142,000	Uniform Rain
Seco Creek at Miller RH near Utopia (USGS gage 08201500)	SecoCk_at_MillerRh_nr_Utopia	45.05	2,430	11,600	25,400	44,600	55,000	66,000	77,000	93,000	Uniform Rain
Seco Creek and Rocky Creek	SecoCk+RockyCk	131.94	3,280	19,400	37,600	64,300	83,000	104,000	124,000	153,000	Uniform Rain
Seco Creek Rowe RH near D'Hanis (USGS gage 08201500)	SecoCk_RoweRh_nr_D'Hanis	165.15	2,990	17,000	32,500	54,700	72,000	90,000	109,000	135,000	Uniform Rain
Seco Creek above Squirrel Creek	SecoCk_abv_SquirrelCk	267.24	1,220	7,630	15,400	27,300	38,000	49,900	61,700	78,700	Uniform Rain
Seco Creek above Hondo Creek	SecoCk_abv_HondoCk	353.95	900	5,670	11,600	21,000	29,800	39,400	49,000	62,900	Uniform Rain

		AEP	50%	20%	10%	4%	2%	1%	0.5%	0.2%	
Location Description	HMS Element Name	Drainage Area (sq mi)	2-yr	5-yr	10-yr	25-yr	50-yr	100-yr	200-yr	500-yr	Method
Hondo Creek below Seco Creek	HondoCk_blw_SecoCk	1019.99	3,650	13,900	27,400	57,000	88,700	121,000	154,000	201,000	Uniform Rain
Hondo Creek above Frio River	HondoCk_abv_FrioRv	1106.85	3,400	12,800	25,400	53,500	84,100	115,000	147,000	193,000	Uniform Rain
Frio River below Hondo Creek	FrioRv_blw_HondoCk	2621.10	8,010	26,900	52,200	109,700	182,000	248,000	324,000	429,000	Uniform Rain
Frio River above Leona River	FrioRv_abv_LeonaRv	2675.30	5,850	25,600	49,500	107,200	180,000	244,000	321,000	427,000	Uniform Rain
Leona River above Taylor Slough	LeonaRv_abv_Taylor_Slough	49.67	300	1,100	1,330	3,450	9,100	13,400	18,200	24,600	Uniform Rain
Leona River below Taylor Slough	LeonaRv_blw_Taylor_Slough	68.61	420	1,510	2,220	5,570	13,700	19,600	26,100	35,000	Uniform Rain
Leona River above Cooks Slough	LeonaRv_abv_Cooks_Slough	68.61	410	1,470	2,150	5,390	13,300	19,100	25,400	34,100	Uniform Rain
Leona River below Cooks Slough	LeonaRv_blw_Cooks_Slough	102.62	470	1,850	2,690	7,560	19,800	29,000	38,700	52,100	Uniform Rain
Leona River near Uvalde (USGS gage 08204005)	LeonaRv_nr_Uvalde	131.15	520	2,020	3,240	9,040	23,300	34,000	45,400	61,300	Uniform Rain
Leona River above Camp Lake Slough	LeonaRv_abv_Camp_Lake_Slough	196.04	450	1,720	2,910	8,920	23,000	33,800	45,400	61,800	Uniform Rain
Leona River below Camp Lake Slough	LeonaRv_blw_Camp_Lake_Slough	234.02	450	1,750	3,050	9,730	24,800	36,400	48,900	66,600	Uniform Rain
Leona River at Highway 57 (USGS gage)	LeonaRv_at_HWY-57	240.99	470	1,850	2,690	7,560	19,800	29,000	38,700	52,100	Uniform Rain
Leona River above Live Oak Creek	LeonaRv_abv_LiveoakCk	380.41	390	1,500	2,740	9,510	23,800	34,900	47,200	64,700	Uniform Rain
Leona River below Live Oak Creek	LeonaRv_blw_LiveoakCk	460.74	400	1,520	2,820	10,540	24,900	36,700	49,600	68,000	Uniform Rain
Leona River above Todos Santos Creek	LeonaRv_abv_Todos_SantosCk	585.22	370	1,400	2,660	10,950	26,000	38,400	51,800	71,500	Uniform Rain
Leona River below Todos Santos Creek	LeonaRv_blw_Todos_SantosCk	660.74	370	1,400	2,670	11,260	26,900	39,700	53,500	73,700	Uniform Rain
Leona River above Frio River	LeonaRv_abv_FrioRv	670.08	360	1,380	2,640	11,130	26,600	39,200	52,900	73,000	Uniform Rain

		AEP	50%	20%	10%	4%	2%	1%	0.5%	0.2%	
Location Description	HMS Element Name	Drainage Area (sq mi)	2-yr	5-yr	10-yr	25-yr	50-yr	100-yr	200-yr	500-yr	Method
Frio River below Leona River	FrioRv_blw_LeonaRv	3345.37	6,190	26,800	51,900	117,400	204,000	283,000	373,000	500,000	Uniform Rain
Frio River near Derby (USGS gage 08215500)	FrioRv_nr_Derby	3447.76	6,190	26,800	51,900	117,500	204,000	286,000	378,000	506,000	Uniform Rain
Frio River at Highway 85	FrioRv_at_HWY-85	3500.89	4,750	24,100	49,000	113,900	200,000	277,000	361,000	488,000	Uniform Rain
Frio River and Ruiz Creek	FrioRv+RuizCk	3653.55	3,930	20,100	42,800	107,700	195,000	273,000	354,000	475,000	Uniform Rain
Frio River above Cibolo Creek	FrioRv_abv_CiboloCk	3698.16	3,450	15,300	34,300	100,200	188,000	266,000	347,000	466,000	Uniform Rain
Cibolo Creek at Highway 85	CiboloCk_at_HWY-85	83.21	740	1,320	4,940	7,780	12,700	18,600	24,800	33,600	Uniform Rain
Cibolo Creek at Purple Heart Trail	CiboloCk_at_Purple_Heart_Trl	174.41	690	1,320	5,760	9,270	15,500	22,900	33,900	47,500	Uniform Rain
Cibolo Creek above Frio River	CiboloCk_abv_FrioRv	394.76	1,680	3,200	9,100	13,700	21,600	31,500	41,900	56,800	Uniform Rain
Frio River below Cibolo Creek	FrioRv_blw_CiboloCk	4092.91	3,500	15,400	36,000	104,000	195,000	275,000	358,000	479,000	Uniform Rain
Frio River above Esperanz Creek	FrioRv_abv_EsperanzaCk	4149.39	3,180	12,500	30,600	95,400	186,000	266,000	348,000	466,000	Uniform Rain
Frio River below Esperanza Creek	FrioRv_blw_EsperanzaCk	4248.12	3,180	12,500	30,600	95,400	186,000	266,000	348,000	466,000	Uniform Rain
Frio River and Galinda Creek	FrioRv+GalindaCk	4337.72	3,060	11,200	26,500	87,100	176,000	255,000	336,000	452,000	Uniform Rain
Frio River above Leoncita Creek	FrioRv_abv_LeoncitaCk	4396.25	3,000	10,700	24,700	81,500	168,000	246,000	325,000	439,000	Uniform Rain
Frio River at Tilden (USGS gage 08206600)	FrioRv_at_Tilden	4462.81	3,000	10,700	24,700	81,500	168,000	246,000	325,000	439,000	Uniform Rain
Frio River above San Miguel Creek	FrioRv_abv_San_MiguelCk	4519.46	3,000	10,700	24,600	80,700	166,000	243,000	322,000	436,000	Uniform Rain
San Miguel Creek above Black Creek	SanMiguelCk_abv_BlackCk	221.57	1,760	5,250	8,610	15,400	22,000	28,700	35,800	47,000	Uniform Rain
San Miguel Creek below Black Creek	SanMiguelCk_blw_BlackCk	348.53	2,280	8,110	13,800	25,300	36,700	47,600	59,400	77,000	Uniform Rain

		AEP	50%	20%	10%	4%	2%	1%	0.5%	0.2%	
Location Description	HMS Element Name	Drainage Area (sq mi)	2-yr	5-yr	10-yr	25-yr	50-yr	100-yr	200-yr	500-yr	Method
San Miguel Creek below Highway 97	SanMiguelCk_blw_HWY-97	516.77	2,180	7,360	13,000	25,300	38,500	51,200	74,600	108,000	Uniform Rain
San Miguel Creek above Lagunillas Creek	SanMiguelCk_abv_LagunillasCk	574.60	2,140	7,210	12,700	24,800	37,700	50,100	66,600	98,000	Uniform Rain
San Miguel Creek below Lagunillas Creek	SanMiguelCk_blw_LagunillasCk	741.44	2,400	8,630	16,500	32,200	49,500	65,500	81,100	118,000	Uniform Rain
San Miguel Creek near Tilden (USGS gage 08206700)	SanMiguelCk_nr_Tilden	782.15	2,960	8,930	15,900	31,200	48,200	63,900	79,900	114,000	Uniform Rain
San Miguel Creek above Frio River	SanMiguelCk_abv_FrioRv	854.80	2,870	8,810	15,300	30,600	47,700	65,100	82,300	113,000	Uniform Rain
Frio River below San Miguel Creek	FrioRv_blw_San_MiguelCk	5374.26	3,780	10,800	24,900	81,400	169,000	248,000	330,000	445,000	Uniform Rain
Choke Canyon Reservoir Inflow	ChokeCanyon_Inflow	5490.45	5,530	11,500	24,900	81,500	169,000	249,000	330,000	445,000	Uniform Rain
Choke Canyon Dam Outflows	Choke Canyon Dam	5490.45	2,510	10,300	23,400	74,100	154,000	187,000	214,000	255,000	Uniform Rain
Frio River below Choke Canyon Dam	ChokeCanyonRes_OWC_nr_3Rv	5490.45	2,510	10,300	23,400	74,100	154,000	187,000	214,000	255,000	Uniform Rain
Frio River above Atascosa River	FrioRv_abv_AtascosaRv	5496.36	2,510	10,300	23,400	74,100	154,000	187,000	214,000	255,000	Uniform Rain
Atascosa River near FM 2904	AtascosaRv_J010	154.50	1,070	5,000	9,200	15,800	22,000	29,000	37,000	47,000	Uniform Rain
Atascosa River at FM 476 (USGS gage 08207290)	AtascosaRv_at_FM-476	315.12	1,280	6,300	11,300	20,700	30,700	42,500	55,300	74,600	Uniform Rain
Atascosa River at Highway 37	AtascosaRv_at_HWY-37	451.31	1,440	7,100	13,800	25,300	37,000	51,000	65,800	87,600	Uniform Rain
Atascosa River near McCoy (USGS gage 08207500)	AtascosaRv_nr_McCoy	510.87	1,250	6,600	13,000	24,800	36,800	52,000	68,100	91,900	Uniform Rain
Atascosa River above Borrego Creek	AtascosaRv_abv_BorregoCk	535.96	1,220	6,350	12,700	24,100	36,100	51,200	67,400	91,500	Uniform Rain
Borrego Creek and Los Cortes Creek	BorregoCk+Los_CortesCk	142.92	1,460	5,140	8,830	14,600	20,000	26,300	32,700	42,700	Uniform Rain

		AEP	50%	20%	10%	4%	2%	1%	0.5%	0.2%	
Location Description	HMS Element Name	Drainage Area (sq mi)	2-yr	5-yr	10-yr	25-yr	50-yr	100-yr	200-yr	500-yr	Method
Borrego Creek above Atascosa River	BorregoCk_abv_AtascosaRv	221.19	1,700	4,540	8,260	14,800	21,400	29,400	37,800	52,400	Uniform Rain
Atascosa River below Borrego Creek	AtascosaRv_blw_BorregoCk	757.15	1,950	8,690	17,800	33,500	50,000	72,000	95,000	129,000	Uniform Rain
Atascosa River above La Parita Creek	AtascosaRv_abv_La_ParitaCK	813.17	2,080	8,470	17,100	32,500	48,000	70,000	93,000	128,000	Uniform Rain
La Parita Creek and Metate Creek	La_ParitaCk+MetateCk	291.40	2,410	7,660	12,900	21,400	29,600	39,000	48,700	63,600	Uniform Rain
La Parita Creek above Atascosa River	La_PartacK_abv_AtascosaRV	311.40	2,260	7,290	12,300	20,600	29,200	38,700	48,400	63,300	Uniform Rain
Atascosa River below La Parita Creek	AtascosaRv_blw_La_PartacK	1124.57	4,300	12,200	20,800	39,900	60,000	88,000	119,000	167,000	Uniform Rain
Atascosa River at Whitsett (USGS gage 0820800)	AtascosaRv_at_Whitsett	1145.77	4,140	12,200	20,500	39,800	60,000	88,000	118,000	166,000	Uniform Rain
Atascosa River above Weedy Creek	AtascosaRv_abv_WeedyCk	1225.28	4,050	11,300	20,200	39,200	59,000	85,700	116,000	163,000	Uniform Rain
Atascosa river below Weedy Creek	AtascosaRv_blw_WeedyCk	1364.40	4,130	11,500	21,000	39,700	60,000	87,600	119,000	169,000	Uniform Rain
Atascosa River above Frio River	AtascosaRv_abv_FrioRv	1395.61	4,100	10,800	20,500	39,300	59,400	86,500	117,000	167,000	Uniform Rain
Atascosa River below Frio River	AtascosaRv_blw_FrioRv	6891.97	6,000	19,900	37,600	81,100	166,000	200,000	230,000	328,000	Uniform Rain
Atascosa River above Nueces River	AtascosaRv_abv_NuecesRv	6911.11	6,000	19,800	37,400	80,700	165,000	200,000	229,000	326,000	Uniform Rain
Nueces River below Atascosa River	NuecesRv_blw_AtascosaRv	15430.54	7,800	26,600	56,700	122,400	207,000	279,000	367,000	465,000	Uniform Rain
Nueces River at Three Rivers (USGS gage 08210000)	NuecesRv_at_Three_Rivers	15430.54	7,790	26,600	56,600	122,300	207,000	278,000	367,000	465,000	Uniform Rain
Nueces River and Sulphur Creek	NuecesRv+SulhpurCk	15619.12	7,730	26,300	56,100	122,200	206,000	277,000	366,000	457,000	Uniform Rain
Nueces River at Highway 59	NuecesRv_at_HWY-59	15715.07	7,600	26,100	55,500	121,900	205,000	275,000	365,000	456,000	Uniform Rain

		AEP	50%	20%	10%	4%	2%	1%	0.5%	0.2%	
Location Description	HMS Element Name	Drainage Area (sq mi)	2-yr	5-yr	10-yr	25-yr	50-yr	100-yr	200-yr	500-yr	Method
Nueces River above Spring Creek	NuecesRv_abv_SpringCk	15733.03	7,580	26,100	55,500	121,900	205,000	275,000	364,000	456,000	Uniform Rain
Nueces River below Spring Creek	NuecesRv_blw_SpringCk	15833.59	7,580	26,100	55,500	122,000	205,000	275,000	364,000	456,000	Uniform Rain
Nueces River and Upper End of Lake Corpus Christi	NuecesRv+UpEnd_LkCorpusChris	15921.68	7,530	25,900	55,300	121,900	205,000	274,000	364,000	456,000	Uniform Rain
Nueces River above Lake Corpus Christi	NuecesRv_abv_LkCorpusCh	16076.35	7,090	24,500	52,400	115,900	195,000	260,000	345,000	433,000	Uniform Rain
Lagarto Creek near George West (USGS gage 08210400)	LagartoCk_nr_George_West	155.28	450	4,080	9,420	16,600	22,300	29,600	37,100	48,100	Uniform Rain
Lagarto Creek above Lake Corpus Christi	LagartoCk_abv_LkCorpusCh	201.87	330	3,470	8,870	16,400	22,800	31,400	40,000	52,600	Uniform Rain
Ramirena Creek at Highway 281	RamirenaCk_at_HWY-281	81.02	590	3,810	8,400	14,400	19,100	24,700	30,300	38,500	Uniform Rain
Ramirena Creek above Lake Corpus Christi	RamirenaCk_abv_LkCorpusCh	119.60	400	4,100	9,600	16,500	22,300	30,100	38,300	50,700	Uniform Rain
Lake Corpus Christi Inflow	Lk_Corpus_Christi_Inflow	16502.10	7,090	24,500	52,500	116,000	195,000	260,000	345,000	433,000	Uniform Rain
Lake Corpus Christi Dam Outflow	Corpus Christi Dam	16502.10	7,060	24,400	52,300	115,400	191,000	257,000	338,000	428,000	Uniform Rain
Nueces River near Mathis (USGS gage 08211000)	NuecesRv_nr_Mathis	16502.10	7,060	24,400	52,300	115,400	191,000	257,000	338,000	428,000	Uniform Rain
Nueces at Bluntzer (USGS gage 08211200)	NuecesRv_at_Bluntzer	16617.60	6,800	23,700	51,000	112,800	186,000	251,000	330,000	419,000	Uniform Rain
Nueces River at Calallen (USGS gage 08211500)	NuecesRv_at_Calallen	16675.30	5,800	22,000	46,400	105,400	175,000	235,000	309,000	392,000	Uniform Rain

**Table 6.9: Peak Reservoir Pool Elevations (feet NAVD88) from the HEC-HMS Uniform Rainfall Frequency Storms**

Location Description	HMS Element Name	Drainage Area (sq mi)	50% AEP	20% AEP	10% AEP	4% AEP	2% AEP	1% AEP	0.5% AEP	0.2% AEP	Hydrologic Method
			2-yr	5-yr	10-yr	25-yr	50-yr	100-yr	200-yr	500-yr	
Choke Canyon Reservoir	Choke Canyon Dam	5490.45	221.1	221.4	221.8	223.3	225.3	229.0	234.5	243.5	Uniform Rain
Lake Corpus Christi	Corpus Christi Dam	16502.10	93.9	94.1	94.3	95.1	96.1	97.8	99.9	101.9	Uniform Rain

### 6.6.3 Uniform Rainfall Frequency Results versus Drainage Area

As a quality check, the peak flows results from the 1% AEP uniform rainfall frequency storms were plotted versus drainage area and outliers were examined, as shown in Figure 6.26. The relative trends in this graph generally make sense. For example, the peak discharges per square mile are highest for the steep headwater reaches of the Nueces, Frio, and Sabinal Rivers along with Hondo and Seco Creeks. Peak discharges on the Atascosa River, on the other hand, tend to be lower relative to their drainage areas as they are located in the middle portion of the basin, which is drier and flatter. The reaches with the highest peak discharges of the entire basin occurred on the Nueces River above Uvalde. This should be expected since USGS stream gages in this area have recorded peak flows of over 600,000 cfs.

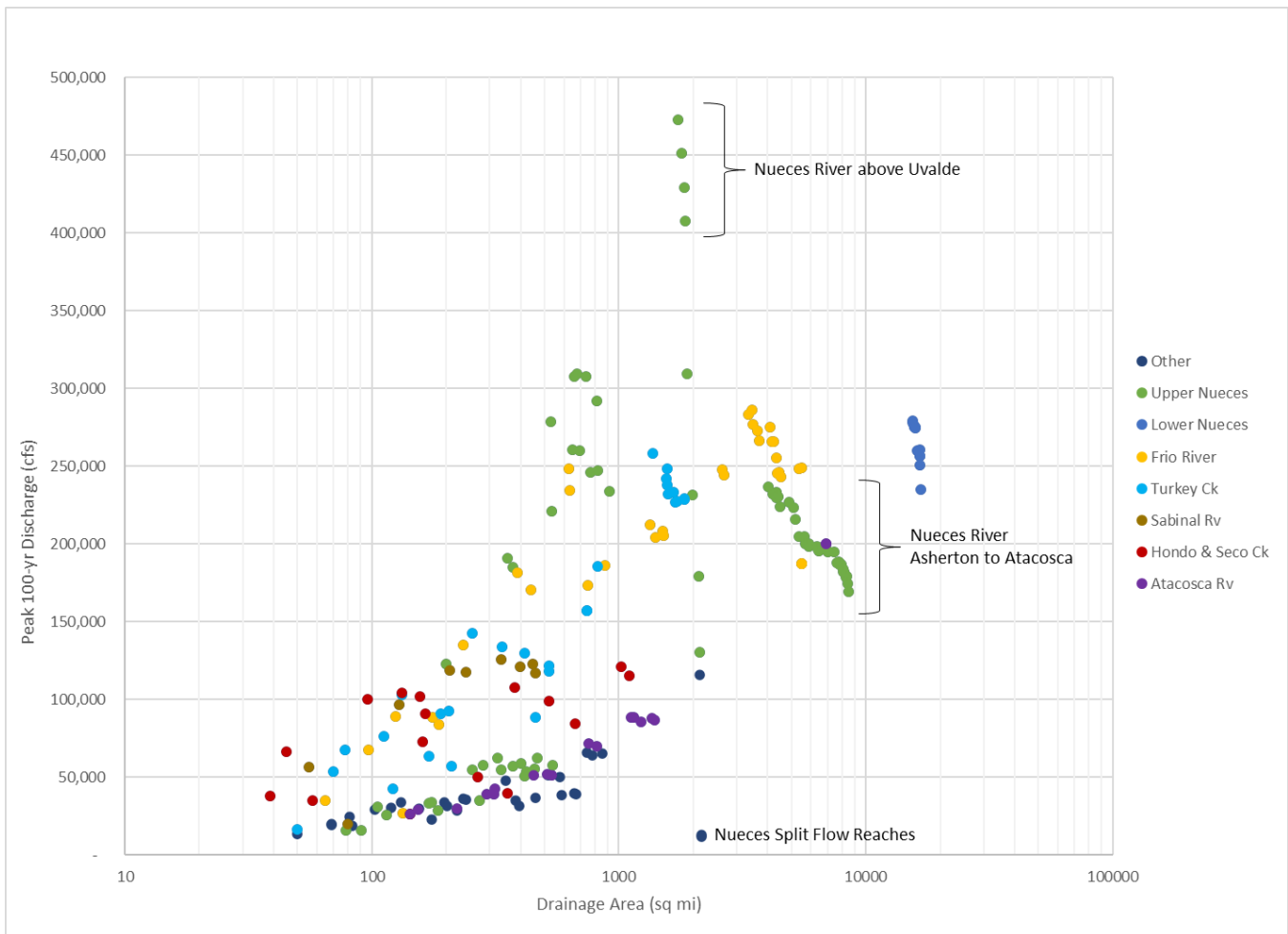


Figure 6.33: NA14 1% AEP Uniform Rain Frequency Storm Results versus Drainage Area

This figure shows that the analyzed junctions followed generally expected patterns of increasing peak flow with drainage area, with some notable exceptions. For example, the observed peak discharges on the Nueces River tend to decrease between the USGS gages at Uvalde and Asherton. Just below Uvalde, the landscape of the

Nueces watershed sharply transitions from steep, narrow valleys to wide, flat irrigated fields. This causes decreasing frequency peak discharges as flood waters spread out into the floodplain and the hydrograph becomes dampened as it moves downstream. In addition, the Nueces River cross several major aquifer outcrops in this area which divert flow from surface water to groundwater. Downstream of Asherton, the peak flows on the Nueces River continue to decrease due to routing attenuation and differences in timing between the main stem and its smaller tributaries. This type of routing attenuation is also observed along the lower Frio and Nueces Rivers.

## 7 Elliptical Frequency Storms in HEC-HMS

### 7.1 INTRODUCTION TO ELLIPTICAL STORMS

Observations of actual storm events show that average precipitation intensity decreases as the area of a storm increases (Meyers, 1980) (Asquith, 2000). The uniform rainfall method results (documented in the previous chapter and Appendix B) use the depth-area analysis in HEC-HMS to produce frequency peak flow estimates (Version 4.4; USACE, 2018). The depth-area analysis in HEC-HMS applies the appropriate depth-area reduction factor to the given point rainfall depths based on the drainage area at a given evaluation point, which are derived from the published depth-area reduction factors from Figure 15 of the National Weather Service TP-40 publication (Hershfield, 1961), as shown in the figure below.

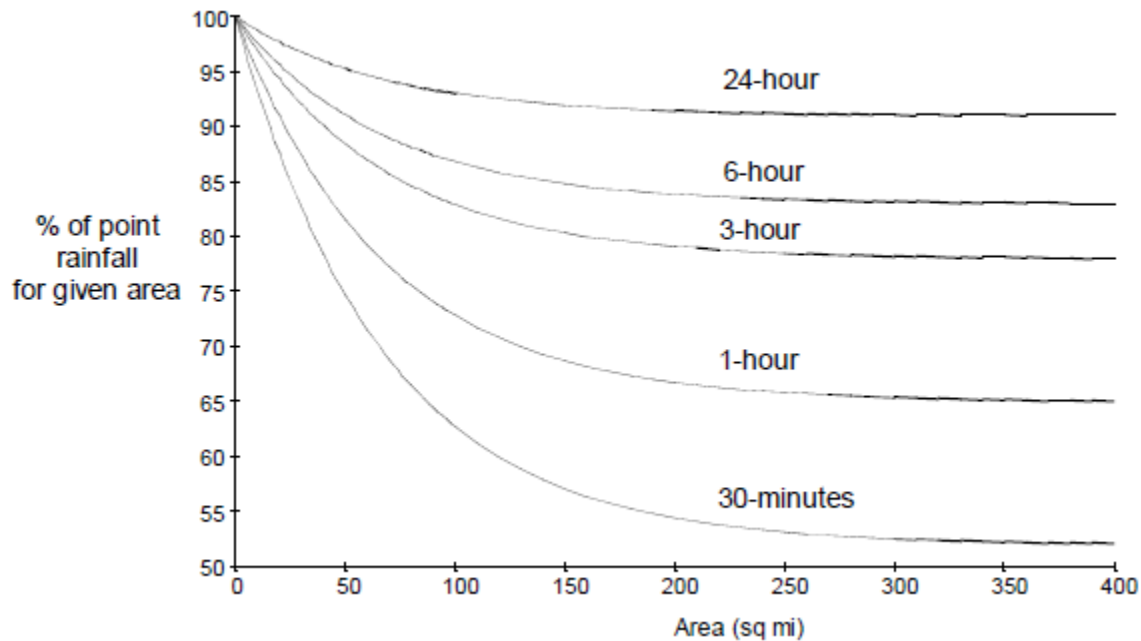


Figure 7.1: Published Depth-Area Reduction Curves from TP-40

When evaluating a stream location with a drainage area greater than 400 square miles, the HEC-HMS software issues a warning that the NWS depth-area reduction factors do not support storms beyond 400 square miles, as seen in the figure above. The program will still calculate the peak discharge, but the warning implies that the calculated volume of the storm may be overestimated for larger drainage areas.

Since the Nueces hydrology study involves calculating frequency discharges for points with over 10,000 square miles of drainage area, the InFRM team developed elliptical frequency storms for gage points and junctions with drainage areas greater than 400 square miles. In these elliptical frequency storms, the same point rainfall depths and durations were applied as in the uniform rainfall method, but the spatial distribution of the rainfall varied in an elliptical shaped pattern with higher rainfall amounts in the center of the ellipse and lesser amounts towards the outer fringes.

Elliptical shaped storms have been used in a variety of hypothetical design applications, including the Probable Maximum Precipitation (PMP) storms from Hydrometeorological Report No 52 (HMR 52) (Hansen, 1982). The elliptical frequency storms constructed for this study are similar to those of HMR 52 in that concentric ellipses are used to construct the storm's spatial pattern, and the storm's location is optimized over the watershed by identifying the storm center location and the angle of its major axis that led to a maximum peak flow at a downstream junction of interest. As an example watershed, Figure 7.2 shows an example of an elliptical 1%

annual exceedance probability (100-yr) storm that was optimized over the watershed above the Frio River above Atascosa gage.

This chapter provides a general summary of the methods and results from the elliptical frequency storm analyses that were completed for the InFRM Watershed Hydrology Assessment of the Nueces River Basin, but additional details on the development and application of the elliptical frequency storms are available in Appendix C: Elliptical Frequency Storms in HEC-HMS.

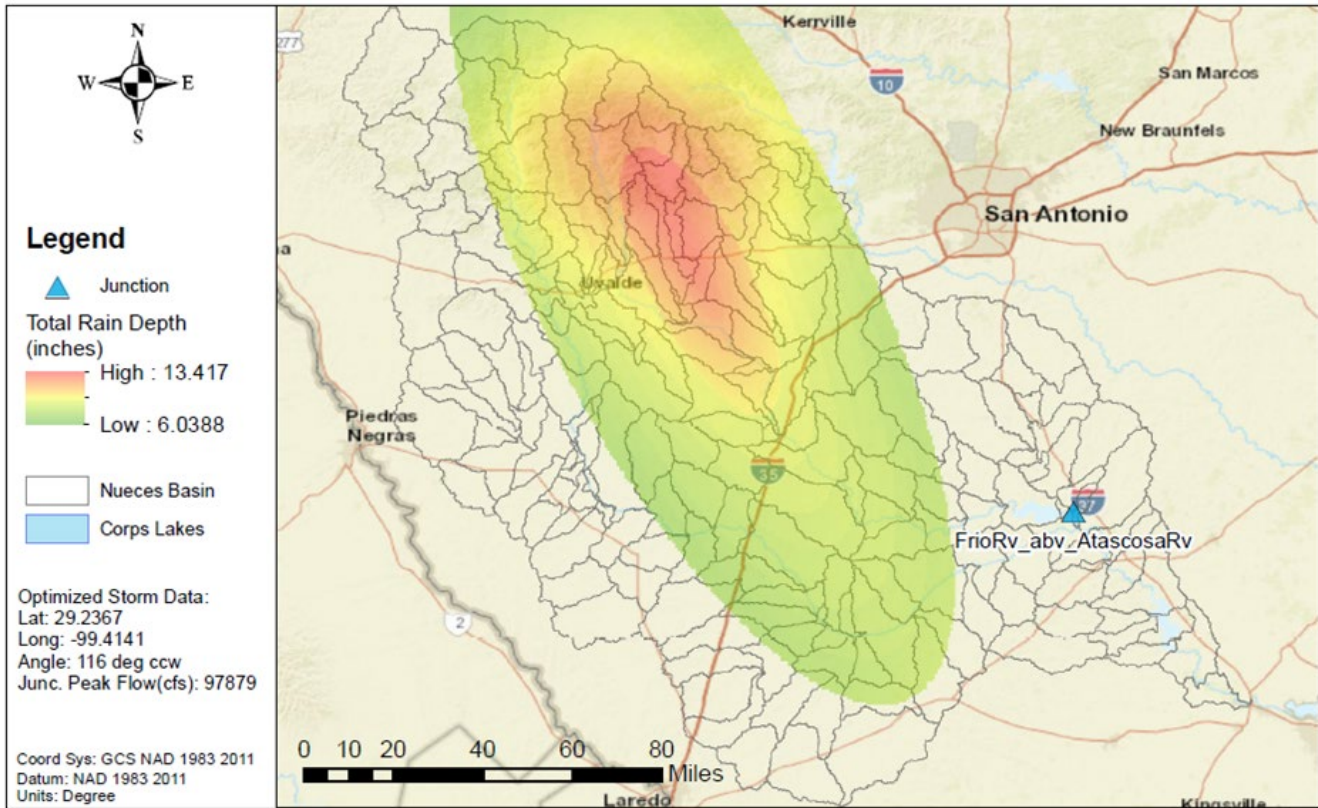


Figure 7.2: Example 1% AEP (100-yr) Elliptical Frequency Storm

## 7.2 ELLIPTICAL STORM PARAMETERS AND METHODOLOGY

The elliptical storm parameters covered below in sections 7.2.1 through 7.2.5 are applicable to the entire Nueces Basin. Unique, optimized elliptical storm configurations were developed for 76 different junction elements within the Nueces HEC-HMS model, 15 of which were USGS stream gage locations.

When comparing the upper reaches of the Nueces Basin with the middle and downstream portions closer to the Gulf of Mexico, the meteorology is noticeably different as demonstrated below in Figure 7.3. The meteorological distinctions across the Nueces River basin were addressed in the sampling of the point precipitation depths and in the development of the depth-area-reduction curves (covered in depth in sections 7.2.3 and 7.2.4, respectively).

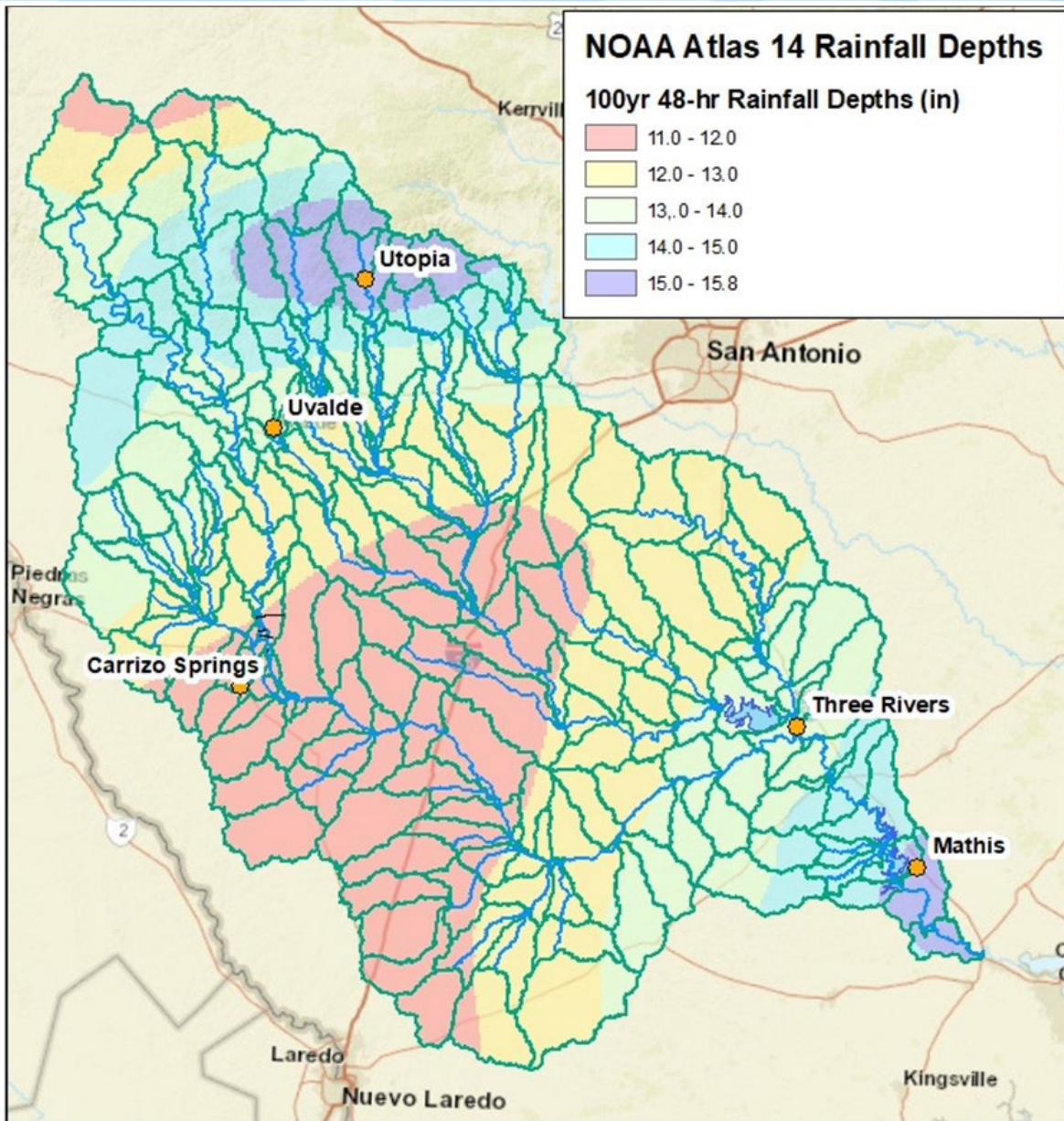


Figure 7.3: NOAA Atlas 14 100-yr 96-hr Precipitation Gradient – Nueces River Basin

## 7.2.1 Elliptical Storm Area

This study uses a storm extent of 10,000 square miles. This is due, in part, to historical rainfall studies rarely including data beyond 10,000 square miles (USACE, 1945). However, many of the more recent, historic storm events analyzed in southeast Texas for this study did extend to 10,000 square miles and beyond in coverage. While this storm extent is somewhat arbitrary, testing was done in previous InFRM studies to limit the storm extent to 3,000 square miles or increase it to 20,000 square miles and the resulting peak discharges were only slightly altered. This is likely because the most intense portion of the storm, which drives the peak discharges on the rivers, occurs within the central 1,000 square miles of the storm. Therefore, even though the drainage area of the Nueces River study area is over 17,000 square miles, a 10,000 square mile storm area was adopted as it produced reasonable and realistic results compared to observed storms.

## 7.2.2 Storm Ellipse Ratio

The HMR-52 study presents the option to design a storm with a major: minor ellipse axis ratio ranging from 2:1 to 3:1. For the final results, a 2.5:1 ellipse was used, as it matched well with the general shape of the Nueces basin. A 3:1 ellipse was tested in several sections within the Nueces basin which led to only nominal differences in regard to optimized storm centerings, storm orientations, and resulting peak flows when compared to the results obtained from using a 2.5:1 ellipse.

## 7.2.3 Elliptical Storm Rainfall Depths

Elliptical storms were designed for each of the following annual exceedance probabilities (AEP): 1 in 2 years, 1 in 5 years, 1 in 10 years, 1 in 25 years, 1 in 50 years, 1 in 100 years, 1 in 200 years and 1 in 500 years. Point rainfall depths and durations were applied directly from NOAA Atlas 14 Volume 11 which contains depth duration frequency estimates of precipitation for the state of Texas (NOAA, 2018). The point precipitation values that were applied to each elliptical storm were based on the storm's optimized location, not the location of the outlet of interest. It is important to note that out of all the design storm parameters that are discussed here, peak flows were most sensitive to adjustments in the NOAA Atlas 14 point frequency depths.

For the Nueces basin, since the precipitation gradient varies significantly across the basin, all of the precipitation depths that fell under the 10,000 sq mi elliptical storm positioning were queried instead of just the one depth at the storm center. Then all of the queried precipitation depths were reduced based on which of the concentric, DAR ellipses they overlapped with (demonstrated in Figure 7.6). In regions where the precipitation depths vary greatly over a short distance, this method performs better since the precipitation gradient is reflected in the makeup of the elliptical storm.

## 7.2.4 Storm Depth Area Reduction (DAR) Factors

The Texas Storm Study (TSS) was completed during the Nueces InFRM WHA and represented a historic breakthrough in DAR factor research. The project analyzed nearly 20,000 storms and measured the DAR curves for each storm. Through analysis of storms and regional weather patterns, the study developed 3 zones that had similar DAR curve characteristics. From the Texas Storm Study, the appropriate DAR curves zone for the Nueces Basin is the Eastern Zone. See Figure 7.4 below.

Note: the Texas Storm Study refers to Depth-Area-Reduction Factors as DARFs but this report will continue to use DAR Curves or DAR factors to be consistent with prior InFRM WHA Studies. There are a few terms used throughout literature on the subject and a few different ways the data can be collected and applied. The Texas Storm Study performed a literature review of the subject and for more information, see the Texas Storm Study on the InFRM Website. <https://webapps.usgs.gov/infrm/>

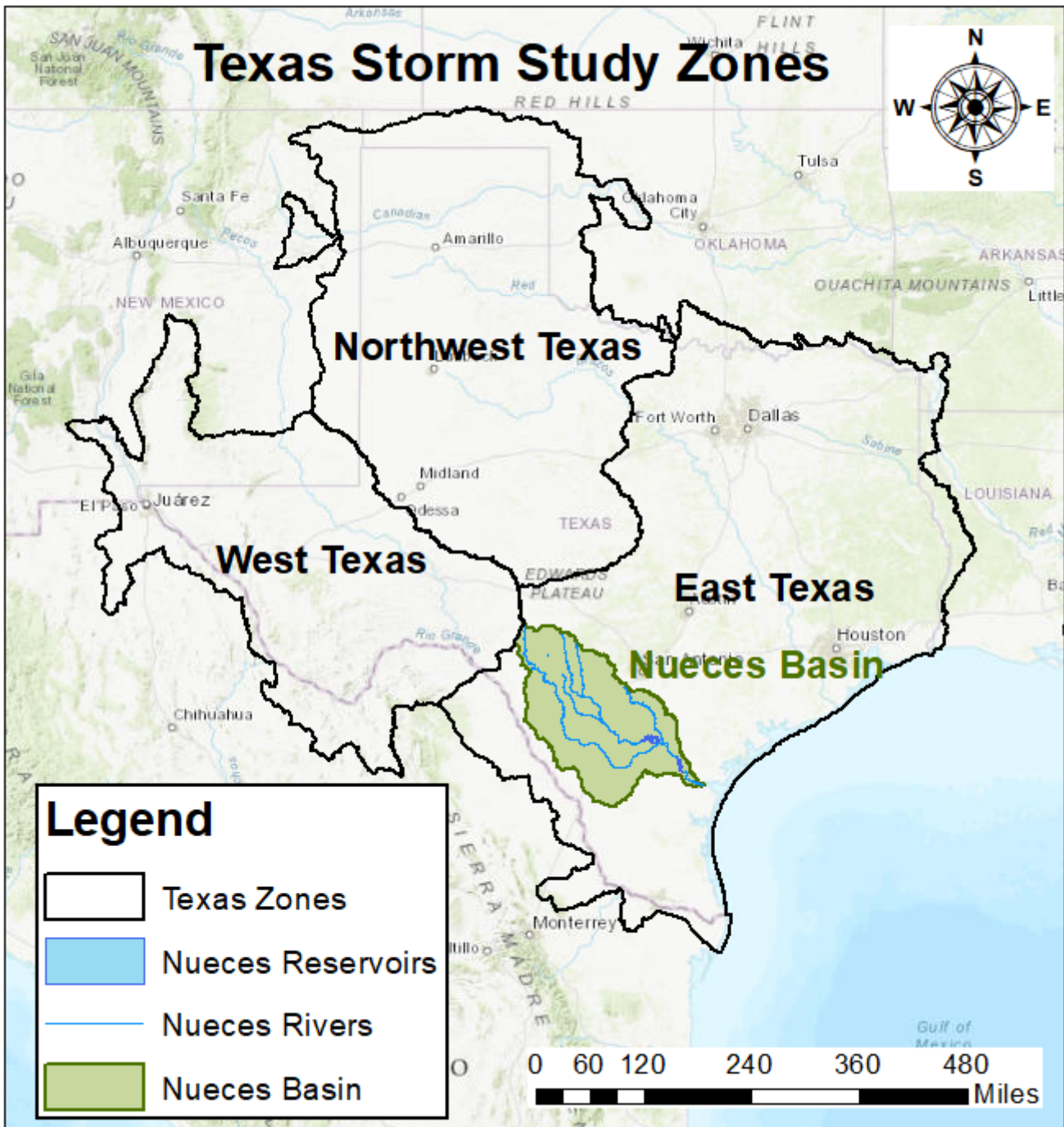


Figure 7.4: Texas Storm Study DAR Factor Zones and the Nueces Basin

The Texas Storm Study found a general relationship between Storm Return Period and DAR curves – the more intense the storm, i.e., the longer the return period, the faster the DAR curve reduces at larger areas. The TSS developed DAR curves for 3 ranges of Return Periods, 2-yr to 50-yr, 50-yr, to 200-yr, and greater than 200-yr. For this study, the 2-yr, 5-yr, 10-yr, and 25-yr elliptical storms utilized the ‘2-yr to 50-yr’ DAR curves, the 50-yr, and 100-yr elliptical storms utilized the ‘50-yr to 200-yr’ DAR curves, and the 200-yr to 500-yr elliptical storm utilized the ‘greater than 200-yr’ DAR curves.

The TSS also developed DAR curves for many storm durations and for areas up to 10,000 square miles. The study provided recommended DAR curves for 1-hr, 2-hr, 3-hr, 6-hr, 12-hr, 24-hr, and 48-hr durations in the East Texas Zone as seen in Figure 7.5.

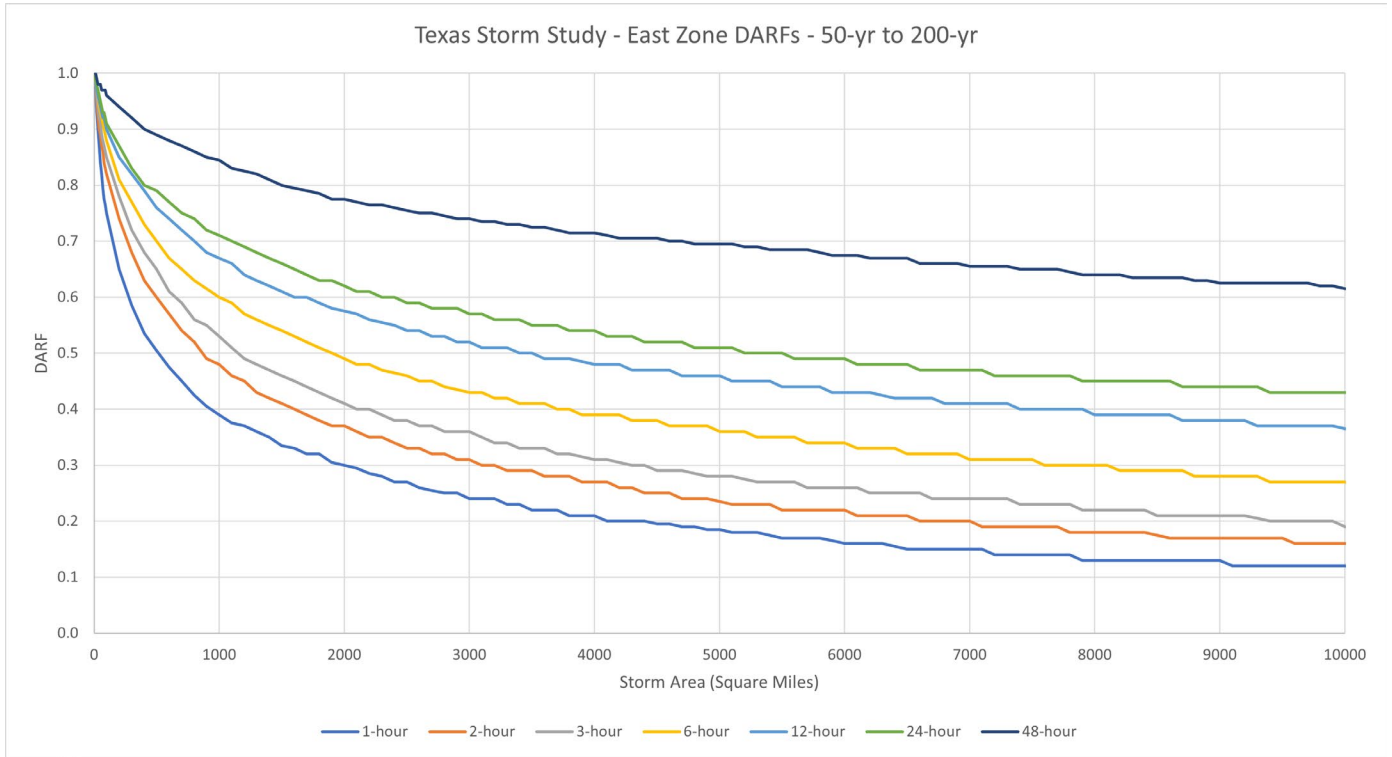


Figure 7.5: Texas Storm Study DAR Factors for the East Texas Zone

The InFRM WHA team utilized all 7 duration DAR factors for each elliptical storm, creating a dynamic storm that emulates an intense storm observed in nature. A total of 21 DAR factor relationships were used, all 7 durations for all 3 return period groups.

Table 7.1: East Texas Zone DAR Factors for Return Periods 2-Yr to 50-Yr

East Texas Zone DARFs							
Area (Sq. Mi.)	2-Yr to 50-yr Return Period						
	1-Hr	2-Hr	3-Hr	6-Hr	12-Hr	24-Hr	48-Hr
1	1.00	1.00	1.00	1.00	1.00	1.00	1.00
10	0.98	0.98	0.98	0.99	0.99	0.99	1.00
100	0.81	0.84	0.86	0.88	0.91	0.94	0.96
200	0.73	0.77	0.79	0.83	0.87	0.91	0.94
300	0.67	0.72	0.74	0.79	0.84	0.88	0.92
400	0.63	0.68	0.71	0.76	0.81	0.86	0.90
500	0.60	0.65	0.68	0.74	0.79	0.85	0.89
600	0.57	0.62	0.66	0.72	0.78	0.84	0.88
700	0.54	0.60	0.64	0.70	0.76	0.82	0.87
800	0.52	0.58	0.62	0.68	0.75	0.81	0.87
900	0.50	0.57	0.60	0.67	0.74	0.80	0.86
1,000	0.49	0.55	0.59	0.65	0.73	0.80	0.85
2,000	0.37	0.44	0.48	0.57	0.65	0.73	0.81
3,000	0.31	0.38	0.42	0.51	0.60	0.69	0.78
4,000	0.27	0.34	0.38	0.47	0.57	0.66	0.75
5,000	0.24	0.30	0.35	0.44	0.54	0.64	0.74
6,000	0.22	0.28	0.32	0.41	0.52	0.62	0.72
7,000	0.20	0.26	0.30	0.39	0.50	0.60	0.70
8,000	0.19	0.24	0.28	0.37	0.48	0.59	0.69
9,000	0.18	0.23	0.27	0.36	0.46	0.57	0.68
10,000	0.17	0.22	0.26	0.34	0.45	0.56	0.67

Table 7.2: East Texas Zone DAR Factors for Return Periods 50-Yr to 200-Yr

East Texas Zone DARFs							
Area (Sq. Mi.)	50-Yr to 200-yr Return Period						
	1-Hr	2-Hr	3-Hr	6-Hr	12-Hr	24-Hr	48-Hr
1	1.00	1.00	1.00	1.00	1.00	1.00	1.00
10	0.98	0.98	0.98	0.99	0.99	0.99	1.00
100	0.81	0.82	0.85	0.88	0.90	0.91	0.96
200	0.73	0.74	0.78	0.81	0.85	0.87	0.94
300	0.67	0.68	0.72	0.77	0.82	0.83	0.92
400	0.63	0.63	0.68	0.73	0.79	0.80	0.90
500	0.60	0.60	0.65	0.70	0.76	0.79	0.89
600	0.57	0.57	0.61	0.67	0.74	0.77	0.88
700	0.54	0.54	0.59	0.65	0.72	0.75	0.87
800	0.52	0.52	0.56	0.63	0.70	0.74	0.86
900	0.50	0.49	0.55	0.62	0.68	0.72	0.85
1,000	0.49	0.48	0.53	0.60	0.67	0.71	0.85
2,000	0.37	0.37	0.41	0.49	0.58	0.62	0.78
3,000	0.31	0.31	0.36	0.43	0.52	0.57	0.74
4,000	0.27	0.27	0.31	0.39	0.48	0.54	0.72
5,000	0.24	0.24	0.28	0.36	0.46	0.51	0.70
6,000	0.22	0.22	0.26	0.34	0.43	0.49	0.68
7,000	0.20	0.20	0.24	0.31	0.41	0.47	0.66
8,000	0.19	0.18	0.22	0.30	0.39	0.45	0.64
9,000	0.18	0.17	0.21	0.28	0.38	0.44	0.63
10,000	0.17	0.16	0.19	0.27	0.37	0.43	0.62

Table 7.3: East Texas Zone DAR Factors for Return Periods Greater than 200-Yr

East Texas Zone DARFs							
Area (Sq. Mi.)	Greater than 200-Yr Return Period						
	1-Hr	2-Hr	3-Hr	6-Hr	12-Hr	24-Hr	48-Hr
1	1.00	1.00	1.00	1.00	1.00	1.00	1.00
10	0.97	0.97	0.97	0.98	0.99	0.99	1.00
100	0.72	0.77	0.79	0.85	0.87	0.88	0.95
200	0.60	0.67	0.71	0.77	0.82	0.82	0.93
300	0.54	0.59	0.64	0.72	0.78	0.78	0.91
400	0.51	0.54	0.58	0.68	0.75	0.76	0.89
500	0.46	0.51	0.55	0.66	0.72	0.74	0.88
600	0.42	0.48	0.53	0.63	0.70	0.72	0.87
700	0.39	0.46	0.51	0.61	0.68	0.70	0.86
800	0.38	0.44	0.49	0.59	0.66	0.69	0.85
900	0.36	0.42	0.48	0.57	0.64	0.67	0.84
1,000	0.35	0.41	0.46	0.55	0.63	0.66	0.83
2,000	0.25	0.31	0.35	0.44	0.52	0.58	0.77
3,000	0.21	0.25	0.30	0.38	0.46	0.52	0.74
4,000	0.18	0.21	0.26	0.33	0.41	0.47	0.71
5,000	0.16	0.19	0.23	0.30	0.38	0.43	0.69
6,000	0.15	0.17	0.20	0.27	0.36	0.40	0.66
7,000	0.13	0.16	0.19	0.25	0.33	0.38	0.65
8,000	0.12	0.15	0.17	0.23	0.32	0.36	0.63
9,000	0.11	0.14	0.16	0.22	0.30	0.34	0.61
10,000	0.10	0.13	0.15	0.20	0.29	0.33	0.59

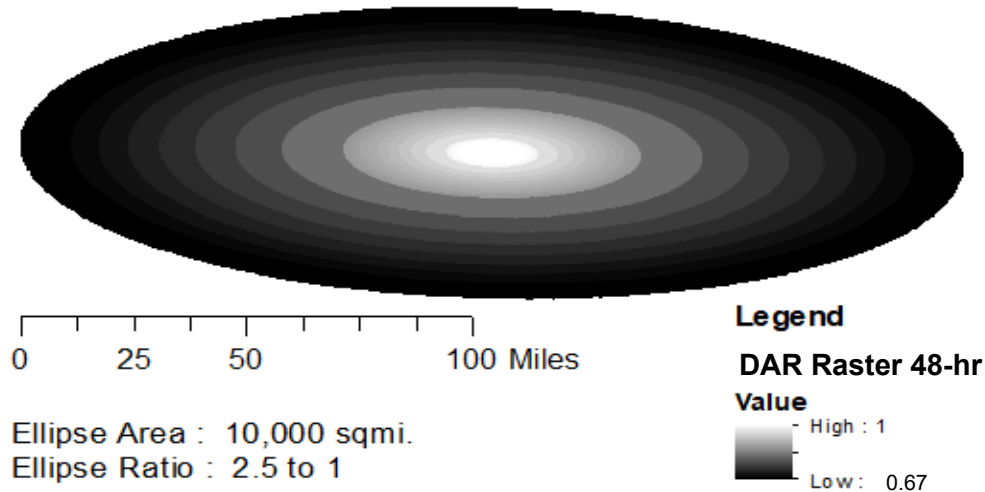


Figure 7.6: Adopted Depth-Area-Reduction Rasterized Ellipse for the 48-hr Duration

### 7.2.5 Storm Temporal Pattern / Hyetograph

Historically, storms have varying intensities and temporal distributions and many studies have been done to document storm patterns. The six storm temporal distributions that were tested for a previous InFRM study on the Guadalupe Basin are shown in Figure 7.7. The Soil Conservation Service (1986) documented different distributions for the United States. Type II is the distribution applicable to Texas; it was included in the testing. Other distributions were also previously tested, including the alternating block Frequency Rainfall temporal distributions from HEC-HMS with the storm centroid occurring at the 25%, 33%, 50%, 67%, and 75% of the total distribution. The HEC-HMS Frequency Rainfall alternating block temporal distributions maintain the appropriate storm intensity for all durations throughout the storm. In other words, the 100 year, 1 hour rainfall depth is maintained within the 100 year, 2 hour rainfall depth and so on all the way through the 100 year, 48 hour rainfall depth. For this Nueces watershed study, a centrally distributed (50%) alternating block temporal distribution was adopted for the final runs.

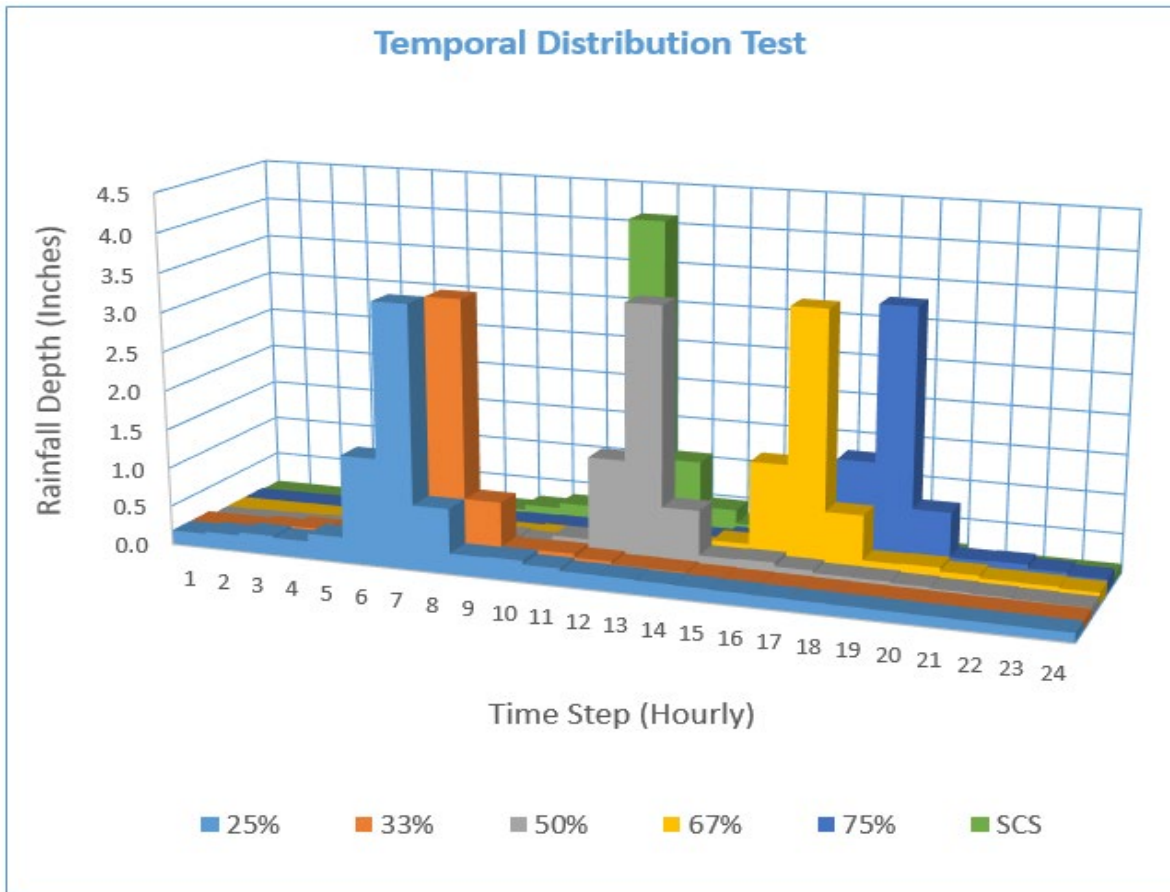


Figure 7.7: Previously Tested Storm Temporal Distributions

During the uniform rainfall analysis covered in Appendix B, storm durations ranging from 24 hours to 7 days were tested on the Nueces basin. A duration of 48-hours was ultimately adopted for the uniform rainfall modeling. The 48-hour results yielded slightly higher peak flows when compared to the 24 hour results, but the difference in peak flows tapered off to less than 1% for durations greater than 48-hours. Furthermore, the 48-hour duration also coincides well with the maximum duration of the Texas Storm Study. In order to be consistent with the uniform rain and with the Texas Storm Study, a 48-hour storm duration was adopted for the elliptical storm modeling on the Nueces.

## 7.2.6 Geospatial Process for Building the Elliptical Storms

For this Nueces InFRM Watershed Hydrology Assessment, a previously developed geospatial method was utilized for creating the rainfall hyetographs that were used as input into the Nueces design storm HEC-HMS model. This new method is built on three principal sources of geospatial data: 1) NOAA Atlas 14 precipitation frequency raster data in ascii format for the 1, 2, 3, 6, 12, 24, and 48-hour durations, 2) rasterized DAR ellipses that are built off of the adopted DAR curves for each of these durations, and 3) a HEC-HMS subbasin delineated shapefile. For each unique storm location and orientation within the Nueces basin, the underlying precipitation data is queried and multiplied by the appropriate rasterized DAR ellipse to get the reduced precipitation for each duration (Figure 7.8). Then zonal statistics are calculated to determine the average reduced precipitation for each subbasin. Using the subbasin-averaged reduced precipitation for the 1, 2, 3, 6, 12, 24, and 48-hour durations, the alternating block method is used to build rainfall hyetographs for each of the subbasins within the design storm HEC-HMS model.

The geospatial algorithm employed builds the storm from the central, maximum intensity duration outwards so that the appropriate storm intensity is maintained throughout the entire storm. For example, the 100 year 1 hour rainfall is maintained within the 100 year 2 hour rainfall and so forth all the way out to 48-hours.

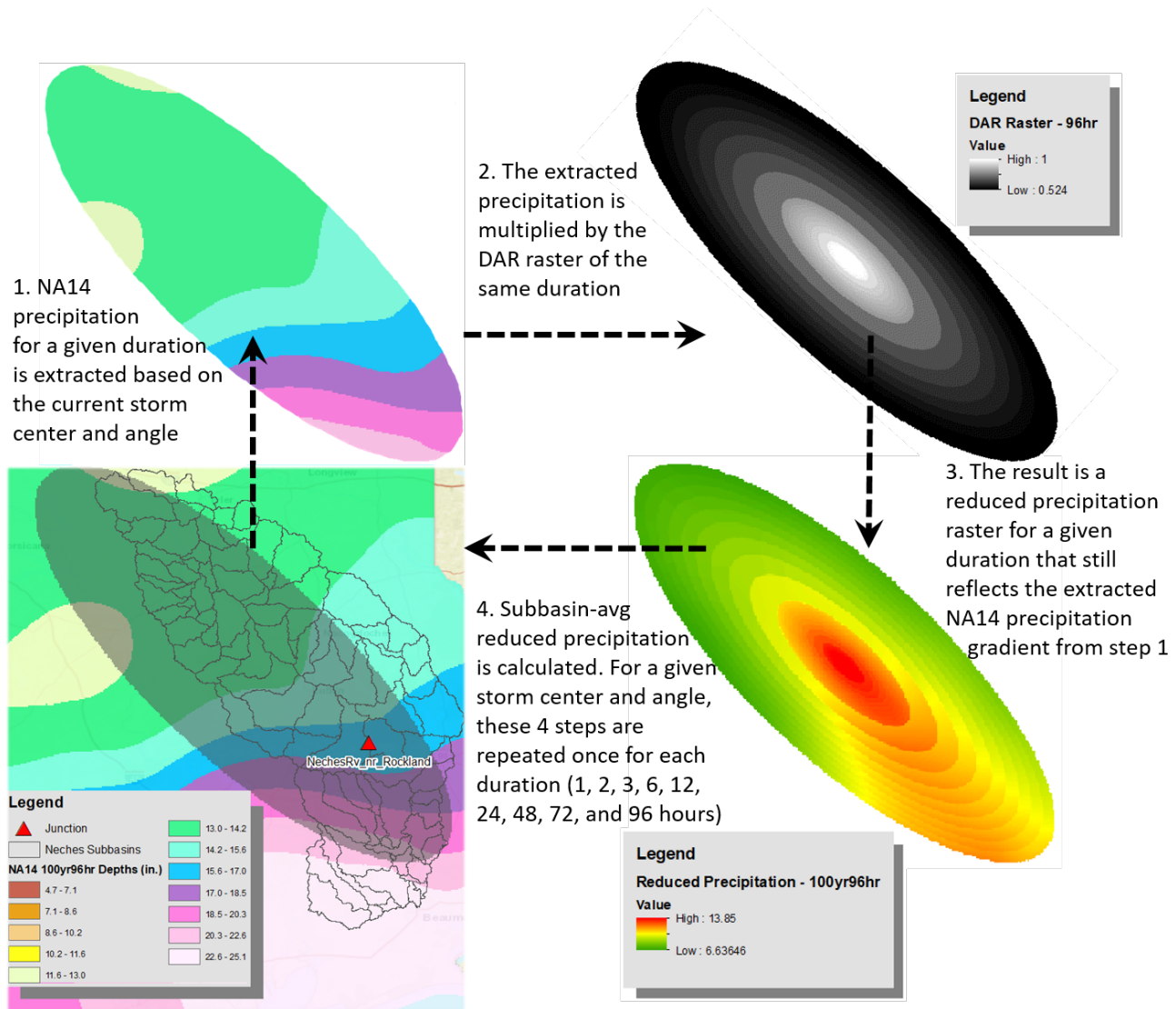


Figure 7.8 Geospatial Process for Building Elliptical Design Storms

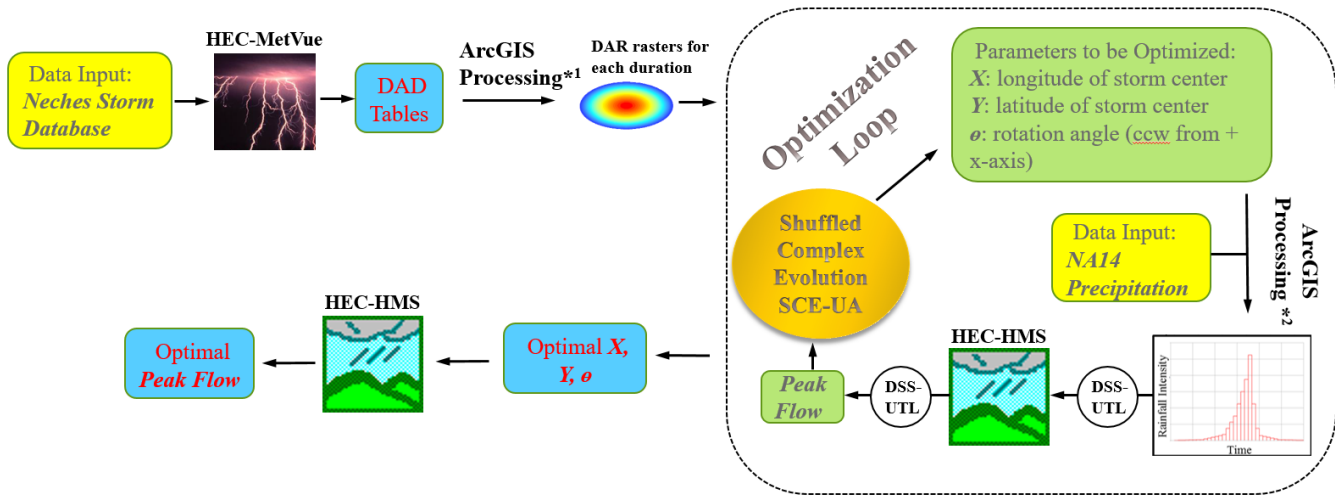
### 7.3 OPTIMIZATION OF THE STORM CENTER LOCATION

For the InFRM Watershed Hydrology Assessments, a script was developed by the University of Texas at Arlington that automatically locates optimal centering locations (x and y) and rotations ( $\theta$ ) of spatially varied elliptical frequency storms for a list of receiving junctions in an HMS basin model. The script was expected to obtain the combination of the three parameters (x, y, and  $\theta$ ) that maximized either peak flow at desired junctions or reservoir pool elevations while achieving the following objectives:

- To complete the task efficiently.
- To allow users to customize the scripts easily based on their needs.
- To generate reasonable results that can be validated manually.
- To outperform the manual grid search method in terms of precision, accuracy and efficiency.

- To function normally on any machine at USACE with the available software and hardware.

The ArcPy Python library, part of Esri's ArcGIS software package, was leveraged for all geospatial operations. The "Optimization Loop" section of Figure 7.8 below illustrates the schematic flow of the storm optimization script. The loop consists of two major components: 1) parameter update/optimization and 2) automatic simulation of the HEC-HMS hydrologic model. In each iteration of the optimization process, the rasterized DAR ellipses for each duration are rotated and shifted to align with the updated parameters ( $x$ ,  $y$ , and  $\theta$ ) and then are applied to the corresponding NOAA Atlas 14 precipitation rasters to create spatially reduced rainfall for each storm duration. The spatially reduced depths are then allocated into each subbasin as mean areal precipitation (MAP). The subbasin MAP values for each duration are then manipulated using the alternating block method to create a complete time series. The time series MAP values, i.e. the hyetographs, are stored in DSS format and transmitted to the HMS model for simulations. After each simulation, the corresponding peak flow value at a desired junction is extracted from the output DSS file. Based on the extracted peak flow value, an optimization algorithm will update the parameters ( $x$ ,  $y$  and  $\theta$ ) and then optimization proceeds into the next iteration. After all optimization iterations for a junction are complete, an optimized storm center ( $x$  and  $y$ ) and orientation ( $\theta$ ) that leads to a peak flow at a given junction is determined. The optimization process can then be repeated for the next junction of interest.



\*1. involves creating rasterized ellipses for each NA14 duration with DAR values of 1 in the center, and decreasing values towards the outer rings.

\*2. involves rotating and shifting each DAR raster, reducing the NA14 precipitation rasters, and calculating zonal statistics for each subbasin.

**Figure 7.9: Schematic Flowchart for the Storm Optimization Script**

Originally, the scripts were designed to automate a grid search, where all possible combinations of parameters (i.e., the 'grids') are exhaustively tested and the optimal combination of the three parameters ( $x$ ,  $y$ , and  $\theta$ ) can then be obtained. Although the approach of grid search seems straightforward, it does suffer from high computational cost because the computational run time depends on the number of grids, which is further constrained by the range and the interval of each parameter. Given the need of maintaining a certain level of precision or keeping constant intervals of the parameters, the UTA team found that the grid search approach might not be appropriate for this project since the computational run time was excessively lengthy – it increases exponentially with greater drainage area (more possible  $x$  and  $y$  values).

In order to overcome this issue, the UTA team selected a global optimization (GO) algorithm entitled shuffled complex evolution (SCE) (Duan et al., 1993) - a random sampling approach. Instead of exhausting all possible grids, the random sampling approach tests the objective function around some sampled grids in an iteration while learning about the structure of the objective function for improving the sampling of grids in the next iteration. More details about GO and SCE are included in the following sections.

### 7.3.1 Global Optimization

The objective of global optimization (GO) is to find the best solution of (possibly nonlinear) models globally, in the (possible or known) presence of multiple local optima. As an example, Figure 7.9 shows a 3-D plot of a continuous objective function of two bounded parameters  $x$  and  $y$ . Suppose the goal is to locate the minimal value globally instead of just locally (Note there are many local minimal values but with only one global minimum value in the chart), a global search in the two-dimensional box region is needed. The theory of GO has been applied to many engineering problems like model calibrations and optimal operations of “black box” systems. The storm optimization here is essentially a constrained GO problem, where the objective is to seek the combination of storm centering locations and rotations yielding the maximal peak flow within the constraints of the possible parameter values.

The level of difficulty in solving a GO problem depends on several major characteristics of the objective function. First, there may be multiple local minima in the parameter space. As illustrated in Figure 7.9, the search of global minimum can be easily “trapped” in the “valleys” of the objective function, depending on the starting point of the search. Second, the objective function in the parameter space may not be smooth or even continuous. In addition, the parameters may exhibit varying degrees of highly nonlinear interaction. In order to deal with these difficulties, the UTA team employed the shuffled complex evolution algorithm (see the following section), which has proven to be effective and efficient for the storm optimization task.

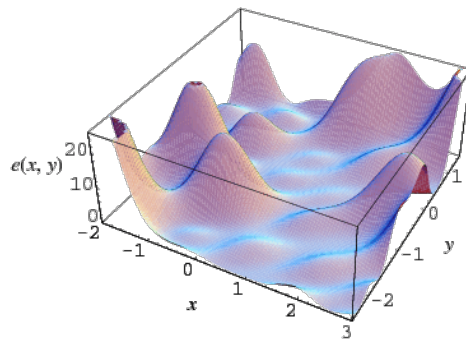


Figure 7.10: Example of a Global Optimization Problem

### 7.3.2 Shuffled Complex Evolution

The shuffled complex evolution works on the basis of four concepts: (1) combination of deterministic and probabilistic approaches; (2) systematic evolution of a complex of grids; (3) competitive evolution; and (4) complex shuffling. The algorithm begins with a randomly selected population of grids from the parameter space. The grids are sorted ascendingly so that the first point represents the smallest value of the objective function and the last point represents the largest. The initial population generated randomly is first partitioned into several complexes. Each complex is allowed to evolve independently to search the parameter space in different dimensions; and each individual grid in a complex has the potential to participate in the process of reproducing new grids. From each complex, some grids are selected to form a sub-complex, where the modified Nelder and Mead Simplex Method (NMSM) (Nelder and Mead, 1965) is applied for global improvement. The grids of higher fitness values have a higher chance of getting selected to generate offspring. The NMSM performs reflection and inside contraction steps to achieve a better fit grid. This new offspring then replaces the grid with the worst performance in the complex. The grids in the evolved complexes are then pooled together and sorted again, shuffled, and finally reassigned to new complexes to enable information sharing. This process is repeated until some convergence criteria are satisfied.

## 7.4 ELLIPTICAL STORM LOCATIONS

The final optimized storm center locations ( $x$ ,  $y$ ) and rotations ( $\theta$ ) for every node of interest in the Nueces watershed are listed in Appendix C. Rotation angles are measured counter-clockwise from the positive  $x$ -axis. These location and rotation parameters were determined from 100yr frequency optimizations and are assumed to be the same for other frequency events in most cases (2yr – 500yr). Sensitivity testing showed that, in general, optimized locations and orientations did not significantly change between frequency events. Once the optimum storm center location and rotation were determined for each location of interest, the elliptical frequency storms for the standard eight frequency events were constructed using the appropriate NOAA Atlas 14 point rainfall depths. See section 1.4 in Appendix C for additional information.

## 7.5 ELLIPTICAL FREQUENCY STORM LOSS RATES

The elliptical frequency storms were then applied to the final HEC-HMS basin model with the same frequency loss rates that were used for the uniform rainfall method which were discussed in Chapter 6 and in Appendix B. In some cases, the 2-yr through 10-yr losses were re-adjusted in order to maintain consistency with the frequent end of the statistical frequency curves at the USGS gages. This final adjustment was performed because of the increased level of confidence in the statistical frequency curve for the 2-yr through 10-yr recurrence intervals. The final 2-yr through 25-yr loss rates used for the elliptical frequency storm events are given in Appendix C. The final 50-yr through 500-yr loss rates are the same as those used for the uniform rainfall method and are also shown in Appendix C.

## 7.6 ELLIPTICAL FREQUENCY STORM RESULTS – PEAK FLOW

The frequency peak flow values were then calculated in HEC-HMS by applying the appropriate, optimized elliptical frequency storms for each junction of interest in the final HEC-HMS basin model. These results will later be compared to the uniform rain results from HEC-HMS along with other methods from this study.

In some cases, one may observe that the simulated peak discharge decreases in the downstream direction. It is not an uncommon phenomenon to see decreasing frequency peak discharges for some river reaches as flood waters spread out into the floodplain and the hydrograph becomes dampened as it moves downstream. This can be due to a combination of peak attenuation due to river routing as well as the difference in timing between the peak of the main stem river versus the runoff from the local tributaries and subbasins.

### 7.6.1 Tabular Results

The final HEC-HMS frequency flows for the locations of interest throughout the watershed model using the NOAA Atlas 14 rainfall depths can be seen below in Table 7.4.

**Table 7.4: Summary of Discharges (cfs) from the HEC-HMS Elliptical Frequency Storm Method**

Location Description	HEC-HMS	HEC-HMS Drainage Area	50% AEP	20% AEP	10% AEP	4% AEP	2% AEP	1% AEP	0.5% AEP	0.2% AEP
	Element Name	(sq mi)	2-yr	5-yr	10-yr	25-yr	50-yr	100-yr	200-yr	500-yr
West Nueces River above Sycamore Creek	W_NuecesRv_abv_SycamoreCk	535.95	4582	30159	70085	119293	152438	197744	229144	293108
West Nueces River Below Sycamore Creek	W_NuecesRv_blw_SycamoreCk	646.40	4571	33093	78060	135144	173078	226452	263543	338382
West Nueces River near Brackettville (USGS gage 08190500)	W_NuecesRv_nr_Brackettville	693.94	4312	32485	77030	133549	171638	225642	263575	340224
West Nueces River above Live Oak	W_NuecesRv_abv_Live OakCk	767.91	4025	30720	72726	126050	161982	212831	250160	324554
West Nueces River Below Live Oak	W_NuecesRv_blw_Live OakCk	820.22	4118	31090	73300	126944	162948	214534	253148	329548
West Nueces River above Nueces River	W_NuecesRv_abv_NuecesRv	918.29	3792	28887	68347	118764	152814	203097	242491	317912
Nueces River below Pulliam Creek	NuecesRv_blw_PulliamCk	529.82	11082	37699	78581	149432	195156	246060	275874	341696
Nueces River at CR414 at Montell (USGS gage 08189998)	NuecesRv_at_Cr414_at_Montell	659.62	10187	37632	79950	155421	205724	263543	298397	373892
Nueces River below Montell Creek	NuecesRv_blw_MontellCk	679.24	10058	37314	79565	155037	205668	263979	299280	375610
Nueces River at Laguna (USGS gage 08190000)	NuecesRv_at_Laguna	736.17	9473	36388	78069	152806	203364	261562	298001	376135
Nueces River above West Nueces River	NuecesRv_abv_W_NuecesRv	815.94	9003	34591	74100	144958	193618	249731	286921	364678
Nueces River Below West Nueces River	NuecesRv_blw_W_NuecesRv	1734.22	9817	46827	109895	213868	281953	375738	439651	573210
Nueces River below Indian Creek	NuecesRv+IndianCk	1802.06	9599	44808	104910	204024	269004	359215	421038	550061
Nueces River at Highway 90	NuecesRv_at_HWY-90	1838.04	9070	42072	98844	192614	254165	339761	398483	521010
Nueces River near Uvalde (USGS gage 08192000)	NuecesRv_nr_Uvalde	1861.45	7861	39076	92551	181005	238919	320289	376722	493324
Nueces River at Highway 83	NuecesRv_at_HWY-83	1885.45	5772	27739	67335	134062	177160	239183	282588	371476
Nueces River at Highway 57	NuecesRv_at_HWY-57	1981.12	2497	16979	38254	88239	122522	166496	200030	269221
Nueces River at FM 1025 nr Crystal City (USGS gage 08192550)	NuecesRv_at_FM-1025_nr_Cryst	2102.48	1896	9629	20300	42410	65742	120263	150795	208127
Nueces River at The Turkey Creek/Espantosa Slough Split	NuecesRv_TurkeyCk_Split	2122.77	1100	6714	13614	27904	38917	66016	104987	152829
Turkey Creek/Espantosa Slough Diversion	TurkeyCk_Diversion	2122.77	835	4888	9305	19195	27834	52907	91146	138656
Nueces River Split	NuecesRv_Split_J010	2165.25	2280	3548	3817	5927	8837	11869	14905	19433
Nueces River above Turkey Creek	NuecesRv_abv_TurkeyCk	2165.25	327	1292	2804	5962	7649	9531	10610	11966
Palo Blanco Creek below Chacon Creek	Palo_BlancoCk_blw_ChaconCk	520.34	9468	17389	23255	32912	52124	70405	89805	108132.84
Palo Blanco Creek above Picoso Creek	Palo_BlancoCk_abv_PicosoCk	520.34	7047	13720	18720	27183	44496	63599	84621	121125.83
Palo Blanco Creek below Picoso Creek	Palo_BlancoCk_blw_PicosoCk	744.76	8538	18865	26459	41221	73000	108128	123440	172629
Palo Blanco Creek above Comanche Creek	Palo_BlancoCk_abv_ComancheC	744.76	8110	17904	25150	39095	69395	102890	117099	164042.78
Palo Blanco Creek Below Comanche Creek	Palo_BlancoCk_blw_ComancheC	822.94	9589	21420	30256	46719	83536	124525	130173	182209.88

Location Description	HEC-HMS	HEC-HMS Drainage Area	50% AEP	20% AEP	10% AEP	4% AEP	2% AEP	1% AEP	0.5% AEP	0.2% AEP
	Element Name	(sq mi)	2-yr	5-yr	10-yr	25-yr	50-yr	100-yr	200-yr	500-yr
Turkey Creek below Chaparrosa Creek	TurkeyCk_blw_ChaparrosaCk	414.59	9131	16388	23418	37075	66876	99641	126576	172589.5
Turkey Creek above Picoso Creek	TurkeyCk_abv_PicosoCk	459.10	4393	8993	12913	20057	34351	50349	64614	90819
Turkey Creek below Picoso Creek	TurkeyCk_blw_PicosoCk	1376.61	10720	23997	33879	52732	94863	140113	175639	197419
Turkey Creek at Highway 83 (New USGS gage)	TurkeyCk_at_HWY-83	1554.98	7624	14939	20209	31476	59803	92969	119369	143767
Turkey Creek above Turkey Split	TurkeyCk_abv_Turkey_Split	1563.55	6137	13433	19350	31267	58982	91769	117685	141941
Turkey Creek below Turkey Split	TurkeyCk_blw_Turkey_Split	1568.83	3258	10555	15677	27315	45794	77624	122248	202459
Turkey Creek above Carrizo Creek	TurkeyCk_abv_CarrizoCk	1581.46	4211	10790	16401	29023	51348	77754	107049	189279
Turkey Creek below Carrizo Creek	TurkeyCk_blw_CarrizoCk	1662.70	4405	11216	16835	29704	53148	80069	107071	189614
Turkey Creek above El Barrosa Creek	TurkeyCk_abv_El_BarrosaCk	1687.81	4416	9986	15392	27769	51169	78254	102751	177632
Turkey Creek below El Barrosa Creek	TurkeyCk_blw_El_BarrosaCk	1718.21	4436	10022	15471	27918	51516	78669	103501	178515
Turkey Creek and El Moro Creek	TurkeyCk+El_MoroCk	1836.07	4917	10063	15480	28362	53083	80689	104354	178352
Turkey Creek above Nueces River	TurkeyCk_abv_NuecesRv	1847.03	4537	9601	15221	27865	51994	79673	103716	178074
Nueces River near Asherton (USGS gage 08193000)	NuecesRv_nr_Asherton	4024.67	4782	10112	16729	30656	53059	82459	108633	185705
Nueces River above Arroyo Negro	NuecesRv_abv_Arroyo_Negro	4213.49	5072	9962	16557	30320	50085	80886	106707	178866
Nueces River below Arroyo Negro	NuecesRv_blw_Arroyo_Negro	4333.02	5469	10343	16965	30840	51598	82145	107114	179262
Nueces River above Appurceon Creek	NuecesRv_abv_AppurceonCk	4333.02	5067	10128	16751	30505	50243	81141	106371	176740
Nueces River below Appurceon Creek	NuecesRv_blw_AppurceonCk	4411.17	5504	10516	17159	31060	51999	82668	107018	177176
Nueces River above San Roque Creek	NuecesRv_abv_San_RoqueCk	4488.43	5426	10508	17042	30647	50638	81385	105342	171730
Nueces River below San Roque Creek	NuecesRv_blw_San_RoqueCk	4903.91	6376	14198	22771	34041	51073	82027	105602	172809
Nueces River and Espio Creek	NuecesRv+EspioCk	5084.65	6410	14066	22467	33517	50282	81064	104276	169301
Nueces River at Cotulla (USGS gage 08194000)	NuecesRv_at_Cotulla	5172.43	6238	12797	20444	31319	50514	80913	103781	165323
Nueces River above La Raices Creek	NuecesRv_abv_La_RaicesCk	5366.43	6518	12876	20165	30654	48939	78199	100207	157644
Nueces River below La Raices Creek	NuecesRv_blw_La_RaicesCk	5638.55	6399	12697	19946	30652	48615	78033	100323	158194
Nueces River above Calman Creek	NuecesRv_abv_CalmanCk	5705.26	6432	12442	19399	30236	47789	76534	98303	154205
Nueces River below Calman Creek	NuecesRv_blw_CalmanCk	5890.78	6422	12474	19448	30426	48204	76998	98866	154701
Nueces River above Los Olmos Creek	NuecesRv_abv_Los_OlmosCk	5898.22	6730	12989	20061	30292	47835	76355	97875	153247
Nueces River below Los Olmos Creek	NuecesRv_blw_Los_OlmosCk	6353.75	8040	18523	28252	42338	70009	97545	119384	157635
Nueces River and Sauz Creek	NuecesRv+SauzCk	6419.66	7795	18077	27563	41347	68390	95455	117169	155429
Nueces River above San Casimiro Creek	NuecesRv_abv_San_CasimiroCk	6445.15	7250	17125	26251	39536	65410	91565	113194	150755

Location Description	HEC-HMS	HEC-HMS Drainage Area	50% AEP	20% AEP	10% AEP	4% AEP	2% AEP	1% AEP	0.5% AEP	0.2% AEP
	Element Name	(sq mi)	2-yr	5-yr	10-yr	25-yr	50-yr	100-yr	200-yr	500-yr
San Casimiro Creek near Freer (USGS gage 08194200)	San_CasimiroCk_nr_Freer	467.65	2591	7818	15916	32312	42865	57261	69929	90799
<b>San Casimiro Creek above Nueces River</b>	San_CasimiroCk_abv_NuecesRv	537.34	2184	6878	14224	29129	38633	51899	63912	83457
Nueces River below San Casimiro Creek	NuecesRv_blw_San_CasimiroCk	6982.49	6899	18406	32891	58396	88594	125183	153121	204133
Nueces River above Black Creek	NuecesRv_abv_BlackCk	7007.66	6773	18041	32087	56864	86383	122162	149762	200105
Nueces River below Black Creek	NuecesRv_blw_BlackCk	7431.13	5976	18689	33503	59668	91787	131351	163212	221346
Nueces River above Ygnacio Creek	NuecesRv_abv_YgnacioCk	7611.07	6326	18564	32037	55401	85573	122411	150655	204993
Nueces River below Ygnacio Creek	NuecesRv_blw_YgnacioCk	7754.47	6160	18440	31994	55503	85706	122661	151095	205604
Nueces River above San Jose Creek	NuecesRv_abv_San_JoseCk	7754.47	6086	18351	31856	55266	85342	122142	150372	204550
Nueces River below San Jose Creek	NuecesRv_blw_San_JoseCk	7857.73	6085	18346	31880	55315	85382	122176	150517	204798
Nueces River above Green Branch	NuecesRv_abv_GreenBr	7857.73	6038	18202	31620	54836	84652	121142	148958	202575
Nueces River below Green Branch	NuecesRv_blw_GreenBr	7943.10	6154	18337	31709	54853	84690	121169	148964	202717
Nueces River near Tilden (USGS gage 08194500)	NuecesRv_nr_Tilden	8105.85	5755	17604	30699	53239	82146	117619	144633	196969
Nueces River above Cow Creek	NuecesRv_abv_CowCk	8105.85	6045	17508	30168	51969	80234	114903	140593	191913
Nueces River below Cow Creek	NuecesRv_blw_CowCk	8182.92	5825	17429	30260	52315	80708	115529	141806	193230
Nueces River above Old River	NuecesRv_abv_OldRv	8275.85	5548	16735	29187	50531	77905	111670	137128	187323
Nueces River below Old River	NuecesRv_blw_OldRv	8354.07	5561	16732	29196	50558	77964	111733	137215	187336
Nueces River and White Creek	NuecesRv+WhiteCk	8464.98	5390	16107	28049	48461	74651	107000	131210	179340
Nueces River above Atascosa River	NuecesRv_abv_AltascosaRv	8519.43	5167	15238	26556	45821	70487	101154	124079	170219
Frio River at Concan (USGS gage 08195000)	FrioRv_at_Concan	389.64	9269	34597	60944	102611	137608	176792	203643	254215
Frio River above Dry Frio River	FrioRv_abv_Dry_FrioRv	441.57	8042	31344	55521	93931	126187	163493	189825	238710
Frio River below Dry Frio River	FrioRv_blw_Dry_FrioRv	628.74	11038	43437	78945	135767	181951	235781	274043	345112
Frio River near Uvalde (USGS gage 08197500)	FrioRv_nr_Uvalde	633.06	10136	40537	73981	127166	170689	221566	257458	324606
Frio River above Blanco Creek	FrioRv_abv_BlancoCk	745.82	3202	21613	41253	74870	101067	130970	155395	201338
Frio River below Blanco Creek	FrioRv_blw_BlancoCk	879.41	4342	22129	41463	76842	106412	140055	167320	218405
Frio River below Sabinal River	FrioRv_blw_SabinalRv	1338.62	5072	21079	39588	77233	114334	155838	191282	257090
Frio River above Elm Creek	FrioRv_abv_ElmCk	1411.00	2300	14903	25959	52309	80446	113687	144611	201228
Frio River below Elm Creek	FrioRv_blw_ElmCk	1499.66	2196	15068	26369	52761	81211	114818	146185	203904
Frio River above Hondo Creek	FrioRv_abv_HondoCk	1514.24	2206	12798	23527	50194	79618	113494	144292	202036

Location Description	HEC-HMS	HEC-HMS Drainage Area	50% AEP	20% AEP	10% AEP	4% AEP	2% AEP	1% AEP	0.5% AEP	0.2% AEP
	Element Name	(sq mi)	2-yr	5-yr	10-yr	25-yr	50-yr	100-yr	200-yr	500-yr
Hondo Creek and Live Oak Creek	HondoCk+Live_OakCk	521.81	8548	16674	25107	50362	75616	102069	121821	157608
Hondo Creek above Seco Creek	HondoCk_abv_SecoCk	666.04	6795	12988	19075	40170	62119	85120	102860	134957
Hondo Creek below Seco Creek	HondoCk_blw_SecoCk	1019.99	7061	17454	29140	57359	84955	116036	138413	181461
Hondo Creek above Frio River	HondoCk_abv_FrioRv	1106.85	6552	16159	26832	53425	79929	109652	131077	172621
Frio River below Hondo Creek	FrioRv_blw_HondoCk	2621.10	6143	21567	36476	79502	121801	173801	212810	282704
Frio River above Leona River	FrioRv_abv_LeonaRv	2675.30	3713	15271	29205	66726	109390	158366	195090	262289
Leona River below Live Oak Creek	LeonaRv_blw_LiveoakCk	460.74	3798	4949	5919	12227	26004	37540	47684	65540
Leona River above Todos Santos Creek	LeonaRv_abv_Todos_SantosCk	585.22	3657	4693	6572	11876	26021	37948	48376	67186
Leona River below Todos Santos Creek	LeonaRv_blw_Todos_SantosCk	660.74	3728	4762	6975	12133	26704	38999	49682	69076
Leona River above Frio River	LeonaRv_abv_FrioRv	670.08	3592	4572	6830	11758	26068	38167	48650	67648
Frio River below Leona River	FrioRv_blw_LeonaRv	3345.37	4541	15689	28645	66087	110072	162174	199771	270376
Frio River near Derby (USGS gage 08215500)	FrioRv_nr_Derby	3447.76	4691	14326	25957	63405	107132	159274	196828	267574
Frio River at Highway 85	FrioRv_at_HWY-85	3500.89	3587	12018	22615	58359	99110	149684	185845	254798
Frio River and Ruiz Creek	FrioRv+RuizCk	3653.55	1941	8650	18226	48136	87636	136769	171972	246178
Frio River above Cibolo Creek	FrioRv_abv_CiboloCk	3698.16	1942	6862	13890	37993	78949	130155	164570	238716
Frio River below Cibolo Creek	FrioRv_blw_CiboloCk	4092.91	2279	11574	19245	40757	80848	134270	169829	246147
Frio River above Esperanz Creek	FrioRv_abv_EsperanzaCk	4149.39	2192	7962	13186	36184	72086	125098	160885	235393
Frio River below Esperanza Creek	FrioRv_blw_EsperanzaCk	4248.12	2498	8502	14061	36305	71740	124538	160363	235180
Frio River and Galinda Creek	FrioRv+GalindaCk	4337.72	2588	8813	13979	33230	64486	115603	151568	225176
Frio River above Leoncita Creek	FrioRv_abv_LeoncitaCk	4396.25	2743	8388	14116	31315	59212	108377	143728	215917
Frio River at Tilden (USGS gage 08206600)	FrioRv_at_Tilden	4462.81	2778	8424	14222	31432	59486	108645	144078	216335
Frio River above San Miguel Creek	FrioRv_abv_San_MiguelCk	4519.46	2713	8339	14074	31371	59252	107583	142835	214796
San Miguel Creek below Highway 97	SanMiguelCk_blw_HWY-97	516.77	2957	7632	13377	25174	35751	46768	58843	90100
San Miguel Creek above Lagunillas Creek	SanMiguelCk_abv_LagunillasCk	574.60	2798	7375	12972	24488	34897	45590	55098	80845
San Miguel Creek below Lagunillas Creek	SanMiguelCk_blw_LagunillasCk	741.44	3357	8724	16569	31906	46153	60375	71451	91766
San Miguel Creek near Tilden (USGS gage 08206700)	SanMiguelCk_nr_Tilden	782.15	3361	8883	15826	30754	44574	58681	69618	90227
San Miguel Creek above Frio River	SanMiguelCk_abv_FrioRv	854.80	7057	11580	16475	30121	43567	58818	70803	92566
Frio River below San Miguel Creek	FrioRv_blw_San_MiguelCk	5374.26	3003	8723	15033	31570	59422	107949	143073	216052
Choke Canyon Reservoir Inflow	ChokeCanyon_Inflow	5490.45	2896	8557	14538	31296	59001	107421	142449	215104

Location Description	HEC-HMS	HEC-HMS Drainage Area	50% AEP	20% AEP	10% AEP	4% AEP	2% AEP	1% AEP	0.5% AEP	0.2% AEP
	Element Name	(sq mi)	2-yr	5-yr	10-yr	25-yr	50-yr	100-yr	200-yr	500-yr
Frio River below Choke Canyon Dam	ChokeCanyonRes_OWC_nr_3Rv	5490.45	1784	8456	14400	29872	53860	97726	130120	177334
Frio River above Atascosa River	FrioRv_abv_AtascosaRv	5496.36	1905	8663	14769	29829	53925	97879	130159	177519
Atascosa River at Highway 37	AtascosaRv_at_HWY-37	451.31	4401	9931	16127	25929	35894	48683	59407	78005
Atascosa River near McCoy (USGS gage 08207500)	AtascosaRv_nr_McCoy	510.87	3915	9191	14934	24735	34352	47774	59026	78260
Atascosa River above Borrego Creek	AtascosaRv_abv_BorregoCk	535.96	3760	8783	14483	23998	33545	46869	58148	78440
Borrego Creek and Los Cortes Creek	BorregoCk+Los_CortesCk	142.92	3780	7327	10551	15809	20971	26996	32265	41337
Borrego Creek above Atascosa River	BorregoCk_abv_AtascosaRv	221.19	3293	6800	10176	16132	22183	29957	36443	48985
Atascosa River below Borrego Creek	AtascosaRv_blw_BorregoCk	757.15	4471	11541	19403	32109	44486	63449	79013	108885
Atascosa River above La Parita Creek	AtascosaRv_abv_La_ParitaCK	813.17	4156	11197	18453	30837	42685	60849	75965	106482
Atascosa River below La Parita Creek	AtascosaRv_blw_La_PartCK	1124.57	4372	12250	20554	35012	48397	70922	88424	127415
Atascosa River at Whitsett (USGS gage 0820800)	AtascosaRv_at_Whitsett	1145.77	4152	11935	19923	34228	47122	68979	86246	124646
Atascosa River above Weedy Creek	AtascosaRv_abv_WeedyCk	1225.28	4688	11817	19689	33601	46460	67877	84598	122019
Atascosa river below Weedy Creek	AtascosaRv_blw_WeedyCk	1364.40	9860	15386	20025	33930	46879	68748	85822	125236
Atascosa River above Frio River	AtascosaRv_abv_FrioRv	1395.61	9341	13957	19481	33061	45718	67068	83748	122237
Atascosa River below Frio River	AtascosaRv_blw_FrioRv	6891.97	16559	29360	42022	57103	65453	94463	112900	161941
Atascosa River above Nueces River	AtascosaRv_abv_NuecesRv	6911.11	3639	11344	20122	29641	52546	98924	130833	183740
Nueces River below Atascosa River	NuecesRv_blw_AltascosaRv	15430.54	5093	14722	27896	47806	78020	121917	147795	199692
Nueces River at Three Rivers (USGS gage 08210000)	NuecesRv_at_Three_Rivers	15430.54	3761	12093	20109	34223	62547	113979	152914	219522
Nueces River and Sulphur Creek	NuecesRv+SulhpurCk	15619.12	5787	16141	30588	49531	75782	119787	145926	203420
Nueces River at Highway 59	NuecesRv_at_HWY-59	15715.07	23738	41670	52769	65112	71411	104792	126510	183773
Nueces River above Spring Creek	NuecesRv_abv_SpringCk	15733.03	4551	13627	25169	44480	74166	115863	139145	189154
Nueces River below Spring Creek	NuecesRv_blw_SpringCk	15833.59	5351	14982	28216	47410	76650	121772	147943	201840
Nueces River and Upper End of Lake Corpus Christi	NuecesRv+UpEnd_LkCorpusChris	15921.68	5432	15137	28978	48040	75712	120595	147914	203605
Nueces River above Lake Corpus Christi	NuecesRv_abv_LkCorpusCh	16076.35	5717	15856	28090	44020	67432	108607	132459	186821
Lake Corpus Christi Inflow	Lk_Corpus_Christi_Inflow	16502.10	5212	12100	24298	43371	70754	111184	134982	182220
Nueces River near Mathis (USGS gage 08211000, Dam Outflow)	NuecesRv_nr_Mathis	16502.10	3997	11847	19324	31990	56894	101267	137361	203390
Nueces at Bluntzer (USGS gage 08211200)	NuecesRv_at_Bluntzer	16617.60	3640	11317	19184	32474	58326	101951	134807	202356
Nueces River at Calallen (USGS gage 08211500)	NuecesRv_at_Calallen	16675.30	2881	9742	17185	28938	51018	93194	123914	187972

**Table 7.5: Peak Reservoir Pool Elevations (feet NAVD88) from the HEC-HMS Elliptical Frequency Storms**

Reservoir Name	HEC-HMS Drainage Area (sq mi)	Lon	Lat	Theta	Reservoir Elevations (ft NAVD 88)							
					50% AEP	20% AEP	10% AEP	4% AEP	2% AEP	1% AEP	0.5% AEP	0.2% AEP
					2-yr	5-yr	10-yr	25-yr	50-yr	100-yr	200-yr	500-yr
Corpus_Christi_Dam	5490.45	-99.2672	28.34891	97.818	93.86	93.98	94.14	94.26	94.49	94.99	95.38	96.01
Choke_Canyon_Dam	16502.1	-99.4247	29.26374	115.501	221	221.33	221.55	222.04	222.73	223.87	224.69	227.13

**Table 7.6: Reservoir Peak Outflow (cfs) from the HEC-HMS Elliptical Frequency Storms**

Reservoir Name	HEC-HMS Drainage Area (sq mi)	Lon	Lat	Theta	Reservoir Peak Outflows (cfs)							
					50% AEP	20% AEP	10% AEP	4% AEP	2% AEP	1% AEP	0.5% AEP	0.2% AEP
					2-yr	5-yr	10-yr	25-yr	50-yr	100-yr	200-yr	500-yr
Corpus_Christi_Dam	5490.45	-99.2672	28.34891	97.818	4865.1	13154.5	24858.5	43805.1	70146	110881.7	136439.5	185549.3
Choke_Canyon_Dam	16502.1	-99.4247	29.26374	115.501	1820.5	8535.7	14470.3	29971.3	54156.7	98231.1	130616.9	177646.6

## 7.6.2 Map Results

The following 'a' figures represent the 100yr 48hr heatmap results for the optimization of each junction of interest in the Elliptical Frequency Storm HEC-HMS model. For each junction of interest, the optimization script ran 300+ times recording the junction flow rate for various storm centerings and orientations. Each of the recorded storm centerings (x,y) and resulting flow rates (z) at the junction of interest were recorded and used to create a rasterized heat map. The red shading represents storm center locations that led to relatively high flow rates at the junction whereas the green shading represents storm center locations that led to relatively low flow rates.

The following 'b' figures show the final, total storm depths and optimized storm configurations for each junction. Note that the peak flow values recorded in the 'a' figures may differ slightly from the final peak flow values recorded in the 'b' figures and in Table 7.4 above. These differences are due to some small adjustments to the elliptical storm and HEC-HMS model parameters that occurred during the review process. The 'b' figures include the final peak flow values after peer review. The figures in this section are generally organized by major tributary and then by alphabetical order junction name. The figures for the reservoir optimizations are in the last subsection.

This section includes the figures for only a small sample of example junctions from the Nueces River basin. The elliptical storm maps for all of the junctions that were analyzed can be found in Appendix C.

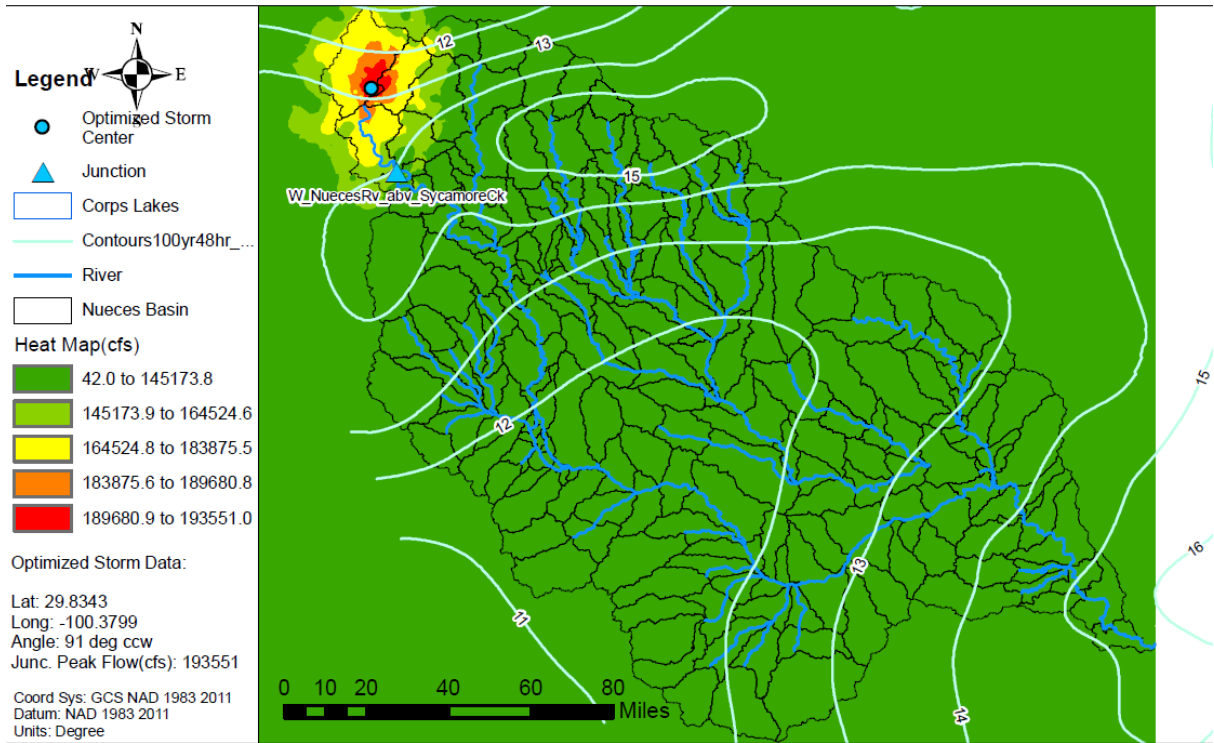


Figure 7.11a: Elliptical Storm Optimization Heat Map for W\_NuecesRv\_abv\_SycamoreCk

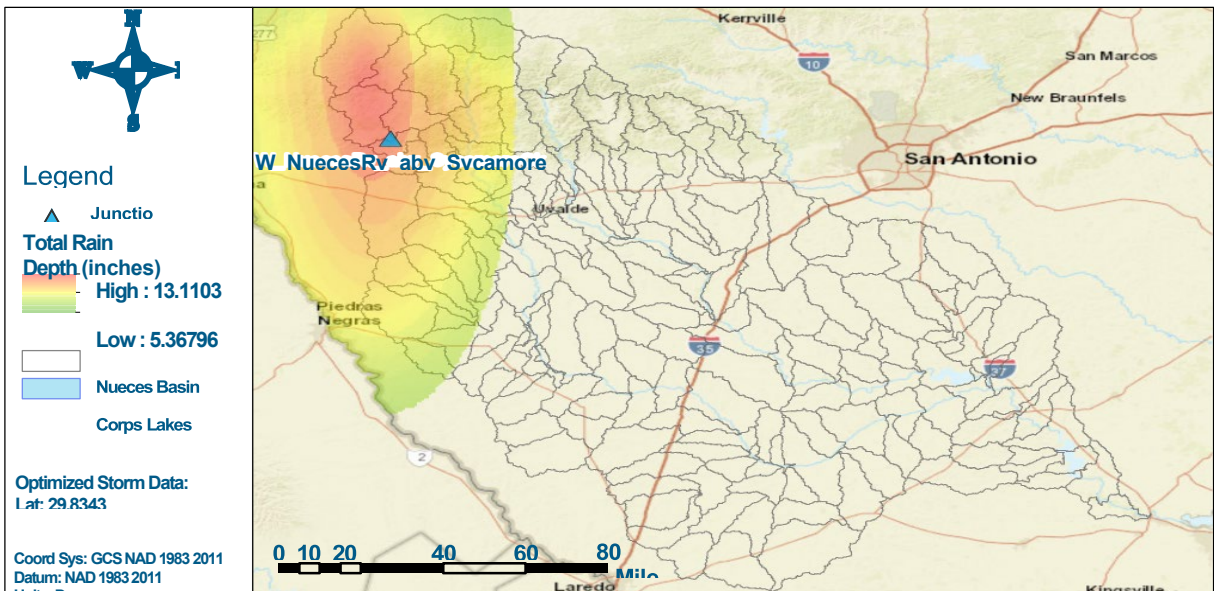


Figure 7.11b: Elliptical Storm Optimization Heat Map for W\_NuecesRv\_abv\_SycamoreCk

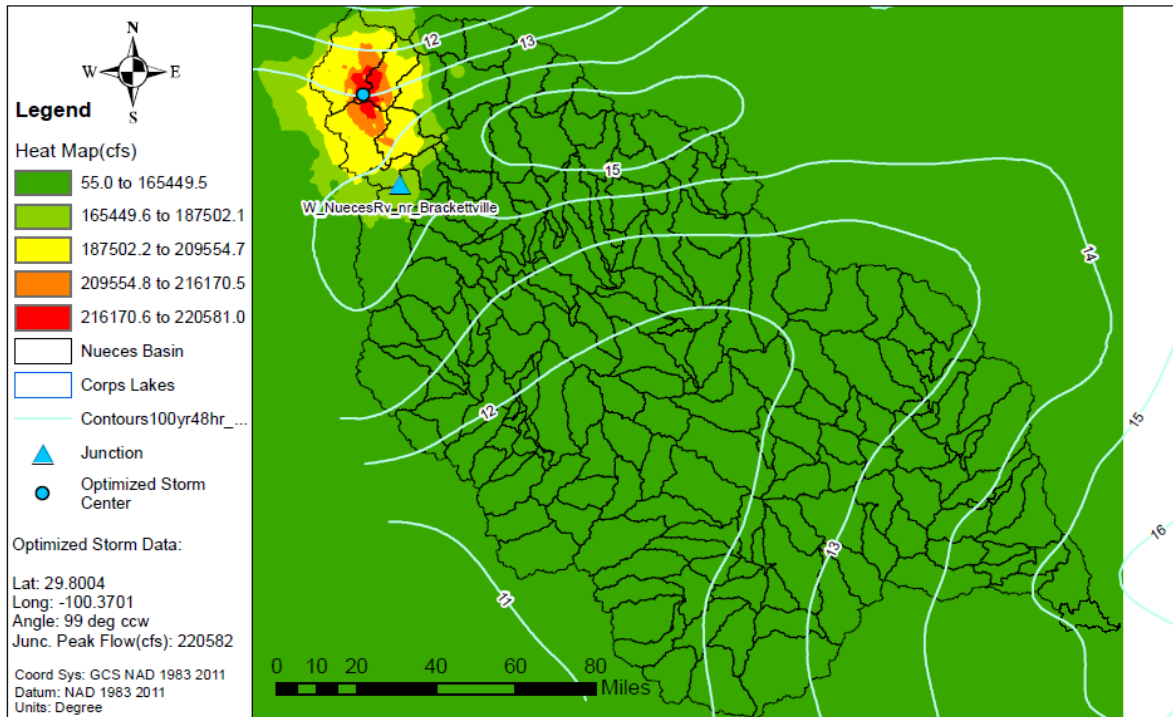


Figure 7.12a: Elliptical Storm Optimization Heat Map for W\_NuecesRv\_nr\_Brackettville

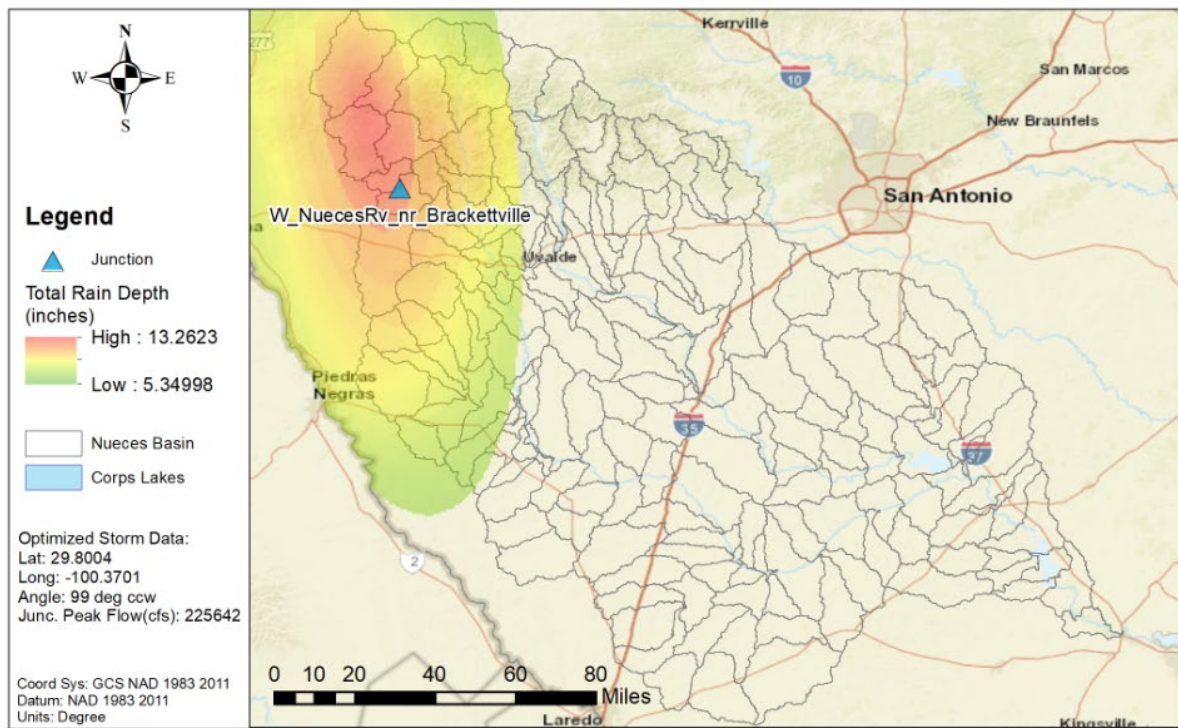


Figure 7.12b: NA14 1% AEP Elliptical Storm for W\_NuecesRv\_nr\_Brackettville

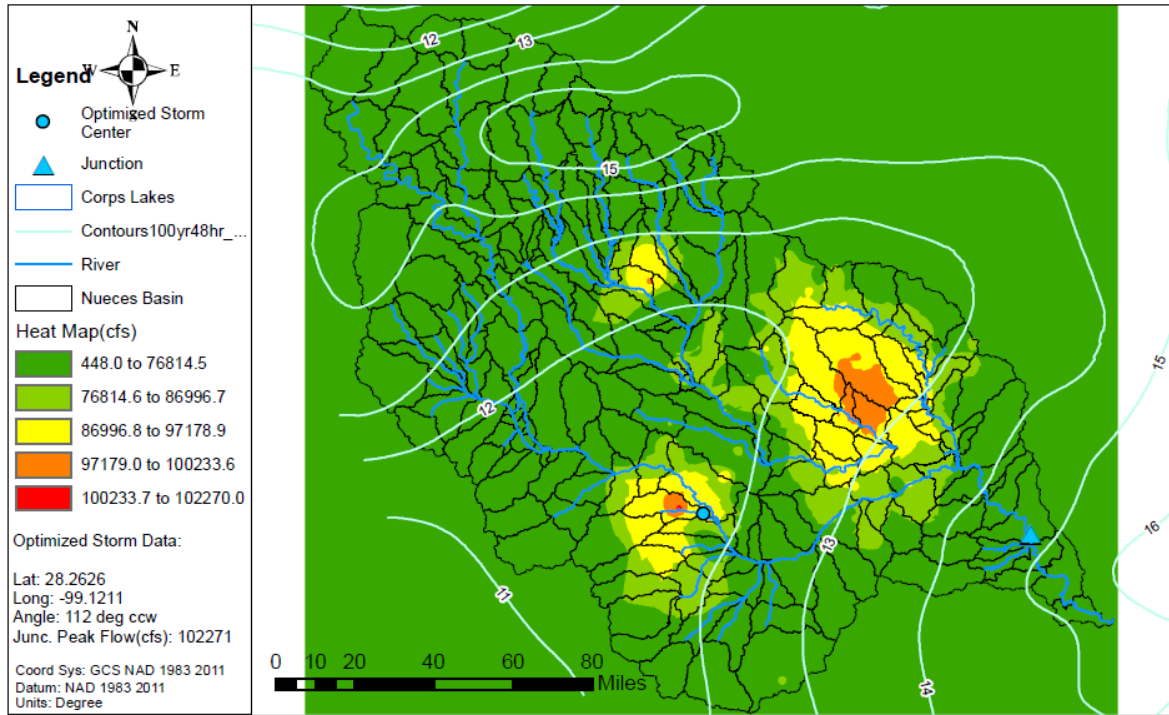


Figure 7.13a: Elliptical Storm Optimization Heat Map for Nueces River above Lake Corpus Christi

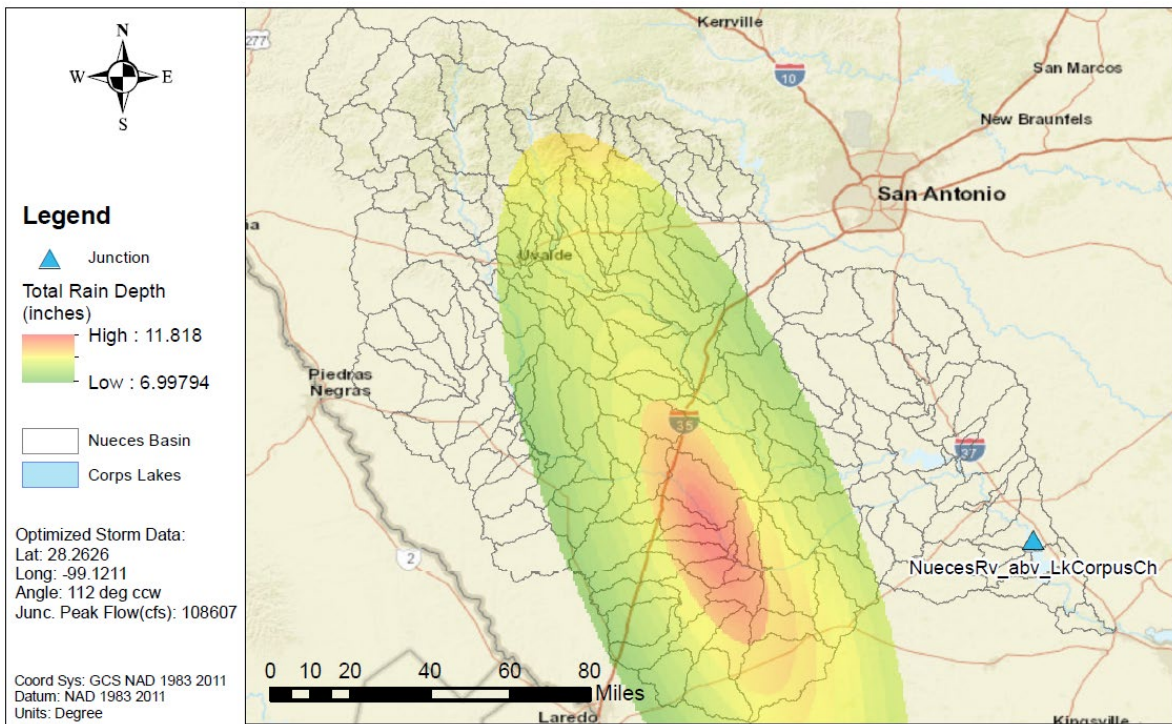


Figure 7.13b: Elliptical Storm Optimization Heat Map for Nueces River above Lake Corpus Christi

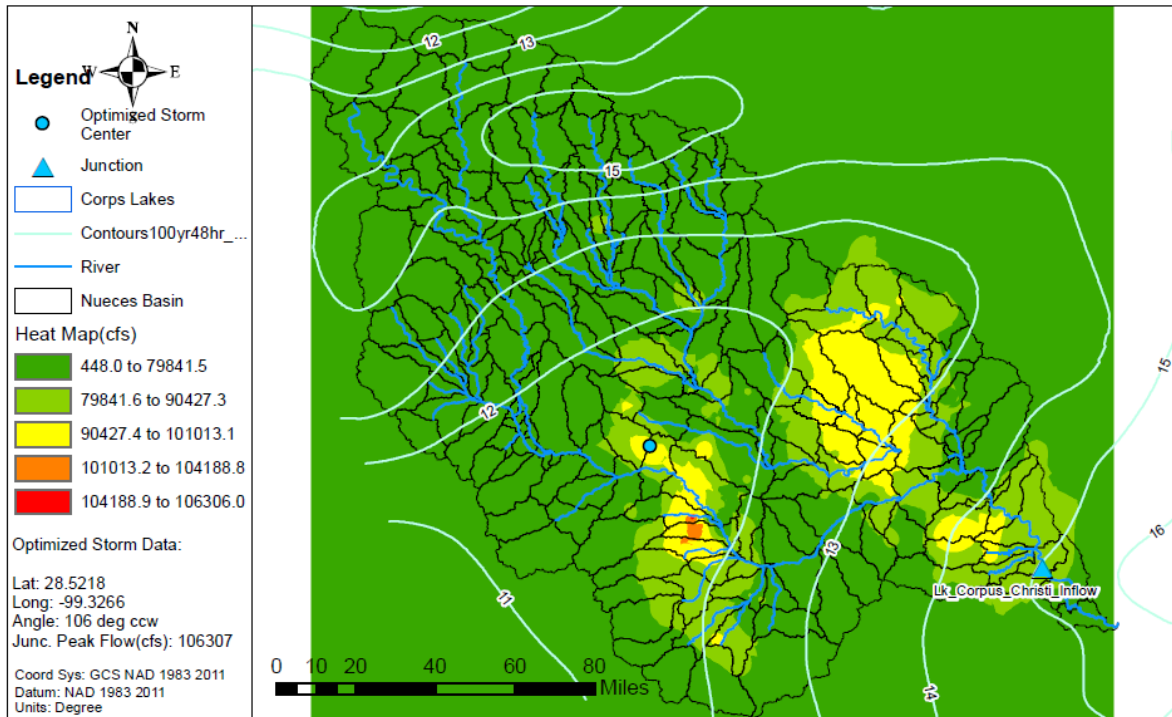


Figure 7.14a: Elliptical Storm Optimization Heat Map for Lake Corpus Christi Inflow

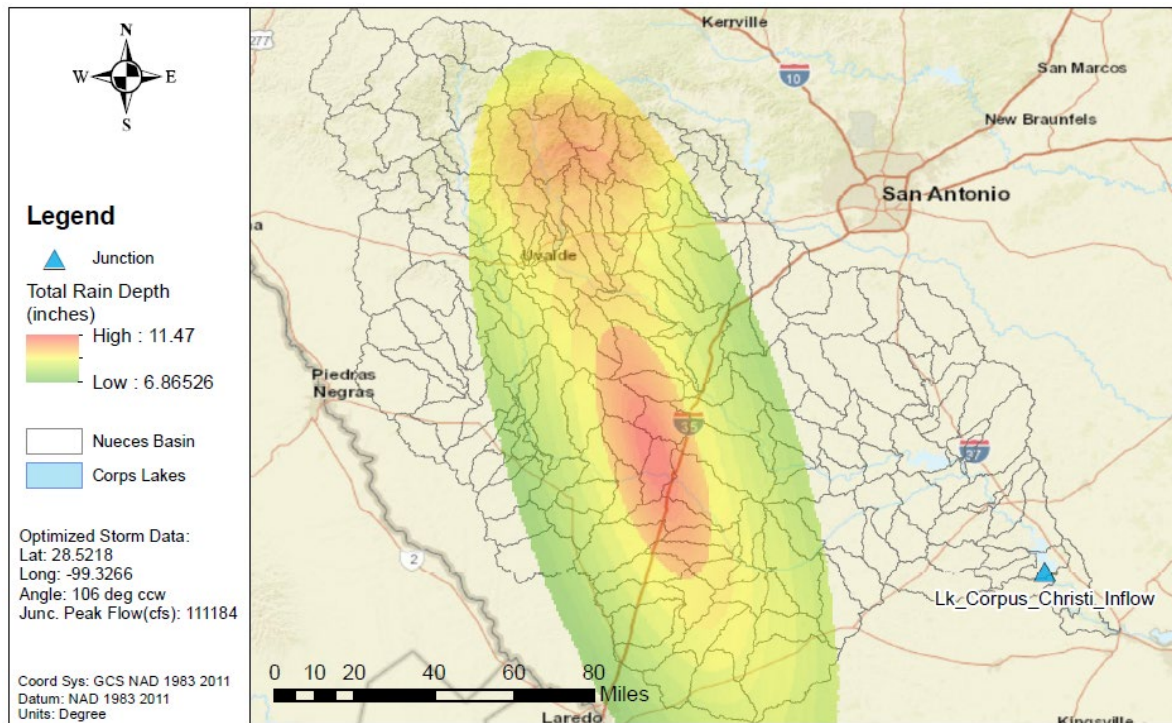


Figure 7.14b: NA14 1% AEP Elliptical Storm for Lake Corpus Christi Inflow

## 7.7 ELLIPTICAL FREQUENCY STORM RESULTS VERSUS DRAINAGE AREA

As a quality check, the peak flow results from the 1% AEP elliptical frequency storms were plotted versus drainage area and outliers were examined, as shown in Figure 7.15. This figure shows that the analyzed junctions followed generally expected patterns of increasing peak flow with drainage area, with exceptions for the effects of large reservoirs. The upper Nueces River and the upper junctions on the Frio River have steeper watersheds and have the highest discharge per area on the plot. This behavior is expected due to the steeper slopes and confirmed by historical flood events which can also be seen in the gage records of Appendix A.

Peak discharges on the middle and lower Nueces River main stem have the lowest peak discharges per area. The middle Nueces River has the lowest NOAA Atlas 14 rainfall depths in the Nueces River basin and is affected by channel losses and irrigation withdrawals, while the lower Nueces River is affected by Choke Canyon and Corpus Christi reservoirs.

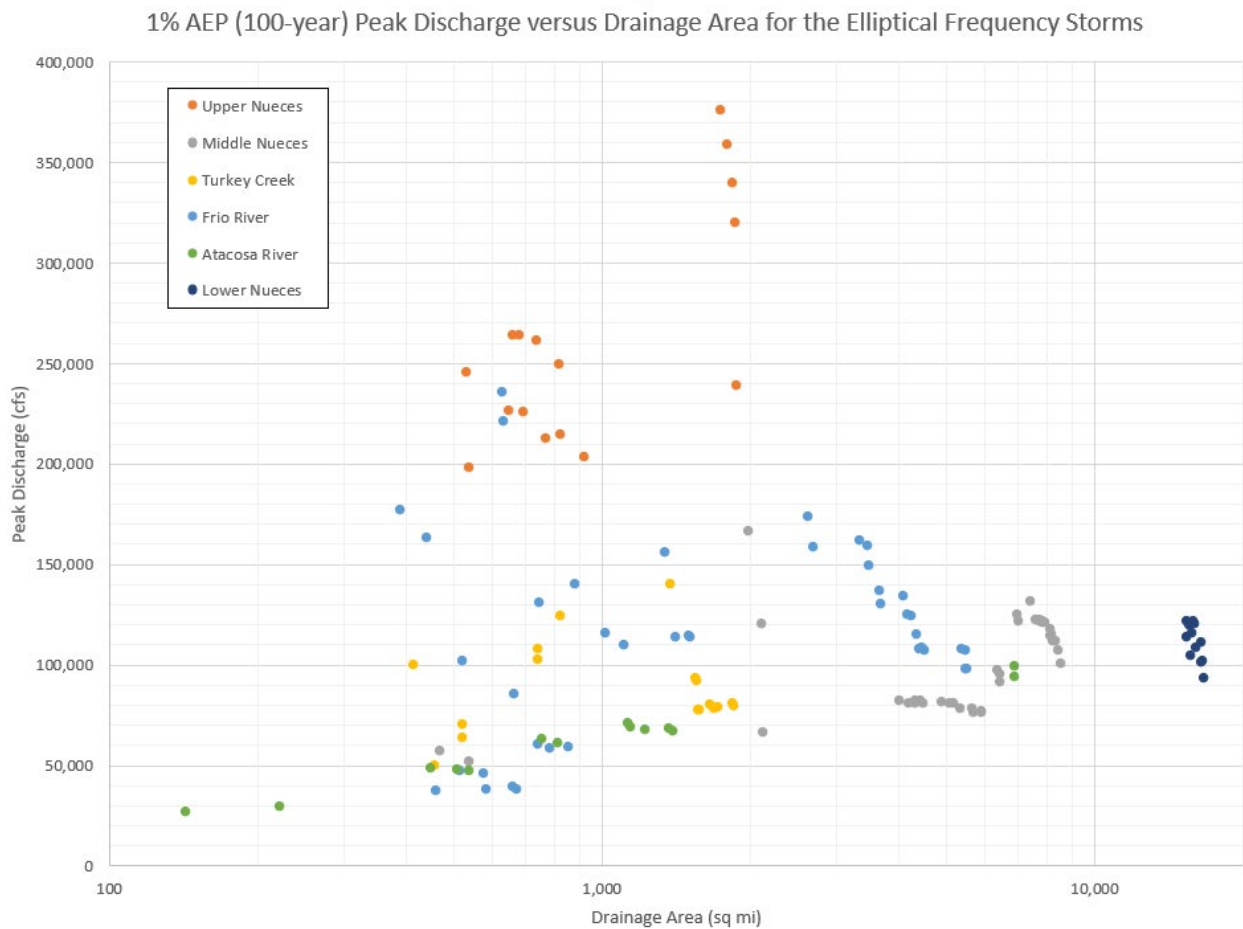


Figure 7.15: NA14 1% AEP Elliptical Storm Frequency Results versus Drainage Area

## 7.8 ELLIPTICAL STORM VERSUS UNIFORM RAIN FREQUENCY RESULTS

As mentioned at the beginning of this appendix, because the published depth-area reduction curves from TP-40 do not extend beyond 400 square miles, the uniform rainfall method may not always be appropriate for larger drainage areas. Therefore, elliptical frequency storms were computed in HEC-HMS as an alternate method to compare to the uniform rain frequency results for larger drainage areas.

Figure 7.16 below gives a comparison of the percent difference in the 1% annual chance (100-yr ) peak flow estimate from the elliptical storms versus the uniform rainfall method. This percent difference is then plotted versus the drainage area of the point of interest. On this plot, a positive value indicates that the elliptical peak flow was higher than the uniform rain peak flow, and conversely, a negative value indicates that the elliptical peak flow was lower than the uniform rain peak flow.

From this figure, one may observe that the percent difference between the two methods generally increases as drainage area increases, which is as expected. For larger drainage areas encompassing several thousand square miles, the total volume of rainfall being applied to the HEC-HMS model is much less for an elliptical storm than for the uniform rainfall method. For drainage areas less than approximately 500 square miles, the results of the two methods generally stay within 10% of one another. For drainage areas greater than 4,000 square miles, the difference can be more than 50%, as shown in Figure 7.16.

This plot also shows that there is a greater difference in the peak flows for the Turkey Creek basin and the Nueces River flow split area than for the rest of the Nueces River basin. This is because the Turkey Creek and upper Nueces headwater watersheds are steep and narrow, but their peak flows quickly attenuate as the streams reach the flat wide floodplains in the middle portions of the basin. As a result, there is a proportionally greater reduction in the peak flow values in these watersheds when comparing elliptical storm to uniform rainfall results.

The lower Nueces River also had a large difference (about a 60% reduction) between the elliptical and uniform rainfall results. This is partially due to the effects of Choke Canyon Reservoir and Lake Corpus Christi. The other reason is that the uniform rainfall method applies an unrealistically large rainfall volume to its 17,000 square mile drainage area by assuming that it is raining on the entire watershed at once. This example illustrates why the elliptical storm method produces more reliable estimates of frequency flows for very large drainage areas.

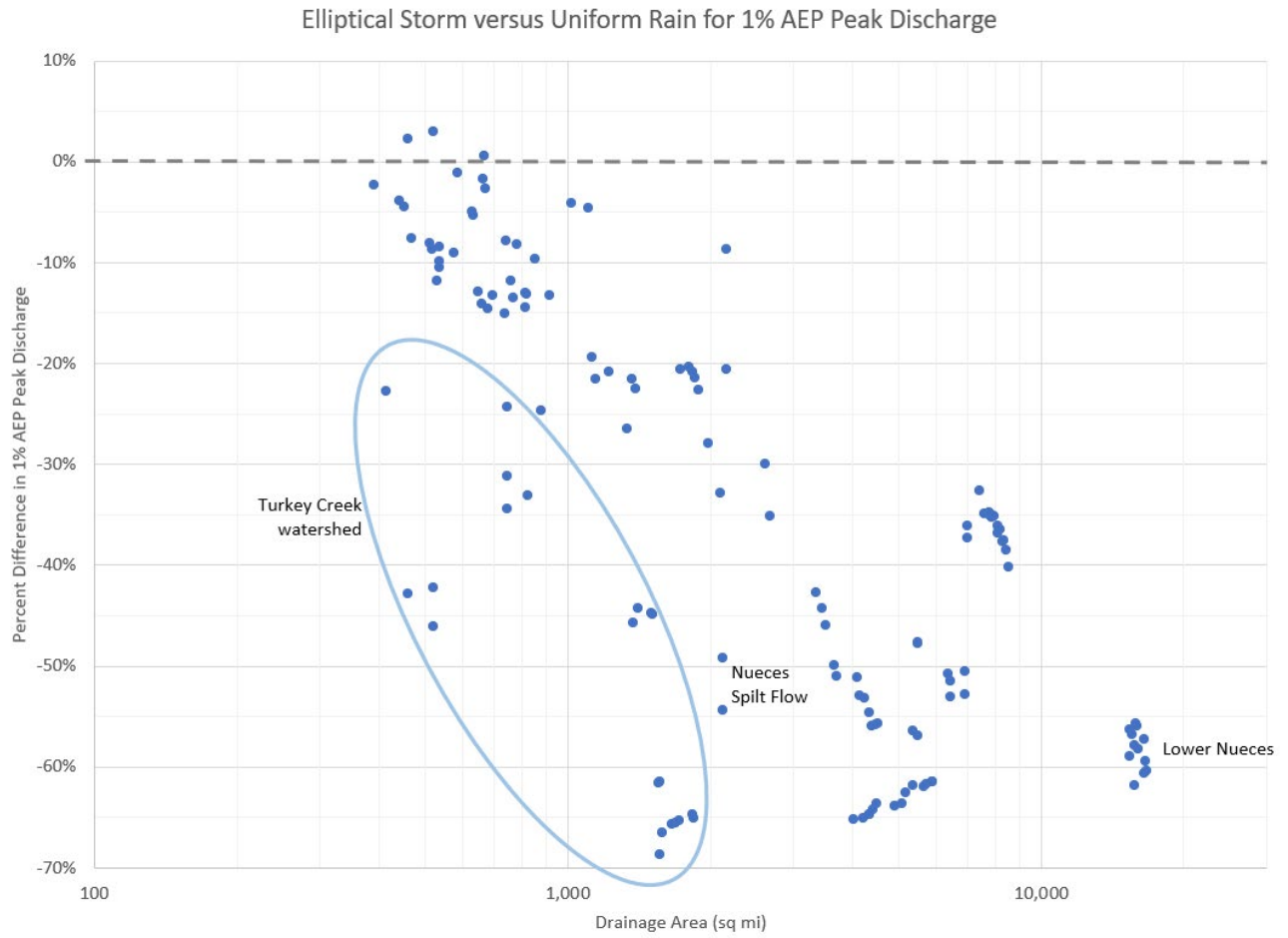


Figure 7.16: Percent Difference between Elliptical and Uniform Rain Estimates of the 1% ACE (100-yr) Peak Flow

## 8 RiverWare Analysis

For the RiverWare portion of the analysis, a new US Army Corps of Engineers (USACE) Period of Record (POR) model in RiverWare (CADSWES, 2020) was created for the Nueces River Basin. The POR data was generated from Water Year (WY) 1942 to 2019. RiverWare was then used to generate a regulated POR by simulating the basin as if the reservoirs and their current rule sets had been present in the basin for the entire time period. This analysis was used to extend flow records at various streamgaging stations within the basin from their observed records, using nearby observed streamgaging stations to an extended simulated record of 1942 to 2019. Statistical flow frequency analyses according to Bulletin 17C were then performed on the extended record. The statistical results from the RiverWare model were later compared with the results of other methods from this study.

This chapter summarizes the RiverWare portion of the hydrologic analysis that was completed for the InFRM Watershed Hydrology Assessment of the Nueces River Basin. Additional details on the model and analyses are available in Appendix D: RiverWare Analyses.

### 8.1 Introduction to Riverware Modeling

RiverWare is a river system modeling tool developed by CADSWES (Center of Advanced Decision Support for Water and Environmental Systems) that allows the user to simulate complex reservoir operations and perform period-of-record analyses for different scenarios. For the InFRM hydrology studies, RiverWare is used to generate a homogeneous regulated POR by simulating the basin as if the reservoirs and their current rule sets had been present in the basin for the entire time period. Statistical analyses can then be performed on the extended records at the gages. This report summarizes the RiverWare portion of the hydrologic analysis being completed for the InFRM Hydrology study of the Nueces River Basin.

The RiverWare model described in this chapter presents development of the Nueces River Basin hydrology, which mimics current operational conditions. The use of the RiverWare program allows for data extension to periods prior to dam construction. The utilization of longer gage record improves discharge frequency results and increases the confidence of the analysis being performed. The modeling evaluation criteria are: (1) evaluate output based on validating policies and functions, and (2) prioritize operation based on surcharge and flood control. A detailed explanation of the Nueces River Basin POR hydrology will be in a later section.

Calibration results will also be shown that illustrate the overall model performance for the POR. The time window simulation run is for October 01, 1942 – September 30, 2019. This time window captures all big events occurred over the Nueces River basin. Each simulated water year was inspected individually to better validate the results.

Historical pool elevations along with observed inflows and outflows were compared against the model simulated results.

#### 8.1.1 USACE Models

Two new RiverWare models were constructed for the Nueces River basin at the onset of this study. The USACE Fort Worth District (SWF) Nueces RiverWare models are: 1) the RiverWare hydrology model, 2) the RiverWare study model. The models were developed with functionalities of algorithms and consolidate object methods, defined functions, and other utilities in the RiverWare program. The hydrology was first simulated (beginning October 01, 1942) utilizing the RiverWare hydrology model, and then simulated results were fed into the RiverWare study model. The latter was used to validate operations and mimic observed data throughout the Nueces River Basin. The concept of using two separate models was to generate local flows from the hydrology model that can be processed in the study model. The algorithmic based functions embedded in the hydrology model, enable the user to apply the right mass balance functions, and route flows throughout the network. The

routing procedures capture lag/travel time and peak attenuation. The parameters applied in the hydrology model are normally set after performing several iterations. Observed flows were used for timing and peaks calibrations. The hydrology model would also provide an accountability of producing incremental and cumulative local flows for further processing. The RiverWare study model network is shown in Figure 8.1.

### 8.1.2 Model Description

The Nueces River Basin model was developed in RiverWare for non-Corps lakes operation. Choke Canyon Reservoir is owned by the Bureau of Reclamation and operated by the City of Corpus Christi. Lake Corpus Christi on the other hand, is owned and operated by the City of Corpus Christi. The upstream modeling boundary is Choke Canyon Dam located on the Frio River. This boundary site is represented in RiverWare as a reservoir object with imported Deterministic Incremental Local Inflow slot values. The downstream modeling boundary is the Nueces River at Calallen, Tex., USGS Streamgaging station 08211500, located near Gulf of Mexico. There are additional local inflow points located throughout the model mainstem.

Rules in the model adapted the RiverWare USACE-SWD regulation policies. The USACE-SWD rules solve the basin as a system and use algorithms for flood control releases, conservation pool operations, and hydropower releases if applicable. The USACE-SWD rules also disaggregate local inflows and forecast cumulative inflows, in which the forecasted flows are used in the network algorithms. Table 8.1 shows model element names and types.

**Table 8.1: Nueces River Basin RiverWare Model Elements and Types**

<b>Element Name</b>	<b>Type</b>	<b>Element Name</b>	<b>Type</b>
Choke Canyon Water Supply	Pump	Lake Corpus Christi _Divert	Diversion
Lake Choke Canyon_Divert	Diversion	Lake Corpus Christi	Storage Reservoir Object
Lake Choke Canyon	Storage Reservoir Object	Lake Corpus Christi Outflow	Control Point
Lake Choke Canyon Outflow	Control point	Near Mathis_Near Bluntzer	Reach
Choke Canyon Outflow_Three Rivers	Reach	Nueces River nr Bluntzer	Control point
Nueces River nr Three Rivers	Control point	Near Bluntzer_At Calallen	Reach
Three Rivers_Corpus Christi Inflow	Reach	Nueces Rv at Calallen	Control Point
Lake Corpus Christi Water Supply	Pump		

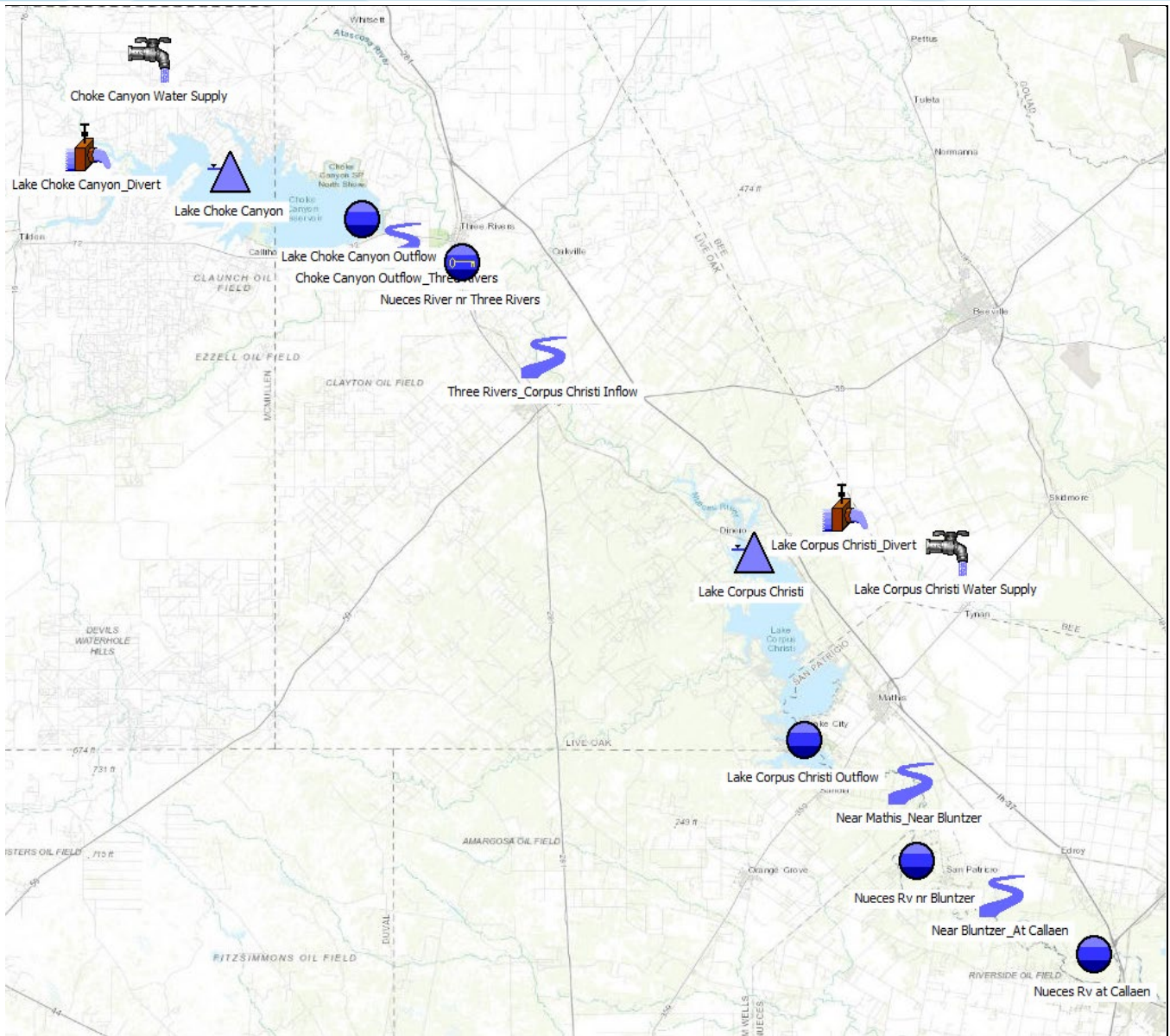


Figure 8.1: RiverWare Nueces River Basin Network

## 8.2 Data Sources Used in the Riverware Model

The modeling efforts in the study area heavily rely upon sound hydrology. Accurate hydrologic analyses reflect more realistic runoff conditions in the watershed, which can change overtime due to urbanization, population growth, agricultural demands, and climate change (e.g., drought or increased flooding due to changes in precipitation conditions). The developed hydrology was based on using the USGS streamgaging stations data at locations of interest. Streamgaging stations with the longest POR were used as the basis for developing gages with missing flow records around the basin. Moreover, data consist of observed USGS discharges, which are measured by the USGS, and pool elevation, adjusted inflow, gated flows, evaporation rates, and water use, which are maintained by the Bureau of Reclamation and the City of Corpus Christi. Table 8.2 lists all gaged data used in the RiverWare models. The locations of the USGS gages in the Nueces River Basin are shown in Figure 8.2.

A significant amount of reservoir volume loss is through evaporation for both lakes. The monthly evaporation rates data were retrieved from the National Oceanic and Atmospheric Administration (NOAA) website. Evaporation rates were then divided and distributed equally over each day of the month before being fed to the RiverWare study model.

In addition, and for Lake Choke Canyon, loss rates through water usage were retrieved from the Bureau of Reclamation Oklahoma-Texas area office water supply data file link (<https://www.usbr.gov/gp-bin/custom.pl?SWE221A&ccdt>). Lake Corpus Christi water use data was obtained from the Nueces River Authority website (<https://www.nueces-ra.org/CP/CITY/pipeline.php>). The monthly water usage data was also divided and distributed equally over each day of the month before being simulated.

Due to some data format limitations in this flood control study, the use of monthly data was justifiable since monthly volumes were preserved regardless of how they were distributed to daily. By inspection, daily loss rates are generally small and have minimum to no impact on flood discharge peaks or flood pool peaks during rare flood events (e.g., 1% ACE or 100-year and greater).

Location	Data Type (Units)	Source
Choke Canyon Dam Site Inflow (San Miguel near Tilden and Frio River at Tilden, Tex.)	Discharge (cubic feet per second)	USGS 08206700 USGS 08206600
Frio Rv at Calliham, Tex.	Discharge (cubic feet per second)	USGS 08207000
Choke Canyon Dam Outflow (Nueces Choke Canyon Res nr Three Rivers, Tex.)	Discharge (cubic feet per second)	USGS 08206910
Atasoca Rv at Whitsett, Tex.	Discharge (cubic feet per second)	USGS 08208000
Nueces Rv nr Tilden, Tex.	Discharge (cubic feet per second)	USGS 08194500
Nueces River nr Three Rivers, Tex.	Discharge (cubic feet per second)	USGS 08210000
Lake Corpus Christi Inflow (Nueces River nr Three Rivers, Tex.)	Discharge (cubic feet per second)	USGS 08210000
Lake Corpus Christi Outflow (Nueces River nr Mathis, Tex.)	Discharge (cubic feet per second)	USGS 08211000
Nueces River nr Bluntzer, Tex.)	Discharge (cubic feet per second)	USGS 08211200

Nueces River at Calallen, Tex.)	Discharge (cubic feet per second)	USGS 08211500
Choke Canyon Pool	Elevation (NGVD-29 feet)	City of Corpus Christi database
Corpus Christi Pool	Elevation (NGVD-29 feet)	City of Corpus Christi database

**Table 8.2: USGS and USACE-SWD Data Used in the RiverWare Model**

Note: NGVD = National Geodetic Vertical Datum of 1929



**Figure 8.2: USGS Streamgauge Locations in the Nueces River Basin**

## 8.3 Period of Record Hydrology Development

### 8.3.1 Methodology Used to Develop Period of Record Hydrology

The important methods used to develop the POR hydrology for the Nueces River Basin in this chapter are the Drainage-Area-ratio method, reservoir inflow calculation, and reservoir inflow smoothing algorithm. This section describes the methodology used in developing the POR.

Rarely is there a POR watershed study where sufficient and consistent gage datasets exist. Incomplete streamgage datasets for streamgaging stations and reservoirs gages can be attributed to budget limitations and anthropogenic changes (*i.e.*, installation of reservoirs). Once discharge estimates were established for each gage, a few years with missing flows were observed. To reconcile the inconsistent dataset, the missing discharges were generated using selected USGS streamgaging stations with continuous records.

Maintenance of Variance extension (MOVE I) (Hirsch, R.M): This method augments daily peak flows using a linear-regression technique to extend gages with short records, utilizing nearby gages of similar hydrologic characteristics with long observed flow records (Equation 1). USGS 08207000 Frio Rv at Calliham, Tex., is a discontinued gage located on the Frio River downstream of the confluence with San Miguel Creek, was used for Choke Canyon Lake inflow from 01 October 1942 to 24 March 1981. Lake inflow for the period of record between 24 March 1981 to 30 September 2019 was the combined flows of USGS 8206600 Frio River at Tilden, Tex., and USGS 8206700 San Miguel near Tilden, Tex. USGS 8206600 Frio River at Tilden was used to extend USGS 8206700 flows from 24 March 1981 to 30 September 1989 since the gage flow recording is missing records (Figure 8.3). Quality control was performed, and the maximum discharge peaks were adjusted to account for attenuation. Extreme discharge peaks greater than the average discharge peak value for the POR were adjusted, by utilizing a correlation resulting from establishing peak to peak flow relationship between the selected USGS gages. The combined inflow was inspected to ensure significant pool elevation rises are directly influenced by high discharge peaks at the lake.

$$Y_i = Y_{Avg} + S_Y / S_X (X_i - X_{Avg})$$

**Equation 1: MOVE I Equation Method**

$Y_i$  is the estimated logarithm of the discharge at the study streamgage for day  $i$  [ $L^3/T$ ].

$Y_{Avg}$  is the mean of the log-transformed observed discharges at the study streamgage [ $L^3/T$ ].

$S_Y$  is the standard deviation of the log-transformed observed discharges at the study streamgages [ $L^3/T$ ].

$S_X$  is the standard deviation of the log-transformed observed discharges at the study streamgage [ $L^3/T$ ].

$X_i$  is the log-transformed daily discharge at the reference streamgage for daily  $i$  [ $L^3/T$ ], and

$X_{Avg}$  is the mean of the log-transformed observed discharge at the reference streamgage [ $L^3/T$ ].

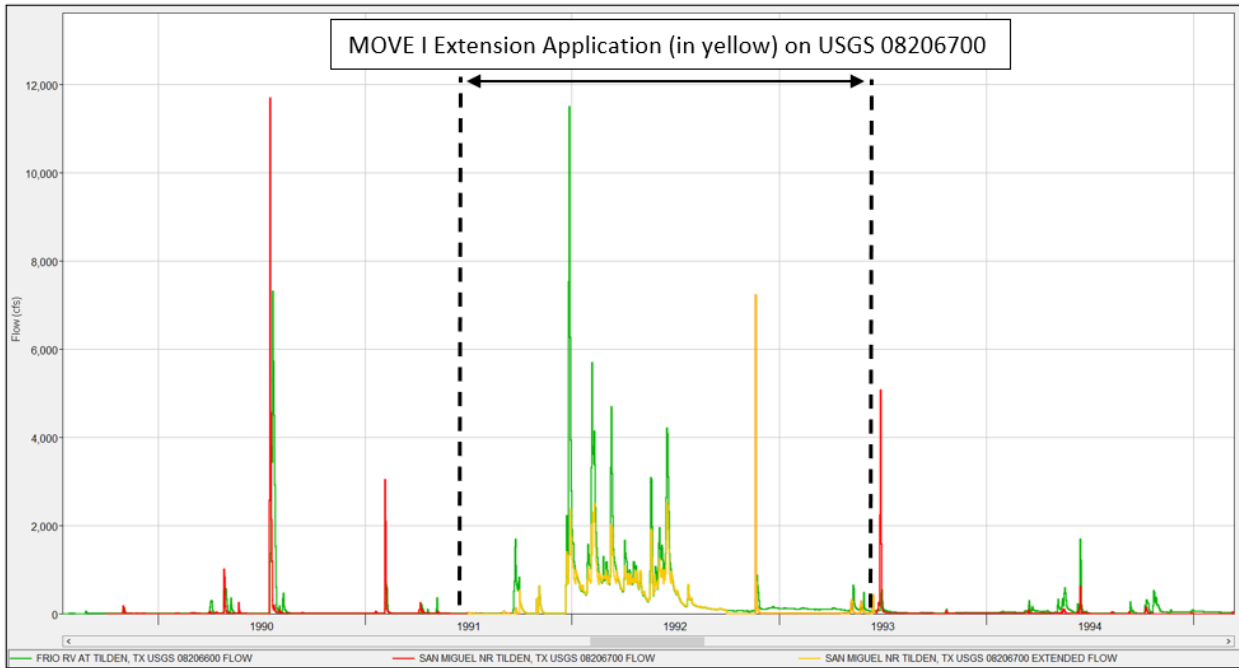


Figure 8.3: Example of USGS 08205500 Gage Record Extension from USGS 08206600 Prior to Mid-Year 1978

The remainder of the discharge peak estimates in the Nueces River Basin were based on applying the Drainage-Area ratio method and routing to capture travel time and attenuation.

The Drainage-Area-ratio method provides a numerical approximation of the missing gage data, using gage datasets upstream or downstream on the same river (Equation 2).

$$Q_y = \frac{Q_x}{A_x} A_y$$

**Equation 2: Drainage-Area-Ratio Method**

$Q_y$  = Flow at gaged site Y of drainage area  $A_y$  [ $L^3 / T$ ]

$Q_x$  = Flow at gaged site X of drainage area  $A_x$  [ $L^3 / T$ ]

$A_y$  = Drainage area of ungaged site [ $L^2$ ]

$A_x$  = Drainage area of available gaged site X [ $L^2$ ]

The numerous arrays of reservoir inflow calculations tolerate for thoroughness, as well as discontinuity. All reservoir inflow calculations share the mass balance approach. The method selection for the calculation of reservoir inflow is subjective and ultimately should be selected on a case-by-case basis. There is one method used to calculate reservoir inflows in this study. It is the “evaporation reservoir inflow method” (method applied to USACE datasets).

$$I = \Delta S + E + R + Q_{total}$$

**Equation 3: Evaporation Reservoir Inflow Method**

$I = \text{Inflow into the reservoir } [L^3 / T]$

$\Delta S = \text{Change in reservoir storage } [L^3 / T]$

$E = \text{Evaporation from the reservoir } [L^3 / T]$

$Q_{total} = \text{Total pumpage out of the reservoir } [L^3 / T]$

The calculated reservoir inflow is subject to measurement error and numerical error. The evaporation parameter is arguably the most difficult parameter to estimate when calculating reservoir inflow. The uncertainty in measurement often leads to negative reservoir inflow values, which violates the conservation of mass theory. Reservoir release rates can also be inaccurate due to the imperfect nature of setting the gate height at the project. To resolve these inconsistencies the reservoir inflow values are numerically smoothed by scaling positive inflows and rectifying negative inflows. The smoothed inflow algorithm is applied over a monthly time period with a daily time step and preserves the volume of the monthly total (Equation 4, Equation 5, Equation 6, and Equation 7). There are additional inflow smoothing methods available, but this method is sufficient to resolve negative reservoir inflows in this case and depending on the month, imparts only minimal positive bias.

$$\text{Monthly Total Inflow} = \sum_i^{i_f} I_i$$

**Equation 4: Monthly Total Inflow Method**

$$\text{Nonnegative Inflow} = \begin{cases} \text{if } I_i < 0 \\ 0 \\ \text{else} \\ I_i \end{cases}$$

**Equation 5: Nonnegative Inflow Method**

$$\text{Monthly Total Nonnegative Inflow} = \sum_i^{i_f} \text{Nonnegative Local}$$

**Equation 6: Monthly Total Nonnegative Inflow Method**

$$\text{Smoothed Inflow} = \begin{cases} \text{if Monthly Total Inflow} < 0 \text{ OR Monthly Total Nonnegative Inflow} = 0 \\ \text{Nonnegative Inflow} * 0 \\ \text{else} \\ \text{Nonnegative Inflow} * \frac{\text{Monthly Total Inflow}}{\text{Monthly Total Nonnegative Inflow}} \end{cases}$$

**Equation 7: Smoothed Inflow Method**

$I = \text{Inflow into the reservoir on the } i^{\text{th}} \text{ day } [L^3 / T]$

$i = i^{\text{th}} \text{ day of the month}$

$i_f = \text{last day of the month}$

*Montly Total Nonnegative Inflow = Summation of the monthly nonnegative inflows  $[L^3 / T]$*

*Montly Total Inflow = Summation of the monthly reservoir inflows  $[L^3 / T]$*

*Nonnegative Inflow = A nonnegative dataset of the reservoir inflows  $[[L^3 / T]: [L^3 / T]]$*

*Smoothed Inflow = A smoothed dataset of the reservoir inflows  $[[L^3 / T]: [L^3 / T]]$*

The methods presented above along with the RiverWare modeling software have permitted for the development of POR hydrology for the Nueces River Basin. The following Application section will describe how these methods were implemented within the framework of the RiverWare modeling software and the precursor to the RiverWare modeling software.

### 8.3.2 Period of Record Hydrology for the Nueces River Basin

The POR hydrology needed to evaluate the Nueces River Basin requires the use of numerical models. RiverWare version 8.0.1 (January 08, 2020) was used to analyze the hydrology and hydraulic processes of Choke Canyon Reservoir and Lake Corpus Christi, and the river reaches within the Nueces River Basin. The hydrology and hydraulic analysis include the use of a multiple-run and simulation-run RiverWare models. The multiple-run RiverWare model produced the POR hydrology from October 01, 1942 to September 30, 2019 for all streams and reservoirs gage sites. The POR hydrology is the naturalized local flows, where major anthropogenic impacts have been removed, including effects of reservoir regulation. The simulation-run RiverWare model used the POR hydrology datasets to simulate the entire Nueces River basin reservoirs pool elevations with reservoir regulation policies incorporated for the entire POR, which will be used in the statistical frequency analysis portion of the study.

The process for developing POR hydrology, for the reservoirs and control points or streamgaging stations of interest, is to assimilate historical reservoir inflow and stream flow datasets, then implement Drainage-Area-ratio methods and reservoir inflow smoothing algorithms in a multiple-run RiverWare model to numerically solve for the POR hydrology. Analyzing pool elevations and operational release over the POR requires the POR hydrology and reservoir operational policies and rule sets to be incorporated into a simulation-run RiverWare model. The reservoir operational policies and rule sets applied to reservoirs can then be compared to historical pool elevations, releases, and local inflows to verify consistency with historical datasets. Ultimately the policies and rule sets can be applied to the POR hydrology to establish synthetic pool elevation and reservoir operation before the reservoirs existed.

## 8.4 Water Control Plans for the Nueces Usace Reservoirs

Table 8.3 lists some main operational procedures, flood control key points, and objectives of each modeled reservoir in RiverWare.

Purpose/Downstream Control points/Pool zones	Choke Canyon	Corpus Christi
<b>Dam Type</b>	Storage	Storage
<b>Purpose</b>	Fish and wildlife, general recreation, and water supply.	Water supply and general recreation
<b>Control Point</b> <b>Located downstream of each project</b>	5,300cfs at USGS 8210000 Nueces River near Three Rivers, Tex.	None, forecast based
<b>Pool zone</b>	Elevation (NGVD-ft)	Elevation (NGVD-ft)
<b>Top of conservation</b>	220.50	Below 94.00
<b>Top of flood</b>	Above 220.5	94.00
<b>Surcharge</b>	220.5	South side 94.00
<b>Top of Spillway Crest</b>		North side 94.50
<b>Top of Dam</b>	241.14	106.0
<b>Initial Impoundment Date</b>	January 1982	January 1952

**Table 8.3: Highlights from the Nueces River Lakes Water Management Plan**

Note: Some pool zone adjustments were made in the model as follows:

- 1- Conservation zone was set at 221 ft-NGVD to match top of observed pool above surcharge.
- 2- Top of flood was set at 222.5 ft-NGVD to mimic observed surcharge.

In RiverWare, policies and functions were written to reflect the current reservoir regulation schedule for each lake. Table 8.4 lists the Lakes' release schedules. Release procedures in this table were also included in the RiverWare model for simulation.

Choke Canyon Reservoir		Lake Corpus Christi	
Pool Elevation (NGVD-feet)	Maximum Allowable Release	Pool Elevation (NGVD-feet)	Maximum Allowable Release
136.40 - 220.50	No flood control release  Low flow requirements of 16cfs.	Below 94.00	No flood control release Daily releases for water supply and bays and estuaries varies from 20 to 110cfs.
220.50	2,000cfs	94.00 - 94.50	Close high-pressure gates (Outlet works) and release according to south side spillway gate operating curve
220.50 - 221.00	Close high-pressure gates (Outlet works) and release according to spillway gate operating curve	Above 94.50	Release according to south side spillway gates operating curve and North side (emergency gates) if needed
Above 221.0	Surcharge release		

**Table 8.4: Nueces River Operated Lakes Release Schedule**

### 8.5 Riverware Operational Model Application

The RiverWare simulation model executes all flood control releases, so as, to maximize flood release within the period of perfect knowledge. This period is defined as: the number of time steps for which the forecast will equal the Deterministic Incremental Local Inflow, *i.e.*, the forecast is known with complete certainty. In real time historical operations, there are numerous and event-specific reasons as to why the reservoir was operated the way it was. Meteorological forecasts from the National Weather Service, as well as river stage forecasts issued by the West Gulf River Forecast Center could both potentially influence the rate of release from the project.

The Nueces River Basin RiverWare model includes policies implemented as rules. Rule number 1 is the highest priority rule and executes last (e.g., hydropower release rule) while the rule with the highest number is the lowest priority rule and executes first (e.g., Surcharge rule). Figure 8.4 below shows the priority list of policies implemented in the model. As seen, the flood control policies execute first and this is mainly to control flooding at damage center locations downstream.

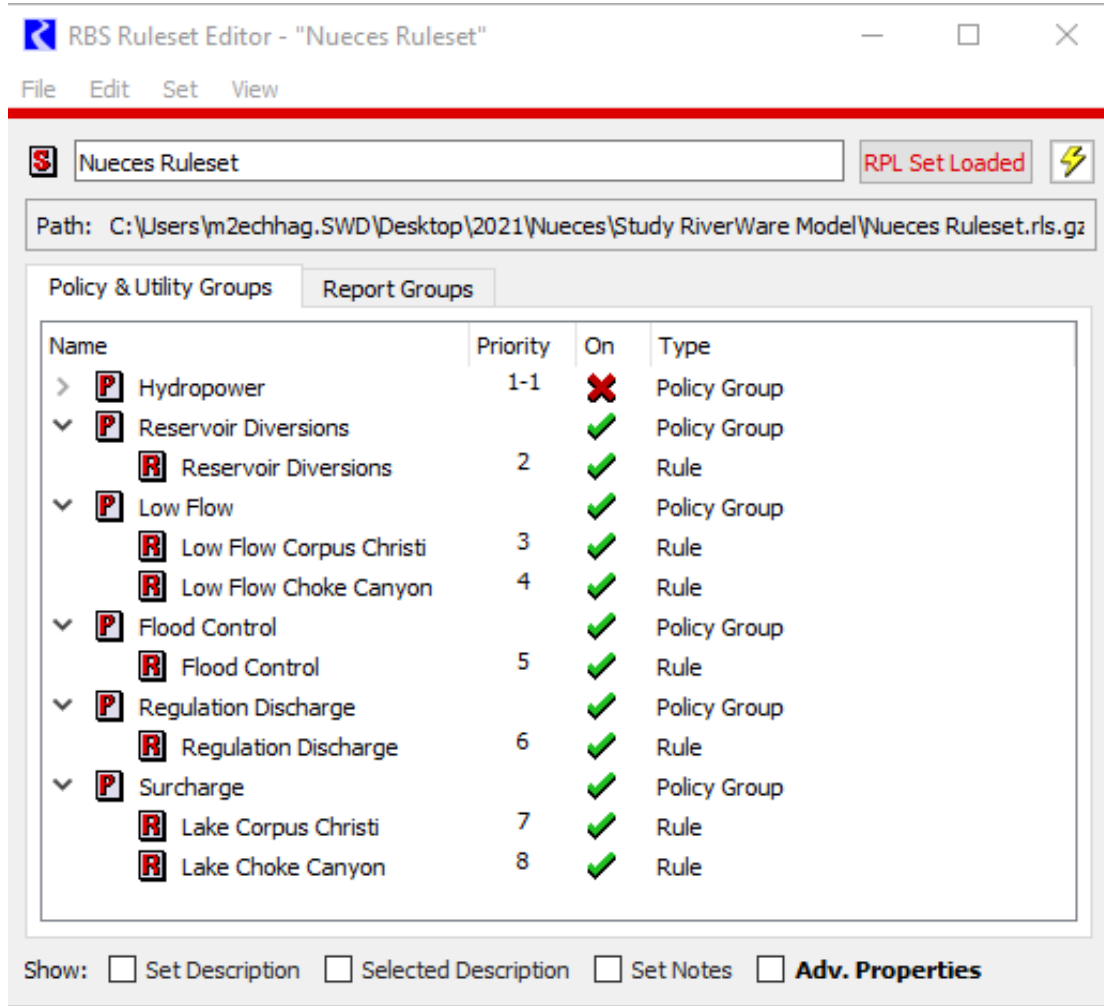


Figure 8.4: Nueces River Basin Rule-based Simulation Groups

The built-in rules in USACE-SWD conservation pool operations apply to Corps and non-Corps dams since RiverWare triggers specific elevations in the operating level table. These generic operating level tables reflect dams' conditions with or without flood storage. The other rules (e.g., Regulation discharge, flood control, reservoir diversion, and hydropower, if applicable, and release rules) kick in based on priority.

## 8.6 Model Calibration Results and Discussion

Overall, the model displays satisfactory results between simulated and observed considering operation limitations. The rules used for simulation do not always produce matching results of the historical (observed) flows, because real-time operation is normally based on real-time forecasting, which causes release deviations from operations' schedule. The model uses the deterministic flow with a simple forecasting technique and a set of policies. The surcharge, regulating discharge, and flood control rules execute first while also accounting for low flows at each reservoir. Data availability can also contribute to deviations from observed conditions.

The following is a discussion of results for Choke Canyon Reservoir and Lake Corpus Christi.

### 8.6.1 Choke Canyon Reservoir Model Performance

The simulated pool for Choke Canyon reservoir showed satisfactory results against observe pool. The comparison is for the period post initial dam impoundment (i.e., 1987) through 2019 (Figure 8.5). To match observed pool, top of pool was set above conservation (221.0ft-NGVD). Although the project has no authorized flood control purposes, a flood control policy that is consistent with the SWD-USACE operation criteria was added to the RiverWare model to mimic observed conditions. The written flood control policy trigger releases based on pool elevations; the assumed pool elevation would be referred to as the flood control pool (222.5ft-NGVD). This flood control pool provides a buffer zone between conservation and surcharge. Releases between 220.5 NGVD-ft and 221.0 NGVD-ft were limited to 2,000cfs. Surcharge conditions mimicked observed pool in the years of 1992, 2002, 2003, 2004, and 2007. Project release was according to the discharge-elevation rating curve for controlled and uncontrolled spill (Table 8.5). For surcharge simulation, the flat top surcharge method was selected. This method uses a perfect knowledge forecast technique and daily time steps. With a minimum timestep of one day being used, the model releases more than observed keeping the peak elevations lower. Release adjustments were made to improve simulated peaks (Table 8.5). Simulated drawdown synchronized well with observed pool. Depletions were according to pumpage data and evaporation rates obtained from water supply monthly reports for January 1983 – October 2019. The simulated pool stayed above observed on the drawdown side. This can be related to the way available data were processed. The monthly evaporation loss rates and water usage data feed are evenly distributed over each day of the month. Lack of data from other losses can add to deviations from observed steep drawdowns.

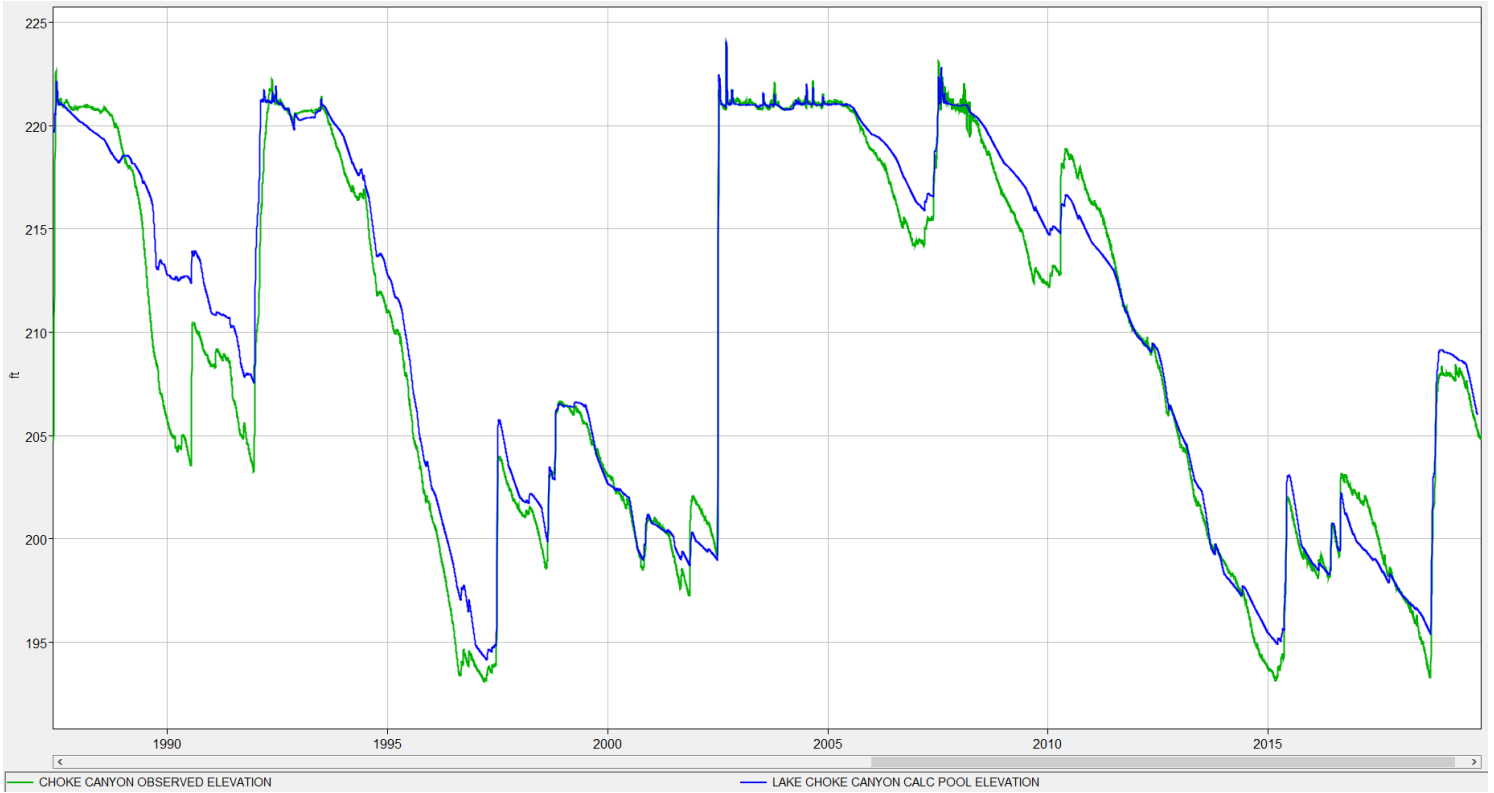


Figure 8.5: Choke Canyon’s Reservoir Simulated Pool Comparison with Observed

**Table 8.5: Choke Canyon Reservoir Controlled and Uncontrolled Maximum Release**

Pool	Release	Pool	Release	Pool	<b>Adjusted Release</b>
NGVD-Feet	CFS	NGVD-Feet	CFS	NGVD-Feet	CFS
135.3	-	217.5	2,000	217.5	2,000
199.5	20	218	2,000	218	2,000
199.9	257	218.5	2,000	218.5	2,000
200	487	219	2,000	219	2,000
200.1	658	219.5	2,000	219.5	2,000
200.2	727	220	2,000	220	2,000
200.4	1,063	220.5	2,000	220.5	2,000
200.6	1,423	221	141,956	221	<b>2,000</b>
200.8	1,794	221.5	145,251	221.5	<b>3,000</b>
201.2	2,000	222	148,473	222	<b>5,000</b>
201.4	2,000	222.5	151,626	222.5	<b>10,000</b>
201.8	2,000	223	154,715	223	<b>15,000</b>
202.6	2,000	223.5	157,744	223.5	<b>25,000</b>
203.5	2,000	224	160,715	224	<b>30,000</b>
204.5	2,000	224.5	163,633	224.5	163,633
205.5	2,000	225	166,499	225	166,499
206.5	2,000	225.5	169,317	225.5	169,317
207.5	2,000	226	172,088	226	172,088
208.5	2,000	226.5	174,816	226.5	174,816
209.5	2,000	227	177,502	227	177,502
210.6	2,000	227.5	180,148	227.5	180,148
211	2,000	228	182,756	228	182,756
211.5	2,000	228.5	185,326	228.5	185,326
212	2,000	229	187,862	229	187,862
212.5	2,000	229.5	190,364	229.5	190,364
213	2,000	230	192,833	230	192,833
213.5	2,000	230.5	195,272	230.5	195,272
214	2,000	231	197,680	231	197,680
214.5	2,000	231.5	200,059	231.5	200,059
215	2,000	232	202,410	232	202,410
215.5	2,000	232.5	204,734	232.5	204,734
216	2,000	233	207,032	233	207,032
216.5	2,000	241	242,200	241	242,200
217	2,000				

NOTE: Some situational releases did occur under 220.5 in previous flood events, but releases are not required below elevation 220.5. Releases in this table were adjusted from the original plan to improve simulation.

USGS 08206910 (Nueces Choke Canyon Reservoir near Three Rivers) is located at the reservoir outlet, but the rating curve of this gage is limited to measuring flows with a maximum stage of 10 feet, which equates to about 2,000cfs. A snippet of discharge at this gage is shown in Figure 8.6. Notice USGS gage flow discontinuity.

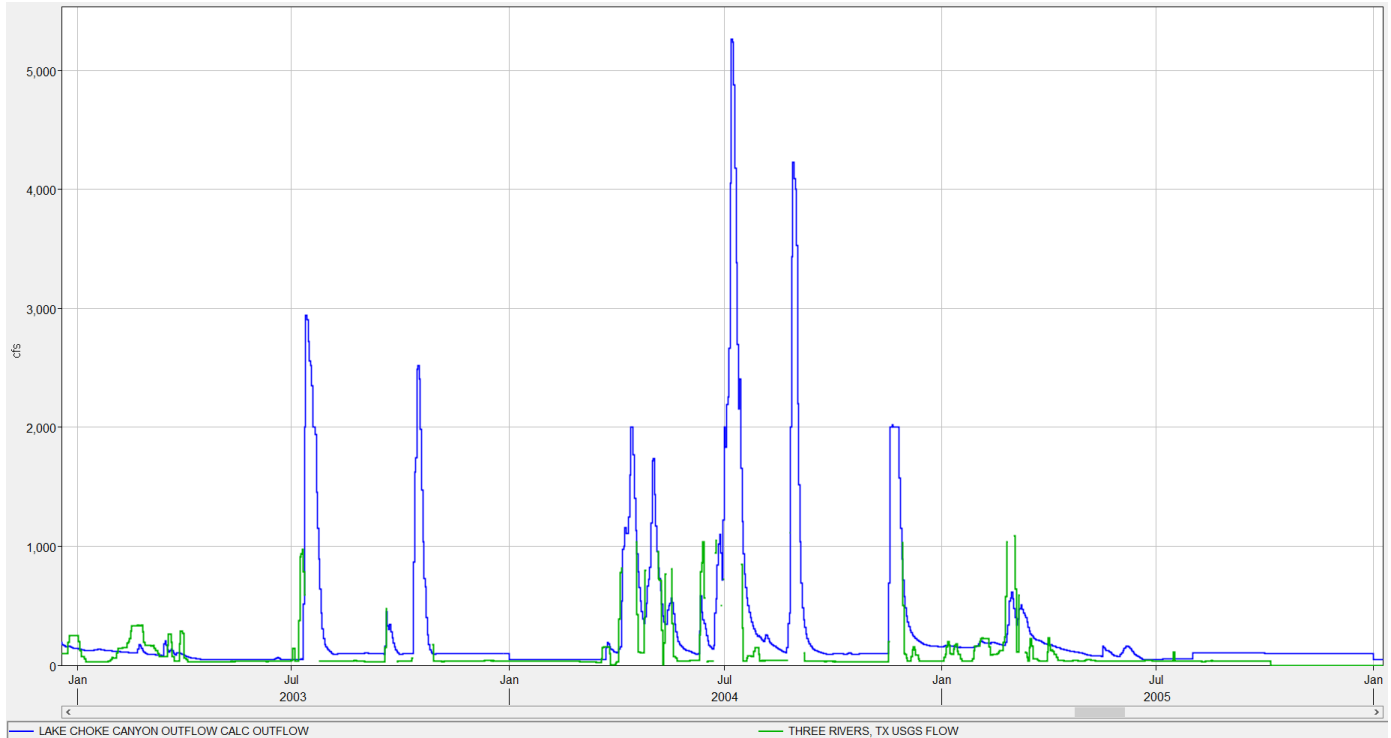


**Figure 8.6: Simulated-Observed Release Comparison at Choke Canyon Reservoir Outlet**

USGS 08210000 (Nueces River near Three Rivers) was also used to evaluate model results. This gage is located between Choke Canyon Reservoir and Lake Corpus Christi. It also captures flows from USGS 08208000 Atascosa Rv at Whitsett and USGS 08194500 Nueces Rv nr Tilden. The validation of simulated releases from Choke Canyon Reservoir captured release routings downstream of the dam, as well as, peaking at USGS 08210000. The flows at this gage were also routed to Lake Corpus Christi. Figure 8.7 and Figure 8.8 illustrate how well the model performs at this location for 2004 – 2019.

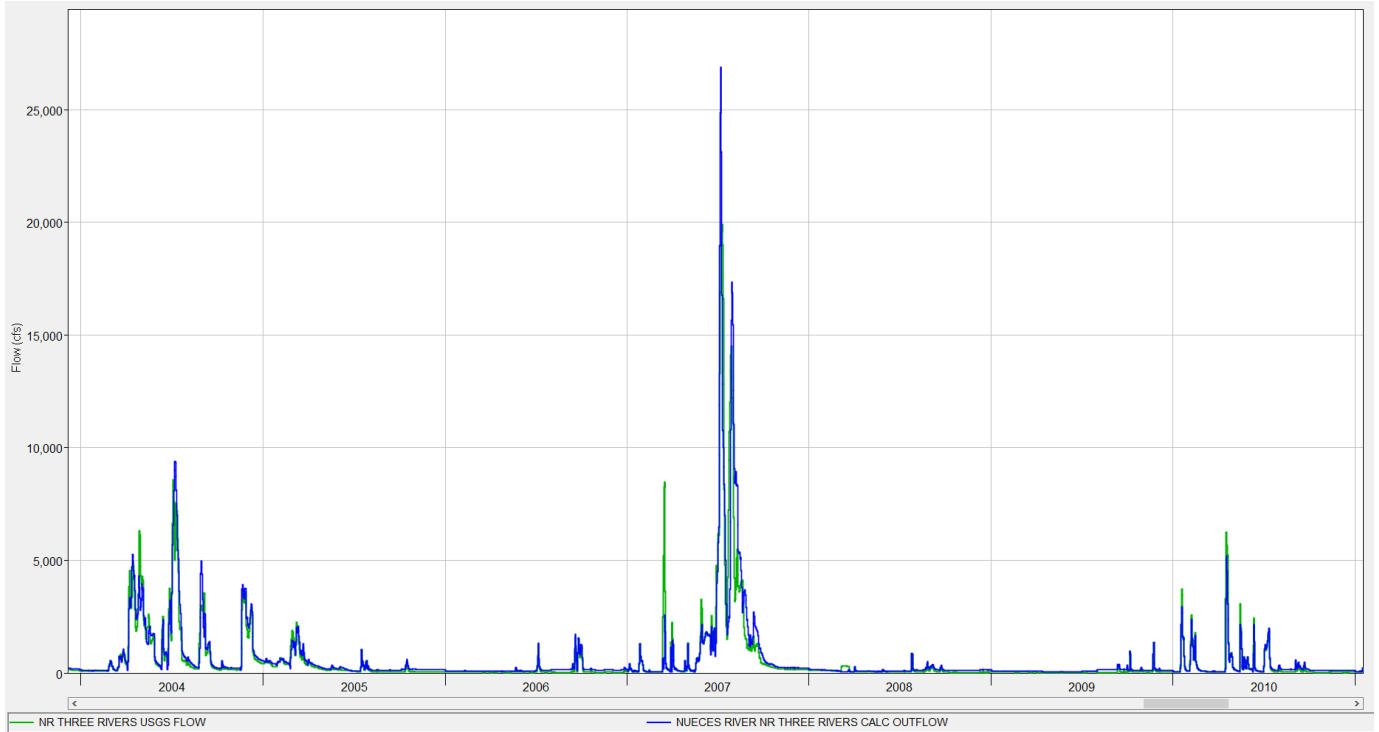


Figure 8.7: (2004-2010) Validation of Simulated Flows at USGS 08210000

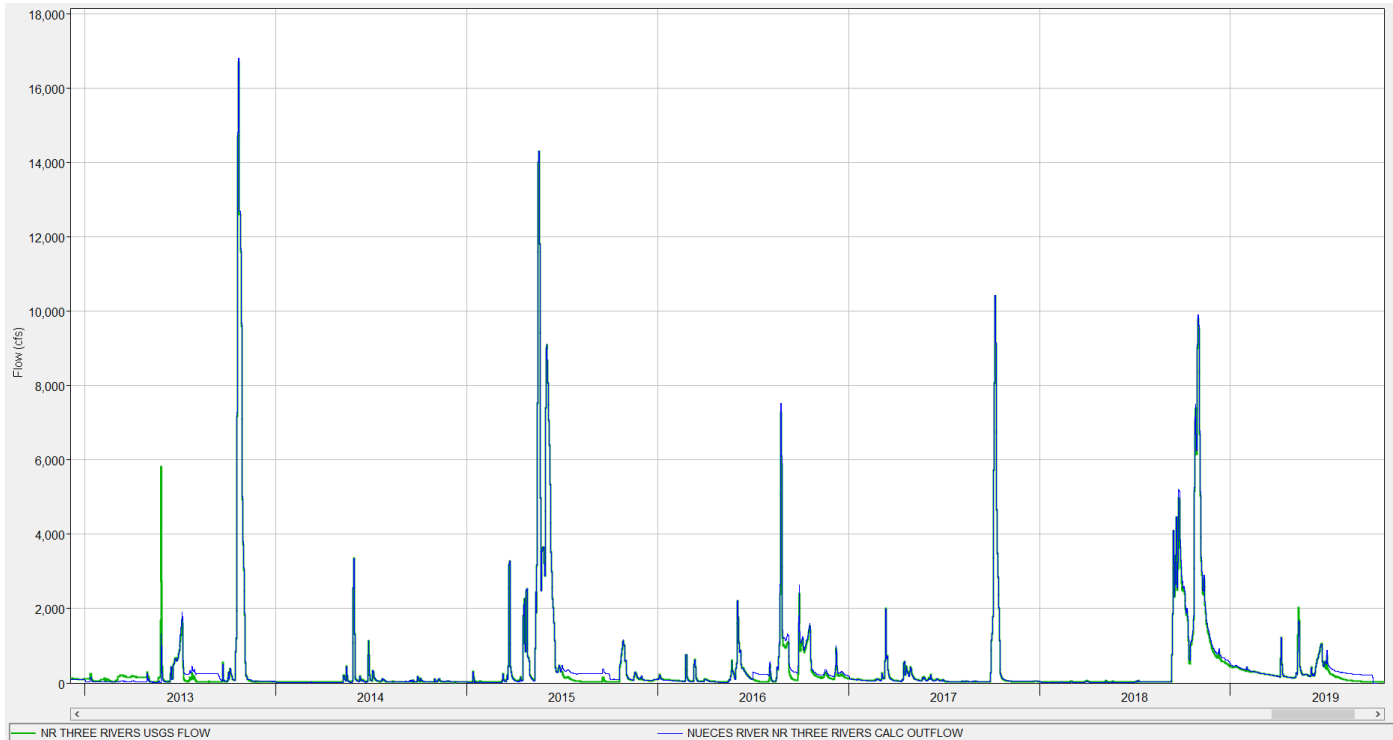
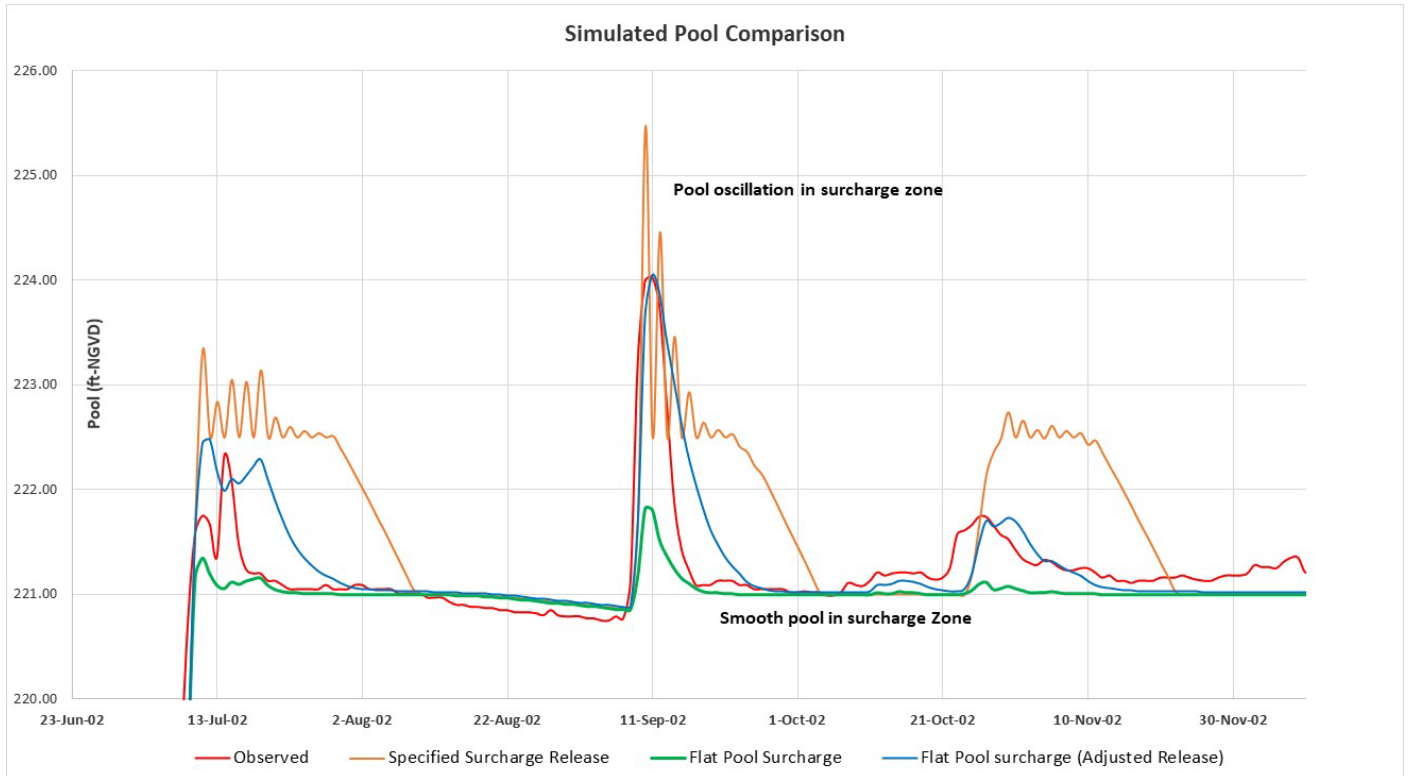


Figure 8.8: (2013-2019) Validation of Simulated Flows at USGS 08210000

Figure 8.9 shows selected sensitivity analysis performed for Choke Canyon Reservoir pool prior to adopting the best performed operation. The flat top surcharge method was selected over the specified surcharge release method. The model tends to be more stable when the flat top surcharge method is selected. The method eliminates oscillations seen in the surcharge zone and reservoir releases. Those oscillations are associated with the specified surcharge release method when selected. The adjusted release flat top surcharge method results associated with the more realistic operation were considered for this study.



**Figure 8.9: Sensitivity Analysis for Choke Canyon Reservoir Pool Simulation**

Figure 8.10 illustrates the Weibull plotting position distribution of the lake between water years 2000 and 2020. The last 20 years of operation were analyzed, because they reflect current operational standards. The simulated peaks above 221.5 ft.-NGVD were lower than observed due to the selected surcharge method, which tends to flatten the top of flood pool. For this lake, the observed pool will be selected over simulated when available during the statistical analysis, but simulated pool peaks will be included for periods prior to dam initial impoundment. Figure 8.11 illustrates the corresponding relationship between observed and simulated pool for Lake Choke Canyon for water years 2000-2020. The strong relationship increases confidence in the adopted simulated results.

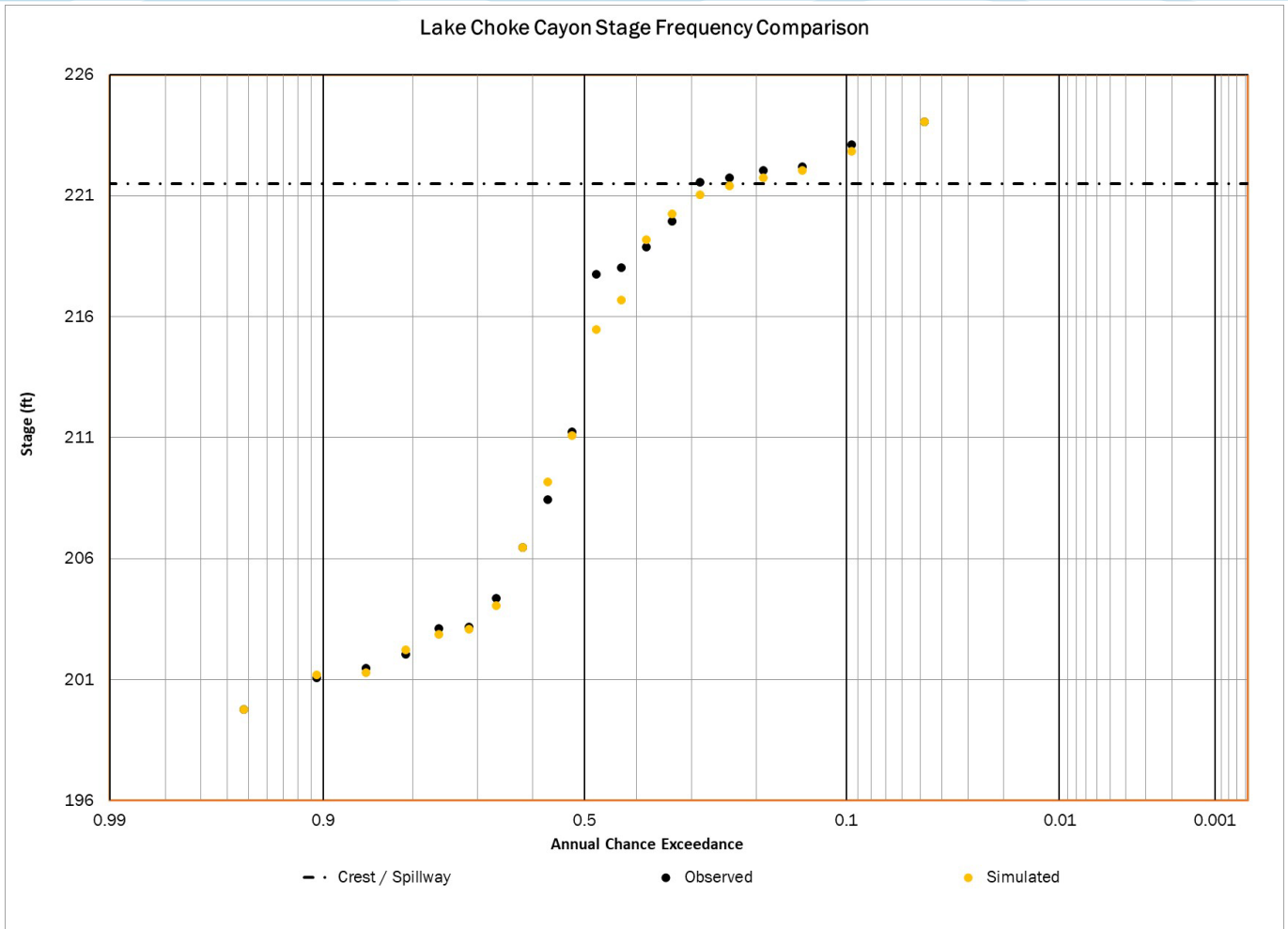


Figure 8.10: Choke Canyon’s Stage Frequency Peak Comparison (Annual Maximum Peaks) for WY 2000-2020

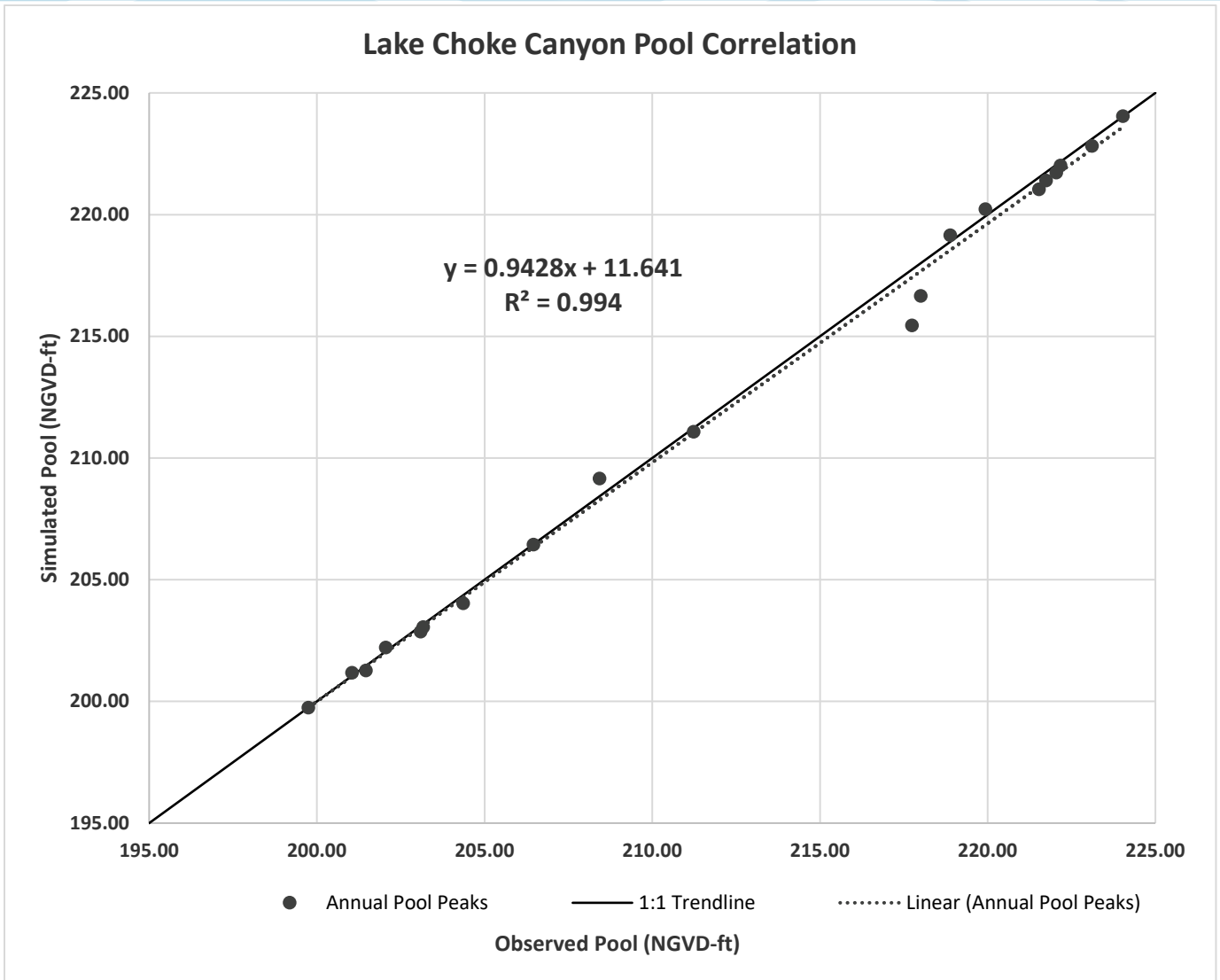


Figure 8.11: Observed Vs. Simulated Pool Annual Maximum Peak for Choke Canyon Lake for WY 2000-2020

Pool simulation for WY (1943-2019) is shown in Figure 8.12. Despite applying the same operation conditions for the entire POR, more drawdowns can be seen during the last 30 years (1987-2019) than the prior 45 years (1943-1987). The last 30 years was the period since dam initial impoundment, where observed loss data were available. Population growth coupled with recent severe droughts due to temperature increase (i.e., increase in evaporation rates) have played major factors in the steep drawdowns seen in the last years. Years prior to 1987, had not seen as many drawdowns. Pool bottom stayed above 211ft-NGVD except during 1967. The simulated pool in those early years were significantly impacted by the assumed losses. Figure 8.13 illustrates observed and assumed water supply demand in cubic feet per second (green line and can be read from the right Y-axis) and the evaporation rates in inches per day (line in brown and can be read from the left Y-axis). Missing data were estimated from the observed using the average. Estimated losses appear with a more consistent trend in the figure. Drawdown operations can be improved in future studies, but there is high confidence in the use of the flood peaks for flood frequency analysis from this study.

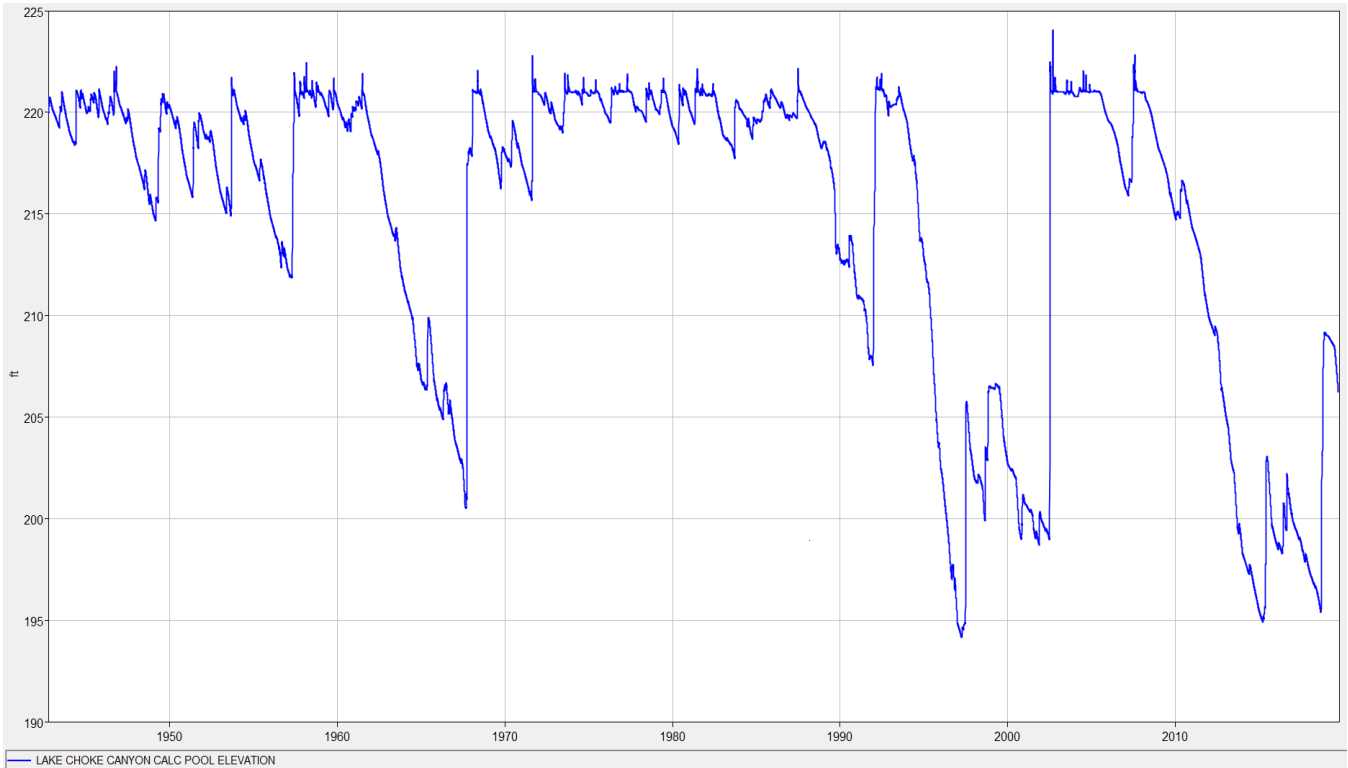


Figure 8.12: Lake Choke Canyon Simulated Pool

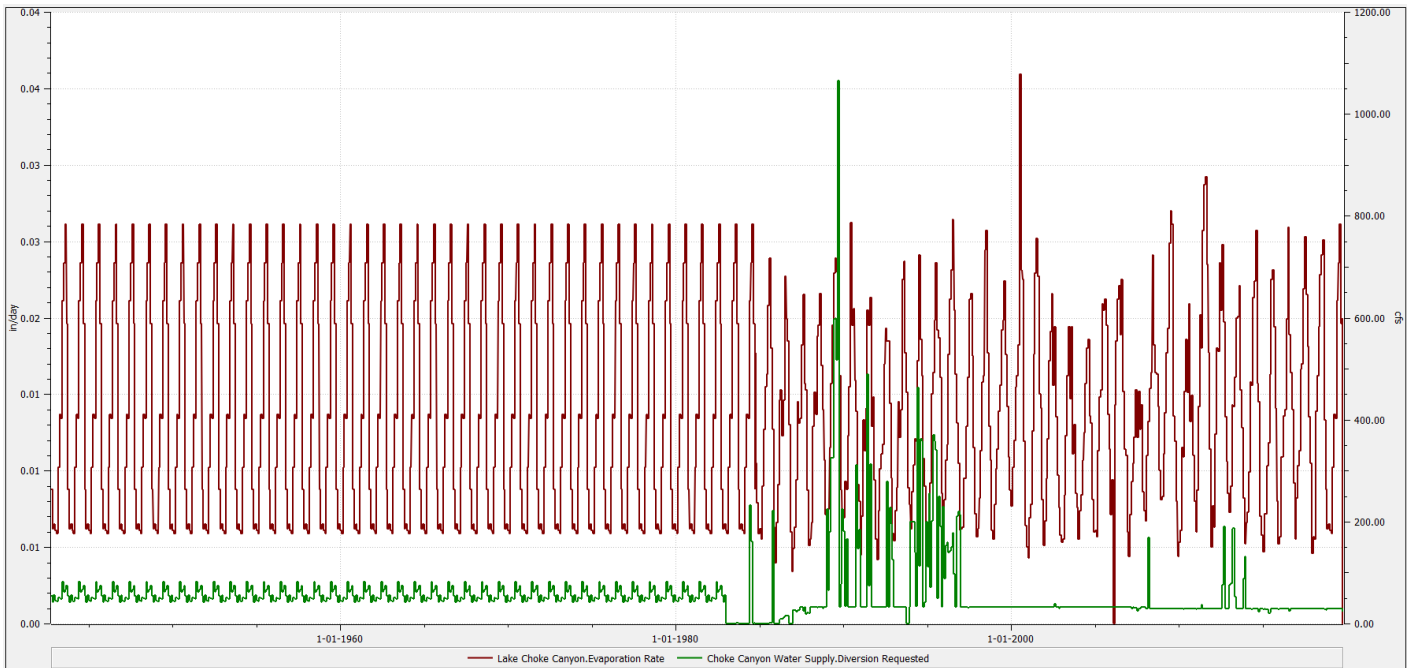


Figure 8.13: Observed and Estimate Water Supply Demand Losses and Evaporation Rates Losses for Lake Coke Canyon

### 8.6.2 Lake Corpus Christi Model Performance

Overall, the simulated results performed well for this lake. The evaluation was based on applying current operation schedules that would reflect normal and flood conditions. For surcharge simulation, the flat top

surcharge method was selected. This method uses a perfect knowledge forecast technique and daily time steps. With a minimum timestep of one day being used, the model releases more than observed keeping the peak elevations lower. Rating curve release adjustments were made to improve simulated release and pool peaks. This method keeps surcharge pool attenuated and somewhat flat near top of flood zone line.

The RiverWare modeling efforts for the Nueces River Basin WHA study in this section were designed to put emphasis on the last 20 years of operations (2000-2020), simulating flood control conditions, rather than rigorously simulate water supply and drought conditions. Plots 8.20-8.25 validate the current operations been applied. The plots show good matching simulation results with observed. The same current rules were then applied across the entire POR to simulate historical events. The following paragraphs illustrate comparisons of historical model simulations with observed. Reasonings behind deviations from historical events are also captured in great details.

It should be noted that background information about the project and a narrative of historical events throughout the life of the project, which were obtained from personnel of the City of Corpus Christi, were used to justify model performances against observed events. The dam has a long history of instability issues, which mandated multiple requests for emergency drawdowns, change in operation, and maintenance. For example, since the dam initial impoundment between 1955 and 1958, and over the years, Lake Corpus Christi was impacted by several droughts that dropped the lake significantly. Damages occurred to the project due to big flood events (e.g., the 1965 flood), instability mandated keeping the pool at low levels. The following figures are comparisons of simulated versus observed pool over the years.

The observed pool in Figure 8.14 shows pool levels of the lake when the project was first constructed. After construction was completed, drought occurred between 1955-1957, which limited reservoir filling. The reservoir essentially started filling post 1958 due to heavy rain and flooding. Since simulation began on 01 October 1942, the simulation does not account for the filling period during initial impoundment and assumes a reasonable starting pool condition. The initial pool was set at conservation (below 94.0ft-NGVD). The simulated pool remained flat and dropped some but stayed above 86.0ft-NGVD. The lake filled quickly, following the flood events occurred between 1958 and 1960, and stayed at conservation through 1960.

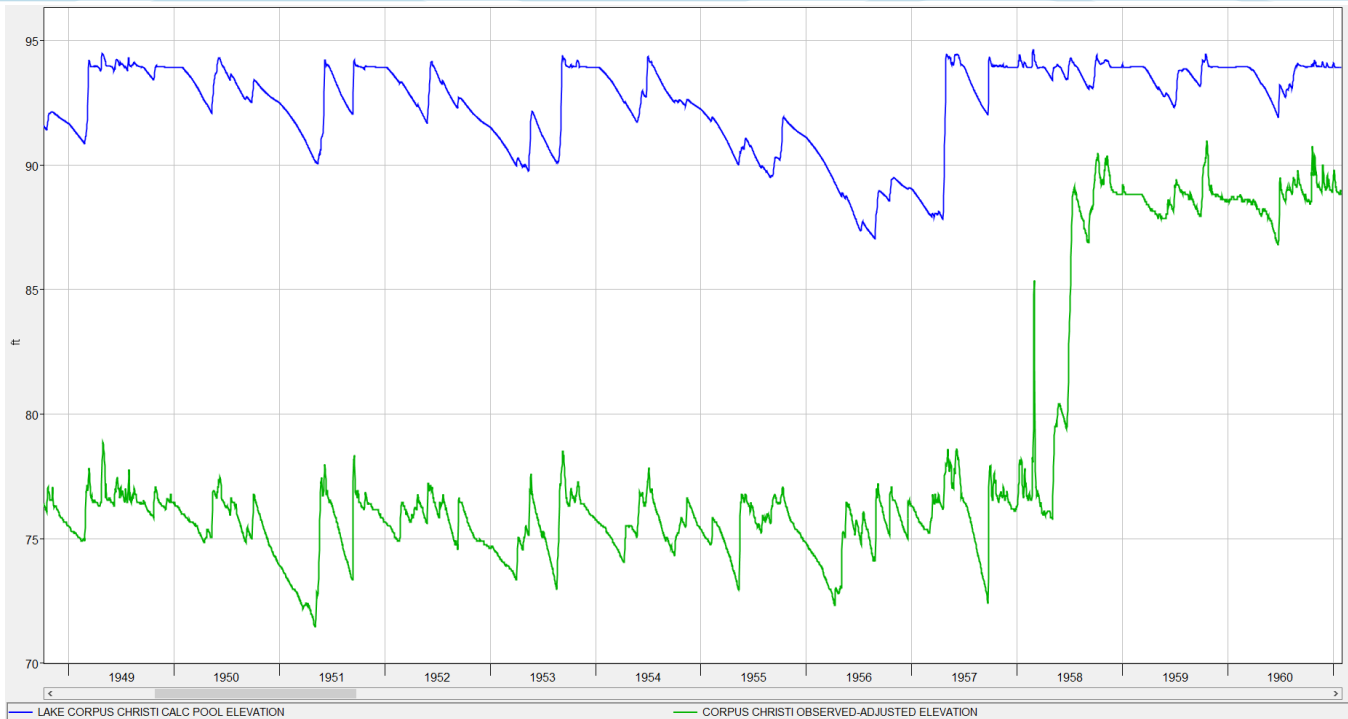


**Figure 8.14: Validation of Lake Corpus Christi Simulated Pool During Dam Initial Impoundment**

Another dry period occurred between 1960 and 1967. This period was captured by the model in 1964. During hurricane Beulah (1967) a high observed water mark was recorded (approximately 96.22ft-NGVD). During the hurricane event, all spillway gates were engaged, and a discharge was approximately 128,000cfs. The model captured the hurricane affect by raising the pool to surcharge (above 94ft-NGVD). The simulated release was about 105,800cfs from the project (Figure 8.16). The peak release difference was associated with the difference between observed and simulated pool (1.40 feet difference) due to the flat top surcharge method being used to simulate reservoir during surcharge. In addition, flood release is based on perfect knowledge that the model trigger releases and keep pool from reaching elevations above 95.0 ft-NGVD. It should also be noted that in 1965, a storm did a significant damage to the system, where the automated gates were replaced by 1967 with manually and hydraulically operated gates. As a result, gate operation policy was developed and a 6 feet drawdown from 1965 until all gates were restored in 1967. Lake was operated according to the 1967 gate operating plan until the stability issues developed. At that time, lake was already low due to drought. It is clear the model is not designed to mimic such unusual conditions, and for that reason the lake wasn't drawn down to the observed level (early 1965 to mid-1967), see Figure 8.15.

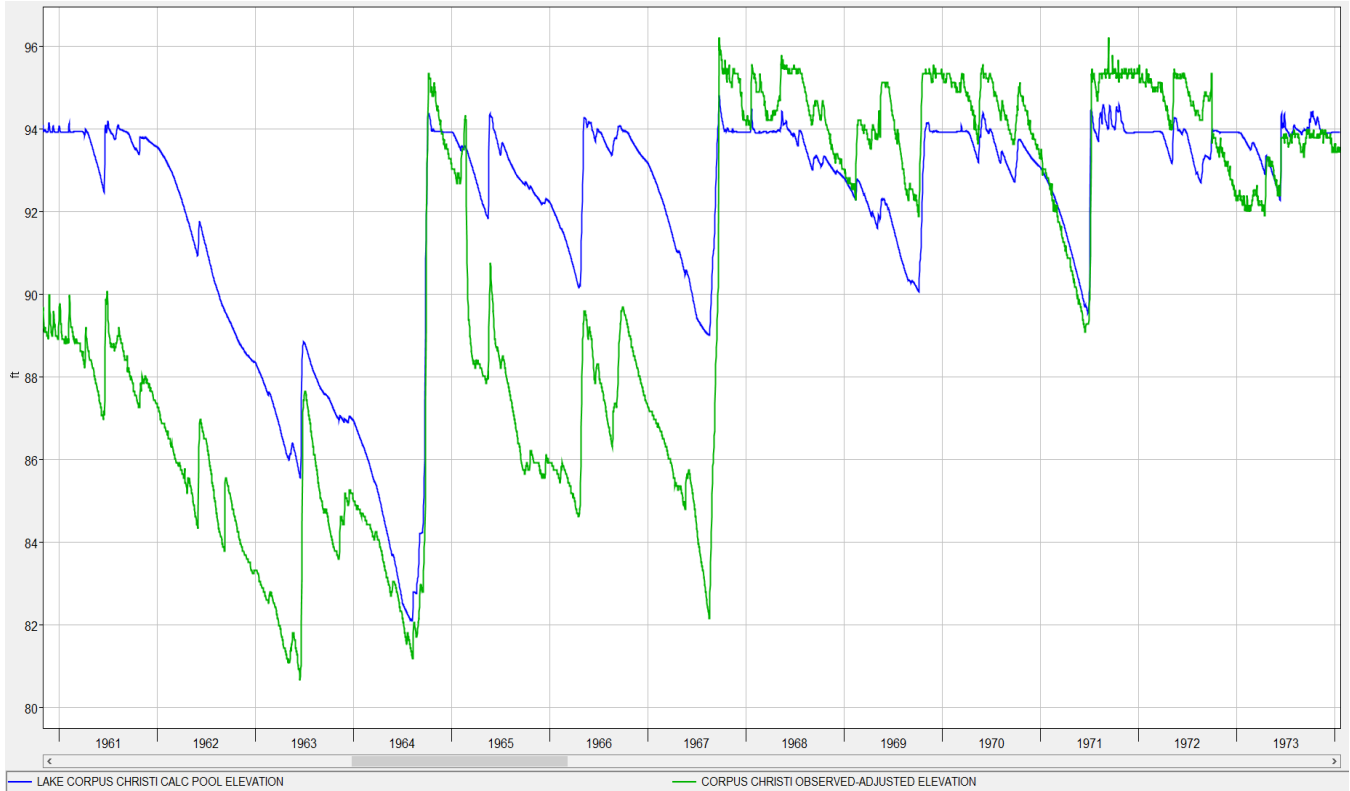


Figure 8.15: Validation of Lake Corpus Christi Simulated Pool During Hurricane Beulah

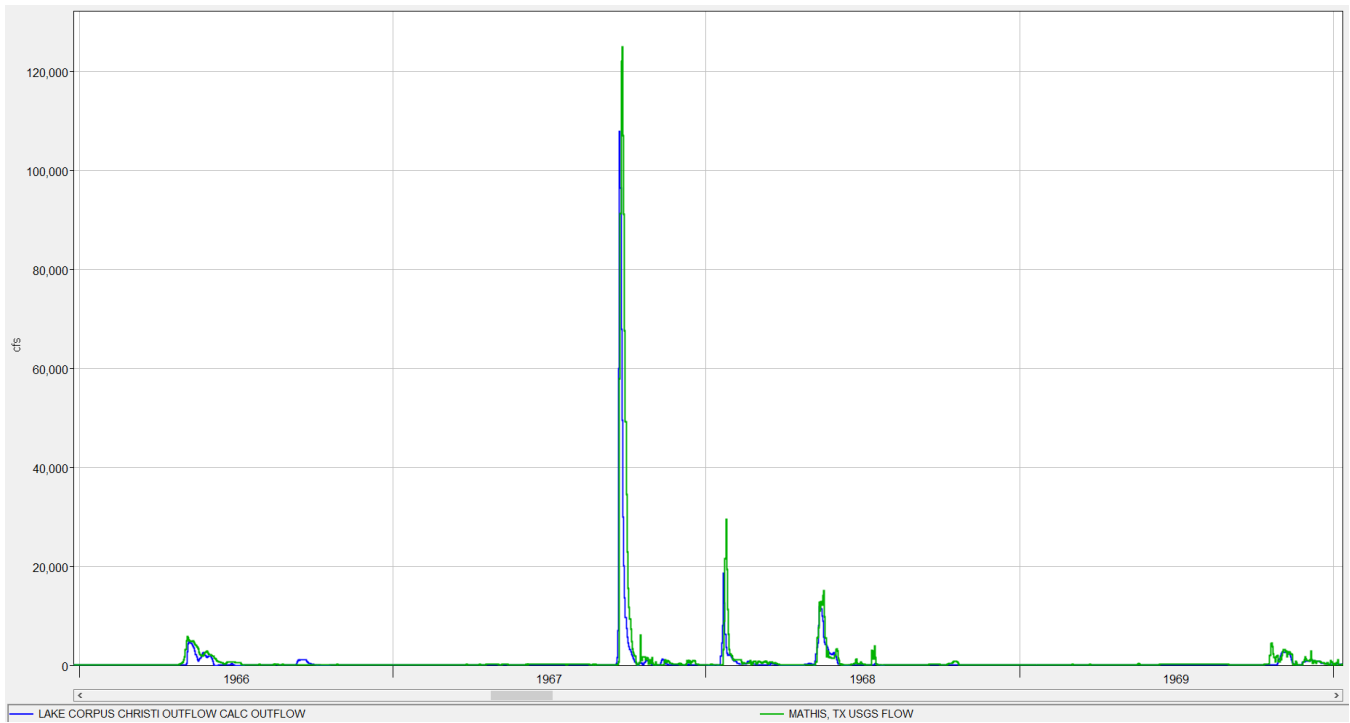
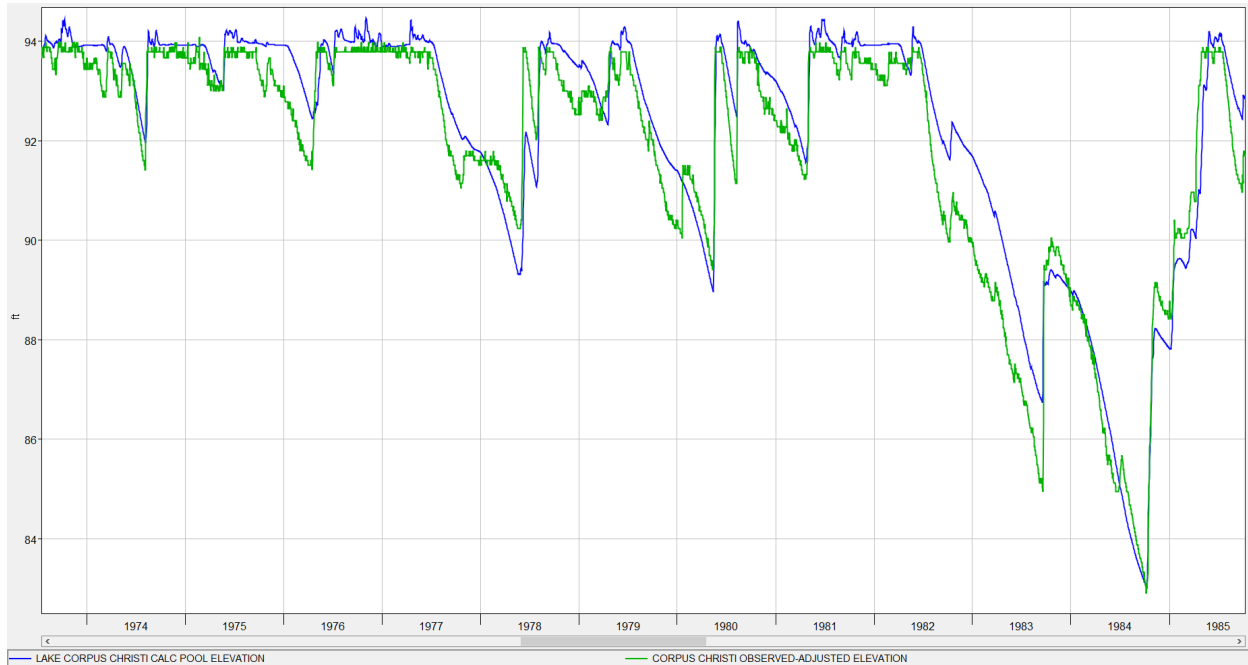


Figure 8.16: Hurricane Beulah Simulated Release from Lake Corpus Christi

The model stays flat at conservation during normal operation years (Figure 8.17). Some simulated pool deviations from observed were seen during 1978, 1980, 1981, 1983, and 1985. Drawdown in those years was high likely due to increased evaporation rates (some 6 feet annually), municipal and industrial use, and required environmental flows. Model results synchronized with observed to mimic drawdown. The differences are associated with the methods being used to develop data and convert from monthly to daily for reservoir depletion rates. Average daily release rates were distributed evenly over the entire period when actual data were not available. Lack of other depletion data may have contributed as well.



**Figure 8.17: Validation of Lake Corpus Christi Simulated Pool During Normal Operating Conditions**

No information is available for the observed period between 1986 and 1996 that would explain operation procedures for those years (Figure 8.18). Drawdown could be related to a period of severe drought in conjunction with high water supply demand during this period. The model deviated some but stayed flat for the most part. More investigation would possibly improve results. A comparison between simulated and observed releases are shown in Figure 8.19 at the project outlet. The 1987 simulated peak was due to surcharge. The model released according to surcharge (Table 8.6), where release is maximum.



Figure 8.18: Validation of Lake Corpus Christi Simulated Pool During Severe Drought Conditions

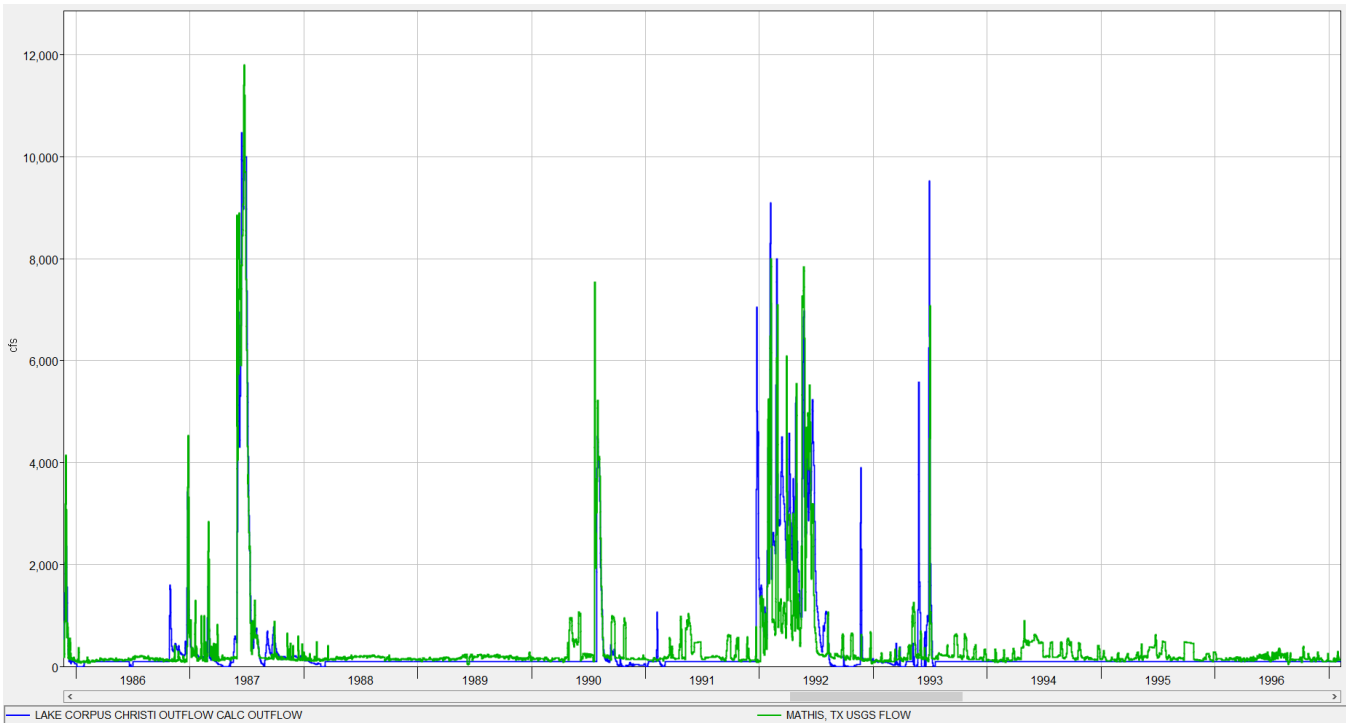


Figure 8.19: Model Results Validation at Lake Corpus Christi Outlet (USGS 0211000 Near Mathis)

**Table 8.6: Lake Corpus Christi Controlled and Uncontrolled Maximum Release**

Pool NGVD-ft	Release CFS	Pool NGVD-ft	Release CFS
38	-	95	142,993
55	1,000	96	177,362
80	10,000	97	215,900
90	20,526	98	254,791
90.85	34,173	99	292,633
91.06	40,514	100	331,800
92.35	67,795	101	380,400
92.56	74,547	102	425,100
92.83	79,211	103	475,500
93.55	97,183	106	620,100
93.58	98,767	108	715,800
94	114,491	110	813,000

The simulated pool for the period between 1995 and 2019 is shown in Figure 8.20. This period reflects changes in operations since Choke Canyon Reservoir was completed in 1982. Choke Canyon Reservoir controls more than 5,000 square miles of Wesley Seale drainage area, holding 700,000 acre-feet versus 256,000 acre-feet in Lake Corpus Christi. The period between 2002 through 2019 shows good match near conservation top pool. Pool levels for 1997-2000 are special case due to instability drawdown. Stability repairs were made and completed in 2000. Yet, the model performed well mimicking drawdown for 2000-2001. During 2010-2011, lake level fell to 17%. Simulated pool dropped below 80ft-NGVD and synchronized with the observed pool moving forward. Environmental flow requirements per 1988 agreed order with TCEQ (Texas Commission of Environmental Quality), required annual release of approximately 95,000 acre-feet, following seasonal rainfall variation. It also dictated flow level as high as 37,000 acre-feet per month. Daily release for water supply and bays and estuaries, are from 20 to 110cfs. Because of the long-simulated POR, an approximate current operation of constant low flow was assumed. This low flow release is an average release value based rather than observed daily rates. The model maintains a minimum flow from the lake to 100cfs (Figure 8.21).

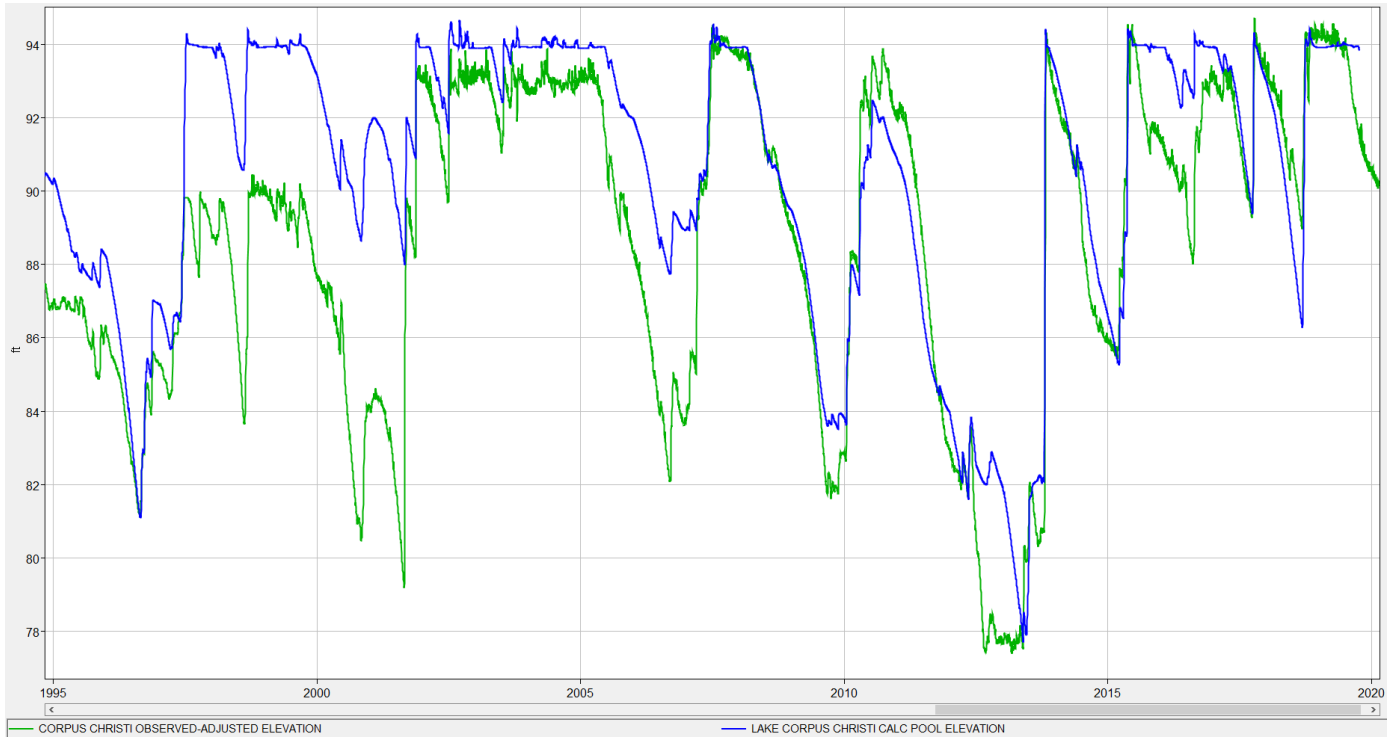


Figure 8.20: Validation of Lake Corpus Christi Simulated Pool for 1996-2019

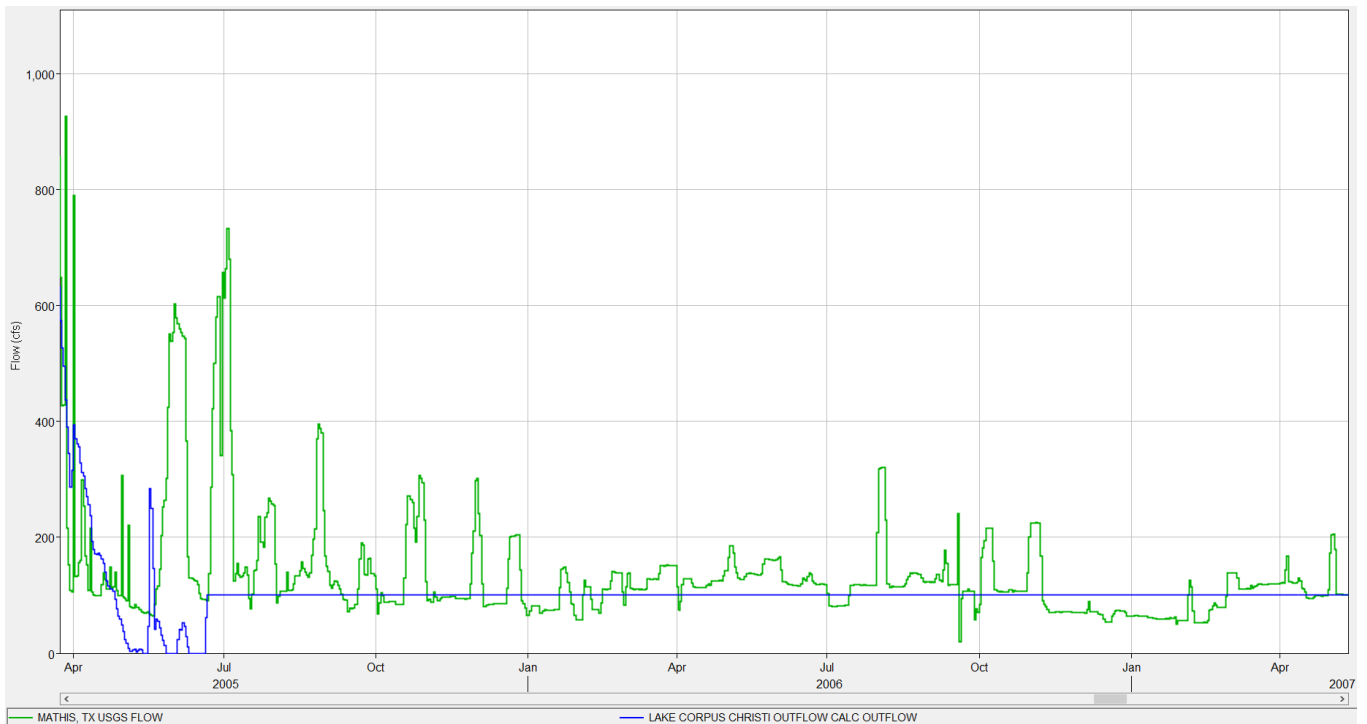


Figure 8.21: Validation of Lake Corpus Christi Minimum Release for Environmental Requirements

Comparisons between the simulated model results and USGS 08211200 Nueces River nr Bluntzer and USGS 08211500 Nueces River at Calallen are shown in Figure 8.22 and Figure 8.23 for the years of 2002 through 2005. The two gages have many years with discontinued discharge records and gaps. However, model routings and peaking compared very well to observed.

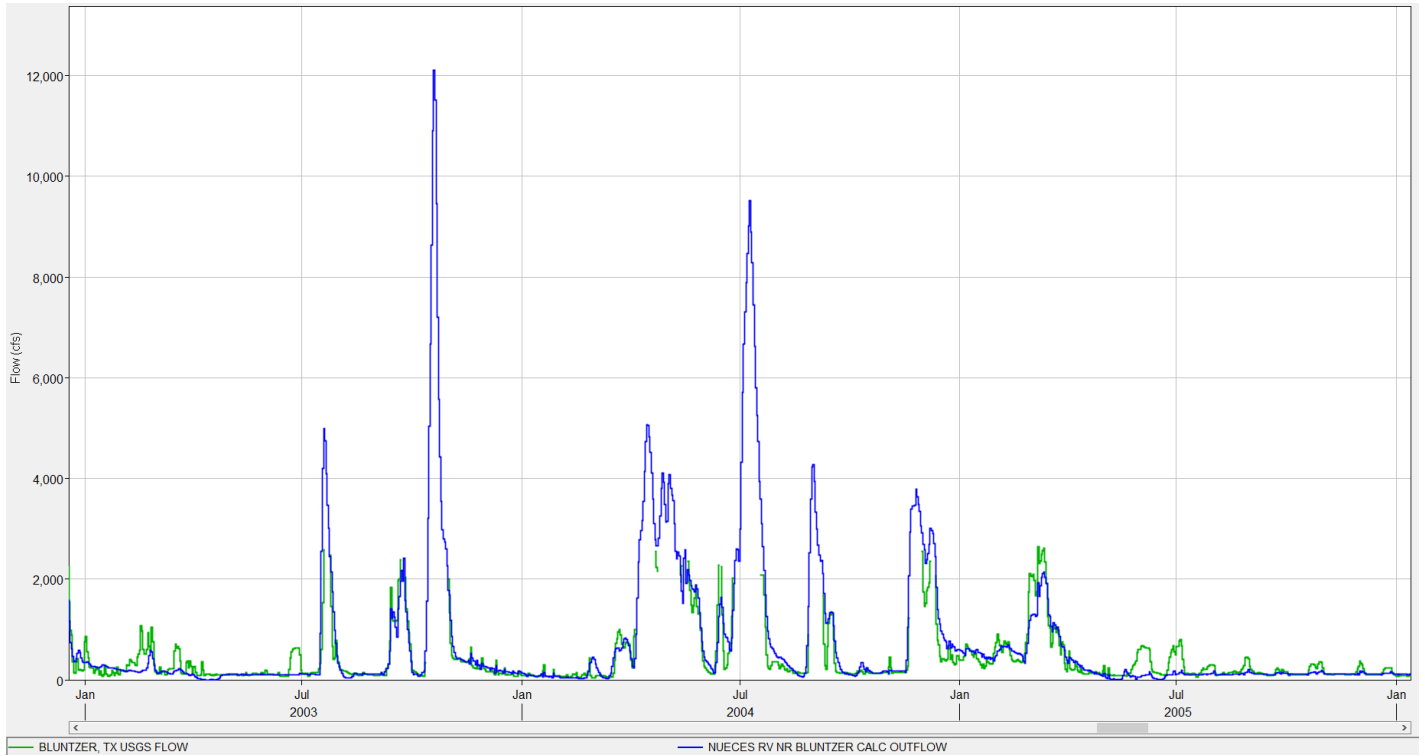


Figure 8.22: Model Results Validation at USGS 0211200 Nueces Rv nr Bluntzer

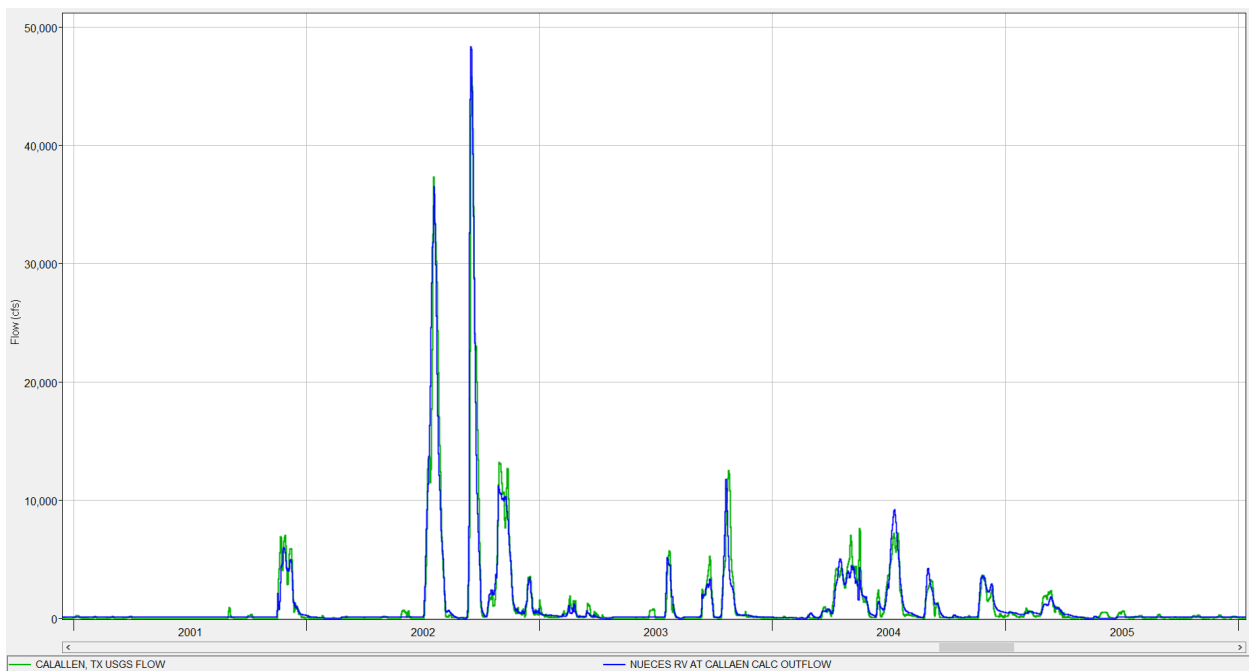


Figure 8.23: Model Results Validation at USGS 0211500 Nueces Rv at Calallen

Figure 8.24 illustrates the Weibull plotting position distribution of Lake Corpus Christi between water years 2000 and 2020. The last 20 years of operation were analyzed, because they reflect current operational standards. Those years were also less impacted by emergency drawdowns, which could impact the analysis. Some of the most extreme simulated peaks near elevation 95.0ft-NGVD were lower than observed due to the selected surcharge method, which tends to flatten the top of flood pool. For this lake, the observed pool for the period of WY2007 through WY2020 will be selected over simulated to perform statistical analysis, but simulated pool peaks will be analyzed for periods prior to WY2007. This approach ensures that the analyzed data is homogenous and valid for statistical analysis. Figure 8.25 illustrates the corresponding relationship between observed and simulated pool for Lake Corpus Christi for water years 2000-2020. The strong relationship increases confidence in the use of selected simulated results prior to WY2000.

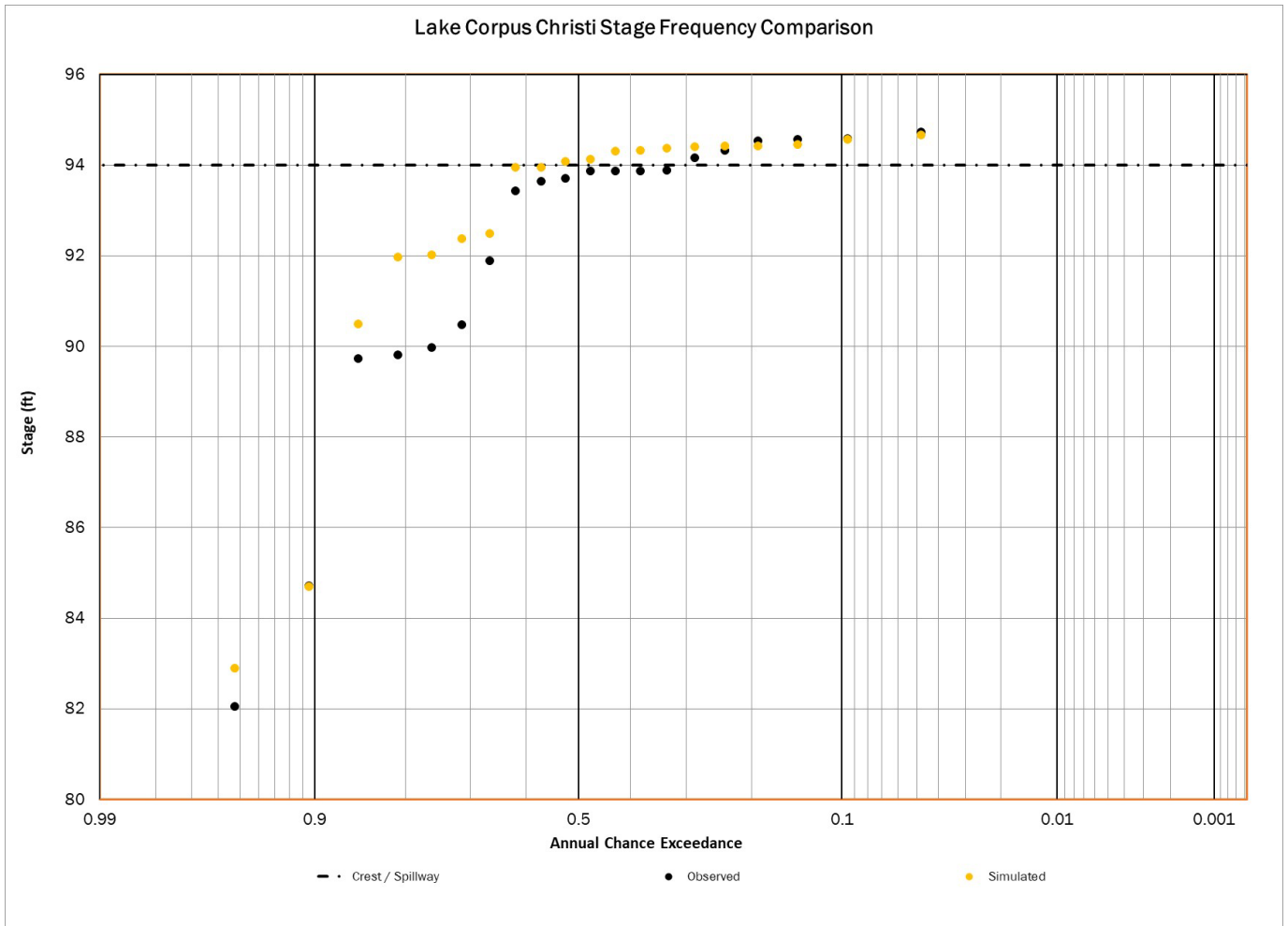


Figure 8.24: Corpus Christi’s Stage Frequency Peak Comparison (Annual Maximum Peaks) for WY 2000-2020

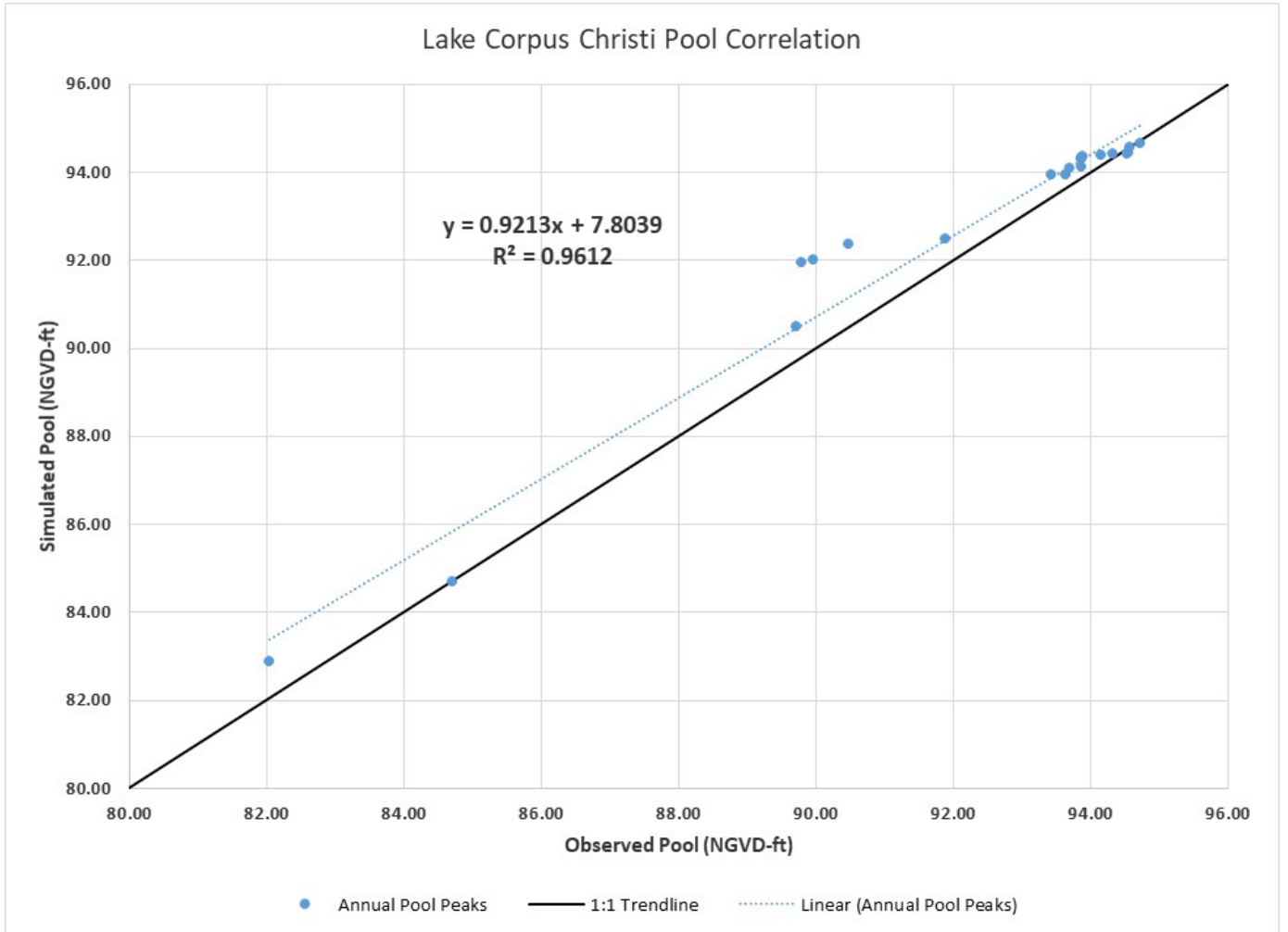


Figure 8.25: Observed Vs. Simulated Pool Annual Maximum Peak for Lake Corpus Christi for WY 2000- 2020

### 8.7 Final Riverware Model Period of Record Results

The final RiverWare simulation runs for the POR (e.g., October 1, 1942 – September 30, 2019) are shown in the following figures. The plots reflect good operational results and similarities with stream gaged (observed) data for the most part.

The data in each plot was used in a tabular format as input to the flow frequency analyses described in the next sections.

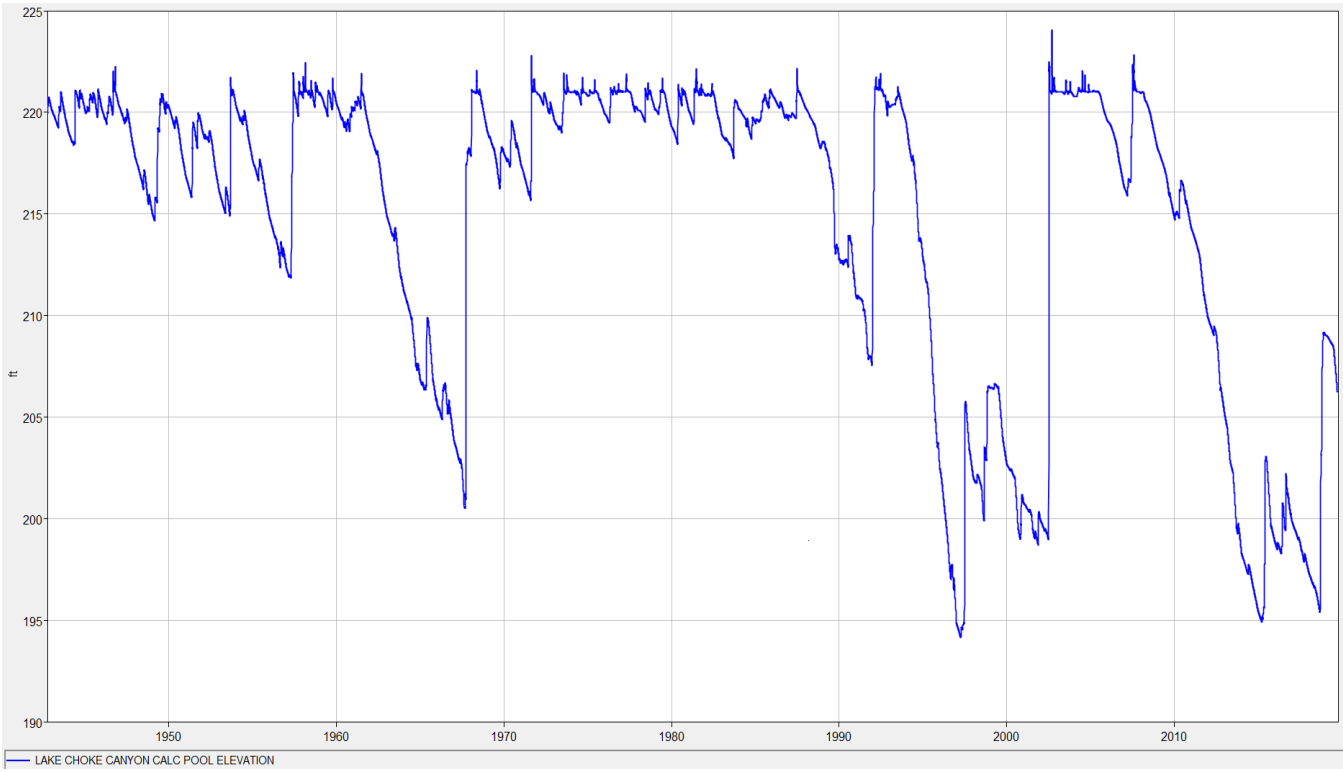


Figure 8.26: Simulated POR Results for Choke Canyon Reservoir

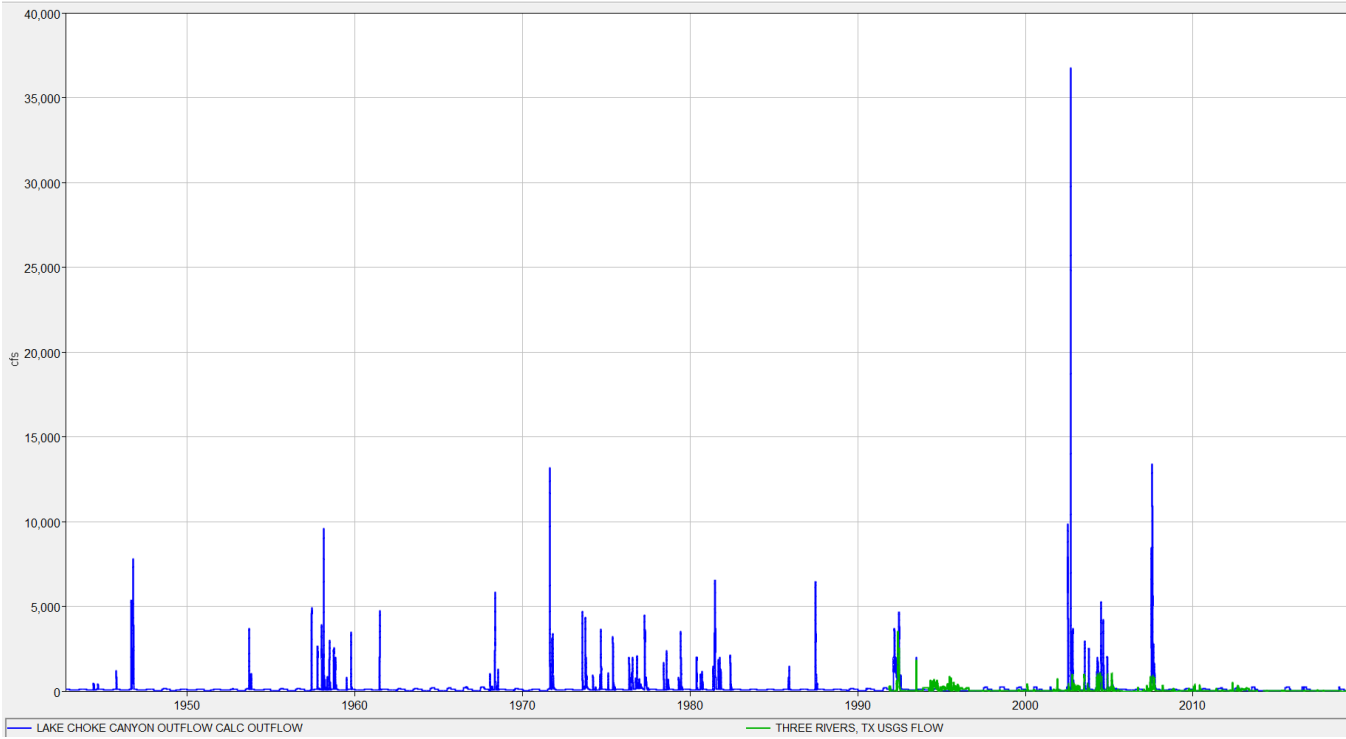


Figure 8.27: RiverWare Model Results Comparison for USGS streamgage station 08206910 Choke Canyon Reservoir nr Three Rivers, Tex.

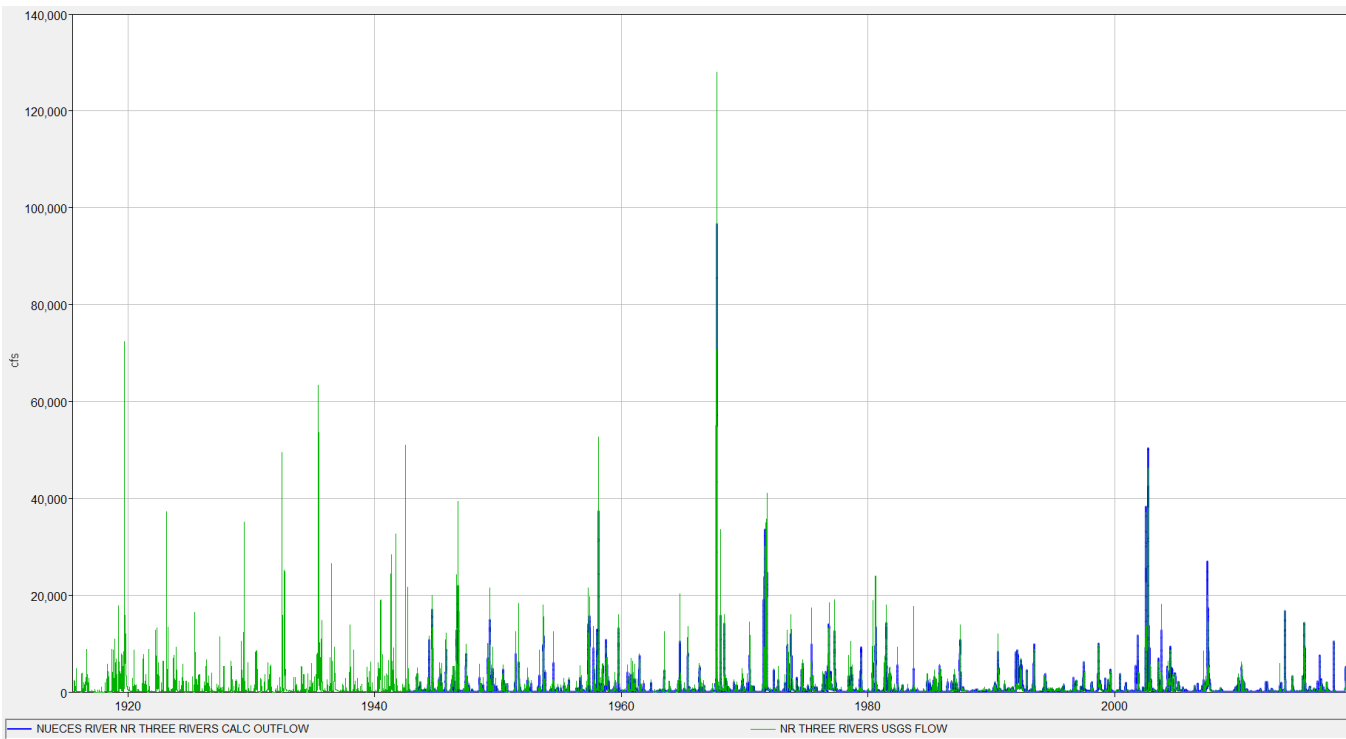


Figure 8.28: RiverWare Model Results Comparison for USGS streamgage station 08210000 Nueces River Near Three Rivers, Tex.

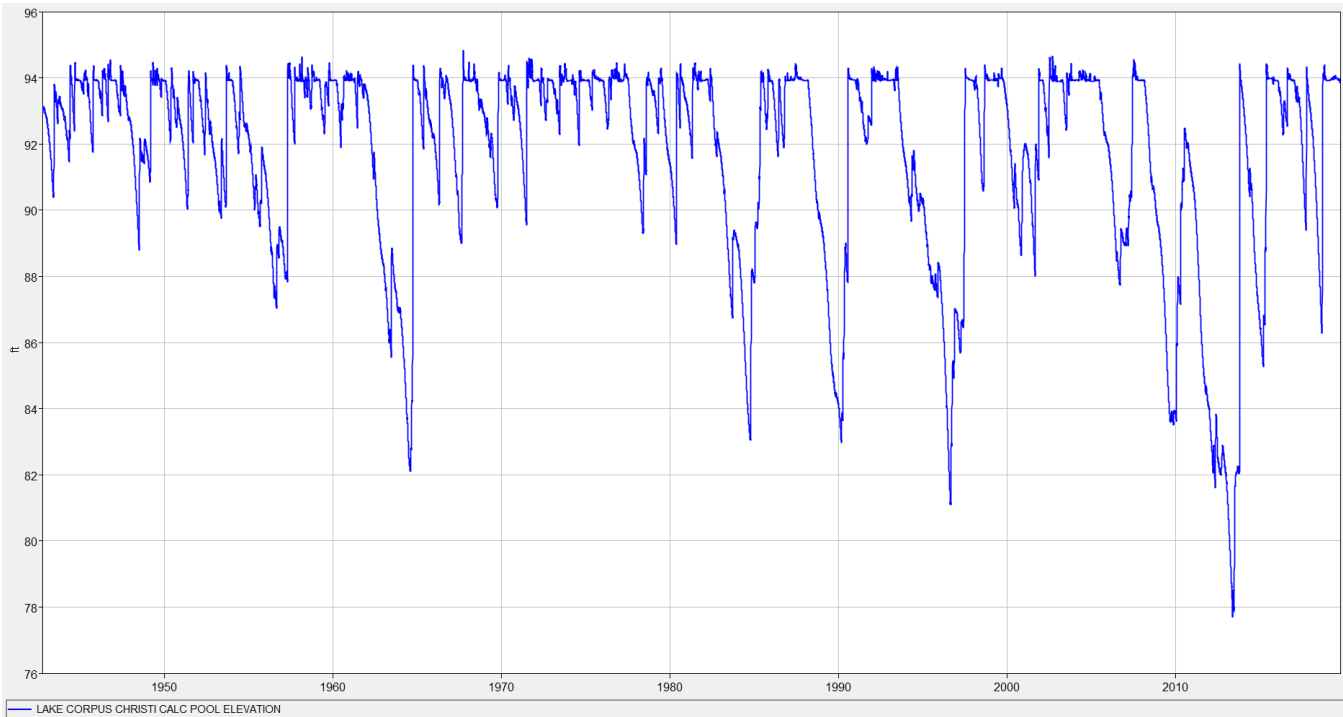


Figure 8.29: Simulated POR Results for Lake Corpus Christi Pool Elevation

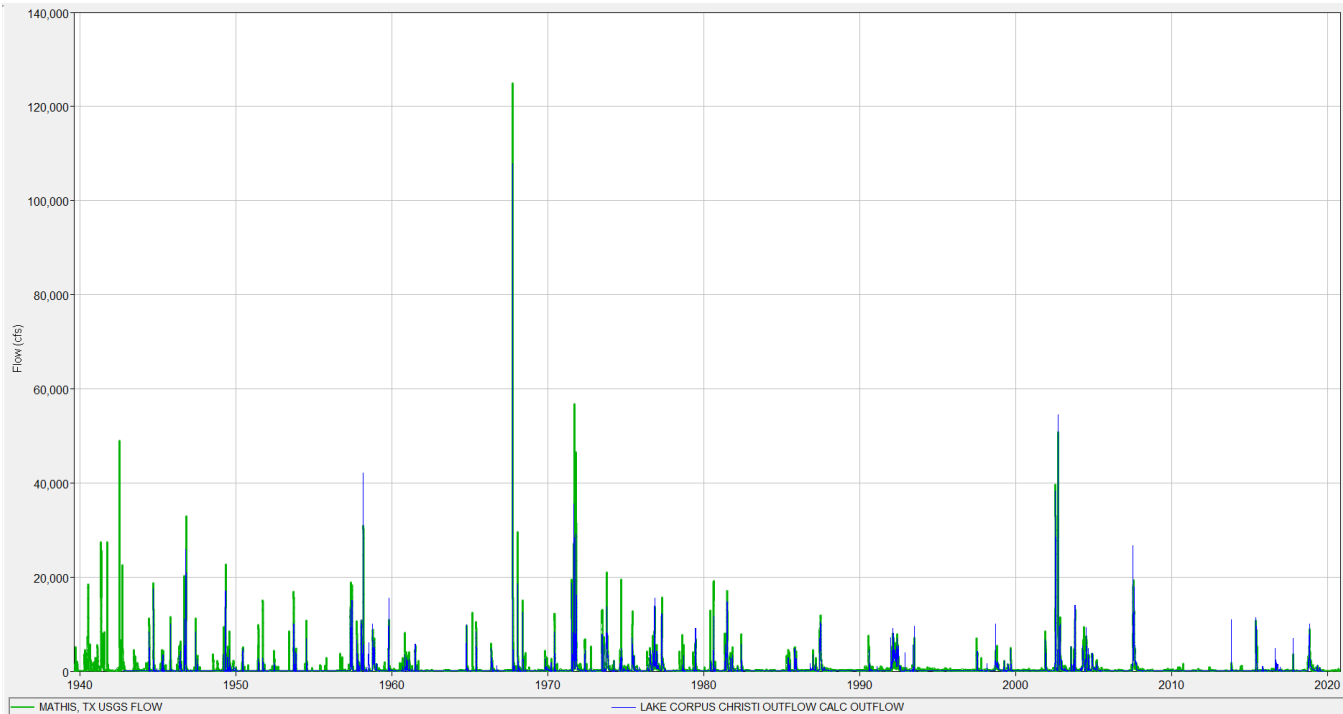


Figure 8.30: RiverWare Model Results Comparison for USGS streamgaging station 08211000 Nueces River near Mathis, Tex.

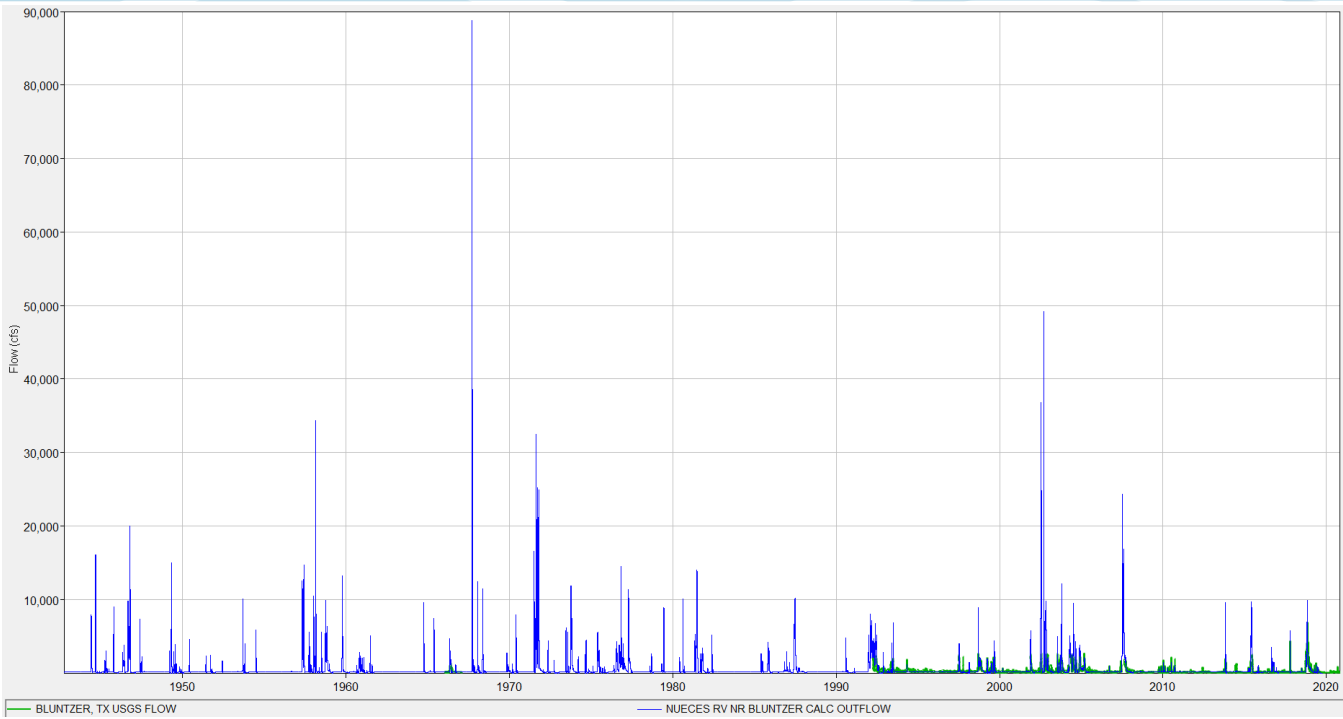


Figure 8.31: RiverWare Model Results Comparison for USGS streamgage Station 08211200 Nueces River near Bluntzer, Tex.

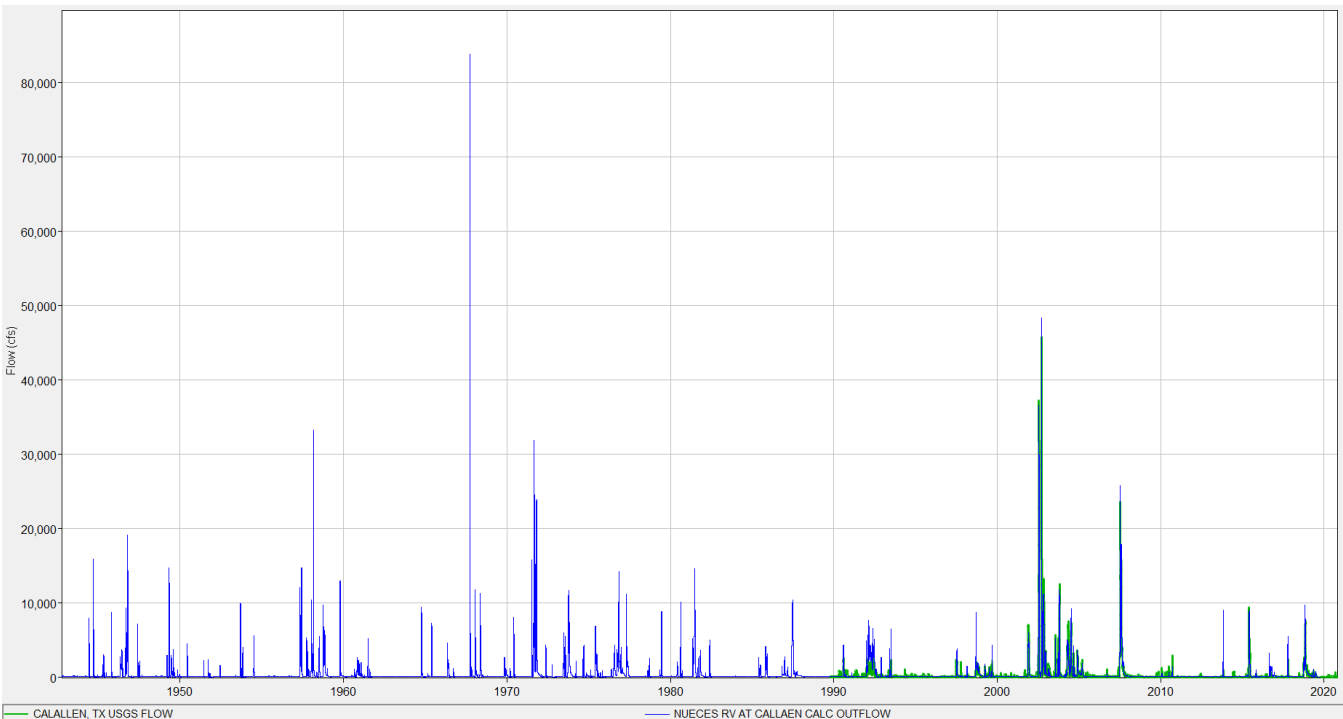
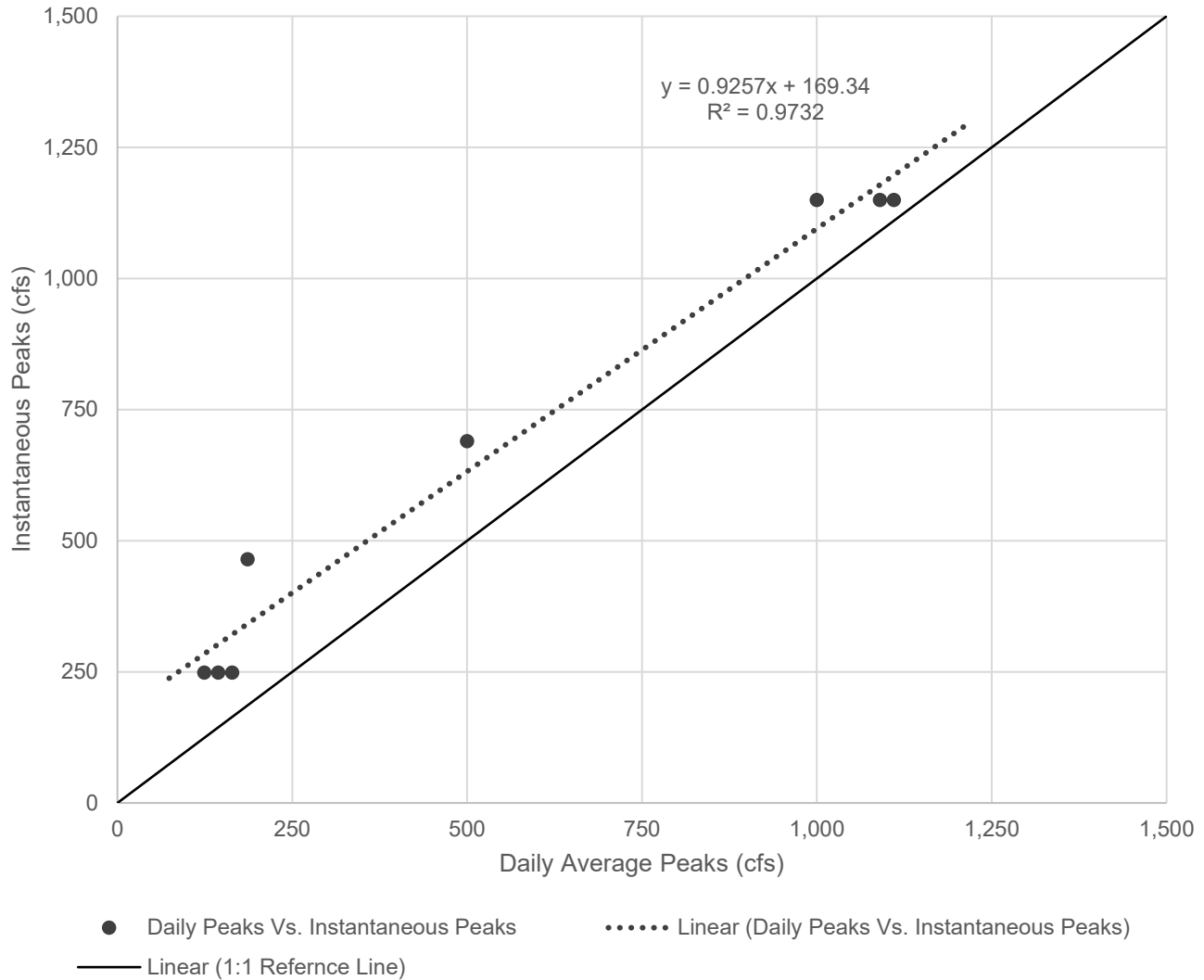


Figure 8.32: RiverWare Model Results Comparison for USGS Streamgage Station 0821500 Nueces River at Calallen, Tex.

## 8.8 Conversion of Daily Discharges to Peak Instantaneous Discharges

While the RiverWare model runs on a daily time step, peak instantaneous discharges are needed for flow frequency analysis. Therefore, a comparison of USGS observed instantaneous peaks and the corresponding USGS daily average discharges were made to convert the RiverWare daily discharges to an equivalent peak instantaneous discharge for each streamgage of interest. A plot of instantaneous discharges versus USGS daily average peak discharges were made, and a regression equation was fit to each dataset. The regression equations were then applied to the daily peak flows from RiverWare to transform them into instantaneous peaks. Figure 8.33 through Figure 8.37 illustrate the corresponding relationship between datasets used to generate peaking factors to transform peaks. The corresponding period of record for each site is indicated below each figure.

### Corresponding Relationship Between Instantaneous and Daily Average Peaks at Choke Canyon reservoir Outlet



**Figure 8.33: Instantaneous vs. Daily Average Peak Discharges for USGS 08206910 Streamgage Station Choke Canyon Reservoir nr Three Rivers, TX., for 2001, 2003-2006, 2008, 2011-2012.**

Since its installment in November 1991, this gage has many gaps and is not reliable to gather high discharge peaks from, especially during mid to high releases. Extreme caution should be used in generating a correlation for its daily average peaks. There are eight (8) discharge peaks used to develop a strong corresponding relationship. The gage should be noted to have high uncertainty with it when developing high discharge frequencies.

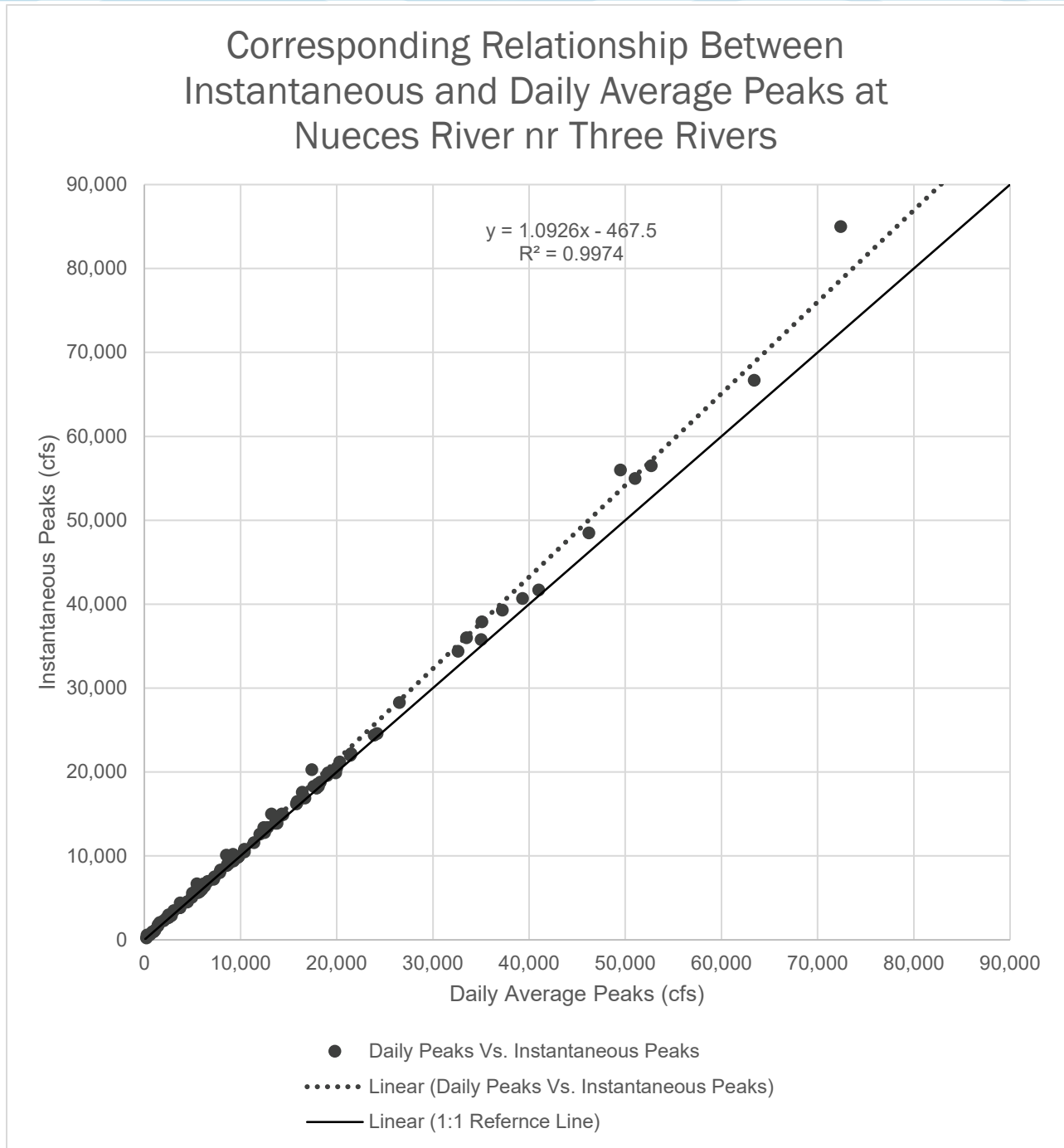


Figure 8.34: Instantaneous vs. Daily Average Peak Discharges for USGS 08210000 Streamgage Station Nueces River nr Three Rivers, TX. POR (1916-2019)

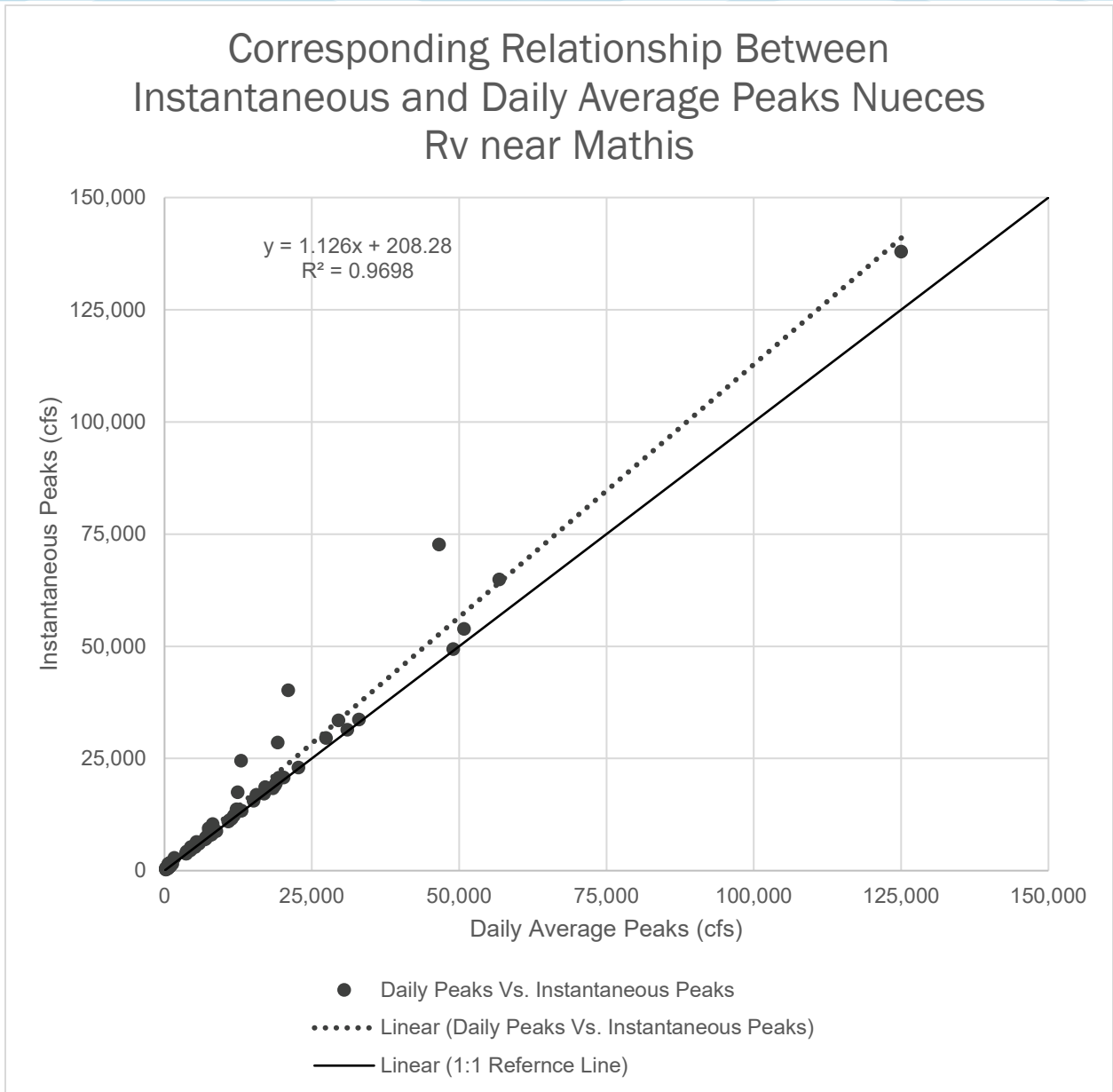
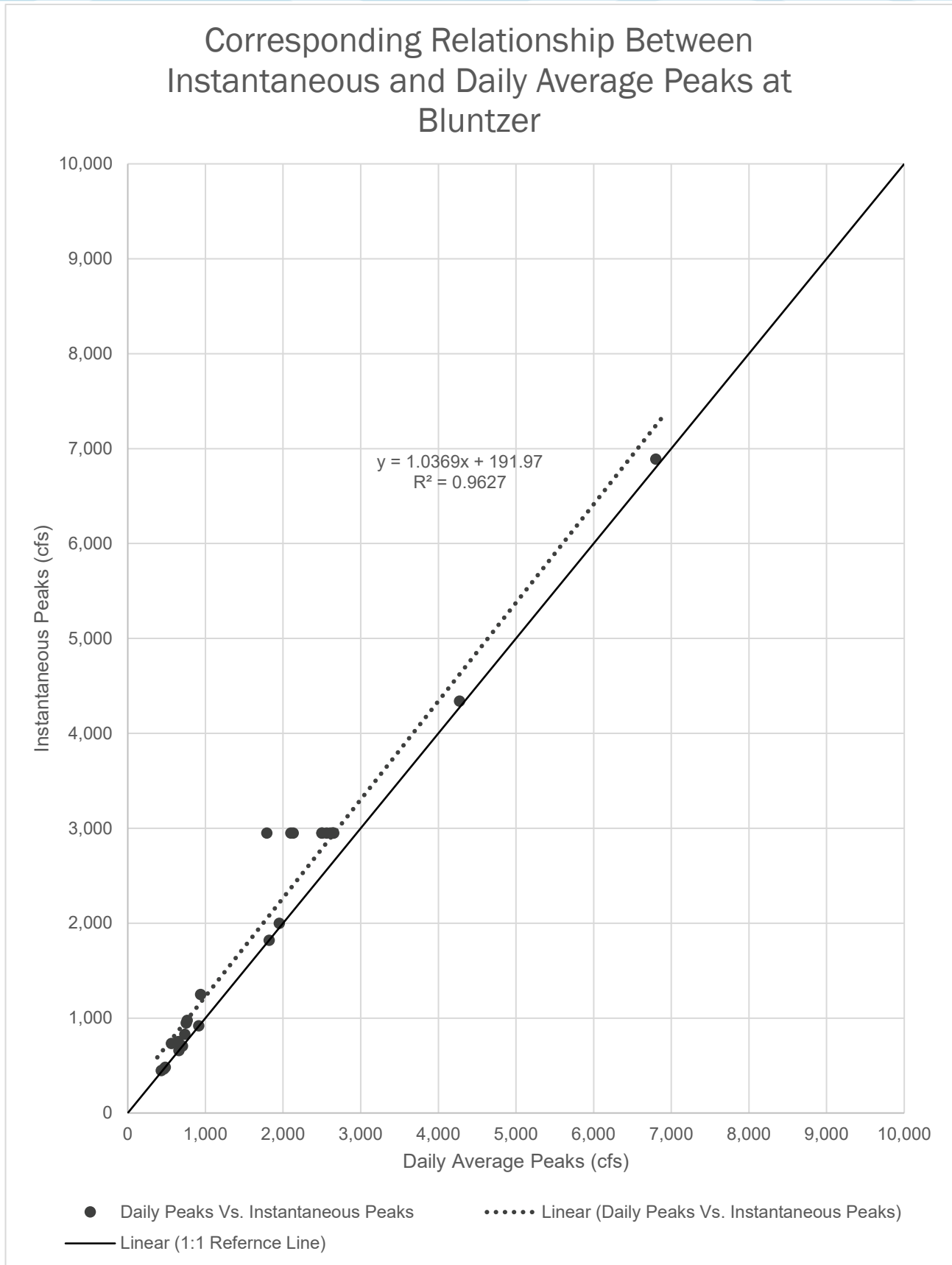


Figure 8.35: Instantaneous vs. Daily Average Peak Discharges for USGS 08211000 Streamgauge Station Nueces River nr Mathis, TX. POR (1940-2019)



**Figure 8.36: Instantaneous vs. Daily Average Peak Discharges for USGS 08211200 Streamgage Station Nueces River near Bluntzer, TX. POR (1994-2019).**

### Corresponding Relationship Between Instantaneous and Daily Average Peaks at Calallen

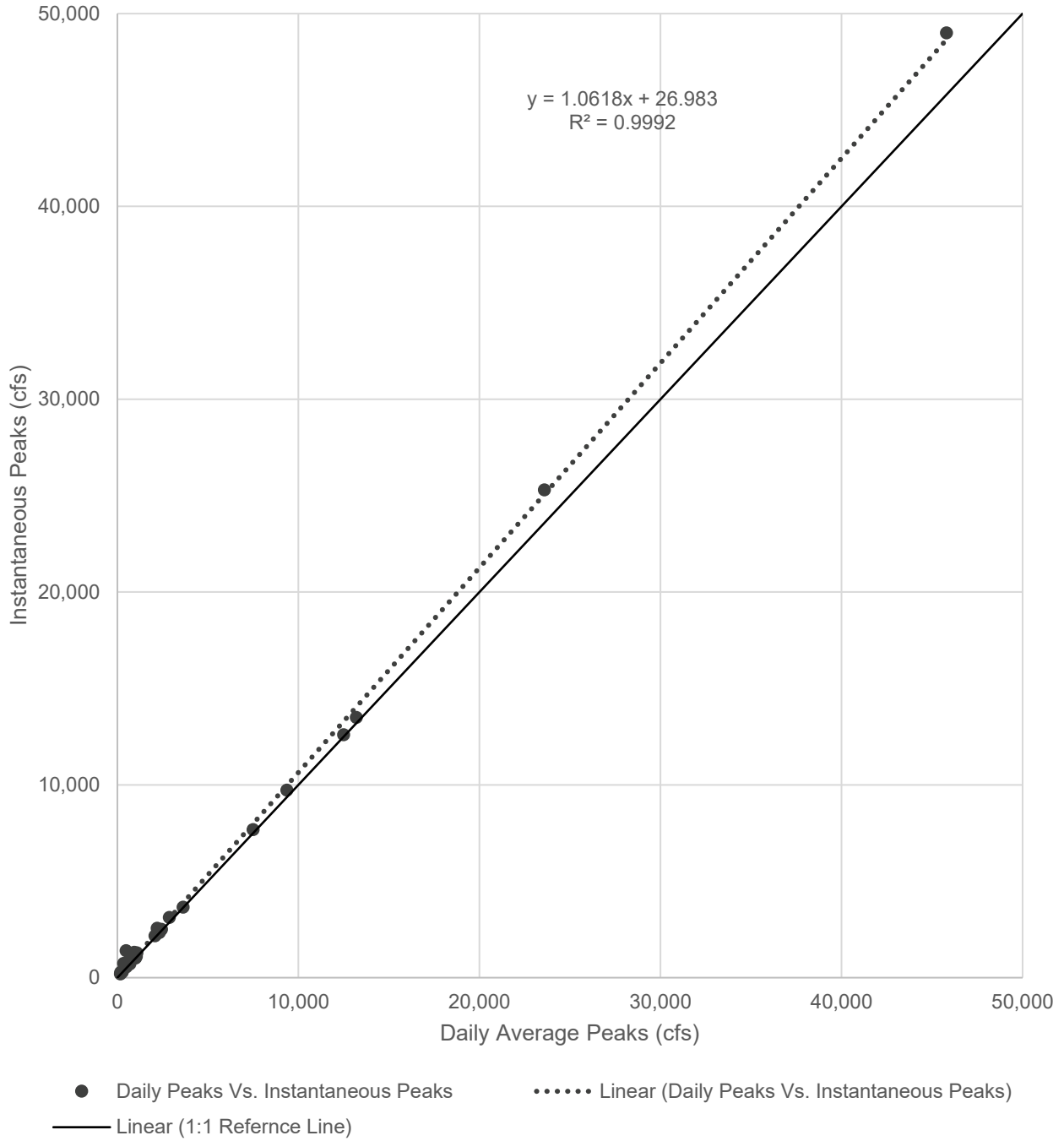


Figure 8.37: Instantaneous vs. Daily Average Peak Discharges for USGS 08211500 Streamgauge Station Nueces River at Calallen, TX. POR (1992-2019).

For more comparisons between simulated and observed annual peaks, see Appendix D.

The finalized discharge peaks, which will be used to develop the instantaneous annual maximum peaks, consist of simulated RiverWare peaks and the USGS instantaneous observed peaks, downloaded from the USGS National Water Information System (NWIS) database (USGS, 2019). The general practice in developing instantaneous annual maximum flow for each water year is to use the observed peaks first but filled with the simulated RiverWare peaks when USGS peaks were missing.

## 8.9 Streamgage Data and Statistical Flood Flow Frequency Results

For the statistical analysis of the RiverWare modeling results, the simulated instantaneous peak discharge was analyzed for five USGS streamgaging stations in the RiverWare model: 08206910 Choke Canyon Reservoir OWC near Three Rivers, 08210000 Nueces River near Three Rivers, 08211000 Nueces River near Mathis, 08211200 Nueces River at Bluntzer, 08211500 Nueces River at Calallen. A peaking factor, described in detail in section 8.8, was applied to the RiverWare daily time-step data to convert the peak discharges to instantaneous peak discharges.

With the aim of providing the best available POR, the USGS observed peak discharge data were substituted for RiverWare simulated record when available. USGS observed peak discharge data are considered to be the most reliable of the two datasets because these data recorded actual events and are not simulated discharge. Simulated RiverWare data, however, supersedes this priority when the USGS record does not reflect the regulated watershed at the time of this analysis. Therefore, in most cases, the POR analyzed in this chapter consists of a combined record of USGS observed and RiverWare simulated peak discharge data. Henceforth, “observed record (or dataset)” refers to only the USGS observed record of peak discharge, whereas “simulated record (or dataset)” refers to the combined RiverWare and USGS peak discharge record. The details of each gage’s POR are described in each gage’s individual section below.

The flood flow frequency analysis was performed following the same methodology as is used in the analysis of the observed POR defined in Chapter 5. Bulletin 17C guidelines (England et al, 2018) were followed, although the usefulness of the expected moments algorithm (EMA) is limited in this analysis, and the sophisticated interpretation of historical peak discharges, thresholds, and so forth is not needed. This is because the combination of USGS and RiverWare peak data results in a fairly homogeneous dataset without these nonstandard forms of information. Flood flow frequency analyses were performed in the USACE Hydrologic Engineering Center’s Statistical Software Package (HEC-SSP), which is a software program designed to perform statistical analyses of hydrologic data including Bulletin17C frequency analyses (England and others, 2018; USACE, 2016). Two especially important options of the HEC-SSP software are the choice of low-outlier threshold and generalized skew and whether to incorporate such skew in the analyses in a weighting between the generalized skew and that computed using the site-specific data (USACE, 2016). Site-specific selection of skew and low-outlier thresholds are discussed in each gage’s individual writeup that follows in this section.

PeakFQ input must conform to specific data formatting requirements (Flynn and others, 2006), which means that constructing a synthetic data input file can be problematic and potentially lead to errors. USGS peak discharge data are available from the [USGS NWIS database \(USGS, 2021\)](#) in a format compatible with PeakFQ, but RiverWare does not provide this formatting option. Therefore, flow frequency analyses performed on RiverWare datasets were done in the USACE HEC-SSP software, which has flexible data input requirements (USACE, 2016). While the program interface might be slightly different than PeakFQ, the basic setup and methodology are the same, and when given identical input both programs will provide the same results. The final results of the simulated record flood flow frequency analyses in this chapter are summarized in Table 8.7.

**08206910 Choke Canyon Reservoir OWC near Three Rivers, Tex.**

The POR used in the flood flow frequency analysis for USGS streamgage 08206910 Choke Canyon Reservoir outlet works channel [OWC] near Three Rivers, Tex. (hereinafter referred to as the “Choke Canyon Outflows gage”) was from 1943 through 2020 (USGS, 2022). RiverWare-simulated annual peak streamflow values were substituted for USGS annual peak values for all years prior to 2017 when annual peak streamflow data became available for the Choke Canyon gage. In the resulting combined dataset of observed and simulated data (hereinafter referred to as the “simulated dataset”), the 1967 simulated peak streamflow of 51,500 cubic feet per second (cfs) is the largest peak of record. A log-normal plot of the peak streamflows for each water year is presented in Figure 8.38. The flood flow frequency for the Choke Canyon Outflows gage-simulated dataset is shown in Figure 8.39, and the tabulated results are listed in Table 8.7.

A low-outlier threshold of 834 cfs was computed by applying the MGBT in HEC-SSP, and the initial station skew computed in HEC-SSP was used as the skew (a regional skew weighting factor was not applied). During the computation of the low-outlier threshold, a total of 39 low outliers (potentially influential low floods) were identified. Streamflow at the Choke Canyon gage is completely regulated as it only measures outflows from Choke Canyon Reservoir, meaning that Bulletin 17C methodology is not well suited to the dataset (England and others, 2019). There were only four observed annual peak streamflow values, and these peaks were all relatively small, ranging from 600 to 1,000 cfs. The bifurcated distribution of the simulated streamflow and the inability to match the observed peaks to the simulated streamflow highlights both the highly regulated nature of the Frio River immediately downstream from the dam and the apparent poor performance of the peaking factor determined for this streamgage.

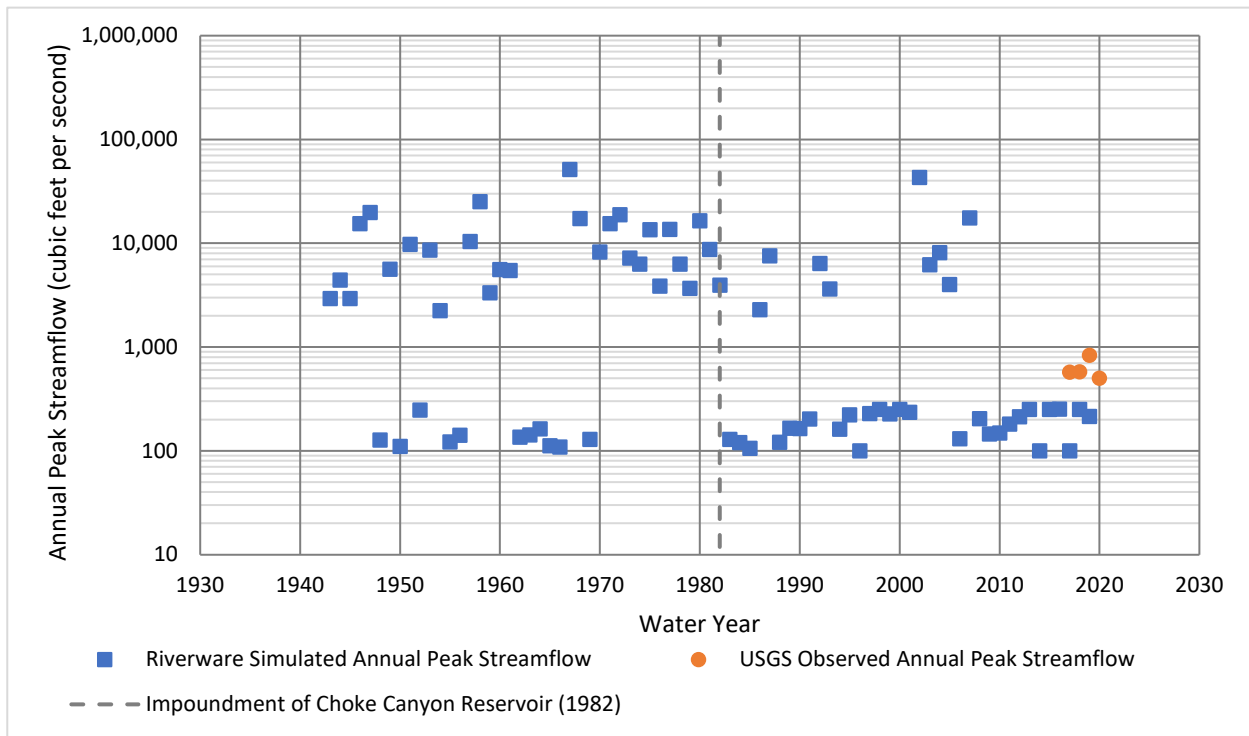


**Figure 8.38: Simulated RiverWare and Observed U.S. Geological Survey (USGS) Annual Peak Streamflow for USGS Streamgage 08206910 Choke Canyon Reservoir OWC near Three Rivers, Texas.**

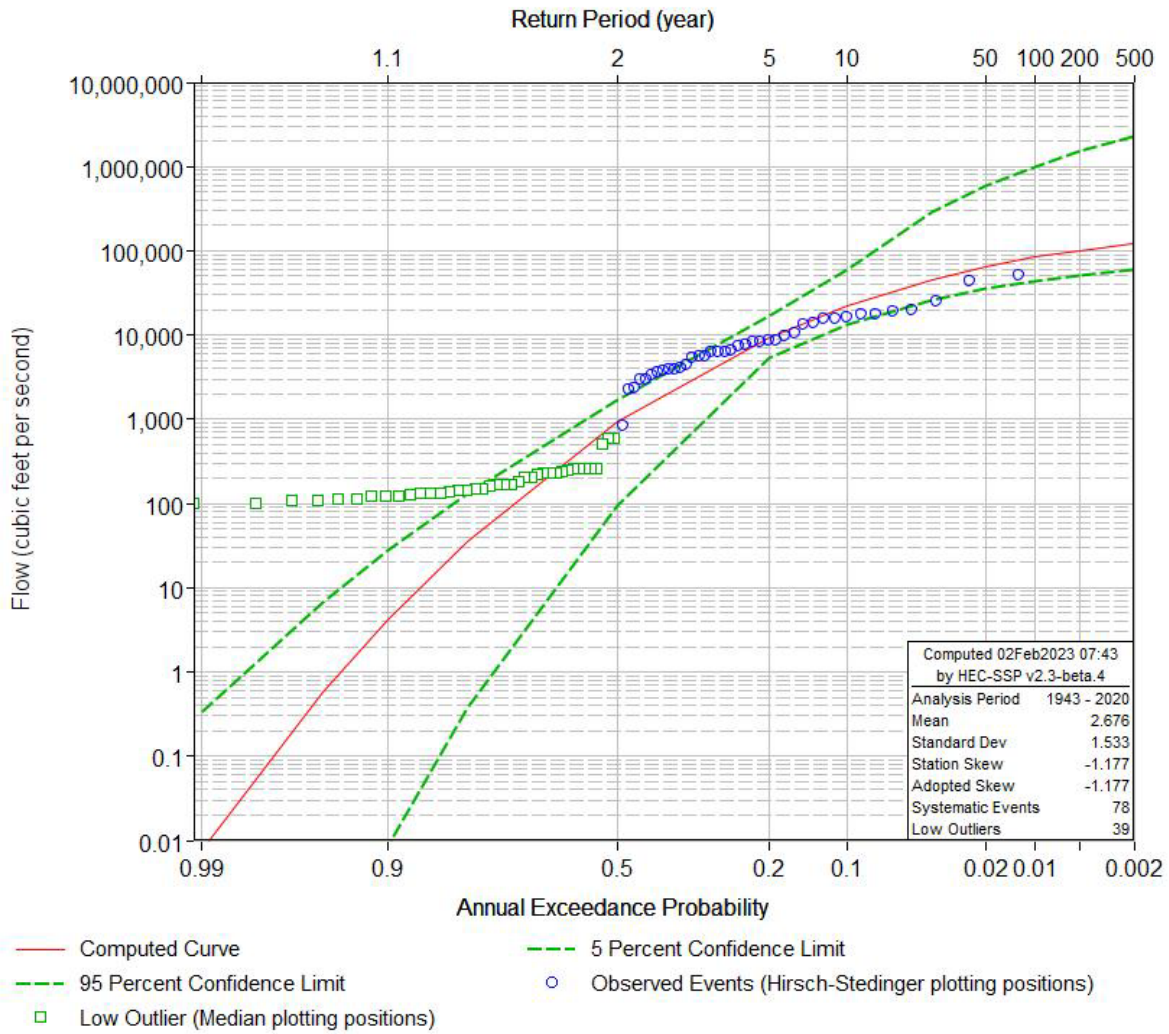
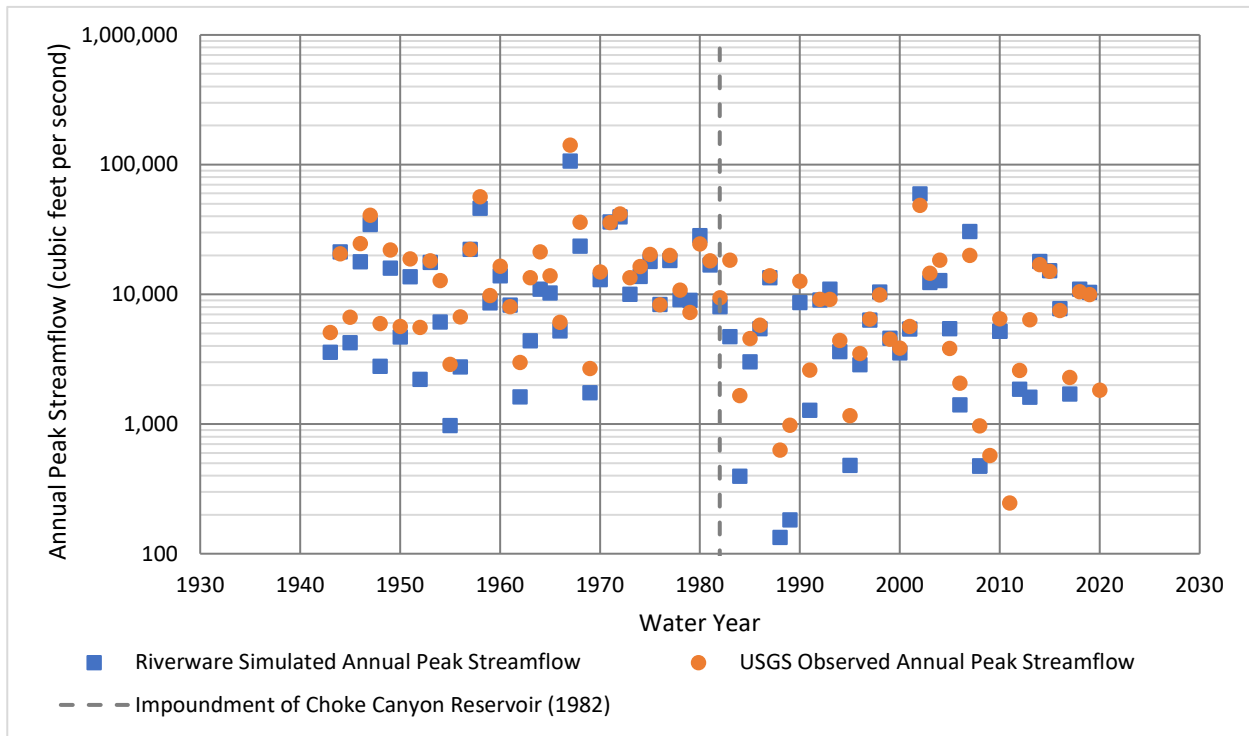


Figure 8.39: Simulated Flood Flow Frequency using log-Pearson Type III Distribution for U.S. Geological Survey Streamgage 08206910 Choke Canyon Reservoir OWC near Three Rivers, Texas.

**08210000 Nueces River near Three Rivers, Tex.**

The POR used in the flood flow frequency analysis for USGS streamgage 08210000 Nueces River near Three Rivers, Tex. (hereinafter referred to as the “Nueces River near Three Rivers gage”) was from 1943 through 2020 (USGS, 2022). RiverWare-simulated annual peak streamflow values were substituted for USGS annual peak values obtained prior to the impoundment of Choke Canyon Reservoir in May of 1982 (TWDB, 2022). In the resulting combined dataset of observed and simulated data, the 1967 simulated peak streamflow of 107,000 cfs is the largest peak of record. A log-normal plot of the peak streamflows for each water year is presented in Figure 8.40. The flood flow frequency for the Nueces River near Three Rivers gage-simulated dataset is shown in Figure 8.41, and the tabulated results are listed in Table 8.7. A low-outlier threshold of 7,000 cfs was manually set in HEC-SSP, and the station skew computed in HEC-SSP was used as the skew. During the computation of the low-outlier threshold, a total of 35 low outliers were identified. The low-outlier threshold of 7,000 cfs is different than the one set for the Nueces River near Three Rivers gage dataset in Appendix A because the inclusion of RiverWare data in this analysis results in a different set of ordered events (Figure 8.39) and therefore a different flood flow frequency analysis.

A comparison of the simulated flood flow frequency analysis from this section and the computed flood flow frequency distribution (curve) from Appendix A is shown in Figure 8.48. The difference between the simulated and observed flood flow frequency curves is substantial. Although RiverWare simulates the operation of Choke Canyon Reservoir prior to its actual impoundment in 1982, it appears that the simulated annual peak streamflow for 1982 and prior years is still higher on average than the observed annual peak streamflow beginning in 1983 (Figure 8.39). The mean simulated annual peak streamflow from 1943 through 1982 is 16,000 cfs, whereas the mean observed annual peak streamflow from 1983 through 2020 is 8,080 cfs.



**Figure 8.40: Simulated RiverWare and Observed U.S. Geological Survey (USGS) Annual Peak Streamflow for USGS Streamgage 08210000 Nueces River near Three Rivers, Texas.**

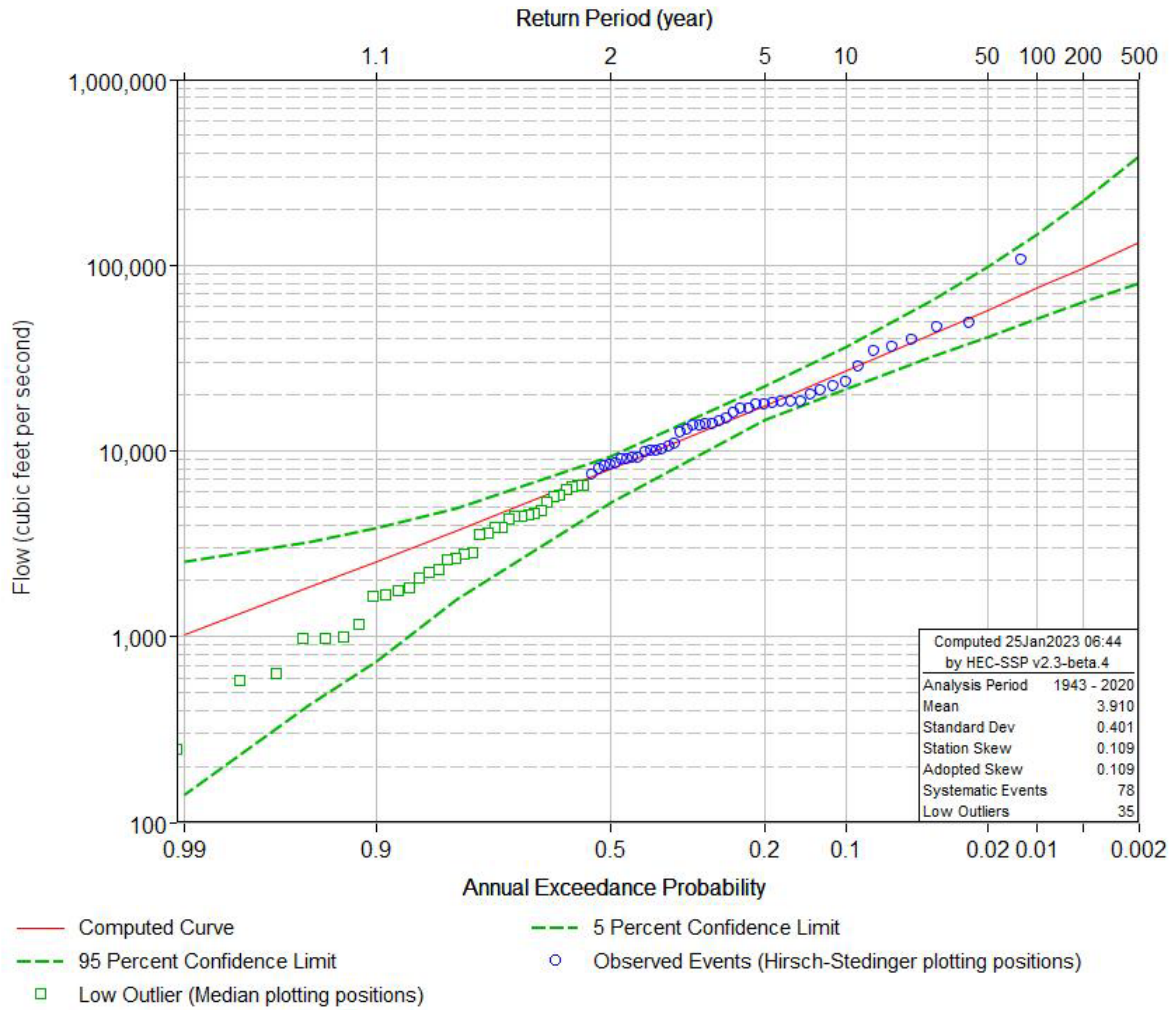


Figure 8.41: Simulated Flood Flow Frequency using log-Pearson Type III Distribution for U.S. Geological Survey Streamgauge 08210000 Nueces River near Three Rivers, Texas.

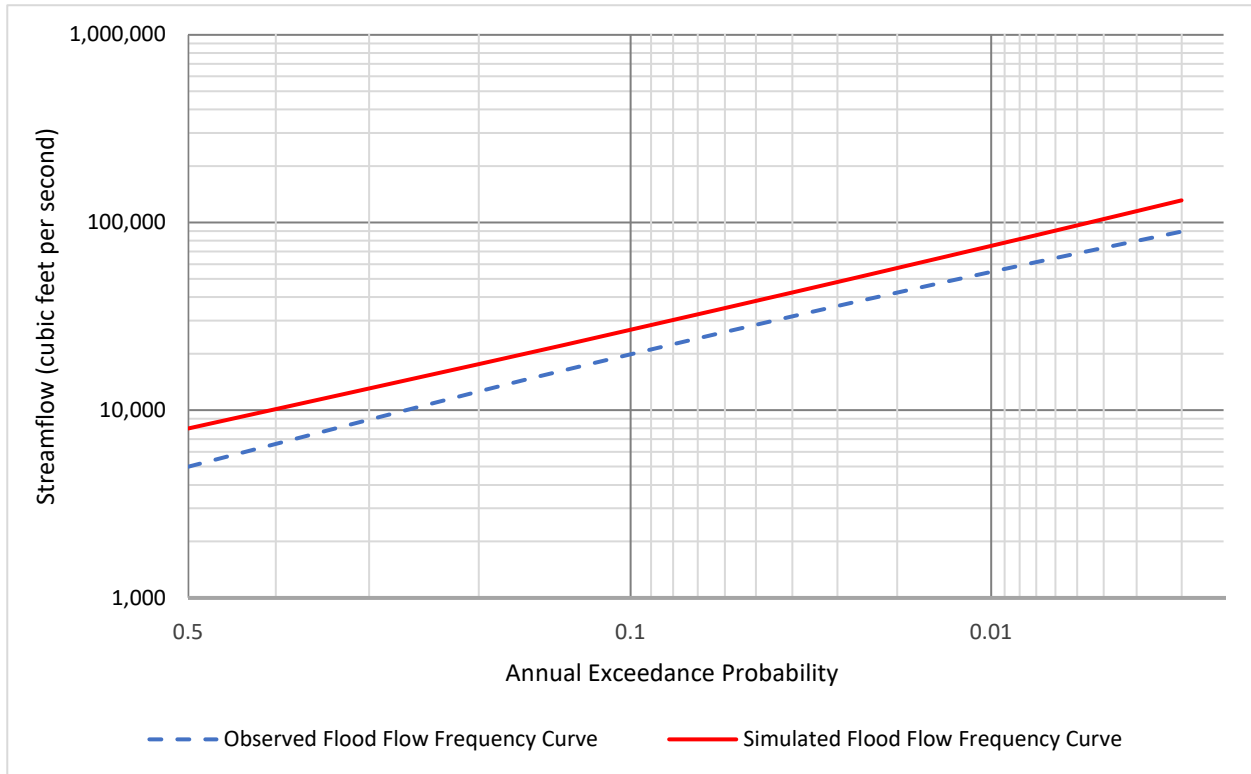


Figure 8.32: Comparison of Flood Flow Frequency Curves for the Observed (1983-2020) and Simulated (1943-2020) Datasets for U.S. Geological Survey Streamgage 08210000 Nueces River near Three Rivers, Texas.

**08211000 Nueces River near Mathis, Tex.**

The POR used in the flood flow frequency analysis for USGS streamgage 08211000 Nueces River near Mathis, Tex. (hereinafter referred to as the “Nueces River near Mathis gage”) was from 1943 through 2020 (USGS, 2022). RiverWare simulated annual peak streamflow values were substituted for USGS annual peak values obtained prior to the impoundment of Choke Canyon Reservoir in May of 1982 (TWDB, 2022). In the resulting combined dataset of observed and simulated data, the 1967 simulated peak streamflow of 119,000 cfs is the largest peak of record. A log-normal plot of the peak streamflows for each water year is presented in Figure 8.43.

The flood flow frequency for the Nueces River near Mathis gage simulated dataset is shown in Figure 8.44, and the tabulated results are listed in Table 8.7. A low-outlier threshold of 4,000 cfs was computed by applying the MGBT in HEC-SSP, and the station skew computed in HEC-SSP was used as the skew. During the computation of the low-outlier threshold, a total of 30 low outliers were identified. The low-outlier threshold of 4,000 cfs is different than the one set for the Nueces River near Mathis gage dataset in Appendix A because the inclusion of RiverWare data in this analysis results in a different set of ordered events and therefore a different flood flow frequency analysis.

A comparison of the simulated flood flow frequency analysis from this section and the computed flood flow frequency distribution (curve) from Appendix A is shown in Figure 8.45. The difference between the simulated and observed flood flow frequency curves is substantial. Although RiverWare was used to simulate the operation of Choke Canyon Reservoir and Lake Corpus Christi prior to its actual impoundment in 1982, it appears as though simulated annual peak streamflow prior to that date is still higher on average than the observed annual peak streamflow beginning in 1983 just as was seen with the Nueces River near Three Rivers gage. The mean simulated annual peak streamflow from 1943 through 1982 is 15,300 cfs, whereas the mean observed annual peak streamflow from 1983 through 2020 is 5,650 cfs. The 0.02 annual exceedance probability (AEP) estimate at the Nueces River near Mathis gage does match better than at the Nueces River near Three Rivers gage, possibly as a result of the more positive skew value at Mathis for the statistical analysis in Appendix A.

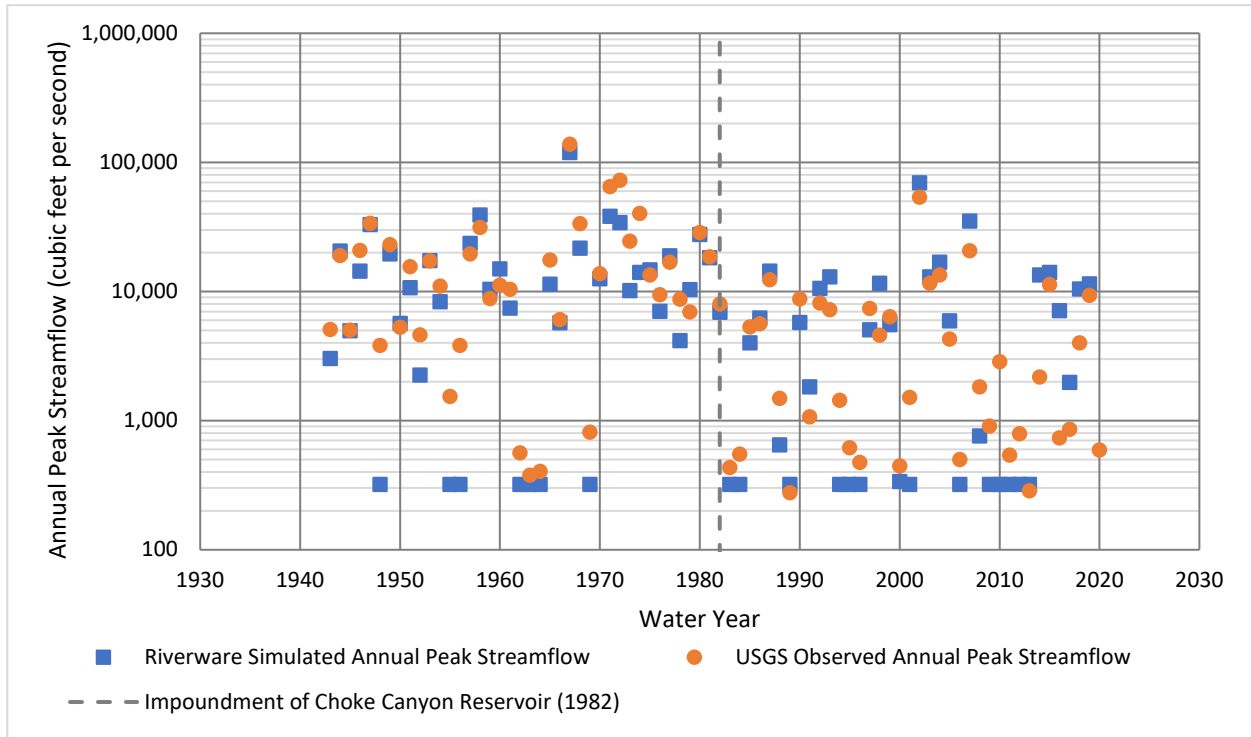


Figure 8.43: Simulated RiverWare and Observed U.S. Geological Survey (USGS) Annual Peak Streamflow for USGS Streamgage 08211000 Nueces River near Mathis, Texas.

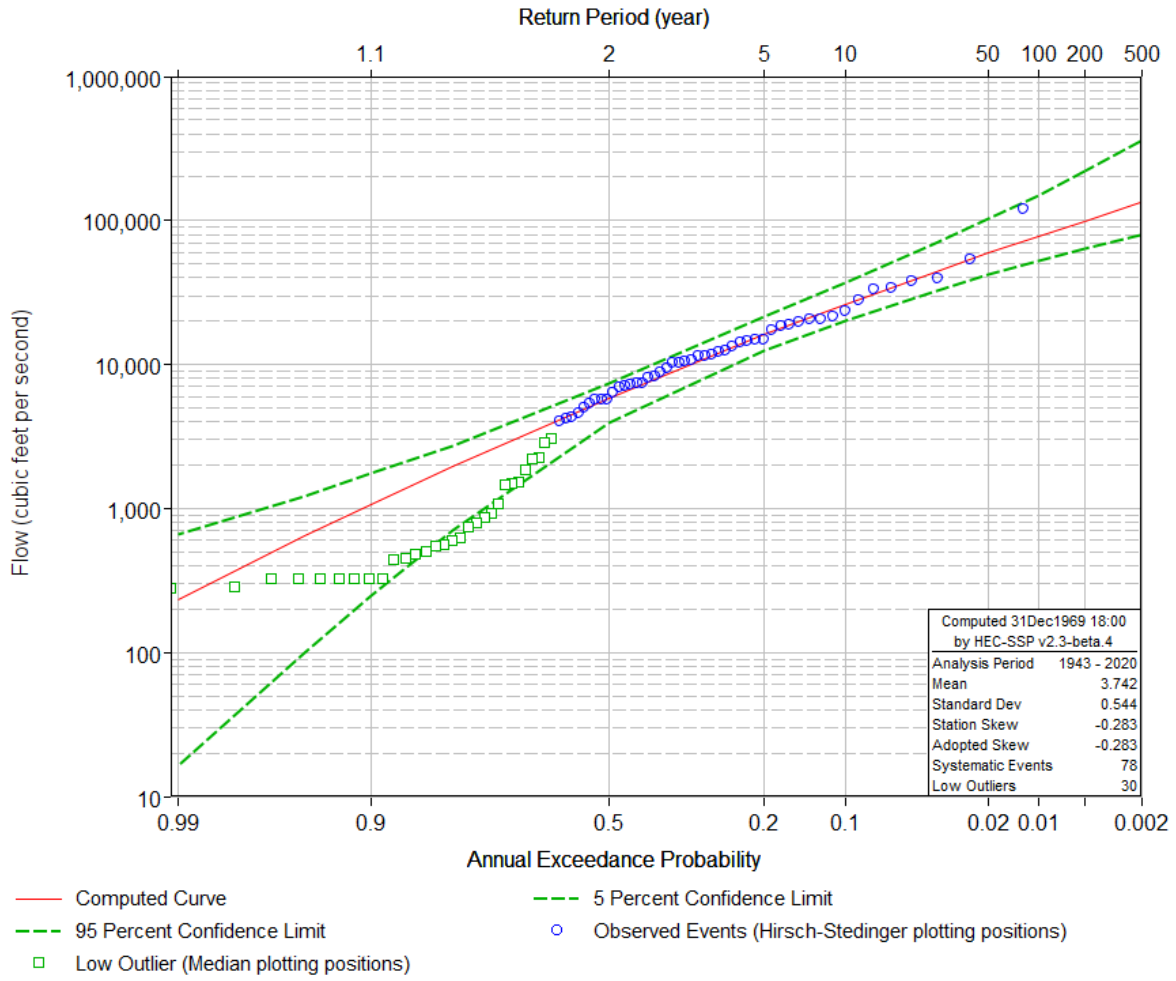


Figure 8.44: Simulated Flood Flow Frequency using log-Pearson Type III Distribution for U.S. Geological Survey Streamgage 08211000 Nueces River near Mathis, Texas.

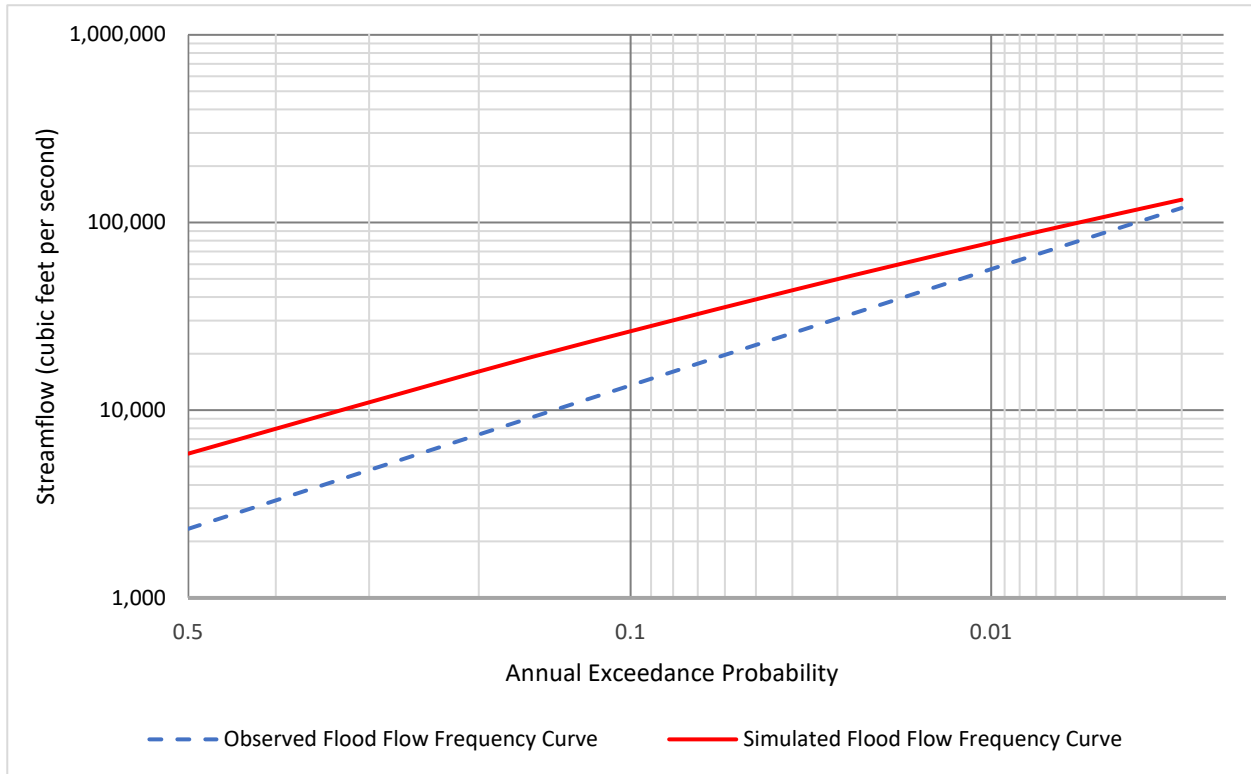
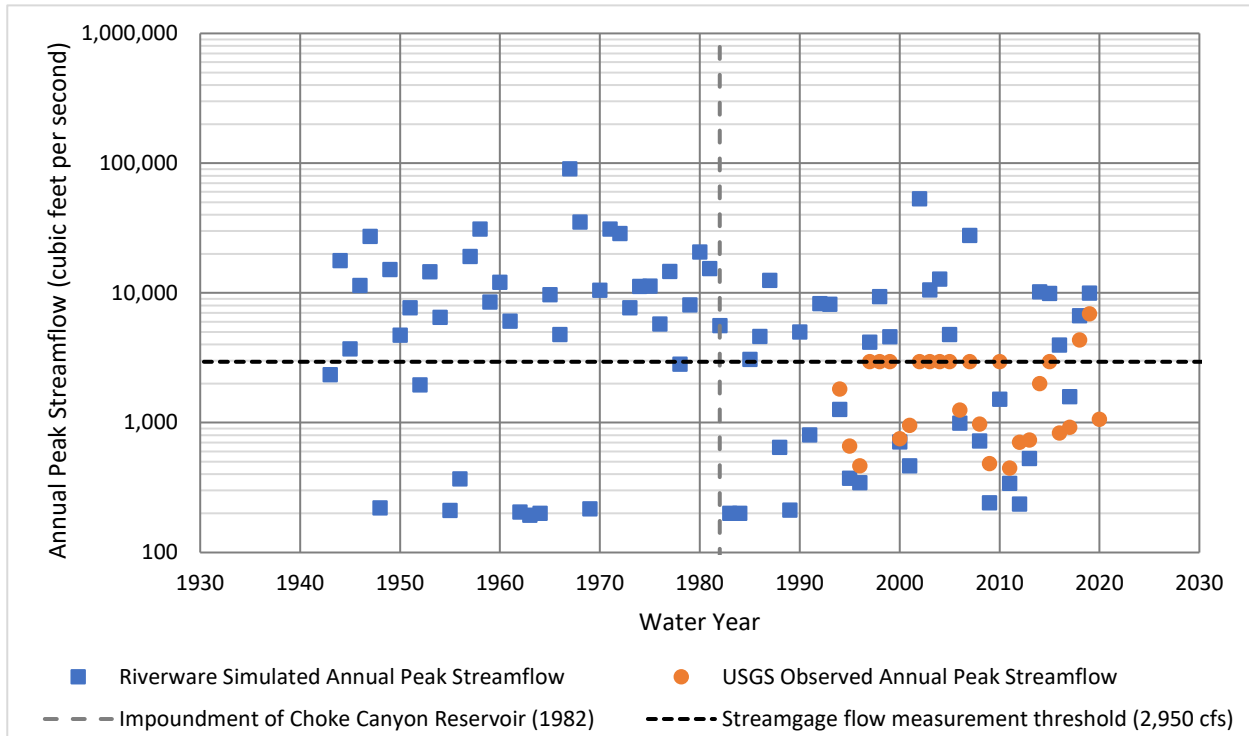


Figure 8.45: Comparison of Flood Flow Frequency Curves for the Observed (1983-2020) and Simulated (1943-2020) Datasets for U.S. Geological Survey Streamgage 08211000 Nueces River near Mathis, Texas.

**08211200 Nueces River at Bluntzer, Tex.**

The POR used in the flood flow frequency analysis for the Nueces River at Bluntzer gage was from 1943 through 2020 (USGS, 2022). RiverWare simulated annual peak streamflow values were substituted for USGS annual peak values obtained prior to the availability of annual peak streamflow data at the gage beginning in water year 1994. Additionally, the Nueces River at Bluntzer gage only measures streamflow beyond a specific threshold, in this case 2,950 cfs. When the annual peak streamflow exceeded this value, it was replaced by the RiverWare simulated annual peak streamflow in the analysis except for two water years, 2018 and 2019, when the peak streamflow was measured by a field crew. In the resulting combined dataset of observed and simulated data, the 1967 simulated peak streamflow of 90,600 cfs is the largest peak of record. A log-normal plot of the peak streamflows for each water year is presented in Figure 8.46.

The flood flow frequency for the Nueces River near Mathis gage-simulated dataset is shown in Figure 8.47, and the tabulated results are listed in Table 8.7. A low-outlier threshold of 2,340 cfs was computed by applying the MGBT in HEC-SSP, and the station skew computed in HEC-SSP was weighted by a regional skew value by Asquith and others (2021). The adopted weighted skew value was -0.40. During the computation of the low-outlier threshold, a total of 28 low outliers were identified. A comparison of the simulated flood flow frequency analysis from this section and the computed flood flow frequency distribution (curve) from Appendix A is not available for the Bluntzer gage because the gage was not analyzed in Appendix A because the period of record was not long enough to perform a reliable flood frequency analysis.



**Figure 8.46: Simulated RiverWare and Observed USGS Annual Peak Streamflow for U.S. Geological Survey (USGS) Streamgage 08211200 Nueces River at Bluntzer, Texas.**

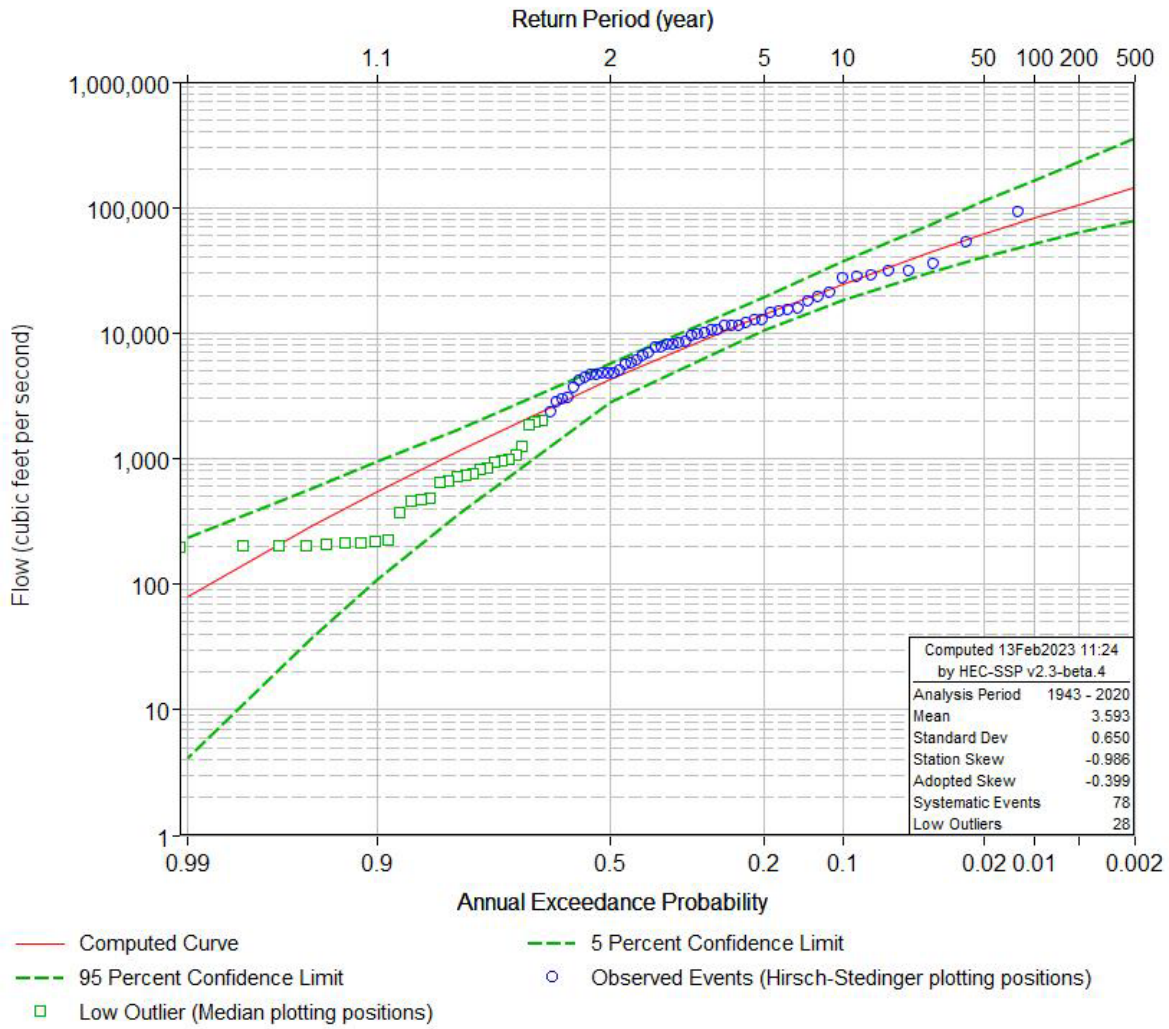


Figure 8.47: Simulated Flood Flow Frequency using log-Pearson Type III Distribution for U.S. Geological Survey Streamgage 08211200 Nueces River at Bluntzer, Texas.

## 08211500 Nueces River at Calallen, Tex.

The POR used in the flood flow frequency analysis for USGS streamgage 08211500 Nueces River at Calallen, Tex. (hereinafter referred to as the “Nueces River at Calallen gage”) was from 1943 through 2020 (USGS, 2022). RiverWare-simulated annual peak streamflow values were substituted for USGS annual peak values obtained prior to the impoundment of Choke Canyon Reservoir in May 1982 (TWDB, 2022). In the resulting combined dataset of observed and simulated data, the 1967 simulated peak streamflow of 92,900 cfs is the largest peak of record. A log-normal plot of the peak streamflows for each water year is presented in Figure 8.48.

The flood flow frequency for the Nueces River at Calallen gage-simulated dataset is shown in Figure 8.49, and the tabulated results are listed in Table 8.7. A low-outlier threshold of 1,940 cfs was computed by applying the MGBT in HEC-SSP, and the station skew computed in HEC-SSP was used as the skew. During the computation of the low-outlier threshold, a total of 27 low outliers were identified. The low-outlier threshold of 1,940 cfs is different than the one set for the Nueces River at Calallen gage dataset in Appendix A because the inclusion of RiverWare data in this analysis results in a different set of ordered events (Figure 8.48) and, as a result, a different flood flow frequency analysis.

A comparison of the simulated flood flow frequency analysis from this section and the computed flood flow frequency distribution (curve) from Appendix A is shown in Figure 8.50. The difference between the simulated and observed flood flow frequency curves is substantial. Although RiverWare simulates the operation of Choke Canyon Reservoir and Lake Corpus Christi from 1940 through 2019, it appears as though simulated annual peak streamflow prior to the impoundment of Choke Canyon Reservoir in 1982 is still higher on average than the observed annual peak streamflow beginning in 1983, just as was seen with the Nueces River near Three Rivers and Nueces River near Mathis gages. The mean simulated annual peak streamflow from 1943 through 1982 is 13,400 cfs, whereas the mean observed annual peak streamflow from 1983 through 2020 is 4,580 cfs.

The 0.002 annual exceedance probability (AEP; 500-year) estimate of 123,000 cfs at the Nueces River at Calallen gage is less than the 0.02 AEP estimate of 187,000 cfs described in Appendix A. The difference in estimates for the 0.002 AEP estimate is likely because a more negative skew value was used in the simulated analysis than in the observed analysis of annual peak streamflows described in Appendix A.

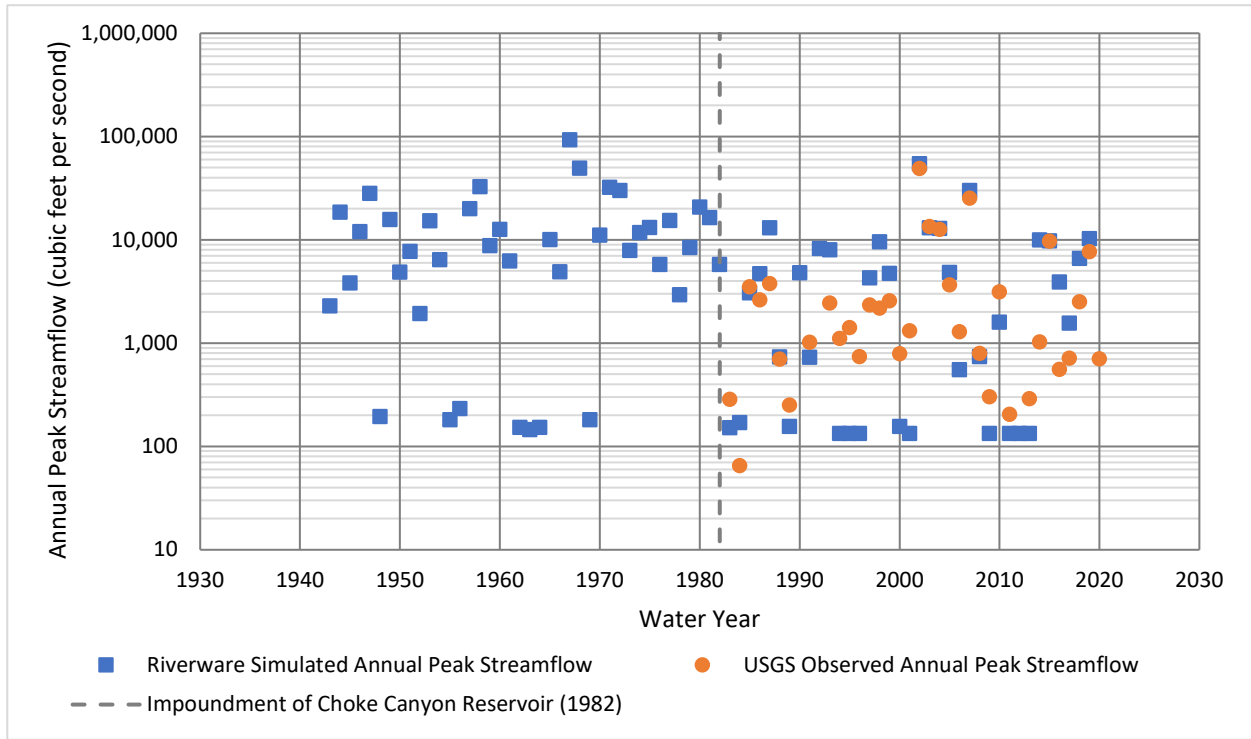


Figure 8.48: Simulated RiverWare and Observed U.S. Geological Survey (USGS) Annual Peak Streamflow for USGS Streamgauge 08211500 Nueces River at Calallen, Texas.

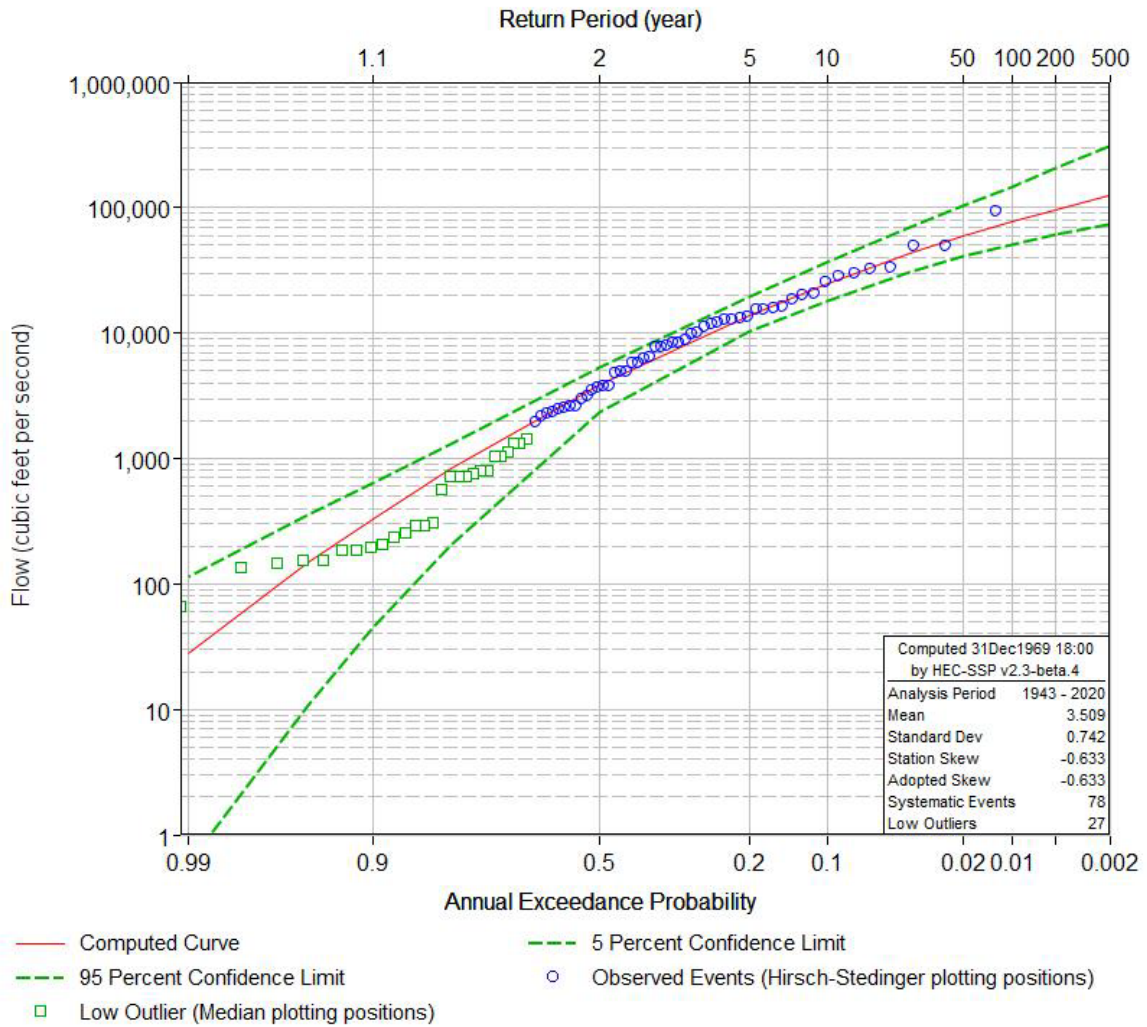


Figure 8.49: Simulated Flood Flow Frequency using log-Pearson Type III Distribution for U.S. Geological Survey Streamgage 08211500 Nueces River at Calallen, Texas.

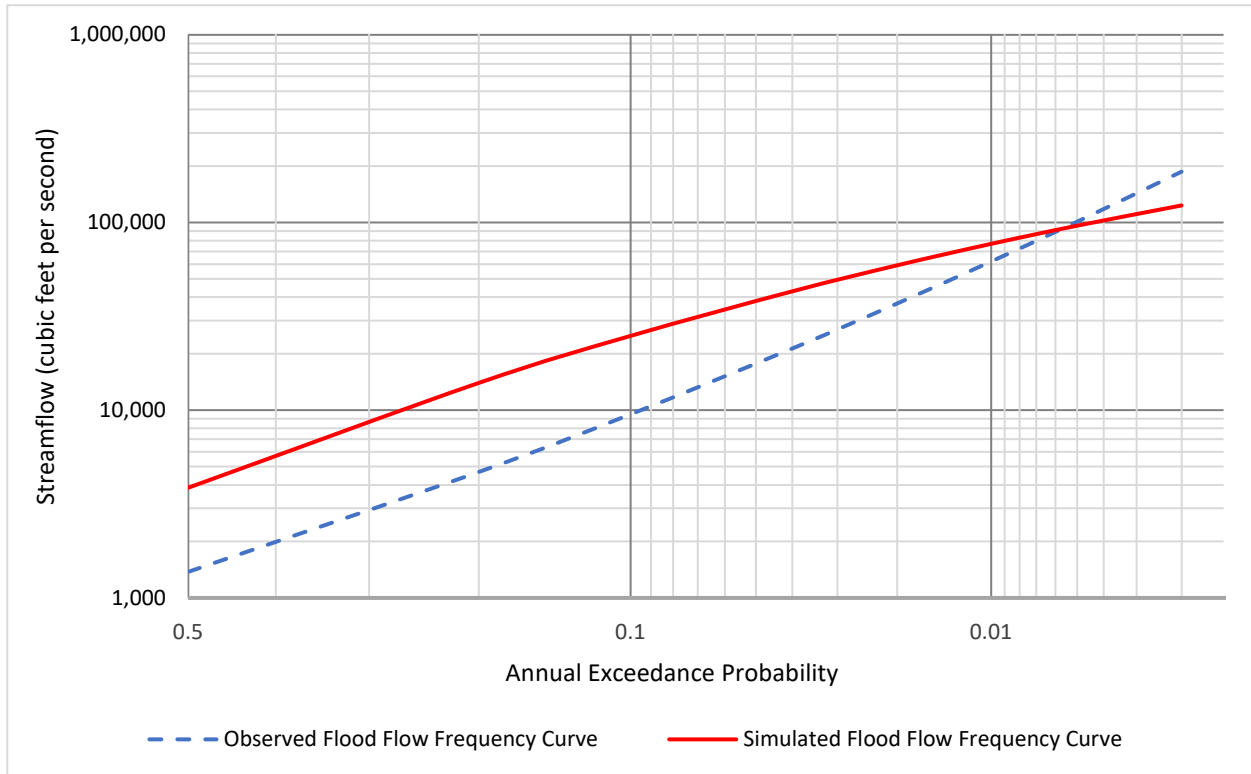


Figure 8.50: Comparison of Flood Flow Frequency Curves for the Observed (1983-2020) and Simulated (1943-2020) Datasets for U.S. Geological Survey Streamgage 08211500 Nueces River at Calallen, Texas.

**Table 8.7: Statistically Estimated Annual Flood Frequency Results and Confidence Intervals Simulated for Five U.S. Geological Survey Streamgaging Stations in the Nueces River Basin, Texas, determined by Hydrologic Engineering Center-Statistical Software Package Software**

[cfs, cubic feet per second; %, percent; CI, confidence interval; Note, table contents derived from EXP file (file extension name) of USACE HEC-SSP software output (USACE, 2016). The estimates are of primary interest and are accentuated using a bold typeface. ]

Station number and name	Flood flow frequency by corresponding average return period (recurrence interval) in years							
	2 year (cfs)	5 year (cfs)	10 year (cfs)	25 year (cfs)	50 year (cfs)	100 year (cfs)	200 year (cfs)	500 year (cfs)
<b>08206910 Choke Canyon Reservoir OWC near Three Rivers, Tex.</b>								
Lower 95%-CI	96	5,330	13,400	25,800	35,100	43,900	51,500	59,800
Estimate	<b>933</b>	<b>9,360</b>	<b>22,300</b>	<b>45,300</b>	<b>64,600</b>	<b>83,600</b>	<b>101,000</b>	<b>121,000</b>
Upper 95%-CI	1,730	16,900	60,100	295,000	595,000	998,000	1,500,000	2,280,000
<b>08210000 Nueces River near Three Rivers, Tex.</b>								
Lower 95%-CI	5,270	14,600	21,400	31,900	41,200	51,600	63,100	79,900
Estimate	<b>8,000</b>	<b>17,600</b>	<b>26,800</b>	<b>42,400</b>	<b>57,200</b>	<b>75,000</b>	<b>96,500</b>	<b>131,000</b>
Upper 95%-CI	9,400	22,300	36,300	64,600	97,600	147,000	221,000	381,000
<b>08211000 Nueces River near Mathis, Tex.</b>								
Lower 95%-CI	3,960	12,600	20,100	31,800	41,800	52,600	64,000	79,600
Estimate	<b>5,860</b>	<b>16,100</b>	<b>26,300</b>	<b>43,500</b>	<b>59,500</b>	<b>78,100</b>	<b>99,500</b>	<b>132,000</b>
Upper 95%-CI	7,400	21,300	36,800	67,400	102,000	150,000	220,000	359,000
<b>08211200 Nueces River at Bluntzer, Tex.</b>								
Lower 95%-CI	2,800	10,600	18,100	30,100	40,300	51,400	62,800	78,400
Estimate	<b>4,330</b>	<b>14,100</b>	<b>24,700</b>	<b>43,300</b>	<b>60,900</b>	<b>81,600</b>	<b>106,000</b>	<b>142,000</b>
Upper 95%-CI	5,710	19,500	37,000	72,700	112,000	164,000	232,000	356,000
<b>08211500 Nueces River at Calallen, Tex.</b>								
Lower 95%-CI	2,320	10,200	18,000	30,300	40,400	50,700	60,700	73,100
Estimate	<b>3,860</b>	<b>14,000</b>	<b>24,900</b>	<b>43,000</b>	<b>59,100</b>	<b>76,900</b>	<b>96,100</b>	<b>123,000</b>
Upper 95%-CI	5,300	19,500	36,400	68,800	103,000	147,000	205,000	309,000

# 9 Reservoir Analyses

## 9.1 Introduction

This section of the report describes the methods used to produce the pool frequency curves for the Nueces River Basin reservoir projects. The reservoir projects that have been analyzed for this section are Choke Canyon Reservoir and Lake Corpus Christi. More details about who owns and operates these projects are listed in section 8.1.3. The frequency curves were developed to represent the current reservoir control plan and watershed conditions (as of 2019). A frequency analysis is a statistical method of prediction that consists of studying past events that are characteristic of a particular hydrology process in order to determine the probabilities of occurrence of these events in the future. A stage-frequency curve estimates the ACE for reservoir pool elevations. For example, if a reservoir pool at the spillway crest has an ACE of 1/50 (1 in 50 years on average), then the reservoir has a 2% chance of the reservoir pool elevation equaling or exceeding the spillway crest elevation in any given year. The stage-frequency curve can be determined using empirical (observed or measured) data; however, the reservoir pool elevations associated with 1% ACE (100-year) or 0.2% (500-year) occurrence are typically beyond the observed reservoir pool elevation period of record (POR). Models serve the purpose of extrapolating reservoir pool elevation frequencies beyond the observed record.

For the presented study, the pool frequency curves presenting current conditions were developed to evaluate the Nueces River Basin projects' pool elevations resulting from the 50% ACE (2-year) to 0.2% (500-year) events. This study incorporates available reservoir daily inflow (historical peaks through 2019) and daily pool data (historical peaks through 2019) into statistical software and applies statistical methods to estimate the critical inflow duration and simulate inflow and elevation period of record for each project. The historical peaks, if available, may be observed and recorded by local residents or seen as water marks on bridge piers or tree trunks; those water elevation marks can be translated into peak inflow or release discharge values via the use of models or by extrapolating rating curves or extrapolation of observed data points. For each project, the Hydrologic Engineering Center-Statistical Software Package (HEC-SSP) (USACE, 2019) was used to compute volume duration frequency curves from the annual maximum peak reservoir inflows. An empirical pool frequency curve was developed from the available reservoir pool Annual Maximum Series (AMS). An event based stochastic Monte Carlo simulation model (USACE, 2018) was used to extrapolate the pool frequency curve beyond the limits of empirical pool frequency curve. RiverWare (CADSWES, 2020) was used to develop a current condition POR for reservoir inflows and elevations. The AMS results derived from RiverWare was used to create the empirical pool frequency curve. The empirical stage-frequency curve was used to validate RFA model simulation results. The results showed adequate validation to the upper tail end of the empirical pool frequency curves and is believed to be a reasonable extrapolation for frequency of rare pool events.

No previous records or pool frequency elevation estimates were made to compare to the results documented in this chapter for the Nueces River Basin Lakes. In this chapter, main emphases were put to accurately capture the 1% ACE (100-year) and 0.2% (500-year) events by utilizing the RMC-RFA program throughout Water Year (WY) 2019 for each project.

## 9.2 Watershed Description

The Nueces River Basin is located in south-central Texas and is the seventh largest river basin in Texas, with a drainage area totaling 16,675 square miles (Figure 9.1). The watershed spans 24 counties and drains all or parts of 24 counties. The basin is approximately 230 miles long, with a maximum width near its center of approximately 115 miles and includes about 6 percent of the total land area of Texas. There are no USACE Reservoirs in the Nueces River Basin, however, the Three Rivers Local Protection Project is located downstream of Choke Canyon Dam on the Frio River. The Nueces River is located in the arid valley of South Texas and empties into the Gulf of Mexico in Corpus Christi, Texas. The Balcones Fault runs East-West through the Northern part of the basin and is responsible for streamflow loss resulting in the groundwater recharge in Edwards Aquifer and the Carrizo-Wilcox Aquifer. Water supply in the Nueces basin relies primarily on groundwater except for the two major lakes in the Southern part of the basin. Both Choke Canyon Reservoir and Lake Corpus Christi provide water supply. The total contributing drainage area to Choke Canyon Reservoir is 5,490 square miles and Lake Corpus Christi is 16,502 square miles.

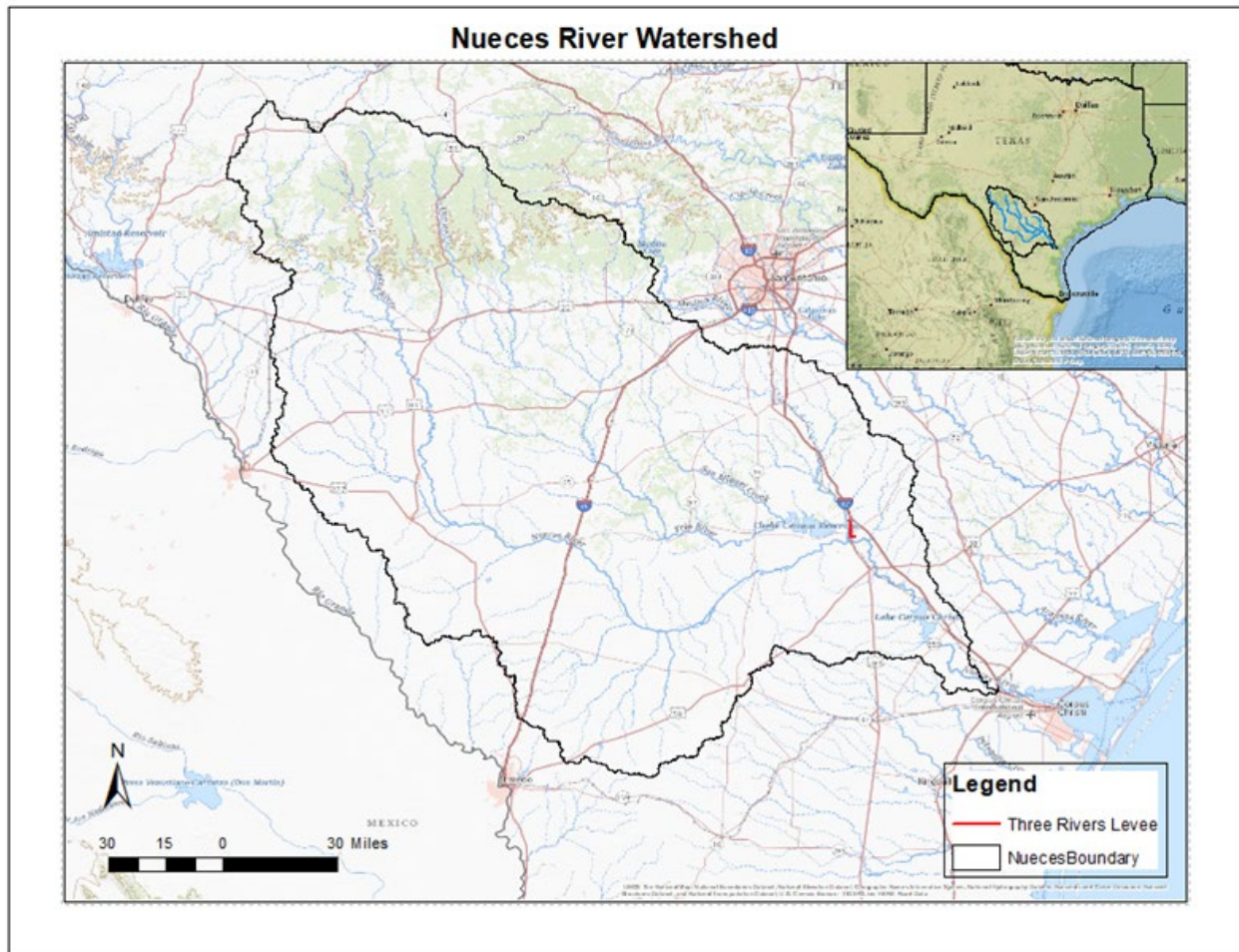


Figure 9.1: Map of the Nueces River Watershed

### 9.2.1 Nueces River Watershed Gages

Figure 9.2 and Table 9.1 show the corresponding reservoir projects and the USGS gages used to develop the Nueces River Basin inflow and release discharges. In many instances, project inflows are estimated from the nearest USGS gage upstream of the dam, especially if the project drainage area does not vary significantly from the nearest USGS gage. The nearest USGS gage rating curve can also be used to estimate the historical inflow and release peak discharges for the projects. Detailed analyses for hydrology development using RiverWare can be found in chapter 8 of this report. The POR for Nueces River Basin Lakes' inflows were obtained from RiverWare.



Figure 9.2: Selected USGS Gage Locations in the Lower Nueces River Basin

Table 9.1: USGS and USACE-SWD Data

Location	Data Type (Units)	Source
San Miguel nr Tilden, Tex.	Discharge (cubic feet per second)	USGS 08206700
Frio River at Tilden, Tex.	Discharge (cubic feet per second)	USGS 08206600
Nueces Choke Canyon Res nr Three Rivers, Tex.	Discharge (Release) (cubic feet per second)	USGS 08206910
Frio Rv at Calliham, Tex.	Discharge (Inflow) (cubic feet per second)	USGS 08207000
Atascosa Rv at Whitsett, Tex.	Discharge (cubic feet per second)	USGS 08208000
Nueces Rv nr Tilden, Tex.	Discharge (cubic feet per second)	USGS 08194500
Nueces River nr Three Rivers, Tex.	Discharge (cubic feet per second)	USGS 08210000
Nueces River nr Mathis, Tex.	Discharge (Release) (cubic feet per second)	USGS 08211000
Nueces River nr Bluntzer, Tex.	Discharge (cubic feet per second)	USGS 08211200
Nueces River at Calallen, Tex.	Discharge (cubic feet per second)	USGS 08211500
Choke Canyon Pool	Elevation (NGVD-29 feet)	City of Corpus Christi database
Corpus Christi Pool	Elevation (NGVD-29 feet)	City of Corpus Christi database

### 9.3 Climate

Climatological conditions (England et al, 2018) (Mansfield, 2013) over the watershed are generally mild and vary from subtropical along the Gulf Coast to semiarid in the upper headwater regions. The rainfall decreases rather uniformly from the Gulf of Mexico to the headwaters. Most of the rainfall in the study area typically occurs in the form of intense, isolated storms during the spring, early summer, and fall. Mean annual rainfall measured in or near the study area ranged from 21.0 to 32.2 inches. About 92 percent of the rainfall in the region evapotranspires each year. The average annual temperatures over the Basin are generally moderate, with the highest at the Gulf and decreasing gradually with the increase in latitude and elevation. Winter months are generally mild, but occasional cold periods of short duration result from the rapid movement of cold high-pressure air masses from the northwest. Snowfall and subfreezing temperatures are rare in the lower portion of the Basin near the Gulf. Summer temperatures are high throughout the Basin. Near the lakes, the average high in January is 65°F and low 45°F. The record low was 11°F and the record high was 109°F.

### 9.4 Runoff

The Nueces River (Mansfield, 2013) Basin is subject to three general types of flood-producing rainfall: thunderstorms, frontal rainfall, and tropical cyclones. Thunderstorms in the watershed are sometimes accompanied by excessive rainfall for periods of up to 8 hours, but rarely produce excessive rainfall over an extensive area. Thunderstorms cause flash flooding in streams and are especially damaging to crops, because they frequently occur during the growing season. The frontal storms result from warm moisture-laden air masses rising from the western Gulf of Mexico and converging with a tropical or polar air mass. These storms may occur in the late summer months and tend to last for several days. The cyclonic storms originate in the Mid-Atlantic Ocean, the Gulf of Mexico, and the Pacific Ocean. When tropical air masses, brought ashore by hurricanes, converge with a cold air mass, torrential rains occur. June through November is considered to be Atlantic hurricane season.

## 9.5 Methods

### 9.5.1 Empirical Stage-Frequency

For the evaluation of a simulated reservoir pool frequency curve predictive capability, an empirical reservoir pool frequency curve is created. An empirical reservoir stage-frequency curve is constructed by ranking the observed/simulated peak annual reservoir stages, assigning the data a plotting position, and then plotting the data on probability paper using a plotting position formula. Many plotting position formulas can be used for the orientation of an empirical reservoir pool frequency curve, but a plotting position formula that is flexible and makes the fewest assumptions is preferred (Cohn et al, 1997) (England et al, 2018). The Weibull plotting position formula was selected. This formula is an unbiased estimator of expected exceedance probability for all distributions and is used to plot the series of peak annual reservoir stages. The formula for Weibull is:

$$P_i = i / (n + 1)$$

Where,  $i$  is the rank of the event,  $n$  is the sample size in years, and  $P_i$  is the exceedance probability for an event with rank  $i$  pool frequency.

### 9.5.2 Risk Management Center - Reservoir Frequency Analysis (RMC-RFA)

RMC-RFA software was developed by the USACE Risk Management Center for use in dam safety risk assessments. It can produce a stage-frequency curve with confidence bounds using a stochastic model with the volume-sampling approach. The model functions best in situations where dam operations are relatively simple, especially when the spillway is not regulated using gates. A simplification of the operational rules is assumed through the use of an elevation-discharge (release) table which is based on a combination of dam discharge structures and calibration to historical releases. Development of model inputs is aided by tools within the program that allow the user to estimate inputs, such as flood seasonality or pool duration curves, in a consistent and automated manner. Other inputs, such as the volume frequency curve or reservoir operations, are developed by the user independently.

### 9.5.3 Volume-Sampling Approach

A common method (Cohn et al, 1997) for estimating a pool frequency curve for a dam is by volume-based sampling. In this method, a large number of flood events is generated using random sampling of flood volumes, the associated flood hydrographs are routed through the reservoir, and the peak reservoir elevation for each event is recorded.

The general workflow for a volume-based pool frequency analysis is as follows:

1. Choose a stage for the reservoir to begin the flood event.
2. Choose an inflow flood hydrograph to scale.
3. Sample a flood volume from the reservoir inflow frequency curve.
4. Scale the selected flood hydrograph to match the sampled flood volume.
5. Route the scaled flood hydrograph through the reservoir using an operations model.
6. Record the peak stage that occurred during the event.

For the stochastic model, RMC-RFA, choices made in steps 1-3 are made using random selection from a probability distribution. The choice is random in the sense that it occurs without pattern, but the relative frequency of the outcomes in the long term is defined by a probability distribution. Reservoir stages for starting the simulation come from a *pool duration curve*, which is a probability distribution for the elevation of the

reservoir pool. They may be seasonally based, in which case first the season of the flood event occurrence is selected at random, and then a starting stage is selected at random from the pool duration curve for that particular season. Sampled flood volumes come from the flow frequency curve produced by fitting an analytical probability distribution to an AMS inflow of N-day river discharges. In the volume-based approach, instead of analyzing instantaneous peak discharge (as is typically the case in a Bulletin 17B/C-type analysis<sup>8</sup>), the analysis is performed on a longer-duration volume (e.g., 15-day average inflow discharge.)

When steps 1-6 are performed a large number of times (for example, 10,000 *samples*), the resulting peak stages are ranked and plotted, producing a stage-frequency curve for the reservoir. However, substantial uncertainty exists in several of the inputs to the model, especially the inflow frequency curve. To account for these uncertainties, steps 1-6 are performed a large number of times with different parameters for the inputs. The input parameters are varied across *realizations*, and for each realization, steps 1-6 are repeated over a large number of *samples*. Thus, the full simulation with uncertainty will contain a number of events equal to the number of realizations times the number of samples. By varying parameters across realizations, the uncertainty in the probability of an event, for example reaching spillway crest elevation, can be better assessed. Each realization will produce an estimate of the probability of reaching this elevation based on the parameters used to drive the realization. Percentiles (for example the 5<sup>th</sup> and 95<sup>th</sup> percentiles) of these probabilities produce a confidence interval for the probability of reaching the spillway. If the mean probability of exceeding any stage is taken, then the result is the *expected frequency curve*, which is the single best estimate for the probability of exceeding a particular stage.

## 9.6 Data Analysis and Model Input

### 9.6.1 Inflow Hydrograph and Pool Stage

Estimate of daily average inflow discharges and pool elevations for the Nueces River Basin projects were retrieved from the City of Corpus Christi water management database system for WY 1943 through WY 2019. Records prior to project construction were simulated using RiverWare. The Nueces River Basin projects impoundment dates are shown in Table 9.2. RiverWare software mimics a watershed by modeling its features as linked objects, including storage or power reservoir objects, stream reach objects, groundwater storage objects, or diversion objects. In a simple model, these objects simulate basic hydrologic processes through mass balance calculations and can be linked to one another through inflow-outflow calculations. More advanced modeling is achieved by selecting object-specific methods that further define the hydrologic processes associated with each object. Additionally, RiverWare may operate under a rule-based simulation, which creates logic-based interdependency of objects through user-defined rules. These rules may look forwards and backwards in time and given priorities in one rule may supersede others depending on the importance defined by the user. These detailed yet simple modeling techniques allow RiverWare to simulate reservoirs' pool elevations and inflow efficiently. The lakes hourly inflow hydrographs are shown in Figure 9.3 and 9.4. Figure 9.5 and 9.6 display selected data of observed and simulated daily average inflow and pool elevations for Lakes Choke Canyon and Corpus Christi.

Table 9.2: Nueces River Basin Dams Deliberate Impoundment Dates

Project	Deliberate Impoundment Date
Choke Canyon Reservoir	October 1984
Lake Corpus Christi	September 1948

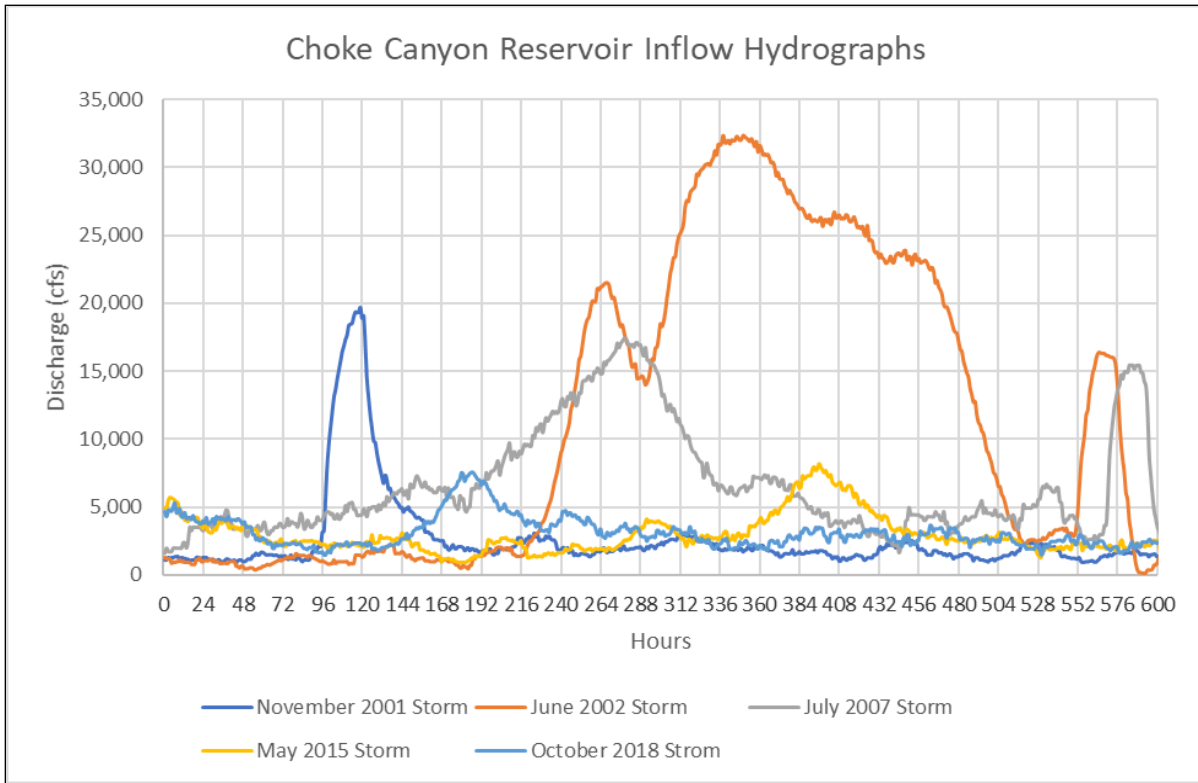


Figure 9.3: Choke Canyon Reservoir Inflow Hydrographs

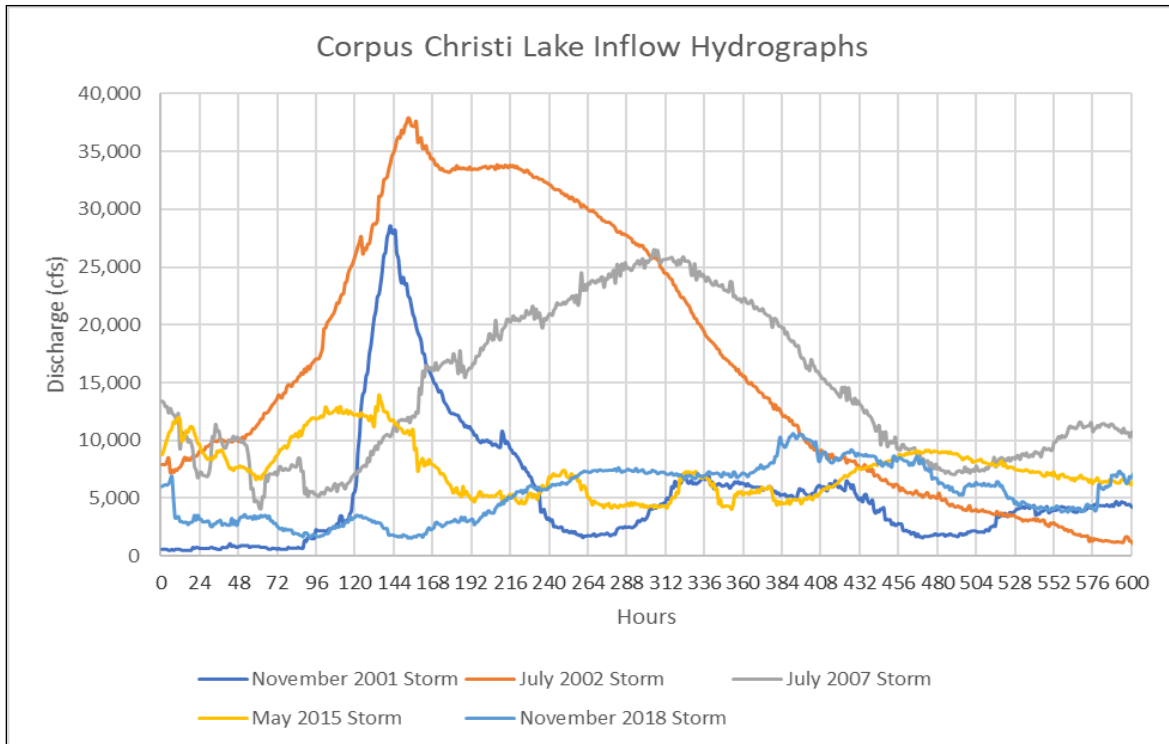


Figure 9.4: Lake Corpus Christi Inflow Hydrographs

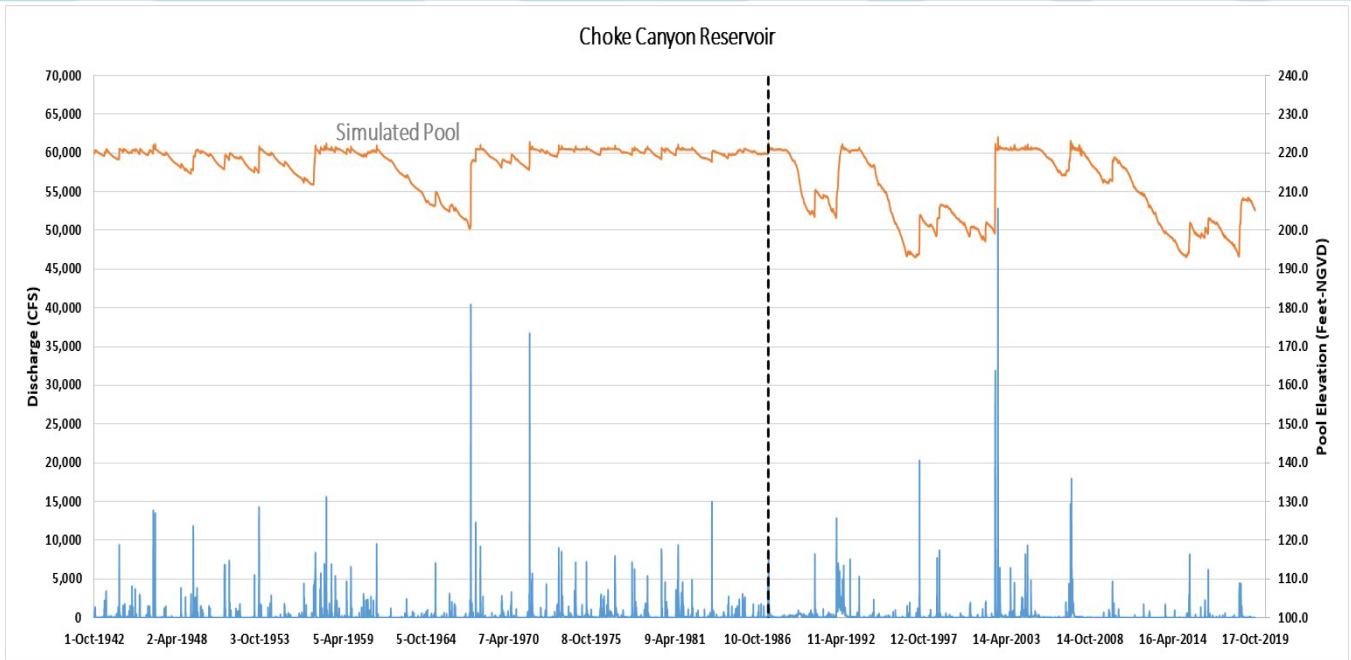


Figure 9.5: Choke Canyon Reservoir Daily Average Inflow and Pool Elevation

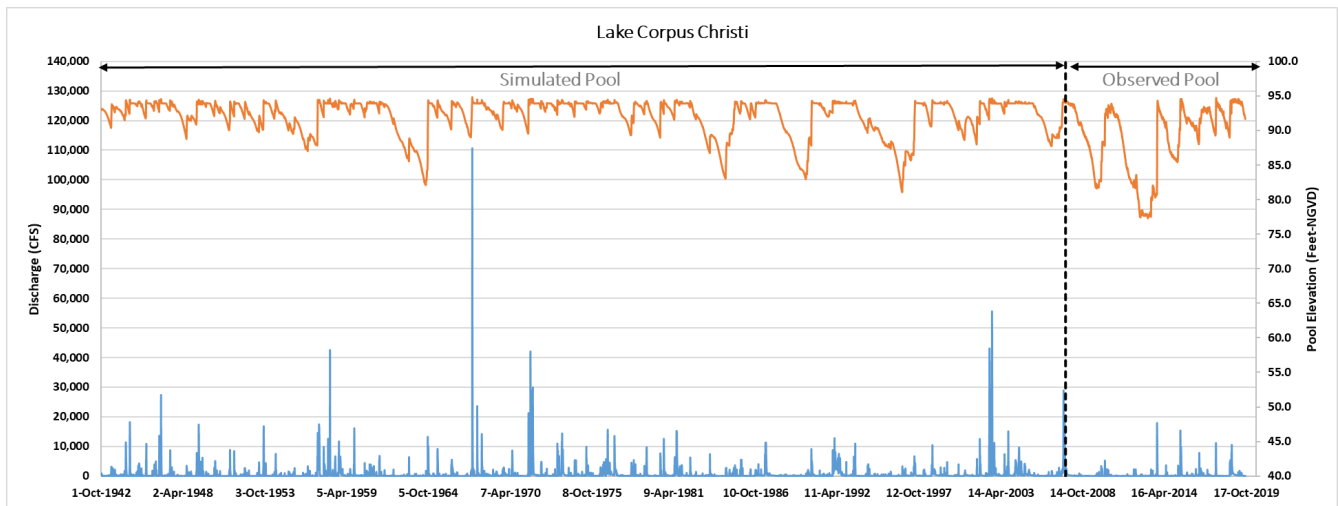


Figure 9.6: Corpus Christi Daily Average Inflow and Pool Elevation

## 9.6.2 Historical Discharge Peak Estimates

The lake inflow systematic record contains observed (recorded) post-dam construction inflow discharges and pre-dam construction synthetic inflow discharge years generated using RiverWare. Choke Canyon Reservoir inflow discharge peaks are annual maximum peaks for the POR 01 October 1915 through 30 September 2019. There were no historical inflow discharge peaks recorded prior to this period. Inflows to Lake Corpus Christi utilized the simulated inflow annual maximum discharge peaks for the POR 01 October 1942 through 30 September 2019. There were no additional independent inflow Historical discharge peaks recorded for the lake. For the simulated record, the largest inflow daily average maximum discharge peaks that stood out for both projects were the September (1967 and 2002) of 40,085cfs and 51,600cfs for Choke Canyon Reservoir; 109,550cfs and 55,140cfs, respectively, for Lake Corpus Christi.

## 9.6.3 Daily Average AMS Estimates

An extract of the n-day inflow discharge average maximum annual peak for each project was made available for the analysis. Choke Canyon Reservoir inflow AMS consists of discharge peaks extracted from USGS 08207000 Frio Rv at Calliham, Tex., USGS 08206700 San Miguel nr Tilden and USGS 08206600 Frio River at Tilden, Tex., combined, whereas Corpus Christi's AMS inflow is RiverWare simulation extract. Inflows to each lake were processed in HEC-DSS Vue to produce the 15-day AMS. The critical duration best estimate in days is shown in section 9.7.

## 9.7 Critical Inflow Duration Analysis

The critical inflow duration can be defined as the inflow duration that tends to produce most consistently the highest water surface elevation for the reservoir. The critical inflow duration accounts for the most significant storm events, which are normally selected based on a screening criterion that capture project inflow hydrographs with a minimum threshold peak determined on a case-by-case basis (*i.e.*, Choke Canyon critical inflow duration minimum threshold peak is 8,000 cfs less than Corpus Christi's). The studied lakes are in the lower portion of the Nueces River Basin, where weather patterns and climate are similar. Rivers flowing to the lakes have flat slopes and wide floodplains, which allow for longer critical durations. The storm duration can also impact critical durations; longer storms result in longer critical durations. To determine critical inflow duration of the observed rainfall-runoff events, extreme rainfall runoff (inflow) events are examined. All large inflow events are independent, meaning that different year hydrographs can be presented in one figure to determine the proper critical duration. The duration peak inflow was used to determine a reasonable value for critical inflow duration. Although this method was found accurate to produce good estimates, the critical duration can be adjusted later during the analysis to reflect the most appropriate frequency curve. Best engineering judgment remains necessary in the final selection of the most appropriate value. For each project, a set of historical inflow events (hydrographs) with daily peak inflows greater than a certain threshold were extracted from USGS gages or RiverWare simulated daily average inflow period of record (*i.e.*, examine the top 20% largest independent inflow events for each project inflow). The best-estimate inflow duration for the reservoir is estimated in two ways. First, by taking the average hydrograph of the major events specified. Figure 9.7 and 9.8 illustrate the lakes inflow critical durations best estimates excluding baseflow. Second, Identify the most extreme historical peak reservoir events as seen in Table 9.3. Then, locate the reservoir inflow, stage, and discharge hydrographs corresponding to each peak stage event. Select events that are consistent with the types of events likely to be the driver of extreme peak stages. Reservoir peak stage occurs when the reservoir outflow equals the inflow on the receding limb of the inflow hydrograph. Figure 9.9 is an example of one selected event, which illustrates the visual procedure of the second method. Best estimates of the n-day critical durations for the projects are listed in Table 9.3. These results were finalized after making several sensitivity analyses while running the RMC-RFA program. The best

critical duration estimate produced the most conservative elevation frequency in the lake. The purpose of this analysis is to have a better understanding of the runoff response from large single rain events that helps establish what inflow volume discharge frequency curves need to be examined.

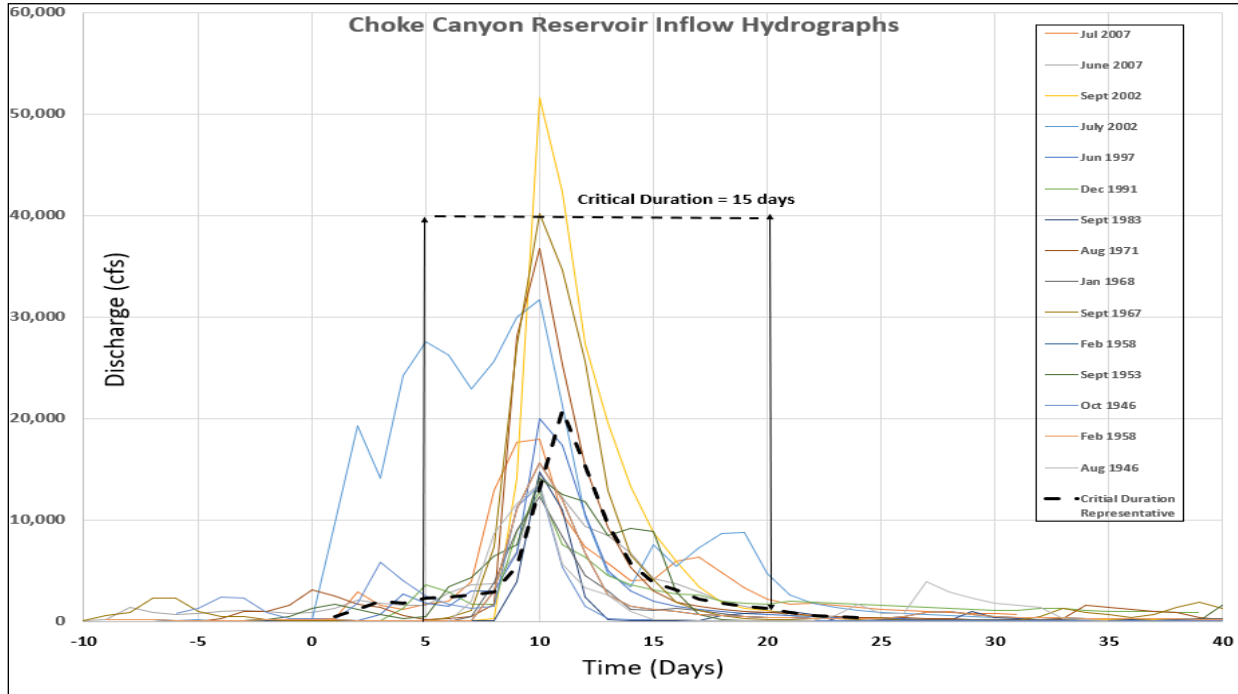


Figure 9.7: Choke Canyon Reservoir Critical Duration Inflow Analysis

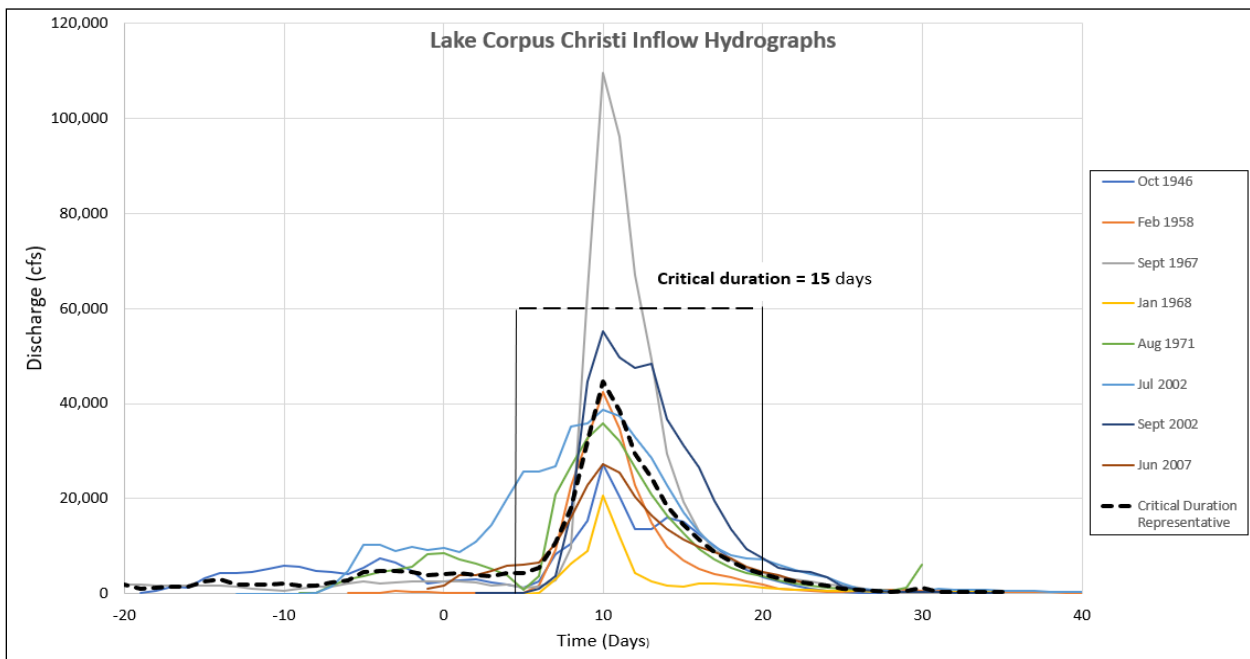
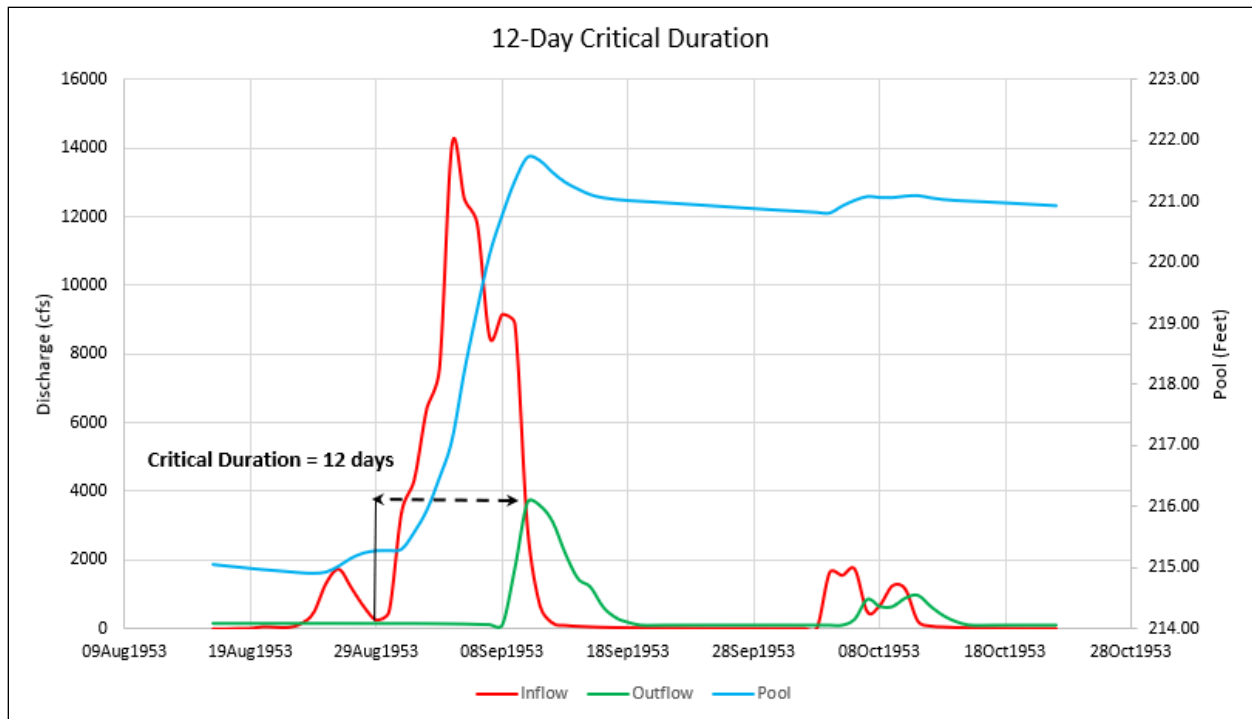


Figure 9.8: Lake Corpus Christi Critical Duration Inflow Analysis

**Table 9.3: Nueces River Basin Inflow Duration Analysis**

Project	Inflow Duration Method		
	Minimum Threshold Peak (CFS)	Number of Analyzed Inflow Events	Critical Duration (Days)
Choke Canyon Reservoir	12,000	15	15
Lake Corpus Christi	20,000	8	15
Project	Inflow-Outflow Coincidental Hydrograph Method		
	Event Date	Number of Analyzed Inflow Events	Critical Duration (Best Estimate, Days)
Choke Canyon Reservoir	Oct46, Sep53, Feb58, Sep67, Jan68, Aug71, Oct83, Dec91, Jun97, Jul02, Sep02, Jul07, Sep07	13	15
Lake Corpus Christi	Feb58, Sep67, Jan68, Aug71, Jul02, Sep02, Jun07	7	15



**Figure 9.9: September 1953 Flood Event for Choke Canyon Reservoir**

### 9.7.1 Volume/Flow Frequency Statistical Analysis

The volume/flow frequency analyses for the Nueces River Basin Lakes were estimated by following Bulletin 17C guidelines and procedures (statistical techniques) to determine exceedance probabilities associated with specific flow rates utilizing HEC-SSP 2.2. The observed and simulated daily average annual maximum peaks were used to establish a relationship between flow magnitude and frequency. In this chapter, the term volume/flow frequency refers to the frequency with which a flow over a given duration, such as 15-Day expected to be equaled or exceeded. The duration selection was based on inspecting the shape of the hydrographs such as those shown in

Figure 9.7, 9.8, and 9.9. The critical durations best estimate are listed in Table 9.3. To adequately assess the risk associated with the Nueces River Basin Dams' structures in question, the 15-Day critical duration was used to construct hypothetical inflow frequency events for Choke Canyon Reservoir and Lake Corpus Christi. The events were routed through the projects to estimate reservoirs' stage-frequency curves.

## 9.7.2 Bulletin 17B/C

The use of bulletin 17C guidance allows for computations of the annual exceedance probability of the instantaneous and daily average inflow discharge peaks, using the Expected Moments Algorithm (EMA). It estimates distribution parameters based on sample moment in a more integrated manner that incorporates non-standard, censored, or historical data at once, rather than as a series of adjustment procedures (Cohn et al, 1997). It should be noted that Bulletin 17B procedures and guidelines would produce similar results if Bulletin 17C procedures were followed since historical interval peaks were not available. In this chapter, Bulletin 17C procedures were followed for the analysis.

## 9.7.3 HEC-SSP Computations

A series of n-day volume duration frequency curves was developed for each of the Nueces River Basin projects. The volume duration frequency results from this analysis were developed using HEC-SSP. The Multiple Grubbs-Beck algorithm was used to perform sensitivity analysis for the low outlier test. Plotting position of the data follow the Log-Pearson III plotting position algorithm distribution. The station skew option was used for the analysis for the projects using the systematic records. For consistency, each developed frequency curve went the same analysis techniques before adoption. Table 9.4 contains skews and record lengths for each project analyzed using HEC-SSP.

**Table 9.4: Summary of HEC-SSP Input Parameters**

<b>Project</b>	<b>Systematic Record (years)</b>	<b>Station Skew (Critical Duration)</b>
Choke Canyon Reservoir	104	-0.347
Lake Corpus Christi	77	+0.109

Note: The actual systematic record length is less than the systematic record length shown in the Table. The actual systematic record length was extended utilizing USGS and RiverWare.

The Nueces River Basin Lakes computed frequency flows from HEC-SSP are listed in Table 9.5. The statistical parameters generated based on applying the Bulletin17C method, station skews, and low outlier tests for Multiple Grubbs-Beck are listed in Table 9.6. Only pertinent critical durations were listed for each project.

**Table 9.5: Nueces River Basin Lakes Bulletin 17C Computed Median Inflows**

N	ACE	Bulletin 17C AMS Computed Average (Median) Peaks (CFS)	
		Choke Canyon Reservoir	Lake Corpus Christi
Years	%	<b>15-Day</b>	<b>15-Day</b>
500	0.2	25,850	74,830
200	0.5	20,260	55,040
100	1	16,435	42,820
50	2	12,970	32,620
20	5	8,935	21,800
10	10	6,310	15,310
5	20	4,050	10,040
2	50	1,615	4,560

**Table 9.6: Nueces River Basin Lakes Bulletin 17C Computed Median Inflow Statistics**

Statistics	Computed Statistics	
	Choke Canyon Reservoir	Lake Corpus Christi
	<b>15-Day</b>	<b>15-Day</b>
Mean	3.180	3.666
Standard Deviation	0.501	0.401
Station Skew	-0.347	+0.109
Historical Events	None	None
Low Outlier	18	17
Missing Flow	0	0
Systematic Events	104	77
Effective Record Length	86	60

## 9.8 RMC-RFA Data Input

### 9.8.1 Inflow Hydrographs

Several inflow hydrographs were selected to route through RMC-RFA. The particular years of which reservoir inflow hydrographs were routed are:

*Choke Canyon Reservoir and Lake Corpus Christi:*

Available hourly inflow hydrographs for November 2001, June 2002, July 2007, May 2015, and October 2018.

The selected hydrographs’ characteristics represent different hydrograph shapes (from peaky to large volume events) seen at the Nueces River Basin Lakes. However, the selection of particular hourly hydrographs was determined by using the hydrographs that influence the best pool frequency curve estimate through RMC-RFA. The selected hourly hydrographs for both lakes are shown in Figure 9.10.

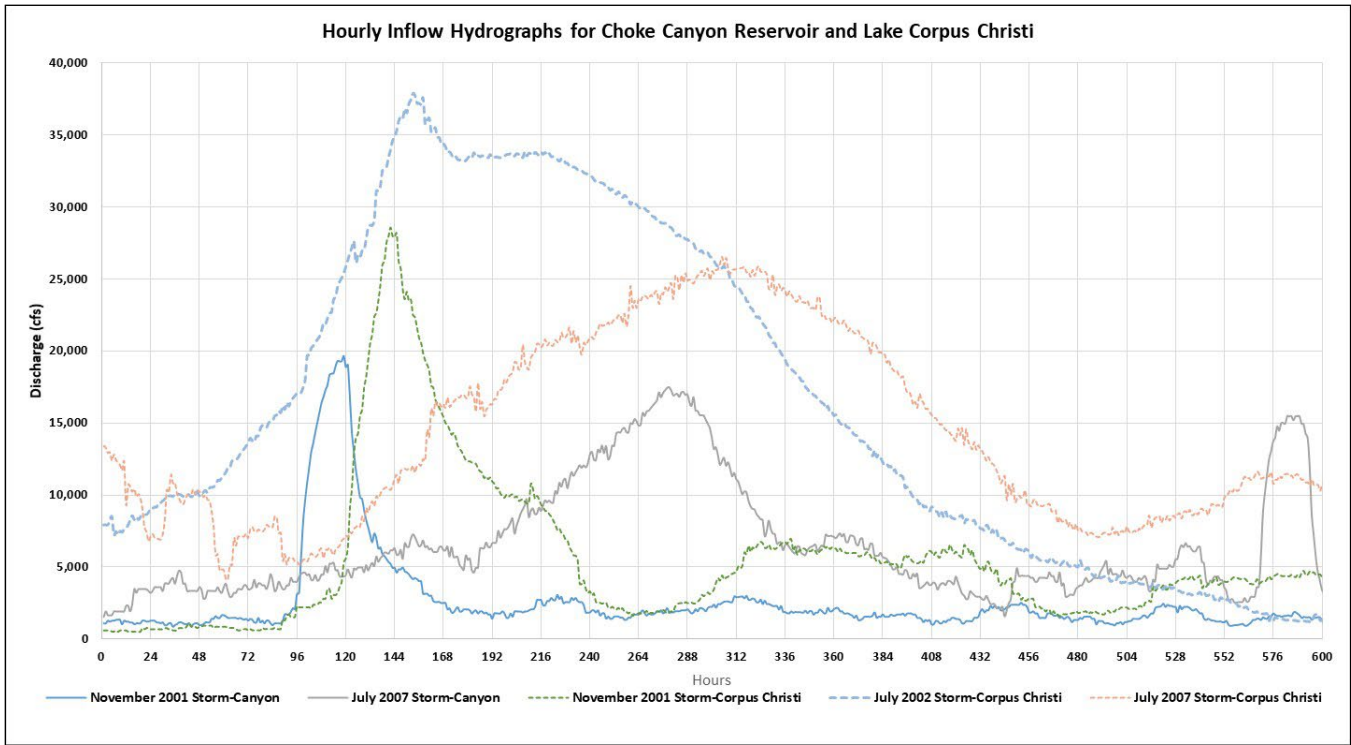


Figure 9.10: Choke Canyon and Lake Corpus Christi Inflow Hydrographs

### 9.8.2 Volume Frequency Curve Computation

The computed volume frequency statistical parameters shown in Table 9.6 were fed into the RMC-RFA program to produce the n-day duration inflows for all projects. As stated in the HEC-SSP computations section, Bulletin 17C procedures and guidelines were followed to produce the inflow volume discharge frequencies. Plots of the 15-Day inflow discharge frequency curves for the Nueces River Basin Lakes are shown in Figure 9.11 and 9.12.

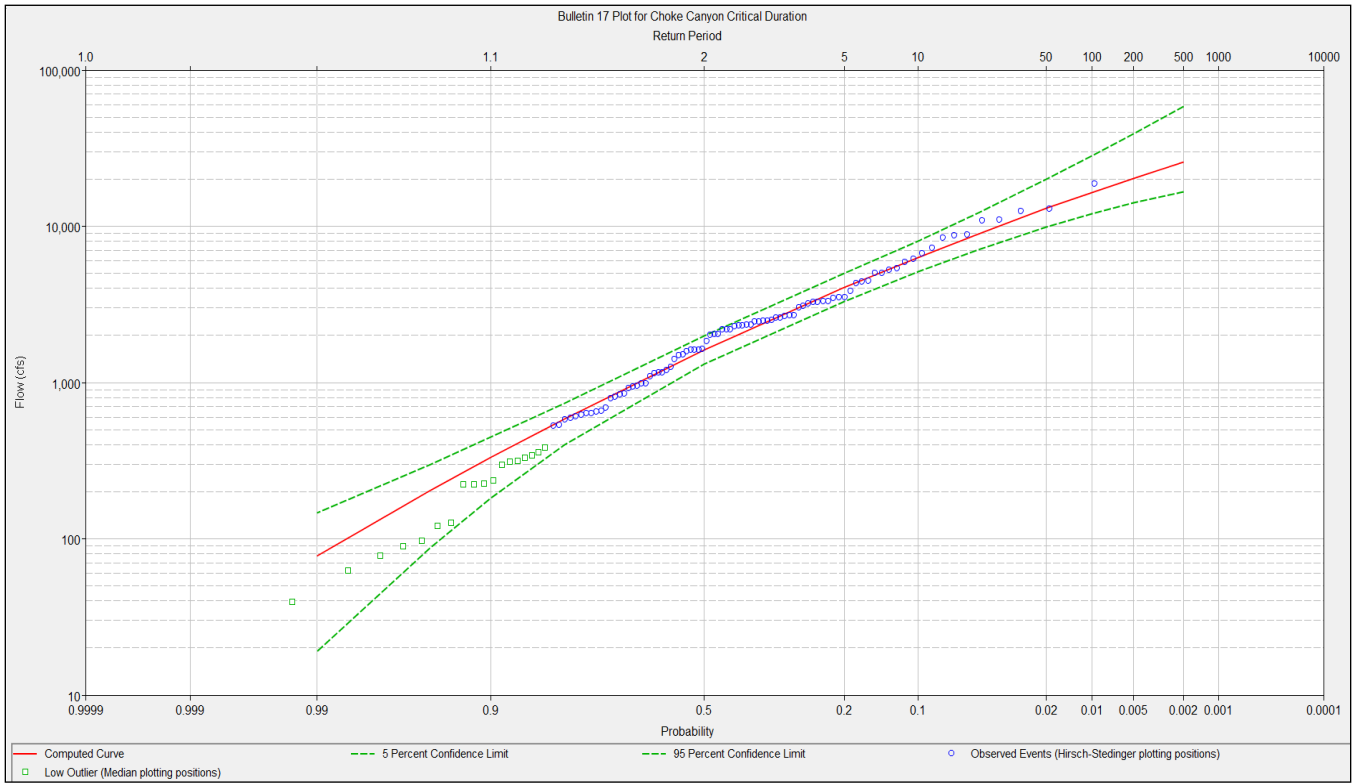


Figure 9.11: Choke Canyon Reservoir Computed 15-Day Volume Frequency Curve

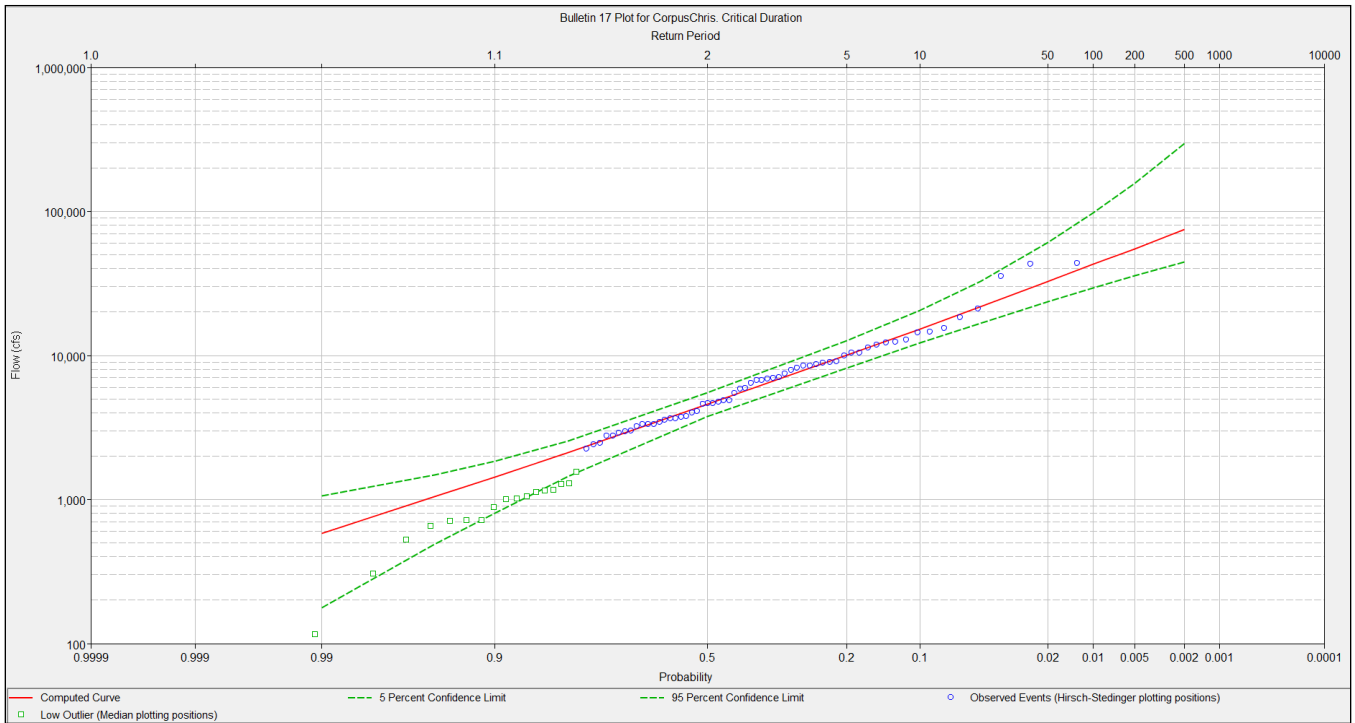


Figure 9.12: Lake Corpus Christi Computed 15-Day Volume Frequency Curve

## 9.9 RMC-RFA Analyses

### 9.9.1 Flood Seasonality

Many reservoirs have operations (pool level) that vary by season in response to the cyclical changes in meteorology and hydrology throughout the year. The inflow pattern at the Nueces River Basin Lakes have three general types of flood-producing rainfall: thunderstorms, frontal rainfall, and tropical cyclones. Generally, the highest 24-hour and monthly precipitation periods have occurred during tropical cyclones. However, there are some instances of heavy precipitation resulting from local thunderstorms. It should be noted that thunderstorms can occur at any time of the year and tropical storms can happen between June and November. Due to meteorological and hydrologic conditions, most significant floods occur during late spring, summer, and fall months.

The term *flood seasonality* is intended to describe the frequency of occurrence of rare floods on a seasonal basis, where a rare flood is defined as any event where the flow exceeds some user specified threshold for a specified flow duration. In the RMC-RFA model operation, a month of flood occurrence is first selected at random according to the relative frequency. Once the month of flood occurrence is specified, a starting pool elevation for the event can be determined from the reservoir stage-duration curve for that particular month. This approach ensures that seasonal variation in reservoir operations is a part of the peak-stage simulation.

The flood seasonality analysis is performed two (2) ways: 1) Assign critical n-day flood seasonality, threshold flow, maximum events per year, and minimum days between events. With these criteria, a total number of events can be calculated. It should be noted that the critical duration used could be different from the volume frequency curve adopted critical duration. 2) Screen out annual maximum peak reservoir pool elevations for the period of record. Peak reservoir pool elevations are the result of significant inflow events and variation of reservoir pool operations. A sensitivity analysis can be done to determine which method applies best when running the RMC-RFA; this is done to obtain the best starting pool answer corresponding to the most frequent events for each month. Projects of which the flood seasonality input parameters were applied (method 1) are listed in Table 9.7. A list of results obtained by method 1 were also included in Table 9.8. The relative frequencies shown in Table 9.8 can be presented in a plot format (Figure 9.13 and 9.14).

**Table 9.7: Flood Seasonality Parameters Input Method**

Project	Critical Duration (Days)	Threshold Flow (CFS)	Minimum Days Between Events	Maximum Number of Events
Choke Canyon Reservoir	15	2,000	4	6
Lake Corpus Christi	15	4,000	6	7

**Table 9.8: Reservoir Stage AMS Peak Analysis and Parameter Input Method Results**

Month	Relative Frequency by Stage (Method 1)			
	Choke Canyon Reservoir		Lake Corpus Christi	
	Freq.	Relative Frequency	Freq.	Relative Frequency
January	2	0.027	2	0.021
February	3	0.041	3	0.031
March	3	0.041	2	0.021
April	0	0.000	0	0.000
May	9	0.123	7	0.073
June	8	0.110	16	0.167
July	21	0.288	16	0.167
August	4	0.055	7	0.073
September	10	0.137	10	0.104
October	10	0.137	21	0.219
November	3	0.041	11	0.115
December	0	0.000	1	0.010

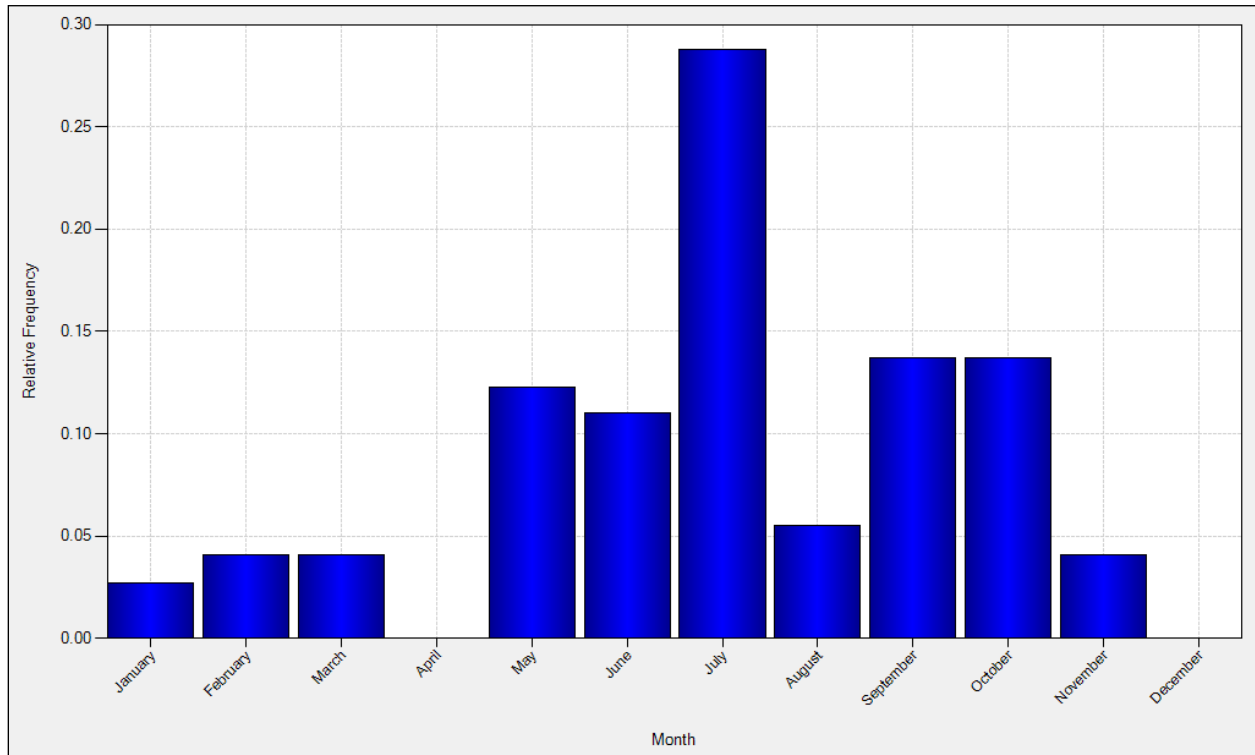


**Figure 9.13: Choke Canyon Reservoir Histogram of RMC-RFA Relative Frequency Output**

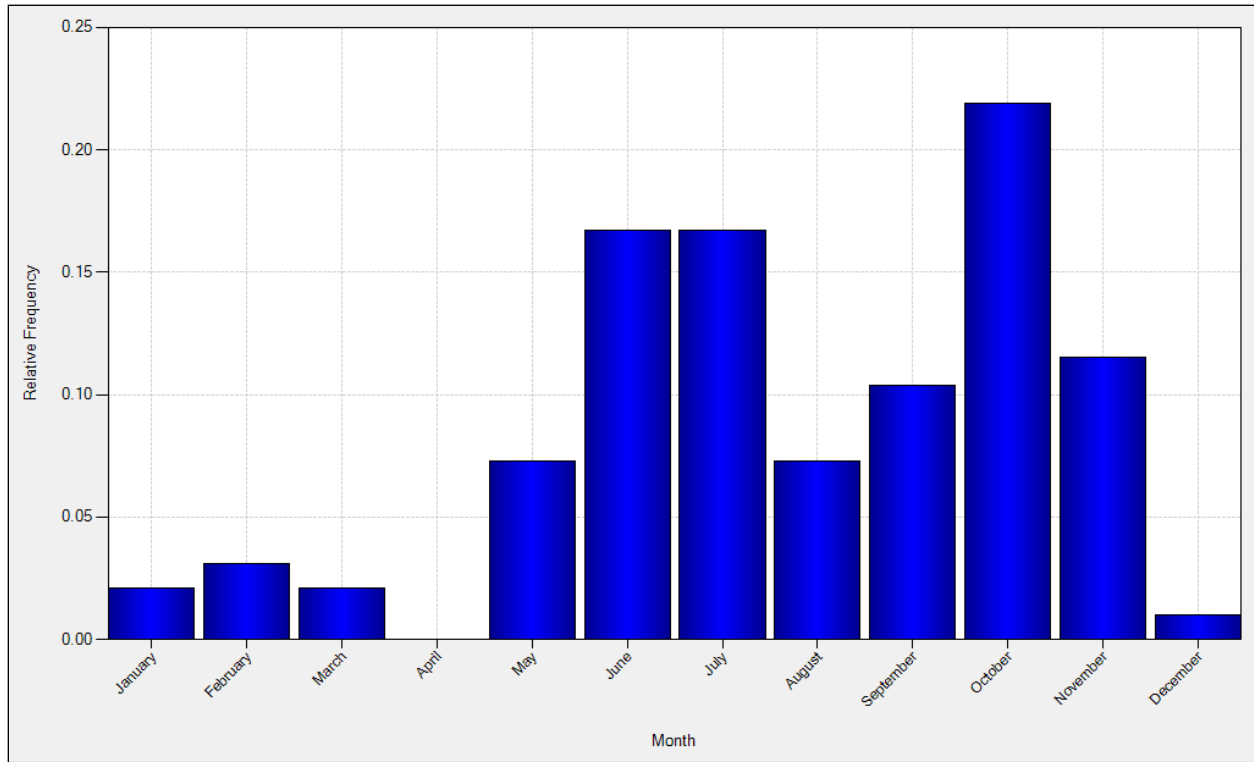


Figure 9.14: Lake Corpus Christi Histogram of RMC-RFA Relative Frequency Output

### 9.9.2 Reservoir Starting Stage

Reservoir starting pool duration curves represent the percent of time during which particular reservoir pools are exceeded. Reservoirs starting stage were estimated by analyzing pool elevations by first filtering observed daily average pools, so that they only represent typical starting pools based on a pool change threshold. Then, the filtered data set is stored by month or season. Because RMC-RFA chooses a starting pool elevation for its simulations based on historic data, the historic data must be filtered so that it is not influenced by flooding events. Starting pool elevations should form the basis for flooding events, not be the result of said events. Therefore, historic pool elevations were filtered with pool change thresholds and typical high (flood) pool durations that are reservoirs dependent (Table 9.9). This filtered stage data now forms the basis for the starting pool elevation for the RMC-RFA reservoir simulation. A sensitivity analysis was performed, and the model’s produced starting stage was not impacted by varying the pool change threshold and typical high pool values. The reservoirs final starting stage duration curves for the lakes are shown in Figure 9.15 and 9.16.

Table 9.9: Nueces River Basin Reservoir Starting Stage Duration Input

Project	Average Pool Change Threshold (Feet)	Typical high Pool duration (Days)
Choke Canyon Reservoir	14	6
Lake Corpus Christi	12	7

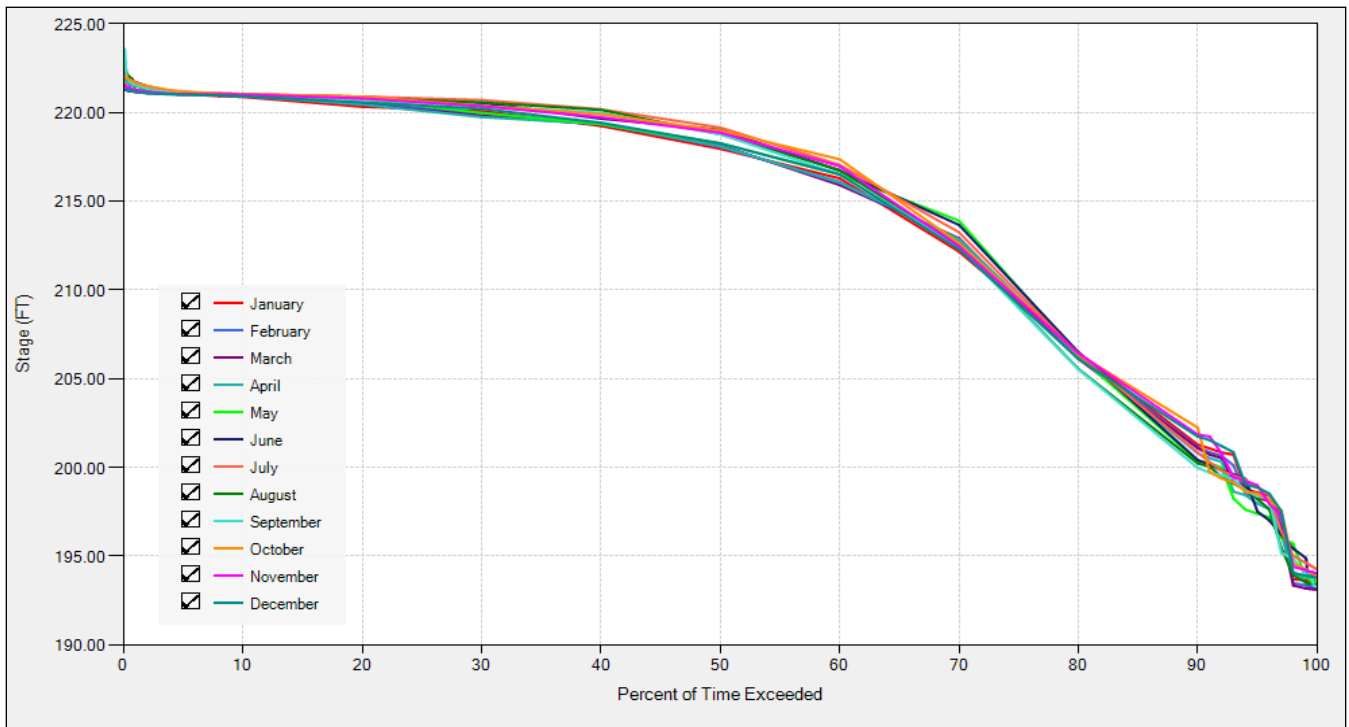


Figure 9.15: Choke Canyon Reservoir Starting Stage Durations

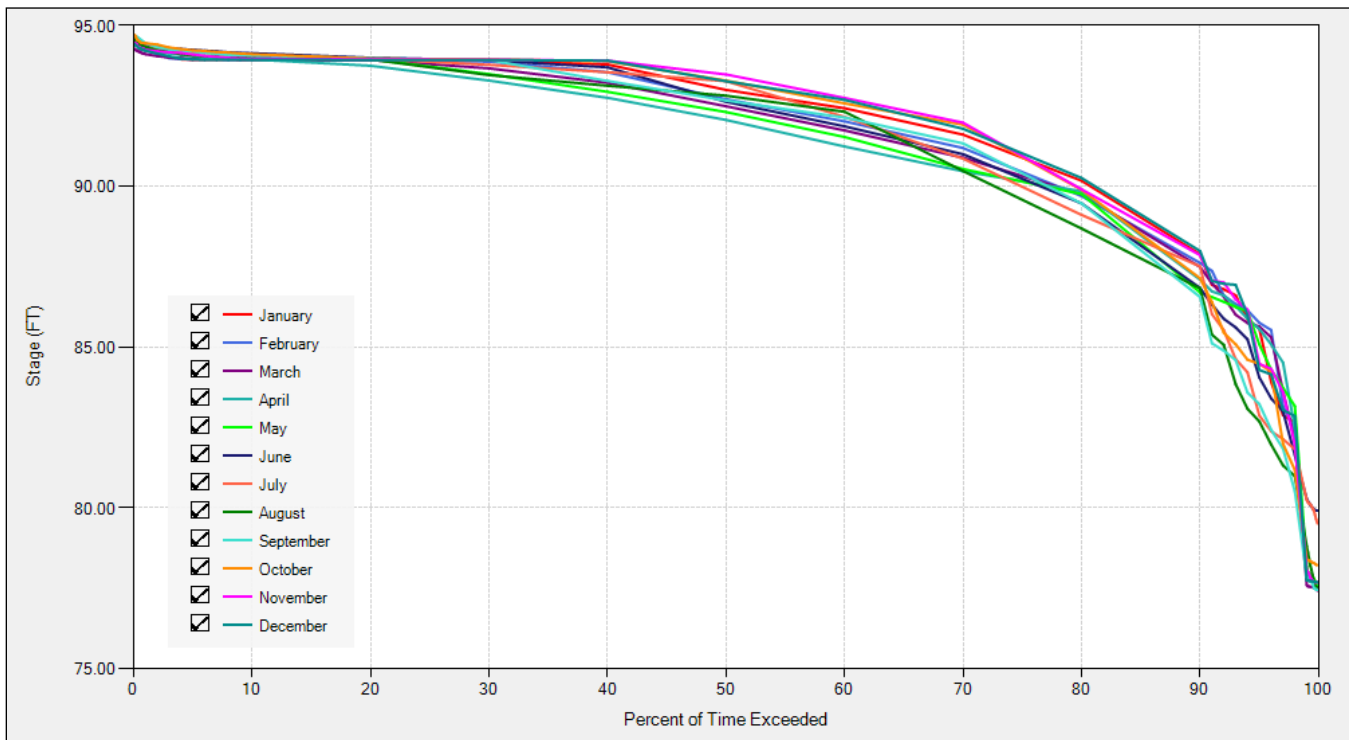


Figure 9.16: Lake Corpus Christi Starting Stage Durations

### 9.9.3 Empirical Frequency Curve

For the evaluation of hydrologic hazards of each project, an extreme-value series of annual maximum stage was generated from the n-year systematic (RiverWare + Observed) period of record. The RiverWare simulated pool elevation peaks were used either prior to dam impoundment dates when the observed pool elevation peaks were not available, or if occurred due to irregular operations (e.g., emergency drawdown), for an intent of extending pool record. Each POR annual maximum series was extracted, the AMS was ranked, and it was plotted on log probability paper using the Weibull plotting position formula shown in Section 9.5.1. Figure 9.17 and 9.18 are Lakes Choke Canyon and Corpus Christi empirical pool frequency relationship, when applying the Weibull plotting positions. The systematic frequency peaks for the projects were plotted against the RMC-RFA expected pool frequency data points, see Section 10.0 plots. The plotting position of the highest and lowest points are the most uncertain due to having insufficient record lengths necessary to inform accurate plotting positions at the extremes. For each project, a duration frequency plot comparison between annual maximum pool elevations for: Observed, simulated (RiverWare), and combined (RiverWare + Observed), were made using the Weibull plotting position formula. Figure 9.19 and 9.20 are illustrations of the distribution comparison for the lakes. In general, longer observed pool record tends to show good distribution and match well when plotted against the extended pool record. Shorter observed pool record increases uncertainty and shifts the distribution from being more representative for rarer frequencies. An example of pool with short record (35 years of observed pool data) is Choke Canyon Reservoir (Figure 9.19). Notice the distribution shifts to the right side and coarser data point plotting position. Selections of pool peaks are based on normal operations to ensure homogeneity. For Lake Corpus Christi, the observed pool for the period of WY2007 through WY2019 will be selected over simulated to perform statistical analysis, but simulated pool peaks will be analyzed for periods prior to WY2007. This approach ensures that the analyzed data is homogenous and valid for statistical analysis. This is also because of changes to reservoir operations were due to structural instability.

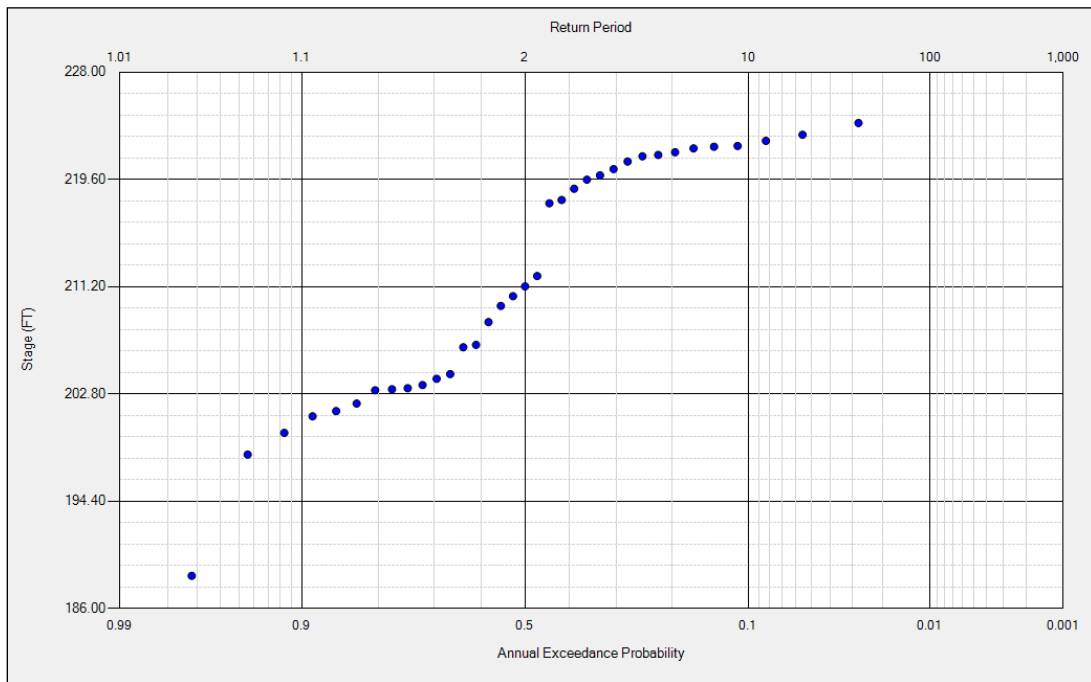


Figure 9.17: Stage Duration Frequency for Choke Canyon Reservoir

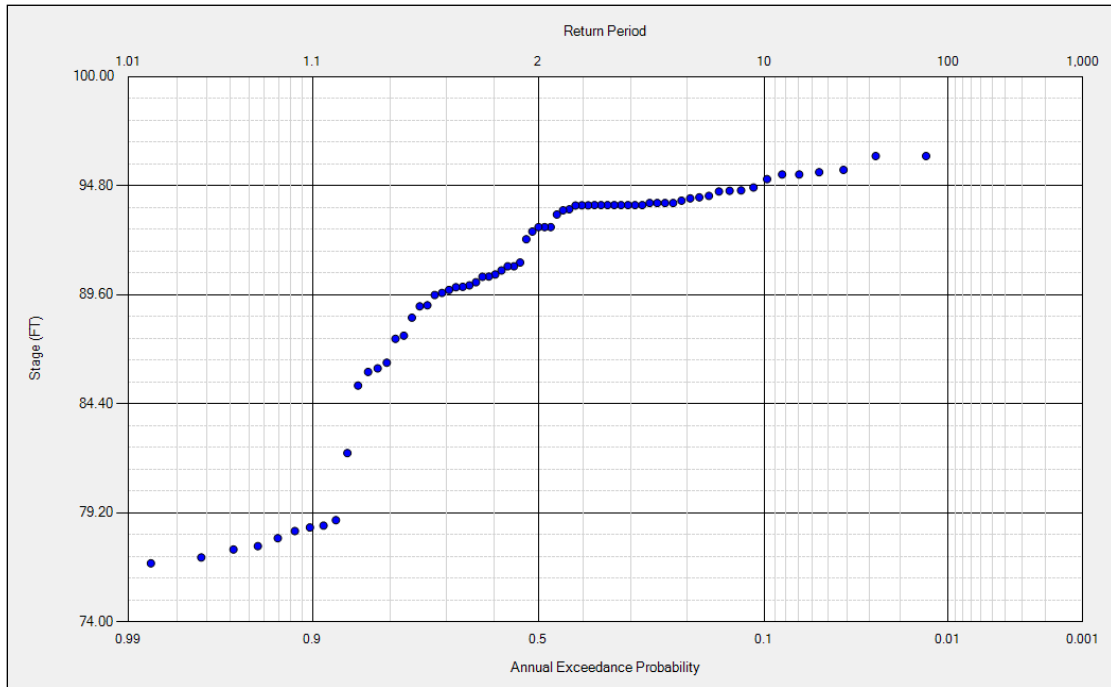


Figure 9.18: Stage Duration Frequency for Lake Corpus Christi

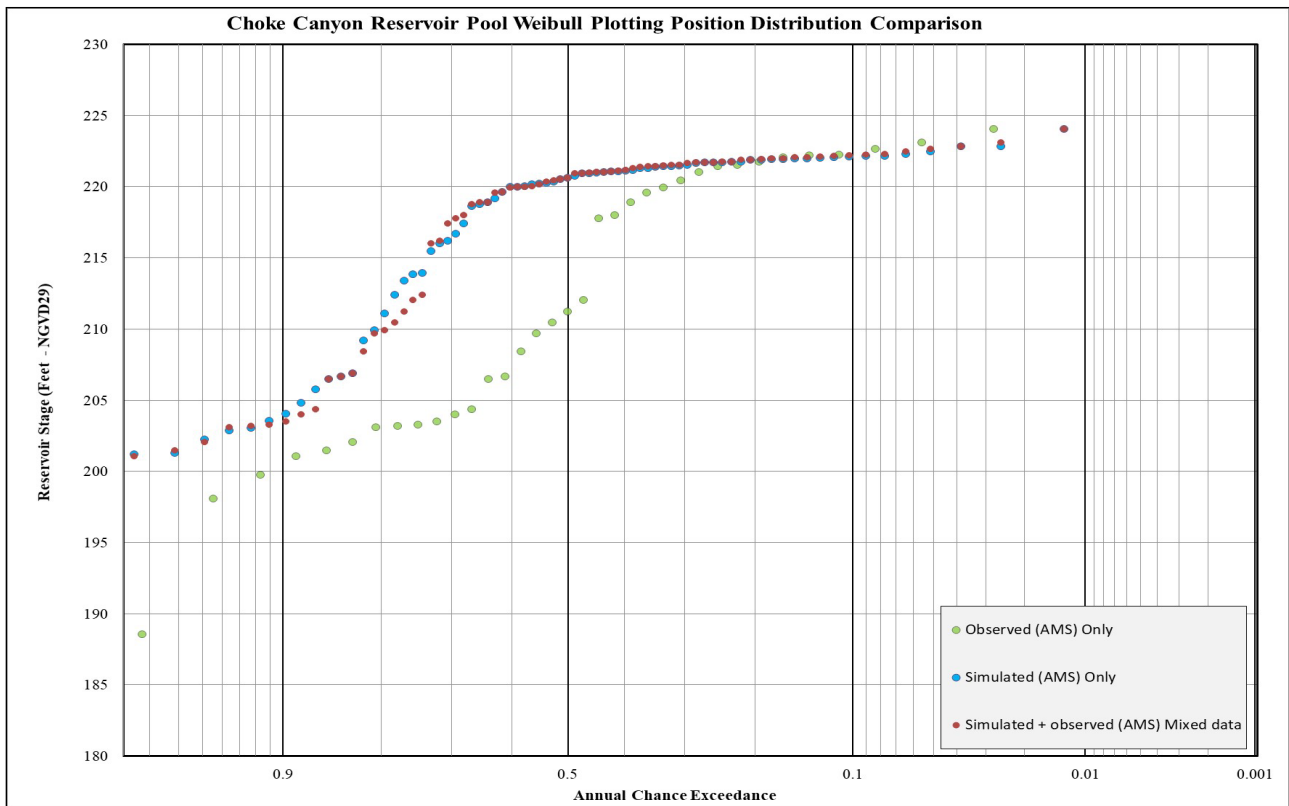


Figure 9.19: Illustration of Choke Canyon Reservoir AMS Pool Weibull Plotting Position Distributions

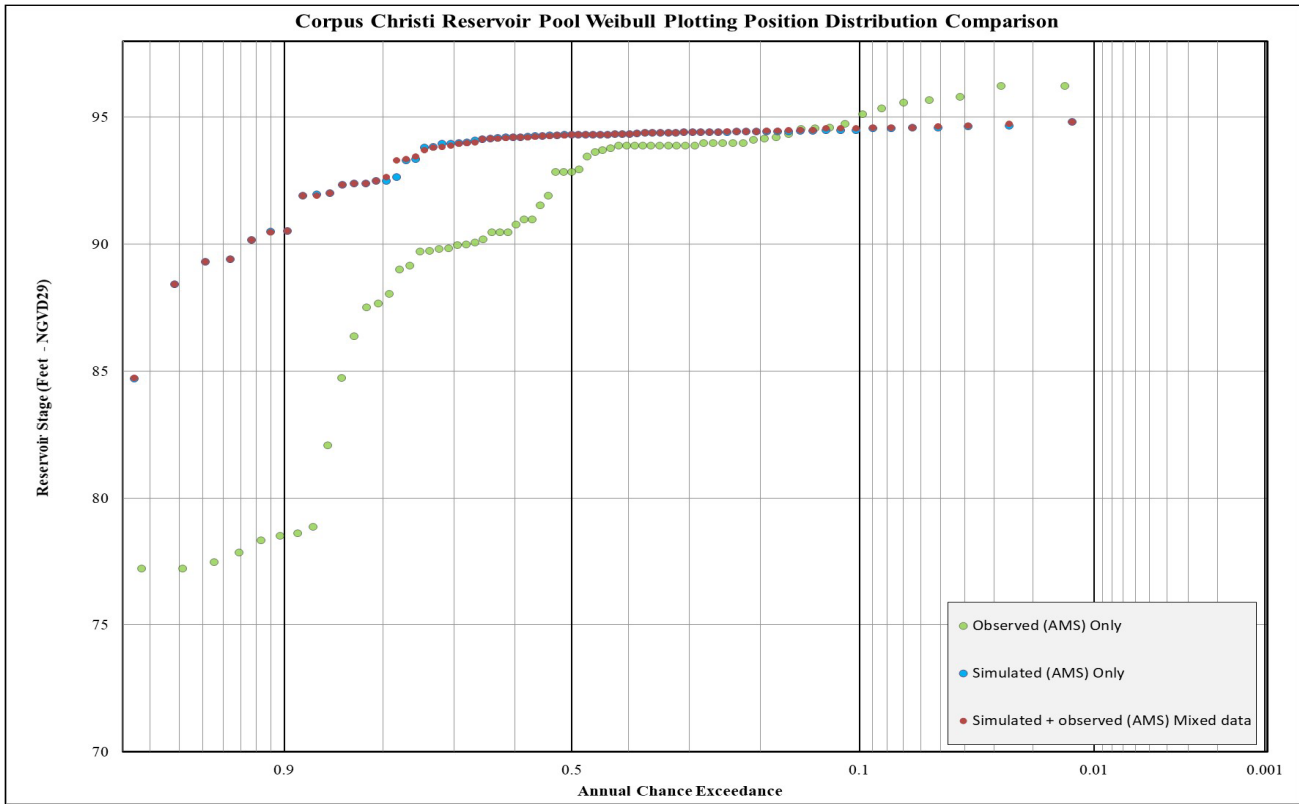


Figure 9.20: Illustration of Lake Corpus Christi AMS Pool Weibull Plotting Position Distributions

### 9.9.4 Reservoir Model

The reservoir details such as top of dam and spillway elevations were obtained from the water data for Texas digital library. Volumetric surveys of both reservoirs were accomplished to update storage information. This was done using current GPS, acoustical depth sounder, and GIS technology. Data was then gathered and processed to generate the stage-storage curves for the reservoirs. The information is needed in order for the simulation to run. The volumetric and sedimentation survey (mostly up to conservation) of the lakes were completed in 2013 for Choke Canyon Reservoir and 2016 for Lake Corpus Christi. The Texas Water Development Board digital library was used to retrieve capacity data for elevation below 220ft-NGVD for Choke Canyon Reservoir, and elevation below 94 ft-NGVD for Lake Corpus Christi. Elevation above 220ft-NGVD for Choke Canyon used the original area (capacity) data of 1992. For Lake Corpus Christi, extension above 94 ft-NGVD was calculated by the SWD studies' group using the area-average method for data obtained from Frees and Nichols. The Nueces River Basin projects' releases are stage dependent. Therefore, a stage-storage-discharge (release) function can be estimated. The Storage-Elevation and Discharge (Release)-Elevation curves for the projects are shown in Figure 9.21 and 9.22. More details about reservoir features are listed in Table 9.10.

**Table 9.10: Nueces River Basin Lakes Features**

Project	Choke Canyon Reservoir	Lake Corpus Christi
<b>Pertinent Feature</b>	Elevation (NGVD-Feet)	
<b>Top of Dam</b>	241.0	106.0
<b>Top of Flood (Control Pool)</b>	> 220.5*	94.0
<b>Spillway Crest</b>	199.5	94.0 South side 94.5 North side
<b>Top of Conservation Pool</b>	220.5	< 94.0

\*This is the surcharge pool for Choke Canyon Reservoir since the lake has no flood pool

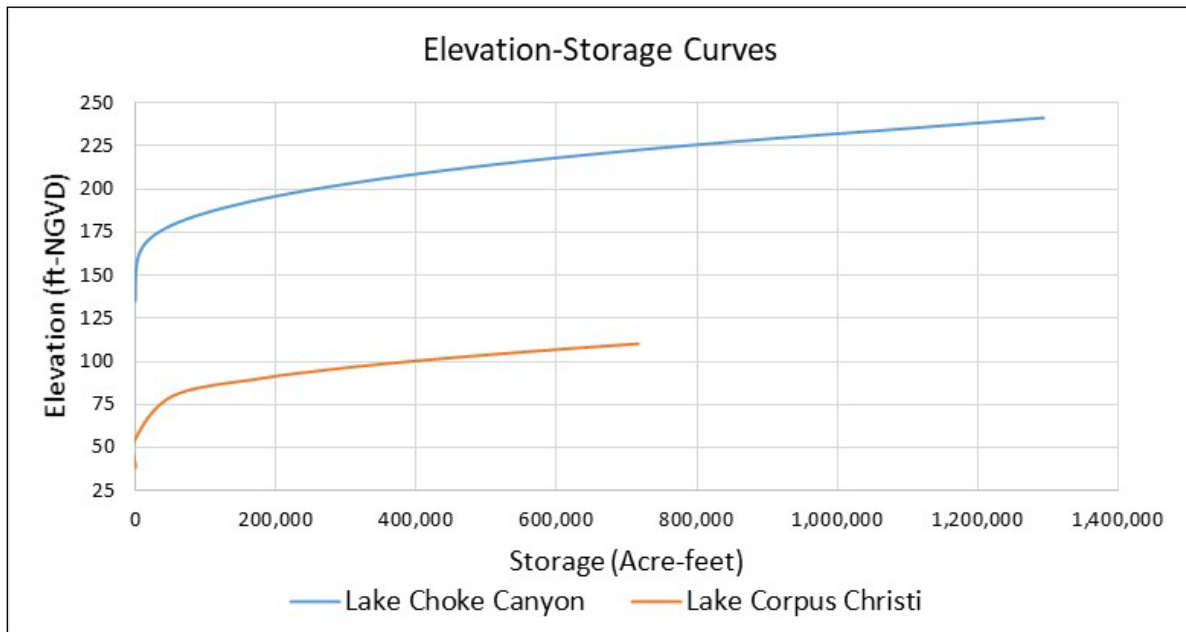


**Figure 9.21: Nueces River Basin Lakes Storage-Elevation Curves**

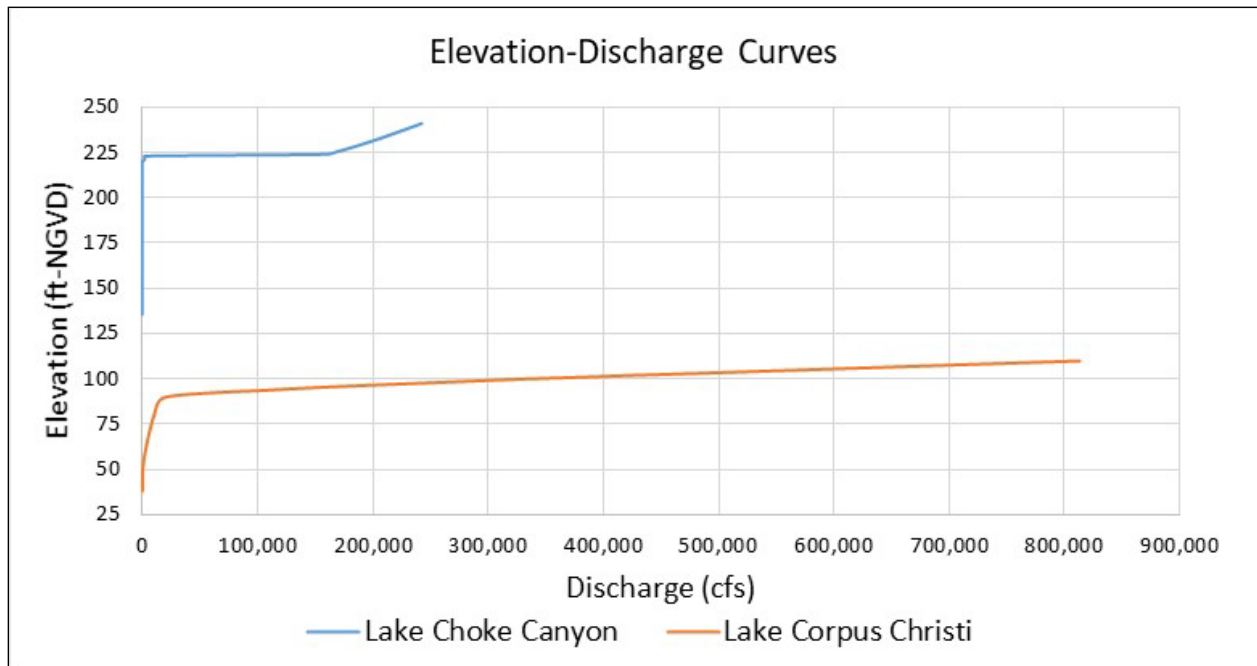


Figure 9.22: Nueces River Basin Lakes Outflow Discharge-Elevation Curves

The importance of using accurate Storage-Discharge-Elevation (Stage) curves is that it results in more accurate estimates of high extreme peak values associated with high degree of uncertainty (*i.e.*, 1% ACE and beyond). Such high peaks are normally observed near or above the spillway crest. Validations of the adopted discharge-elevation curves used in RMC-RFA for the Nueces River Basin Lakes, are shown in Figure 9.23 and 9.24. The plots show that model releases are within range of operations. The adopted elevation-release curve for Choke Canyon Reservoir maintained no release up to elevation 220.0ft-NGVD. Release was then increased by 500cfs at pool elevation 221.ft-NGVD, to 4,000cfs (222.ft-NGVD), 20,000cfs (223.0ft-NGVD), and followed the spillway release rating curve for pool elevations above 224ft-NGVD. To achieve best estimate frequency curve for Lake Corpus Christi, Release is interpolated from the spillway rating curve between pool elevations 94ft-NGVD and 95-ft-NGVD; above elevation 95ft-NGVD, follow the spillway release rating curve, where releases were through the north and south side spillways.

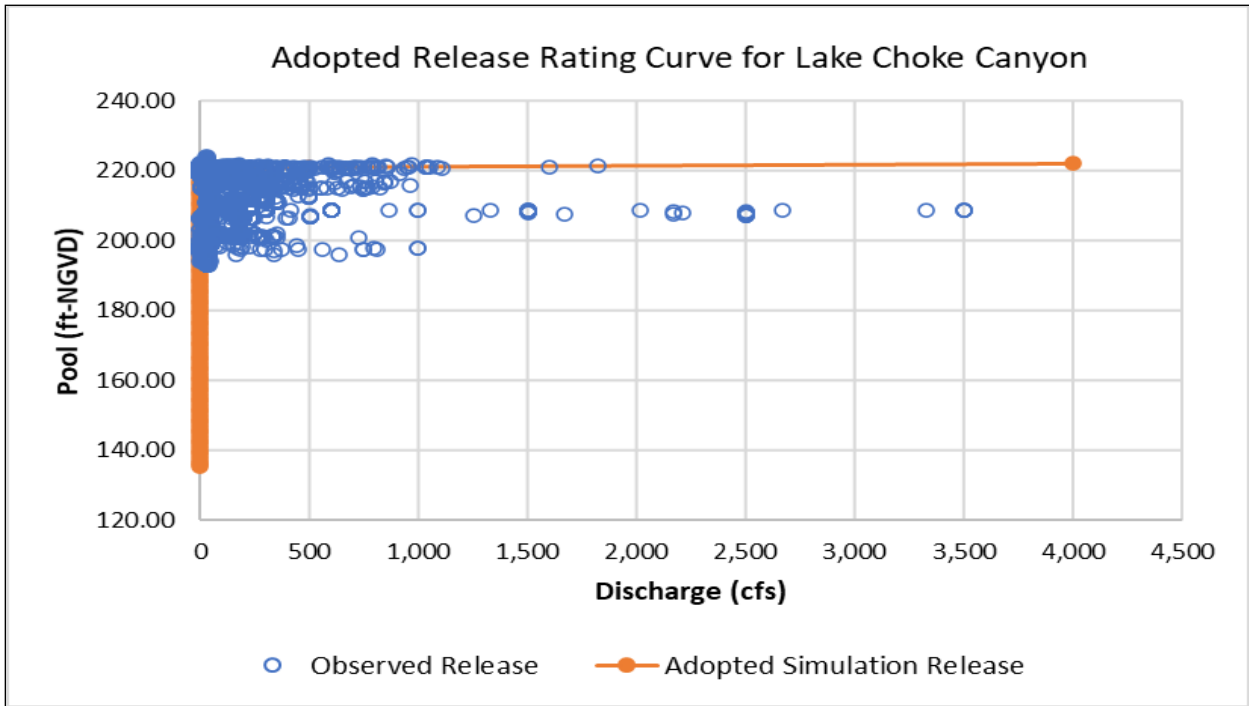


Figure 9.23: Validation of the Adopted Elevation-Discharge (Release) Curve for Choke Canyon Reservoir

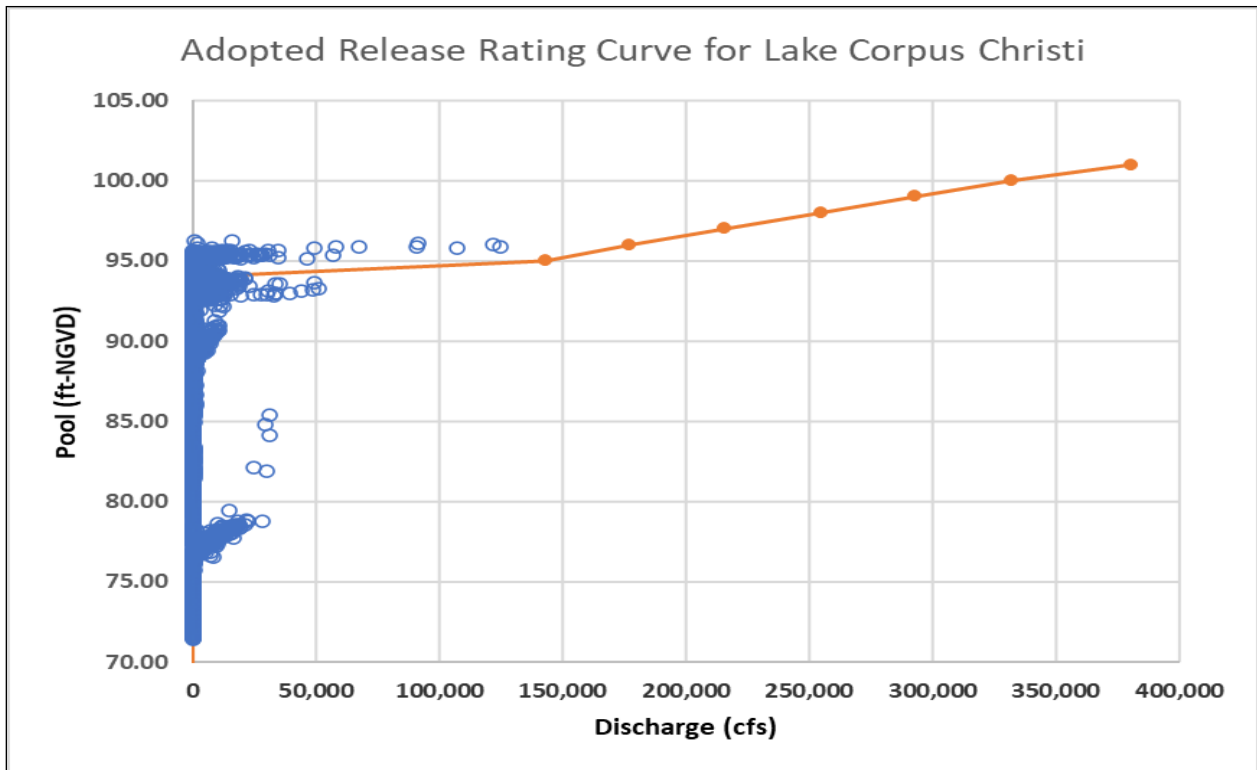


Figure 9.24: Validation of the Adopted Elevation-Discharge (Release) Curve for Lake Corpus Christi

## 9.10 Results

The RMC-RFA program was used to simulate rainfall-runoff floods using the inflow-frequency curve and the adopted flood seasonality. The specified hourly inflow hydrographs in Section 9.8.1 and those found in the RMC-RFA program, are weighted equally to account for each unique shape (*i.e.*, volume and peak) and to have the same probability. Appropriate routing time windows were specified to calculate the full size of floods routed through the reservoir on hourly basis. The RMC-RFA model was simulated using the expected pool frequency curve only model option. This runs 10,000 realizations with 1,000,000 events per realization. This means RMC-RFA simulates a total of 10 billion events (10,000 x 1,000,000) to produce its best estimate of the expected curve. The following sections list detailed results about each project's new simulated expected stage-frequency curve.

To assess regulation, the total release for each project corresponding to each pool frequency, was developed by analyzing each project's observed and simulated releases, where annual maximum peaks were plotted using the Weibull position distribution and applying a graphical curve, which would approximately fit through the data points. Sets of the Weibull plotting position distribution figures for the projects are shown in sections 9.10.1 and 9.10.2.

The regulated (simulated/observed) releases were used to best estimate release frequencies below the spillway crest. High flood events that may exceed spillway crest elevation, would follow the discharge-elevation curve illustrated in Figure 9.22.

Several iterations were made, using the RMC-RFA program to obtain the best simulated pool frequency curves. The best fit is defined as the curve that fits well through the more frequent events (*i.e.*, 10% ACE (10-year) through 2% ACE (50-year)) through the empirical stage points. The best estimate curve is a result of applying release schedules that would not violate the most upper and lower bounds of discharge peaks. As a result, and with degrees of uncertainty, the curves are believed to have captured good estimates beyond the 1% ACE (100-year) events. Adopted pool frequency curves are shown below.

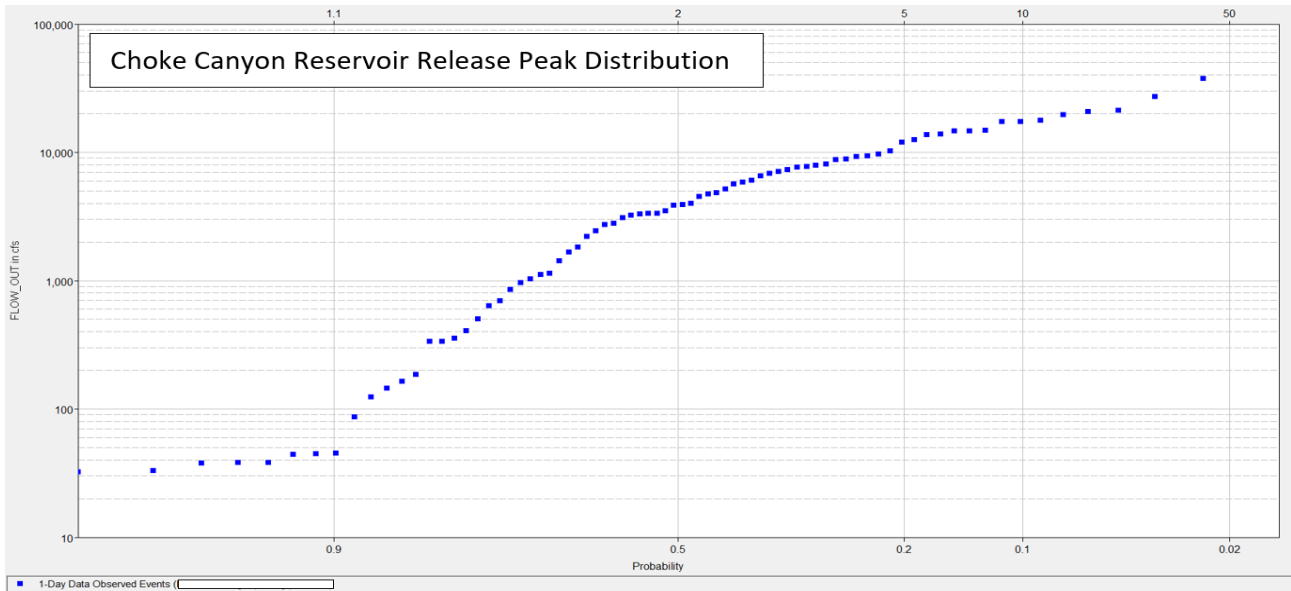
### 9.10.1 Choke Canyon Reservoir

Table 9.11: 2021 Choke Canyon Reservoir Computed Pool Frequency Estimate

Choke Canyon Reservoir		RMC-RFA Best Estimate
N-Years	ACE %	Feet-NGVD
2	50	220.57
5	20	221.89
10	10	222.46
25	4	223.02
50	2	223.34
100	1	223.62
250	0.4	224.01
500	0.2	224.39

**Table 9.12: 2021 Choke Canyon Reservoir Computed Frequency Discharge Release**

Choke Canyon Reservoir		RMC-RFA Best Estimate (Expected)			
N-Years	ACE %	Elevation-NGVD	Spillway Release (CFS)	Gate Release (CFS)	Total Release (CFS)
2	50	220.57	0	2,900	2,900
5	20	221.89	0	12,050	12,050
10	10	222.46	0	22,000	22,000
25	4	223.02	0	37,950	37,950
50	2	223.34	50,500	0	50,500
100	1	223.62	69,660	0	69,660
250	0.4	224.01	102,774	0	102,774
500	0.2	224.39	123,160	0	123,160



**Figure 9.25: Choke Canyon Reservoir Simulated Total Release Following Weibull Plotting Distribution**

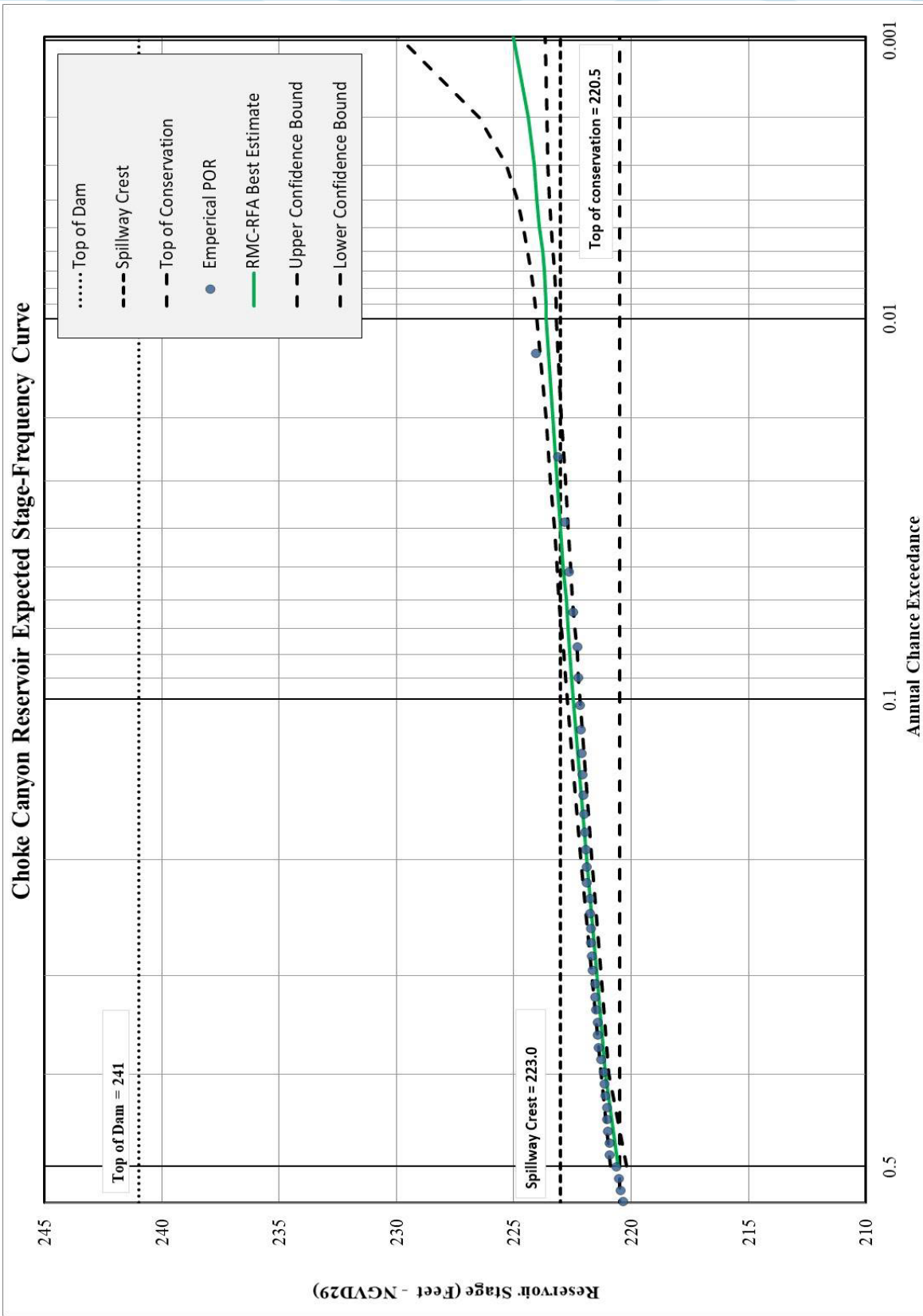


Figure 9.26: Choke Canyon Reservoir Current Condition (2021) Stage-Frequency Curve for Rainfall Simulations

## 9.10.2 Lake Corpus Christi

Table 9.13: 2021 Lake Corpus Christi Computed Pool Frequency Estimate

Lake Corpus Christi		RMC-RFA Best Estimate
N-Years	ACE %	Feet-NGVD
2	50	94.06
5	20	94.24
10	10	94.39
25	4	94.48
50	2	94.67
100	1	94.85
250	0.4	95.50
500	0.2	96.83

Table 9.14: 2021 Lake Corpus Christi Computed Frequency Discharge Release

Lake Corpus Christi		RMC-RFA Best Estimate (Expected)			
N-Years	ACE %	Elevation-NGVD	Spillway Release (CFS)	Gate Release (CFS)	Total Release (CFS)
2	50	94.06	6,200	0	6,200
5	20	94.24	17,000	0	17,000
10	10	94.39	28,600	0	28,600
25	4	94.48	48,550	0	48,550
50	2	94.67	67,800	0	67,800
100	1	94.85	91,000	0	91,000
250	0.4	95.50	128,825	0	128,825
500	0.2	96.83	163,200	0	163,200

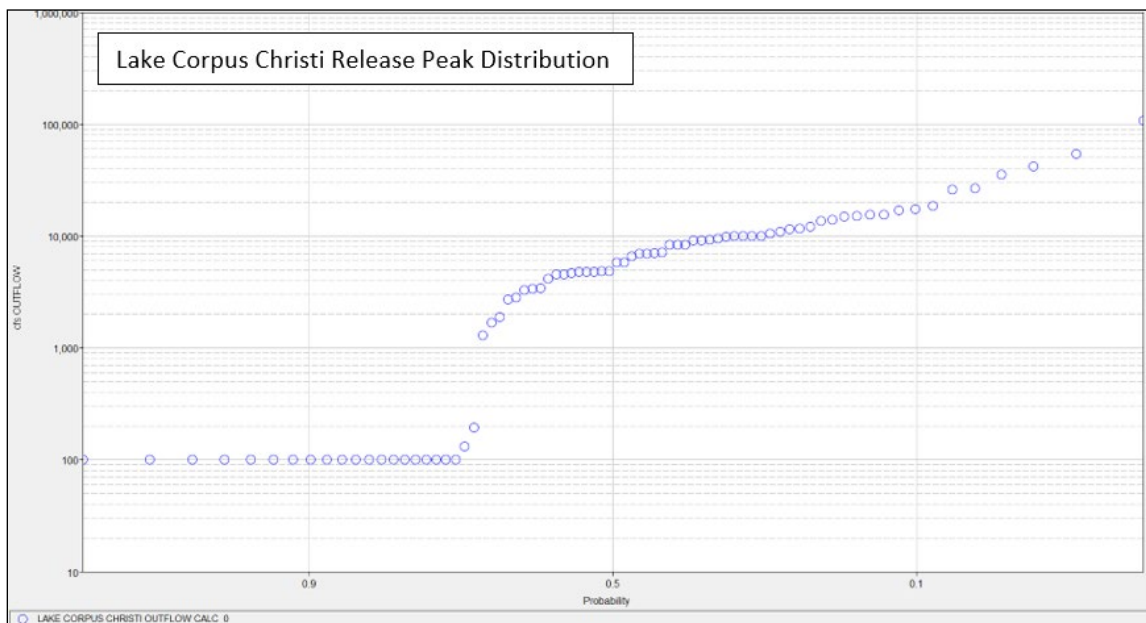


Figure 9.27: Lake Corpus Christi Simulated Release Following Weibull Plotting Distribution

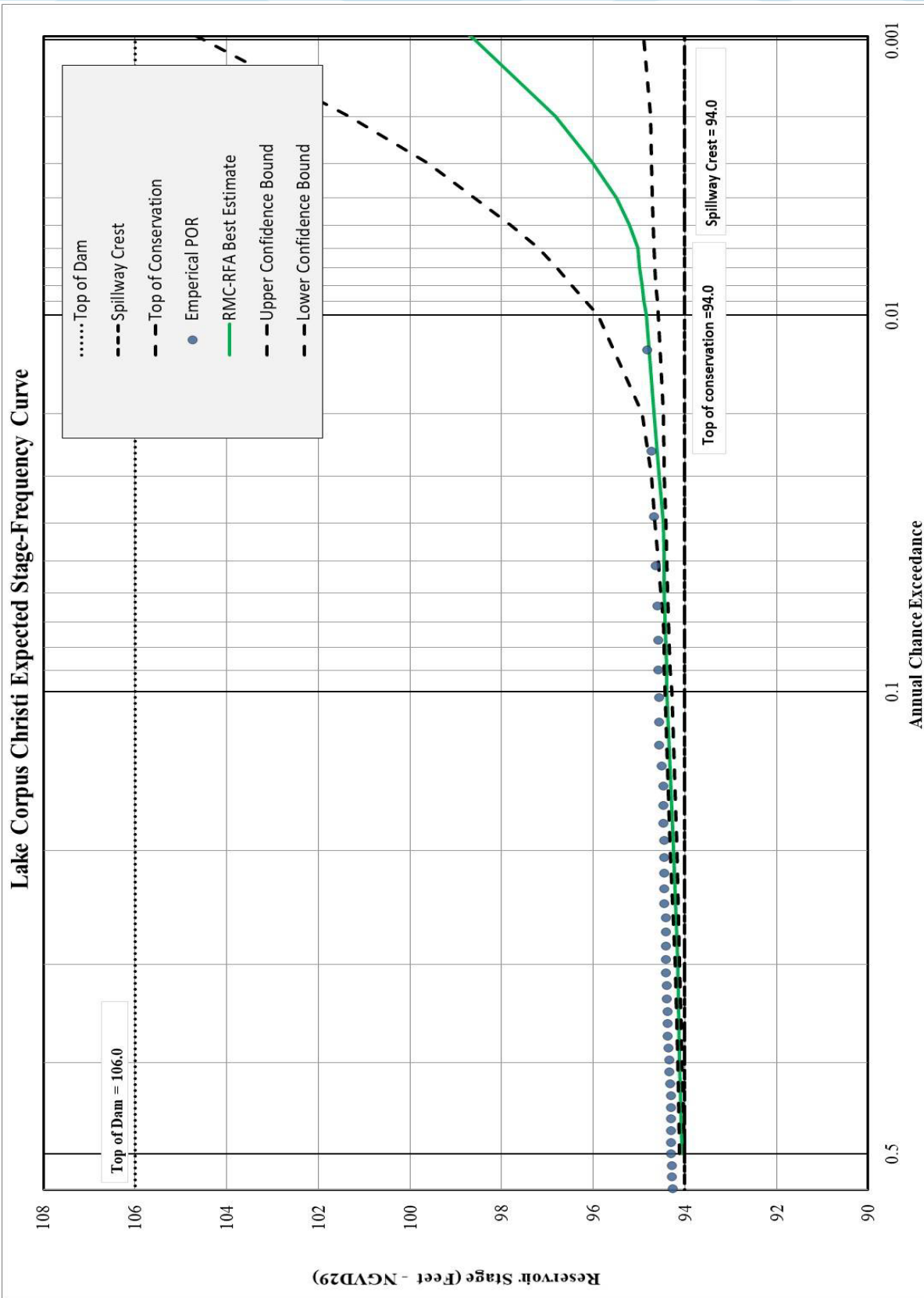


Figure 9.28: Lake Corpus Christi Current Condition (2021) Stage-Frequency Curve for Rainfall Simulations

## 9.11 Results Validation

The pool frequency results displayed in section 9.10 went through rigorous analyses before being finalized. Appendix E describes some sensitivity analyses performed on both lakes to validate selections of the best estimate pool frequency results.

# 10 2-Dimensional HEC-RAS Analysis of the Turkey Creek Watershed

## 10.1 Introduction

Turkey Creek is a rural watershed in South Texas that is located within the Nueces River basin upstream of the USGS gage near Asherton, TX (0819300), as shown in Figure 10.1. The Turkey Creek watershed encompasses approximately 2,000 square miles of drainage area, and it is entirely ungaged. With no observed data available to help calibrate the HEC-HMS model, the rainfall runoff response of this portion of the Nueces basin is largely unknown. In addition, no existing hydraulic models were available within the Turkey Creek watershed to develop Modified Puls routing data for HEC-HMS. The lack of observed data and hydraulic modeling data within the Turkey Creek watershed made this portion of the study area a prime candidate for a 2 dimensional (2D) analysis. This appendix will describe the development of a new 2D HEC-RAS model of the Turkey Creek watershed upstream of Highway 83. The 2D HEC-RAS model was used to estimate Modified Puls routing parameters and to calibrate the Snyder's subbasin transform parameters.

Unit hydrograph theory is a commonly utilized method among the hydrologic community that transforms excess precipitation into runoff hydrographs. The Nueces InFRM HEC-HMS hydrology model (covered in detail in Appendix B) uses the Snyder's unit hydrograph method to transform excess rainfall into direct runoff hydrographs. For the Turkey Creek portion of the Nueces River basin, no observed data was available to calibrate the transform parameters. Literature indicates that the lag time (and consequently the time of concentration) of a unit hydrograph generally tend to decrease as storm intensity increases (Snyder, 1938 and Minshall, 1960). Due to the availability of physically based routing routines/methods, HEC-RAS 2D has commonly been utilized by the USACE dam safety community to develop variable unit hydrograph parameters for different rainfall intensities (USACE RMC, 2017).

A primary purpose of this analysis is to utilize a HEC-RAS 2D model to calibrate the unit hydrograph parameters used in the HEC-HMS model for the purpose of improving flood frequency estimates within the Nueces River / Turkey Creek watershed. The 2D diffusion wave transform method in HEC-RAS, which is based on the momentum and continuity equations and is not tied to the assumption of linearity, was used to inform the Snyder's unit hydrograph transform parameters in HEC-HMS particularly for rare, intense rainfall events that have not yet been observed in this portion of the basin. A secondary purpose of the 2D HEC-RAS analysis was to develop storage volumes for a range of discharges that could be applied in the HEC-HMS routing reaches as Modified Puls storage-discharge curves.

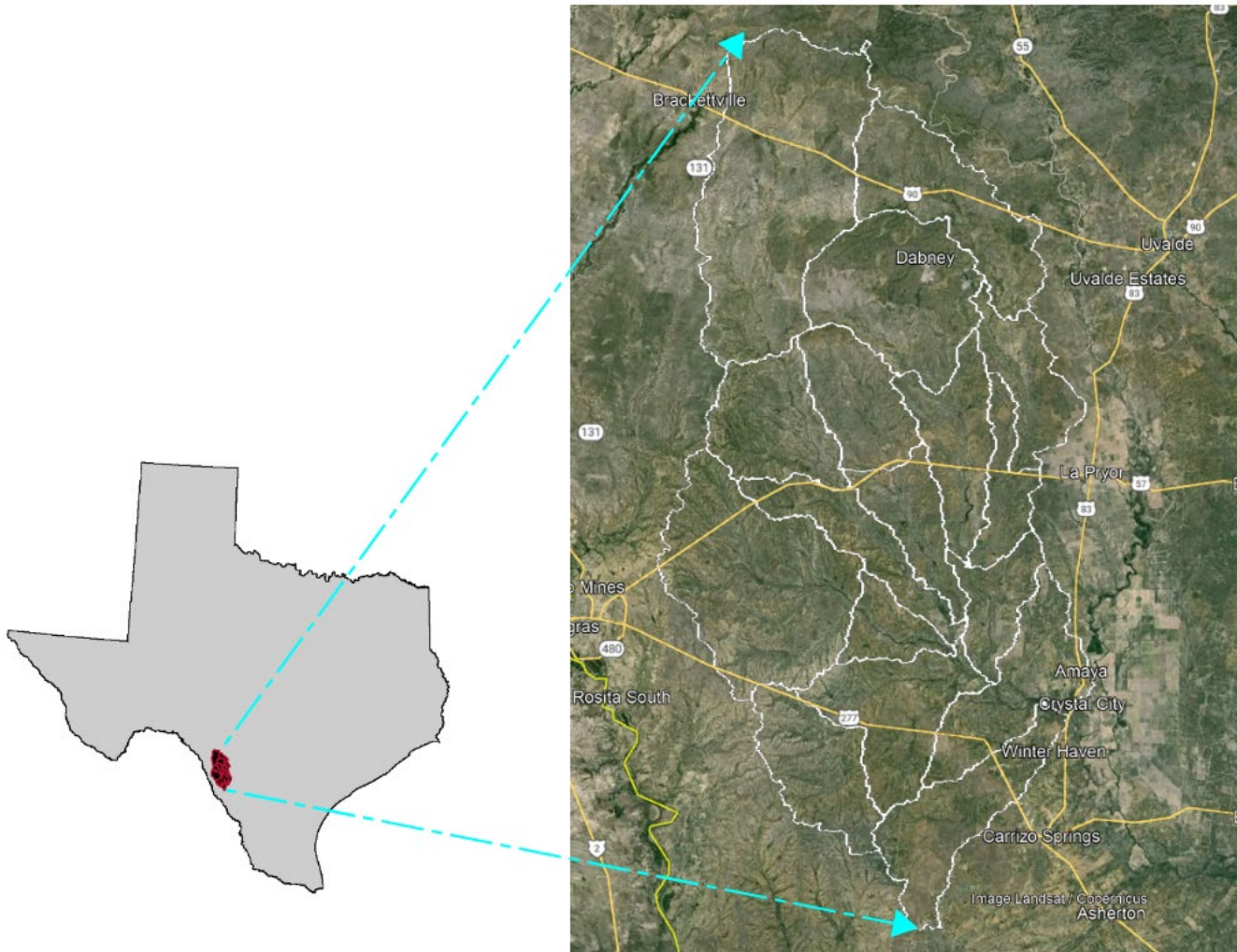


Figure 10.1: Turkey Creek Watershed and 2D Modeling Domain

## 10.2 HEC-HMS Model Development and Calibration

The Nueces InFRM HEC-HMS model consists of subbasins that utilize the Snyder's transform method and associated parameters (lag time and peaking coefficient) to model how excess precipitation transforms into a direct runoff hydrograph at each subbasin outlet. HEC-HMS calibration was performed for the downstream gage at the Nueces River near Asherton, but for those available calibration events, very little runoff originated from the Turkey Creek basin. See Figure 10.2 for the layout of the HEC-HMS subbasins relative to the Asherton gage.

The relevant HEC-HMS subbasins along with their preliminary lag times and peaking coefficients are shown in Table 10.1. Prior to the 2D analysis, the preliminary lag times and peaking coefficients in Table 10.1 were selected for the 2 through 500-year recurrence intervals based on the preliminary HEC-HMS calibration results. More information on the uniform HEC-HMS model development and calibration can be found in Appendix B.

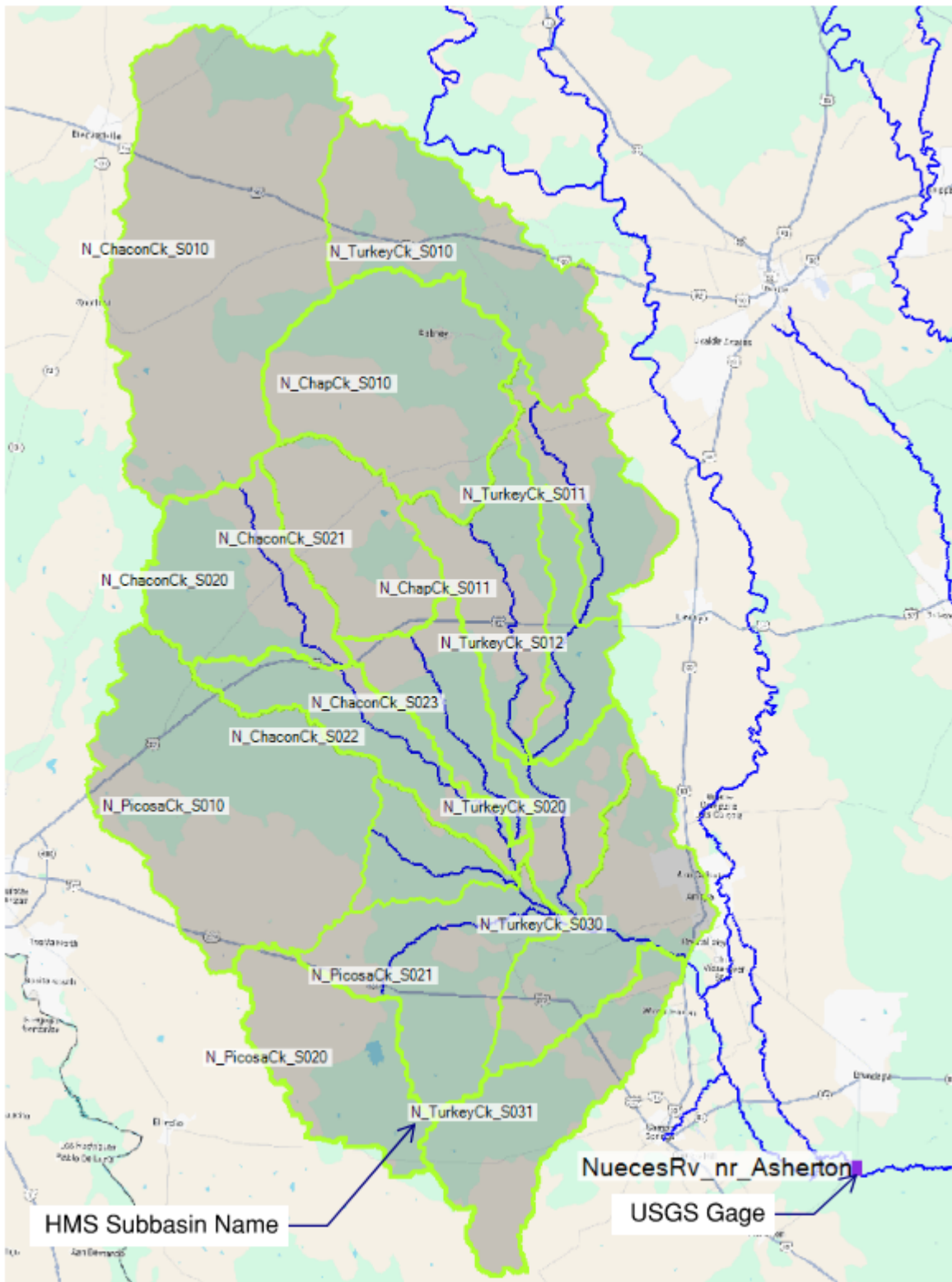


Figure 10.2: Nueces InFRM HEC-HMS Model – Relevant Subbasins for 2D Analysis

**Table 10.1: Turkey Creek Preliminary HEC-HMS Subbasin Parameters**

Subbasin Name	Drainage Area (sqmi)	Lag Time (hr)	Peaking Coefficient
N_ChaconCk_S010	254.90	17.39	0.7
N_ChaconCk_S020	82.65	12.09	0.7
N_ChaconCk_S021	69.98	10.83	0.7
N_ChaconCk_S023	51.26	14.07	0.7
N_ChaconCk_S022	61.55	16.48	0.7
N_PicosaCk_S010	190.28	17.5	0.7
N_PicosaCk_S011	34.14	9.21	0.7
N_PicosaCk_S020	78.18	7.7	0.7
N_TurkeyCk_S010	111.93	13.54	0.7
N_TurkeyCk_S011	58.59	11.57	0.7
N_TurkeyCk_S012	39.53	11.97	0.7
N_ChapCk_S010	132.77	11.9	0.7
N_ChapCk_S011	71.77	14.69	0.7
N_TurkeyCk_S020	44.51	10.41	0.7
N_PicosaCk_S021	94.57	13.57	0.7
N_TurkeyCk_S030	89.43	9.92	0.7
N_TurkeyCk_S031	88.95	16.11	0.7

## 10.3 2D HEC-RAS Model Development and Calibration

At the time of this analysis, the official HEC-RAS release version was 6.4.1. In this version, precipitation can be applied as a boundary condition to the 2D computational mesh. The excess precipitation applied to the HEC-RAS model was taken directly from the HEC-HMS model. The primary purpose of building the 2D HEC-RAS model was to use the 2D diffusion wave method to transform excess precipitation into runoff, everything else being the same as the HEC-HMS model for a direct comparison.

### 10.3.1 Terrain and 2D Computational Mesh

For the terrain, the seamless statewide LiDAR dataset from the Texas Water Development Board was used (TWDB, 2021). This dataset included the best available 1-meter LiDAR data as of August 2021 for the whole state of Texas, which was then processed into seamless DEMs with 3-meter cell sizes. For the Turkey Creek study area, the TWDB terrain was processed into a single DEM with a 10-foot cell size, and its vertical units were then converted from meters to feet. The final Turkey Creek DEM was re-projected into the same projection as the HEC-HMS model, which was USA Contiguous Albers Equal Area Conic USGS version in feet.

A total of sixteen HEC-RAS 2D flow areas were created with perimeters that exactly matched the subbasin delineations used in HEC-HMS. Next, a 2D computational mesh was developed with 500-foot cell sizes throughout most of the model. A stream centerline file as well as roads that had significant embankments were inserted as breaklines.

An overall view of the terrain and 2D computational mesh can be seen in Figure 10.3. Figure 10.4 shows a zoomed-in view near the confluence of Chacon Creek with Palo Blanco Creek.

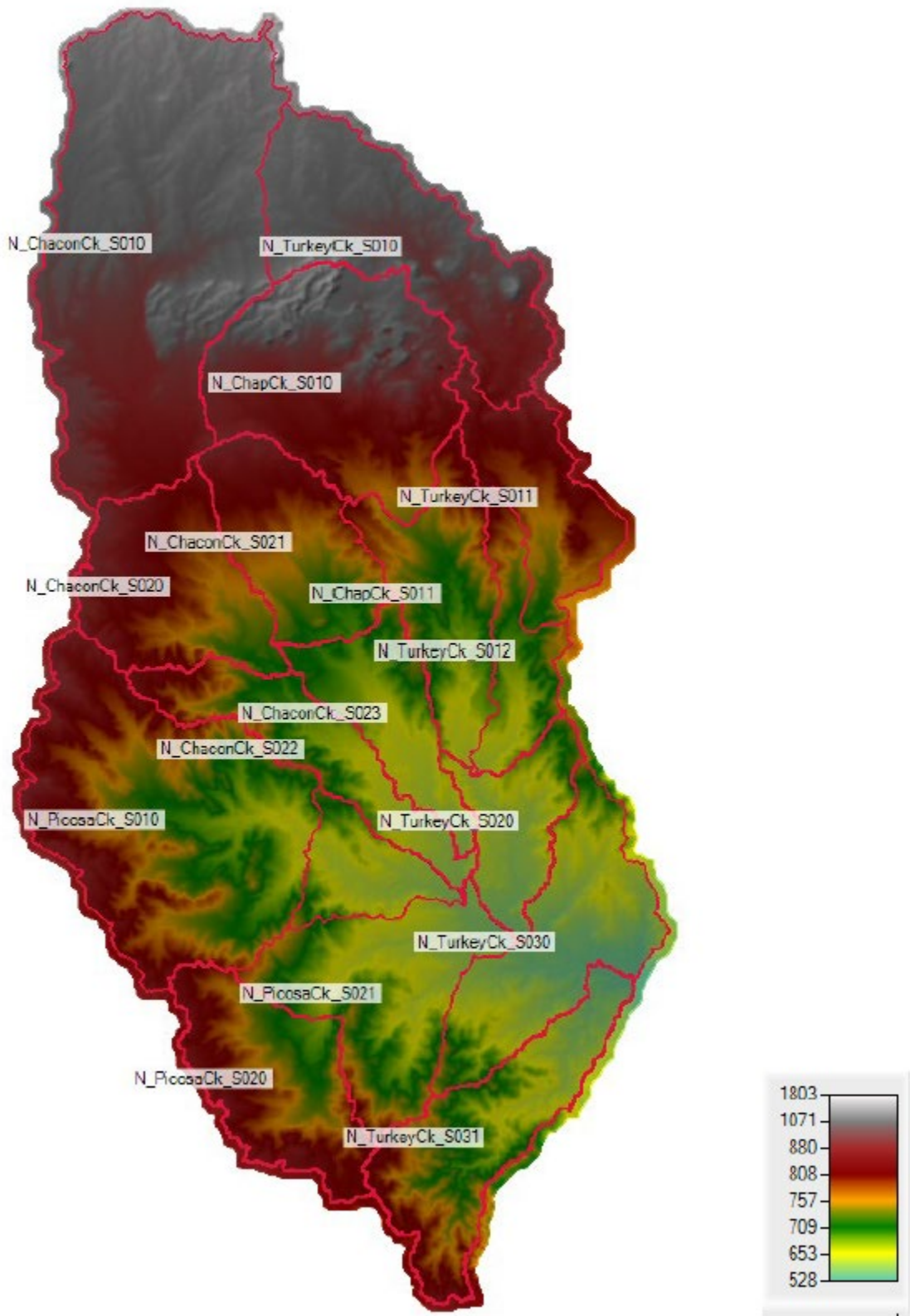


Figure 10.3: Overall Terrain Model with Sixteen Subbasin Areas

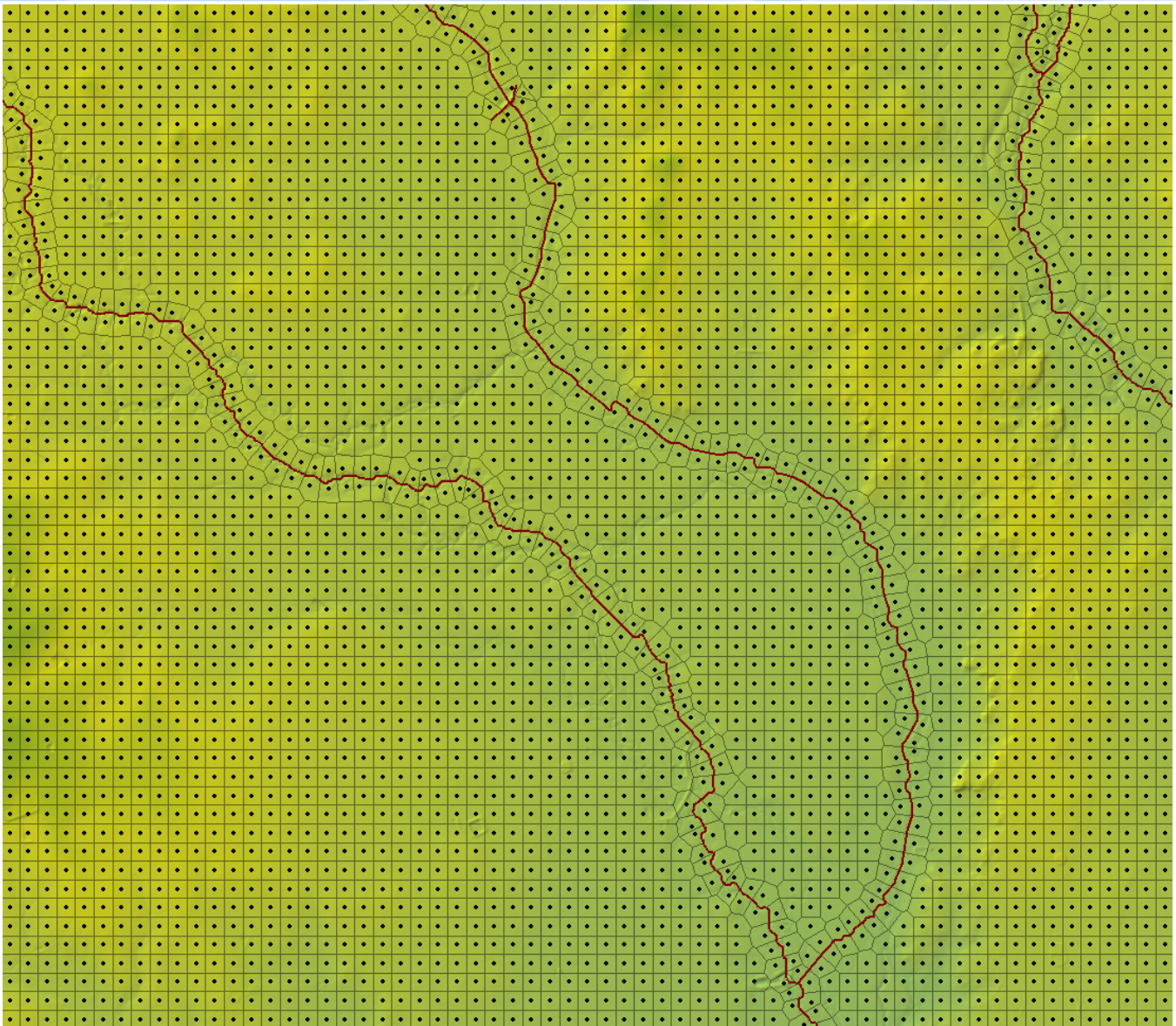


Figure 10.4: Terrain Model and 2D Mesh near ChaconCk\_R020 (breaklines shown in red)

### 10.3.2 Unsteady Flow Files and Boundary Conditions

Two separate unsteady flow files were created for this analysis: one for the transform parameters and one for the routing parameters. For the transform parameters, HEC-RAS 2D rain on mesh method was used. Excess precipitation from the HEC-HMS model (losses removed) was applied as a precipitation boundary condition. These conditions were applied for subbasins N\_TurkeyCk\_S010, N\_ChacónCk\_S020, and N\_PicosakCk\_S020 basins in the HEC-RAS unsteady flow data. These subbasins were selected as representative subbasins for the rest of the Turkey Creek watershed. A normal depth based on the river bed profile was used as the downstream boundary condition. The excess precipitation from the Uniform Rain 100-yr storm for the gage of the Nueces River near Asherton junction was applied to the HEC-RAS model.

For calculating routing parameters, the unsteady flow hydrograph method was used in HEC-RAS. A normal depth was used as the downstream boundary condition. A stepped inflow hydrograph was developed for each reach as an inflow boundary condition at the upstream end of each reach. See below Figure 10.5 for Turkey creek's

stepped inflow hydrograph. The stepped flow hydrograph had 20 constant flow “steps” ranging from in-channel flows to a maximum flow that is greater than the expected 500-yr flow for each reach. Similar stepped inflow hydrographs were also developed for the other routing reach tributaries in the Turkey Creek basin. Additional information on the initial conditions for these simulations can be found in Appendix F.

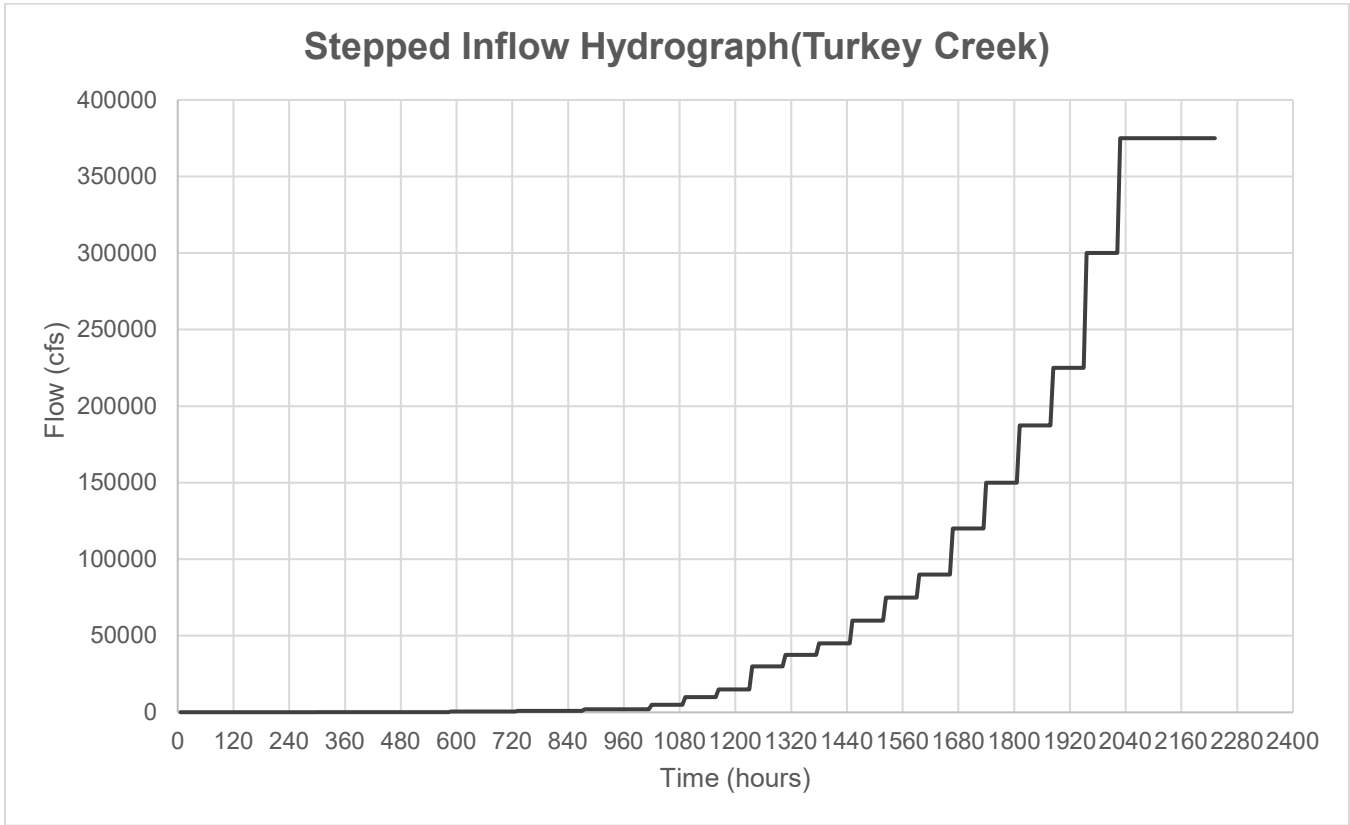


Figure 10.5: Stepped Inflow Hydrograph – Upstream Boundary Condition

### 10.3.3 National Land Cover Database (NLCD)

2021 National Land Cover Database (NLCD) data were imported into RAS as a Land Cover Layer to establish initial Manning’s ‘n’ estimates based on land cover categories (Figure F.6). Shrub-Scrub was the dominant land use type within the Turkey Creek floodplains; therefore, that is the category that had the greatest impact on the routing of flows within the floodplain.

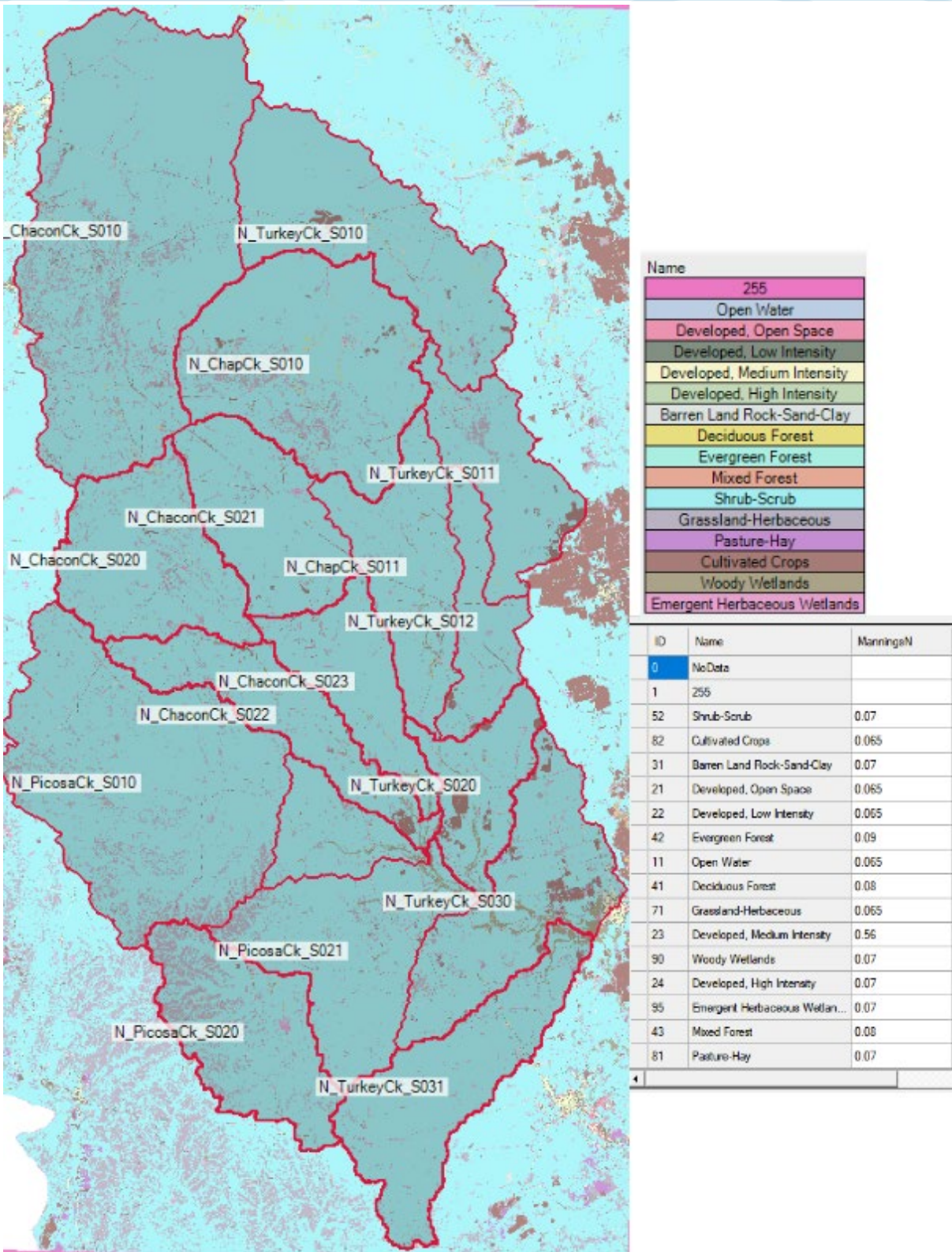


Figure 10.6: Nueces River – Turkey Creek: NLCD Categories

### 10.3.4 Manning's n Values

Manning's n values were developed for the different land uses and flow regimes throughout the watershed. The final Manning's n included one Manning's 'n' override region for the channel. These values were based on guidance from HEC-RAS Hydraulic Reference Manual (USACE, 2020). The base 'n' values and channel zones can be seen in Table 10.2.

**Table 10.2: Final Manning's 'n' Values**

Land Use Category	Base Mann 'n'	Channel Mann 'n'
Shrub-Scrub	0.07	0.05
Cultivated Crops	0.065	0.045
Barren Land Rock-Sand-Clay	0.07	0.05
Developed, Open Space	0.065	0.045
Developed, Low Intensity	0.065	0.045
Evergreen Forest	0.09	0.07
Open Water	0.065	0.045
Deciduous Forest	0.08	0.06
Grassland-Herbaceous	0.065	0.045
Developed, Medium Intensity	0.065	0.045
Woody Wetlands	0.07	0.05
Developed, High Intensity	0.07	0.05
Emergent Herbaceous Wetlands	0.07	0.045
Mixed Forest	0.08	0.05
Pasture-Hay	0.07	0.048

## 10.4 HEC-RAS Results And Adjusting Parameters In Hec-Hms

### 10.4.1 Transform Parameter Analysis

For the transform parameter analysis, a 2D excess rain-on-mesh method was used to simulate the rainfall runoff process. The excess precipitation, which is precipitation minus the losses, was extracted from the HEC-HMS model for the 1% AEP (100-year) storm. This excess precipitation time series was then applied to the 2D HEC-RAS model as a precipitation boundary condition in the unsteady flow file. The HEC-RAS 2D diffusion wave model was then run with the excess precipitation. The resulting flow hydrograph at the downstream end of each 2D subbasin was then extracted and compared to the HEC-HMS results for the corresponding subbasins. The lag times and peaking coefficients in HEC-HMS were then adjusted to match flow hydrograph from the 2D HEC-RAS results at the subbasin outlets.

N\_TurkeyCK\_S010 is a representative of the steep headwater subbasins. The HEC-RAS results from this subbasin were used to develop transform parameters for subbasins N\_TurkeyCK\_S010, N\_ChaconCk\_S010 and NChapCk\_S010. Subbasins N\_Chancnck\_S020 and N\_PicosaCk\_S020 are representative of the rest of the subbasins in the Turkey Creek watershed. The average of the results from subbasins N\_Chancnck\_S020 and N\_PicosaCk\_S020 were then used to adjust the lag times and peaking coefficients for the rest of the Turkey Creek subbasins. A summary of Snyder's Transform adjusted parameters are shown below in Table 10.3.

**Table 10.3: Summary of Snyder's Transform Parameters**

Subbasin	Previous HEC-HMS Parameters		New HEC-HMS Parameters from 2D RAS		Subbasin Type	Percentage Reduction in Lag Time
	Lag Time(hrs)	Peaking Coeff.	Lag Time(hrs)	Peaking Coeff.		
N_ChaconCk_S010	17.39	0.7	5.77	0.75	Steep headwaters	67%
N_ChaconCk_S020	12.09	0.7	4.5	0.75	Normal slope	63%
N_ChaconCk_S021	10.83	0.7	4.33	0.75	Normal slope	60%
N_ChaconCk_S023	14.07	0.7	5.63	0.75	Normal slope	60%
N_ChaconCk_S022	16.48	0.7	6.59	0.75	Normal slope	60%
N_PicosaCk_S010	17.5	0.7	7.00	0.75	Normal slope	60%
N_PicosaCk_S011	9.21	0.7	3.68	0.75	Normal slope	60%
N_PicosaCk_S020	7.7	0.7	3.25	0.75	Normal slope	58%
N_TurkeyCk_S010	13.54	0.7	4.50	0.75	Steep headwaters	67%
N_TurkeyCk_S011	11.57	0.7	4.63	0.75	Normal slope	60%
N_TurkeyCk_S012	11.97	0.7	4.79	0.75	Normal slope	60%
N_ChapCk_S010	11.9	0.7	3.95	0.75	Steep headwaters	67%
N_ChapCk_S011	14.69	0.7	5.88	0.75	Normal slope	60%
N_TurkeyCk_S020	10.41	0.7	4.16	0.75	Normal slope	60%
N_PicosaCk_S021	13.57	0.7	5.43	0.75	Normal slope	60%
N_TurkeyCk_S030	9.92	0.7	3.97	0.75	Normal slope	60%
N_TurkeyCk_S031	16.11	0.7	6.44	0.75	Normal slope	60%

### 10.4.2 Routing Parameter Analysis

A second HEC-RAS 2D diffusion wave model simulation was used to generate storage discharge curves for thirteen routing reaches which corresponded to the thirteen routing reaches in HEC-HMS that fall within the 2D modeling domain. For each of these thirteen reaches, an unsteady flow hydrograph was applied as an upstream boundary condition and normal depth was applied as the downstream boundary condition. A range of flows from in channel flows to greater than the expected 500-year flow were applied to the reaches in the form of a stepped flow hydrograph, and the resulting flow hydrograph at the downstream end of each reach was extracted from the HEC-RAS output. The incremental storage volume for a given flow value was then calculated as the area between the inflow and outflow time series for that reach, as shown in Figure 10.7. The cumulative sum of the incremental storage values were then used to calculate the storage-discharge curve for each reach. Figure 10.8 shows the resulting storage-discharge curves for the Turkey Creek mainstem. Tabular and graphical results of all the reaches in the routing analysis are available in Appendix F.

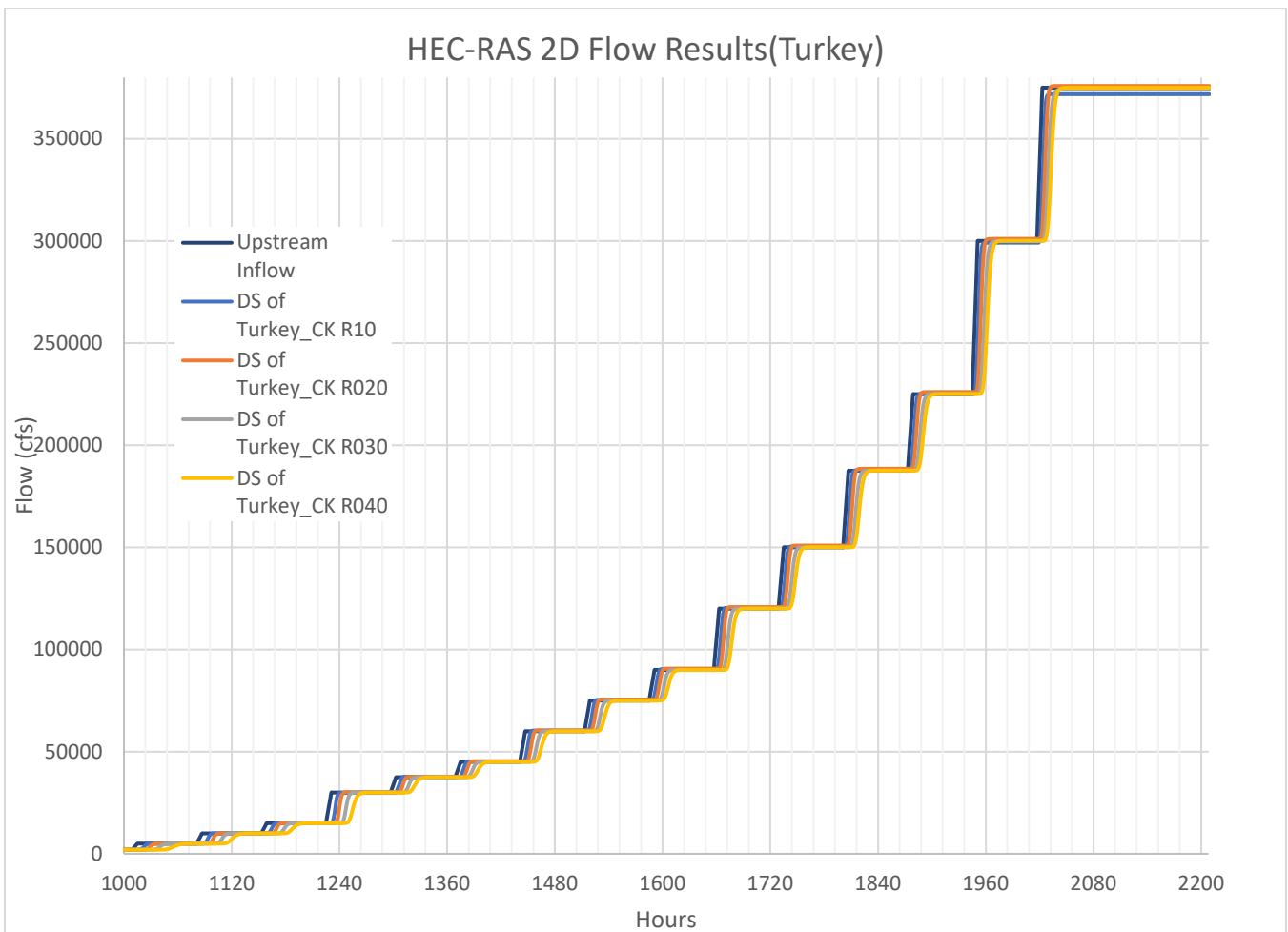


Figure 10.7: Reach Inflow and Outflow Hydrographs from 2D HEC-RAS

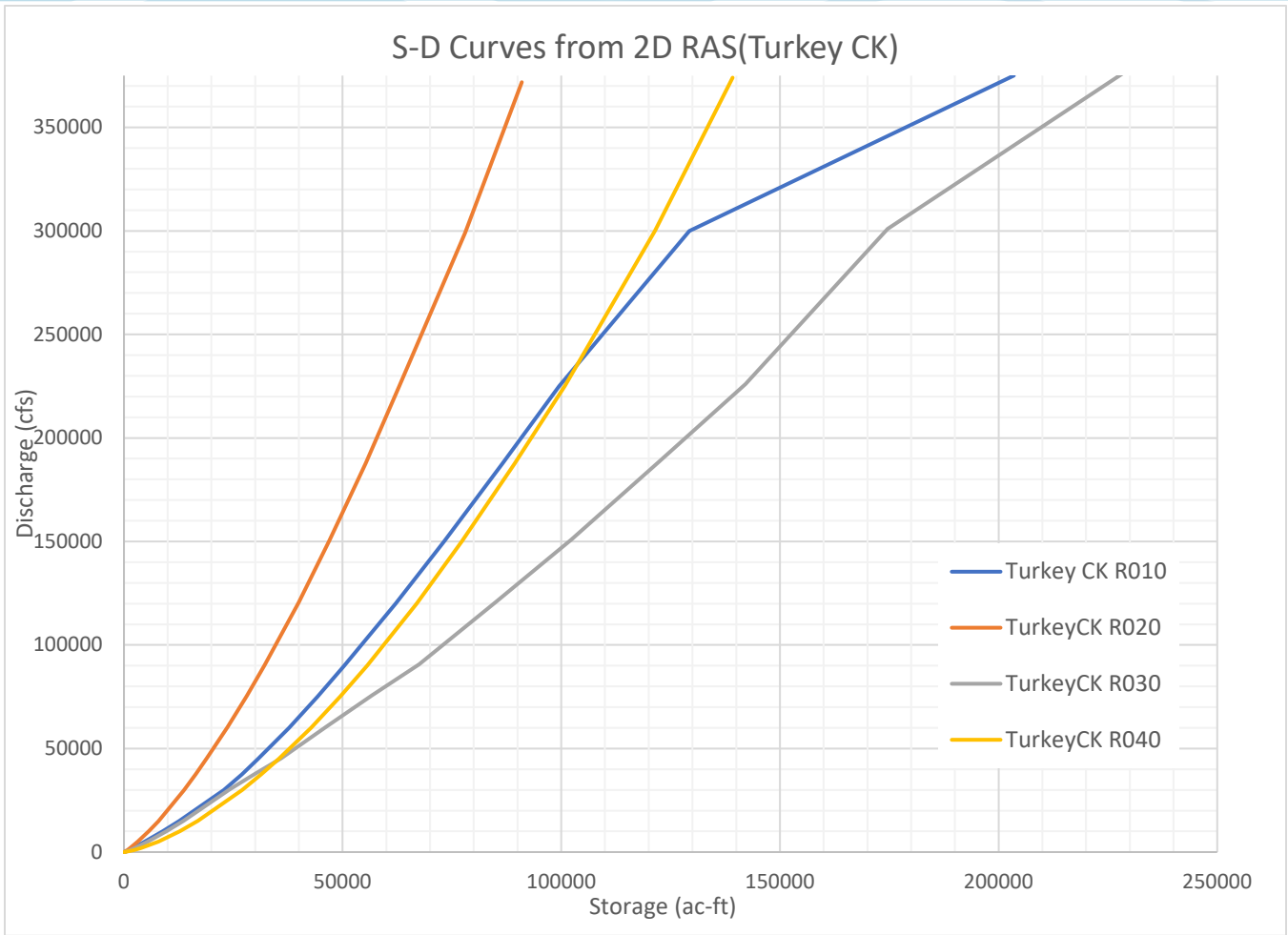


Figure 10.8: 2D HEC-RAS Turkey Creek Storage-Discharge Curves

### 10.4.3 2D-Informed Updates to the InFRM HEC-HMS Model

The thirteen storage-discharge curves computed from the 2D HEC-RAS model were adopted in the InFRM final HEC-HMS model as parameters to the Modified Puls routing reaches in the Turkey Creek watershed.

After updating the routing reaches, the 2D transform results were used to update the Snyder's transform parameter estimates in HEC-HMS. It is important to note that the 2D diffusion wave equations in HEC-RAS have no notion of Lag time and Peaking coefficient parameters which are specific to the HEC-HMS Snyder's transform method. However, the peak magnitude, peak timing, and overall shape of the 2D transform hydrographs can be used to inform Snyder's transform parameters. The subbasin lag time and peaking coefficient parameters were adjusted in HEC-HMS until the Snyder's transform hydrographs more closely matched the 2D HEC-RAS downstream hydrographs. The final adjusted HEC-HMS transform parameters were shown in Table F.3.

The InFRM Uniform and Elliptical storm HEC-HMS models were then recomputed with the final 2D storage-discharge curves and the final Tc and R parameters. Figure 10.9- through 10.11 compare the 100-yr flow hydrograph results for subbasins N\_TurkeyCK, N\_ChanconCk\_S020 and N\_PicosaCk\_S020 from 2D HEC-RAS, from the preliminary HEC-HMS transform parameters and from the final HEC-HMS transform parameters. Likewise, Figure 10.12 compares the 100-yr preliminary and final HEC-HMS flow hydrograph results at the Turkey Creek at Highway 83 junction, which is at the downstream end of the 2D HEC-RAS analysis. This figure uses the results from the 100-yr elliptical storm for the downstream Asherton gage.

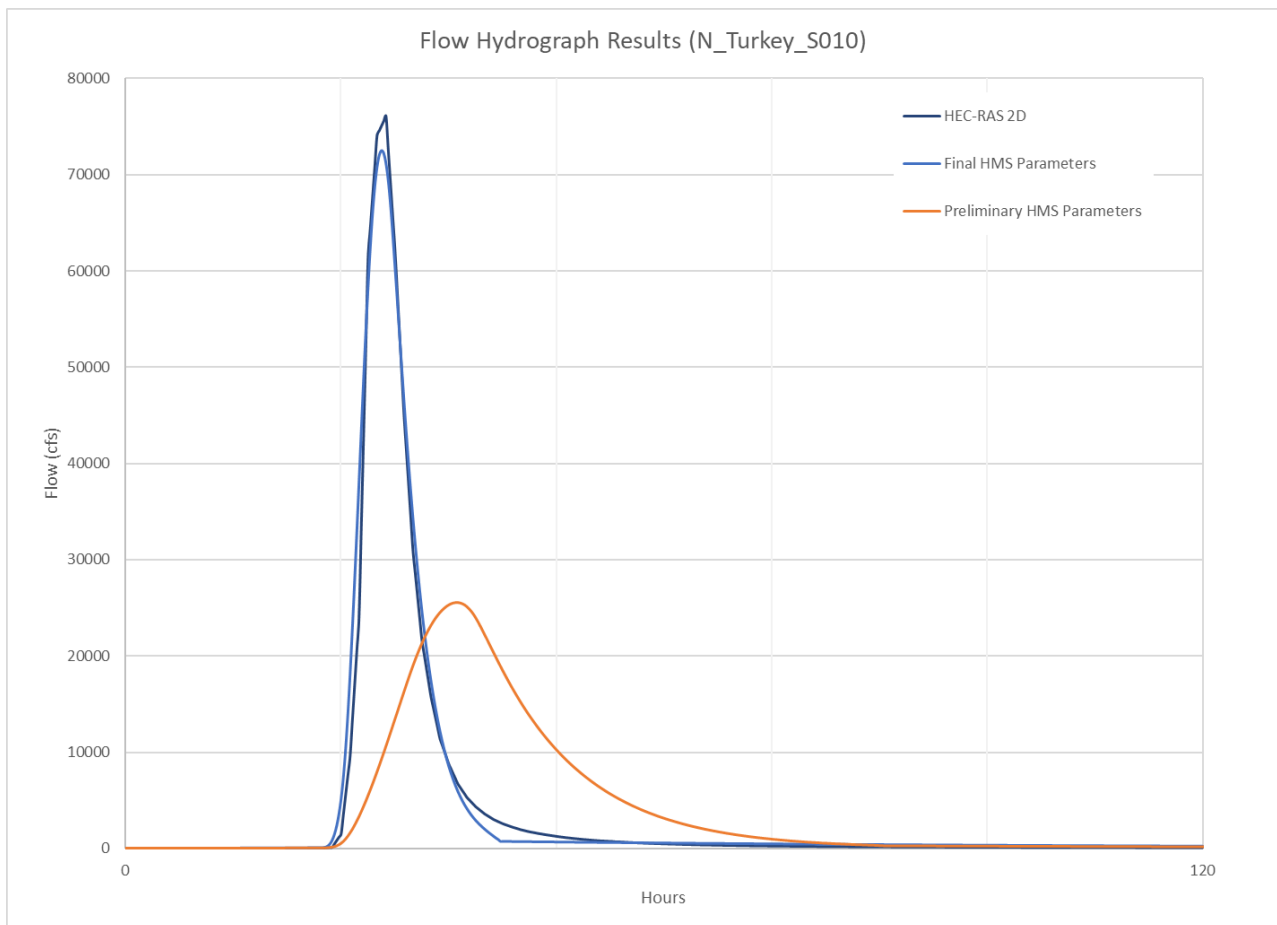


Figure 10.9: Comparison of Flow Hydrograph Results for Subbasin N\_Turkey\_S010

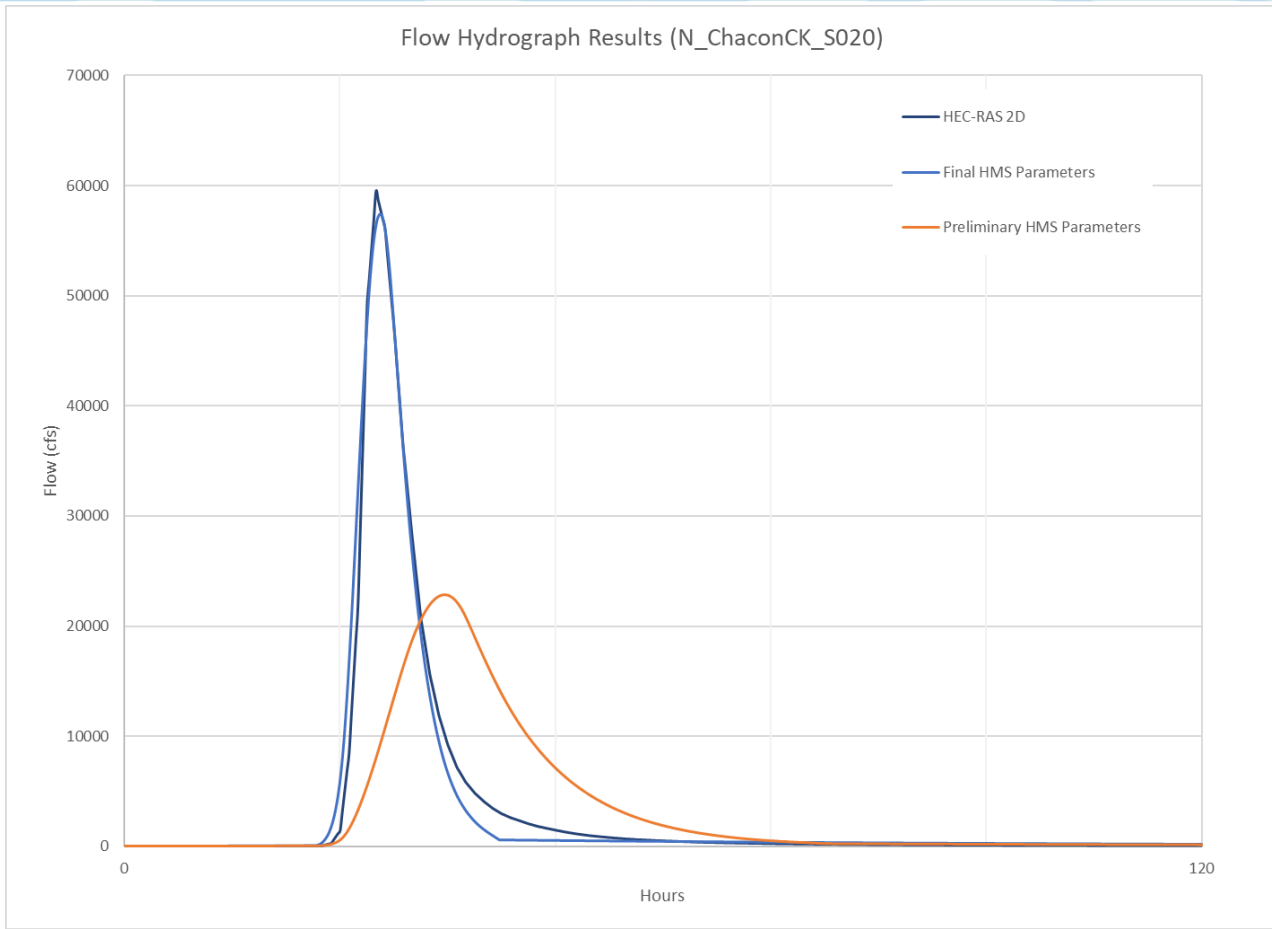


Figure 10.10: Comparison of Flow Hydrograph Results For Subbasin N\_ChacoCk\_S020

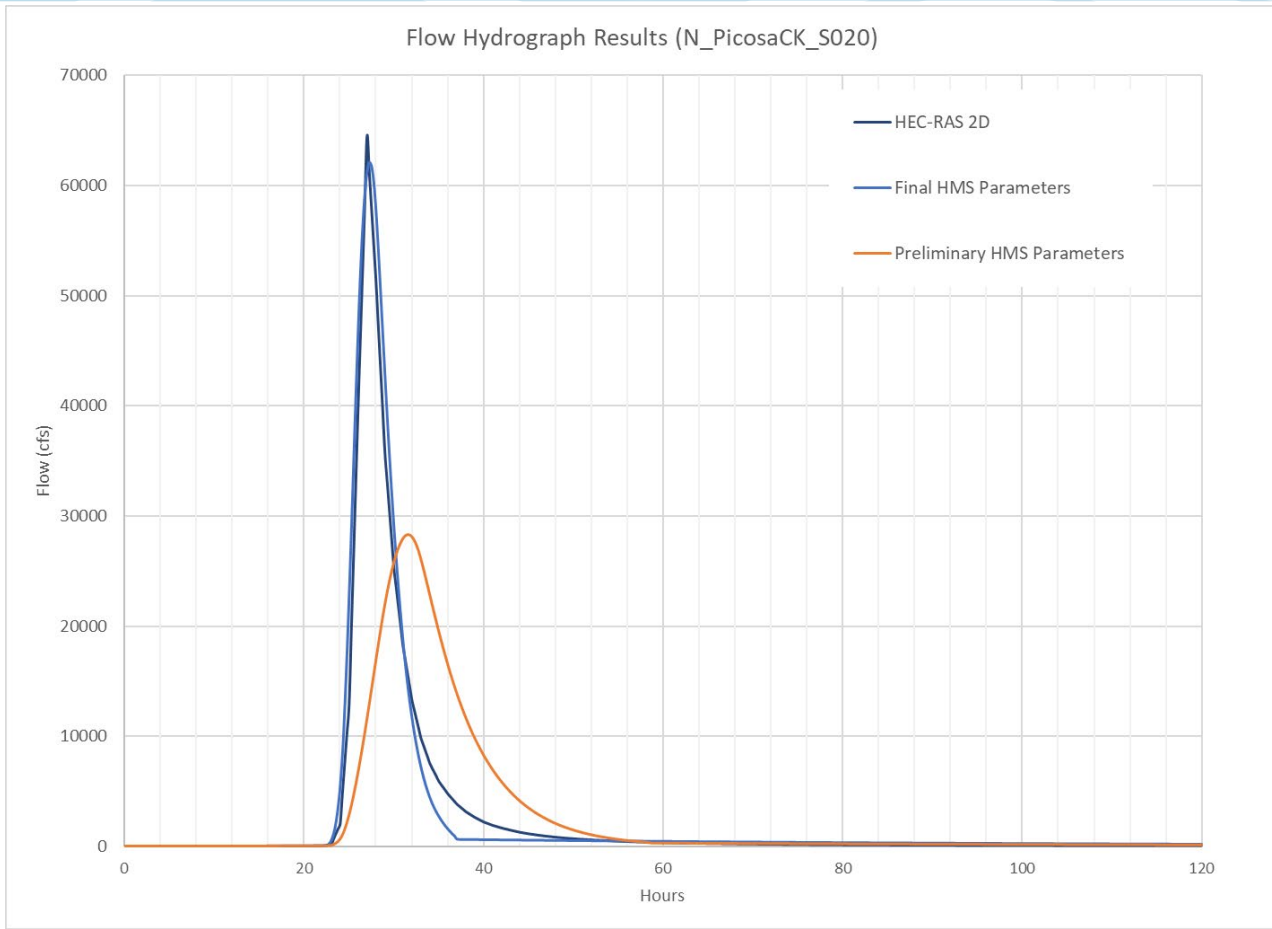


Figure 10.11: Comparison of Flow Hydrograph Results For Subbasin N\_PicosaCk\_S020

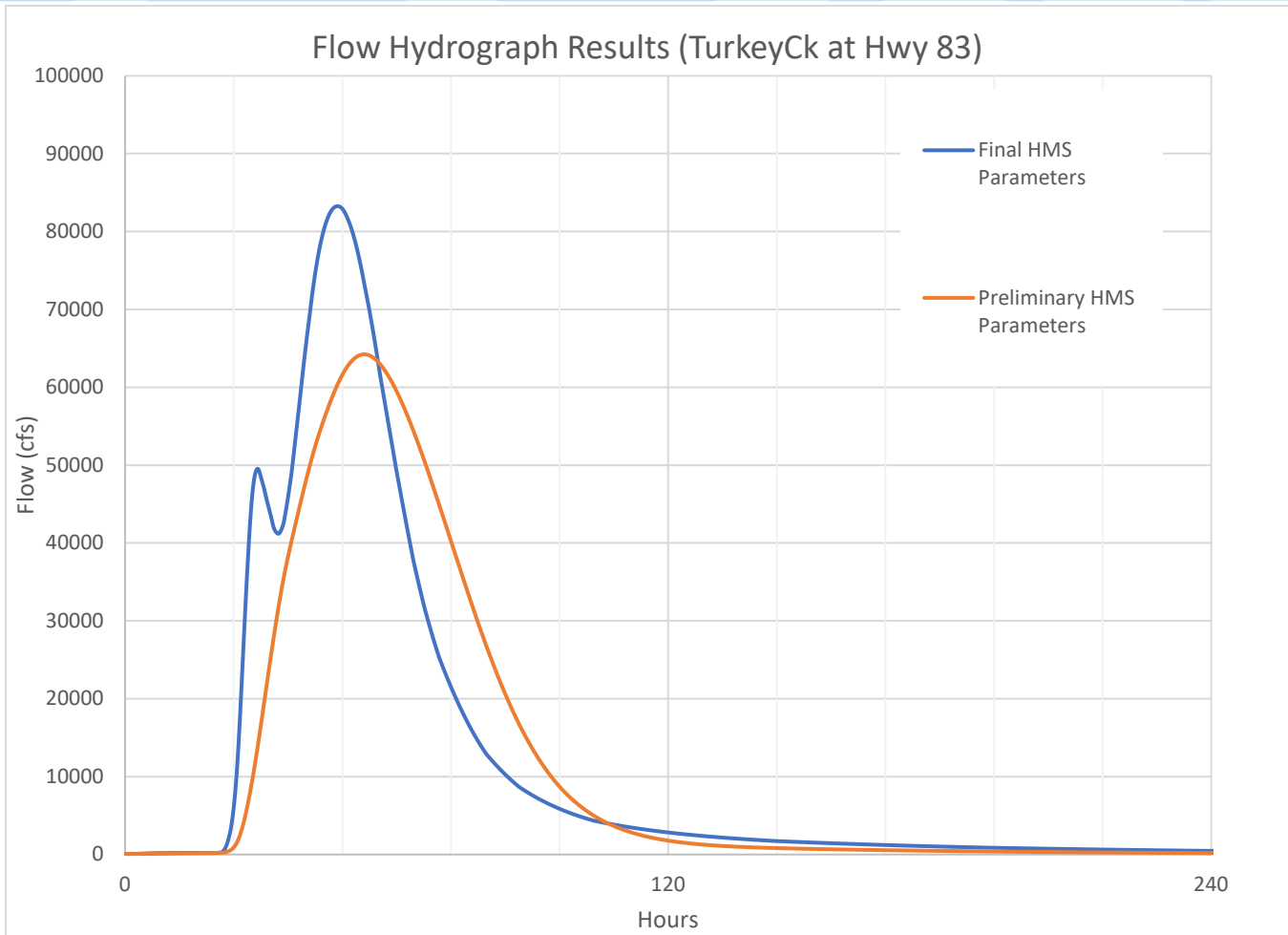


Figure 10.12: Comparison of Flow Hydrograph Results For Subbasin Turkey Creek at Hwy 83

## 10.5 Limitations and Opportunities for Improvement

Since there was no observed data to assist in calibrating the HEC-HMS model, this analysis utilized 2D HEC-RAS as a calibration and verification tool instead. The modeling domain of the 2D analysis consisted of a drainage area of approximately 2,000 square miles. Given a watershed of this size, it was cost and time-prohibitive to include bridges, culverts, and other structures that could affect the arrival time and peak magnitudes of flows downstream. However, the overall accuracy of the model over a larger range of event intensities would most likely be improved if the influence of structures would have been specifically accounted for during model development.

In addition, for the sake of efficiency, subbasin transform parameters were directly estimated in HEC-RAS for only three representative subbasins. Proportional adjustments were then applied to the remaining subbasins in the Turkey Creek watershed. Some improvement in accuracy could have been obtained by repeating the same analysis for all 17 subbasins; however, the degree of improvement may have been relatively small relative to the information already gained from this analysis.

Additional sensitivity testing to the mesh cell sizes might also help improve the accuracy of the model, particularly near the main channel. While a finer cell resolution of about 500-feet was implemented, additional refinement could be done so that the cell sizes better fit the varying channel widths observed throughout the terrain model.

This would allow for a more accurate designation of in-bank versus out-of-bank Manning's 'n' values which could have some effect on the computed arrival times and peak water surface elevations.

## 10.6 Conclusions

One of the acknowledged limitations of unit hydrograph theory is the assumption of linearity, which implies that a watershed would have the same time of concentration when receiving a very low intensity rain event as it would when receiving a high intensity rainfall event. Concerns with this assumption can be reduced by calibrating the model to storms of similar intensity to the storm of primary interest (i.e., the 1% AEP or 100-yr recurrence interval).

In this analysis, the 2D diffusion wave transform method in HEC-RAS, which is based on the momentum and continuity equations and is not tied to the assumption of linearity, was used to inform the Snyder's unit hydrograph transform parameters in HEC-HMS particularly for rare, intense rainfall events such as the 1% AEP storm. In fact, the results of this analysis led to an average decrease of 60% in the Snyder's lag times for the 1% AEP storm event on the Turkey Creek watershed. These decreases in lag times generally led to higher peak discharges downstream. The results from this analysis were also consistent with those found in literature such as Snyder and Minshall (Snyder, 1938 and Minshall, 1962). However, these increases in individual subbasin peak discharges were tempered by the floodplain storage added to the model in the Modified Puls routing reaches.

The 2D HEC-RAS analysis was used to calculate the storage volumes in the HEC-HMS routing reaches of Turkey Creek above HWY-83. The analysis from 2D model of the Turkey Creek watershed was used to estimate Modified Puls Routing parameters and Snyder's subbasins transform parameters. The results of this 2D analysis were used to update the transform and routing reach parameters in the final InFRM HEC-HMS model. This analysis helped to overcome the lack of observed data in the Turkey Creek watershed and helped to reduce the uncertainty in the flood frequency estimates of the HEC-HMS model for rare events such as the 1% AEP (100-yr) storm.

# 11 Comparison of Frequency Flow Estimates

As each of the hydrologic analyses was completed, their results were compared to one another in terms of frequency peak discharge estimates at the USGS stream gage locations. These comparisons of frequency flow estimates were made in table format as well as graphs of peak discharge versus probability. The estimated frequency curves from each method were plotted along with their associated confidence limits and the previous published discharges from the effective FEMA Flood Insurance Studies (FIS) or the Base Level Engineering (BLE) data for the Nueces River basin. For gages where a statistical change over time plot was generated, as described in Section 5.3, the results from the other methods were also compared against the range of flow values in those graphs.

Wherever there were significant differences in the resulting flood magnitudes, the InFRM team made an effort to investigate and understand the reasons for those differences to the extent practicable. The investigation process often uncovered one or more adjustments that should be made to the assumptions in a particular method that improved the results. These adjustments may or may not have led to better agreement in the results, but at the very least, the strengths and weaknesses of each method at a particular location were more fully understood through the process of investigation.

## 11.1 FREQUENCY FLOW COMPARISONS

The final comparisons of the frequency flow estimates are given in Table 11.1 to 11.25. Blank cells indicate data was not available at that specific location. Figures 11.1 through 11.25 include plots of the estimated frequency curves at each gage along with their confidence limits and the previous published discharges from the BLE data and the effective FEMA Flood Insurance Studies (FIS).

**Table 11.1: Frequency Flow (cfs) Results Comparisons for West Nueces River nr Brackettville, TX**

Annual Exceedance Probability (AEP)	Return Period (years)	Currently Effective FEMA FIS	BLE Data-Statistical Analysis	Statistical Analysis of the Gage Record (81 years)	HEC-HMS Uniform Rain Frequency Storm	HEC-HMS Elliptical Frequency Storm
0.002	500			717,000	411,532	340,224
0.005	200			537,000	321,031	263,575
0.01	100			408,000	259,775	225,642
0.02	50			291,000	197,317	171,638
0.04	25			189,000	146,976	133,549
0.1	10			86,100	84,434	77,030
0.2	5			35,800	36,785	32,485
0.5	2			4,370	4,051	4,312

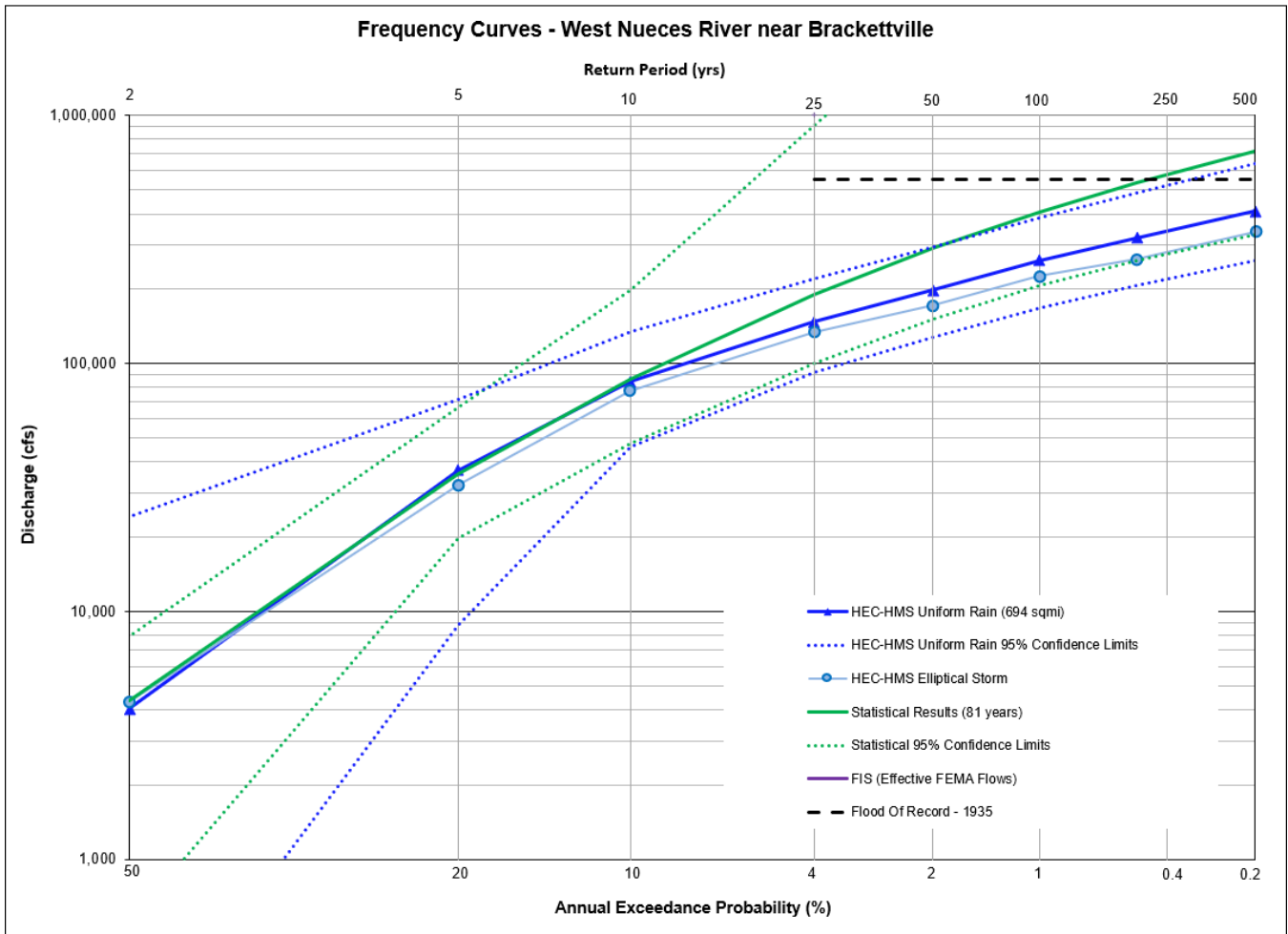


Figure 11.1: Flow Frequency Curve Comparison for West Nueces River nr Brackettville, TX

The West Nueces River near Brackettville USGS gage has a steep, hill country watershed with a drainage area of almost 700 square miles. The period of record at USGS streamgage 08190500 West Nueces River near Brackettville, Texas was from 1940 through 2020. This gives the gage a relatively long period of record of approximately 80 years.

Figure 11.1 shows that the HEC-HMS results are substantially lower than the current statistical analysis of the gage record based on 80 years of record. However, the HEC-HMS results are still well within the confidence bounds of the statistical results. Figure 11.1 also shows that the HEC-HMS results are similar to the current statistical analysis of the gage record based on 80 years of record at the 4% AEP (25-yr) frequency, but the HEC-HMS results start becoming significantly lower than the statistical results at the 2% AEP (50-yr) frequency. As we approach the 0.2% AEP, the statistical estimate is largely driven by the 1935 flood of record. The 1935 flood was an extreme event at this location, which likely far exceeded a 1,000-year event. The 1935 peak discharge on the West Nueces River was estimated at 550,000 cfs, which was the highest discharge ever recorded anywhere for a watershed of that size. As a result of the influence of that flood, the 1% and 0.2% AEP statistical estimates are likely still high, even after 80 years. The HEC-HMS results, on the other hand, are based on the regional rainfall statistics of NOAA Atlas 14, which tend to make their frequency flood estimates more consistent over time and less subject to change.

**Table 11.2: Frequency Flow (cfs) Results Comparisons for Nueces River at Laguna, TX**

Annual Exceedance Probability (AEP)	Return Period (years)	Currently Effective FEMA FIS	BLE Data-Statistical Analysis	Statistical Analysis of the Gage Record (91 years)	HEC-HMS Uniform Rain Frequency Storm	HEC-HMS Elliptical Frequency Storm
0.002	500			546,000	467,906	376,135
0.005	200			412,000	373,479	298,001
0.01	100			320,000	307,795	261,562
0.02	50			237,000	240,677	203,364
0.04	25			164,000	171,634	152,806
0.1	10			87,800	86,925	78,069
0.2	5			45,300	42,862	36,388
0.5	2			10,300	9,086	9,472

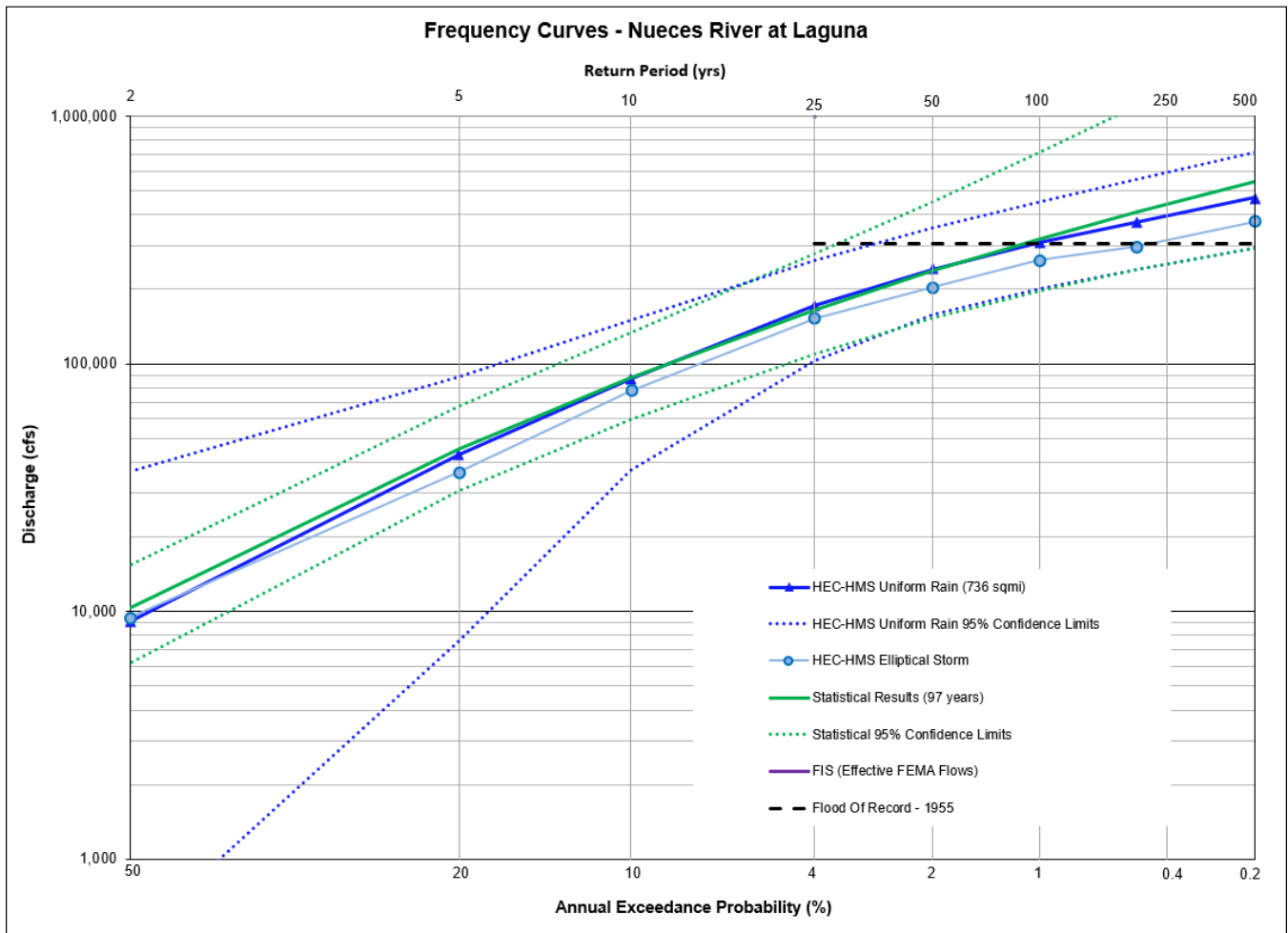


**Figure 11.2a: Flow Frequency Curve Comparison for Nueces River at Laguna, TX**

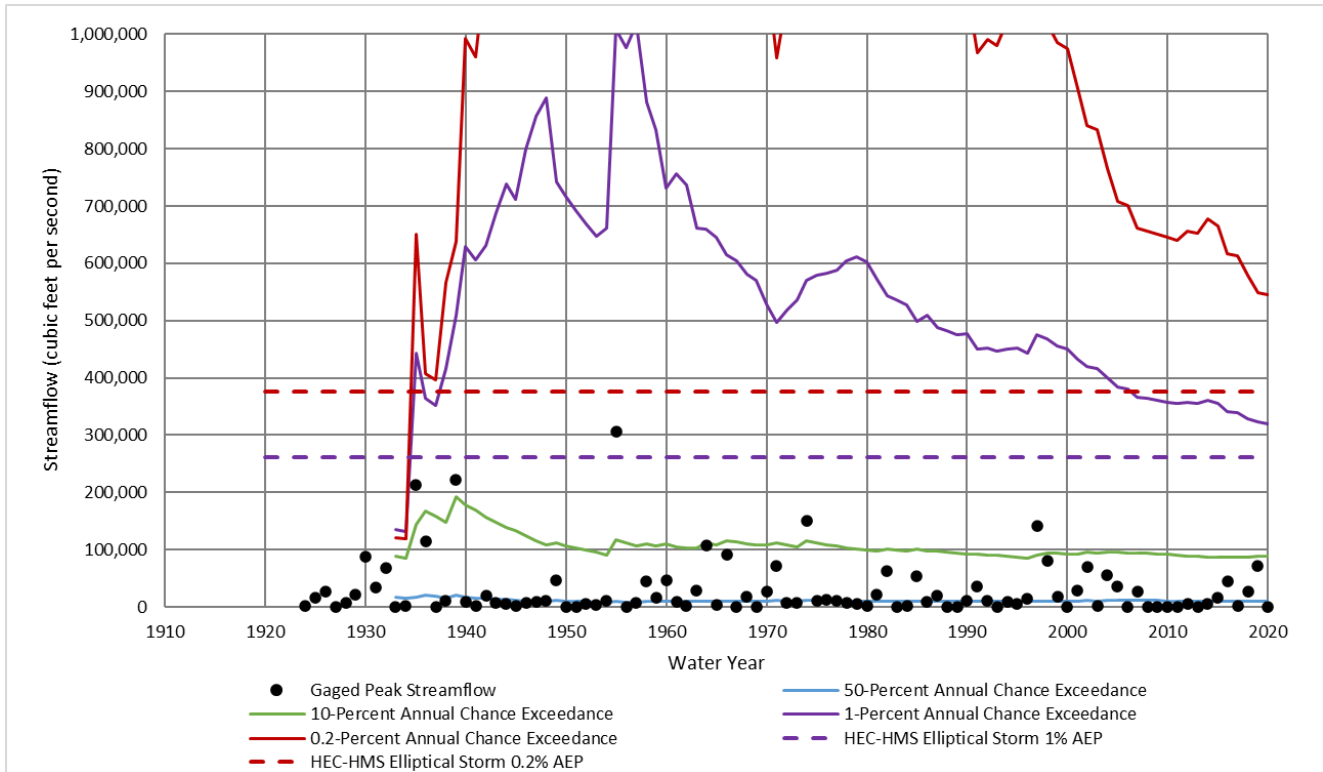


**Figure 11.2b: Statistical Change Over Time Comparison for Nueces River at Laguna, TX**

The Nueces River at Laguna USGS gage has a steep, hill country watershed with a drainage area of just over 700 square miles. The period of record for USGS streamgage 08190000 Nueces River at Laguna, Texas was from 1924 through 2020. This gives the gage a relatively long period of record of approximately 90 years.

Figure 11.2a shows that the HEC-HMS results from both uniform rain and the elliptical storms are lower than the statistical analysis of the gage record at the 1% AEP event, but the results generally show good agreement and are still well within one another's confidence bounds. Figure 11.2b illustrates the degree to which the statistical estimates for the 1% and 0.2% AEP are still changing over time, even after 90 years of record. The 10% AEP statistical estimate, on the other hand, is relatively stable, although it does show a slight downward trend. The HEC-HMS results, on the other hand, are relatively stable due to the regional rainfall statistics of NOAA Atlas 14. The 1% AEP elliptical storm estimate from HEC-HMS is also slightly lower than the 1955 flood of record.

**Table 11.3: Frequency Flow (cfs) Results Comparisons for Nueces River nr Uvalde, TX**

Annual Exceedance Probability (AEP)	Return Period (years)	Currently Effective FEMA FIS	BLE Data-Statistical Analysis	Statistical Analysis of the Gage Record (93 years)	HEC-HMS Uniform Rain Frequency Storm	HEC-HMS Elliptical Frequency Storm
0.002	500			686,000	659,615	493,324
0.005	200			519,000	509,965	376,722
0.01	100			401,000	407,871	320,289
0.02	50			294,000	307,157	238,919
0.04	25			201,000	219,317	181,005
0.1	10			103,000	116,152	92,551
0.2	5			49,500	54,602	39,076
0.5	2			9,310	9,319	7,861

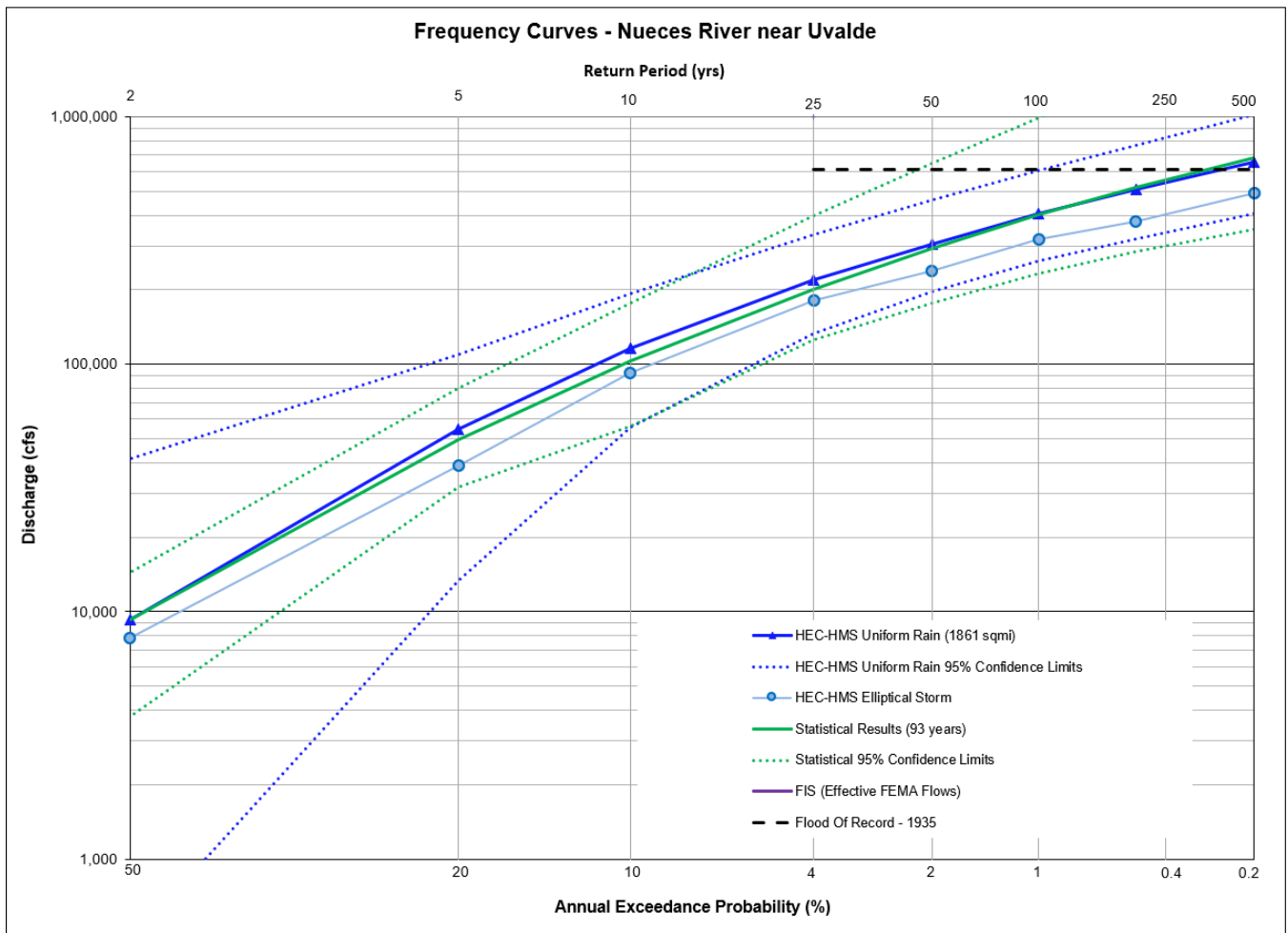


**Figure 11.3a: Flow Frequency Curve Comparison for Nueces River nr Uvalde, TX**

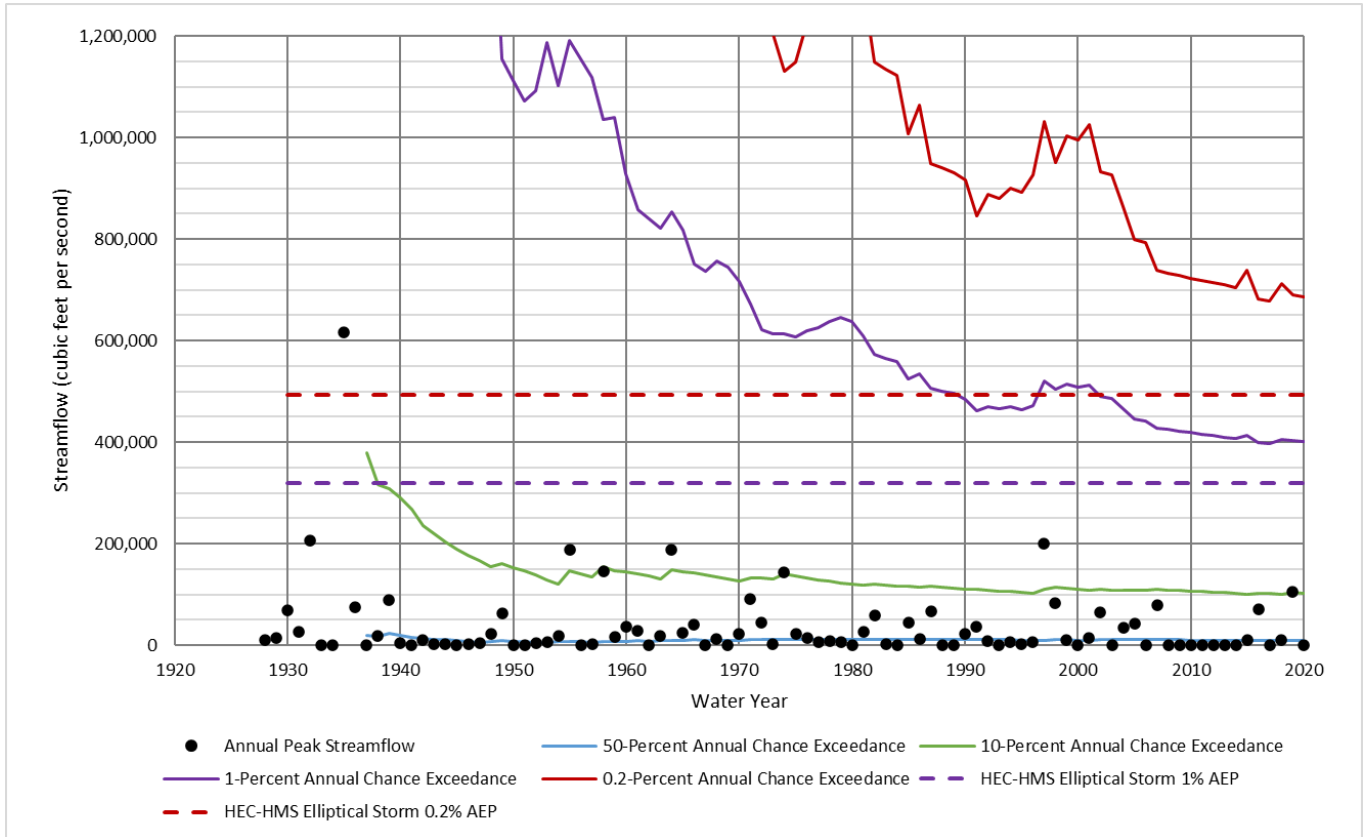


**Figure 11.3b: Statistical Change Over Time Comparison for Nueces River nr Uvalde, TX**

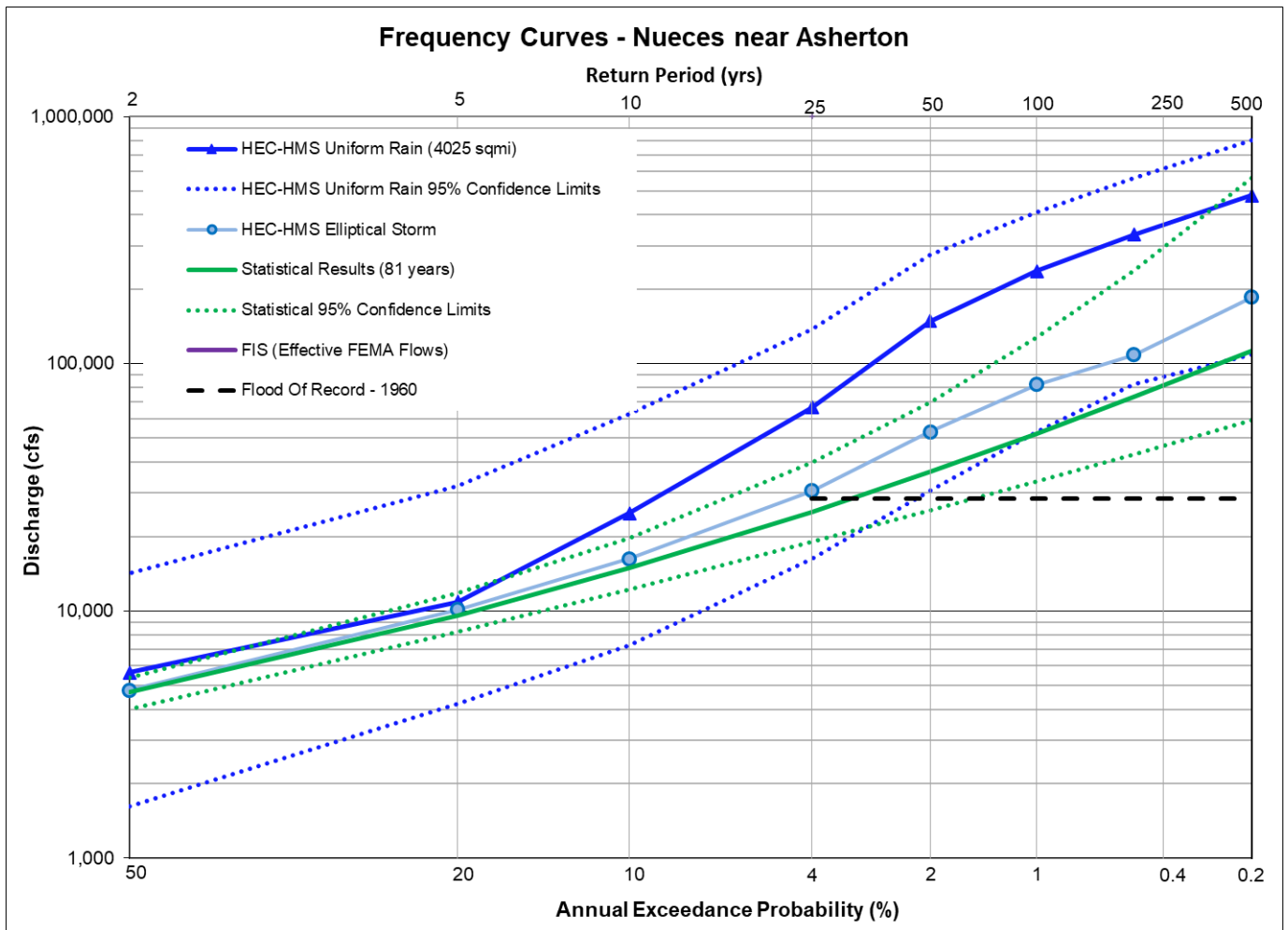
The Nueces River near Uvalde USGS gage has a steep, hill country watershed with a drainage area of just over 1800 square miles. The period of record at USGS streamgage 08192000 Nueces River below Uvalde, Texas was from 1928 through 2020. This gives the gage a relatively long period of record of approximately 90 years. However, the statistical results for the rare floods are likely being overestimated due to the influence of the 1935 flood of record. The 1935 flood was an extreme event with a peak discharge of 616,000 cfs at this location.

Figure 11.3a shows that there is a very good agreement between the statistical analysis and the HEC-HMS Uniform Analysis throughout all of the AEPs, from the 50% (2-Year) frequency through the 0.2% (500-Year) frequency. However, the uniform rain results are likely overestimating the rainfall volume on this 1,800 square mile watershed. The HEC-HMS Elliptical storm results are lower than both the uniform and statistical results but show reasonably good agreement and are well within the confidence limits of both analyses.

Figure 11.3b illustrates the extreme influence of the 1935 flood on the statistical estimates, and it shows that even after 90 years of record, the statistical estimates of the 1% and 0.2% AEP peak discharges still have not stabilized.

**Table 11.4: Frequency Flow (cfs) Results Comparisons for Nueces River nr Asherton, TX**

Annual Exceedance Probability (AEP)	Return Period (years)	Currently Effective FEMA FIS	BLE Data - Statistical Analysis	Statistical Analysis of the Gage Record (81 years)	HEC-HMS Uniform Rain Frequency Storm	HEC-HMS Elliptical Frequency Storm
0.002	500			113,000	478,211	185,705
0.005	200			73,100	332,587	108,633
0.01	100			51,900	236,542	82,459
0.02	50			36,500	148,741	53,059
0.04	25			25,200	66,485	30,656
0.1	10			14,900	24,869	16,279
0.2	5			9,590	10,866	10,112
0.5	2			4,710	5,620	4,782



**Figure 11.4a: Flow Frequency Curve Comparison for Nueces River nr Asherton, TX**

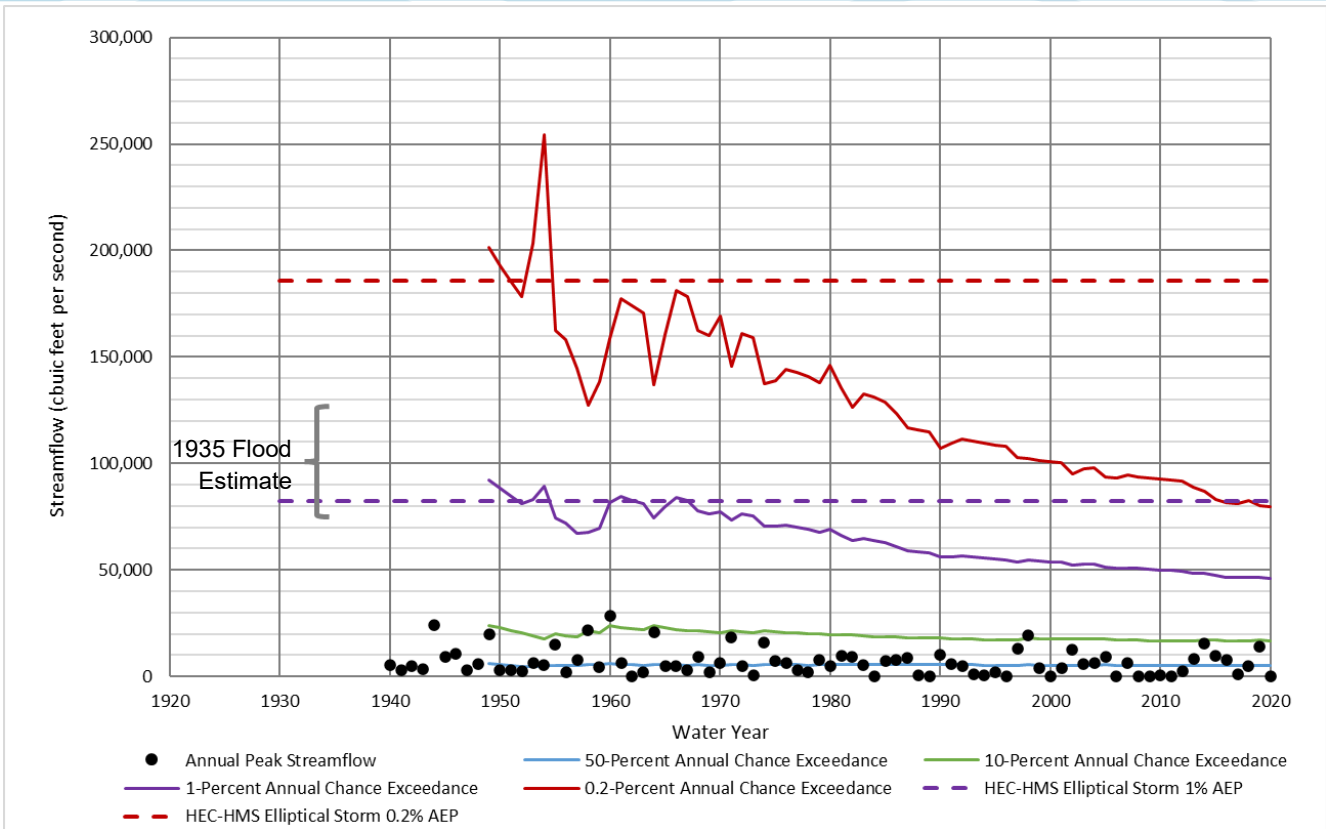


**Figure 11.4b: Statistical Change Over Time Comparison for Nueces River nr Asherton, TX**

The Nueces River near Asherton has a drainage area of 4,000 square miles and is located in an area with wide expanses of irrigated fields. The hydrology of the Nueces River near Asherton is probably the most complicated of any location in the Nueces River basin. It is located just downstream of the split flow area discussed in the Chapter 6 as well as the 2,000 square miles of ungaged watershed for Turkey Creek. It is also located downstream of the Edwards and Carrizo aquifer outcrops. As a result of the aquifers and the wide irrigated floodplains, large volumes of floodwater that have been observed at upstream gages never appear at the Asherton gage. For example, during the October 1996 flood on the Nueces River, there was a 90% reduction in observed peak flow and an 80% reduction in observed streamflow volume between the Uvalde and Asherton USGS gages. The channel losses and routing parameters of the HEC-HMS model were calibrated to reproduce the large reductions in observed peak flows between Uvalde and Asherton.

The period of record at USGS streamgage 08193000 Nueces River near Asherton, Texas was from 1940 through 2020. gives the gage a relatively long period of record of approximately 80 years. However, the largest flood of record had a peak flow of only 28,500 cfs, which is an order of magnitude smaller than the upstream gages. This gage was not recording for the 1935 flood, which was the flood of record at both the upstream and downstream gages. Therefore, an interval estimate of the 1935 flood was incorporated into the statistical analysis.

Figure 11.4a shows that the HEC-HMS results from both uniform rain and the elliptical storms are significantly higher than the statistical analysis of the gage record at the 1% AEP event. The uniform rain results are high due to the rainfall volume being overestimated on the 4,000 square mile drainage area. The elliptical storm results are significantly higher than the statistics but still well within the confidence bounds. Figure 11.4b shows that no floods larger than a 10-year (10% AEP) event have been recorded at this location in the past 60 years. As a result, the current statistical results are likely underestimating the 1% AEP (100-Year) flood potential. In addition, the elliptical storm results line up well with the interval estimate of the 1935 flood, as shown in Figure 11.4b.

**Table 11.5: Frequency Flow (cfs) Results Comparisons for Nueces River at Cotulla, TX**

Annual Exceedance Probability (AEP)	Return Period (years)	Currently Effective FEMA FIS	BLE Data-Statistical Analysis	Statistical Analysis of the Gage Record (97 years)	HEC-HMS Uniform Rain Frequency Storm	HEC-HMS Elliptical Frequency Storm
0.002	500			100,000	423,013	165,323
0.005	200			76,300	298,522	103,781
0.01	100			60,600	215,574	80,913
0.02	50			46,900	140,288	50,514
0.04	25			35,000	64,724	31,319
0.1	10			22,000	24,913	20,444
0.2	5			14,000	14,572	12,797
0.5	2			5,610	5,935	6,238

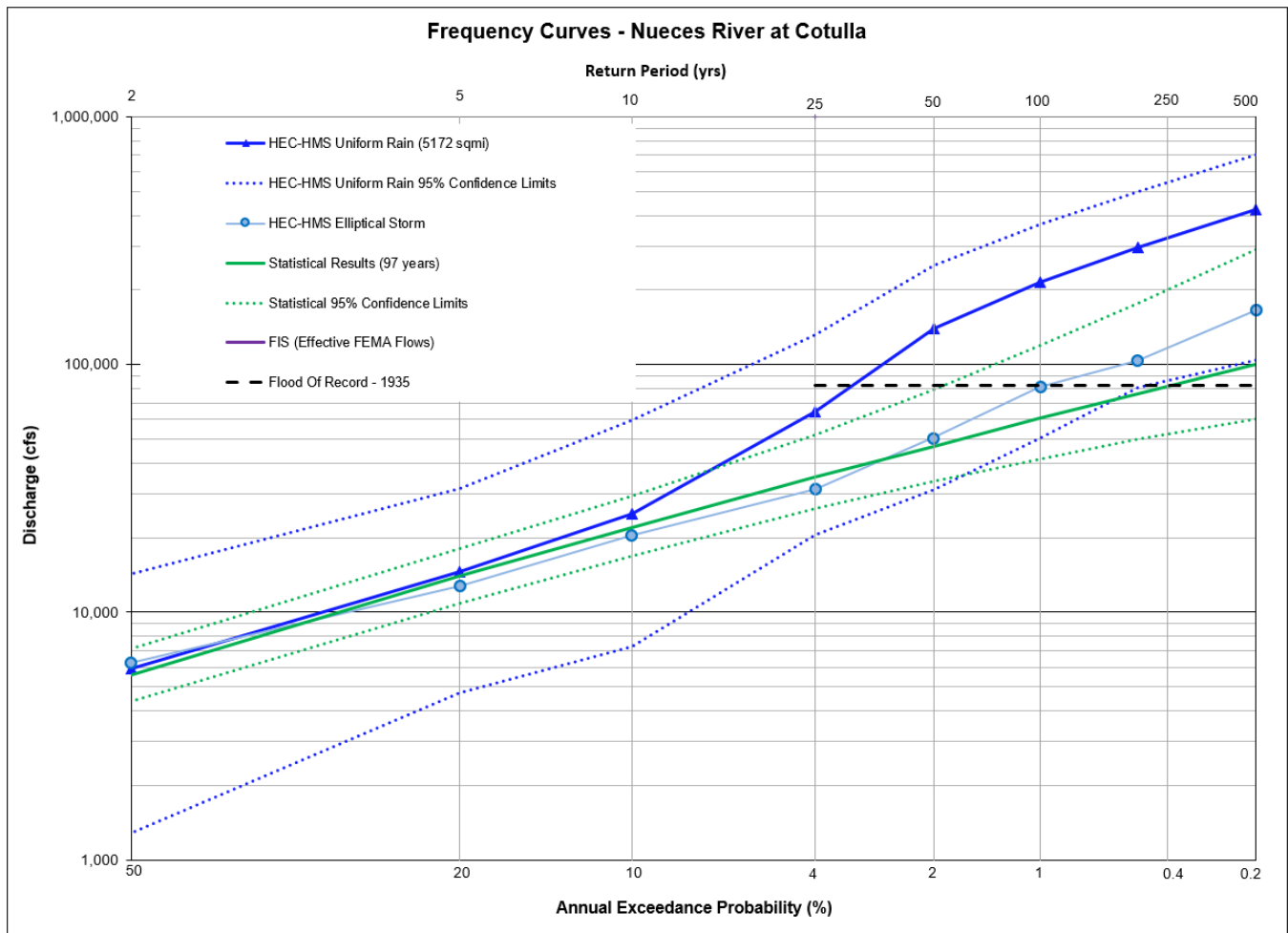


**Figure 11.5a: Flow Frequency Curve Comparison for Nueces River at Cotulla, TX**

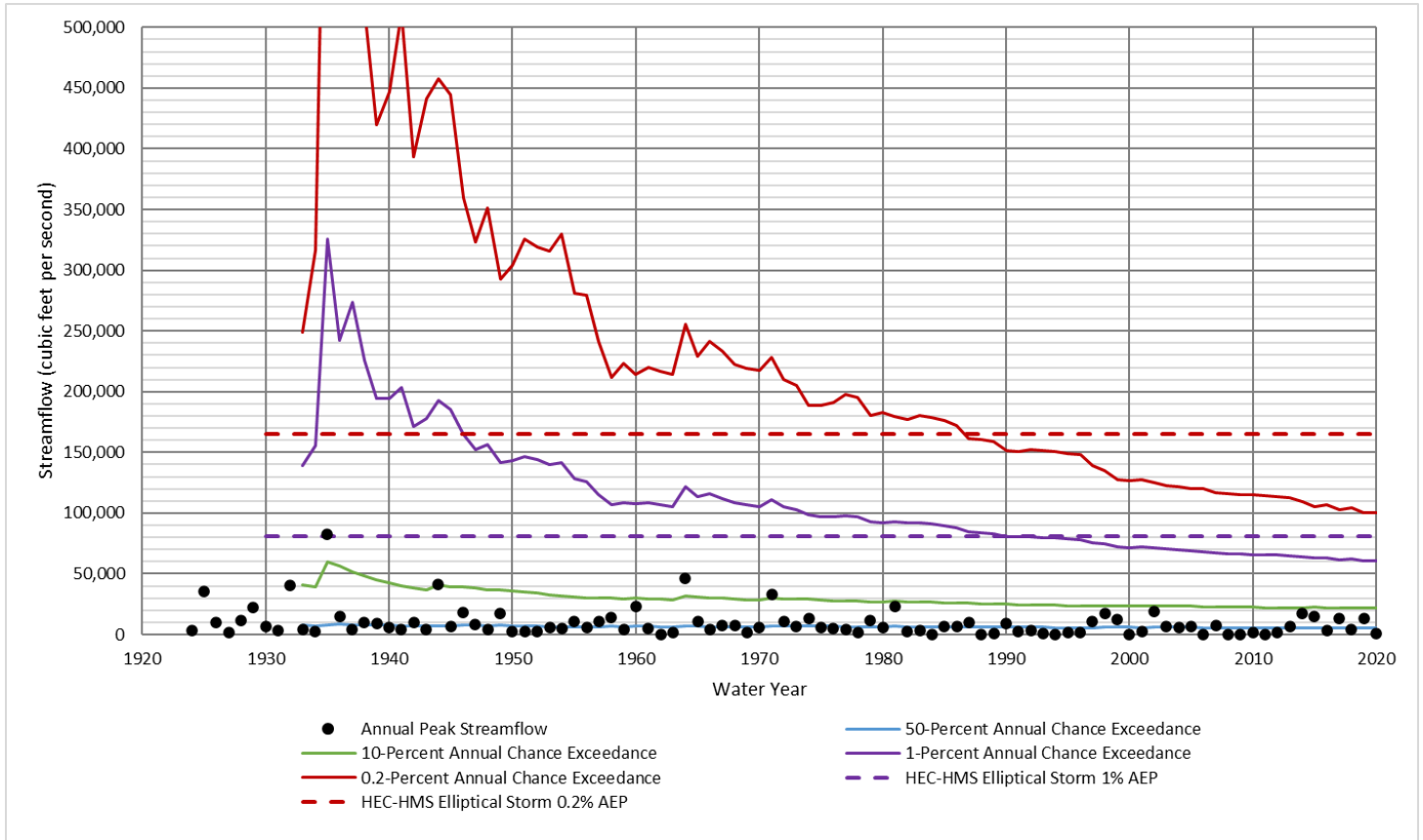


**Figure 11.5b: Statistical Change Over Time Comparison for Nueces River at Cotulla, TX**

The Nueces River at Cotulla has a drainage area of over 5,000 square miles and is located in an area of wide floodplains and irrigated fields. The period of record at USGS streamgauge 08194000 Nueces River at Cotulla, Texas was from 1924 through 2020. This gives the gage a relatively long period of record of 97 years.

Figure 11.5a shows that the HEC-HMS uniform rain results are significantly higher than both the statistical analysis of the gage record and the elliptical storm results at the 1% AEP event. This is to be expected since the uniform rain method overestimates the rainfall volume for large watersheds. The Elliptical storms results, on the other hand, show good agreement with the statistical estimates while diverging slightly higher for the rare frequencies.

Figure 11.5b shows a consistent downward trend in the statistical estimates starting in the 1930s, especially for the 1% and 0.2% AEP events. This is probably partially due to the fact that there have been no floods greater than a 10-year return interval since the 1970s, and as a result, the currently statistical estimates may be underestimating the 1% AEP flood potential of this location. This is another example of a location where the statistical estimates of the 1% AEP event still have not stabilized, even after almost 100 years of record. Figure 11.5b also shows that the HEC-HMS elliptical storm results for the 1% AEP event lines up well with the largest flood recorded in almost 100 years and with the center of the variation in statistical estimates over the past 60 years.

Table 11.6: Frequency Flow (cfs) Results Comparisons for San Casimiro Creek nr Freer, TX

Annual Exceedance Probability (AEP)	Return Period (years)	Currently Effective FEMA FIS	BLE Data-Statistical Analysis	Statistical Analysis of the Gage Record (59 years)	HEC-HMS Uniform Rain Frequency Storm	HEC-HMS Elliptical Frequency Storm
0.002	500			231,000	100,219	90,799
0.005	200			137,000	78,567	69,929
0.01	100			89,900	62,042	56,916
0.02	50			57,000	46,497	42,865
0.04	25			34,600	33,553	32,312
0.1	10			16,200	16,291	15,916
0.2	5			8,100	7,844	7,818
0.5	2			2,250	2,309	2,591

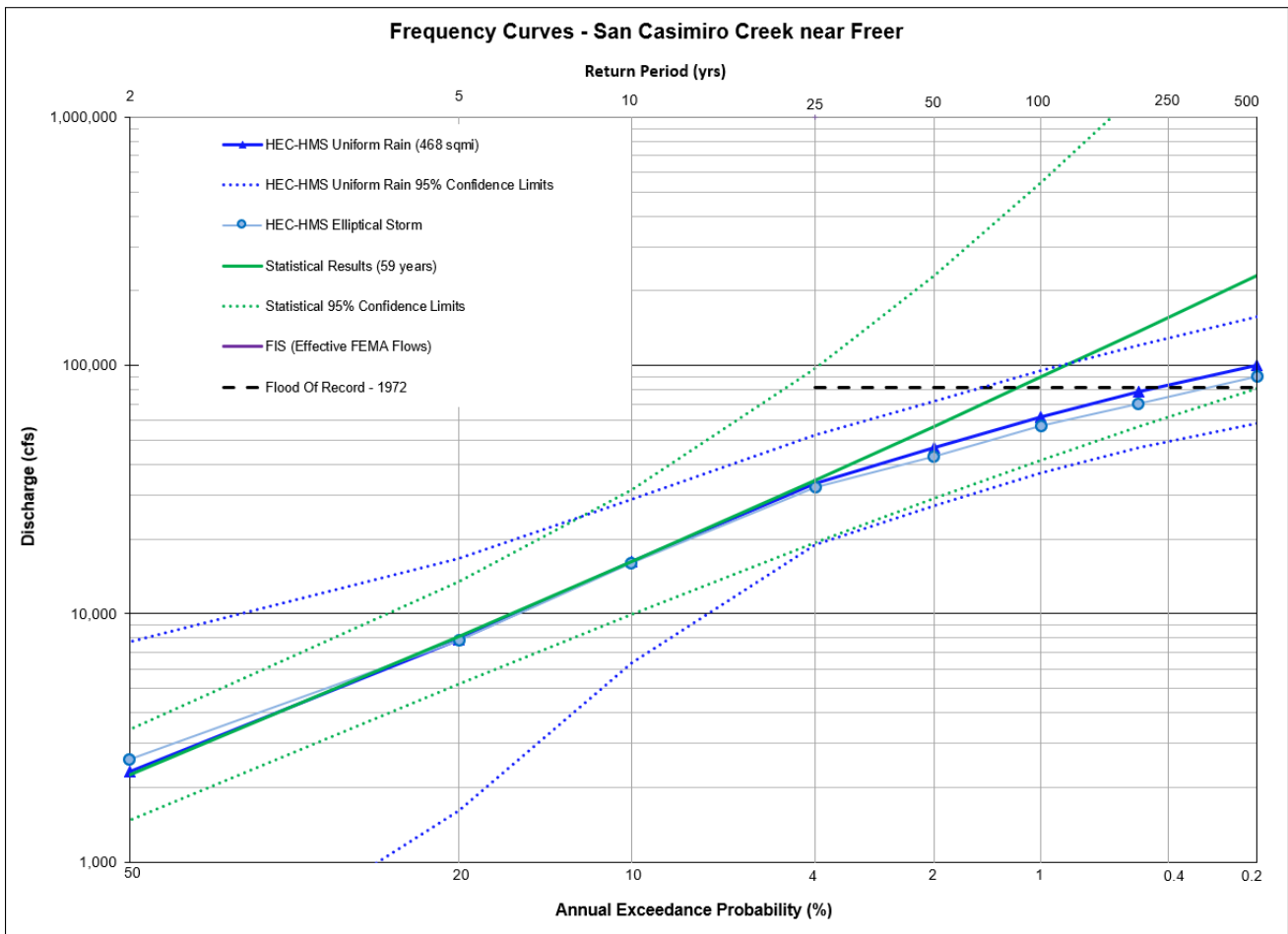
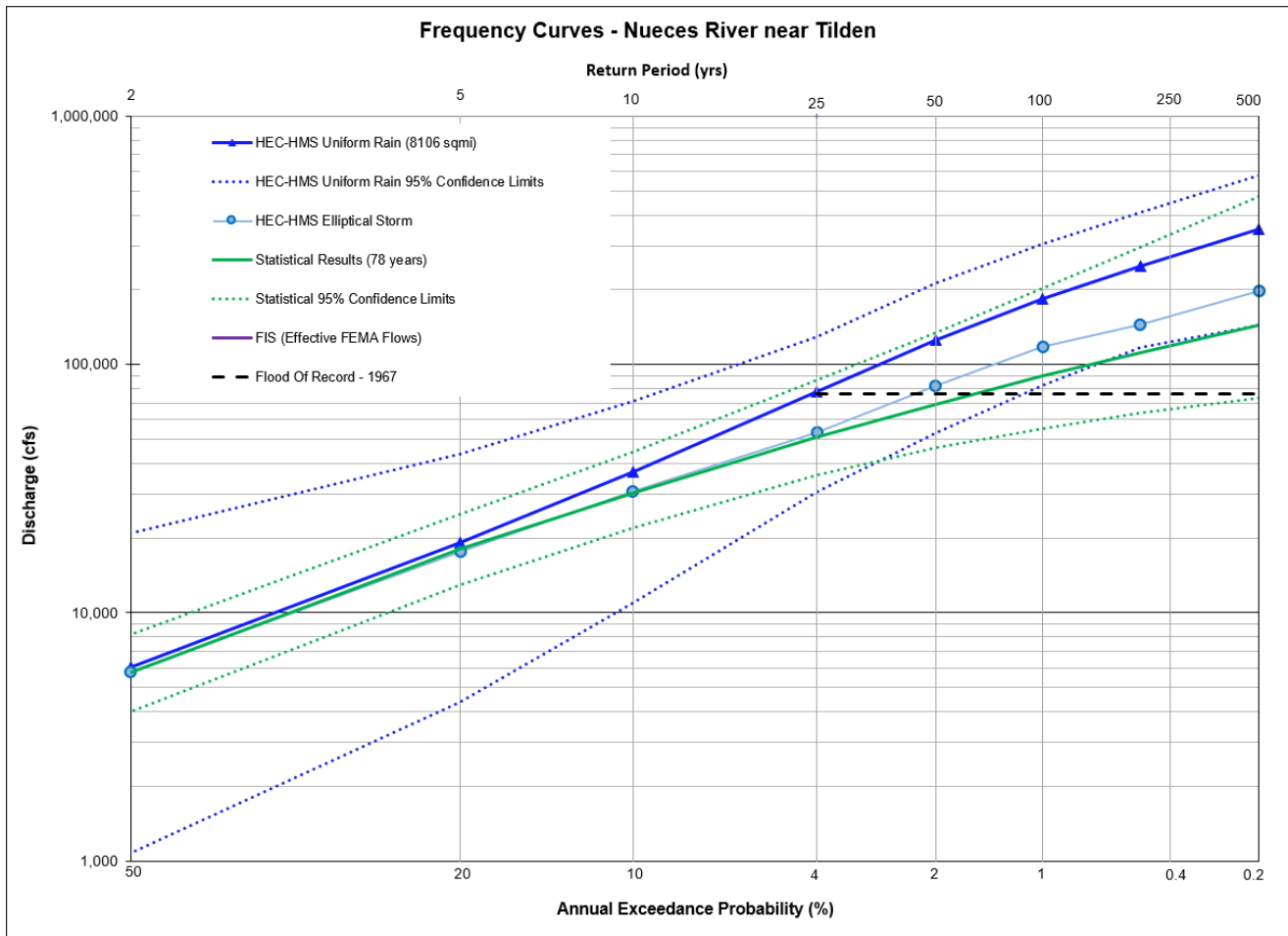


Figure 11.6: Flow Frequency Curve Comparison for San Casimiro Creek nr Freer, TX

San Casimiro Creek nr Freer has a drainage area of over 400 square miles and is located in the southern portion of the basin in an area with several irrigation dams upstream. The period of record at USGS streamgage 08194200 San Casimiro Creek near Freer, Texas was from 1962 through 2020. This gives the gage a moderate period of record of 59 years. Figure 11.6 shows that the HEC-HMS results from both uniform rain and the elliptical storms are significantly lower than the statistical analysis of the gage record at the 1% AEP event, but the results of both are still well within the statistical confidence bounds. The statistical analysis is showing good agreement with HEC-HMS through the 4% AEP (25-Year) frequency, only showing divergence at lesser frequencies, likely due to the limited period of record at this gage.

**Table 11.7: Frequency Flow (cfs) Results Comparisons for Nueces River nr Tilden, TX**

Annual Exceedance Probability (AEP)	Return Period (years)	Currently Effective FEMA FIS	BLE Data-Statistical Analysis	Statistical Analysis of the Gage Record (78 years)	HEC-HMS Uniform Rain Frequency Storm	HEC-HMS Elliptical Frequency Storm
0.002	500			144,000	349,374	196,969
0.005	200			112,000	249,840	144,633
0.01	100			89,600	183,670	117,619
0.02	50			69,200	125,132	82,146
0.04	25			51,000	77,814	53,142
0.1	10			30,500	36,996	30,699
0.2	5			18,000	19,112	17,604
0.5	2			5,770	6,040	5,755



**Figure 11.7a: Flow Frequency Curve Comparison for Nueces River nr Tilden, TX**

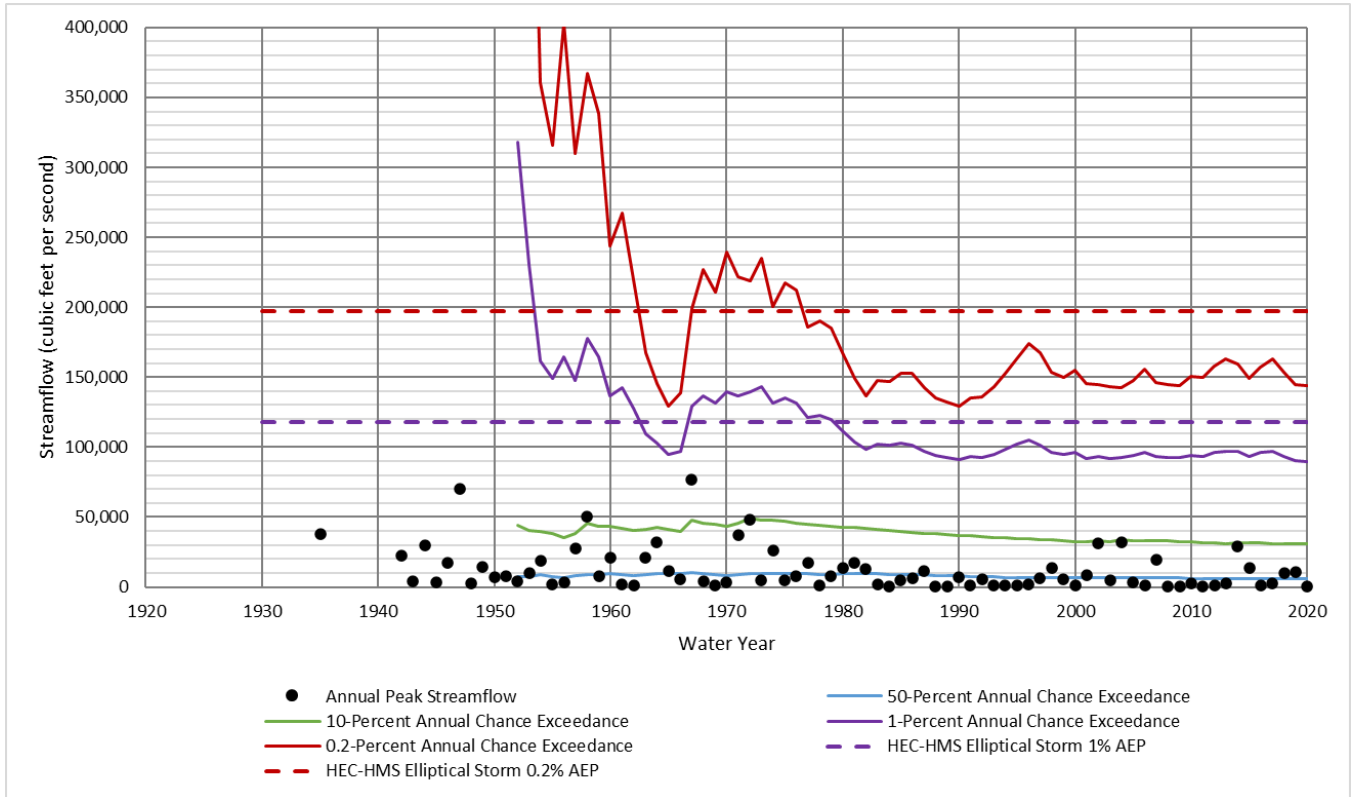


**Figure 11.7b: Statistical Change Over Time Comparison for Nueces River nr Tilden, TX**

The Nueces River near Tilden has a drainage area of over 8,000 square miles and is located in an area of wide floodplains and irrigated fields. The period of record at USGS streamgage 08194500 Nueces River near Tilden, Texas was from 1943 through 2020. This gives the gages a moderate period of record of 78 years. Both the HEC-HMS Uniform and Elliptical results are higher than the current statistical results based on 78 years of gage record, as shown in Figure 11.7a. This is likely because the largest flood of record occurred in 1967, and statistical estimates tend to trend downward if there are several decades without a large flood. However, as Figure 11.7a shows, the HEC-HMS results are still well within the confidence limits of the statistical analysis. Figure 11.7b shows that the HEC-HMS 1% AEP elliptical storm results fall within the range of variation in the statistical estimate over the past 70 years. While the 1% and 0.2% AEP statistical estimates on Figure 11.7b appear relatively stable over the past 30 years, one large flood event could significantly increase those estimates in the future.

**Table 11.8: Frequency Flow (cfs) Results Comparisons for Frio River at Concan, TX**

Annual Exceedance Probability (AEP)	Return Period (years)	Currently Effective FEMA FIS	BLE Data-Statistical Analysis	Statistical Analysis of the Gage Record (98 years)	HEC-HMS Uniform Rain Frequency Storm	HEC-HMS Elliptical Frequency Storm
0.002	500			190,000	271,833	254,215
0.005	200			163,000	219,180	203,643
0.01	100			140,000	181,245	176,792
0.02	50			116,000	142,434	137,608
0.04	25			89,900	103,368	102,611
0.1	10			55,800	60,214	60,944
0.2	5			32,000	33,259	34,597
0.5	2			8,030	7,958	9,269

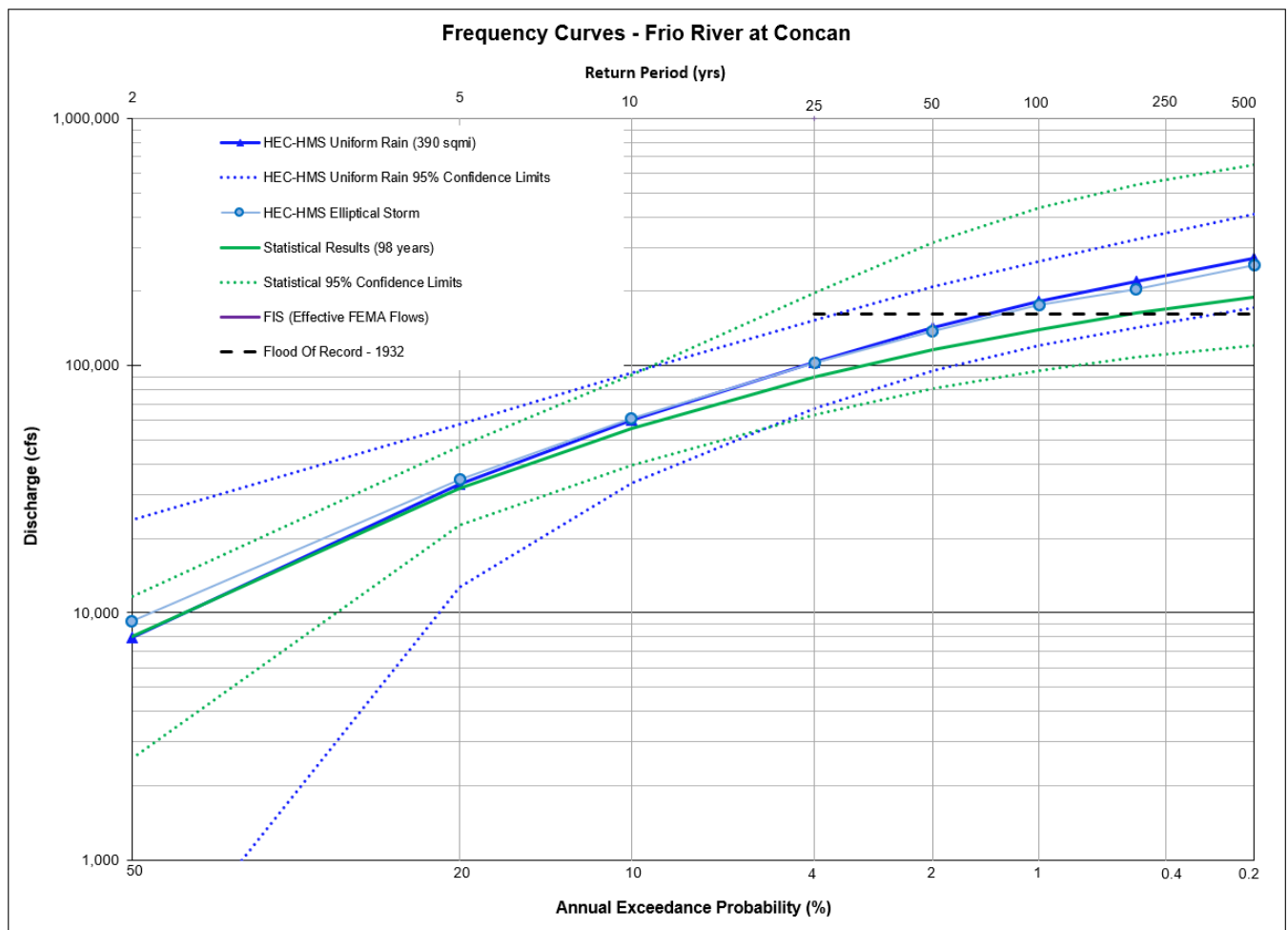


**Figure 11.8a: Flow Frequency Curve Comparison for Frio River at Concan, TX**

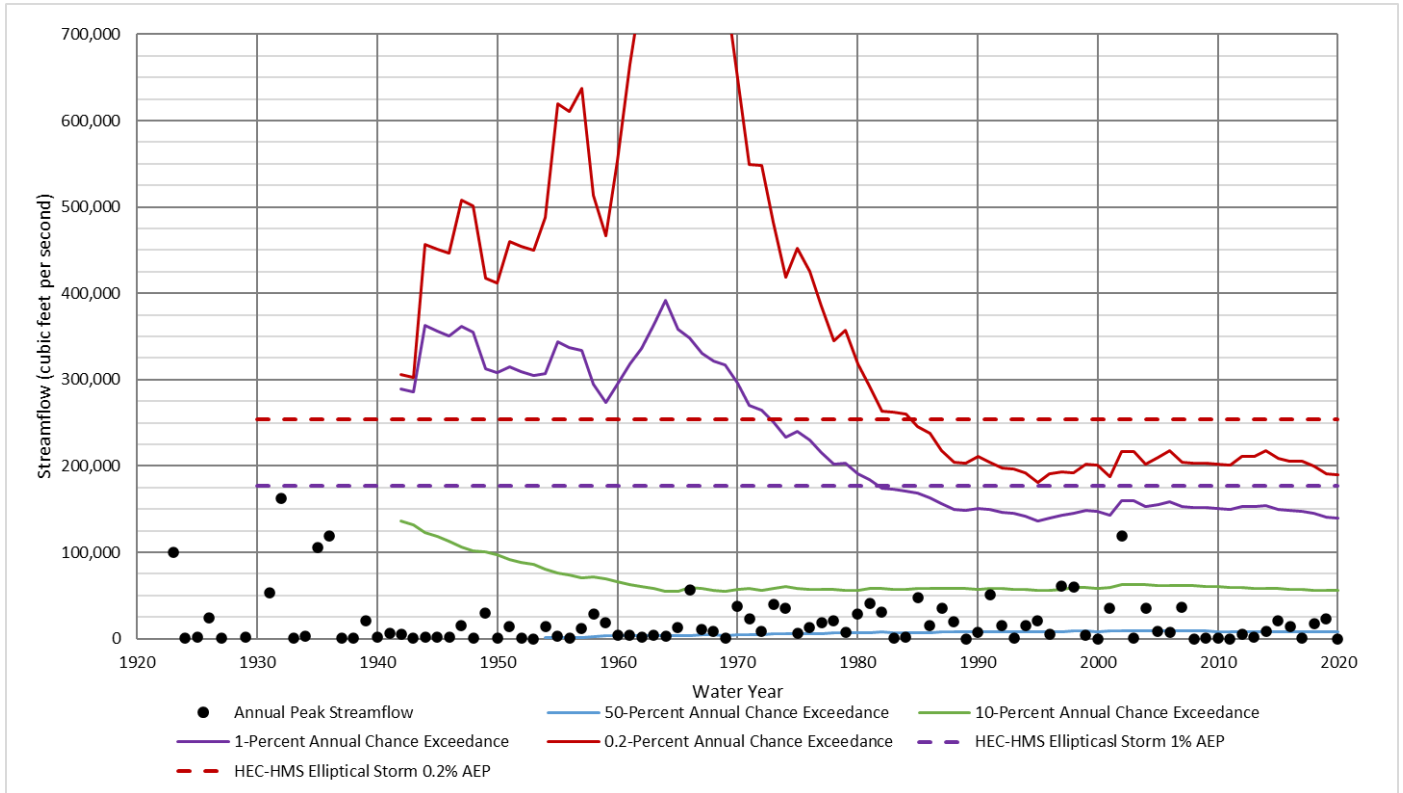


**Figure 11.8b: Statistical Change Over Time Comparison for Frio River at Concan, TX**

The Frio River at Concan has a drainage area of 390 square miles and is located in the steep headwaters portion of the basin. The period of record at USGS streamgage 08195000 Frio River at Concan, Texas was from 1923 through 2020. This gives the gage a relatively long period of record of 98 years. Figure 11.8a shows that the statistical analysis of the gage record based on 98 years of record are slightly lower than the HEC-HMS results for both uniform rainfall and elliptical storms. However, both sets of results generally show good agreement with each other and are still well within one another's confidence bounds.

Figure 11.8b illustrates the variation in the statistical estimates over the period of record and compares those results to the HEC-HMS results. As shown, the HEC-HMS results are well within the range of variation in the statistical estimates.

**Table 11.9: Frequency Flow (cfs) Results Comparisons for the Dry Frio River nr Reagan Wells, TX**

Annual Exceedance Probability (AEP)	Return Period (years)	Currently Effective FEMA FIS	BLE Data-Statistical Analysis	Statistical Analysis of the Gage Record (68 years)	HEC-HMS Uniform Rain Frequency Storm	HEC-HMS Elliptical Storm
0.002	500			232,000	132,003	
0.005	200			166,000	106,576	
0.01	100			123,000	88,957	
0.02	50			87,700	70,688	
0.04	25			58,700	52,968	
0.1	10			30,000	29,987	
0.2	5			15,100	15,220	
0.5	2			3,440	3,510	

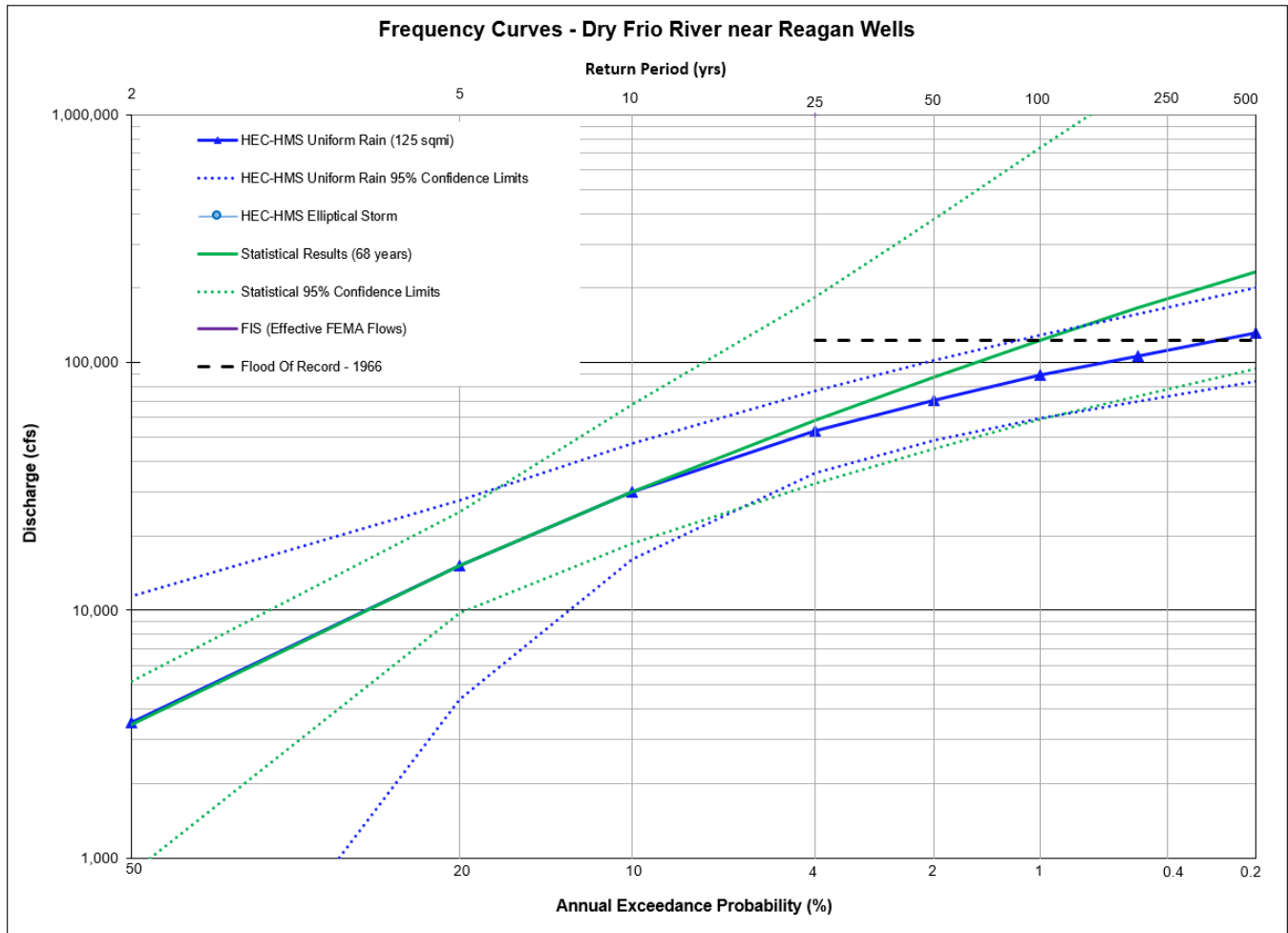


**Figure 11.9: Flow Frequency Curve Comparison for the Dry Frio River nr Reagan Wells, TX**

The Dry Frio River near Reagan Wells has a drainage area of 125 square miles and is located in the steep headwaters portion of the basin. The period of record at USGS streamgage 08196000 Dry Frio River near Reagan Wells, Texas was from 1953 through 2020. This gives the gage a moderate period of record of 68 years.

The statistical and HEC-HMS uniform rainfall analysis showed good agreement through the 10% AEP (10-Year) frequency and then started to slightly diverge. HEC-HMS uniform rain is within the statistical confidence limits, but the statistical results are slightly higher than the HEC-HMS confidence limits. This is likely due to the fact the largest peak in the gaged period of record is the 1966 peak streamflow of 123,000 cfs at a stage of 27.60 ft and it may be skewing the statistical results high due to a period of record of only 68 years.

**Table 11.10: Frequency Flow (cfs) Results Comparisons for the Frio River nr Uvalde, TX**

Annual Exceedance Probability (AEP)	Return Period (years)	Currently Effective FEMA FIS	BLE Data-Statistical Analysis	Statistical Analysis of the Gage Record (69 years)	HEC-HMS Uniform Rain Frequency Storm	HEC-HMS Elliptical Frequency Storm
0.002	500			266,000	358,897	324,606
0.005	200			228,000	286,033	257,458
0.01	100			195,000	234,073	221,566
0.02	50			159,000	181,018	170,689
0.04	25			122,000	130,654	127,166
0.1	10			72,900	74,502	73,981
0.2	5			39,800	39,832	40,537
0.5	2			8,560	8,590	10,136

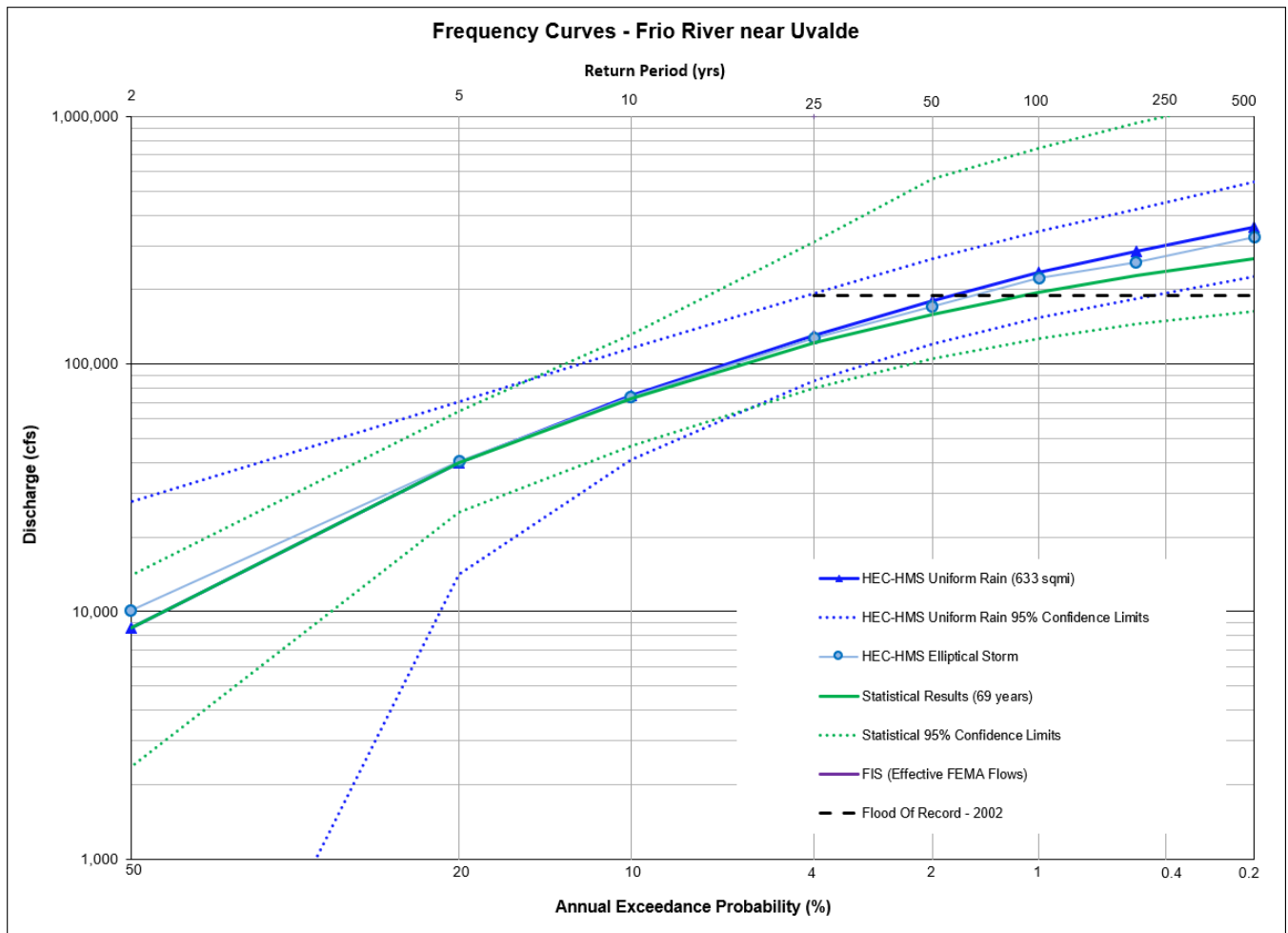


**Figure 11.10a: Flow Frequency Curve Comparison for the Frio River nr Uvalde, TX**

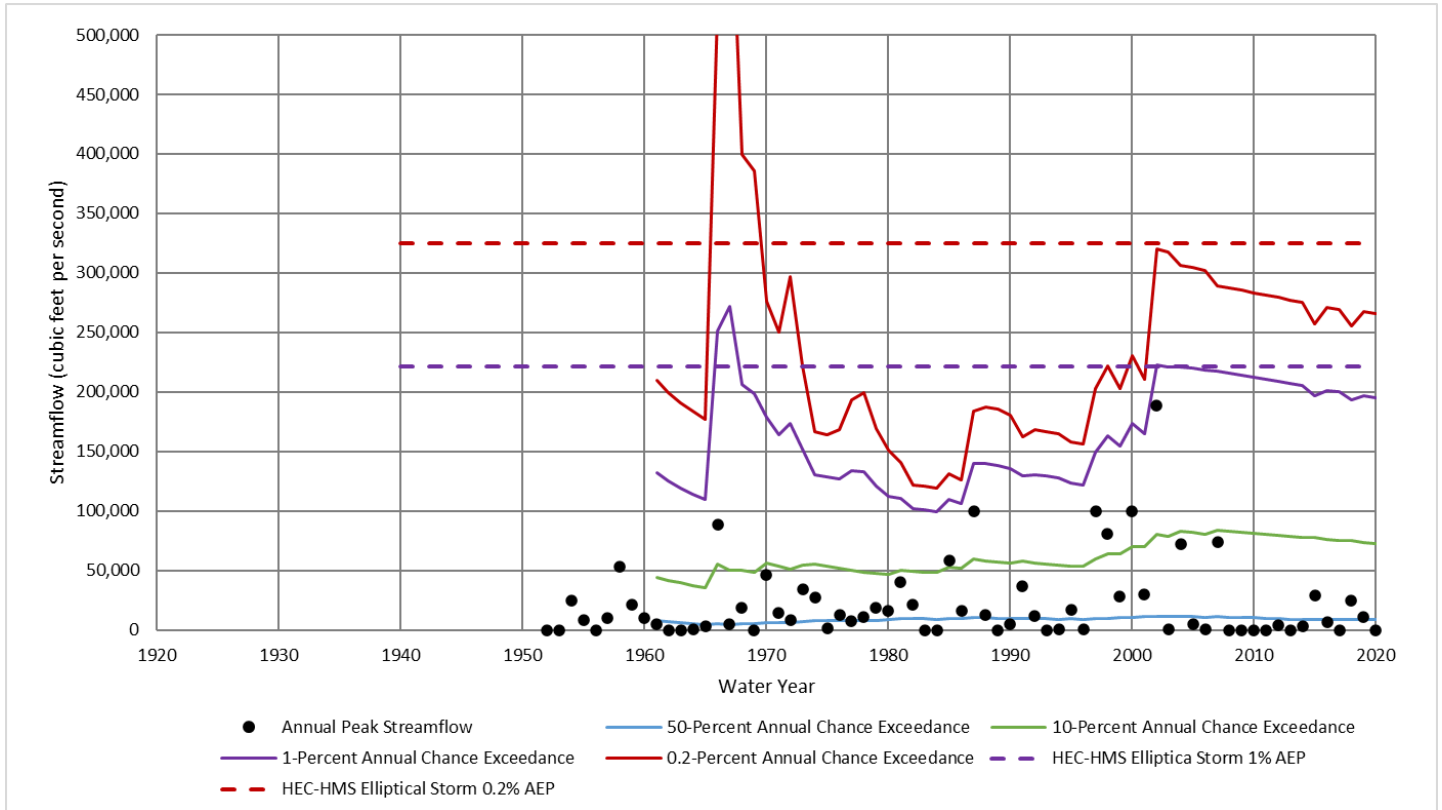


**Figure 11.10b: Statistical Change Over Time Comparison for the Frio River nr Uvalde, TX**

The Frio River nr Uvalde has a drainage area of over 600 square miles and is located in the steep headwaters portion of the basin. The period of record at USGS streamgauge 08197500 Frio River below Dry Frio River near Uvalde, Texas was from 1952 through 2020. This gives the gage a moderate period of record of 69 years.

The statistical analysis, the HEC-HMS uniform rainfall, and HEC-HMS elliptical storms are all showing relatively good agreement with another, as shown on Figure 11.10a. The HEC-HMS uniform rain is well within the confidence boundaries for the statistical analysis, and the statistical analysis falls within the confidence boundaries of HEC-HMS uniform rain. As seen in Figure 11.10a, the HEC-HMS elliptical storm falls right in between those two analyses for the 1% AEP (100-Year) frequency. Figure 11.10b shows that after 68 years, there is still quite a bit of variation in the statistical estimates over time, and the HEC-HMS results fall within that range of variation.

**Table 11.11: Frequency Flow (cfs) Results Comparisons for the Sabinal River nr Sabinal, TX**

Annual Exceedance Probability (AEP)	Return Period (years)	Currently Effective FEMA FIS	BLE Data-Statistical Analysis	Statistical Analysis of the Gage Record (78 years)	HEC-HMS Uniform Rain Frequency Storm	HEC-HMS Elliptical Frequency Storm
0.002	500			142,000	179,307	
0.005	200			103,000	143,564	
0.01	100			78,400	118,374	
0.02	50			58,400	92,318	
0.04	25			42,100	59,472	
0.1	10			25,400	31,294	
0.2	5			15,800	18,385	
0.5	2			6,320	6,589	

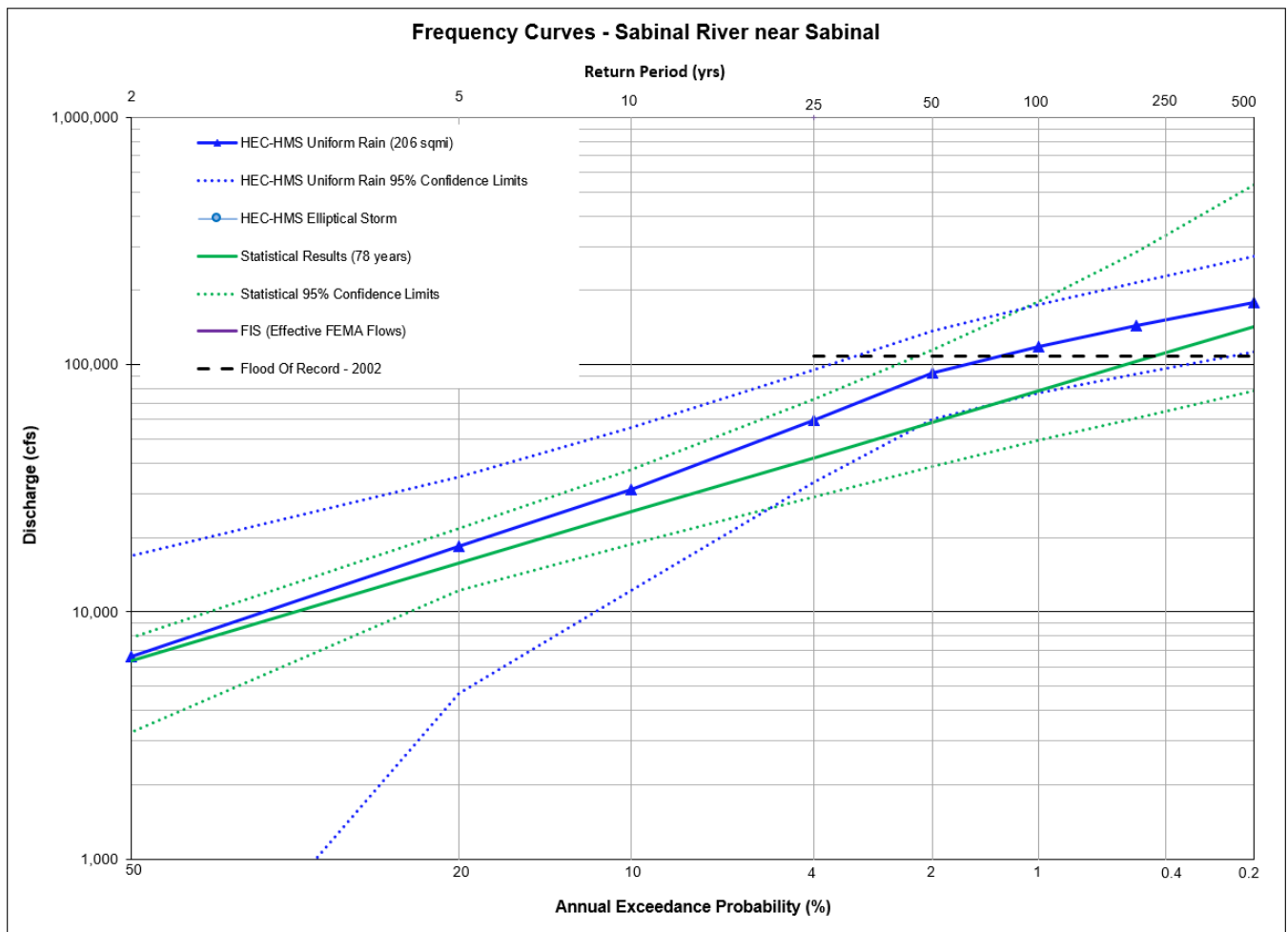


**Figure 11.11: Flow Frequency Curve Comparison for the Sabinal River nr Sabinal, TX**

The Sabinal River nr Sabinal has a drainage area of over 200 square miles and is located in the steep headwaters portion of the basin. The period of record at USGS streamgage 08198000 Sabinal River near Sabinal is from 1943 through 2020. This gives the gage a moderate period of record of 78 years.

The statistical analysis and the HEC-HMS uniform rainfall results are showing good agreement with one another. As seen in Figure 11.11, the HEC-HMS uniform rain is well within the confidence boundaries for the statistical analysis, and the statistical analysis falls within the confidence boundaries of HEC-HMS uniform rain.

**Table 11.12: Frequency Flow (cfs) Results Comparisons for the Sabinal River at Sabinal, TX**

Annual Exceedance Probability (AEP)	Return Period (years)	Currently Effective FEMA FIS	BLE Data-Statistical Analysis	Statistical Analysis of the Gage Record (68 years)	HEC-HMS Uniform Rain Frequency Storm	HEC-HMS Elliptical Frequency Storm
0.002	500			177,000	180,214	
0.005	200			134,000	143,304	
0.01	100			105,000	117,451	
0.02	50			79,300	90,811	
0.04	25			57,100	58,582	
0.1	10			33,200	30,982	
0.2	5			19,200	18,032	
0.5	2			5,990	6,077	

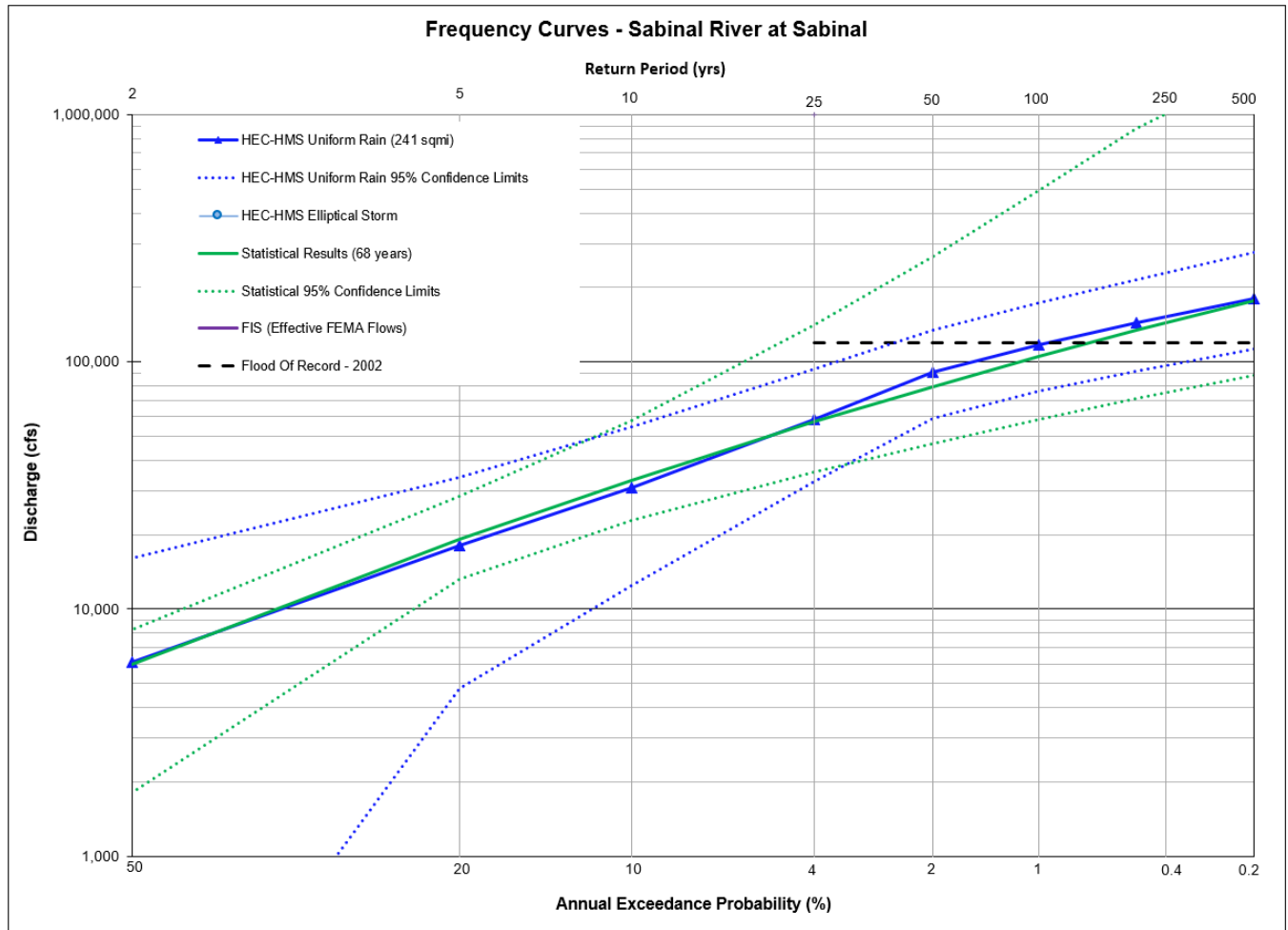


**Figure 11.12: Flow Frequency Curve Comparison for the Sabinal River at Sabinal, TX**

The Sabinal River at Sabinal has a drainage area of over 240 square miles and is located in the steep headwaters portion of the basin. The period of record at USGS streamgage 08198500 Sabinal River at Sabinal, Texas was from 1953 through 2020. This gives the gage a moderate period of record of 68 years.

The statistical analysis and the HEC-HMS uniform rainfall results show excellent agreement with one another. As seen in Figure 11.12, the HEC-HMS Uniform rain is well within the confidence boundaries for the statistical analysis, and the statistical analysis falls within the confidence boundaries of HMS Uniform rain.

**Table 11.13: Frequency Flow (cfs) Results Comparisons for Hondo Creek nr Tarpley, TX**

Annual Exceedance Probability (AEP)	Return Period (years)	Currently Effective FEMA FIS	BLE Data-Statistical Analysis	Statistical Analysis of the Gage Record (68 years)	HEC-HMS Uniform Rain Frequency Storm	HEC-HMS Elliptical Frequency Storm
0.002	500			152,000	142,791	
0.005	200			123,000	117,810	
0.01	100			100,000	99,869	
0.02	50			78,600	80,840	
0.04	25			58,100	63,130	
0.1	10			33,900	37,593	
0.2	5			18,900	19,988	
0.5	2			4,820	4,841	

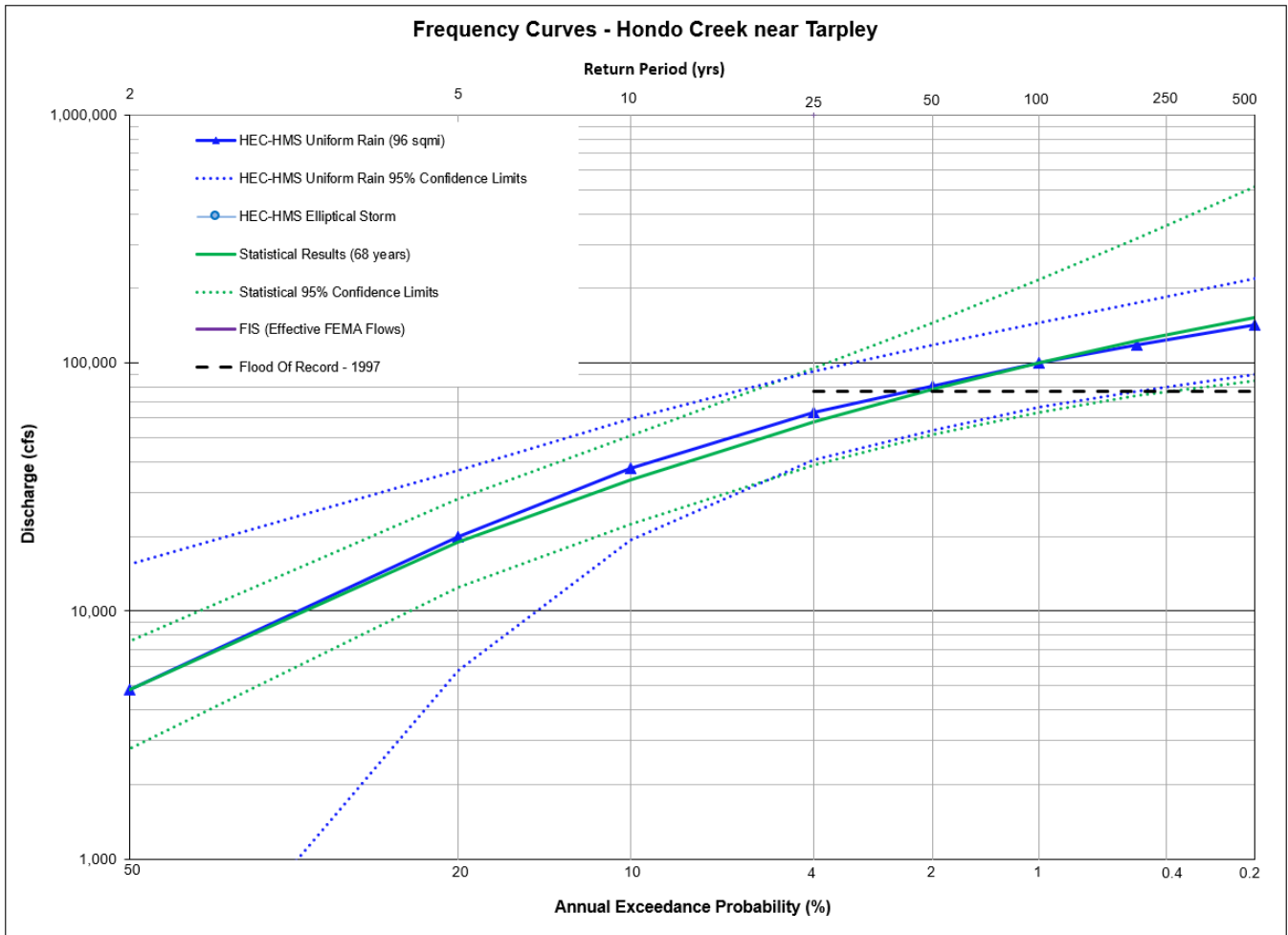


**Figure 11.13: Flow Frequency Curve Comparison for Hondo Creek nr Tarpley, TX**

The Hondo Creek nr Tarpley has a drainage area of just under 100 square miles and is located in the steep headwaters portion of the basin. The period of record at USGS streamgage 08200000 Hondo Creek near Tarpley, Texas was from 1953 through 2020. This gives the gage a moderate period of record of 68 years.

The statistical analysis and the HEC-HMS uniform rainfall show excellent agreement with one another. As seen in Figure 11.13, the HMS Uniform rain is well within the confidence boundaries for the statistical analysis, and the statistical analysis falls within the confidence boundaries of HMS Uniform rain.

**Table 11.14: Frequency Flow (cfs) Results Comparisons for Hondo Creek nr Hondo, TX**

Annual Exceedance Probability (AEP)	Return Period (years)	Currently Effective FEMA FIS	BLE Data-Statistical Analysis	Statistical Analysis of the Gage Record (45 years)	HEC-HMS Uniform Rain Frequency Storm	HEC-HMS Elliptical Frequency Storm
0.002	500	125,000		126,000	150,096	
0.005	200			110,000	121,859	
0.01	100	76,080		96,500	101,632	
0.02	50	57,970		81,000	80,344	
0.04	25			64,200	61,134	
0.1	10	30,010		41,100	36,046	
0.2	5			24,200	19,853	
0.5	2			6,370	5,175	

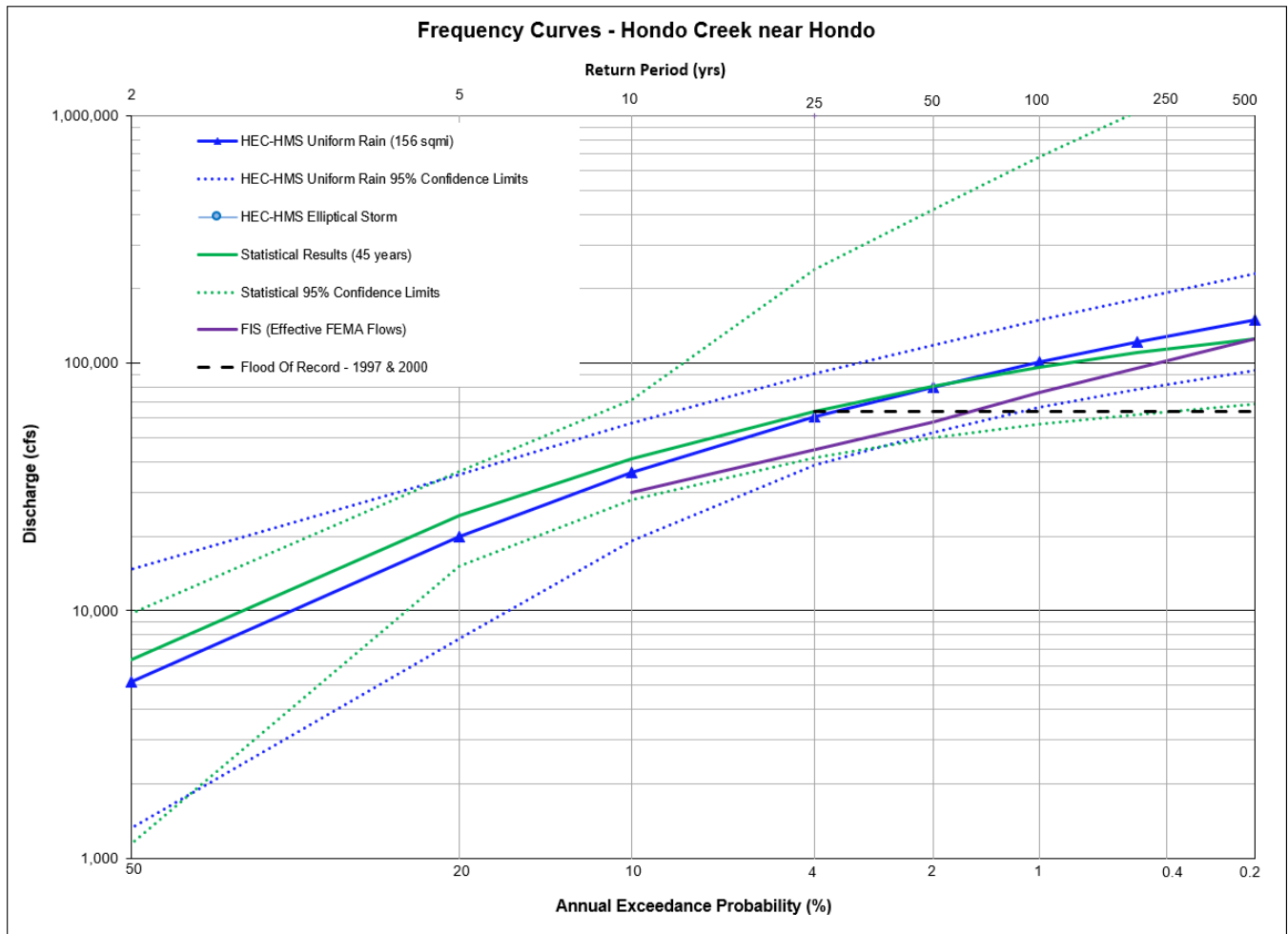


**Figure 11.14: Flow Frequency Curve Comparison for Hondo Creek nr Hondo, TX**

Hondo Creek near Hondo has a drainage area of over 150 square miles and is located in the steep headwaters portion of the basin. The period of record at USGS streamgage 08200720 Hondo Creek at S.H. 173 near Hondo, Texas was from 1961 through 2005. This gives the gage a moderate period of record of 45 years.

The statistical analysis and the HEC-HMS uniform rainfall results show excellent agreement with one another. As seen in Figure 11.14, the HMS Uniform rain is well within the confidence boundaries for the statistical analysis, and the statistical analysis falls within the confidence boundaries of HEC-HMS uniform rain. Both of these analyses are significantly higher than the currently effective FEMA FIS flows. The effective FEMA flows at this location were from the Medina County FIS and were based on a 1978 HEC-1 rainfall runoff analysis which did not have the benefit of modern rainfall or gage data for calibration.

**Table 11.15: Frequency Flow (cfs) Results Comparisons for Seco Creek at Miller RH nr Utopia, TX**

Annual Exceedance Probability (AEP)	Return Period (years)	Currently Effective FEMA FIS	BLE Data-Statistical Analysis	Statistical Analysis of the Gage Record (59 years)	HEC-HMS Uniform Rain Frequency Storm	HEC-HMS Elliptical Frequency Storm
0.002	500	150,000		132,000	92,663	
0.005	200			103,000	77,412	
0.01	100	91,000		81,000	66,346	
0.02	50	68,200		60,800	55,346	
0.04	25			42,700	44,588	
0.1	10	36,100		22,800	25,420	
0.2	5			11,500	11,601	
0.5	2			2,340	2,429	

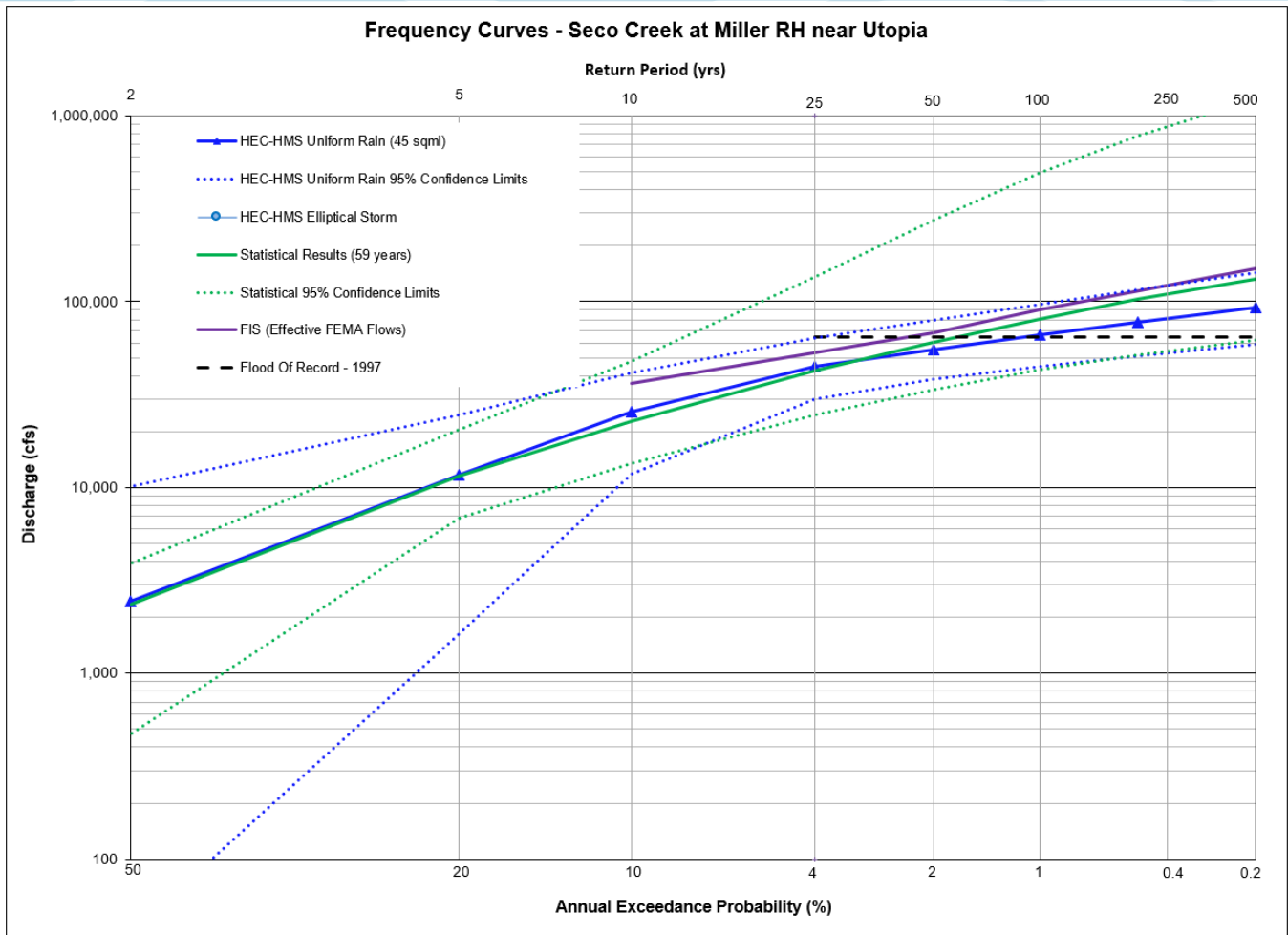


**Figure 11.15: Flow Frequency Curve Comparison for Seco Creek at Miller RH nr Utopia, TX**

Seco Creek at Miller RH near Utopia has a drainage area of just 45 square miles and is located in the steep headwaters portion of the basin. The period of record at USGS streamgauge 08201500 Seco Creek at Miller Ranch near Utopia, Texas was from 1962 through 2020. This gives the gage a moderate period of record of 59 years.

The statistical analysis and the HEC-HMS uniform rainfall results show excellent agreement through the 2% AEP (50-yr) event. For the rarer 1% and 0.2% AEP events, the HEC-HMS results are slightly lower than the current statistical results. Both analyses are well within one another’s confidence bounds. The 1% AEP HEC-HMS estimate also coincides well with the 1997 flood of record, which was one of the calibration events.

The currently effective FEMA flows are higher than both the statistical and HEC-HMS results. The effective FEMA flows at this location were from the Medina County FIS and were based on a 1978 HEC-1 rainfall runoff analysis which did not have the benefit of modern rainfall or gage data for calibration.

**Table 11.16: Frequency Flow (cfs) Results Comparisons for Seco Creek Rowe RH nr D'Hanis, TX**

Annual Exceedance Probability (AEP)	Return Period (years)	Currently Effective FEMA FIS	BLE Data-Statistical Analysis	Statistical Analysis of the Gage Record (60 years)	HEC-HMS Uniform Rain Frequency Storm	HEC-HMS Elliptical Frequency Storm
0.002	500			154,000	134,588	
0.005	200			127,000	108,642	
0.01	100			105,000	90,484	
0.02	50			82,600	71,688	
0.04	25			60,200	54,656	
0.1	10			33,100	32,474	
0.2	5			16,600	17,003	
0.5	2			2,940	2,994	

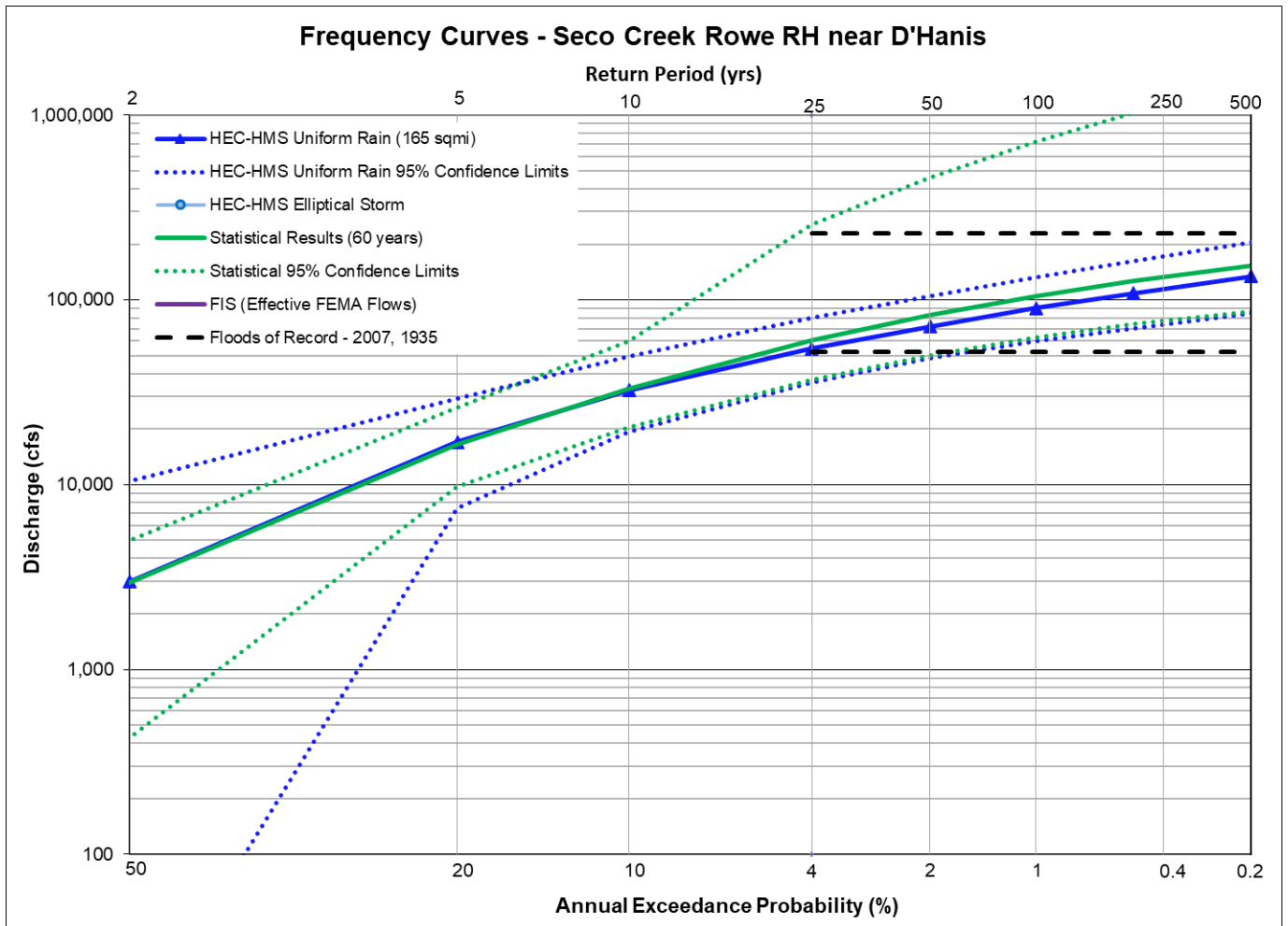


**Figure 11.16: Flow Frequency Curve Comparison for Seco Creek Rowe RH nr D'Hanis, TX**

Seco Creek at Miller Rowe RH near D'Hanis has a drainage area of 165 square miles and is located in the steep headwaters portion of the basin. The period of record at USGS streamgage 08202700 Seco Creek at Rowe Ranch near D'Hanis, Texas was from 1961 through 2020. This gives the gage a moderate period of record of 60 years. The peak streamflow for the 1935 flooding event was computed as 230,000 cfs by Dalrymple (1939). However, the 1935 flood was an extreme event at this location, as over 22 inches of rain fell in less than 3 hours near D'Hanis, Texas (Dalrymple, 1939).

The statistical analysis and the HEC-HMS uniform rainfall results show good agreement one another. The HEC-HMS results for the 1% AEP are slightly lower than the statistical results. As seen in Figure 11.16, the HEC-HMS uniform rain is well within the confidence boundaries for the statistical analysis, and the statistical analysis falls within the confidence boundaries of HEC-HMS uniform rain.

**Table 11.17: Frequency Flow (cfs) Results Comparisons for Frio River nr Derby, TX**

Annual Exceedance Probability (AEP)	Return Period (years)	Currently Effective FEMA FIS	BLE Data-Statistical Analysis	Statistical Analysis of the Gage Record (105 years)	HEC-HMS Uniform Rain Frequency Storm	HEC-HMS Elliptical Frequency Storm
0.002	500		166000	245,000	505,982	267,574
0.005	200			159,000	377,514	196,828
0.01	100		93,500	112,000	286,002	159,274
0.02	50		69,100	76,100	204,470	107,132
0.04	25		48,700	49,900	117,508	63,405
0.1	10		27,500	26,200	52,047	25,957
0.2	5			14,400	26,801	14,326
0.5	2			4,740	6,190	4,691

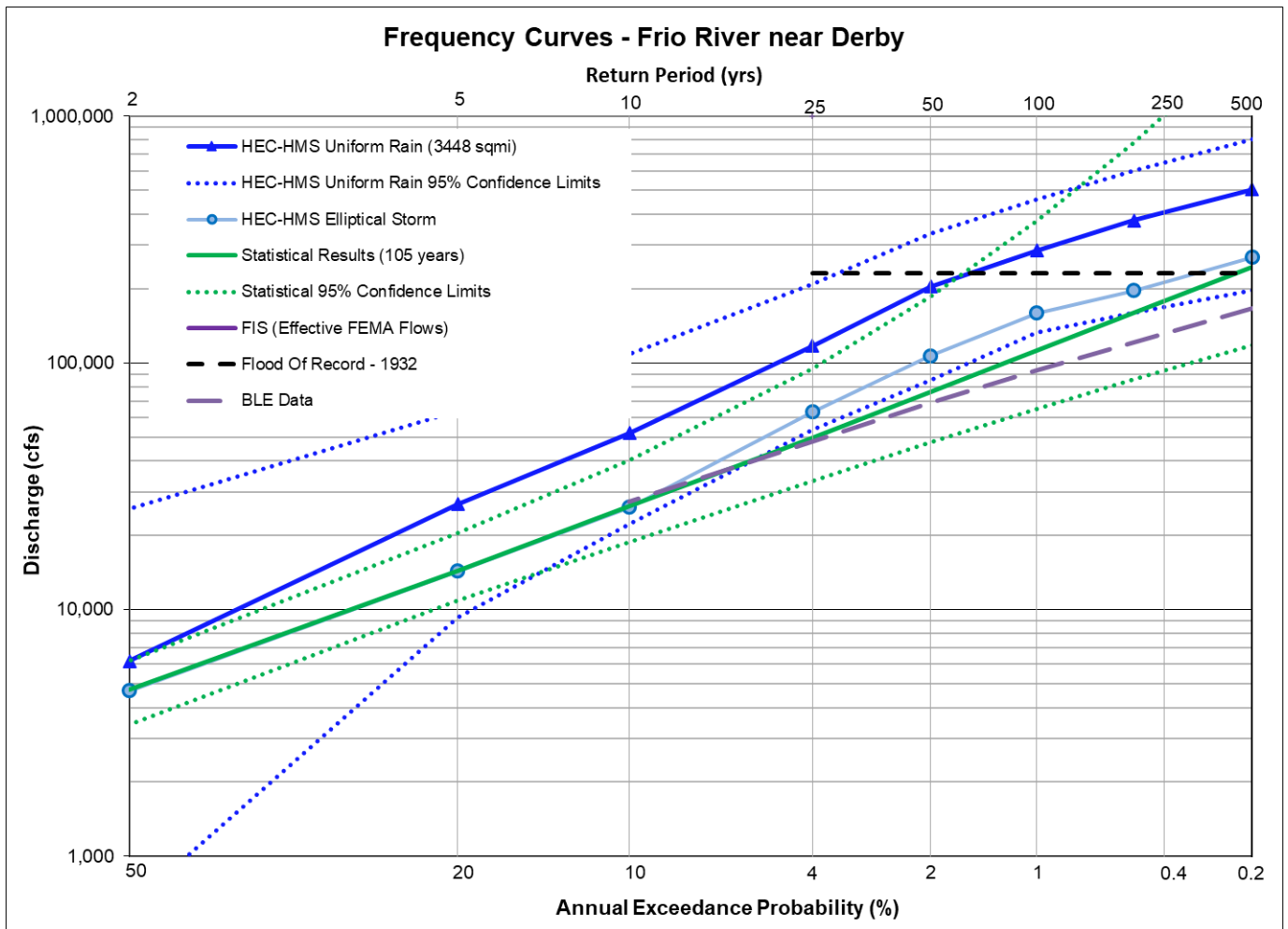


**Figure 11.17a: Flow Frequency Curve Comparison for Frio River nr Derby, TX**

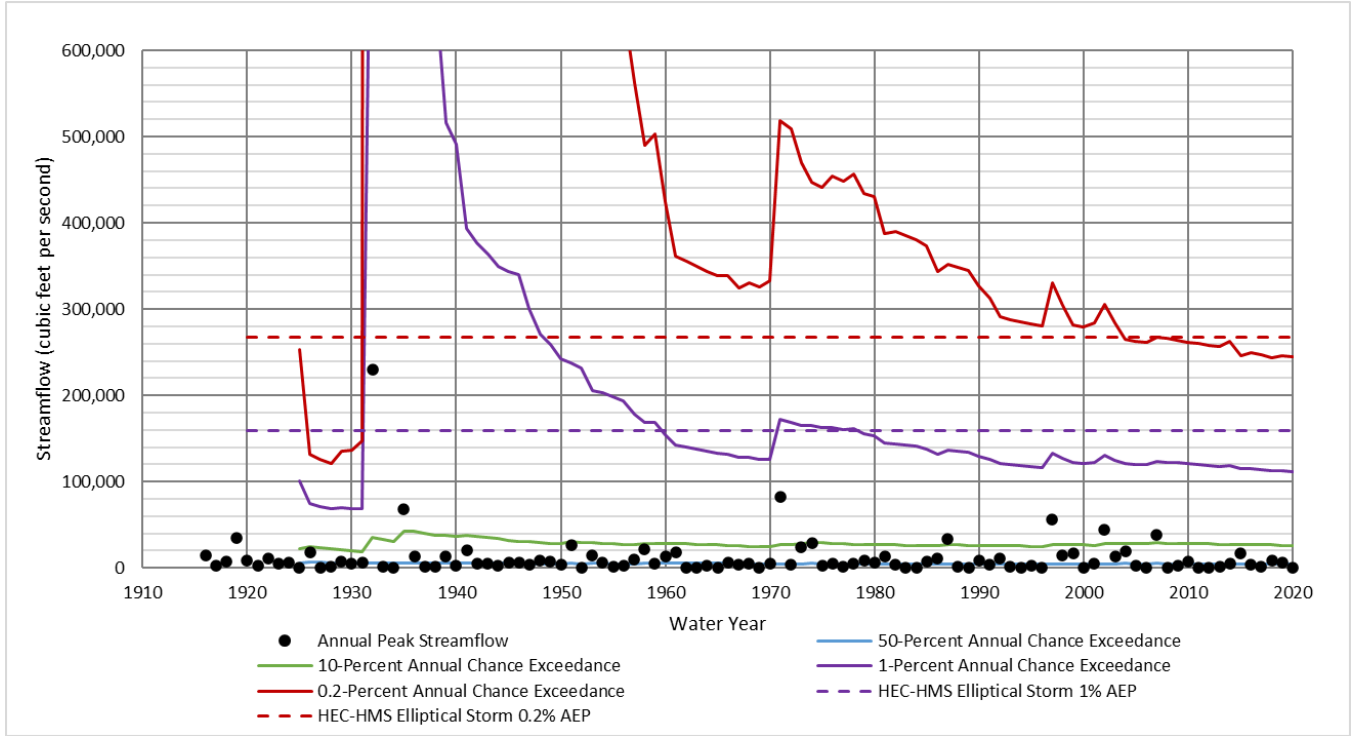


**Figure 11.17b: Statistical Change Over Time Comparison for Frio River nr Derby, TX**

The Frio River near Derby has a drainage area of over 3,000 square miles and is located in an area of wide, irrigated floodplains downstream of the aquifer outcrops. The period of record at USGS streamgage 08205500 Frio River near Derby, Texas was from 1916 through 2020. This gives the gage a relatively long period of record of 104 years.

The statistical analysis and the HEC-HMS elliptical storm results show good agreement with one another, the HEC-HMS results being slightly higher for the 1% AEP event. As seen in Figure 11.17a, the HEC-HMS elliptical storm results are well within the confidence boundaries for the statistical analysis. Figure 11.17b shows the variation in the statistical estimates over time. From this figure, one can see that even with 100 years of record, the statistical estimates for the 1% and 0.2% AEPs are still a moving target. This figure also shows that the HEC-HMS elliptical storm results fall within the range of variation in the statistical estimates over the past 60 years.

**Table 11.18: Frequency Flow (cfs) Results Comparisons for the Frio River at Tilden, TX**

Annual Exceedance Probability (AEP)	Return Period (years)	Currently Effective FEMA FIS	BLE Data-Statistical Analysis	Statistical Analysis of the Gage Record (42 years)	Alternate Statistical Analysis of the Gage Record (96 years)	HEC-HMS Uniform Rain Frequency Storm	HEC-HMS Elliptical Frequency Storm
0.002	500		47400	67,000	96,700	439,273	216,335
0.005	200			53,000	72,500	325,378	144,078
0.01	100		32,000	43,000	56,700	245,682	108,645
0.02	50		25,700	33,700	43,200	168,043	59,486
0.04	25		19,800	25,200	31,600	81,531	31,432
0.1	10		12,700	15,300	19,100	24,827	14,222
0.2	5			9,150	11,700	10,742	8,424
0.5	2			2,950	4,350	3,005	2,778

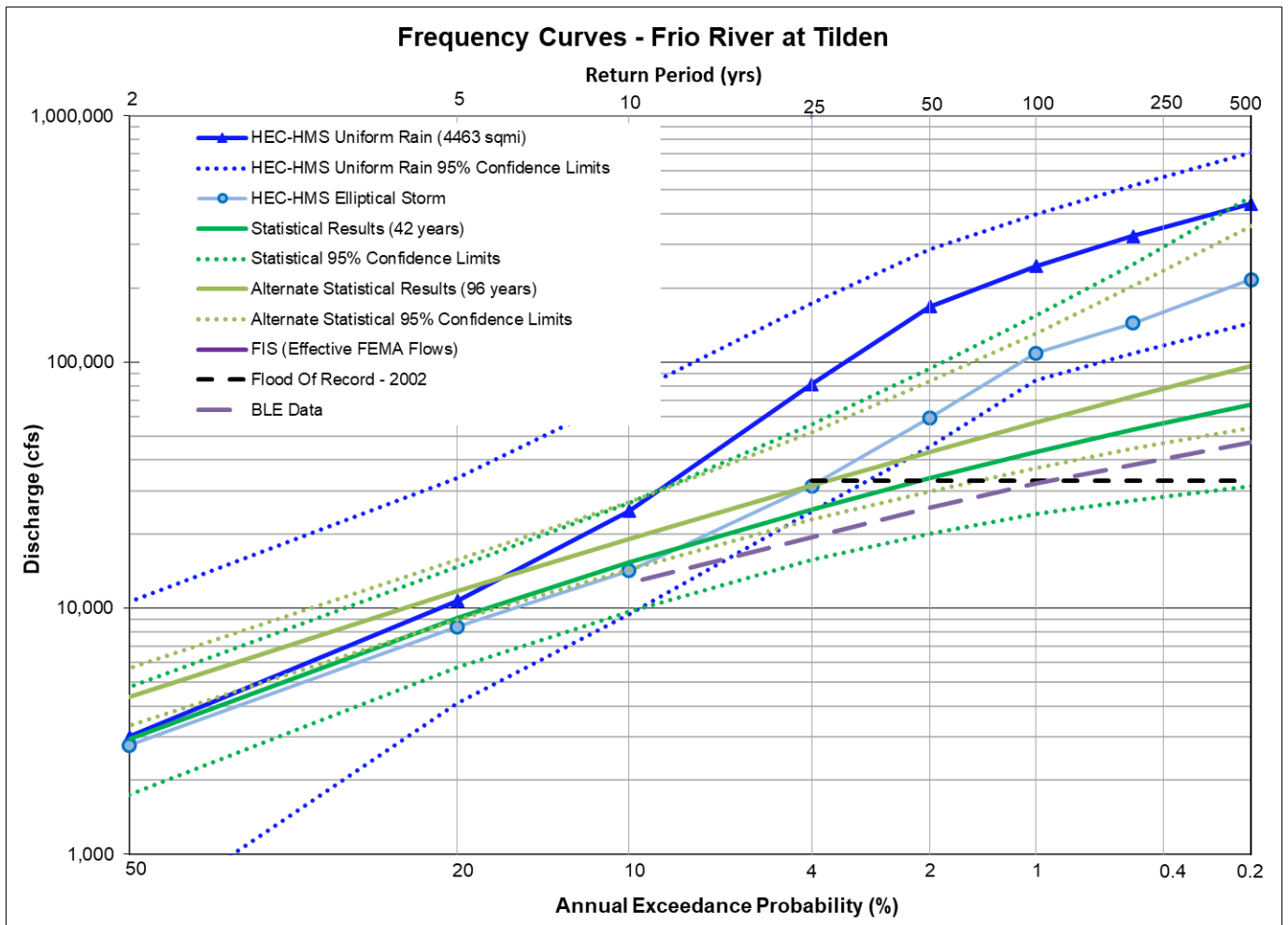


**Figure 11.18: Flow Frequency Curve Comparison for the Frio River at Tilden, TX**

The Frio River at Tilden has a drainage area of over 4,400 square miles and is located in an area of wide, irrigated floodplains. The period of record at USGS streamgage 08206600 Frio River at Tilden, Texas was from 1979 through 2020. This gives the gage a moderate period of record of 42 years. An alternate statistical analysis was performed at this site which used the upstream and downstream gage records to extend the period of record at Tilden to 96 years, as shown on Figure 11.18. The extended period of record analysis increased the frequency discharge estimates across the board.

The HEC-HMS uniform rainfall results overestimate the peak discharges due to the large drainage area at this location. The HEC-HMS elliptical storm results are very similar to the statistical results for the frequent events, and then they trend higher than the statistical results for the rare frequencies. However, the elliptical storm results are still well within the uncertainty bounds of the statistical estimates. In addition, the current statistical estimates may be underestimated since the gage has not experienced a large flood in recent decades.

Peak discharges from Base Level Engineering (BLE) data were also available at this location. Figure 11.18 shows that the BLE peak discharges were significantly lower than all of the other analyses. In fact, the BLE peak discharges fall below the lower confidence bounds of some of the statistical and HEC-HMS results. This is an indication that the BLE discharges are significantly underestimated at this location. The BLE data for the Frio River was published using 1D HEC-RAS models and hydrology from a gage statistical analysis.

**Table 11.19: Frequency Flow (cfs) Results Comparisons for San Miguel Creek nr Tilden, TX**

Annual Exceedance Probability (AEP)	Return Period (years)	Currently Effective FEMA FIS	BLE Data-Statistical Analysis	Statistical Analysis of the Gage Record (57 years)	HEC-HMS Uniform Rain Frequency Storm	HEC-HMS Elliptical Frequency Storm
0.002	500		48,200	67,700	113,770	90,227
0.005	200			52,800	79,942	69,618
0.01	100		31,300	42,400	63,896	58,681
0.02	50		25,200	33,000	48,235	44,574
0.04	25		19,200	24,500	31,210	30,754
0.1	10		12,200	14,900	15,878	15,826
0.2	5			8,940	8,926	8,883
0.5	2			3,000	2,963	3,361

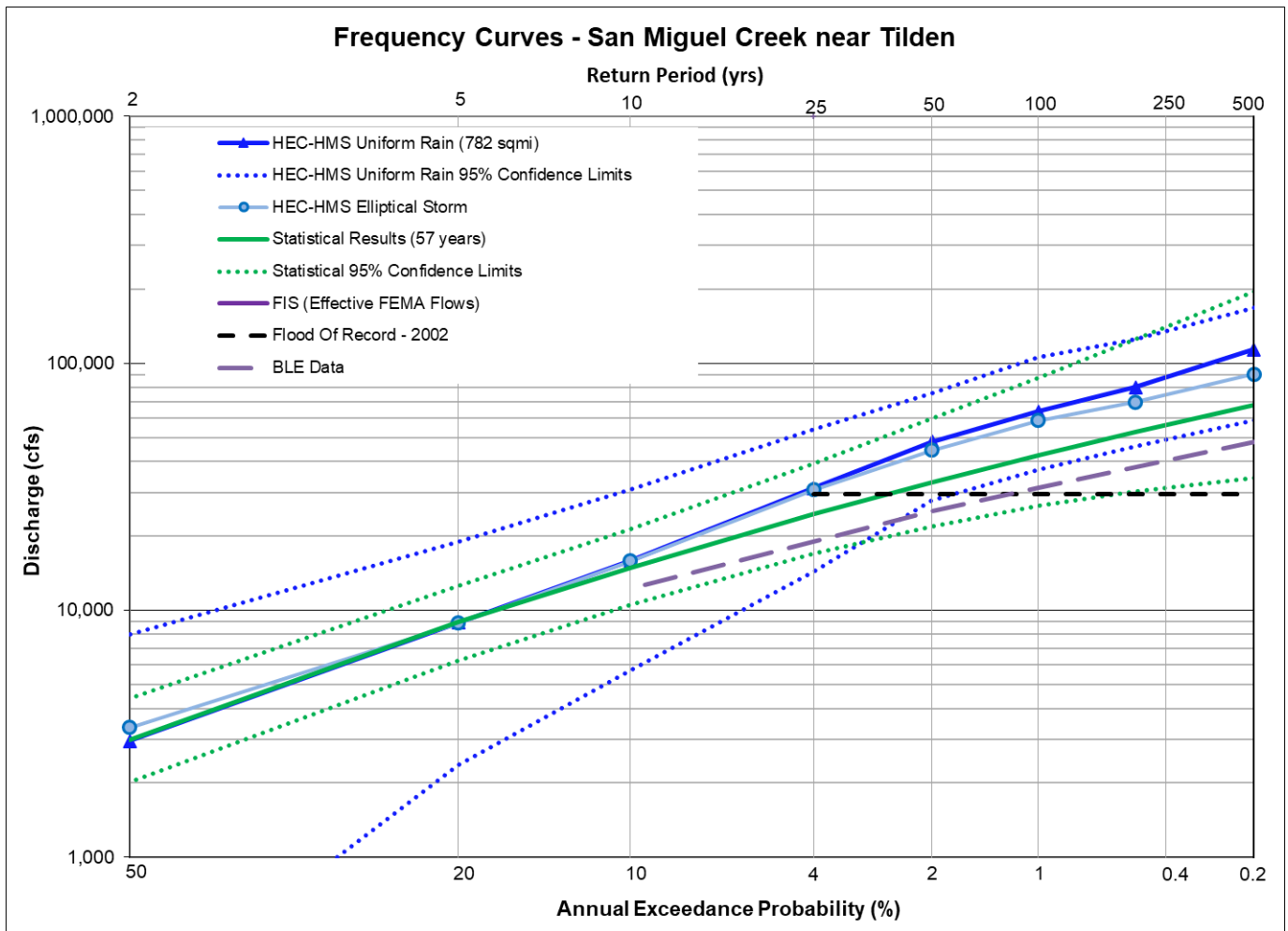


**Figure 11.19: Flow Frequency Curve Comparison for San Miguel Creek nr Tilden, TX**

San Miguel Creek near Tilden has a drainage area of over 780 square miles and is located in an area of wide, irrigated floodplains. The period of record at USGS streamgage 08206700 San Miguel Creek near Tilden, Texas was from 1964 through 2020. This gives the gage a moderate period of record of 57 years.

As seen in Figure 11.19, the HEC-HMS uniform rain and elliptical storm results are quite similar to one another and are well within the confidence boundaries for the statistical analysis, and the statistical analysis falls within the confidence boundaries of HEC-HMS uniform rain. Once again, the 1D BLE data have the lowest discharges out of all of the analyses.

Choke Canyon Reservoir is Bureau of Reclamation reservoir whose deliberate impoundment began in 1984. It is located on the Frio River downstream of Tilden and has a drainage area of approximately 5,500 square miles. RiverWare was used to extend the period of record for Choke Canyon back to 1943. The simulated period of record used in the RiverWare flood flow frequency analysis for USGS streamgage 08206910 Choke Canyon Res OWC near Three Rivers, Texas was 78 years, while the observed USGS peaks were not recorded until 2017. Due to this short period of record, the traditional statistical analysis was substituted for the RiverWare simulation data analysis.

As seen in Figure 11.20, the HEC-HMS Elliptical Storms, the RiverWare statistical analysis and the RFA Reservoir Analysis results all showed very good agreement with one another. These analyses are all well within one another's confidence bounds.

**Table 11.20: Frequency Flow (cfs) Results Comparisons for Choke Canyon Reservoir**

Annual Exceedance Probability (AEP)	Return Period (years)	Currently Effective FEMA FIS	BLE Data-Regression Equations	Statistical Analysis of the Extended RiverWare Record (78 years)	HEC-HMS Uniform Rain Frequency Storm	HEC-HMS Elliptical Frequency Storm	Reservoir Analysis in RMC-RFA
0.002	500		99539	121,000	255,318	177,647	123,160
0.005	200			101,000	214,044	130,617	102,774
0.01	100		59,271	83,600	187,209	98,231	69,660
0.02	50		45,953	64,600	154,356	54,157	50,500
0.04	25		34,556	45,300	74,106	29,971	37,950
0.1	10		22,355	22,300	23,474	14,400	22,000
0.2	5			9,360	10,306	8,536	12,050
0.5	2			933	2,507	1,821	2,900

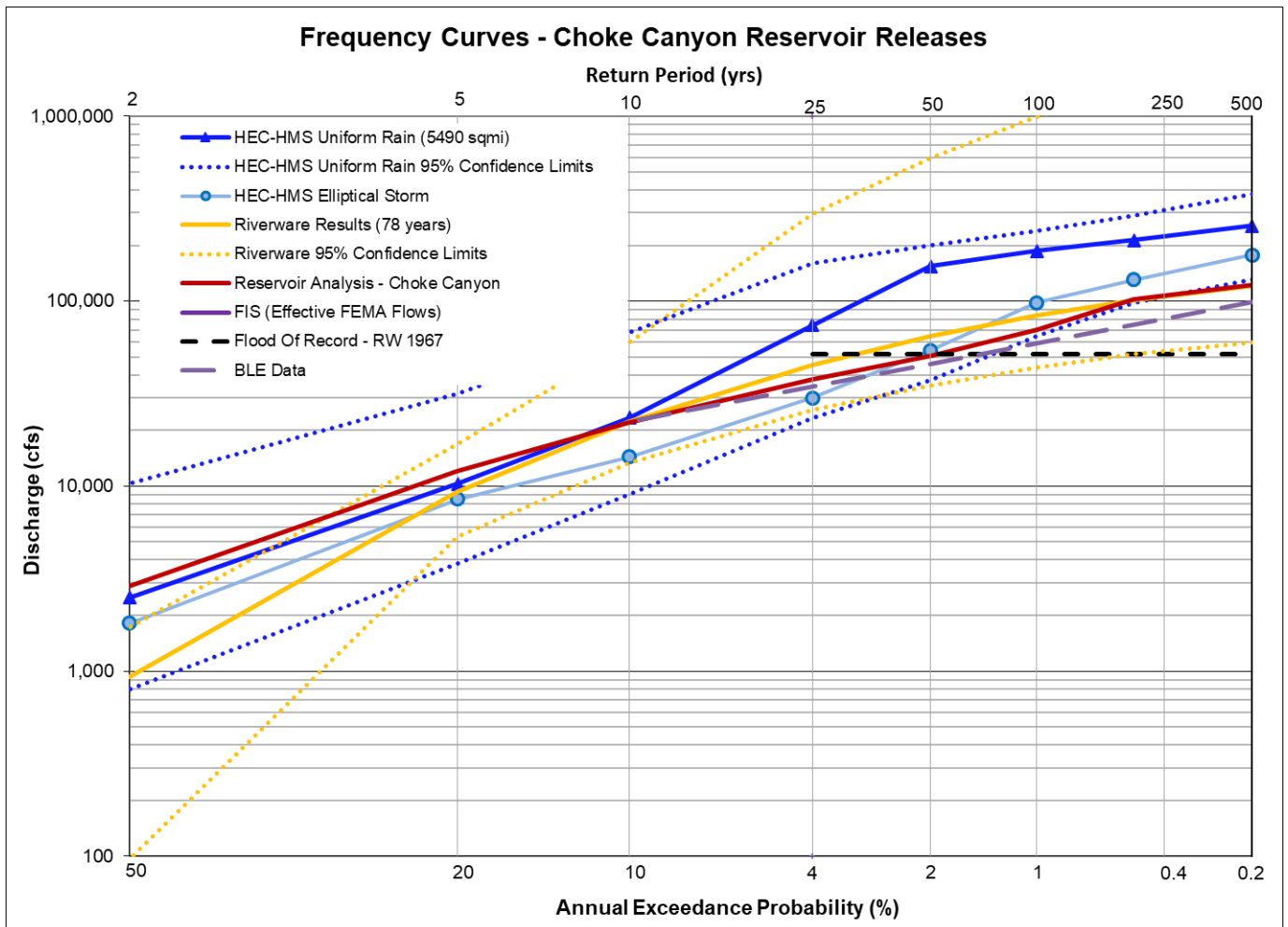


**Figure 11.20: Flow Frequency Curve Comparison for Choke Canyon Reservoir**

**Table 11.21: Frequency Flow (cfs) Results Comparisons for Atascosa River at Whitsett, TX**

Annual Exceedance Probability (AEP)	Return Period (years)	Currently Effective FEMA FIS	BLE Data-Statistical Analysis	Statistical Analysis of the Gage Record (96 years)	HEC-HMS Uniform Rain Frequency Storm	HEC-HMS Elliptical Frequency Storm
0.002	500		121000	151,000	166,047	124,646
0.005	200			104,000	118,353	86,246
0.01	100		52,400	76,000	88,160	68,979
0.02	50		35,500	54,200	60,139	47,122
0.04	25		23,700	37,200	39,810	34,228
0.1	10		14,100	20,700	20,535	19,923
0.2	5			12,000	12,154	11,935
0.5	2			4,190	4,139	4,152

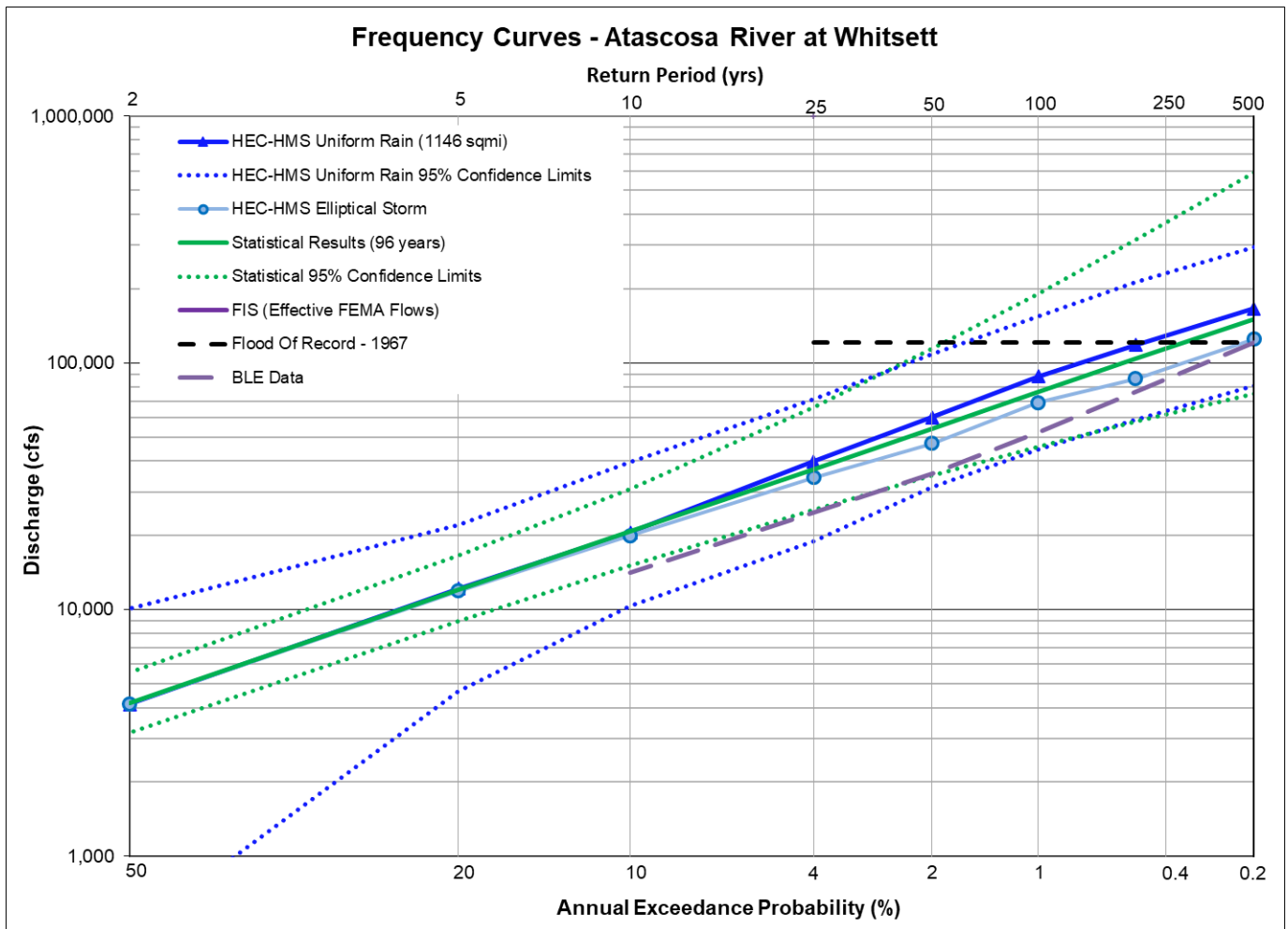


**Figure 11.21a: Flow Frequency Curve Comparison for Atascosa River at Whitsett, TX**

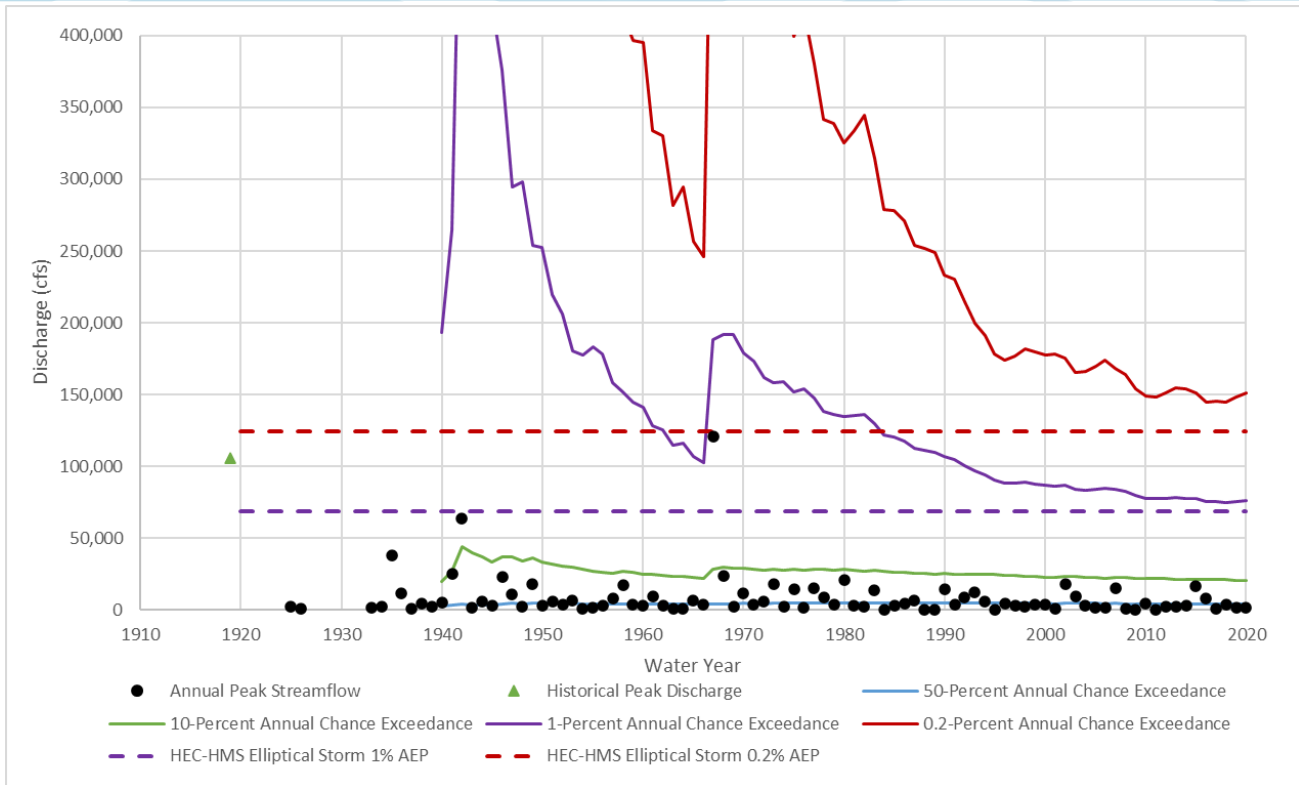


**Figure 11.21b: Statistical Change Over Time Comparison for Atascosa River at Whitsett, TX**

Atascosa River at Whitsett has a drainage area of over 1,100 square miles and is located in an area of wide, irrigated floodplains. The period of record at USGS streamgauge 08208000 Atascosa River at Whitsett, Texas was from 1925 through 2020. This gives the gage a relatively long period of record of 95 years. The largest peak in the gaged period of record is the 1967 peak streamflow of 121,000 cfs.

The statistical analysis, the HEC-HMS Uniform Rainfall, and HEC-HMS Elliptical storms are all showing very good agreement with one another, as seen in figure 11.21a. They are also well within one another’s confidence bounds.

Figure 11.21b shows the variation in the statistical estimates over time. From this figure, one can see that even within almost 100 years of record, the statistical estimates for the 1% and 0.2% AEP frequencies still have not stabilized. They are being heavily affected by several large flood events which occurred between 1940 and 1970. The 1967 flood of record in particular, which the HEC-HMS model estimates as close to a 500-year storm event, dramatically increased statistical estimates, and they may still be overestimating peak discharges at this location. The HEC-HMS results, on the other hand, are based on the regional rainfall statistics of NOAA Atlas 14, which tend to make their frequency flood estimates more stable over time.

**Table 11.22: Frequency Flow (cfs) Results Comparisons for the Nueces River at Three Rivers, TX**

Annual Exceedance Probability (AEP)	Return Period (years)	Currently Effective FEMA FIS	BLE Data-Statistical Analysis	Statistical Analysis of the Gage Record (38 years)	Statistical Analysis of the Extended RiverWare Record (78 years)	HEC-HMS Uniform Rain Frequency Storm	HEC-HMS Elliptical Frequency Storm
0.002	500		130960	89,400	131,000	465,060	219,522
0.005	200			68,400	96,500	366,842	152,914
0.01	100		71,728	54,500	75,000	278,099	113,979
0.02	50		50,140	42,300	57,200	206,630	62,547
0.04	25		41,499	31,600	42,400	122,338	34,223
0.1	10		31,111	19,900	26,800	56,726	20,109
0.2	5			12,600	17,600	26,563	12,093
0.5	2			5,010	8,000	7,792	3,761

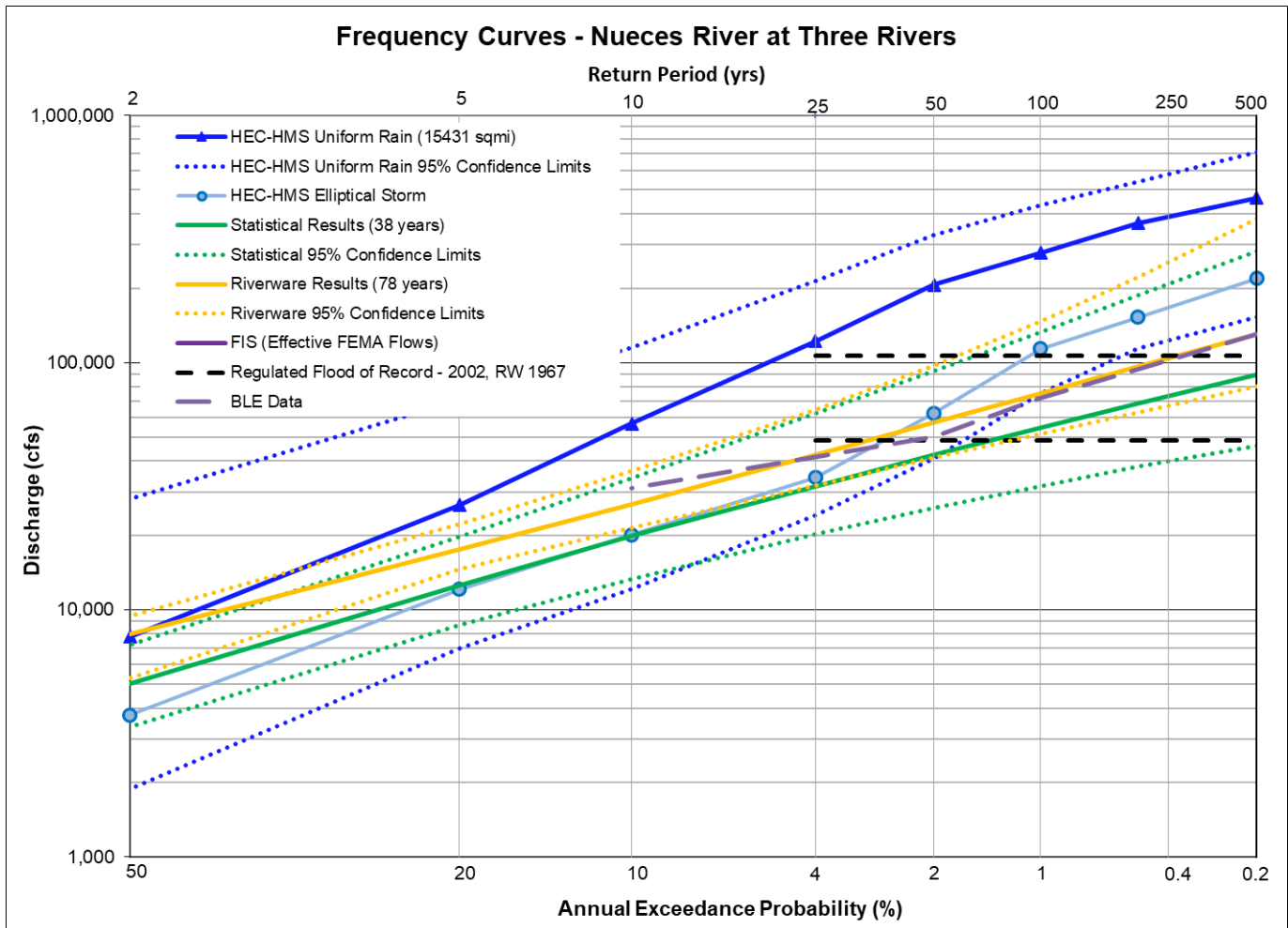


**Figure 11.22: Flow Frequency Curve Comparison for the Nueces River at Three Rivers, TX**

Nueces River at Three Rivers has a drainage area of over 15,000 square miles and is located downstream of the confluence of the Nueces River with the Frio River and the Atascosa River. The period of record at USGS streamgage 08210000 Nueces River near Three Rivers, Texas was from 1916 through 2020. However, the Pettitt test identified a statistically significant change point in water year 1984 corresponding to the beginning of deliberate impoundment of Choke Canyon Reservoir in 1984 (TWDB, 2022). Peaks prior to 1983 were removed from the statistical analysis to account for streamflow regulation caused by the reservoir. This gives the gage a relatively short period of record of 38 years.

As seen in Figure 11.22, there was a significant spread of flow frequency estimates across the four analyses. The HEC-HMS uniform rain results were the highest, but these results should be ignored due to the rainfall volume being overestimated for this very large drainage area. Due to the relatively short period of record in the statistical analysis with no major floods during the 38 years, the frequency flows for this analysis came in the lowest. With the extended period of record that was simulated in RiverWare, the frequency flows were increased significantly. The HEC-HMS elliptical storm results show very good agreement with the statistical results for the 50% through 4% AEP frequencies, but then are significantly higher than statistical analyses for the 1% and 0.2% AEP frequencies. This makes sense given the fact that no large floods were recorded during the observed period of record. However, the HEC-HMS elliptical storm results are still well within the confidence bounds of the statistical and RiverWare analyses.

**Table 11.23: Frequency Flow (cfs) Results Comparisons for Nueces River nr Mathis, TX**

Annual Exceedance Probability (AEP)	Return Period (years)	Currently Effective FEMA FIS	BLE Data-Statistical Analysis	Statistical Analysis of the Gage Record (81 years)	Statistical Analysis of the Extended RiverWare Record (78 years)	HEC-HMS Uniform Rain Frequency Storm	HEC-HMS Elliptical Frequency Storm	Reservoir Analysis in RMC-RFA
0.002	500	161,700	239,820	119,000	132,000	428,019	185,549	163,200
0.005	200			79,100	99,500	338,492	136,440	128,800
0.01	100	115,200	128,302	56,300	78,100	256,548	110,882	91,000
0.02	50	95,600	88,487	38,900	59,500	190,659	70,146	67,800
0.04	25		72,114	25,700	43,500	115,442	43,805	48,550
0.1	10	51,900	52,846	13,600	26,300	52,330	24,859	28,600
0.2	5			7,420	16,100	24,376	13,155	17,000
0.5	2			2,340	5,860	7,065	4,865	6,200

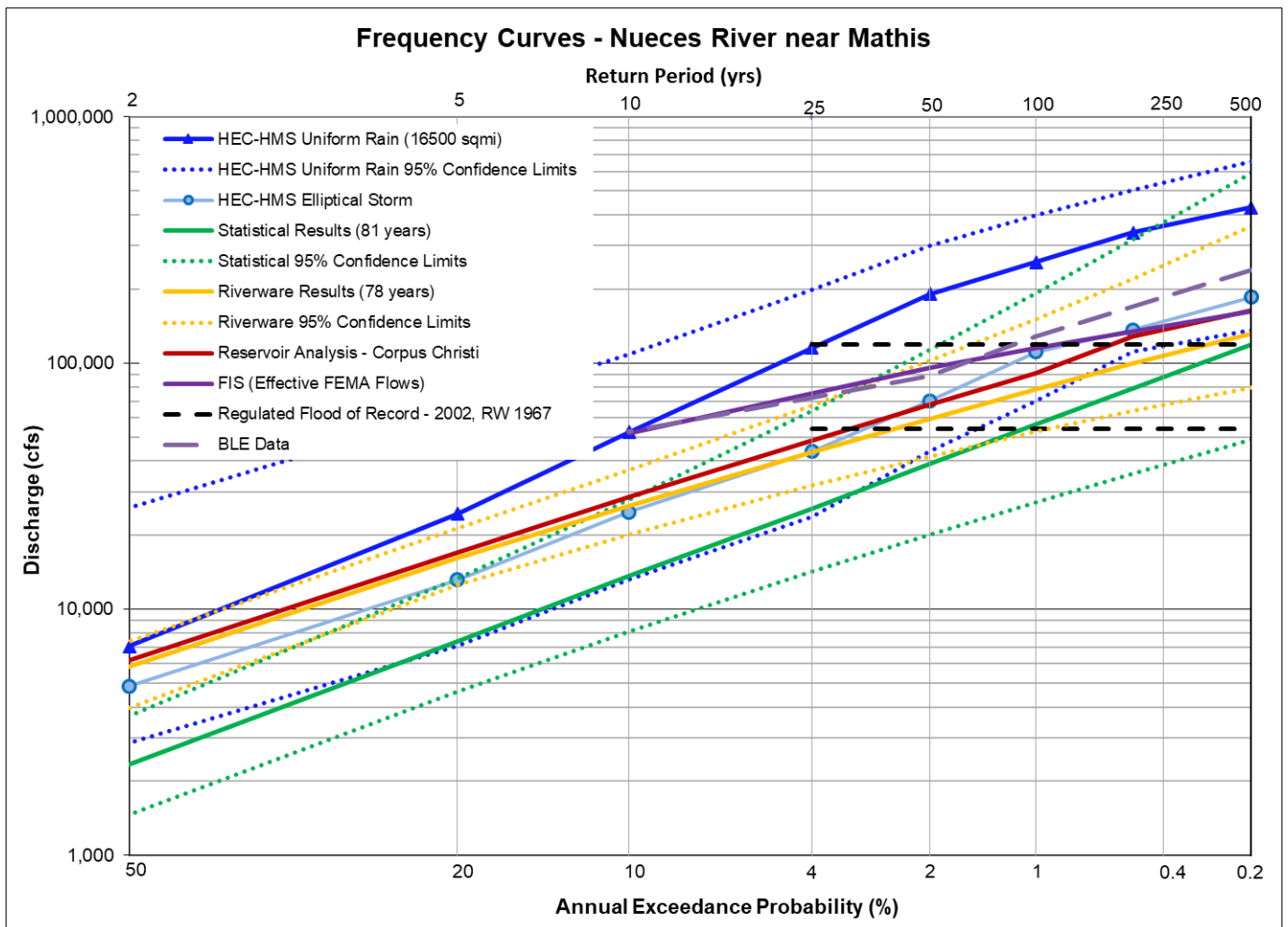


**Figure 11.23: Flow Frequency Curve Comparison for Nueces River nr Mathis, TX**

Nueces River near Mathis has a drainage area of over 16,500 square miles and is located just downstream of the dam for Lake Corpus Christi. The period of record at USGS streamgage 08211000 Nueces River near Mathis, Texas was from 1940 through 2020. This gives the gage a relatively long period of record of 80 years. However, the Pettitt test identified a significant change point in water year 1982 corresponding to the construction of Choke Canyon Reservoir upstream in 1982. Peaks prior to 1983 were removed from the analysis to account for streamflow regulation caused by Choke Canyon Reservoir. The RiverWare analyses extends the regulated period of record to 78 years by modeling the basin as if both Choke Canyon and Lake Corpus Christi were in operation for the entire period of record.

As seen in Figure 11.23, there was a significant spread of flow frequency estimates across the five analyses. However, there is good agreement between the RiverWare analyses, the RFA reservoir analysis, and the HEC-HMS elliptical storm results. The HEC-HMS elliptical storm results were also very similar to the effective FEMA flows at the 1% AEP frequency, while the 1D BLE flows were a bit higher.

Nueces River at Bluntzer has a drainage area of over 16,600 square miles and is located on the Lower Nueces River downstream of Lake Corpus Christi. The simulated period of record used in the RiverWare flood flow frequency analysis for USGS streamgage 08211200 Nueces River at Bluntzer, Texas was from 1943 through 2020. Observed USGS peaks were not recorded until 1994. Due to this short period of record, the traditional statistical analysis was substituted for the RiverWare simulation data analysis. As seen in Figure 11.24, the HEC-HMS Elliptical Storms and the RiverWare statistical analysis were reasonably in agreement with one another.

**Table 11.24: Frequency Flow (cfs) Results Comparisons for Nueces River at Bluntzer, TX**

Annual Exceedance Probability (AEP)	Return Period (years)	Currently Effective FEMA FIS	BLE Data- Interpolated between Other Gages	Statistical Analysis of the Extended RiverWare Record (78 years)	HEC-HMS Uniform Rain Frequency Storm	HEC-HMS Elliptical Frequency Storm
0.002	500		245,472	142,000	418,510	202,356
0.005	200			106,000	330,181	134,807
0.01	100		131,909	81,600	250,704	101,951
0.02	50		91,150	60,900	186,484	58,326
0.04	25			43,300	112,776	32,474
0.1	10		54,623	24,700	51,073	19,184
0.2	5			14,100	23,698	11,317
0.5	2			4,330	6,800	3,640

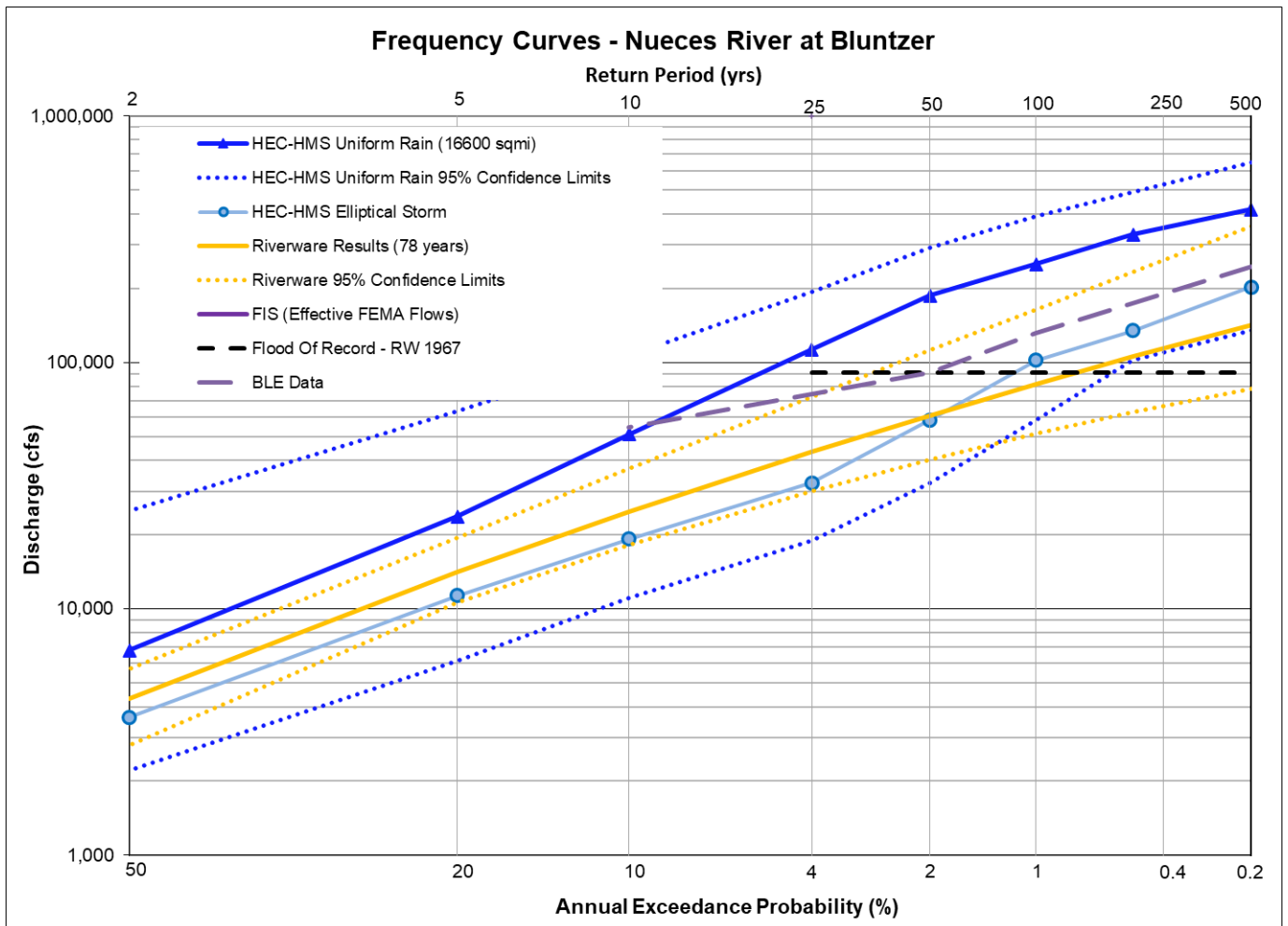


**Figure 11.24: Flow Frequency Curve Comparison for Nueces River at Bluntzer, TX**

**Table 11.25: Frequency Flow (cfs) Results Comparisons for the Nueces River at Calallen, TX**

Annual Exceedance Probability (AEP)	Return Period (years)	Currently Effective FEMA FIS	BLE Data- Statistical Analysis	Statistical Analysis of the Gage Record (38 years)	HEC-HMS Uniform Rain Frequency Storm	HEC-HMS Elliptical Frequency Storm	Statistical Analysis of the Extended RiverWare Record (78 years)
0.002	500	237,180	245,472	187,000	392,440	187,972	123,000
0.005	200			101,000	308,786	123,914	96,100
0.01	100	144,790	131,909	62,000	235,081	93,194	76,900
0.02	50	110,930	91,150	37,000	175,043	51,018	59,100
0.04	25			21,300	105,363	28,938	43,000
0.1	10	47,720	54,623	9,510	46,491	17,185	24,900
0.2	5			4,690	22,011	9,742	14,000
0.5	2			1,380	5,796	2,881	3,860

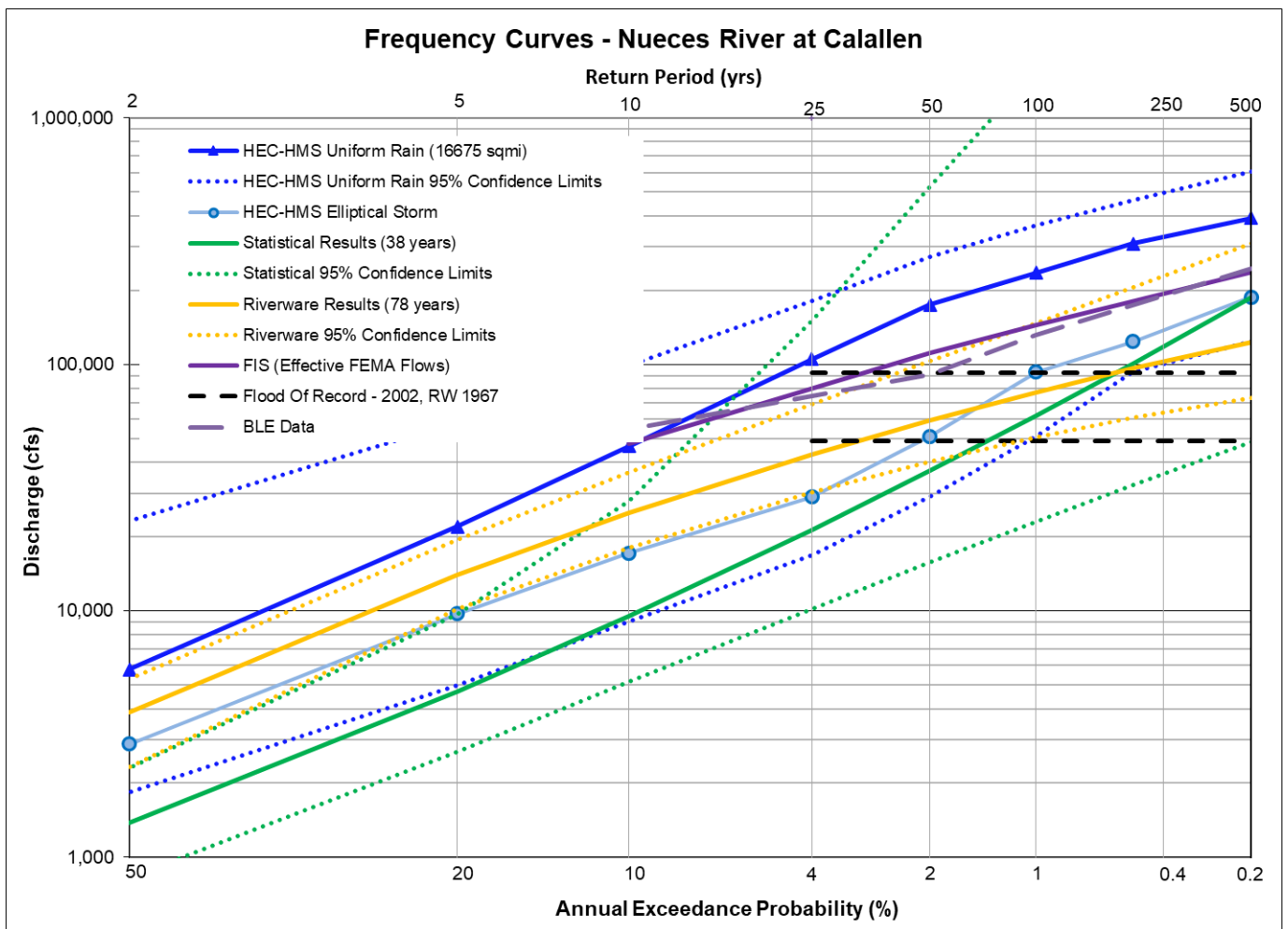


**Figure 11.25a: Flow Frequency Curve Comparison for Nueces River at Calallen, TX**

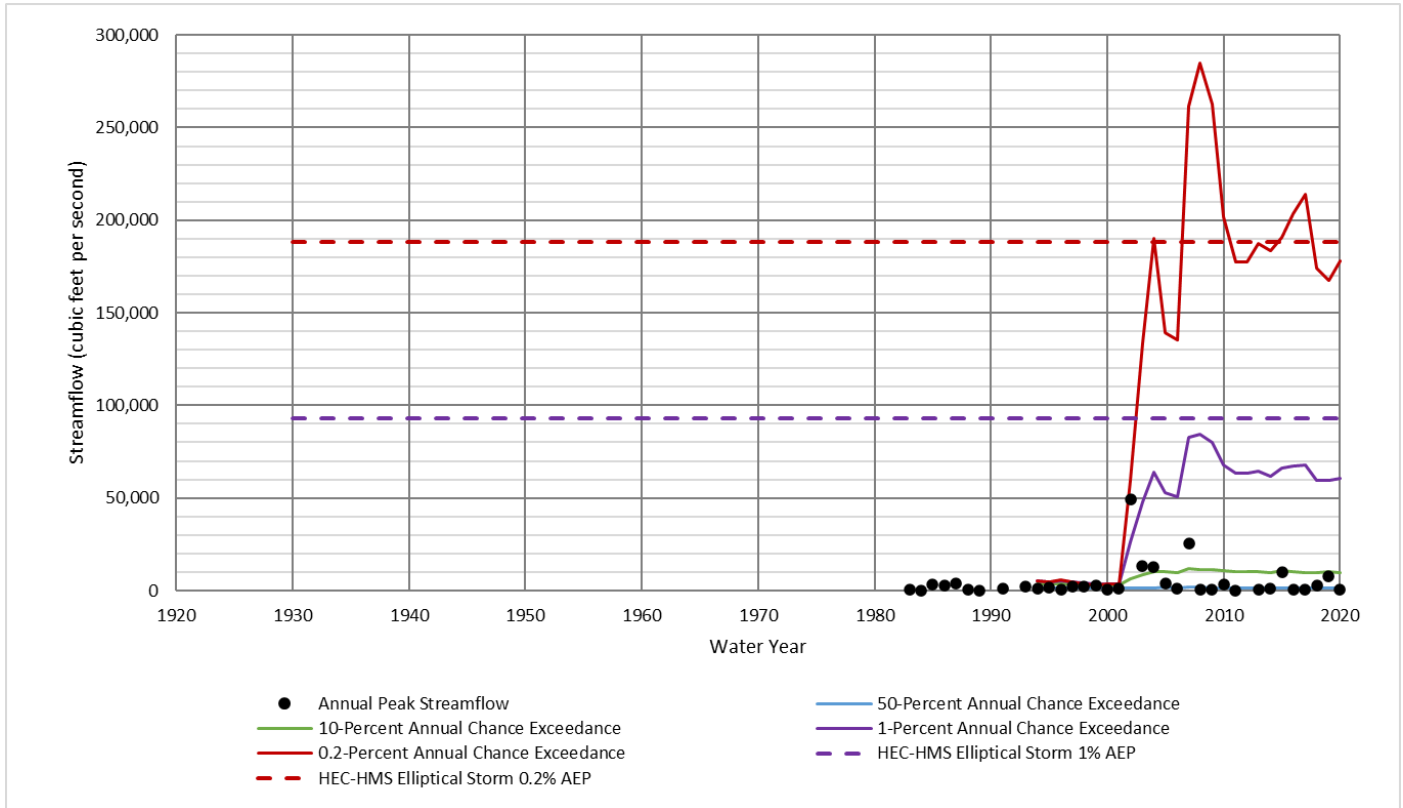


**Figure 11.25b: Statistical Change Over Time Comparison for Nueces River at Calallen, TX**

Nueces River At Calallen has a drainage area of over 16,700 square miles and is located on the Nueces River downstream of Lake Corpus Christi. The period of record at USGS streamgage 08211500 Nueces River at Calallen, Texas was from 1983 through 2020. This gives the gage a relatively short period of record of 38 years.

As seen in Figure 11.25a, there was a significant spread of flow frequencies across the four analyses, but there was much better agreement between the RiverWare results and the HEC-HMS elliptical storms. However, the effective FIS flows at this location were significantly higher, trending along the upper confidence bound of the RiverWare analysis. The FIS flows came from a 2006 Bulletin 17B statistical analysis based on a very limited period of record. Therefore, the current analyses should be more reliable than the effective FIS flows at this location. Figure 11.25b shows the variation in the statistical frequency estimates based on the available data, and as one can see, the 1% and 0.2% estimates are still quite unstable.

## 11.2 LAKE ELEVATION COMPARISONS

The final comparisons of the reservoirs frequency pool elevation estimates are given in the tables and figures of this section of the report. Blank cells indicate data was not available at that specific location. The figures in this section of the report include plots of the estimated pool frequency curves at each reservoir.

**Table 11.26: Frequency Pool Elevation (ft NAVD88) Comparison for Choke Canyon**

Annual Exceedance Probability (AEP)	Return Period (years)	Currently Effective FEMA FIS	HEC-HMS Uniform Rain Frequency Storm	HEC-HMS Elliptical Frequency Storm	Reservoir Analysis in RMC-RFA
0.002	500		243.4	227.13	224.49
0.005	200		234.5	224.69	224.11
0.01	100		228.9	223.87	223.72
0.02	50		225.2	222.73	223.44
0.04	25		223.2	222.04	223.12
0.1	10		221.7	221.55	222.56
0.2	5		221.3	221.33	221.99
0.5	2		221.0	221.00	220.67

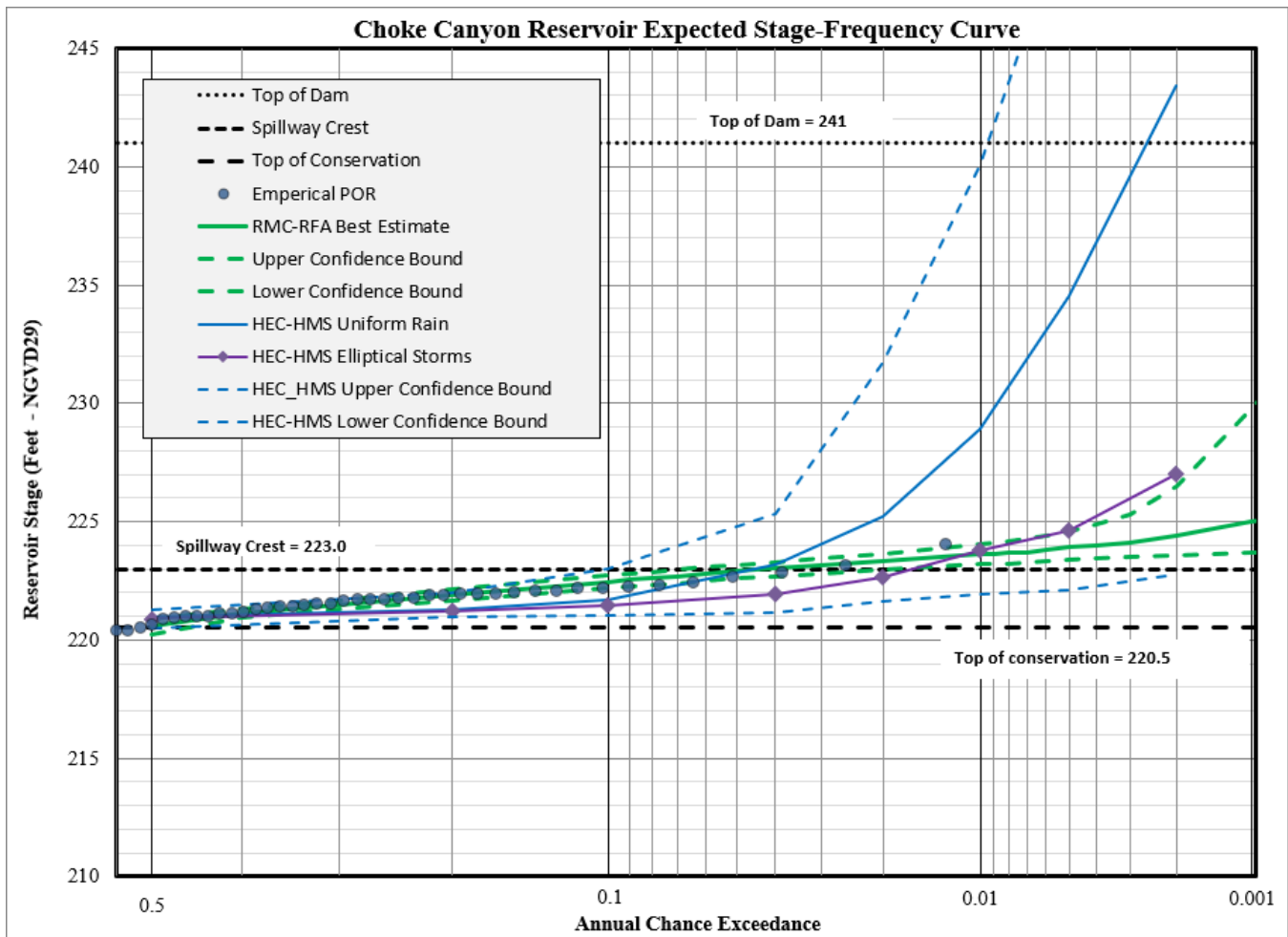


**Figure 11.26: Pool Elevation Frequency Curve Comparison for Choke Canyon Reservoir**

Choke Canyon Reservoir is owned by the Bureau of Reclamation and operated by the City of Corpus Christi. As seen in Figure 11.26 above, RMC-RFA and the HEC-HMS Elliptical storms are showing reasonable agreement, with the elliptical storm results staying within one foot of the RFA reservoir analysis results from the 50% to the 0.5% AEP. For the 0.2% AEP, the HEC-HMS elliptical storm results trend significantly higher than the reservoir analysis.

Lake Corpus Christi is owned and operated by the City of Corpus Christi. As seen in Figure 11.26 below, RMC-RFA and the HMS Elliptical storms are showing good agreement with both sets of results staying within a few tenths of a foot of each other for all frequencies.

**Table 11.27: Frequency Pool Elevation (feet NAVD88) Comparison for Lake Corpus Christi**

Annual Exceedance Probability (AEP)	Return Period (years)	Currently Effective FEMA FIS	HEC-HMS Uniform Rain Frequency Storm	HEC-HMS Elliptical Frequency Storm	Reservoir Analysis in RMC-RFA
0.002	500		102.1	96.01	96.63
0.005	200		100.1	95.38	95.3
0.01	100		98.0	94.99	94.65
0.02	50		96.3	94.49	94.47
0.04	25		95.3	94.26	94.28
0.1	10		94.5	94.14	94.19
0.2	5		94.3	93.98	94.04
0.5	2		94.1	93.86	93.86

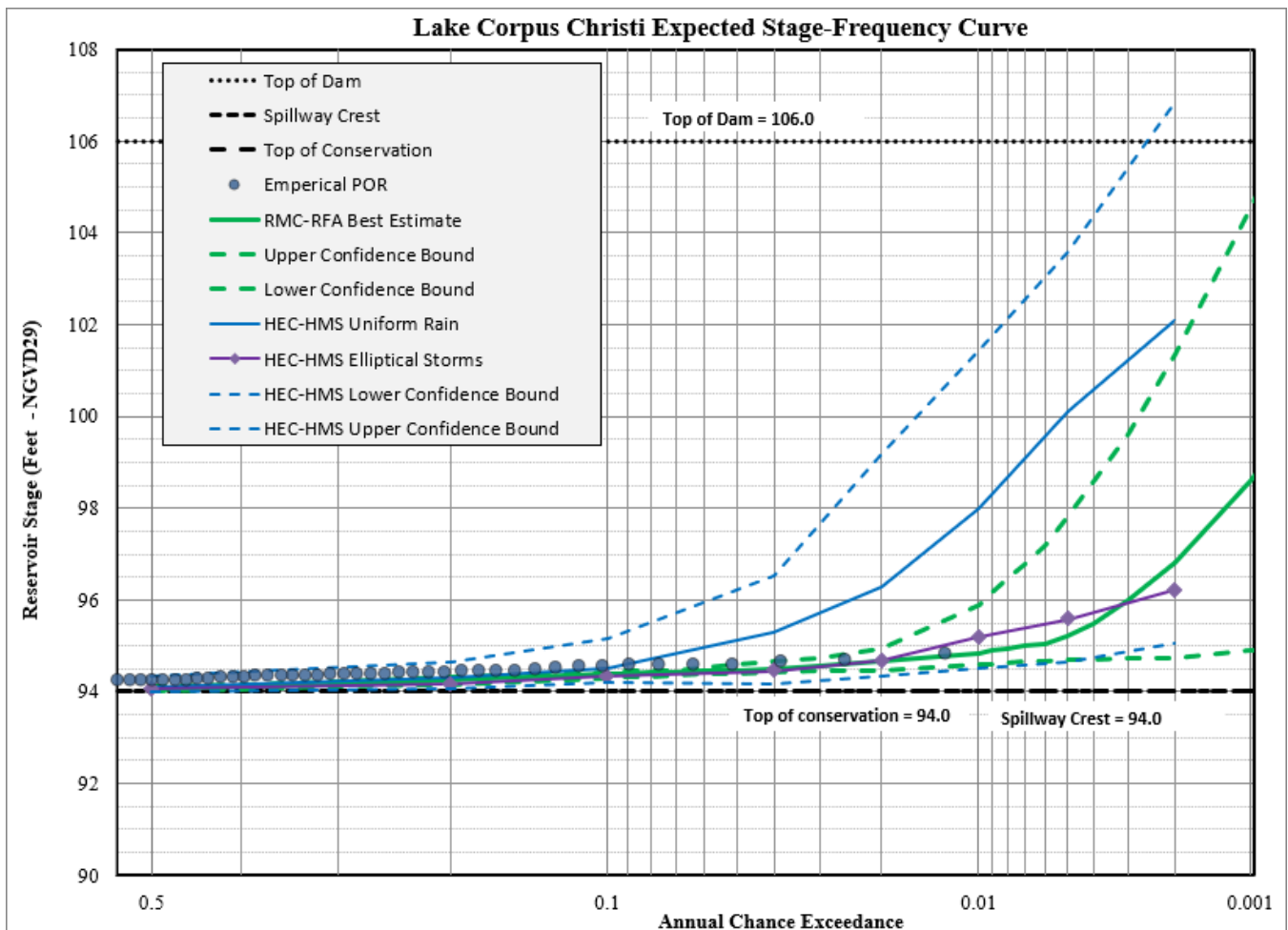


**Figure 11.27: Pool Elevation Frequency Curve Comparison for Lake Corpus Christi**

## 12 Frequency Flow Recommendations

The final recommendations for the InFRM Watershed Hydrology Assessments are formulated through a rigorous process which requires technical feedback and collaboration between all of the InFRM subject matter experts. This process includes the following steps at a minimum: (1) comparing the results of the various hydrologic methods to one another, (2) performing an investigation into the reasons for any significant differences in results at each location in the watershed, (3) selecting the draft recommended methods, (4) performing internal and external technical reviews of the hydrologic analyses and the draft recommendations, and finally, (5) finalizing the study recommendations.

After completing this process for the Nueces River basin, the frequency discharges that were recommended for adoption by the InFRM team were a combination of the results from the following methods: HEC-HMS uniform rain frequency storms (Chapter 6), HEC-HMS elliptical frequency storms (Chapter 7), and RMC-RFA Reservoir Analyses (Chapter 9). Detailed breakouts of the recommended frequency discharges and pool elevations for each location in the watershed are given in Tables 12.1 and 12.2.

The statistical results from Chapter 5 and the RiverWare statistical results from Chapter 8 were used as points of comparison, especially at the frequent end of the curves, but the InFRM team chose not to adopt the statistical flow frequency results directly. One reason for this decision was the tendency of the statistical results to change after each significant flood event, as demonstrated in the statistical change over time comparison figures in Chapter 11. In addition, climate variability can result in non-representative samples in the gage record. The statistical frequency analyses and RiverWare results support the HEC-HMS results by demonstrating that they are generally within one another's confidence limits, especially for the 1% and 0.2% AEP events of interest for FEMA floodplain mapping.

Rainfall runoff modeling, on the other hand, is based on physical watershed characteristics, such as drainage area and stream slope, that do not tend to change as much over time. Climate variability can also be accounted for in the watershed model by using regional rainfall information from NOAA Atlas 14 and by adjusting soil loss rates to be consistent with observed storms and appropriate for the rarity of the event in question. Another reason for the selection of the HEC-HMS modeling discharges was the ability to directly calculate frequency discharges for locations within the Nueces River watershed that do not coincide with a stream gage.

Rainfall-runoff modeling in HEC-HMS was used to simulate the physical processes that occur in the Nueces watershed during intense storm events, including the movement of water across the land surface and through the streams and rivers. The HEC-HMS model for the Nueces River basin underwent extensive calibration to accurately simulate the response of the watershed to a range of observed flood events, including large events similar to a 1% ACE (100-yr) flood. In fact, a total of sixteen recent storm events were used to fine tune the HEC-HMS model: thereby bestowing a high degree of confidence in the HEC-HMS model's results.

In addition to extensive calibration, best available precipitation frequency estimates from NOAA Atlas 14 (NOAA, 2018) were used to build frequency storms within the HEC-HMS model. NOAA Atlas 14 is the most accurate, up-to-date, and comprehensive study of rainfall depths in Texas. NOAA Atlas 14 used a regional statistical approach that incorporated at least 1,000 cumulative years of daily data and 500 cumulative years of sub-daily data into each station's rainfall frequency estimate. This regional approach yielded better estimates of rare rainfall depths such as the 1% and 0.2% AEP (100-yr and 500-yr) depths. For these reasons, the calibrated HEC-HMS watershed modeling with the NOAA Atlas 14 rainfall depths was adopted as having the most complete accounting of both the historic rainfall data and the physical processes at work in the watershed.

Between the uniform rain and the elliptical frequency storms in HEC-HMS, the uniform rain method is simpler and well suited for smaller drainage areas, while the elliptical storm method is more complex and better suited for larger drainage areas. Both this study and the previous InFRM Watershed Hydrology Assessments have confirmed that the uniform rainfall method can produce reasonable results up to about 1,500 square miles (InFRM, 2019) (InFRM, 2021) (InFRM, 2022) (InFRM, 2024). For larger drainage areas in the Nueces River basin, the elliptical storm results from HEC-HMS did a better job of producing reasonable runoff volumes and subsequently peak stream flows. Table 12.1 indicates the locations where the recommended results transitioned from uniform rainfall results to elliptical storm results on each stream and river. The exact locations of the transitions between uniform and elliptical storms generally occurred at locations with drainage areas between 400 and 1,400 square miles and were placed at significant confluences to avoid any jumps or dips in the peak flows due to a change in the rainfall method.

For the major reservoirs in the Nueces River basin, the recommended frequency pool elevations were calculated in the RMC-RFA reservoir analyses from Chapter 9. These reservoir analyses were performed for the two major reservoirs within the basin: Choke Canyon Reservoir and Lake Corpus Christi. The RMC-RFA analyses utilized stochastic techniques and had the most comprehensive accounting for the operations of the dam, the frequency of its inflow volumes, and the range of its starting pool elevations. This type of detailed reservoir analysis lends a higher level of confidence to the resulting frequency estimates of its pool elevations. The resulting recommended frequency pool elevations are shown in Table 12.2. The recommended frequency outflows from the reservoir analyses as well as frequency peak flows for the rest of the watershed are presented in Table 12.1.

Table 12.1: Summary of Recommended Frequency Peak Discharges (cfs) for the Nueces River Basin

	AEP	50%	20%	10%	4%	2%	1%	0.5%	0.2%	
Location Description	Drainage Area (sq mi)	2-yr	5-yr	10-yr	25-yr	50-yr	100-yr	200-yr	500-yr	Hydrologic Method
West Nueces River at Indian Creek	373.49	3,070	28,900	66,300	111,800	146,000	185,000	224,000	281,000	HEC-HMS Uniform Rain
West Nueces River above Sycamore Creek	535.95	3,440	32,300	74,200	128,000	170,000	221,000	271,000	345,000	HEC-HMS Uniform Rain
West Nueces River Below Sycamore Creek	646.40	4,060	37,000	85,100	148,200	199,000	260,000	320,000	409,000	HEC-HMS Uniform Rain
West Nueces River near Brackettville (USGS gage 08190500)	693.94	4,050	36,800	84,400	147,000	197,000	260,000	321,000	412,000	HEC-HMS Uniform Rain
West Nueces River above Sycamore Creek	767.91	3,820	34,900	79,900	139,000	187,000	246,000	304,000	391,000	HEC-HMS Uniform Rain
West Nueces River Below Sycamore Creek	820.22	3,830	35,100	80,400	139,700	188,000	247,000	307,000	396,000	HEC-HMS Uniform Rain
West Nueces River above Nueces River	918.29	3,590	33,000	75,500	131,300	177,000	234,000	292,000	379,000	HEC-HMS Uniform Rain
Hackberry Creek at East Prong Nueces River	199.93	4,300	19,900	40,200	76,800	101,000	123,000	144,000	172,000	HEC-HMS Uniform Rain
Nueces River above Pulliam Creek	354.34	6,520	29,300	58,900	113,600	154,000	191,000	226,000	276,000	HEC-HMS Uniform Rain
Nueces River below Pulliam Creek	529.82	8,830	41,400	83,800	162,500	222,000	279,000	334,000	411,000	HEC-HMS Uniform Rain
Nueces River at CR414 at Montell (USGS gage 08189998)	659.62	9,170	43,200	87,600	172,700	241,000	307,000	372,000	463,000	HEC-HMS Uniform Rain
Nueces River below Montell Creek	679.24	9,190	43,300	87,800	173,200	242,000	309,000	374,000	467,000	HEC-HMS Uniform Rain
Nueces River at Laguna (USGS gage 08190000)	736.17	9,090	42,900	86,900	171,600	241,000	308,000	373,000	468,000	HEC-HMS Uniform Rain
Nueces River above West Nueces River	815.94	8,520	40,600	82,300	162,400	228,000	292,000	356,000	449,000	HEC-HMS Uniform Rain
Nueces River below West Nueces River	1734.22	9,820	46,800	110,000	214,000	282,000	376,000	440,000	573,000	HEC-HMS Elliptical Storms

	AEP	50%	20%	10%	4%	2%	1%	0.5%	0.2%	
Location Description	Drainage Area (sq mi)	2-yr	5-yr	10-yr	25-yr	50-yr	100-yr	200-yr	500-yr	Hydrologic Method
Nueces River below Indian Creek	1802.06	9,600	44,800	105,000	204,000	269,000	359,000	421,000	550,000	HEC-HMS Elliptical Storms
Nueces River at Highway 90	1838.04	9,070	42,100	98,800	193,000	254,000	340,000	398,000	521,000	HEC-HMS Elliptical Storms
Nueces River near Uvalde (USGS gage 08192000)	1861.45	7,860	39,100	92,600	181,000	239,000	320,000	377,000	493,000	HEC-HMS Elliptical Storms
Nueces River at Highway 83	1885.45	5,770	27,700	67,300	134,000	177,000	239,000	283,000	371,000	HEC-HMS Elliptical Storms
Nueces River at Highway 57	1981.12	2,500	17,000	38,300	88,200	123,000	166,000	200,000	269,000	HEC-HMS Elliptical Storms
Nueces River at FM 1025 nr Crystal City (USGS gage 08192550)	2102.48	1,900	9,630	20,300	42,400	65,700	120,000	151,000	208,000	HEC-HMS Elliptical Storms
Nueces River at The Turkey Creek/Espantosa Slough Split	2122.77	1,100	6,710	13,600	27,900	38,900	66,000	105,000	153,000	HEC-HMS Elliptical Storms
Turkey Creek/Espantosa Slough Diversion	2122.77	835	4,890	9,310	19,200	27,800	52,900	91,100	139,000	HEC-HMS Elliptical Storms
Nueces River Split	2165.25	2,280	3,550	3,820	5,930	8,840	11,900	14,900	19,400	HEC-HMS Elliptical Storms
Nueces River above Turkey Creek	2165.25	327	1,290	2,800	5,960	7,650	9,530	10,600	12,000	HEC-HMS Elliptical Storms
Elm Creek and Stricklin Creek	254.90	1,590	4,200	15,600	46,000	103,000	143,000	182,000	233,000	HEC-HMS Uniform Rain
Chacon Creek at Highway 57	337.55	1,770	4,220	10,800	35,200	90,000	134,000	177,000	233,000	HEC-HMS Uniform Rain
Palo Blanco Creek at Highway 57	69.98	2,430	5,170	10,700	22,200	41,000	53,000	66,000	82,000	HEC-HMS Uniform Rain
Palo Blanco Creek above Chacon Creek	121.24	1,120	2,650	6,500	15,100	31,000	42,000	55,000	73,000	HEC-HMS Uniform Rain
Palo Blanco Creek below Chacon Creek	520.34	1,690	4,220	10,600	30,100	78,000	122,000	170,000	234,000	HEC-HMS Uniform Rain
Palo Blanco Creek above Picoso Creek	520.34	1,280	3,360	8,900	29,300	76,000	118,000	166,000	230,000	HEC-HMS Uniform Rain

	<b>AEP</b>	<b>50%</b>	<b>20%</b>	<b>10%</b>	<b>4%</b>	<b>2%</b>	<b>1%</b>	<b>0.5%</b>	<b>0.2%</b>	
<b>Location Description</b>	<b>Drainage Area (sq mi)</b>	<b>2-yr</b>	<b>5-yr</b>	<b>10-yr</b>	<b>25-yr</b>	<b>50-yr</b>	<b>100-yr</b>	<b>200-yr</b>	<b>500-yr</b>	<b>Hydrologic Method</b>
Picosa Creek and Chueco Creek	190.28	2,020	5,890	13,500	31,900	66,000	91,000	115,000	148,000	HEC-HMS Uniform Rain
Palo Blanco Creek below Picosa Creek	744.76	8,540	18,900	26,500	41,200	73,000	108,000	123,000	173,000	HEC-HMS Elliptical Storm
Palo Blanco Creek above Comanche Creek	744.76	8,110	17,900	25,200	39,100	69,400	103,000	117,000	164,000	HEC-HMS Elliptical Storm
Comanche Creek at Highway 277	78.18	1,430	3,940	10,300	24,900	51,000	68,000	83,000	105,000	HEC-HMS Uniform Rain
Palo Blanco Creek Below Comanche Creek	822.94	9,590	21,400	30,300	46,700	83,500	125,000	130,000	182,000	HEC-HMS Elliptical Storm
Turkey Creek and Wood Slough	111.93	1,380	3,190	9,480	26,100	56,000	76,000	95,000	120,000	HEC-HMS Uniform Rain
Turkey Creek at Highway 57	170.51	1,090	2,360	6,210	16,200	41,000	64,000	88,000	122,000	HEC-HMS Uniform Rain
Turkey Creek above Chaparrosa Creek	210.04	780	1,680	4,490	14,000	36,000	57,000	81,000	117,000	HEC-HMS Uniform Rain
Chaparrosa Creek and Muela Creek	132.77	3,370	7,290	18,300	41,900	80,000	103,000	126,000	157,000	HEC-HMS Uniform Rain
Chaparrosa Creek above Turkey Creek	204.55	1,120	2,980	9,800	26,300	63,000	93,000	122,000	161,000	HEC-HMS Uniform Rain
Turkey Creek below Chaparrosa Creek	414.59	1,730	3,800	13,000	35,800	87,000	129,000	174,000	248,000	HEC-HMS Uniform Rain
Turkey Creek above Picosa Creek	459.10	1,070	2,710	8,800	25,700	60,000	88,000	124,000	179,000	HEC-HMS Uniform Rain
Turkey Creek below Picosa Creek	1376.61	10,700	24,000	33,900	52,700	94,900	140,000	176,000	197,000	HEC-HMS Elliptical Storm
Turkey Creek at Highway 83 (New USGS gage)	1554.98	7,620	14,900	20,200	31,500	59,800	93,000	119,000	144,000	HEC-HMS Elliptical Storm
Turkey Creek above Turkey Split	1563.55	6,140	13,400	19,400	31,300	59,000	91,800	118,000	142,000	HEC-HMS Elliptical Storm
Turkey Creek below Turkey Split	1568.83	3,260	10,600	15,700	27,300	45,800	77,600	122,000	202,000	HEC-HMS Elliptical Storm
Turkey Creek above Carrizo Creek	1581.46	4,210	10,800	16,400	29,000	51,300	77,800	107,000	189,000	HEC-HMS Elliptical Storm

	<b>AEP</b>	<b>50%</b>	<b>20%</b>	<b>10%</b>	<b>4%</b>	<b>2%</b>	<b>1%</b>	<b>0.5%</b>	<b>0.2%</b>	
<b>Location Description</b>	<b>Drainage Area (sq mi)</b>	<b>2-yr</b>	<b>5-yr</b>	<b>10-yr</b>	<b>25-yr</b>	<b>50-yr</b>	<b>100-yr</b>	<b>200-yr</b>	<b>500-yr</b>	<b>Hydrologic Method</b>
Carrizo Creek at Highway 83	49.73	1,790	3,030	3,640	7,400	12,800	16,500	20,400	26,200	HEC-HMS Uniform Rain
Turkey Creek below Carrizo Creek	1662.70	4,410	11,200	16,800	29,700	53,100	80,100	107,000	190,000	HEC-HMS Elliptical Storm
Turkey Creek above El Barrosa Creek	1687.81	4,420	9,990	15,400	27,800	51,200	78,300	103,000	178,000	HEC-HMS Elliptical Storm
Turkey Creek below El Barrosa Creek	1718.21	4,440	10,000	15,500	27,900	51,500	78,700	104,000	179,000	HEC-HMS Elliptical Storm
Turkey Creek and El Moro Creek	1836.07	4,920	10,100	15,500	28,400	53,100	80,700	104,000	178,000	HEC-HMS Elliptical Storm
Turkey Creek above Nueces River	1847.03	4,540	9,600	15,200	27,900	52,000	79,700	104,000	178,000	HEC-HMS Elliptical Storm
Nueces River near Asherton (USGS gage 08193000)	4024.67	4,780	10,100	16,300	30,700	53,000	82,500	109,000	186,000	HEC-HMS Elliptical Storms
Nueces River above Arroyo Negro	4213.49	5,070	9,960	16,600	30,300	50,100	80,900	107,000	179,000	HEC-HMS Elliptical Storms
Nueces River below Arroyo Negro	4333.02	5,470	10,300	17,000	30,800	51,600	82,100	107,000	179,000	HEC-HMS Elliptical Storms
Nueces River above Appurceon Creek	4333.02	5,070	10,100	16,800	30,500	50,200	81,100	106,000	177,000	HEC-HMS Elliptical Storms
Nueces River below Appurceon Creek	4411.17	5,500	10,500	17,200	31,100	52,000	82,700	107,000	177,000	HEC-HMS Elliptical Storms
Nueces River above San Roque Creek	4488.43	5,430	10,500	17,000	30,600	50,600	81,400	105,000	172,000	HEC-HMS Elliptical Storms
San Roque Creek and Canyon Creek	255.77	3,650	11,100	14,500	28,800	41,000	55,000	69,000	90,000	HEC-HMS Uniform Rain
San Roque Creek below Highway 83	333.91	3,550	10,900	14,300	28,500	40,000	54,000	69,000	90,000	HEC-HMS Uniform Rain
San Roque Creek above Nueces River	415.48	3,250	10,000	13,100	26,300	37,000	51,000	65,000	84,000	HEC-HMS Uniform Rain
Nueces River below San Roque Creek	4903.91	6,380	14,200	22,800	34,000	51,100	82,000	106,000	173,000	HEC-HMS Elliptical Storms
Nueces River and Espio Creek	5084.65	6,410	14,100	22,500	33,500	50,300	81,100	104,000	169,000	HEC-HMS Elliptical Storms

	AEP	50%	20%	10%	4%	2%	1%	0.5%	0.2%	
Location Description	Drainage Area (sq mi)	2-yr	5-yr	10-yr	25-yr	50-yr	100-yr	200-yr	500-yr	Hydrologic Method
Nueces River at Cotulla (USGS gage 08194000)	5172.43	6,240	12,800	20,400	31,300	50,500	80,900	104,000	165,000	HEC-HMS Elliptical Storms
Nueces River above La Raices Creek	5366.43	6,520	12,900	20,200	30,700	48,900	78,200	100,000	158,000	HEC-HMS Elliptical Storms
La Raices Creek at IH-35	175.31	560	2,500	6,040	14,100	24,700	33,900	43,200	56,100	HEC-HMS Uniform Rain
La Raices Creek above Nueces River	272.12	560	2,500	6,090	14,400	25,200	34,800	44,500	58,100	HEC-HMS Uniform Rain
Nueces River below La Raices Creek	5638.55	6,400	12,700	19,900	30,700	48,600	78,000	100,000	158,000	HEC-HMS Elliptical Storms
Nueces River above Calman Creek	5705.26	6,430	12,400	19,400	30,200	47,800	76,500	98,300	154,000	HEC-HMS Elliptical Storms
Tecolote Creek and Chucareto Creek	115.03	690	2,340	4,990	11,000	19,000	26,000	33,000	42,000	HEC-HMS Uniform Rain
Calman Creek above Nueces River	185.52	890	2,840	5,520	12,100	21,000	28,000	36,000	47,000	HEC-HMS Uniform Rain
Nueces River below Calman Creek	5890.78	6,420	12,500	19,400	30,400	48,200	77,000	98,900	155,000	HEC-HMS Elliptical Storms
Nueces River above Los Olmos Creek	5898.22	6,730	13,000	20,100	30,300	47,800	76,400	97,900	153,000	HEC-HMS Elliptical Storms
Carrizitos Creek above Venado Creek	90.70	780	2,190	3,670	7,250	11,900	16,000	20,000	25,800	HEC-HMS Uniform Rain
Los Olmos Creek and Carrizitos Creek	322.57	1,720	6,100	12,100	26,700	46,000	62,000	78,000	101,000	HEC-HMS Uniform Rain
Los Olmos Creek above TX-44	403.09	1,700	5,900	11,500	25,100	43,100	58,900	74,600	97,100	HEC-HMS Uniform Rain
Los Olmos Creek above Nueces River	455.53	1,660	5,600	10,800	23,600	40,500	55,200	70,100	91,400	HEC-HMS Uniform Rain
Nueces River below Los Olmos Creek	6353.75	8,040	18,500	28,300	42,300	70,000	97,500	119,000	158,000	HEC-HMS Elliptical Storms
Nueces River and Sauz Creek	6419.66	7,800	18,100	27,600	41,300	68,400	95,500	117,000	155,000	HEC-HMS Elliptical Storms
Nueces River above San Casimiro Creek	6445.15	7,250	17,100	26,300	39,500	65,400	91,600	113,000	151,000	HEC-HMS Elliptical Storms

	AEP	50%	20%	10%	4%	2%	1%	0.5%	0.2%	
Location Description	Drainage Area (sq mi)	2-yr	5-yr	10-yr	25-yr	50-yr	100-yr	200-yr	500-yr	Hydrologic Method
Salado Creek and Gato Creek	170.00	800	3,300	7,800	17,300	24,600	33,100	42,300	53,500	HEC-HMS Uniform Rain
Beccerra Creek and Pato Creek	105.24	1,870	5,100	9,400	17,800	23,800	30,900	37,900	47,500	HEC-HMS Uniform Rain
San Casimiro Creek near Freer (USGS gage 08194200)	467.65	2,590	7,820	15,900	32,300	42,900	57,300	69,900	90,800	HEC-HMS Elliptical Storms
San Casimiro Creek above Nueces River	537.34	2,180	6,880	14,200	29,100	38,600	51,900	63,900	83,500	HEC-HMS Elliptical Storms
Nueces River below San Casimiro Creek	6982.49	6,900	18,400	32,900	58,400	88,600	125,000	153,000	204,000	HEC-HMS Elliptical Storms
Nueces River above Black Creek	7007.66	6,770	18,000	32,100	56,900	86,400	122,000	150,000	200,000	HEC-HMS Elliptical Storms
Black Creek near Biel Lake	282.58	1,760	6,030	12,000	25,600	43,000	57,600	72,600	92,800	HEC-HMS Uniform Rain
Black Creek at Highway 44	373.84	1,760	5,990	11,900	25,300	42,600	57,300	72,700	94,200	HEC-HMS Uniform Rain
Black Creek above Nueces River	423.47	1,670	5,600	11,000	23,400	39,500	53,400	68,100	88,700	HEC-HMS Uniform Rain
Nueces River below Black Creek	7431.13	5,980	18,700	33,500	59,700	91,800	131,000	163,000	221,000	HEC-HMS Elliptical Storms
Nueces River above Ygnacio Creek	7611.07	6,330	18,600	32,000	55,400	85,600	122,000	151,000	205,000	HEC-HMS Elliptical Storms
Nueces River below Ygnacio Creek	7754.47	6,160	18,400	32,000	55,500	85,700	123,000	151,000	206,000	HEC-HMS Elliptical Storms
Nueces River above San Jose Creek	7754.47	6,090	18,400	31,900	55,300	85,300	122,000	150,000	205,000	HEC-HMS Elliptical Storms
Nueces River below San Jose Creek	7857.73	6,090	18,300	31,900	55,300	85,400	122,000	151,000	205,000	HEC-HMS Elliptical Storms
Nueces River above Green Branch	7857.73	6,040	18,200	31,600	54,800	84,700	121,000	149,000	203,000	HEC-HMS Elliptical Storms
Nueces River below Green Branch	7943.10	6,150	18,300	31,700	54,900	84,700	121,000	149,000	203,000	HEC-HMS Elliptical Storms

	AEP	50%	20%	10%	4%	2%	1%	0.5%	0.2%	
Location Description	Drainage Area (sq mi)	2-yr	5-yr	10-yr	25-yr	50-yr	100-yr	200-yr	500-yr	Hydrologic Method
Nueces River near Tilden (USGS gage 08194500)	8105.85	5,750	17,600	30,700	53,100	82,100	118,000	145,000	197,000	HEC-HMS Elliptical Storms
Nueces River above Cow Creek	8105.85	6,050	17,500	30,200	52,000	80,200	115,000	141,000	192,000	HEC-HMS Elliptical Storms
Nueces River below Cow Creek	8182.92	5,830	17,400	30,300	52,300	80,700	116,000	142,000	193,000	HEC-HMS Elliptical Storms
Nueces River above Old River	8275.85	5,550	16,700	29,200	50,500	77,900	112,000	137,000	187,000	HEC-HMS Elliptical Storms
Old River and Hill Creek	78.22	310	1,560	4,320	8,710	12,200	15,900	19,900	26,000	HEC-HMS Uniform Rain
Nueces River below Old River	8354.07	5,560	16,700	29,200	50,600	78,000	112,000	137,000	187,000	HEC-HMS Elliptical Storms
Nueces River and White Creek	8464.98	5,390	16,100	28,000	48,500	74,700	107,000	131,000	179,000	HEC-HMS Elliptical Storms
Nueces River above Atascosa River	8519.43	5,170	15,200	26,600	45,800	70,500	101,000	124,000	170,000	HEC-HMS Elliptical Storms
Frio River and East Frio River	96.68	4,670	16,000	27,200	41,900	55,000	68,000	81,000	98,000	HEC-HMS Uniform Rain
Frio River at Leakey (USGS gage 08194840)	235.06	6,840	27,600	49,300	81,500	108,000	135,000	160,000	196,000	HEC-HMS Uniform Rain
Frio River at Concan (USGS gage 08195000)	389.64	7,960	33,300	60,200	103,400	142,000	181,000	219,000	272,000	HEC-HMS Uniform Rain
Frio River above Dry Frio River	441.57	7,150	30,800	55,700	95,700	132,000	170,000	207,000	259,000	HEC-HMS Uniform Rain
Dry Frio River near Reagan Wells (USGS gage 08196000)	124.55	3,510	15,200	30,000	53,000	71,000	89,000	107,000	132,000	HEC-HMS Uniform Rain
Dry Frio River at FM 2690 (USGS gage 08196300)	176.10	2,790	14,000	27,900	50,500	69,000	88,000	107,000	135,000	HEC-HMS Uniform Rain
Dry Frio River above Frio River	187.17	2,490	13,100	26,100	47,500	65,000	84,000	102,000	129,000	HEC-HMS Uniform Rain
Frio River below Dry Frio River	628.74	11,000	43,400	78,900	136,000	182,000	236,000	274,000	345,000	HEC-HMS Elliptical Storm

	AEP	50%	20%	10%	4%	2%	1%	0.5%	0.2%	
Location Description	Drainage Area (sq mi)	2-yr	5-yr	10-yr	25-yr	50-yr	100-yr	200-yr	500-yr	Hydrologic Method
Frio River near Uvalde (USGS gage 08197500)	633.06	10,100	40,500	74,000	127,000	171,000	222,000	257,000	325,000	HEC-HMS Elliptical Storm
Frio River above Blanco Creek	745.82	3,200	21,600	41,300	74,900	101,000	131,000	155,000	201,000	HEC-HMS Elliptical Storm
Blanco Creek at Highway 90	64.51	310	1,790	3,910	12,800	24,900	35,100	45,000	57,800	HEC-HMS Uniform Rain
Blanco Creek above Frio River	133.59	210	990	2,440	9,100	18,600	26,900	35,500	47,400	HEC-HMS Uniform Rain
Frio River below Blanco Creek	879.41	4,340	22,100	41,500	76,800	106,000	140,000	167,000	218,000	HEC-HMS Elliptical Storm
Sabinal River near Vanderpool (USGS gage 08197936)	55.75	4,070	9,800	16,400	31,300	46,000	56,000	67,000	81,000	HEC-HMS Uniform Rain
Sabinal River at Utopia (USGS gage 08197970)	129.54	6,430	16,600	27,400	50,600	77,000	97,000	116,000	143,000	HEC-HMS Uniform Rain
Sabinal River near Sabinal (USGS gage 08198000)	205.92	6,590	18,400	31,300	59,500	92,000	118,000	144,000	179,000	HEC-HMS Uniform Rain
Sabinal River at Sabinal (USGS gage 08198500)	240.56	6,080	18,000	31,000	58,600	91,000	117,000	143,000	180,000	HEC-HMS Uniform Rain
Rancheros Creek and Elm Creek	79.64	430	1,180	2,190	7,060	13,800	19,600	25,800	34,200	HEC-HMS Uniform Rain
Sabinal River and Rancheros Creek	333.99	5,410	16,800	29,300	58,800	95,000	125,000	156,000	198,000	HEC-HMS Uniform Rain
Sabinal River above East Elm Creek	398.47	4,810	15,200	27,000	55,300	91,000	121,000	151,000	194,000	HEC-HMS Uniform Rain
Sabinal River below East Elm Creek	446.58	4,830	15,200	27,000	55,700	92,000	123,000	154,000	198,000	HEC-HMS Uniform Rain
Sabinal River above Frio River	459.21	4,490	14,300	25,500	52,600	87,000	117,000	147,000	190,000	HEC-HMS Uniform Rain
Frio River below Sabinal River	1338.62	5,070	21,100	39,600	77,200	114,000	156,000	191,000	257,000	HEC-HMS Elliptical Storm
Frio River above Elm Creek	1411.00	2,300	14,900	26,000	52,300	80,400	114,000	145,000	201,000	HEC-HMS Elliptical Storm

	<b>AEP</b>	<b>50%</b>	<b>20%</b>	<b>10%</b>	<b>4%</b>	<b>2%</b>	<b>1%</b>	<b>0.5%</b>	<b>0.2%</b>	
<b>Location Description</b>	<b>Drainage Area (sq mi)</b>	<b>2-yr</b>	<b>5-yr</b>	<b>10-yr</b>	<b>25-yr</b>	<b>50-yr</b>	<b>100-yr</b>	<b>200-yr</b>	<b>500-yr</b>	<b>Hydrologic Method</b>
Frio River below Elm Creek	1499.66	2,200	15,100	26,400	52,800	81,200	115,000	146,000	204,000	HEC-HMS Elliptical Storm
Frio River above Hondo Creek	1514.24	2,210	12,800	23,500	50,200	79,600	113,000	144,000	202,000	HEC-HMS Elliptical Storm
Hondo Creek near Tarpley (USGS gage 8200000)	96.07	4,840	20,000	37,600	63,100	81,000	100,000	118,000	143,000	HEC-HMS Uniform Rain
Hondo Creek at Hwy 173 nr Hondo, TX (USGS Gage 08200720)	156.45	5,180	19,900	36,000	61,100	80,000	102,000	122,000	150,000	HEC-HMS Uniform Rain
Hondo Creek above Verde Creek	160.76	3,890	13,900	24,900	42,600	57,000	73,000	88,000	109,000	HEC-HMS Uniform Rain
Middle Verde Ck at SH 173 nr Bandera (USGS gage 08200977)	38.90	1,180	2,900	6,300	16,600	29,000	38,000	46,000	56,000	HEC-HMS Uniform Rain
Middle Verde Creek and East Verde Creek	57.54	1,090	2,330	5,130	14,200	25,700	35,100	43,600	54,300	HEC-HMS Uniform Rain
Verde Creek below Quihi Creek	143.13	1,190	1,870	3,110	9,700	18,600	26,100	33,500	43,600	HEC-HMS Uniform Rain
Hondo Creek below Verde Creek	379.80	4,480	14,700	27,400	54,300	81,000	107,000	133,000	168,000	HEC-HMS Uniform Rain
Hondo Creek and Live Oak Creek	521.81	3,710	11,300	21,400	45,800	72,700	99,100	126,000	163,000	HEC-HMS Uniform Rain
Hondo Creek above Seco Creek	666.04	2,890	8,700	16,700	37,500	61,200	84,600	109,000	142,000	HEC-HMS Uniform Rain
Seco Creek at Miller RH near Utopia (USGS gage 08201500)	45.05	2,430	11,600	25,400	44,600	55,000	66,000	77,000	93,000	HEC-HMS Uniform Rain
Seco Creek and Rocky Creek	131.94	3,280	19,400	37,600	64,300	83,000	104,000	124,000	153,000	HEC-HMS Uniform Rain
Seco Creek Rowe RH near D'Hanis (USGS gage 08201500)	165.15	2,990	17,000	32,500	54,700	72,000	90,000	109,000	135,000	HEC-HMS Uniform Rain

	<b>AEP</b>	<b>50%</b>	<b>20%</b>	<b>10%</b>	<b>4%</b>	<b>2%</b>	<b>1%</b>	<b>0.5%</b>	<b>0.2%</b>	
<b>Location Description</b>	<b>Drainage Area (sq mi)</b>	<b>2-yr</b>	<b>5-yr</b>	<b>10-yr</b>	<b>25-yr</b>	<b>50-yr</b>	<b>100-yr</b>	<b>200-yr</b>	<b>500-yr</b>	<b>Hydrologic Method</b>
Seco Creek above Squirrel Creek	267.24	1,220	7,630	15,400	27,300	38,000	49,900	61,700	78,700	HEC-HMS Uniform Rain
Seco Creek above Hondo Creek	353.95	900	5,670	11,600	21,000	29,800	39,400	49,000	62,900	HEC-HMS Uniform Rain
Hondo Creek below Seco Creek	1019.99	3,650	13,900	27,400	57,000	88,700	121,000	154,000	201,000	HEC-HMS Uniform Rain
Hondo Creek above Frio River	1106.85	3,400	12,800	25,400	53,500	84,100	115,000	147,000	193,000	HEC-HMS Uniform Rain
Frio River below Hondo Creek	2621.10	6,140	21,600	36,500	79,500	122,000	174,000	213,000	283,000	HEC-HMS Elliptical Storm
Frio River above Leona River	2675.30	3,710	15,300	29,200	66,700	109,000	158,000	195,000	262,000	HEC-HMS Elliptical Storm
Leona River above Taylor Slough	49.67	300	1,100	1,330	3,450	9,100	13,400	18,200	24,600	HEC-HMS Uniform Rain
Leona River below Taylor Slough	68.61	420	1,510	2,220	5,570	13,700	19,600	26,100	35,000	HEC-HMS Uniform Rain
Leona River above Cooks Slough	68.61	410	1,470	2,150	5,390	13,300	19,100	25,400	34,100	HEC-HMS Uniform Rain
Leona River below Cooks Slough	102.62	470	1,850	2,690	7,560	19,800	29,000	38,700	52,100	HEC-HMS Uniform Rain
Leona River near Uvalde (USGS gage 08204005)	131.15	520	2,020	3,240	9,040	23,300	34,000	45,400	61,300	HEC-HMS Uniform Rain
Leona River above Camp Lake Slough	196.04	450	1,720	2,910	8,920	23,000	33,800	45,400	61,800	HEC-HMS Uniform Rain
Leona River below Camp Lake Slough	234.02	450	1,750	3,050	9,730	24,800	36,400	48,900	66,600	HEC-HMS Uniform Rain
Leona River at Highway 57 (USGS gage)	240.99	470	1,850	2,690	7,560	19,800	29,000	38,700	52,100	HEC-HMS Uniform Rain
Leona River above Live Oak Creek	380.41	390	1,500	2,740	9,510	23,800	34,900	47,200	64,700	HEC-HMS Uniform Rain
Leona River below Live Oak Creek	460.74	400	1,520	2,820	10,540	24,900	36,700	49,600	68,000	HEC-HMS Uniform Rain
Leona River above Todos Santos Creek	585.22	370	1,400	2,660	10,950	26,000	38,400	51,800	71,500	HEC-HMS Uniform Rain

	<b>AEP</b>	<b>50%</b>	<b>20%</b>	<b>10%</b>	<b>4%</b>	<b>2%</b>	<b>1%</b>	<b>0.5%</b>	<b>0.2%</b>	
<b>Location Description</b>	<b>Drainage Area (sq mi)</b>	<b>2-yr</b>	<b>5-yr</b>	<b>10-yr</b>	<b>25-yr</b>	<b>50-yr</b>	<b>100-yr</b>	<b>200-yr</b>	<b>500-yr</b>	<b>Hydrologic Method</b>
Leona River below Todos Santos Creek	660.74	370	1,400	2,670	11,260	26,900	39,700	53,500	73,700	HEC-HMS Uniform Rain
Leona River above Frio River	670.08	360	1,380	2,640	11,130	26,600	39,200	52,900	73,000	HEC-HMS Uniform Rain
Frio River below Leona River	3345.37	4,540	15,700	28,600	66,100	110,000	162,000	200,000	270,000	HEC-HMS Elliptical Storm
Frio River near Derby (USGS gage 08215500)	3447.76	4,690	14,300	26,000	63,400	107,000	159,000	197,000	268,000	HEC-HMS Elliptical Storms
Frio River at Highway 85	3500.89	3,590	12,000	22,600	58,400	99,100	150,000	186,000	255,000	HEC-HMS Elliptical Storms
Frio River and Ruiz Creek	3653.55	1,940	8,650	18,200	48,100	87,600	137,000	172,000	246,000	HEC-HMS Elliptical Storms
Frio River above Cibolo Creek	3698.16	1,940	6,860	13,900	38,000	78,900	130,000	165,000	239,000	HEC-HMS Elliptical Storms
Cibolo Creek at Highway 85	83.21	740	1,320	4,940	7,780	12,700	18,600	24,800	33,600	HEC-HMS Uniform Rain
Cibolo Creek at Purple Heart Trail	174.41	690	1,320	5,760	9,270	15,500	22,900	33,900	47,500	HEC-HMS Uniform Rain
Cibolo Creek above Frio River	394.76	1,680	3,200	9,100	13,700	21,600	31,500	41,900	56,800	HEC-HMS Uniform Rain
Frio River below Cibolo Creek	4092.91	2,280	11,600	19,200	40,800	80,800	134,000	170,000	246,000	HEC-HMS Elliptical Storms
Frio River above Esperanz Creek	4149.39	2,190	7,960	13,200	36,200	72,100	125,000	161,000	235,000	HEC-HMS Elliptical Storms
Frio River below Esperanza Creek	4248.12	2,500	8,500	14,100	36,300	71,700	125,000	160,000	235,000	HEC-HMS Elliptical Storms
Frio River and Galinda Creek	4337.72	2,590	8,810	14,000	33,200	64,500	116,000	152,000	225,000	HEC-HMS Elliptical Storms
Frio River above Leoncita Creek	4396.25	2,740	8,390	14,100	31,300	59,200	108,000	144,000	216,000	HEC-HMS Elliptical Storms
Frio River at Tilden (USGS gage 08206600)	4462.81	2,780	8,420	14,200	31,400	59,500	109,000	144,000	216,000	HEC-HMS Elliptical Storms
Frio River above San Miguel Creek	4519.46	2,710	8,340	14,100	31,400	59,300	108,000	143,000	215,000	HEC-HMS Elliptical Storms

	<b>AEP</b>	<b>50%</b>	<b>20%</b>	<b>10%</b>	<b>4%</b>	<b>2%</b>	<b>1%</b>	<b>0.5%</b>	<b>0.2%</b>	
<b>Location Description</b>	<b>Drainage Area (sq mi)</b>	<b>2-yr</b>	<b>5-yr</b>	<b>10-yr</b>	<b>25-yr</b>	<b>50-yr</b>	<b>100-yr</b>	<b>200-yr</b>	<b>500-yr</b>	<b>Hydrologic Method</b>
San Miguel Creek above Black Creek	221.57	1,760	5,250	8,610	15,400	22,000	28,700	35,800	47,000	HEC-HMS Uniform Rain
San Miguel Creek below Black Creek	348.53	2,280	8,110	13,800	25,300	36,700	47,600	59,400	77,000	HEC-HMS Uniform Rain
San Miguel Creek below Highway 97	516.77	2,180	7,360	13,000	25,300	38,500	51,200	74,600	108,000	HEC-HMS Uniform Rain
San Miguel Creek above Lagunillas Creek	574.60	2,140	7,210	12,700	24,800	37,700	50,100	66,600	98,000	HEC-HMS Uniform Rain
San Miguel Creek below Lagunillas Creek	741.44	2,400	8,630	16,500	32,200	49,500	65,500	81,100	118,000	HEC-HMS Uniform Rain
San Miguel Creek near Tilden (USGS gage 08206700)	782.15	2,960	8,930	15,900	31,200	48,200	63,900	79,900	114,000	HEC-HMS Uniform Rain
San Miguel Creek above Frio River	854.80	2,870	8,810	15,300	30,600	47,700	65,100	82,300	113,000	HEC-HMS Uniform Rain
Frio River below San Miguel Creek	5374.26	3,000	8,720	15,000	31,600	59,400	108,000	143,000	216,000	HEC-HMS Elliptical Storm
Choke Canyon Reservoir Inflow	5490.45	2,900	8,560	14,500	31,300	59,000	107,000	142,000	215,000	HEC-HMS Elliptical Storm
Choke Canyon Dam Outflows	5490.45	1,780	8,460	14,400	29,900	53,900	97,700	130,000	177,000	HEC-HMS Elliptical Storm
Frio River below Choke Canyon Dam	5490.45	1,780	8,460	14,400	29,900	53,900	97,700	130,000	177,000	HEC-HMS Elliptical Storm
Frio River above Atascosa River	5496.36	1,910	8,660	14,800	29,800	53,900	97,900	130,000	178,000	HEC-HMS Elliptical Storms
Atascosa River near FM 2904	154.50	1,070	5,000	9,200	15,800	22,000	29,000	37,000	47,000	HEC-HMS Uniform Rain
Atascosa River at FM 476 (USGS gage 08207290)	315.12	1,280	6,300	11,300	20,700	30,700	42,500	55,300	74,600	HEC-HMS Uniform Rain
Atascosa River at Highway 37	451.31	1,440	7,100	13,800	25,300	37,000	51,000	65,800	87,600	HEC-HMS Uniform Rain
Atascosa River near McCoy (USGS gage 08207500)	510.87	1,250	6,600	13,000	24,800	36,800	52,000	68,100	91,900	HEC-HMS Uniform Rain

	AEP	50%	20%	10%	4%	2%	1%	0.5%	0.2%	
Location Description	Drainage Area (sq mi)	2-yr	5-yr	10-yr	25-yr	50-yr	100-yr	200-yr	500-yr	Hydrologic Method
Atascosa River above Borrego Creek	535.96	1,220	6,350	12,700	24,100	36,100	51,200	67,400	91,500	HEC-HMS Uniform Rain
Borrego Creek and Los Cortes Creek	142.92	1,460	5,140	8,830	14,600	20,000	26,300	32,700	42,700	HEC-HMS Uniform Rain
Borrego Creek above Atascosa River	221.19	1,700	4,540	8,260	14,800	21,400	29,400	37,800	52,400	HEC-HMS Uniform Rain
Atascosa River below Borrego Creek	757.15	1,950	8,690	17,800	33,500	50,000	72,000	95,000	129,000	HEC-HMS Uniform Rain
Atascosa River above La Parita Creek	813.17	2,080	8,470	17,100	32,500	48,000	70,000	93,000	128,000	HEC-HMS Uniform Rain
La Parita Creek and Metate Creek	291.40	2,410	7,660	12,900	21,400	29,600	39,000	48,700	63,600	HEC-HMS Uniform Rain
La Parita Creek above Atascosa River	311.40	2,260	7,290	12,300	20,600	29,200	38,700	48,400	63,300	HEC-HMS Uniform Rain
Atascosa River below La Parita Creek	1124.57	4,300	12,200	20,800	39,900	60,000	88,000	119,000	167,000	HEC-HMS Uniform Rain
Atascosa River at Whitsett (USGS gage 0820800)	1145.77	4,140	12,200	20,500	39,800	60,000	88,000	118,000	166,000	HEC-HMS Uniform Rain
Atascosa River above Weedy Creek	1225.28	4,050	11,300	20,200	39,200	59,000	85,700	116,000	163,000	HEC-HMS Uniform Rain
Atascosa river below Weedy Creek	1364.40	4,130	11,500	21,000	39,700	60,000	87,600	119,000	169,000	HEC-HMS Uniform Rain
Atascosa River above Frio River	1395.61	4,100	10,800	20,500	39,300	59,400	86,500	117,000	167,000	HEC-HMS Uniform Rain
Atascosa River below Frio River	6891.97	16,600	29,400	42,000	57,100	65,500	94,500	113,000	162,000	HEC-HMS Elliptical Storm
Atascosa River above Nueces River	6911.11	3,640	11,300	20,100	29,600	52,500	98,900	131,000	184,000	HEC-HMS Elliptical Storm
Nueces River below Atascosa River	15430.54	5,090	14,700	27,900	47,800	78,000	122,000	148,000	200,000	HEC-HMS Elliptical Storm
Nueces River at Three Rivers (USGS gage 08210000)	15430.54	3,760	12,100	20,100	34,200	62,500	114,000	153,000	220,000	HEC-HMS Elliptical Storms

	<b>AEP</b>	<b>50%</b>	<b>20%</b>	<b>10%</b>	<b>4%</b>	<b>2%</b>	<b>1%</b>	<b>0.5%</b>	<b>0.2%</b>	
<b>Location Description</b>	<b>Drainage Area (sq mi)</b>	<b>2-yr</b>	<b>5-yr</b>	<b>10-yr</b>	<b>25-yr</b>	<b>50-yr</b>	<b>100-yr</b>	<b>200-yr</b>	<b>500-yr</b>	<b>Hydrologic Method</b>
Nueces River and Sulphur Creek	15619.12	5,790	16,100	30,600	49,500	75,800	120,000	146,000	203,000	HEC-HMS Elliptical Storms
Nueces River at Highway 59	15715.07	23,700	41,700	52,800	65,100	71,400	105,000	127,000	184,000	HEC-HMS Elliptical Storms
Nueces River above Spring Creek	15733.03	4,550	13,600	25,200	44,500	74,200	116,000	139,000	189,000	HEC-HMS Elliptical Storms
Nueces River below Spring Creek	15833.59	5,350	15,000	28,200	47,400	76,700	122,000	148,000	202,000	HEC-HMS Elliptical Storms
Nueces River and Upper End of Lake Corpus Christi	15921.68	5,430	15,100	29,000	48,000	75,700	121,000	148,000	204,000	HEC-HMS Elliptical Storms
Nueces River above Lake Corpus Christi	16076.35	5,720	15,900	28,100	44,000	67,400	109,000	132,000	187,000	HEC-HMS Elliptical Storms
Lagarto Creek near George West (USGS gage 08210400)	155.28	450	4,080	9,420	16,600	22,300	29,600	37,100	48,100	HEC-HMS Uniform Rain
Lagarto Creek above Lake Corpus Christi	201.87	330	3,470	8,870	16,400	22,800	31,400	40,000	52,600	HEC-HMS Uniform Rain
Ramirena Creek at Highway 281	81.02	590	3,810	8,400	14,400	19,100	24,700	30,300	38,500	HEC-HMS Uniform Rain
Ramirena Creek above Lake Corpus Christi	119.60	400	4,100	9,600	16,500	22,300	30,100	38,300	50,700	HEC-HMS Uniform Rain
Lake Corpus Christi Inflow	16502.10	5,210	12,100	24,300	43,400	70,800	111,000	135,000	182,000	HEC-HMS Elliptical Storms
Lake Corpus Christi Dam Outflow	16502.10	4,000	11,800	19,300	32,000	56,900	101,000	137,000	203,000	HEC-HMS Elliptical Storm
Nueces River near Mathis (USGS gage 08211000)	16502.10	4,000	11,800	19,300	32,000	56,900	101,000	137,000	203,000	HEC-HMS Elliptical Storm
Nueces at Bluntzer (USGS gage 08211200)	16617.60	3,640	11,300	19,200	32,500	58,300	102,000	134,800	202,400	HEC-HMS Elliptical Storms
Nueces River at Calallen (USGS gage 08211500)	16675.30	2,880	9,740	17,200	28,900	51,000	93,200	124,000	188,000	HEC-HMS Elliptical Storms

**Table 12.2: Recommended Frequency Peak Pool Elevations (feet NAVD88) for Reservoirs in the Nueces River Basin**

Reservoir Name	Drainage Area	50%	20%	10%	4%	2%	1%	0.50%	0.20%	Hydrologic Method
	sq mi	2-YR	5-YR	10-YR	25-YR	50-YR	100-YR	200-YR	500-YR	
Choke Canyon Reservoir	3451.8	220.57	221.89	222.46	223.02	223.34	223.62	224.01	224.39	RMC-RFA Reservoir Analysis
Lake Corpus Christi	7569.3	94.06	94.24	94.39	94.48	94.67	94.85	95.50	96.83	RMC-RFA Reservoir Analysis

## 13 Conclusions

This report summarizes new analyses that were completed as part of an InFRM Watershed Hydrology Assessment (WHA) to estimate the 1% annual chance (100-yr) flow, along with other frequency flows, for various stream reaches throughout the Nueces River Basin in Texas. In addition to the partnered federal agencies of the InFRM team, regional stakeholders such as the Nueces River Authority, Bureau of Reclamation (BoR), City of Corpus Christi, and the Texas Water Development Board (TWDB) also participated in the updates and review process for this study. This study represents a significant step forward towards increasing resiliency against flood hazards in the Nueces River basin.

The flow results that were recommended for adoption came from a combination of the watershed model results using NOAA Atlas 14 uniform rain, elliptical storms, and reservoir analysis techniques. Other methods, such as the statistical and RiverWare results, were used as points of comparison to fine tune the model for the frequent storms, but they were not adopted directly due to their tendency to change after each significant flood event. Since the calibrated watershed model simulates the physical processes that occur during a storm event, it can produce more reliable and consistent estimations of the flow expected during a 1% annual chance (100-yr) storm. In addition, NOAA Atlas 14's recent study of rainfall depths in Texas shed new light on the depths and frequency of rainfall that could be expected in the Nueces River basin. Both uniform rain and elliptical shaped frequency storms were run in the watershed model. The elliptical frequency storm results were generally recommended for river reaches with large drainage areas, while the uniform rain results were recommended for the smaller drainage areas. The expected impacts of reservoir operations for Choke Canyon Reservoir and Lake Corpus Christi were also analyzed in detail for this study, and the frequency dam pool elevations that resulted from the reservoir analyses were recommended for the reaches immediately upstream of the dams.

Previously published frequency discharges from effective FEMA Flood Insurance Studies (FIS) and Base Level Engineering (BLE) data in the Nueces River Basin differ from the new flow frequency results of this study in many locations. For the large majority of the Nueces River basin, no effective FEMA FIS flows have been published, so the results from this study provide a significant step forward in accurately mapping flood risk in the Nueces River basin. The BLE data that was available in the Nueces River basin at the time of this report publication was only from 1D HEC-RAS modeling using regional regression equations. The results of this study showed that the 1D BLE data was grossly underestimating the flood risk for the unregulated areas of Nueces River basin while overestimating the frequency discharges on some of the reaches downstream of the major reservoirs.

The statistical analyses of the gage records and the RiverWare results are generally consistent with the recommended results from this study but may be slightly higher or lower than the recommended results at a given location, depending on whether or not large storms have hit that particular watershed during the observed period of record. For the two reservoirs in the basin, Choke Canyon Reservoir and Lake Corpus Christi, the recommended results of this study came from detailed reservoir analyses that utilized stochastic techniques to account for the operations of the dam, the frequency and volume of its inflows, and the possible range of its starting pool elevations. Once again, the areas near these reservoirs have not been previously studied in detail; therefore, there are no effective FEMA FIS pool elevations available for comparison.

Given the severe loss of life and property due to flooding that has occurred multiple times throughout the history of Texas, it is imperative that future updates to the published flood insurance rate maps for the Nueces River Basin accurately reflect the levels of flood risk in the basin. The recommended results from this study represent the best available estimate of flood risk for the larger streams in the Nueces River basin, based on a range of hydrologic methods performed by an expert team of engineers and scientists from multiple federal agencies. For smaller tributaries in the Nueces basin, the recommended results from the watershed model provide a good

starting point which could be further refined by adding additional subbasins and using methodologies that are consistent with this study.

As a result of the level of investment, analyses, and collaboration that went into this Watershed Hydrology Assessment, the flood risk estimates contained in this report are recommended as the basis for future NFIP studies or other federal flood risk studies within the Nueces River basin. These federally developed modeling results form a consistent understanding of hydrology across the Nueces watershed, which is a key requirement outlined in FEMA's General Hydrologic Considerations Guidance. Furthermore, the models and data used to produce these flood risk estimates are available upon request, at no charge, to communities, local stakeholders, and architecture engineering firms. Models can be requested through the InFRM website at [www.InFRM.us](http://www.InFRM.us).

While the results from this study should be considered the best available estimates of flood risk for many areas of the Nueces River basin, significant uncertainty still remains, as it does in any hydrologic study. Because of this uncertainty and because of the potential impacts these estimates can have on life and property, the InFRM team strongly recommends and supports local communities that implement higher standards, such as additional freeboard requirements, floodplain management practices based on standards greater than the 1% annual chance flood, and/or "no valley storage loss" criteria.

# 14 References and Resources

## 14.1 REFERENCES

- Asquith, W.H., *Effects of regulation on L-moments of annual peak streamflow in Texas*: U.S. Geological Survey Water-Resources Investigations Report 01-4243, 66 p., <http://pubs.usgs.gov/wri/wri014243/>; 2001.
- Asquith, W.H., *Distributional analysis with L-moment statistics using the R environment for statistical computing*: Ph.D. dissertation, Texas Tech University, accessed on June 3, 2016 at <https://ttu-ir.tdl.org/ttu-ir/handle/2346/ETD-TTU-2011-05-1319>; 2011a.
- Asquith, W.H., *Distributional analysis with L-moment statistics using the R environment for statistical computing*: CreateSpace, [print-on-demand], ISBN 978-146350841-8, [reprinting of Asquith (2011a), with errata]; 2011b.
- Asquith, W.H., and Roussel, M.C., *Regression equations for estimation of annual peak-streamflow frequency for undeveloped watersheds in Texas using an L-moment-based, PRESS-minimized, residual-adjusted approach*: U.S. Geological Survey Scientific Investigations Report 2009-5087, 48 p., <http://pubs.usgs.gov/sir/2009/5087/>; 2009.
- Asquith, W.H. and Famiglietti, J.S. *Precipitation Areal-Reduction Factor Estimation Using an Annual-Maxima Centered Approach*. Journal of Hydrology. 2000.
- Asquith, W.H., Roussel, M.C., Atlas of *Depth-Duration Frequency of Precipitation Annual Maxima for Texas*; U.S. Geological Survey Scientific Investigations Report 2004-5041; 2009.
- Asquith, W.H., Roussel, M.C., and Vrabel, Joseph, *Statewide analysis of the drainage-area ratio method for 34 streamflow percentile ranges in Texas*: U.S. Geological Survey Scientific Investigation Report 2006-5286, 34 p., 1 appendix, <http://pubs.usgs.gov/sir/2006/5286/>; 2006.
- Asquith, W.H., and Slade, R.M., *Regional equations for estimation of peak-streamflow frequency for natural basins in Texas*: U.S. Geological Survey Water-Resources Investigations Report 96-4307, 68p., accessed September 21, 2017 at <https://doi.org/10.3133/wri964307>; 1997
- Asquith, W.H., and Thompson, D.B., *Alternative regression equations for estimation of annual peak-streamflow frequency for undeveloped watersheds in Texas using PRESS minimization*: U.S. Geological Survey Scientific Investigations Report 2008-5084, 40 p., <http://pubs.usgs.gov/sir/2008/5084/>; 2008.
- Asquith, W.H., Yesildirek, M.V., Landers, R.N., Cleveland, T.G., Fang, Z.N., Zhang, J. *Technique to estimate generalized skew coefficients of annual peak streamflow for natural basins in Texas*, in Cleveland, T.G., Fang, Z.N., Zhang, J., and Landers, R.N., 2021, Develop a generalized skew update and regional study of other measures of distribution shape for Texas flood frequency analyses: Texas Department of Transportation Research Report 0-6977-1, chapter N, pp. 1-19, accessed Jun. 1, 2022, at <https://rosap.nrl.bts.gov/view/dot/60662>; 2021.
- Cohn, T. A., Lane, W. L., and Baier, W. G. *An algorithm for computing moments-based flood quantile estimates when historical flood information is available*. Water Resources Research, 33(9):2089-2096. 1997.
- Cohn, T. A., Lane, W. L., and Stedinger, J. R. *Confidence intervals for Expected Moments Algorithm flood quantile estimates*. Water Resources Research, 37(6):1695-1706. 2001.

Dalrymple, T., 1939, Major Texas floods of 1935: U.S. Geological Survey Water Supply Paper 796-G, 81 p., accessed Dec. 1, 2021, at <https://doi.org/10.3133/wsp796G>.

Duan, Q. Y., Gupta, V. K., & Sorooshian, S. *Shuffled complex evolution approach for effective and efficient global minimization. Journal of optimization theory and applications*, 76(3), 501-521. 1993.

England, J.F., Jr.; Cohn, T.A.; Faber, B.A.; Stedinger, J.R.; Thomas, W.O., Jr.; Veilleux, A.G.; Kiang, J.E.; and Mason, R.R., Jr. *Guidelines for determining flood flow frequency—Bulletin 17C (ver. 1.1, May 2019): U.S. Geological Survey Techniques and Methods*, book 4, chap. B5, 148 p., accessed June 29, 2022, at <https://doi.org/10.3133/tm4B5>; 2019.

Faber, B. *Flood Frequency Analysis. "Lecture 3.4 Uncertainty in Frequency Estimates,"* Training at the USACE Hydrologic Engineering Center (HEC), May 2018.

FEMA, *Base Level Engineering (BLE) Analysis, Region 6 Nueces River Watershed.* <https://webapps.usgs.gov/infrm/estBFE/>. August 2019.

Flynn, K.M., Kirby, W.H., and Hummel, P.R. *User's Manual for Program PeakFQ Annual Flood-Frequency Analysis Using Bulletin 17B Guidelines: U.S. Geological Survey, Techniques and Methods Book 4, Chapter B4; 42 p*, accessed March 30, 2018 at <https://pubs.usgs.gov/tm/2006/tm4b4/>. 2006.

Good, P.I., and Hardin, J.W., *Common errors in statistics (and how to avoid them):* New York, John Wiley, ISBN 0-471-46068-0, 2006.

Gumbel, E. J., 1958, *Statistics of extremes*, Columbia Univ. press, New York. 1958.

Gupta, R. D. *Hydrology and Hydraulic Systems.* Long Grove: Waveland Press. 2008.

Hansen, E.M., L.C. Schreiner, and J.F. Miller. *Application of Probable Maximum Precipitation Estimates – United States East of the 105<sup>th</sup> Meridian. Hydrometeorological Report No. 52.* National Weather Service, Washington D.C. 1982.

Helsel, D.R., and Hirsch, R.M., *Statistical methods in water resources: U.S. Geological Survey Techniques of Water-Resources Investigations book 4, chap. A3,* <http://pubs.usgs.gov/twri/twri4a3>; 2002.

Hershfield, D.M. *Rainfall-Intensity-Duration-Frequency Curves for Selected Stations in the United States, Alaska, Hawaiian Islands, and Puerto Rico. Technical Paper 25.* U.S. Weather Bureau. 1955.

Hershfield, D.M. *Rainfall Intensity-Frequency Regime. Technical Paper 29, Part 1 The Ohio Valley, Part 2 Southeastern United States.* U.S. Weather Bureau. 1957, 1958.

Hershfield, D.M. *Rainfall frequency atlas of the United States for durations from 30 minutes to 24 hours and return periods from 1 to 100 years, TP 40.* National Weather Service. 1961.

Hirsh, R.M. *A Comparison of Four Streamflow Record Extension Techniques.* US Geological Survey, Water Resources Research, Vol. 18, No. 4, Pages 1081-1088, Aug 1982.

Hirsch, R.M., and Gilroy, E.J., 1984, Methods of fitting a straight line to data—examples in water resources: *Water Resources Bulletin*, v. 20, no. 5, p. 705–711, accessed Jul. 12, 2021, at <https://doi.org/10.1111/j.1752-1688.1984.tb04753.x>.

Hirsch, R.M. and Stedinger, J.R. *Plotting positions for historical floods and their positions,* *Water Resources Research*, Vol 23, No. 4, p. 715–727, accessed on March 30, 2018 at <https://doi.org/10.1029/WR023i004p00715>. 1987.

- Hollander, M., and Wolfe, D.A., *Nonparametric statistical procedures*: John Wiley and Sons, New York, 503 p. 1973.
- Interagency Advisory Committee on Water Data [IACWD], *Guidelines for determining flood flow frequency: Bulletin 17B*, Reston, Virginia, U.S. Department of the Interior, Geological Survey, accessed on May 10, 2016 at [http://water.usgs.gov/osw/bulletin17b/dl\\_flow.pdf](http://water.usgs.gov/osw/bulletin17b/dl_flow.pdf); 1982.
- Interagency Flood Risk Management (InFRM). *Watershed Hydrology Assessment for the Guadalupe River Basin*. 2019.
- Interagency Flood Risk Management (InFRM). *Watershed Hydrology Assessment for the Trinity River Basin*. 2021.
- Interagency Flood Risk Management (InFRM). *Watershed Hydrology Assessment for the Neches River Basin*. 2022.
- Interagency Flood Risk Management (InFRM). *Watershed Hydrology Assessment for the Lower Colorado River Basin*. 2024.
- Judd, L., Asquith, W.H., and Slade, R.M., *Techniques to estimate generalized skew coefficients of annual peak streamflow for natural basins in Texas*: U.S. Geological Survey Water Resource Investigations Report 96-4117, 28 p., <http://pubs.usgs.gov/wri/wri97-4117/>; 1996.
- Kang, B., Kim, E., Kim, J., & Moon, S. *Comparative study on spatiotemporal characteristics of fixed-area and storm-centered ARFs*. 2019.
- Kloesel, K., B., et al. *Southern Great Plains. In Impacts, Risks, and Adaptation in the United States: Fourth National Climate Assessment, Volume II*. U.S. Global Change Research Program, Washington, DC, USA, pp. 987-1035. doi: 10.7930/NCA4.2018.CH23, 2018.
- Kunkel, K.E. *Incorporation of the Effects of Future Anthropogenically-Forced Climate Change in Intensity-Duration-Frequency Design Values*. Department of Defense Strategic Environmental Research and Development Project (SERDP), RC-2517. 2020.
- McEnroe, B. and Gonzalez, P. *Storm Duration and Antecedent Moisture Conditions for Flood Discharge Estimation*. Kansas Department of Transportation. November 2003.
- Minshall, N.E. *Predicting Storm Runoff on Small Experimental Watersheds*. Paper No. 3333, ASCE. 1962.
- Moriasi, D.N., et al. *Model Evaluation Guidelines for Systematic Quantification of Accuracy in Watershed Simulations*. American Society of Agricultural and Biological Engineers. 2007.
- Moriasi, D.N., et al. *Hydrologic and Water Quality Models: Performance Measures and Evaluation Criteria*. American Society of Agricultural and Biological Engineers. 2012.
- Meyers, V.A., Zehr, R.M., *A Methodology for Point-to-Area Rainfall Frequency Ratios*. NOAA Technical Report NWS 24. National Weather Service. 1980.
- Natural Resources Conservation Service (NRCS), United States Department of Agriculture (USDA). *Web Soil Survey*. Available online at <https://websoilsurvey.nrcs.usda.gov/>. Accessed December 2009.
- National Centers for Environmental Information (NCEI), U.S. climatological divisions: National Oceanic and Atmospheric Administration, accessed on July 24, 2016 at <https://www.ncdc.noaa.gov/monitoring-references/maps/images/us-climate-divisions-names.jpg>; 2016a.

- NCEI, Climate indices: National Oceanic and Atmospheric Administration, accessed on July 24, 2016 at <http://www7.ncdc.noaa.gov/CDO/CDODivisionalSelect.jsp>; 2016b.
- NCEI. State Summaries 149-TX, NOAA Technical Report NESDIS 149-TX. <https://statesummaries.ncics.org/chapter/tx/> 2017.
- NCEI, U.S. climate divisions—History of the U.S. climate divisional dataset: National Oceanic and Atmospheric Administration, accessed on May 10, 2016 at <http://www.ncdc.noaa.gov/monitoring-references/maps/us-climate-divisions.php>; 2016d.
- Nelder, J. A., & Mead, R. *A simple method for function minimization*. The computer journal, 7(4), 308-313. 1965.
- Nelson, T.L. *Synthetic Unit Hydrograph Relationships Trinity River Tributaries, Fort Worth-Dallas Urban Area*, 1970.
- NOAA, Hydrometeorological Design Studies Center, *Precipitation Frequency Data Server (PFDS)*. <https://hdsc.nws.noaa.gov/hdsc/pfds/> Accessed Aug 2022.
- NOAA, *NOAA Atlas 14 Precipitation Frequency Atlas of the United States: Volume 11 Version 2.0: Texas*, 2018.
- Nueces River Authority. *Lower Nueces River Watershed Protection Plan*. 2015.
- PRISM, *Time Series Values for Individual Locations*: data product of the Northwest Alliance for Computational Science and Engineering, accessed on July 30, 2018 at <http://www.prism.oregonstate.edu/explorer/>. 2015.
- RiverWare. *Technical Documentation Version 7.4, USACE-SWD Methods*, Center for Advanced Decision Support for Water and Environmental Systems (ADSWES), University of Colorado Boulder. 2019.
- Rodman, P.K. *Effects of Urbanization on Various Frequency Peak Discharges*, 1977.
- Slade, R.M., Tasker, G.D., and Asquith W.H., *Multiple-regression equations to estimate peak-flow frequency for streams in Hays County, Texas*: U.S. Geological Survey Water Resources Investigations Report 95-4019; 1995.
- State of Texas, Board of Water Engineers. *Texas Floods of April – May – June 1957*. October 1957.
- Snyder, F.F. *Synthetic Unit Graphs*. Transactions. American Geophysical Union. 1938.
- Texas Water Development Board (TWDB), *Chapter 4: Climate of Texas, Water for Texas 2012 State Water Plan*. 2012.
- USACE. *Corps Water Management System (CWMS) Final Report for the Nueces River Watershed*. March 2020.
- USACE. Engineer Manual 1110-3-1411, “Standard Project Flood Determinations.” Available from: [http://www.publications.usace.army.mil/Portals/76/Publications/EngineerManuals/EM\\_1110-2-1411.pdf](http://www.publications.usace.army.mil/Portals/76/Publications/EngineerManuals/EM_1110-2-1411.pdf)
- USACE. *Hydrologic Hazard Curves for Success Dam*, Sacramento District, 26 p. 2017.
- USACE. *Inflow Design Floods for Dam and Reservoirs*. ER 110-8-2(FR). 1991.
- USACE. *National Inventory of Dams (NID)*. <https://nid.sec.usace.army.mil/ords/f?p=105:1> Accessed June 2016.
- USACE. *Storm rainfall in the United States, depth, area, duration data*. Revised January 2, 1962. 1945.
- USACE. *The Texas Storm Study*. [www.InFRM.us](http://www.InFRM.us); 2024.

USACE, Fort Worth District. *Determination of Percent Sand in Watersheds*. 1986.

USACE, Fort Worth District. *SWFHYD "NUDALLAS" Documentation*, 1989.

USACE, Fort Worth District *Texas Storm Study*. 2024

USACE, Risk Management Center (RMC). *Probable maximum flood analysis for Whittier Narrows Dam*. 2017.

U.S. Department of Agriculture (USDA). *Urban hydrology for small watersheds*. Soil Conservation Service, Engineering Division. Technical Release 55 (TR-55). 1986.

U.S. Geological Survey (USGS), *PeakFQ—Flood Frequency Analysis Based on Bulletin 17B and recommendations of the Advisory Committee on Water Information (ACWI) Subcommittee on Hydrology (SOH) Hydrologic Frequency Analysis Work Group (HFAWG)*: accessed on May 7, 2016 at <http://water.usgs.gov/software/PeakFQ/>. 2014.

U.S. Geological Survey (USGS). *3DEP LiDAR Explorer*. Available from: <https://prd-nm.s3.amazonaws.com/LidarExplorer/index.html#/>. Accessed 2018. 2018a.

U.S. Geological Survey, *Computation of annual exceedance probability (AEP) for characterization of observed flood peaks*: U.S. Geological Survey Office of Surface Water Technical Memorandum 2013.01 accessed on July 1, 2015 at <http://water.usgs.gov/admin/memo/SW/sw13.01.pdf>; 2012.

U.S. Geological Survey (USGS), *Floods in Southeast Texas, October 1994*. Fact Sheet 94-073. January 1995.

U.S. Geological Survey [USGS], 2021, USGS Water data for the Nation: U.S. Geological Survey National Water Information System database: accessed Feb. 24, 2021, at <https://doi.org/10.5066/F7P55KJN>.

Veilleux, A.G., Cohn, T.A., Kathleen M. Flynn, K.M., Mason, R.R., Jr., and Hummel, P.R., *Estimating magnitude and frequency of floods using the PeakFQ 7.0 program*: U.S. Geological Survey Fact Sheet 2013-3108, 2 p., <http://pubs.usgs.gov/fs/2013/3108/>; 2013.

Vogel, R.M., and Stedinger, J.R., 1985, Minimum variance streamflow record augmentation procedures: *Water Resources Research*, v. 21, no. 5, p. 715–723, accessed Jul. 12, 2021, at <https://doi.org/10.1029/WRO21i005p00715>.

## 14.2 SOFTWARE

ArcGIS, Environmental Systems Research Institute, Inc., ArcMap 10.2.2: Retrieved from <http://www.esri.com/>.

CWMS, US Army Corps of Engineers, Corps Water Management System, CWMS 2.1, retrieved from <http://www.hec.usace.army.mil>.

HEC-DSSVue, US Army Corps of Engineers, HEC-DSSVue 2.0.1: Retrieved from <http://www.hec.usace.army.mil>.

HEC-GeoHMS, US Army Corps of Engineers, HEC-GeoHMS 10.2: Retrieved from <http://www.hec.usace.army.mil>

HEC-HMS, US Army Corps of Engineers, Hydrologic Engineering Center Hydrologic Modeling System, [HEC-HMS 4.6.1 and 4.11](#): Retrieved from <http://www.hec.usace.army.mil>

HEC-MetVue, US Army Corps of Engineers, Hydrologic Engineering Center Meteorological Visualization Utility Engine, HEC-MetVue 3.1 (2019): Retrieved from <http://www.hec.usace.army.mil>

HEC-RAS, US Army Corps of Engineers, Hydrologic Engineering Center River Analysis System, [HEC-RAS 6.4.1](#): Retrieved from <http://www.hec.usace.army.mil>.

HEC-SSP, US Army Corps of Engineers, Hydrologic Engineering Center Statistical Software Package, [HEC-SSP 2.2](#): Retrieved from <http://www.hec.usace.army.mil>

PeakFQ, U.S. Geological Survey (USGS), Hydrologic Frequency Analysis Work Group (HFAWG). [PeakFQ 7.2](#) retrieved from <http://water.usgs.gov/software/PeakFQ/>

Python Software Foundation. Python Language Reference, version 2.7. Retrieved from <http://www.python.org>.

RiverWare, Center of Advanced Decision Support for Water and Environmental System (CADSWES), University of Colorado Boulder, [RiverWare 8.0.1](#), retrieved from [www.Riverware.org](http://www.Riverware.org).

RMC-RFA, UA Army Corps of Engineers, *Risk Management Center Reservoir Frequency Analysis (RMC-RFA)*, [Version 1.1.0](#), obtained from the USACE Risk Management Center. [2018](#).

## 14.3 DATA SOURCES, GUIDANCE & PROCEDURES

Environmental Systems Research Institute, Inc. (ESRI). United States National Boundary, County Boundaries, Street Centerlines.

Available from: <http://www.esri.com/software/arcgis/arcgisonline/services/map-services>

Environmental Systems Research Institute, Inc. (ESRI),

[http://www.esri.com/software/arcgis/arcgisonline/map\\_services.html](http://www.esri.com/software/arcgis/arcgisonline/map_services.html)

ESRI Streetmap2D Image Service - ESRI basemap data, DeLorme basemap layers, Automotive Navigation Data (AND) road data, U.S. Geological Survey (USGS) elevation data, UNEP-WCMC parks and protected areas for the world, Tele Atlas Dynamap® and Multinet® street data for North America and Europe and First American (CoreLogic) parcel data for the United States.

ESRI World Imagery Service - Imagery from NASA, icubed, U.S. Geological Survey (USGS), U.S. Department of Agriculture Farm Services Agency (USDA FSA), GeoEye, and Aerials Express.

ESRI. ArcGIS software. Application reference available from: <http://www.esri.com/>

Federal Emergency Management Agency (FEMA). Publication 64, "Federal Guidelines for Dam Safety, Emergency Action Planning for Dam Owners," Federal Emergency Management Agency (FEMA) U.S. Department of Homeland Security (DHS), Washington, D.C., 2004.

Available from: <http://www.fema.gov/library/viewRecord.do?id=1672>

Gesch, D., Oimoen, M., Greenlee, S., Nelson, C., Steuck, M., and Tyler, D. "The National Elevation Dataset: Photogrammetric Engineering and Remote Sensing," v. 68, no. 1, p. 5-11, 2002.

Texas Department of Transportation (TxDOT). 2019 Roadway Inventory. Available from:

<https://www.txdot.gov/inside-txdot/division/transportation-planning/roadway-inventory.html>

USACE. Engineering and Construction Bulletin 2008-10, CECW-CE, March 24, 2008.

USACE. Guideline RD-13, "Flood Emergency Plans – Guidelines for Corps Dams," USACE Hydrologic Engineering Center, Davis, CA, June 1980.

Available from: [http://www.hec.usace.army.mil/publications/pub\\_download.html](http://www.hec.usace.army.mil/publications/pub_download.html)

USACE, HEC. HEC-GeoRAS software.

Available from: [http://www.hec.usace.army.mil/software/hec-ras/hec-georas\\_downloads.html](http://www.hec.usace.army.mil/software/hec-ras/hec-georas_downloads.html)

USACE, HEC. HEC-RAS software.

Available from: <http://www.hec.usace.army.mil/software/hecras/hecras-download.html>

USACE, HEC. "HEC-GeoRAS User's Manual," Davis, CA, September 2005.

USACE, HEC. "HEC-HMS Hydrologic Modeling System User's Manual," USACE, Davis, CA, November 2006.

USACE, HEC. "HEC-RAS River Analysis System, Hydraulic Reference Manual," Davis, CA, November 2002.

USACE, HEC. "HEC-RAS River Analysis System User's Manual," Davis, CA, November 2006.

U.S. Department of Agriculture, Farm Service Agency. National Agriculture Imagery Program Images.

Available from: <http://www.fsa.usda.gov/FSA/apfoapp?area=home&subject=prog&topic=nai>

U.S. Geological Survey (USGS). 3DEP LiDAR Explorer. Available from: [https://prd-tnm.s3.amazonaws.com/LidarExplorer/index.html#/.](https://prd-tnm.s3.amazonaws.com/LidarExplorer/index.html#/)

U.S. Geological Survey (USGS). National Elevation Dataset. Available from: <http://ned.usgs.gov/>

U.S. Geological Survey (USGS). National Hydrography Dataset. Available from: <http://nhd.usgs.gov/data.html>

# 15 Terms of Reference

Acronym	Definition
2D	two-dimensional
3DEP	three-dimensional Elevation Program
AEP	annual exceedance probability
BFE	base flood elevations
cfs	cubic feet per second
CWMS	Corps Water Management System
DDF	Depth Duration Frequency
DEM	digital elevation model
DSS	data storage system
EM	Engineering Manual
ER	Engineering Regulation
EMA	expected moment algorithm
ERDC	Engineering Research & Development Center of USACE
FEMA	Federal Emergency Management Agency
FIS	flood insurance study
GeoHMS	Geospatial Hydrologic Model System extension
GIS	Geographic Information Systems
HEC	Hydrologic Engineering Center
HMS	Hydrologic Modeling System
IACWD	Interagency Advisory Committee on Water Data
InFRM	Interagency Flood Risk Management
LiDAR	Light (Laser) Detection and Range
LPIII	Log Pearson III
MMC	Modeling, Mapping, and Consequences Production Center
NA14	NOAA Atlas 14
NAD 83	North American Datum of 1983
NCDC	National Climatic Data Center
NED	National Elevation Dataset
NGVD 29	National Geodetic Vertical Datum of 1929
NHD	National Hydrography Dataset
NID	National Inventory of Dams
NLCD	National Land Cover Database
NOAA	National Oceanic and Atmospheric Administration
NRCS	Natural Resources Conservation Service
NSE	Nash Sutcliffe Efficiency
NWIS	National Water Information System
NWS	National Weather Service
PeakFQ	Peak Flood Frequency
PFDS	Precipitation Frequency Data Server
PMP	Probable Maximum Precipitation
QPF	Quantitative Precipitation Forecast
RAS	River Analysis System
ResSim	Reservoir System Simulation
RFA	Reservoir Frequency Analysis
RFC	River Forecast Center
RMC	Risk Management Center
RMSE	root mean square error
RSR	observed standard deviation ratio
SCS	Soil Conservation Service
SHG	Standard Hydrologic Grid

<b>Acronym</b>	<b>Definition</b>
SME	subject matter expert
SOP	Standard Operating Procedures
sq mi	square miles
SSURGO	Soil Survey Geographic Database
TxDOT	Texas Department of Transportation
USACE	U.S. Army Corps of Engineers
USDA	U.S. Department of Agriculture
USGS	U.S. Geological Survey
WCM	Water Control Manual
WGRFC	West Gulf River Forecast Center

